REPORT DOCUMENTATION PAGE

Form Approved OMB No. 0704-0188

Public reporting burden for this collection of information is estimated to average 1 hour per response, including the time for reviewing instructions, searching existing data sources, gathering and maintaining the data needed, and completing and reviewing the collection of information. Send comments regarding this burden estimate or any other aspect of this collection of information, including suggestions for reducing the burden, to Department of Defense, Washington Headquarters Services, Directorate for Information Operations and Reports (0704-0188), 1215 Jefferson Davis Highway, Suite 1204, Arlington, VA 22202-4302. Respondents should be aware that notwithstanding any other provision of law, no person shall be subject to any penalty for failing to comply with a collection of information if it does not display a currently valid OMB control number.
PLEASE DO NOT RETURN YOUR FORM TO THE ABOVE ADDRESS.

1. REPORT DATE *(DD-MM-YYYY)* 24-06-2005	2. REPORT TYPE Final Report	3. DATES COVERED *(From – To)* 01-Apr-02 - 22-Jul-05

4. TITLE AND SUBTITLE

Nanoscale Mechanism of Composite Reinforcement by Fibers and Filler, Theoretical Computation and Experimental Validation of the Theory Using Rubber/Short Carbon Fiber Compounds

5a. CONTRACT NUMBER
ISTC Registration No: 2154p

5b. GRANT NUMBER

5c. PROGRAM ELEMENT NUMBER

6. AUTHOR(S)

Professor Sergey A. Lurie

5d. PROJECT NUMBER

5d. TASK NUMBER

5e. WORK UNIT NUMBER

7. PERFORMING ORGANIZATION NAME(S) AND ADDRESS(ES)
Computing Center of Academy of Sciences
Vavilova 40
Moscow 117967
Russia

8. PERFORMING ORGANIZATION REPORT NUMBER

N/A

9. SPONSORING/MONITORING AGENCY NAME(S) AND ADDRESS(ES)

EOARD
PSC 821 BOX 14
FPO 09421-0014

10. SPONSOR/MONITOR'S ACRONYM(S)

11. SPONSOR/MONITOR'S REPORT NUMBER(S)
ISTC 00-7044

12. DISTRIBUTION/AVAILABILITY STATEMENT

Approved for public release; distribution is unlimited.

13. SUPPLEMENTARY NOTES

14. ABSTRACT

This report results from a contract tasking Computing Center of Academy of Sciences as follows: The description of the mechanical characteristics and prediction of the behavior of composite materials reinforced by short carbon fibers and fillers is the goal of the project. The development of the theoretical techniques of the research of reinforced composite materials with taking into account of interphasic interactions between carbon fibers and the matrix represents the task of the project. The experimental validation of the theoretical research by using the measured mechanical properties of reinforced composite materials is also the task of the project.
The accomplishment of such tasks has been possible thanks to the recent program of mathematical description and modeling of interfacial interactions and also to the appropriate experimental test.
To describe the effective medium characteristics with nanoscale structures the homogenization problem is solved. The methods of solutions of the identification problems are developed within framework of the Project for designed models with nanoscale structures.
A strong impact on the knowledge of composite theoretical behavior is expected as a result of this Project. The obtained experimental results should support the extension of the mathematical description to other kinds of composites, mainly fiber/epoxy, carbon/carbon etc.

15. SUBJECT TERMS
EOARD, Materials, Laminates and Composite Materials

16. SECURITY CLASSIFICATION OF:			17. LIMITATION OF ABSTRACT	18, NUMBER OF PAGES	19a. NAME OF RESPONSIBLE PERSON JOAN FULLER
a. REPORT UNCLAS	b. ABSTRACT UNCLAS	c. THIS PAGE UNCLAS	UL	268	19b. TELEPHONE NUMBER *(Include area code)* +44 (0)20 7514 3154

Standard Form 298 (Rev. 8/98)
Prescribed by ANSI Std. Z39-18

ANNUAL TECHNICAL REPORT

FINAL REPORT

Project Title #2154 p

Nanoscale Mechanism of Composite Reinforcement by Fibers and Filler, Theoretical Computation and Experimental Validation of the Theory Using Rubber/Short Carbon Fiber Compounds
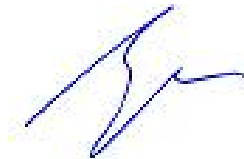
Participating Institutions:

1. Leading Institution: Dorodnicyn Computing Centre of Russian Academy of Sciences (CCAS)

2. Supporting Institution: Institute of Applied Mechanics of Russian Academy of Sciences RAS (IPRIM)

Project Manager   S.A. Lurie

Director
of the Dorodnicyn Computing Centre
of Russian Academy of Sciences (CCAS)   Y.G. Evtushenko

Moscow 2005

1. Title of the Project / Number of Annual Report

1. Project **N 2154 p**   The Final Annual Report

Title:

"Nanoscale Mechanism of Composite Reinforcement by Fibers and Filler, Theoretical Computation and Experimental Validation of the Theory Using Rubber/Short Carbon Fiber Compounds"

2. Contracting Institute:

> Dorodnicyn Computing Centre of Russian Academy of Sciences (CCAS)

3. Participating Institutes:

> Institute of Applied Mechanics of Russian Academy of Sciences RAS (IPRIM)

4. Project Manager:

Sergey A. Lurie,

Phone number: 7(095)135-6190,   Fax numbers: 7(095)135-6190   and   7(095)135-6159

E-mail address: lurie@ccas.ru

5. Commencement Date: 01.04.2002,

> Duration: 36 months

6. Brief description of the work plan: objective, expected results, technical approach

Objective:

- The aim of the project is to determine effective mechanical characteristics and to predict behavior of the composite enforced with carbon fibers and nanoparticles, from the point of view of enhanced methods of classical continuum mechanics and composite mechanics.

The following statements determine aims of the current stage:

- Modeling of adhesion interaction of the polymer and inclusions, estimation of properties of the interface layer, its thickness, and dependence of its properties on the properties of the matrix and inclusion.
- Development of the theoretical basis of modeling of disperse enforced composites accounting for the scale effects.
- Theoretical and numerical modeling of deformation of composite as a whole accounting for cohesion and adhesion interactions.
- Writing and testing algorithms and methods of calculations of effective characteristics of the disperse composites.
- Development of quantum-mechanical and quantum-chemical modeling.
- Description and predictions of properties of the composites.
- Experimental verification of the theoretical statements and results, which is one of the main aims.

Expected results:

- To obtain the dependence of the change of elastic parameters of the composites reinforced with both isotropic and anisotropic inclusions (nanotubes) for various types of particles distributions over orientation.
- To write the dependence of the composite elastic moduli accounting for the finiteness of inclusions concentration (the solutions are obtained in the form of dependences of the moduli on concentration for various relative nanotubes lengths).
- To give the algorithm of an approximate calculation of the effective characteristics of nano-composite, consisting of the matrix, nano-inclusions taking into account interphase layer of the inclusions and of the matrix surrounding the nano-particles.
- To write a mechanical model of the nanotube, surrounded by the polymer matrix, and to obtain the distribution of the shear stresses, which depend on behavior of the material in the interface layer.
- To develop the interphase layer theory of cohesion-adhesion interactions as a display of non-classical phases properties in the contact zone, and apply its to the mechanics of disperse composites.

- To estimate the properties of the interface layer and effective properties of the equivalent homogeneous medium and to give an example of the solution for the problem of identifying non-classical properties of the composite. To find analytical approximation formulas for the composite characteristics allowing to forecast the composite properties for the wide range of volumetric concentration and diameters of the inclusions.
- To obtain the generalized of the integral Eshelby's formulas, which allows determining the increase in the energy in the fragment due to inclusion of another material and to obtain the solution of the generalized of the fundamental Eshelby's problem for an isolated inclusion in the framework of the theory of the interphase layer (adhesion-cohesion model).
- To describe physical and mechanical properties of the composite with high-elastic matrix on the base of investigations of microstructure.
- With the help of direct numerical modeling:
  o to study interaction of polymer molecules with the surfaces of technical carbon;
  o to describe structural and energetic characteristics of mixtures of polymer and carbon microclasters;
  o to investigate the structure as well as energetic and mechanical properties of model particles of technical carbon;
  o to determine influence of the mentioned physical-chemical factors to micromechanical behavior and properties of the model composite media and the related effect of enforcement.

Technical Approach:

The following approaches were used:

Variational methods and methods of variational calculus, tensor algebra, methods of mathematical physics, methods of mechanics of solids, methods of mechanics of composites (methods of equivalent inclusions of Eshelby, method Mori-Tanaka, mechanical model of a nanotube embedded to polymer matrix, development of Kelly-Tyson model) were used to develop mathematical micro- and macro-models of composite materials, investigation influence of structural parameters to behavior of heterogeneous media, enhanced study of of properties of new composites. Numerical modeling on the base of a new blocked analytical-numerical method was applied to 2-D and 3-D domains. Physical molecular modeling and Monte-Carlo method were applied to investigate molecular interactions and transformations. Methods of parameters identification on the base of experimental data were used for visco-elastic media. Experimental investigations of the composite samples (field resins) were also used.

7. Technical progress during the second year (for 3nd annual reports)

- A set of particular solutions was obtained for composite reinforced both isotropic and anisotropic inclusions (nanotubes). Three types of space distributions of inclusions were studied: unidirectional, isotropic and in-plane distribution of the inclusions. The solutions were obtained in the form of dependences of moduli versus volumetric effective concentration of the inclusions for various aspect ratios of the latter.
- It was shown that according to Mori-Tanaka's method within the diapason of concentrations of interest the dependences of moduli on the concentration very slightly deviate from the linear ones. Hence, for all configurations of interest the linearised (on concentration) dependences were obtained for the changes of elastic moduli due to presence of inclusions according to the theory of dilute concentrations, which simplifies the procedure and visualization significantly.
- An algorithm for approximate calculating the effective characteristics of three phase composite material formed by the matrix, nano-tubes (or disk-like nano-particles) and surrounding them regions of the third phase was presented.

- The mechanical model of the nanotube embedded in the polymer matrix was proposed. The model takes into attention the dependence of the interface shear stresses (and, therefore, the adhesion parameters) on the displacements of the nanotube axis, the elastic properties of the polymer matrix and the nanotube, and on the thickness of the adhesion layer between the matrix and the nanotube.

- The theory of interphase layer was constructed which models the interactions of adhesion and cohesion types on the base of a continuum model accounting for scale effects.

- Approximate analytical estimations of Young's and shear moduli of the interphase layer are given. In addition to the previous stages of the work, a model of adhesion interaction is given. The example is given illustrating that the effect of adhesion may lead to both increase (for an ideal contact) and decrease (for the case of damage) of the effective stiffness of a two-phases sample.

- Composite materials are considered taking into account the theory of interphase layer (local cohesion and adhesion effects). The account of these local effects allows to model effect of strengthening of the filled composite materials

- Approximate analytical estimations of Young's modulus of the composite materials taking into account the local cohesion and adhesion effects are established. It was shown, that usage of simple enough modelling statements of the problems within the framework of the theory of an interphase layer allows to describe characteristics of composites well enough. Such solutions give a good consent with results that are submitted in work (Odegard et al, 2002) and experimental dates.

- The consecutive concept of the quantum-mechanical description of materials was formulated. The suggested concept allows to connect macro- and micro-characteristics of materials with parameters of potentials used for modelling continuum mediums as ensemble of the particles connected by special character of interactions.

- The effective block analytical-numerical method was developed. A generalization of algorithm of a block analytical-numerical method is performed for spatial problems (3D problem) with an inclusion of an arbitrary shape and its partial realization is made. Test calculations were made for the classical component, confirming efficiency of a method.

- The problem of the identification of the model parameters on the base of more complete description was considered. The identification problem of determining of mathematical model parameters was investigated using experimental data. The diapason of parameters (concentration and sizes of the inclusions) for which the model agrees well with experimental dates.

- On the basis of molecular models of saturated hydrocarbonic polymers (prototype of elastomers) and nano-model of technical carbon by means of quantum-mechanical approach and direct quantum-chemical numerical simulation, the computational experiments for polymer composites filled with disperse particles were gone on. An interconnection between texture and properties of surface for pure graphite fillers and for hydrogen terminated graphite surfaces is ascertained.

- The method of identification of constitutive material parameters of heterogeneous viscoelastic media was elaborated for description of geometrical non-linear behavior of considered systems under finite deformations. It was shown, that on the base of evaluation of alteration some material parameters, one can adequate characterize an ability to damage of this materials.

- For modeling reinforcement effect for polymer high-elastic composites (rubbers) multiscale hierarchical approach has been used. The approach had some important steps, that are:

    -Atomic-molecular computer description the behavior of nano- and mesostructures for representative elements of volume of heterogeneous polymer composites media.

    -Atomic-molecular experimental investigations of the properties of surface of reinforced media by means of complex of atomic-forced, tunnel-scanning, dynamic-forced microscopes.

    -Physical description micro- and macromechanics of composite high-elastic heterogeneous media taking into account the properties of interphase layers.

-Phenomenological description of behavior of high-elastic heterogeneous media by small (linear) and finite (large) deformations and an identification of non-linear models for description of behavior by deformation.

-Experimental evaluation of the complex of viscoelastic mechanical properties for model rubber compounds on the basis of natural rubber filled with black and white soot (ten different sorts) by small (linear) and finite (up to destruction) deformation modes. Evaluation of relaxation properties. Juxtaposition with prognosis of previous levels.

- By modeling of atomic-molecular mesoscopic systems a set of new algorithms and programs based on quantum-mechanical approach, Monte-Carlo method and molecular dynamics methods, developed by the authors, were used. An influence of different physico-chemical factors, that is, properties of surface of solid phase, the nature of polymer molecules, some important reinforced additives end etc., on character of interaction of constituents of heterogeneous media were analyzed.

- A comparison of viscoelastic behavior of rubber compounds filled with different sorts of reinforced particles by small and finite (up to destruction) deformation was done experimentally and theoretically, during the procedure of identification. Validity of effect of reinforcement on the basis of the analysis of relaxation properties of materials content the different sorts of technical carbons and silica had also been made.

8. <u>Technical progress during the year of reference</u>

For the last year the work was conducted in full agreement with the problems and main stages formulated in the Research Plan. In addition to the problems pointed in the Research Plan, additional work was done discussed with the employer.

The key achievements are related mainly to the following results:

According to the Working Plan the following works have been done and the following main results achieved:

- The algorithm for calculating the effective characteristics of three phase composite material formed by the matrix, nano-tubes (or disk-like nano-particles) and surrounding them regions of the third phase is developed. Variants of both direct and inverse problems are considered for both thick and thin intermediate layer. In the frame of the approach the effects caused by anisotropy are accounted. An example of solving inverse problem has been presented: estimation of the properties of intermediate layer

- During the reported period we proposed a mechanical model of the interface adhesion of polymer matrix and nanotubes accounting for the dependencies of the shear stresses between matrix and nanotube versus the main physical-mechanical parameters of the nanocomposite material: -the parametric analysis of the model parameters on the nanotubes and the interface layer stresses states was performed; -the asymptotic cases of the stresses states were considered and analyzed; -the multi-parametric model was proposed for the analysis of properties of new nanocomposite materials and for analysis of the experimental data.

- On the basis of the previous researches the consistent and correct theory of interphase layer was formulated and analyzed as whole. The theory of interphase layer includes the following moments: -the formal mathematical statement, -the physical constitutive equations, - the identification problem of the parameters determining nonclassical effects, -the qualitative analysis of the theory-analytical estimations of properties of an interphase layer, -the qualitative analysis of the theory-estimation of an interphase layer influence on the effective characteristics of a composite, -some application for fracture mechanics, quantum mechanical approaches, -numerical modeling of the stress state of the cell with inclusions and some notes about specific averaging procedures for filled composites, previously results of the generalized Eshelby problem and its application.

- A new general kinematic theory of defects in continuous media, the general mechanisms of existence of defects, their generation (or birth) and disappearance (or healing) were establish.
- The generalized model of pseudocontinuums are obtained for which a surface tension, static friction bodies with ideally smooth surface of contact, the meniscus, wettability and capillarity are modeled as special effects within the framework of unified continual description. All these special effects are united by one property, they are the scale effects in continuums.
- Using asymptotic approach the correct algorithm for the account of damage is proposed on the base strong generalized model of the mediums with reserved dislocation.
- On the basis of procedure of asymptotic homogenization of composite materials with a periodic microstructure it was received the formula for effective characteristics of composite materials with account of the local effects.
- With the help of a block method of multipoles distribution of energy density and components of stress tensor in micro cell with inclusion is simulated. The features of the current realization of algorithm of a block method are shown, which require its technical modification in the way of improvement of block system of the equations solver and more accurate normalization of joining functionals.
- The algorithm of the solution of a problem of model parameters identification has been developed according to experimental researches for the general three-dimensional case. The series of the calculations has been made.
- A new approach to model and investigation both the texture and the mechanical characteristics of large molecular systems by Monte-Carlo method has been developed. As a base of the method is an unorthodox algorithm allowed to make a classical Metropolis procedure for a few polymer molecules. Algorithm under consideration belongs to class of program which use space decomposition and has high grade of calibration. The structures of model mixtures of n-pentane and carbon microclusters C_{38} (graphite type) as prototype of reinforced rubber composites have been investigated. It was shown the strong dependence the grade of associate of carbons microclusters on form of its surface. Chemical modification of components of mixture substantially influences on structure and mechanical properties of materials under study. So, aquation of carbon microclusters leads to decreasing of middle value of potential energy of particles. We proposed the method and investigated the mobility of polymer molecules close to surface of particle of filler. It was fixed the presence of layer with limited mobility around area of contact "polymer – graphite". It was developed the method of evaluation of shear modulus for composite microcluster during the model by Monte-Carlo method. Quantum-Chemical Approach.
- At given stage of work in course of modelling it was obtained that maximal shear force for polymer particle adsorbed on carbon surface was found approximately 3 times higher than for polymer in a polymeric matrix. Owing to rather weak however quite sufficient for immobilization of polymeric chain segments on the carbon surface Van-der-Waals forces, around carbon filler particles some condensed layer of rubber is formed with the lowered mobility of chain segments which most likely is responsible for strengthening of organic polymers by filling them with high dispersed carbon. Summarizing in should be mentioned, that in the given section the technique offered earlier is tested on an example of calculation of molecular friction in the complex system consisting of organic polymer and carbon filler. The reinforcing effect of pure nonterminated carbon fillers is the best. Some conclusions about impact of chemical nature of the polymer matrix on the interaction of the polymer segments with surface of soot fillers have been done. Aggregation of the soot particles can be prevented by adsorption interlayer of polymer between the soot particles. Adsorption of water in the interparticle interface can be considered as competitive process for polymer adsorption. For the formation of the contact polymer-filler water layer on the soot surface has to be removed. Hence the best reinforcement can be reported for the combination of isoprene-amorphous carbon and the worth

for system polyethylene-amorphous carbon. Obtained dependencies of polymer molecule cohesion with carbon particle surface (or of the highest forces of microscopic friction) are in a good accordance with calculated geometrical and energetic characteristics. The best cohesion of isoprene chain with filler particle surface (the highest forces of microscopic friction) was obtained for the system isoprene-silica. A little worth is cohesion of isoprene with carbon black or soot. Such fillers as fullerene and high dispersed carbon tubes represent lower forces of adhesion. As it is seen from the obtained results enthalpy of binding of rubber chains on a clay surface and force of microscopical friction in this system, which interconnected with cohesion is strongly depended on modification of clay surface by hydrophobic agent (organic cation). The best case can be observed if use organic cations with middle-sized chains at about 15-20 monomer units and various modification of uncharged end providing better hydrophobic binding with rubber chains.

- During the molecular-dynamic modelling it was shown, there is the discrepancy between behaviour of polyethylene and polyisoprene chains under their interaction with carbon fillers. The polyethylene chains sharply change their configuration on time and always furls into ball both in case of contact to carbon particles and without. Materials with polyethylene matrix practically do not keep an initial configuration and quickly jump in amorphous condition, aggregated around carbon particle. Polyisoprene chains, contrariwise, keep initial structure and injection into system of carbon filler deepens this tendency. Polyisoprene's component is stabilized in presence of carbon filler. As structural so energetic results of molecular dynamic calculation testify about. Injection into composite system polyisoprene – carbon filler some water destabilizes appropriate adsorption complexes, but at this case the system keeps the shape of its structure pretty long.

- To investigate the microstructure of rubber composites the method of dynamic forced microscopy and 3D-optical interferential microscope have been used. Different sorts of technical carbons and samples of rubber compounds filled with active particles have been analyzed. Microstructure investigations of geometry of surface of particles of disperse filler and aggregations of those inside elastomeric matrix gave us very useful information for verification of theoretical and model evaluations of parameters of microclusters of composite polymeric structures. The samples of natural rubber filled with montmorillonite (5, 20, 40, 60% vol.) and samples of natural rubber filled with combined particles (technical carbon and montmorillonite) have been investigated. Rheological data which have been made during full-scale investigations let us to evaluate some important relaxation parameters and, first of all, the spectrum of relaxation time distribution. It was systematize the data about influence of different sorts of filler on complex of rheological and relaxation parameters, which govern to viscoelastic behavior above media under deformation. Such information is important for the setup of optimal processing technology of the composite compounds into articles.

- It was accomplished the task of identification of nonlinear model for viscoelastic media on the basis of the nonlinear integrated Hammerstein's operator. Is shown, that this operator with a nucleus synthesized on calculation of a relaxation spectrum, not always provides qualitative identification of model at the large deformations. The lacks of application of concept of a relaxation spectrum in models force us to pass to other type of models based on neural networks. The technique of synthesis of neural networks for the decision of a concrete mathematical task is given. The detailed block diagrams of neural networks for the decision of the specified kind of tasks are given. It is established, that during training and adaptation of neural network are frequently observed long convergence iterative procedures to extremal of functional. Last circumstance compels to use methods of regularization by training of neural models. Synthesis and analysis of neural work model to describe the behavior of viscoelastic media shows, that to accomplishment of required workable accuracy of neural network without using the feedback (small mistake of training), it is necessary to interpolate the experimental data in order to expand a dimension of vectors.

- The algorithm for designation strength characteristics of heterogeneous media has been proposed. Justification of entered idea about stress and strain concentration tensors is shown. Consideration of properties of symmetry for periodicity cells allows to simplify a calculation the effective stiffness tensor of those.

See at the end of the report the following forms:
9. Current technical status , 10.Cooperation with foreign collaborators, 11. Problems encountered and suggestions to remedy, 12. Perspectives of future developments of the research/technology developed

PREFACE
(Compliance with tasks and milestones as described in the work plan)

The final report contains work executed according to the plan and also brief generalization of the results received at the previous stages of work under Project.

The investigations were elaborated in the complete correspondence with coordinated and authorized Plan of Work , within the framework of following tasks and subtasks of the Project

Problem 1
Development of molecular models of the interface layers for reinforced composites and development of molecular models of interphase layers for reinforced matrix composites and description of physico-mechanical properties of the composites with viscoelastic matrix. The methods of description of physico-mechanical properties of the composites with polymeric matrix on the base of microstructural approach.

Problem 2
Development of the block structure and realization of the analytic-numerical method for the media with nanoinclusions and of an effective method of calculation of the average properties for the heterogeneous media and its realization. Development of the analytic-numerical method for the media with nanoinclusions, arbitrarily oriented in the space and containing a boundary layer: -calculation of the stress distribution and the average properties of the media based on the complete version of the program for calculation and optimization of heterogeneous media reinforced by nanoinclusions with a boundary layer

Problem 3
The experimental and theoretical assessment of the physico-mechanical properties of the disperse composites. Studying of the macromechanical properties (effective and strength parameters etc.) of the heterogeneous media as a whole. Verifications of some hypothesis and approaches used in the calculations and reconsideration of some hypothesis and approaches used in the calculations.

Problem 4
Estimation of an influence of the shape, dimensions, of rigid inclusions and spatial distribution of the inclusions (its statistical characteristics) of to the increase in the material stiffness. The comparison with the experimental data and development of preliminary recommendations for improving composite deformation characteristics by adjusting its microstructure.

Problem 5
Modeling and prediction of macroscopic properties of materials fabricated from polymer matrix and nanoparticles or nanotubes. Analysis of the adhesion strength at the nanotube - polymer matrix interface. Prediction of macroscopic properties of materials fabricated from polymer matrix and nanoparticles or nanotubes. Calculating of the stress-strain state characteristics.

Task 6. Simulation of the continuum behavior with internal degree of freedoms for a description of the composite materials reinforced by fillers. Calculating of the nano-particles stiffness. Formulation of the relations for moment continuums with an additional kinematics degree of freedom (the set models of the Cossera type). Simulation of mediums with a continuous field of defects (damage accumulation models) by variation procedures. Simulation of composites as a heterogeneous continuum with a field of defects (fillers). Prediction of the mechanical effective properties of composites with shot fibers compounds.

Problem 7

Definition of the unknown parameters of the model to fit the experimental data. Development of the numerical algorithm for the calculation of Gradient of cost functional and the development of the appropriate approximation for the conjugate problem (with the aid of Fast Automatic Differentiation technique); the choice suitable numerical code for the optimization of functional

Present Final Technical Report includes complete discussion of these products:
- Development of numerical methods for a calculation of the media with inclusions.
- The experimental and theoretical assessment of the physico-mechanical properties of the disperse composites.
- Simulation of the continuum behavior with internal degree of freedoms for a description of the composite materials reinforced by fillers.
- Definition of the unknown parameters of the model to fit the experimental data.

SUMMARY

A number of important particular cases, for which asymptotical representations are possible, were pointed out: flat inclusions (nano-plates), and needle-like inclusions (nano-tubes). The combined influence of the shape and relative stiffness of inclusions was investigated; it was shown that the presence of two parameters (the ratio of maximal an minimal dimensions of the inclusion and relative stiffness of inclusions) leads to non-uniform limit transition, which restricts the area of applicability of known classical asymptotical formulae. The areas of applicability of asymptotical formulae were obtained (appears to be for the first time). It was shown that the main influence is due to some particular combinations of elastic parameters of inclusions, and these combinations were pointed out. For the composites on the base of nano-tubes three types of space distribution were considered: random, aligned and transverse (all inclusions lay in parallel planes). The solution for last case appears to be obtained for the first time.

Originally, all the solutions were obtained for the small concentration of inclusions. The influence of concentration were then accounted for with the help of differential self-consistent method and the method of effective field (Mori-Tanaka). The former appears to be more strict and physically justified, however it leads to necessity to solve systems of differential equations. The obtained results appear to be important as it are, as well as an useful tool for constructing more advanced models such as three-phases models, accounting for the presence of an intermediate layer between the matrix and inclusions.

The current report continues research of properties of composite materials, determined by the parameters of the matrix and filler. An algorithm for approximate calculating the effective characteristics of three phase composite material formed by the matrix, nano-tubes (or disk-like nano-particles) and surrounding them regions of the third phase is presented. Variants of solutions for both direct and inverse problems have been suggested.

According to the working plan the modeling of the nanotube-polymer matrix adhesion was. we continued studies modeling of the nanotube-polymer matrix adhesion. The statement of the problem and all equations were presented in the preceding reports in details. In this final report the analysis of the computation results, obtained according to the model proposed in the preceding reports is presented.

A new general theory of defects in continuous media is introduced. The general mechanisms of generation and healing of defects are established. The kinematic description of continuum media with defects is presented. The definition of defects of different levels is given, and the classification of continuous media with defects is introduced. The hierarchic structure of the theory of defects is discussed. A new broad class of defects of new types is established and interpreted. It is shown that the existence of new classes of defects is directly connected with some known theoretical and experimental data on the possibility of generation of such defects as dislocations and disclinations. In particular, it is shown that the generation of dislocations is necessarily connected with the existence of disclinations. The formal class of defects being a source of disclinations is specified. A formal generalization of classification of defects is developed to include the defects of any finite level. The development of consistent theory of defects is very important from both, fundamental and applied viewpoints. The potential applications include, in particular, the modeling of dispersed composite materials, porous media, dynamics of surface effects, crackling, cavitation and turbulence.

The correct medium models with the microstructure (by the Mindlin's definition) investigated in this part of work. The set of constitutive equations is determined and the corresponding boundary problem statement is formulated. It's demonstrated, that concerned medium models are not only model the scale effects, but also are the base for description of rather wide spectrum of the adhesion interactions. In this work the principal attention is focused on analysis of the physical part of the model. For the first time the interpretation of all the physical characteristics is given, which are described the non-classical effects, as well as description of adhesion mechanical parameters is given. The submitted generalized model of mechanics of continua as a whole is theoretical model in which a surface tension, static friction bodies with ideally smooth surface of contact, the meniscus, wettability and capillarity are modeled as special effects within the framework of unified continual description. All these special effects are united by one signature they are the scale effects in continuums.

The test problems allowing to define all spectrum of modules of elasticity are established. Thus, formulas for definition of characteristics of a researched material both damaged, and the non-damaged mediums are established. In essence, algorithms of definition of all spectrum of physical constants for mediums with fields of defects - dislocations (the filled composites, porous environments), taking into account scale effects are offered.

The Klapeiron's and Dupre's theorems were proved for the pseudocontinuum model with scale effects of the cohesion and adhesion types.

The algorithm of the damage accumulation estimation (development of porosity and so on), was proposed on the base strong generalized model of the mediums with reserved dislocation. The asymptotic method of the reduced loadings was proposed, as theoretically proved way of the account of the damage accumulation in the filled composites and anisotropic composite materials under various conditions of loading.

On the basis of the previous researches the consistent and correct theory of interphase layer as whole was formulated and analyzed. The analytical estimations of the interphase layer properties, composite properties were done, some particular tasks (Eshelby problem) and applications were considered and identification problem for the model parameters were solved.

With the help of a block method of multipoles distribution of energy density and components of stress tensor in micro cell with inclusion is simulated at variation of cohesion field parameters and of inclusion orientation inside a cell that has significance for quality evaluation of influence of cohesion fields and for calculation of effective characteristics of materials with random distribution of inclusions.

On the basis of procedure of asymptotic homogenization of composite materials with a periodic microstructure it was received the formula for effective characteristics of composite materials with account of the local effects.

As a fundamental background of theory of reinforcement of rubber composites the multiscale hierarchical model (from nano- to mega-) and approach, which consider rubber composite as non-linear heterogeneous multicomponent medium is proposed. Description of the properties of above medium is made taking into account the physico-chemical and micromechanical peculiarities of its components. The unorthodox algorithms for description of nano- and mezo- structural and mechanical properties of given sorts of medium have been developed by the authors. On the base of above algorithms in parallel regimes of calculations by supercomputer numerous computational experiments (methods of Monte-Carlo, molecular dynamics, quantum mechanics) have been made. Representative volumes of medium under consideration have kept up to 106 atoms and molecules that correspond to microclusters of real composite's structures. The general peculiarities of formation the microstructure of polymeric composites, consisted of different polymeric matrixes (the thermoplastics, the elastomers, the thermoreactoplastics) and the active fillers (black and white soot, fullerens, nanotubes, montmorillonite), terminated by different chemical groups have been elaborated. It was separately investigated an influence

of molecular water inside a microcluster on the micromechanical behavior of above media. A correctness of atomic-molecular computational model under study is verified by means of nano- and microstructure experiments. Constitutive micromechanical rheological equations have been constructed on the base of unorthodox integral models of viscoelastic media, using non-linear Hammerstein's type operators. In this view the method of theoretical and experimental identification have been developed. The availability of neural network models for identification of viscoelastic and relaxation properties of composite's polymer media has also been discussed. The results of theoretical and numerical description have verified by means of numerous experimental investigations of model elastomeric compounds on the base of natural rubber filled with different sorts of disperse particles (black and white soot, montmorillonite). Both the structure characteristics (methods of dynamic forced microscopy and 3D optical interferential microscopy) and the viscoelastic (rheological) properties have been tested. The last one has investigated in wide range of regimes and parameters of deformations and temperatures. To estimate the efficient (average) macrocharacteristics of strength properties of heterogeneous media (rubber composites, particularly) a new method has been proposed. The evaluation of effective mechanical and strength properties of composites appoints the operational merits of those. Above stage of work logically finalizes the multiscale hierarchical description of behavior of reinforcement rubber composite.

All of the stages of work according to scientific schedule for the four quarters have made consummately.

ANNUAL TECHNICAL REPORT

FINAL REPORT

SUMMARY

Project Title #2154 p

Nanoscale Mechanism of Composite Reinforcement by Fibers and Filler, Theoretical Computation and Experimental Validation of the Theory Using Rubber/Short Carbon Fiber Compounds

Participating Institutions:

1. Leading Institution: Dorodnicyn Computing Centre of Russian Academy of Sciences (CCAS)

2. Supporting Institution: Institute of Applied Mechanics of Russian Academy of Sciences RAS (IPRIM)

Project Manager   S.A. Lurie

Director
of the Dorodnicyn Computing Centre
of Russian Academy of Sciences (CCAS)   Y.G. Evtushenko

Moscow 2005

1. Title of the Project / Number of Annual Report

1. Project **N 2154 p**   The Final Annual Report

Title:

"Nanoscale Mechanism of Composite Reinforcement by Fibers and Filler, Theoretical Computation and Experimental Validation of the Theory Using Rubber/Short Carbon Fiber Compounds"

2. Contracting Institute:

Dorodnicyn Computing Centre of Russian Academy of Sciences (CCAS)

3. Participating Institutes:

Institute of Applied Mechanics of Russian Academy of Sciences RAS (IPRIM)

4. Project Manager:

Sergey A. Lurie,

Phone number: 7(095)135-6190,   Fax numbers: 7(095)135-6190   and   7(095)135-6159

E-mail address: lurie@ccas.ru

5. Commencement Date: 01.04.2002,

Duration: 36 months

6. Objectives of the Project:

-   The aim of the project is to determine effective mechanical characteristics and to predict behavior of the composite enforced with carbon fibers and nanoparticles, from the point of view of enhanced methods of classical continuum mechanics and composite mechanics.

The following statements determine aims of the current stage:

-   Modeling of adhesion interaction of the polymer and inclusions, estimation of properties of the interface layer, its thickness, and dependence of its properties on the properties of the matrix and inclusion.
-   Development of the theoretical basis of modeling of disperse enforced composites accounting for the scale effects.
-   Theoretical and numerical modeling of deformation of composite as a whole accounting for cohesion and adhesion interactions.
-   Writing and testing algorithms and methods of calculations of effective characteristics of the disperse composites.
-   Development of quantum-mechanical and quantum-chemical modeling.
-   Description and predictions of properties of the composites.
-   Experimental verification of the theoretical statements and results, which is one of the main aims.

for visco-elastic media. Experimental investigations of the composite samples (field resins) were also used.

7. Scope of Work and Technical Approach:

The final report contains work executed according to the plan and also brief generalization of the results received at the previous stages of work under Project.

The investigations were elaborated in the complete correspondence with coordinated and authorized Plan of Work , within the framework of following tasks and subtasks of the Project

Problem 1

Development of molecular models of the interface layers for reinforced composites and development of molecular models of interphase layers for reinforced matrix composites and description of physico-mechanical properties of the composites with viscoelastic matrix. The methods of description of physico-mechanical properties of the composites with polymeric matrix on the base of microstructural approach.

Problem 2

Development of the block structure and realization of the analytic-numerical method for the media with nanoinclusions and of an effective method of calculation of the average properties for the heterogeneous media and its realization. Development of the analytic-numerical method for the media with

nanoinclusions, arbitrarily oriented in the space and containing a boundary layer: -calculation of the stress distribution and the average properties of the media based on the complete version of the program for calculation and optimization of heterogeneous media reinforced by nanoinclusions with a boundary layer

Problem 3

The experimental and theoretical assessment of the physico-mechanical properties of the disperse composites. Studying of the macromechanical properties (effective and strength parameters etc.) of the heterogeneous media as a whole. Verifications of some hypothesis and approaches used in the calculations and reconsideration of some hypothesis and approaches used in the calculations.

Problem 4

Estimation of an influence of the shape, dimensions, of rigid inclusions and spatial distribution of the inclusions (its statistical characteristics) of to the increase in the material stiffness. The comparison with the experimental data and development of preliminary recommendations for improving composite deformation characteristics by adjusting its microstructure.

Problem 5

Modeling and prediction of macroscopic properties of materials fabricated from polymer matrix and nanoparticles or nanotubes. Analysis of the adhesion strength at the nanotube - polymer matrix interface. Prediction of macroscopic properties of materials fabricated from polymer matrix and nanoparticles or nanotubes. Calculating of the stress-strain state characteristics.

Task 6. Simulation of the continuum behavior with internal degree of freedoms for a description of the composite materials reinforced by fillers. Calculating of the nano-particles stiffness. Formulation of the relations for moment continuums with an additional kinematics degree of freedom (the set models of the Cossera type). Simulation of mediums with a continuous field of defects (damage accumulation models) by variation procedures. Simulation of composites as a heterogeneous continuum with a field of defects (fillers). Prediction of the mechanical effective properties of composites with shot fibers compounds.

Problem 7

Definition of the unknown parameters of the model to fit the experimental data. Development of the numerical algorithm for the calculation of Gradient of cost functional and the development of the appropriate approximation for the conjugate problem (with the aid of Fast Automatic Differentiation technique); the choice suitable numerical code for the optimization of functional

8. Technical Progress During the Year of Reference

For the last year the work was conducted in full agreement with the problems and main stages formulated in the Research Plan. In addition to the problems pointed in the Research Plan, additional work was done discussed with the employer.

The key achievements are related mainly to the following results:

According to the Working Plan the following works have been done and the following main results achieved:

- The algorithm for calculating the effective characteristics of three phase composite material formed by the matrix, nano-tubes (or disk-like nano-particles) and surrounding them regions of the third phase is developed. Variants of both direct and inverse problems are considered for both thick and thin intermediate layer. In the frame of the approach the effects caused by anisotropy are accounted. An example of solving inverse problem has been presented: estimation of the properties of intermediate layer

- During the reported period we proposed a mechanical model of the interface adhesion of polymer matrix and nanotubes accounting for the dependencies of the shear stresses between matrix and nanotube versus the main physical-mechanical parameters of the nanocomposite material: -the parametric analysis of the model parameters on the nanotubes and the interface layer stresses states

was performed; -the asymptotic cases of the stresses states were considered and analyzed; -the multi-parametric model was proposed for the analysis of properties of new nanocomposite materials and for analysis of the experimental data.

- On the basis of the previous researches the consistent and correct theory of interphase layer was formulated and analyzed as whole. The theory of interphase layer includes the following moments: -the formal mathematical statement, -the physical constitutive equations, - the identification problem of the parameters determining nonclassical effects, -the qualitative analysis of the theory-analytical estimations of properties of an interphase layer, -the qualitative analysis of the theory-estimation of an interphase layer influence on the effective characteristics of a composite, -some application for fracture mechanics, quantum mechanical approaches, -numerical modeling of the stress state of the cell with inclusions and some notes about specific averaging procedures for filled composites, previously results of the generalized Eshelby problem and its application.

- A new general kinematic theory of defects in continuous media, the general mechanisms of existence of defects, their generation (or birth) and disappearance (or healing) were establish.

- The generalized model of pseudocontinuums are obtained for which a surface tension, static friction bodies with ideally smooth surface of contact, the meniscus, wettability and capillarity are modeled as special effects within the framework of unified continual description. All these special effects are united by one property, they are the scale effects in continuums.

- Using asymptotic approach the correct algorithm for the account of the accumulation damage is proposed on the base strong generalized model of the mediums with reserved dislocation.

- On the basis of procedure of asymptotic homogenization of composite materials with a periodic microstructure it was received the formula for effective characteristics of composite materials with account of the local effects.

- With the help of a block method of multipoles distribution of energy density and components of stress tensor in micro cell with inclusion is simulated. The features of the current realization of algorithm of a block method are shown, which require its technical modification in the way of improvement of block system of the equations solver and more accurate normalization of joining functionals.

- The algorithm of the solution of a problem of model parameters identification has been developed according to experimental researches for the general three-dimensional case. The series of the calculations has been made.

- A new approach to model and investigation both the texture and the mechanical characteristics of large molecular systems by Monte-Carlo method has been developed. As a base of the method is an unorthodox algorithm allowed to make a classical Metropolis procedure for a few polymer molecules. Algorithm under consideration belongs to class of program which use space decomposition and has high grade of calibration. The structures of model mixtures of n-pentane and carbon microclusters C_{38} (graphite type) as prototype of reinforced rubber composites have been investigated. It was shown the strong dependence the grade of associate of carbons microclusters on form of its surface. Chemical modification of components of mixture substantially influences on structure and mechanical properties of materials under study. So, aquation of carbon microclusters leads to decreasing of middle value of potential energy of particles. We proposed the method and investigated the mobility of polymer molecules close to surface of particle of filler. It was fixed the presence of layer with limited mobility around area of contact "polymer – graphite". It was developed the method of evaluation of shear modulus for composite microcluster during the model by Monte-Carlo method. Quantum-Chemical Approach.

- At given stage of work in course of modelling it was obtained that maximal shear force for polymer particle adsorbed on carbon surface was found approximately 3 times higher than for polymer in a polymeric matrix. Owing to rather weak however quite sufficient for immobilization of polymeric

chain segments on the carbon surface Van-der-Waals forces, around carbon filler particles some condensed layer of rubber is formed with the lowered mobility of chain segments which most likely is responsible for strengthening of organic polymers by filling them with high dispersed carbon. Summarizing in should be mentioned, that in the given section the technique offered earlier is tested on an example of calculation of molecular friction in the complex system consisting of organic polymer and carbon filler. The reinforcing effect of pure nonterminated carbon fillers is the best. Some conclusions about impact of chemical nature of the polymer matrix on the interaction of the polymer segments with surface of soot fillers have been done. Aggregation of the soot particles can be prevented by adsorption interlayer of polymer between the soot particles. Adsorption of water in the interparticle interface can be considered as competitive process for polymer adsorption. For the formation of the contact polymer-filler water layer on the soot surface has to be removed. Hence the best reinforcement can be reported for the combination of isoprene-amorphous carbon and the worth for system polyethylene-amorphous carbon. Obtained dependencies of polymer molecule cohesion with carbon particle surface (or of the highest forces of microscopic friction) are in a good accordance with calculated geometrical and energetic characteristics. The best cohesion of isoprene chain with filler particle surface (the highest forces of microscopic friction) was obtained for the system isoprene-silica. A little worth is cohesion of isoprene with carbon black or soot. Such fillers as fullerene and high dispersed carbon tubes represent lower forces of adhesion. As it is seen from the obtained results enthalpy of binding of rubber chains on a clay surface and force of microscopical friction in this system, which interconnected with cohesion is strongly depended on modification of clay surface by hydrophobic agent (organic cation). The best case can be observed if use organic cations with middle-sized chains at about 15-20 monomer units and various modification of uncharged end providing better hydrophobic binding with rubber chains.

- During the molecular-dynamic modelling it was shown, there is the discrepancy between behaviour of polyethylene and polyisoprene chains under their interaction with carbon fillers. The polyethylene chains sharply change their configuration on time and always furls into ball both in case of contact to carbon particles and without. Materials with polyethylene matrix practically do not keep an initial configuration and quickly jump in amorphous condition, aggregated around carbon particle. Polyisoprene chains, contrariwise, keep initial structure and injection into system of carbon filler deepens this tendency. Polyisoprene's component is stabilized in presence of carbon filler. As structural so energetic results of molecular dynamic calculation testify about. Injection into composite system polyisoprene – carbon filler some water destabilizes appropriate adsorption complexes, but at this case the system keeps the shape of its structure pretty long.

- To investigate the microstructure of rubber composites the method of dynamic forced microscopy and 3D-optical interferential microscope have been used. Different sorts of technical carbons and samples of rubber compounds filled with active particles have been analyzed. Microstructure investigations of geometry of surface of particles of disperse filler and aggregations of those inside elastomeric matrix gave us very useful information for verification of theoretical and model evaluations of parameters of microclusters of composite polymeric structures. The samples of natural rubber filled with montmorillonite (5, 20, 40, 60% vol.) and samples of natural rubber filled with combined particles (technical carbon and montmorillonite) have been investigated. Rheological data which have been made during full-scale investigations let us to evaluate some important relaxation parameters and, first of all, the spectrum of relaxation time distribution. It was systematize the data about influence of different sorts of filler on complex of rheological and relaxation parameters, which govern to viscoelastic behavior above media under deformation. Such information is important for the setup of optimal processing technology of the composite compounds into articles.

- It was accomplished the task of identification of nonlinear model for viscoelastic media on the basis of the nonlinear integrated Hammerstein's operator. Is shown, that this operator with a nucleus synthesized on calculation of a relaxation spectrum, not always provides qualitative identification of model at the large deformations. The lacks of application of concept of a relaxation spectrum in models force us to pass to other type of models based on neural networks. The technique of synthesis of neural networks for the decision of a concrete mathematical task is given. The detailed block diagrams of neural networks for the decision of the specified kind of tasks are given. It is established, that during training and adaptation of neural network are frequently observed long convergence iterative procedures to extremal of functional. Last circumstance compels to use methods of regularization by training of neural models. Synthesis and analysis of neural work model to describe the behavior of viscoelastic media shows, that to accomplishment of required workable accuracy of neural network without using the feedback (small mistake of training), it is necessary to interpolate the experimental data in order to expand a dimension of vectors.
- The algorithm for designation strength characteristics of heterogeneous media has been proposed. Justification of entered idea about stress and strain concentration tensors is shown. Consideration of properties of symmetry for periodicity cells allows to simplify a calculation the effective stiffness tensor of those.

9. Plan for Following Years: Final Report

10. References of papers and reports published.

1. Lurie S., Belov P., Tuchkova N. The Application of the multiscale models for description of the dispersed composites// Int. Journal "Computational Materials Science" A., 2004, 36(2):145-152.
2. Lurie S. A. and Kalamkarov A. L.   General Theory of Defects in Continuous Media// Solid and structures, 2005,(accepted for print)
3. Evtushenko Y.G, Lurie S., Volkov-Bogorodsky D, Zubov V. I. Numerical - analytical modelling of scale effects at research of deformations for disperse reinforced nanocomposites with use of the block method of multifields//Comput. Math. And Math Phys. 2005 (accepted for publication)
4. Obraztsov I.F., Lurie S.A., Belov P.A., Volkov-Bogorodsky D.B., Yanovsky Yu.G., Kochemasova E.I., Dudchenko A.A., Potupcik E.M., Shumova N.P. Elements of theory of interphase layer. Composite Mechanics and Design, 2004, v.10, N3, pp.596-612.
5. Lurie S, Belov P, Volkov-Bogorodsky D, Tuchkova N, Nanomechanical Modeling of the Nanostructures and Dispersed Composites, Int. J. Comp Mater Scs 2003; 28(3-4):529-539
6. Lurie, P.A. Volkov-Bogorodskii D.B.and N.P. Tuchkova N. P, Mathematical model of the interphase layer. Mathematical and numerical modeling of the composites// Int. Symp. On Trend in applications of Mathematics to Mechanics (STAMP"2004) Aug. 2004, Seeheim, Germany. pp.28-29
7. Lurie S., Hui D. and Kireitseu M. Multiscale Modeling of the Interphase Layers in the Mechanics of Materials, Proceedings Book of 11th International Conference on Composites/Nano Engineering, Hilton Head, S. Carolina, August 8-14, 2004. pp. 784-786
8. Lurie S., Leontiev A., Tuchkova N. One algorithm of the solution of the fracture mechanics problems for the finite elastic bodies//Mechanics of composite materials and structures. 2004, v.10. N3
9. S A Lurie, N P Tuchkova, V I Zubov The Application of the Interphase Model for the Description of the Filled Composite Properties with Nanoparticles. Identification of the Parameters of the Model // The 2nd International Conference on Composites Testing and ModelIdentification Comptest 2004 held on the 21st - 23rd September 2004, hosted by the Department of Aerospace Engineering, University of Bristol, U.K. (http://www.aer.bris.ac.uk/comptest2004/proceedings)
10. Vlasov A.N. Averaging of mechanical properties of heterogeneous media. Composite Mechanics and Design, 2004, v.10, N3, pp.424-441.
11. Yanovsky Yu.G., Zgaevskii V.E. Mechanical properties of high elastic polymer matrix composites filled with rigid particles: Nanoscale consideration of the interfacial problem. Composite Interfaces, 2004, v.11,N3, pp.245-261.
12. Yanovsky Yu.G. Multiscale Modeling of Polymer Composite Properties. International. Journal for Multiscale Computational Engineering, 2005, v.3, N2.

13. Obraztsov I.F., Vlasov A.N., Yanovsky Yu.G. Calculating Method of Strength Properties of Heterogeneous Media. Doklady Physics, Moscow, 2005 (in press).
14. Yanovsky Yu.G. Multiscale Modeling of Polymer Composite Properties. Proceedings of the Sixth World Congress on Computational Mechanics, Tsinghua University Press and Springer, Beijing, China, Eds. Z.Yao, M.Yuan, W.Zhong, 2004, pp.758-762.
15. Nikitina E.A., Yanovsky Yu.G. Quantum Mechanical Investigation of the Microstructure and Mechanical Characteristics of Nano-Structured Composites. Abstracts of the Sixth World Congress on Computational Mechanics, Tsinghua University Press and Springer, Beijing, China, Eds. Z.Yao, M.Yuan, W.Zhong, 2004, p.626.
16. Teplukhin A.V. Monte-Carlo Modeling of Atomic and Molecular Mesoscopic Composite Systems. Abstracts of the Sixth World Congress on Computational Mechanics, Tsinghua University Press and Springer, Beijing, China, Eds. Z.Yao, M.Yuan, W.Zhong, 2004, p.627.
17. Vlasov A.N., Yanovsky Yu.G. Numerical Modeling to Determine Constitutive Relations of Jointed Rock. Abstracts of the Sixth World Congress on Computational Mechanics, Tsinghua University Press and Springer, Beijing, China, Eds. Z.Yao, M.Yuan, W.Zhong, 2004, p.628.
18. Yanovsky Yu.G., Basistov Yu.A., Filipenkov P.A. Problem of identification of rheological behavior of heterogeneous polymeric media under finite deformation. Proceedings of the XIV International Congress on Rheology, ISBN 89-950057-5-0, The Korean Society of Rheology, 2004, SO18-1 – SO18-3.
19. Yanovsky Yu.G. Multiscale Modeling of Polymer Composite Mechanical Properties and Behavior. Abstracts of the International Conference on Heterogeneous Material Mechanics, Chongqing University and Yangtze River/Three Gorges, China, 2004, p.252.

1. INFLUENCE OF INCLUSIONS ON EFFECTIVE PROPERTIES OF MATERIALS

It is well known that the presence of inclusions may lead to significant changes in effective properties of materials, the properties of the obtained composites determined not only by the physical properties of the phases (matrix and inclusions), but also by the characteristic of space distribution of particles and their shape and size. The last aspect became extremely important when dealing with very fine inclusions: at nano-scale. Below, the main results of the investigation of the influence of the above characteristic on both elastic and strength properties of composites are given.

1.1.   INFLUENCE OF INCLUSIONS ON EFFECTIVE ELASTIC PROPERTIES OF MATERIALS. TWO-PHASE MODELS

According to the Working Plan the literature review of the problem was presented (Final Report, 2002).

On the base of the classical Eshelby's approach the effective solutions for determining effective properties of the composites formed by the elastic matrix and isolated inclusions were obtained in the closed form. The solutions were presented both in tensor form (Final Report, 2002), and in more convenient, although less physical matrix form (Final Report, 2003.

A number of important particular cases, for which asymptotical representations are possible, were pointed out: flat inclusions (nano-plates), and needle-like inclusions (nano-tubes). The combined influence of the shape and relative stiffness of inclusions was investigated; it was shown that the presence of two parameters (the ratio of maximal an minimal dimensions of the inclusion and relative stiffness of inclusions) leads to non-uniform limit transition, which restricts the area of applicability of known classical asymptotical formulae. The areas of applicability of asymptotical formulae were obtained (appears to be for the first time).

The influence of anisotropy of the inclusions to the effective composite properties was investigated (Final Report, 2003). It was shown that the main influence is due to some particular combinations of elastic parameters of inclusions, and these combinations were pointed out.

The influence of the orientation of inclusions in space were investigated both for isotropic and anisotropic inclusions (Final Report, 2003). For the composites on the base of nano-tubes three types of space distribution were considered: random, aligned and transverse (all inclusions lay in parallel planes). The solution for last case appears to be obtained for the first time.

Originally, all the solutions were obtained for the small concentration of inclusions. The influence of concentration were then accounted for with the help of differential self-consistent method and the method of effective field (Mori-Tanaka). The former appears to be more strict and physically justified, however it leads to necessity to solve systems of differential equations. Besides, now it is inapplicable for solving the problems of anisotropic distribution of inclusions, because expressions of Eshelby's tensor for anisotropic media in closed form are not obtained yet. Mori-Tanaka's method, although, may be, resulting to some (not significant) systematical error, is more simple and allows obtaining generalizations for anisotropic distribution of the (anisotropic) inclusions in space.

The obtained results were compared with the results known from the literature.

The above results were presented in the previous reports (Final Report, 2002; Final Report, 2003).

The obtained results appear to be important as it are, as well as an useful tool for constructing more advanced models such as three-phases models, accounting for the presence of an intermediate layer between the matrix and inclusions.

1.2.   INFLUENCE OF THE INTERMEDIATE PHASE TO THE EFFECTIVE ELASTIC PROPERTIES OF THE COMPOSITE

1.2.1. General

Generally, during polymerization process in addition to matrix and inclusions the third, Intermediate, phase appears in the form of thin or thick shells surrounding nano-particles. If such a situation takes place, the influence of this Intermediate phase to the effective properties of the composite has to be taken into accounts. The presence of such a phase is indicated by the following facts:

- abnormal increase of elastic modulii of nano-composites;
- dependence of the effective elastic properties of sizes of inclusions;
- increase in strength of the composite with the decrease of the inclusions sizes.

Indeed, the changes in the composite properties with the decrease of the inclusions sizes, which are not predicted by the classical theories, may be explained by the existence of the intermediate phase at the matrix-inclusions contacts. Since the contact area grows with the decrease of the inclusions sizes, the influence of the size became reasonable.

In the frame of the current research plan we continued our study on the modeling of the influence of the intermediate phase to the effective moduli of the composite. Earlier (Final Report, 2003; Intermediate Report, 2004) a method of estimation of the intermediate phase properties is suggested, and the example of estimation of the properties of intermediate layer is given.

The following problems may be formulated. First, knowing mechanical and geometrical properties of all phases to calculate the effective properties of the composite (the direct problem). Second, knowing elastic properties of the matrix and the composite, to estimate the properties of the Intermediate phase and/or the inclusions (inverse problem).

Two alternative approaches may be suggested to address the problem. The first one consists in solving the complete three phase problem and calculating the effective moduli in question. However, this way, although being rigorous, leads to enormous computational difficulties (e.g. Riccardi and Montheillet, 1999). Moreover, the method used in the cited above paper is restricted by the case of co-focal spheroids bounding the inclusion and the third phase. In reality, the shapes of the phase boundaries are more complex (see below). Rigorous calculations for this case are thought to be much more complicated.

An alternative simplified model were suggested consisting in separating the problem into two sub-problems and solving each of them consecutively. **First**, to consider the original nano-inclusion and the surrounding layer of the third phase and to calculate the effective properties of such a uniform equivalent inclusion. **Second**, to calculate the effective properties of the composite consisting of the matrix and embedded inclusions of such an equivalent material. This approach, although being just an approximation, leads to essential simplification of the problem and allows relatively simple analytical estimations. It is believed that the errors involved due to such a simplification are in agreement with the accuracy of the experimental data.

The idea of the suggested approach was outlined previously (Final Report, 2003). Below, more detailed description is given accounting for such effects as anisotropy of nanoparticles and influence of the relative thickness of the intermediate layer. An example of the inversed problem is considered: knowing properties of matrix and inclusions to find properties of the intermediate layer.

1.2.2. Real object and proposed model; statements of direct problems

Let us consider a composite consisting of a matrix and nano-partiles embedded to it, each nano-tube being surrounded by the material of the intermediate phase that appeared during polymerization process and possesses properties different from the properties of the matrix, as it is shown in Figure 1.1. Generally, the properties of the third phase may be non-uniform and the surface bounding it from the matrix may be rather uncertain. However it is naturally to suppose that the thickness of the layer formed by the intermediate phase is approximately constant. Therefore the boundary between the matrix and the intermediate phase may be considered as being close to the surface surrounding the nano-particle equidistantly. If the regions of the intermediate phase occupy quite large relative volume, then these regions may overlap as it is shown in the Figure 1.1.

In order to simplify further considerations, the real structure of the intermediate phase, which is unknown, but supposed to be close to the described ones, is modeled by possessing rather uniform elastic properties and being bounded from the matrix by rather regular distinguishable surface (Figure 1.2).

Let us introduce the following notation

V_1, V_2, V_3 are the volumes occupied by the nano-particles, intermediate phase and matrix, respectively;

$\Lambda^{ijkl}_1, \Lambda^{ijkl}_2, \Lambda^{ijkl}_3, -$	are tensors of elastic moduli of nano-particles, intermediate phase and matrix, respectively;
$k_1, E_1, \mu_1, \lambda_1, \nu_1 -$	are compressive, Young's and shier moduli, lame constant and Poisson's ratio of nano-particles, respectively (in case of isotropy);
$k_2, E_2, \mu_2, \lambda_2, \nu_2 -$	are compressive, Young's and shier moduli, lame constant and Poisson's ratio of the intermadiate phase, respectively (in case of isotropy);
$k_3, E_3, \mu_3, \lambda_3, \nu_3 -$	are compressive, Young's and shier moduli, lame constant and Poisson's ratio of the matrix, respectively (in case of isotropy);
$\Lambda^{ijkl}_{12} -$	is tensor of equivalent elastic moduli of the particle formed by nanoinclusion and the intermediate layer;
$\Lambda^{ijkl}_{13} -$	is tensor of equivalent elastic moduli of the composite;
$k_{12}, E_{12}, \mu_{12}, \lambda_{12}, \nu_{12} -$	are equivalent compressive, Young's and shier moduli, lame constant and Poisson's ratio of the particle formed by nanoinclusion and the intermediate layer (in case of isotropy);
$k_{13}, E_{13}, \mu_{13}, \lambda_{12}, \nu_{13} -$	are equivalent compressive, Young's and shier moduli, lame constant and Poisson's ratio of the composite (in case of isotropy);
$\Omega -$	is the volume concentrations of the nano-particles within the composite.

The last quantity is defined, obviously, as

$$\Omega = \frac{V_1}{V_1 + V_2 + V_3} \tag{1.1}$$

For further calculation we will need some additional quantities: relative concentration of the nano-particles within the third phase, which is

$$\Omega_{12} = \frac{V_1}{V_1 + V_2} \tag{1.2}$$

and relative concentration of the nano-particles and third phase within the matrix, which is

$$\Omega_{23} = \frac{V_1 + V_2}{V_1 + V_2 + V_3} \tag{1.3}$$

The obvious relation for the introduced quantities follows directly from definitions (1.1) – (1.3)

$$\Omega = \Omega_{12}\Omega_{23} \tag{1.4}$$

Following the outlined procedure, let us consider the original inclusion and the surrounding layer of the third phase and calculate the effective properties of such a uniform equivalent inclusion. In general case the problem may be solved for an arbitrary concentration Ω_{12} and shapes of the regions occupied by the third phase at least numerically.

Then consider a medium, constituted by the matrix and equivalent particles, which properties are supposed to be equal to the properties calculated at the previous stage.

1.2.3. The first stage

Let us apply the following approach, being the more rigorous the less is the relative concentration Ω_{12}. Namely, ***consider the two phases media consisting of nano-particles scattered within the matrix of the third phase with concentration Ω_{12}***, and calculate the effective moduli of such a media, assuming these moduli to be the moduli of the equivalent inclusion.

Two particular extreme cases may be distinguished: the thick and thin intermediate layer (Figure 1.2).

1.2.3.1. Thick intermediate layer; general

For the case of relatively thick intermediate layer the volume occupied by it is much larger then the volume of the nanoparticle. Therefore, the condition of small concentration is satisfied

$$\Omega_{12} \equiv \frac{V_1}{V_1 + V_2} \ll 1 \tag{1.5}$$

and the applied method is justified. Tensor of elastic moduli, in that case is determined by the following expression (Final Report, 2003):

$$\Lambda_{12} = \Lambda_2 + \left(\left(\Lambda_1 - \Lambda_2\right)^{-1} + S\Lambda_2^{-1}\right)^{-1}\Omega_{12} \tag{1.6}$$

The matrix form is adopted hereafter for all tensor quantities. Here S is Eshelby's matrix, composed by the elements of Eshelby's tensor. The particular expressions for its components for the particles under consideration are given in previous reports (Final Report, 2003; Final Report, 2003).

Assuming the nanoparticles and equivalent particles to be isotropic, the following simple formulae are obtained (Final Report, 2003)< which are valid for small relative concentration Ω_{12}:

$$k_{12} = k_2\left[1 + A\,\Omega_{12}\right]$$
$$\mu_{12} = \mu_2\left[1 + B\,\Omega_{12}\right] \tag{1.7}$$

1.2.3.2. Thick intermediate layer; isotropic model

Assuming the nanoparticles and equivalent particles to be isotropic, the following simple formulae are obtained (Final Report, 2003) for the parameters A and B, determined by elastic moduli of matrix and inclusions and the shape of the inclusions:

For nanotubes, represented as prolated spheroids they are

$$A = \frac{(k_1 - k_2)(3k_2 + \mu_1 + 3\mu_2)}{k_2(3k_1 + \mu_1 + 3\mu_2)} =$$
$$= \frac{(k_1 - k_2)\left[k_1(1 - 2\nu_1)(1 + \nu_2) + k_2(1 + \nu_1)(5 - 4\nu_2)\right]}{3k_2\left[k_1(1 + \nu_2) + k_2(1 - 2\nu_2)(1 + \nu_1)\right]}$$

$$B = \frac{3k_2(\mu_1 - \mu_2)}{5\mu_2(\mu_1 + \mu_2)(3k_1 + \mu_1 + 3\mu_2)(3k_2\mu_1 + 3k_2\mu_2 + 7\mu_1\mu_2 + \mu_2^2)} *$$
$$\left[(\mu_1 + \mu_2)(4\mu_2(3\mu_1 + 7\mu_2) + 3k_1(\mu_1 + 9\mu_2)) + \right.$$
$$+ \mu_2\left(8\mu_2(9\mu_1^2 + 23\mu_1\mu_2 + 8\mu_2^2) + 3k_1(7\mu_1^2 + 52\mu_1\mu_2 + 21\mu_2^2)\right)\right] =$$
$$= \frac{2(\mu_1 - \mu_2)}{15\mu_2(\mu_1 + \mu_2)(\mu_1 + \mu_2(1 - 2\nu_1))(\mu_2 + \mu_1(3 - 4\nu_2))} *$$
$$\left[4\mu_2^3(1 - 2\nu_1)(5 - 3\nu_2) + \mu_1^3(1 + \nu_1)(3 - 4\nu_2) + \right.$$
$$+ \mu_1\mu_2^2(57 - \nu_1(75 - 88\nu_2) - 56\nu_2) + 4\mu_1^2\mu_2(10 - 2\nu_1 - 12\nu_2 + 3\nu_1\nu_2)\right] \tag{1.8}$$

For nanoplates, represented as oblated spheroids they are

$$A = \frac{(k_1 - k_2)(3k_2 + 4\mu_1)}{k_2(3k_1 + 4\mu_1)} = \frac{(k_1 - k_2)\left[k_2(1 + \nu_1) + 2k_1(1 - 2\nu_1)\right]}{3k_2k_1(1 - \nu_1)}$$
$$B = \frac{(\mu_1 - \mu_2)(9k_1\mu_1 + 8\mu_1^2 + 6k_1\mu_2 + 12\mu_1\mu_2)}{5\mu^*\mu^0(3k^* + 4\mu^*)} =$$
$$= \frac{(\mu_1 - \mu_2)\left[\mu_1(7 - 5\nu_1) + 2\mu_2(4 - 5\nu_1)\right]}{5\mu_1\mu_2(1 - \nu_1)} \tag{1.9}$$

1.2.3.3. Thick intermediate layer; anisotropic model

However, representation of the equivalent inclusions as anisotropic appeared to be more realistic, sinse, even neglecting anisotropy of the nanoparticles itself, their distribution within the intermediate phase (position of the single inclusion) is ordered.

For strongly prolonged inclusions, such as nanotubes, by making limit transition to infinitesimally thin spheroids in the formulas for components of Eshelby's tensor (written in Final report, 2003, formulae (1.10)-

(1.11)), and then substituting the result into (1.6) we obtain an asypmtotic representation for the effective elastic moduli of a composite enforced with aligned prolonged inclusions

$$
\Lambda_{12} =
\begin{pmatrix}
\lambda_2+2\mu_2 & \lambda_2 & \lambda_2 & 0 & 0 & 0 \\
\lambda_2 & \lambda_2+2\mu_2 & \lambda_2 & 0 & 0 & 0 \\
\lambda_2 & \lambda_2 & \lambda_2+2\mu_2 & 0 & 0 & 0 \\
0 & 0 & 0 & \mu_2 & 0 & 0 \\
0 & 0 & 0 & 0 & \mu_2 & 0 \\
0 & 0 & 0 & 0 & 0 & \mu_2
\end{pmatrix}
+
\begin{pmatrix}
D_{11} & D_{12} & D_{13} & 0 & 0 & 0 \\
D_{12} & D_{11} & D_{13} & 0 & 0 & 0 \\
D_{13} & D_{13} & D_{33} & 0 & 0 & 0 \\
0 & 0 & 0 & D_{44} & 0 & 0 \\
0 & 0 & 0 & 0 & D_{44} & 0 \\
0 & 0 & 0 & 0 & 0 & \dfrac{D_{11}-D_{12}}{2}
\end{pmatrix}
\Omega_{12}
\qquad (1.10)
$$

where

$$
\begin{aligned}
D_{11} = &\, 2\mu_2(1-\nu_2)\big[-4\Lambda^1_{11}\mu_2(1-\nu_2)+4\Lambda^1_{12}\mu_2\nu_2(5-8\nu_2)-\Lambda^{1}_{12}{}^2(1-2\nu_2)(5-8\nu_2)+ \\
&+\Lambda^{1}_{11}{}^2(5-18\nu_2+16\nu_2{}^2)-4\mu_2{}^2(3-8\nu_2+8\nu_2{}^2)\big]/ \\
&\big(\Lambda^1_{11}+\Lambda^1_{12}+2\mu_2\big)(1-2\nu_2)^2\big[2\mu_2+(\Lambda^1_{11}-\Lambda^1_{12})(3-4\nu_2)\big]
\end{aligned}
$$

$$
\begin{aligned}
D_{12} = &\, 2\mu_2(1-\nu_2)\big[\Lambda^{1}_{11}{}^2(1-2\nu_2)-4\Lambda^1_{11}\mu_2(1-\nu_2)-\Lambda^{1}_{12}{}^2(1-2\nu_2)+ \\
&4\mu_2{}^2(1-8\nu_2+8\nu_2{}^2)+4\Lambda^1_{12}\mu_2(4-11\nu_2+8\nu_2{}^2)\big]/ \\
&\big(\Lambda^1_{11}+\Lambda^1_{12}+2\mu_2\big)(1-2\nu_2)^2\big[2\mu_2+(\Lambda^1_{11}-\Lambda^1_{12})(3-4\nu_2)\big]
\end{aligned}
$$

$$
D_{13} = 4\mu_2(1-\nu_2)\frac{\Lambda^1_{13}-2\nu_2(\Lambda^1_{13}+\mu_2)}{(1-2\nu_2)^2(\Lambda^1_{11}+\Lambda^1_{12}+2\mu_2)}
\qquad (1.11)
$$

$$
\begin{aligned}
D_{33} = &\, \big\{(\Lambda^1_{33}-2\mu_2)(\Lambda^1_{11}+\Lambda^1_{12}+2\mu_2)-2\Lambda^{1}_{13}{}^2(1-2\nu_2)^2- \\
&-2\nu_2(2\Lambda^1_{33}-3\mu_2)(\Lambda^1_{11}+\Lambda^1_{12}+2\mu_2)+8\Lambda^1_{13}\mu_2\nu_2(1-2\nu_2)+ \\
&+4\nu_2{}^2\big[(\Lambda^1_{11}+\Lambda^1_{12})\Lambda^1_{33}-(\Lambda^1_{11}+\Lambda^1_{12}-2\Lambda^1_{33})\mu_2-4\mu_2{}^2\big]\big\}/ \\
&\big(\Lambda^1_{11}+\Lambda^1_{12}+2\mu_2\big)(1-2\nu_2)^2
\end{aligned}
$$

$$
D_{44} = \frac{2\mu_2(\Lambda^1_{44}-\mu_2)}{\Lambda^1_{44}+\mu_2}
$$

Here moduli is related to the Cartesian coordinate frame with x_3 axis directed along the axis of rotation of the nanotube.

This result, obtained here as a particular case coinsides with the result by Walpole (1969). It has to be noted, that as it was mentioned in the previous reports (Final Report 2002; Final Report 2003), such asymptotics stop working for extremely rigid inclusions, for which condition

$$
\frac{\Lambda^1_{ij}}{\mu_2} << \frac{b}{a}; \quad \frac{b}{a} >> 1.
\qquad (1.12)
$$

are not satisfied. Here $\dfrac{b}{a}$ is the ratio of semi-axes of the spheroid.

In case of relatively rigid inclusions, however condition (1.12) is not violated, in the frame of the considered case the following particular case may be distinguished, namely

$$
\frac{b}{a} >> \frac{\Lambda^1_{ij}}{\mu_2} >> 1
\qquad (1.13)
$$

For this case the result may be obtained by the limit transition $(\Lambda_1 - \Lambda_2)^{-1}\Lambda_2 \to 0$ in (1.11).). In case of the aligned inclusions the result is

$$\Lambda_{12} = \begin{pmatrix} \lambda_2 + 2\mu_2 & \lambda_2 & \lambda_2 & 0 & 0 & 0 \\ \lambda_2 & \lambda_2 + 2\mu_2 & \lambda_2 & 0 & 0 & 0 \\ \lambda_2 & \lambda_2 & \lambda_2 + 2\mu_2 & 0 & 0 & 0 \\ 0 & 0 & 0 & \mu_2 & 0 & 0 \\ 0 & 0 & 0 & 0 & \mu_2 & 0 \\ 0 & 0 & 0 & 0 & 0 & \mu_2 \end{pmatrix} + \begin{pmatrix} 0 & 0 & 0 & 0 & 0 & 0 \\ 0 & 0 & 0 & 0 & 0 & 0 \\ 0 & 0 & E_{33} & 0 & 0 & 0 \\ 0 & 0 & 0 & 0 & 0 & 0 \\ 0 & 0 & 0 & 0 & 0 & 0 \\ 0 & 0 & 0 & 0 & 0 & 0 \end{pmatrix} \Omega_{12} \tag{1.14}$$

where E_{33} is the elastic modulus along the inclusions

$$E_{33} = \Lambda^1_{33} - \frac{2\Lambda^1_{23}{}^2}{\Lambda^1_{11} + \Lambda^1_{12}} \tag{1.15}$$

Thus, if condition (1.13) is satisfied, the effective elastic properties essentially depend on elastic modulus along the inclusions only.

In case of oblate spheroids, by making limit transition to infinitesimally thin spheroids in the formulas for components of Eshelby's tensor (written in Final report, 2003, formulae (1.10)-(1.11)), and then substituting the result into (1.6) we obtain an asypmtotic representation for the effective elastic moduli of a composite enforced with aligned nano-plates. Similar to the case of nano-tubes, the result is still given by (1.10), where

$$D_{11} = \frac{\Lambda^1_{11}\Lambda^1_{33} - \Lambda^1_{13}{}^2}{\Lambda^1_{33}} + 2\mu_2 \frac{2\Lambda^1_{13}\nu_2 - \Lambda^1_{33}(1-\nu_2)}{\Lambda^1_{33}(1-2\nu_2)} - \frac{4\mu_2{}^2\nu_2{}^2}{\Lambda^1_{33}(1-2\nu_2)^2}$$

$$D_{12} = \frac{\Lambda^1_{12}\Lambda^1_{33} - \Lambda^1_{13}{}^2}{\Lambda^1_{33}} + 2\mu_2\nu_2 \frac{2\Lambda^1_{13} - \Lambda^1_{33}}{\Lambda^1_{33}(1-2\nu_2)} - \frac{4\mu_2{}^2\nu_2{}^2}{\Lambda^1_{33}(1-2\nu_2)^2}$$

$$D_{13} = \frac{2\mu_2(1-\nu_2)\left[\Lambda^1_{13} - 2\nu_2\left(\Lambda^1_{13} + \mu_2\right)\right]}{\Lambda^1_{33}(1-2\nu_2)^2} \tag{1.16}$$

$$D_{33} = \frac{2\mu_2(1-\nu_2)\left[\Lambda^1_{33}(1-2\nu_2) - 2\mu_2(1-\nu_2)\right]}{\Lambda^1_{33}(1-2\nu_2)^2}$$

$$D_{44} = \frac{\mu_2\left(\Lambda^1_{44} - \mu_2\right)}{\Lambda^1_{44}}$$

Here moduli is related to the Cartesian coordinate frame with x_3 axis directed normally to the the plane of the nano-plate.

This result, obtained here as a particular case coinsides with the result by Walpole (1969). It has to be noted, that as it was mentioned in the Final report (2002, 2003), such asymptotics stop working for extremely rigid inclusions, for which condition

$$\frac{\Lambda^1_{ij}}{\mu_2} << \frac{a}{b}; \quad \frac{a}{b} >> 1. \tag{1.17}$$

where $\frac{a}{b}$ is the ratio of semi-axes of the spheroid representing the nano-plate.

In case of relatively rigid inclusions, however condition (1.17) is not violated, in the frame of the considered case the following particular case may be distinguished, namely

$$\frac{a}{b} >> \frac{\Lambda^1_{ij}}{\mu_2} >> 1 \tag{1.18}$$

For this case the result may be obtained by the limit transition $(\Lambda_1 - \Lambda_2)^{-1}\Lambda_2 \to 0$ in (1.16). In case of the aligned inclusions the result is

$$\Lambda_{12} = \begin{pmatrix} \lambda_2 + 2\mu_2 & \lambda_2 & \lambda_2 & 0 & 0 & 0 \\ \lambda_2 & \lambda_2 + 2\mu_2 & \lambda_2 & 0 & 0 & 0 \\ \lambda_2 & \lambda_2 & \lambda_2 + 2\mu_2 & 0 & 0 & 0 \\ 0 & 0 & 0 & \mu_2 & 0 & 0 \\ 0 & 0 & 0 & 0 & \mu_2 & 0 \\ 0 & 0 & 0 & 0 & 0 & \mu_2 \end{pmatrix} + \begin{pmatrix} \Lambda_{11}^1 - \dfrac{\Lambda_{13}^{1\ 2}}{\Lambda_{33}^1} & \Lambda_{12}^1 - \dfrac{\Lambda_{13}^{1\ 2}}{\Lambda_{33}^1} & 0 & 0 & 0 & 0 \\ \Lambda_{12}^1 - \dfrac{\Lambda_{13}^{1\ 2}}{\Lambda_{33}^1} & \Lambda_{11}^1 - \dfrac{\Lambda_{13}^{1\ 2}}{\Lambda_{33}^1} & 0 & 0 & 0 & 0 \\ 0 & 0 & 0 & 0 & 0 & 0 \\ 0 & 0 & 0 & 0 & 0 & 0 \\ 0 & 0 & 0 & 0 & 0 & 0 \\ 0 & 0 & 0 & 0 & 0 & \dfrac{\Lambda_{11}^1 - \Lambda_{12}^1}{2} \end{pmatrix}\Omega_{12} \tag{1.19}$$

Note, that if the condition of small relative concentration (1.5) is satisfied, according to the described technique, the effective moduli of the equivalent inclusions are determined solely by the relative concentration of the nano-particles within the material of the third phase Ω_{12}, effective moduli of nano-inclusions and the third phase and geometry of nano-particles, and do not depend on the particular shape of regions occupied by the third phase. That seems reasonable, taking into account the assumption.

1.2.3.4. Thin intermediate layer; anisotropic model

In case of a thin intermediate layer, representation of the effective particle formed by nono-inclusion and the intermediate layer as an isotropic particle seems too inaccurate. Besides, the shapes of these particles are not close to spherical any longer; the shape of the effective particles rather reflect the shape of the original nano-inclusions (oblate, or prolate spheroids).

In case of violating condition (1.5), one of approximate schemes of calculating effective characteristics should be applied. The most attractive for the case in question appears to be considering the periodical structures. However, for the sake of simplicity, Mori-Tanaka's approach may be applied. According to this approach, (1.6) have to be replaced with the following expression (Final report, 2003)

$$\Lambda_{12} = \Lambda_2 + \left(\left(\Lambda_1 - \Lambda_2 \right)^{-1} + \left(1 - \Omega_{12} \right) S \Lambda_2^{-1} \right)^{-1} \Omega_{12} \tag{1.20}$$

Here the components of Eshelby's tensor, S, have to be chosen corresponding either prolate, or oblate spheroids for nano-tubes and nano-plates, respectively.

It is also use the differential scheme. This approach seems preferable if the analytical solution is known for the case under consideration.

Thus, the first part of the problem is solved.

1.2.4. The second stage

Let us consider now the second part of the problem: namely, ***to determine the effective properties of the composite consisting of the matrix and embedded inclusions of the equivalent material with the above calculated properties***. We restrict ourselves with considering isotropic in space distribution of particles only.

To address this problem we again may use Eshelby's method of determining effective characteristics of the composite with ellipsoidal inclusions (Final Report, 2002; Final Report 2003). Similar to (1.6), (1.20) we may write

$$\Lambda_{13} = \Lambda_3 + \left(\left(\Lambda_{12} - \Lambda_{12} \right)^{-1} + S \Lambda_3^{-1} \right)^{-1} \Omega_{23} \tag{1.21}$$

for small relative concentrations Ω_{23}, or

$$\Lambda_{13} = \Lambda_3 + \left(\left(\Lambda_{12} - \Lambda_{12} \right)^{-1} + \left(1 - \Omega_{23} \right) S \Lambda_3^{-1} \right)^{-1} \Omega_{23} \tag{1.22}$$

for final concentrations.

In case of isotropic distribution of the inclusions (even anisotropic) in the isotropic matrix, the composite remains. In case of small relative concentration, Ω_{23} we have:

$$k_{13} = k_3 \left[1 + A^* \Omega_{23} \right] \tag{1.23}$$
$$\mu_{13} = \mu_3 \left[1 + B^* \Omega_{23} \right]$$

Here A^* and B^* are some constants, determined by modulus of the matrix and inclusions, as well as by the shape of the inclusions.

1.2.4.1. Thick intermediate layer

Keeping in mind that the thickness of the layer of the third phase between the nano-tube and the matrix is approximately constant, we may conclude that increase of the relative concentration Ω_{12} leads to the configuration, for which the shape of zone occupied by the intermediate phase approach to the shape of the nanoparticle (flat, or needle-like spheroid); and the decrease of Ω_{12} leads to approaching this zone a sphere. It is this considerations that has determined the choice of the cases considered in figure 1.2.

Therefore, for small relative concentrations Ω_{12} the constants A^* and B^* may be chosen corresponding to the spherical inclusions (Figure 1.2). Corresponding expressions for isotropic inclusions have the form (Roscoe, 1973, Finale Report 2002; Finale Report 2003)

$$A^* = \frac{(k_{12} - k_3)(3k_3 + 4\mu_3)}{k_3(3k_{12} + 4\mu_3)} \tag{1.24}$$

$$B^* = \frac{5(\mu_{12} - \mu_3)(3k_3 + 4\mu_3)}{4\mu_3(3\mu_{12} + 2\mu_3) + 3k_3(2\mu_{12} + 3\mu_3)}$$

For anisotropic inclusions substituting components of Eshelby's tensor for spherical inclusions and the values of effective elastic constants, calculated on previous stage into (1.21) or (1.22) yields the effective elastic properties of composite. In case of isotropic distribution, they may be found with the help of methods of (Kroner, 1958; Finale Report 2002; Finale Report 2003). In this case the constants in equations (1.23) are determined as follows

$$A^* = 2\mu_3(1 - v_3)\big[2(\Lambda_{11}^{12} + \Lambda_{12}^{12})(2\Lambda_{33}^{12} + \mu_3) - \mu_3(3\Lambda_{33}^{12} + 14\mu_3) -$$
$$(13\Lambda_{33}^{12} + 12\mu_3)v_3(\Lambda_{11}^{12} + \Lambda_{12}^{12}) - (5\Lambda_{33}^{12} + 4\mu_3)\mu_3 v_3 +$$
$$10(\Lambda_{11}^{12} + \Lambda_{12}^{12} + \mu_3)(\Lambda_{33}^{12} + \mu_3)v_3^2 + 4\Lambda_{13}^{12}\mu_3(5 - 7v_3) - 2\Lambda_{13}^{12^2}(4 - 13v_3 + 10v_3^2)\big] /$$
$$(1 - 2v_3)^2\big[13\Lambda_{33}^{12}\mu_3 + 2(\Lambda_{11}^{12} + \Lambda_{12}^{12})(2\Lambda_{33}^{12} + 5\mu_3) - 5\Lambda_{33}^{12}v_3(\Lambda_{11}^{12} + \Lambda_{12}^{12} + 3\mu_3) -$$
$$- 2\Lambda_{13}^{13^2}(4 - 5v_3) - 4\Lambda_{13}^{12}\mu_3(3 - 5v_3) + 28\mu_3^2 - 10\mu_3 v_3(\Lambda_{11}^{12} + \Lambda_{12}^{12} + 2\mu_3)\big]$$

$$B^* = 15\mu_3(1 - v_3)$$
$$\Big\{\Lambda_{11}^{12^2}\big[-\Lambda_{13}^{12}(4 - 5v_3)(2\Lambda_{44}^{12}(4 - 5v_3) + \mu_3(1 + v_3)) +$$
$$4\mu_3(1 - v_3)(-4\Lambda_{44}^{12}(4 - 5v_3) + \mu_3(1 - 5v_3))\big] +$$
$$\Lambda_{12}^{12^2}\big[\Lambda_{33}^{12}(4 - 5v_3)(2\Lambda_{44}^{12}(4 - 5v_3) + \mu_3(1 + v_3)) -$$
$$4\mu_3(1 - v_3)(-4\Lambda_{44}^{12}(4 - 5v_3) + \mu_3(1 - 5v_3))\big] +$$
$$\Lambda_{11}^{12}\big[2\Lambda_{13}^{12^2}(4 - 5v_3)(2\Lambda_{44}^{12}(4 - 5v_3) + \mu_3(1 + v_3)) +$$
$$+ 8\Lambda_{13}^{12}\mu_3(\mu_3(5 - 7v_3) + 2\Lambda_{44}^{12}(2 - 3v_3)(4 - 5v_3)) +$$
$$+ \mu_3(\Lambda_{33}^{12}(1 - v_3)(-26\Lambda_{44}^{12}(4 - 5v_3) + \mu_3(29 - 55v_3)) +$$
$$+ 8\mu_3(\mu_3(3 - 4v_3)(7 - 5v_3) - \Lambda_{44}^{12}(15 - 22v_3 + 5v_3^2)))\big] +$$

$$+ 2\mu_3 \left[-4\Lambda_{13}^{12}\mu_3\left(\mu_3(1-3v_3)(7-5v_3)-2\Lambda_{44}^{12}(5-7v_3)\right) - \right.$$

$$- \Lambda_{13}^{12\,2}\left(\mu_3(7-5v_3)(5-7v_3)-2\Lambda_{44}^{12}\left(4-v_3-5v_3^{\;2}\right)\right)+$$

$$+ 4\mu_3^{\;2}(7-5v_3)\left(2\Lambda_{44}^{12}(1-2v_3)+\mu_3(7-5v_3)\right)+$$

$$+ \mu_3\Lambda_{33}^{12}\left(\mu_3(7-5v_3)(9-11v_3)-2\Lambda_{44}^{12}\left(3+5v_3-10v_3^{\;2}\right)\right)\Big]+$$

$$+ \Lambda_{12}^{12}\Big[2\Lambda_{13}^{12\,2}(4-5v_3)\left(-2\Lambda_{44}^{12}(4-5v_3)-\mu_3(1+v_3)\right)-$$

$$- 8\Lambda_{13}^{12}\mu_3\left(2\Lambda_{44}^{12}(2-3v_3)(4-5v_3)+\mu_3(5-7v_3)\right)+$$

$$+ \mu_3\Lambda_{33}^{12}\left(2\Lambda_{44}^{12}(4-5v_3)(11-15v_3)+\mu_3\left(41-64v_3+15v_3^{\;2}\right)\right)+$$

$$+ 8\mu_3^{\;2}\left(\mu_3(7-5v_3)+\Lambda_{44}^{12}\left(17-34v_3+15v_3^{\;2}\right)\right)\Big]\Big]\Big\}\bigg/$$

(1.25)

$$2\left[\left(\Lambda_{11}^{12}-\Lambda_{12}^{12}\right)(4-5v_3)+\mu_3(7-5v_3)\right]\left[2\Lambda_{44}^{12}(4-5v_3)+\mu_3(7-5v_3)\right]$$

$$\left[-13\Lambda_{33}^{12}\mu_3-2\left(\Lambda_{11}^{12}+\Lambda_{12}^{12}\right)\left(2\Lambda_{33}^{12}+5\mu_3\right)+2\Lambda_{13}^{12\,2}(4-5v_3)+\right.$$

$$\left. + 5\Lambda_{33}^{12}v_3\left(\Lambda_{11}^{12}+\Lambda_{12}^{12}+3\mu_3\right)+4\Lambda_{13}^{12}\mu_3(3-5v_3)-28\mu_3^{\;2}+10\mu_3 v_3\left(\Lambda_{11}^{12}+\Lambda_{12}^{12}+2\mu_3\right)\right]$$

Applicability of formulae (1.24) and (1.25) is restricted with the small relative concentrations.

$$\Omega_{23} \equiv \frac{V_1+V_2}{V_1+V_2+V_3} << 1 \qquad (1.26)$$

Simultaneous satisfying both conditions (1.5) and (1.26) seems unlikely. For higher concentration of the equivalent inclusions within the matrix the differential scheme of calculating the effective characteristic may be applied (Roscoe, 1973; Salganik, 1973; see also Ustinov, 2002, 2003; Final Report 2003). Therefore, according to this scheme, condition (1.26) may be withdrawn, and as the retribution, linear algebraic equations (1.23) have to be replaced with the differential ones. For the case in question these equations are (Roscoe, 1973; Final Report, 2002; Final Report, 2003)

$$\frac{dk_{13}}{d\Omega_{23}} = \frac{(k_{12}-k_{13})(3k_{13}+4\mu_{13})}{(3k_{12}+4\mu_{13})(1-\Omega_{23})}$$

$$\frac{d\mu_{13}}{d\Omega_{23}} = \frac{5(\mu_{12}-\mu_{13})(3k_{13}+4\mu_{13})\mu_{13}}{4\mu(3\mu_{12}+2\mu_{13})+3k_{13}(2\mu_{12}+3\mu_{13})}\frac{1}{(1-\Omega_{23})} \qquad (1.27)$$

Here moduli k_{13}, μ_{13} are considered as functions of concentration Ω_{23}. The obvious initial conditions

$$k_{13}\big|_{\Omega_{23}=0} = k_3$$

$$\mu_{13}\big|_{\Omega_{23}=0} = \mu_3 \qquad (1.28)$$

have to be satisfied for the system (1.27).

If it is not necessary to obtain more accurate solution, the differential scheme may be replaced with the scheme of Mori-Tanaka, considered above.

As was mentioned previously (Final Report, 2003), if the relative volume occupied by the intermediate phase become close to unity, regions occupied by the third phase may overlap. When the number of such overlapped regions reaches some critical value, the effect of percolation would take place. This means that the results obtained may loose their accuracy and an alternative model has to be applied. In the limiting case, where "the intermediate layer" occupy all the space and there is no original matrix remained, there is no need to consider the second stage.

1.2.4.2. Thin intermediate layer

In case of thin intermediate layer (high relative concentrations Ω_{12}) for real composites with small concentration Ω, owing to (1.4) Ω_{23} is also small. Therefore, this case may be considered in the frame of small concentration approach.

In case of isotropic distribution of nano-tubes surrounded by thin intermediate layer, considering the nanotube and surrounding them layers of the third phase as isotropic particles, we may use formulae (1.7), (1.8), formally replacing indexes 2 to 3, and 1 to 12. In case of nano-plates, using the same approach, we may use formulae (1.7), (1.9) with the same formal replacement.

According to a more rigorous approach, the nanotubes surrounded by thin intermediate layer should be considered as anisotropic particles. Therefore, instead of (1.8) the following formulae obtained on the base of method of invariants (Final Report, 2003) have to be used

$$A = \frac{1}{9}\left(2D_{11}^{12} + D_{33}^{12} + 2D_{12}^{12} + 4D_{13}^{12}\right)$$

$$B = \frac{1}{30}\left(7D_{11}^{12} + 2D_{33}^{12} + 12D_{44}^{12} - 5D_{12}^{12} - 4D_{13}^{12}\right) \qquad (1.29)$$

where D_{ij}^{12} are determined:
- for nano-tubes, by formulae (1.11) with formal replacing indexes 2 to 3, and 1 to 12;
- for nano-plates, by formulae (1.16) with the same formal replacing.

Thus, the second stage of the problem is completed.

1.2.5. Inverse problem; an example

Here, the algorithm is applied for calculating effective modulus of composite reinforced by nanoplates.

While solving the direct problem is straightforward, and its solution is stable, the solution of the inversed problem may cause some difficulties due to instability and possible absence of the exact outcome within the reasonable range of parameters. Therefore the procedure is suggested, consisting in consider the influence of the parameters of the third phase to the Young's modulus of composite only.

Consider an example, rather typical for nanocomposites: matrix is field with 0.5% volumetric concentration of nanoplates, which Young's modulus is 200 times higher then the modulus of the matrix; Poisson's ratio of the matrix and nanoplates being 0.45 and 0.33 respectively; the increase of composite modulus comparing to the matrix modulus being 70%. If there would be no intermediate layer the theory predicts the increase of 50%. To explain the additional increase we suppose that the additional intermediate layer has appeared while casting.

Let us seek for the solution assuming the intermediate layer to be thin.

For the first stage (the problem of a thin plate embedded in a material of the intermediate phase) the analytical solution for the differential scheme is known (Final Report, 2003), therefore it is natural to make use of it.

$$\frac{1}{E_{12}} = \frac{3(1-\nu_1)(9+5\nu_1) - (1+\nu_1)(13-15\nu_1)\Omega_{12}}{2(1-\nu_1)E_1\Omega_{12}} -$$
$$\frac{3(1-\nu_1)^2 E_2(1-\Omega_{12})}{6(1-\nu_1)E_1E_2\Omega_{12} + 4[E_1(1-2\nu_2) - E_2(1-2\nu_1)]E_1\Omega_{12}^2} -$$
$$\frac{150(1-\nu_1^2)^2 E_2(1-\Omega_{12})}{(7-5\nu_1)E_1\Omega_{12}[15E_2(1-\nu_1^2) + (7-5\nu_1)\Omega_{12}(E_1(1+\nu_2) - E_2(1+\nu_1))]} \qquad (1.30)$$

The expression for the effective modulus of the composite may be obtained by formal replacement E_1, ν_1, E_2, ν_2, Ω_{12} with E_{12}, ν_{12}, E_3, ν_3, Ω_{23}.

The solution in question is obtained by resolving equation (1.30) and the one obtained by the above mentioned formal replacement with respect to Young's modulus of the intermediate phase E_2 and relative concentration Ω_{12}.

The possible combination of its thickness (directly related to the relative concentration of the nanoplates within the volume of the layers) and Young's modulus, which is able to explain the additional increase, is shown in the Figure 1.3. Concentration $\Omega_{12}=0.1$ corresponds to the thickness of the layer about 4.5 times higher then the thickness of nanoplates; concentration $\Omega_{12}=0.6$ corresponds to the thickness of the layer about 3 times lower then

the thickness of nanoplates. It is seen that such a parameter as Poisson's ratio of the intermediate layer has a minor effect on the results.

1.2.6. Summary

During the three years period and according to the Working Plan the following works have been done and the following main results achieved:

- The literature review of the problem has been performed.
- On the base of the classical Eshelby's approach the effective solutions for determining effective properties of the composites formed by the elastic matrix and isolated inclusions have been obtained in the closed form. The solutions have been presented both in tensor and matrix forms.
- A number of important particular cases, for which asymptotical representations are possible, have been pointed out: flat inclusions (nano-plates), and needle-like inclusions (nano-tubes). The combined influence of the shape and relative stiffness of inclusions has been investigated; it has been shown that the presence of two parameters (the ratio of maximal an minimal dimensions of the inclusion and relative stiffness of inclusions) leads to non-uniform limit transition, which restricts the area of applicability of known classical asymptotical formulae. The areas of applicability of asymptotical formulae have been obtained (appears to be for the first time).
- The influence of anisotropy of the inclusions to the effective composite properties has been investigated (Final Report, 2003). It has been shown that the main influence is due to some particular combinations of elastic parameters of inclusions, and these combinations have been pointed out.
- The influence of the orientation of inclusions in space have been investigated both for isotropic and anisotropic inclusions. For the composites on the base of nano-tubes three types of space distribution have been considered: random, aligned and transverse (all inclusions lay in parallel planes). The solution for last case appears to be obtained for the first time.
- The nonlinear influence of concentration has been accounted for with the help of differential self-consistent method and the method of effective field (Mori-Tanaka).
- The obtained results were compared with the results known from the literature. The obtained results appear to be important as it are, as well as an useful tool for constructing more advanced models such as three-phases models, accounting for the presence of an intermediate layer between the matrix and inclusions.
- An algorithm for approximate calculating the effective characteristics of three phase composite material formed by the matrix, nano-tubes (or disk-like nano-particles) and surrounding them regions of the third phase is suggested.
- For the three-phase composite the following problems have been formulated. First, knowing mechanical and geometrical properties of all phases to calculate the effective properties of the composite (the direct problem). Second, knowing elastic properties of the matrix and the composite, to estimate the properties of the Intermediate phase and/or the inclusions (inverse problem).
- Variants of solutions of both direct and inverse problems have been suggested.
- Examples of solving both direct and inverse problems have been presented.

The above results were presented in the current and previous reports (Final Report, 2002; Final Report, 2003).

During the last year and according to the Working Plan the following works have been done and the following main results achieved:

- The algorithm for calculating the effective characteristics of three phase composite material formed by the matrix, nano-tubes (or disk-like nano-particles) and surrounding them regions of the third phase is developed. Variants of both direct and inverse problems are considered for both thick and thin intermediate layer.
- In the frame of the approach the effects caused by anisotropy are accounted.
- An example of solving inverse problem has been presented: estimation of the properties of intermediate layer.

Suggestions on prolongation of the works on the theme.

It is suggested to continue the study of the mechanical properties of nanocomposite in the following directions:

1. To continue studying the influence of the intermediate phase to the effective properties of the composite. Such a phase may appear during polymerization process in the form of thin or thick shells surrounding nano-particles. The study was commenced during the project and a method of estimation the influence of the intermediate phase properties was suggested, based on consequent consideration of contribution of the inclusions and intermediate phase into the effective properties. It is suggested to develop this approach to account for anisotropy effects and various types of space distribution.

2. To study the influence of the area of contact between the matrix and inclusions. Researches on this and previous point may help to understand such processes as intercolation and exfoliation and their influences to the effective mechanical properties of the composite.

3. To study the influence of the matrix anisotropy and to obtain a solution for effective elastic properties of composite with anisotropic matrix (at least for some important particular cases of anisotropy). For the last years, a lot of attention has been devoted to the problem of influence of inclusions of various shapes to the effective properties of composites with *isotropic* matrices. At the same time much less attention has been given to consideration the anisotropic matrices. This is mainly due to the fact that the latter case need much more complicated calculations involved, such that the general analytical solution for this case in the closed form is still unknown. Meanwhile, to obtain such a such a solution, at least for some important particular cases of matrix anisotropy, would be of great interest due to:
    -   such a solution is of importance itself;
    -   for calculating effective elastic properties of composite even on the base of isotropic matrix such methods as self consistent method and differential self consistent method involve solutions for an inclusion in the anisotropic matrix.

1.3. ESTIMATES OF NANOCOMPOSITES SHEAR STRENGTH

According to the working plan we continued studies modeling of the nanotube-polymer matrix adhesion. The statement of the problem and all equations were presented in the preceding reports in details.

In this final report the analysis of the computation results, obtained according to the model proposed in the preceding reports is presented.

The main relations essential for understanding the computation results are briefly outlined below.

Let's define the average shear stress τ_a along of a nanotube part of the length L_c as follows

$$\tau_a = \frac{1}{L_c} \int_0^{L_c} \tau_i(x)dx \qquad (1.31)$$

For a case when the shear stresses $\tau_i(x)$ in the all range of the external loading are linearly depend on the axis displacements u

$$\tau_i = \frac{G_1}{H_1}u \qquad (1.32)$$

and at the nanotube sections $x = 0$ and $x = L_c$ (see Fig. 1.4) are adopted the following boundary conditions

$$\sigma(L_c) = E_f \left. \frac{\partial u_1}{\partial x} \right|_{x=L_c} = \sigma_f, \quad \sigma(0) = E_f \left. \frac{\partial u_1}{\partial x} \right|_{x=0} = 0 \qquad (1.33)$$

we can obtain the dependence of the shear stresses over the nanotube axis:

$$\tau_i(t) = \frac{\sigma_f}{2\delta}\sqrt{\mu_1}\,\frac{\cosh\left(\dfrac{2\delta L_c\sqrt{\mu_1}}{D}t\right)}{\sinh(\lambda_1)} \qquad (1.34)$$

The following notations are used in the formulas (1.31)-(1.34):

H is the interface layer thickness (see Fig. 1.4);

G_1 is the shear modulus of the interface layer on the elastic branch of the deformation law (see Fig. 1.5);

E_f is the elastic modulus of the fiber;

σ_f is the external normal stress applied at the end of the nanofiber;

μ_1 is the relative stiffness of the interface layer between nanotubes and polymer matrix;

$t = {x}/{L_c}$ is dimensionless distance along of the nanotube axis;

D, d are outer and inner nanotube diameters, respectively (see Fig. 1.4).

The following parameters were also introduced above (and similar will be used later):

$$\mu_{1,2} = \frac{G_{1,2}}{E_f}\frac{D}{H}, \quad \beta_{1,2} = \frac{2\delta\sqrt{\mu_{1,2}}}{D}, \quad \lambda_{1,2} = \beta_{1,2}L_c, \quad \delta = \frac{D}{\sqrt{D^2 - d^2}} \qquad (1.35)$$

By using formula (1.34) and notations (1.35) we can write

$$\tau_a = \frac{\sigma_f\sqrt{\mu_1}}{2\delta L_c\sinh(\lambda_1)}\int_0^{L_c}\cosh(\beta_1 x)\,dx = \frac{\sigma_f D}{4L_c\delta^2} = \sigma_f\left[\frac{D}{4L_c}\left(1 - \frac{d^2}{D^2}\right)\right] \qquad (1.36)$$

Let's note, that the average value of the shear stresses (1.36) coincides with the value of the shear stress for an ideally-plastic matrix (Kelly and Tyson,1965; Wagner, 2002).

The dimensionless shear stresses (the shear stress concentration factor, SCCF) can be defined as follow

$$\tau_R(t) = \frac{\tau_i}{\tau_a} \qquad (1.37)$$

By incorporating Eqs (1.34) and (1.36) we obtain for the linear deformation law (1.32)

$$\tau_R(t) = \frac{\tau_i}{\tau_a} = \lambda_1\frac{\cosh(\lambda_1 t)}{\sinh(\lambda_1)} = \frac{2\delta L_c}{D}\sqrt{\mu_1}\,\frac{\cosh\left(\dfrac{2\delta L_c\sqrt{\mu_1}}{D}t\right)}{\sinh(\lambda_1)} \qquad (1.38)$$

Within the framework of the current model the maximal value of the shear stresses is observed on loaded end of the nanotube ($x = L_c$).

For displacements given at the nanotube end ($x = L_c$)

$$u_1(L_c) = u_f \qquad (1.39)$$

where u_f is the nanotube limit stretching, the dependency of the shear stress over nanotube length is

$$\tau_i(t) = u_f\frac{G_1}{H}\frac{\cosh(\lambda_1 t)}{\cosh(\lambda_1)} \qquad (1.40)$$

In this case the average shear stress τ_A is defined as

$$\tau_A = u_f \frac{G_1}{H} \int_0^1 \frac{\cosh(\lambda_1 t)}{\cosh(\lambda_1)} dt = u_f \frac{G_1}{H} \frac{\tanh(\lambda_1)}{\lambda_1} \tag{1.41}$$

and SCCF coincides with (1.38)

$$\tau_R(t) = \frac{\tau_i}{\tau_A} = \lambda_1 \frac{\cosh(\lambda_1 t)}{\sinh(\lambda_1)} \tag{1.42}$$

Let's evaluate the physical-mechanical parameters in (1.31)-(1.42). According to the data presented in (Wagner, 2002) the wall thickness ($h = 0.5(D - d)$) of single-wall nanotubes is $h = 0.34\,nm$ and the external diameter D is about $2 - 5\,nm$. Supposing that $D = 5\,nm$ then the internal diameter is $d = 4.32\,nm$ and

$$\delta = \frac{D}{\sqrt{D^2 - d^2}} \approx 1.986 \tag{1.43}$$

According to (Wagner, 2002) the critical length of a nanofiber is about $L_c \approx 100 - 500\,nm$ and the critical external stress σ_f vary between 20 and $150\,GPa$. The elastic modulus of the nanotubes is in the range $E_f = 0.8 - 1,8\,TPa$ (Wagner, 2002; Lau, 2003).

Information regarding other parameters of the model is rather undetermined. The thickness of the interface layer H strongly depends on the types of adhesion. There are several methods to improve interaction between nanotubes and polymeric matrix. For example, chemical attachment or cross linking of nanotube walls and polymeric matrix (functionalization) has been proposed as one of the techniques to improve the interfacial bonding. Based on molecular dynamics simulation it was shown (Wong, 2003; Frankland and Harik,2003; Frankland et al, 2002) that the shear strength of nanotubes-matrix interface and the critical length for load transfer are essentially improved by chemical cross-linking the nanotubes and matrix. The length of a functionalization group is about $0.1 - 0.2\,nm$ (Wong, 2003). Therefore, the lower bound of the thickness of the interface layer is $H = (0.04 - 0.1)D$ and the upper reasonable bound of this parameter is not more then the nanotube diameter $H \approx D$. Let's proceed to the determination other parameters of the deformation law (Fig. 1.5). The equations of the deformation law for the cases of the elastic deformation and hardening along the nanotube axis can be written as follow

$$\tau_i(x) = \begin{cases} \kappa_1 u(x), & 0 < u(x) \le u_m \\ \tau_2 + \kappa_2 u(x), & u_m < u(x) \end{cases} \tag{1.44}$$

where

$$\kappa_1 = \frac{G_1}{H}, \quad \kappa_2 = \frac{G_2}{H}, \quad \tau_2 = u_m(\kappa_1 - \kappa_2) \tag{1.45}$$

We can evaluate the bounds for the shear modulus G_1 supposing that the distance between the functionalize attached groups is not more then the nanotube diameter as in the numerical simulation (Wong, 2003; Frankland and Harik,2003; Frankland et al, 2002) and the thickness of the functionalize group is less then the nanotube wall thickness $h = 0.34\,nm$. In this case the upper bound for the elastic modulus of the interface layer is

$$E_1 < \frac{h}{D + h} E_f \tag{1.46}$$

If Poisson's ratio for the interface layer equals $\nu = 0.25$ and $D = 2 - 5\,nm$ we obtain

$$G_1 < \frac{0.5h}{(D + h)} \frac{E_f}{(1 + \nu)} \approx 0.05 E_f \tag{1.47}$$

The elastic modulus of the polymer matrix is about $E_m = 2 \div 3.5\,GPa$, therefore the bounds for the shear modulus of the interface layer are

$$\psi G_m \le G_1 \le \frac{\varepsilon E_f}{2(1+\nu)}, \quad \varepsilon < \frac{h}{D+h} \tag{1.48}$$

where the parameter $\psi < 1$ is determined by the equality of the adhesion without the functionalization and G_m is the shear modulus of the matrix.

We also can choose the parameter (G_2) of the hardening part of the deformation law supposing that

$$0 \le G_2 \le G_1 \tag{1.49}$$

The case $G_2 = 0$ corresponds to the ideal plastic flow. Note, that for this case the formulas (1.38)-(1.43) need to be modified.

Finally, we will use the following parameters for the computation:

the nanotube external diameter - $D = 5\,nm$;

the nanotube internal diameter - $d = 4.32\ nm$;

the wall thickness of single-wall nanotube - $h = 0.34\ nm$;

the critical length of the nanofiber - $L_c = 100\ nm$;

the elastic modulus of the nanotubes - $E_f = 1\,TPa$;

the Poisson ratio - $\nu = 0.25$;

the critical external stress - $\sigma_f = 50\,GPa$ (Wong, 2003; Frankland and Harik, 2003; Frankland et al, 2002);

the thickness of the intermediate layer - $H = D$.

The values of the parameter ε in (1.48) are chosen as $\varepsilon = 0.0005,\ 0.00025,\ 0.000125$ and the shear modulus of the interface layer is calculated according to

$$G_1 = \frac{\varepsilon E_f}{2(1+\nu)} \tag{1.50}$$

The values of the relative stiffness of the interface layer for the given values of D, H, E_f and ε are determined as follows

$$\mu_1 = \frac{G_1}{E_f}\frac{D}{H} = 2.0 \cdot 10^{-4}; 1.0 \cdot 10^{-4}; 0.5 \cdot 10^{-4} \tag{1.51}$$

The average shear stress for deformation law (1.32) and given above values of parameters σ_f, L_c, D, d equals:

$$\tau_a \approx 158,44\,MPa$$

The dependencies of the shear stress over the nanotube length for different values of the layer relative stiffness, see (1.51) are given in Fig. 1.6. Note, that the results in Fig. 1.6 are close to the experimental results (Wong, 2003; Frankland and Harik, 2003; Frankland et al, 2002) where the shear stresses for nanotube based composites were investigated: 138 MPa (epoxy matrix) and 186 MPa for polystyrene matrix.

One can also see in Fig. 1.6 that when the relative stiffness of the interface layer is decreasing then the distribution of the shear stresses tends toward the uniform state.

For a small parameter μ_1 we can write

$$\lambda_1 = \frac{2\delta L_c \sqrt{\mu_1}}{D} \approx 1$$

and therefore from (1.34) и (1.38) we obtain

$$\tau_i(t) \to \sigma_f\left[\frac{D}{4L_c}\left(1 - \frac{d^2}{D^2}\right)\right], \quad \tau_R = \frac{\tau_i}{\tau_a} \to 1 \tag{1.52}$$

which is close to ideally-plastic case (Kelly and Tyson, 1965; Wagner, 2002).

The distributions of the dimensionless shear stress (SCCF) along the nanotube axis for the values of relative stiffness μ_1 from (1.51) and for relative stiffness $\mu_{1\alpha} = 10\mu_1$ are shown in Fig. 1.7-1.8. It is seen that when the relative stiffness of the interface layer is increasing by 10 times then the distribution of the shear stresses

tend toward more non-uniform state. For example, if $\mu_1 = 0.5 \cdot 10^{-4}$ (see Fig. 1.7) then $\tau_R(1)/\tau_R(0) \approx 1.085$ and for $\mu_{1\alpha} = 2 \cdot 10^{-3} = 40\mu_1$ (see Fig. 1.8) we obtain $\tau_R(1)/\tau_R(0) \approx 17.75$. It should be noted, that if the stiffness of polymer matrix is decreasing then the shear stresses tend to uniform state.

The dependencies of the shear stresses at the breaking point $(x = 0)$ versus the relative length of the broken part of nanotube are given in Fig. 1.9. It is seen that if the relative length of the broken part is increasing then the shear stress is decreasing. It is easy to show from (1.4) that if $\mu_1 \to \infty$ then $\tau_i(0) \to 0$.

The shear stresses at the loading zone ($x = L_c$) are also decreasing if the relative length of the broken part of nanotube increases (see Fig. 1.10) and

$$\tau_i(1) = \frac{\sigma_f}{2\delta}\sqrt{\mu_1}, \quad \frac{L_c}{D} \to \infty \tag{1.53}$$

The dependencies of the dimensionless shear stress (SCCF) at the breaking point $(x = 0)$ and at the loading edge ($x = L_c$) versus the relative length of the broken part of the nanotube are given in Fig. 1.11-1.12. If the relative length of the broken part is increased then the parameter $\tau_R(1)/\tau_R(0)$ also increases.

It's interesting to note, that the average value of the dimensionless shear stress (SCCF) along the nanotube axis is not depend on the relative stiffness

$$\overline{\tau}_R = \lambda_1 \int_0^1 \frac{\cosh(\lambda_1 t)}{\sinh(\lambda_1)} dt = 1 \tag{1.54}$$

Let's consider the displacement u_f given at the nanotube end ($x = L_c$) as the boundary condition

$$u_1(L_c) = u_f \tag{1.55}$$

The normal critical stress at the ($x = L_c$) for the boundary conditions (1.55) can be written as follows

$$\sigma_f(\frac{L_c}{D}) = \frac{2u_f E_f \delta}{D}\sqrt{\mu_1} \tanh\left(2\delta\sqrt{\mu_1}\frac{L_c}{D}\right) \tag{1.56}$$

The dependencies of the normal critical stress (1.56) on the relative length of the broken part of nanotube are given in Figs 1.13-1.14 $\left(u_f = 2\,nm\right)$. If $\dfrac{L_c}{D} \to \infty$ then the normal critical stress is tends to

$$\sigma_f^{\min} = \frac{2u_f E_f \delta}{D}\sqrt{\mu_1} \tag{1.57}$$

To continue the solution of the problem let us consider the bilinear interface law with elastic and hardening parts (Fig. 1.5). To obtain the distribution of the shear stresses over the nanotube length one needs to consider the inverse problem. For deformation law (1.44), boundary conditions (1.33) and the additional conditions of continuity and compatibility at the point x_m of the deformation law changing

$$u_m = u_1(x_m) = u_2(x_m), \quad \left.\frac{\partial u_1}{\partial x}\right|_{x=x_m} = \left.\frac{\partial u_2}{\partial x}\right|_{x=x_m} \tag{1.58}$$

and the shear stresses can be written as follow

$$\tau_i(t) = \begin{cases} G_1 \dfrac{u_m}{H}\dfrac{\cosh(\lambda_1 t)}{\cosh(\lambda_1 \rho_m)}, & 0 \le t \le \rho_m \\[4mm] G_2 \dfrac{u_m}{H}\dfrac{\eta\cosh\left[\lambda_2(t-1)\right] + \dfrac{\xi\sigma_f}{E_f\lambda_2}\sinh\left[\lambda_2(t-\rho_m)\right]}{\cosh\left[\lambda_2(\rho_m-1)\right]}, & \rho_m < t \le 1 \end{cases} \tag{1.59}$$

where $u_1(x), u_2(x)$ are displacements of the nanotube axis on the parts with different stress-displacement law, u_m is the critical axis displacements (Fig. 1.4),

$$\rho_m = \frac{x_m}{L_c}, \quad \frac{1}{\xi} = \frac{u_m}{L_c} \tag{1.60}$$

Suppose that the relative size of the hardening zone $(1 - \rho_m)$ is given then the parameter of the deformation u_m can be obtain from the condition of continuity of stresses

$$\frac{1}{\xi} = \frac{\dfrac{\sigma_f}{E_f \lambda_2}}{\sqrt{\eta} \tanh(\lambda_1 \rho_m) \cosh\left[\lambda_2 (\rho_m - 1)\right] - \eta \sinh\left[\lambda_2 (\rho_m - 1)\right]} \tag{1.61}$$

The parameters $1/\xi$ and $u_m = L_c / \xi$ are computed from (1.61) for given values of $(1 - \rho_m)$ and the external stresses σ_f. Then the distribution of the shear stresses along of the nanotube axis computed from (1.59) for given values ξ, u_m and ρ_m. The following parameters of the model were used for the calculation of the results which are shown in Figs 1.15-1.18

$$\eta = \frac{G_1}{G_2} = 2, \ 4, \ 20; \quad \mu_1 = 1.0 \cdot 10^{-4} \tag{1.62}$$

The distributions of the shear stresses along the nanotube axis for fixed value of $\rho_m = 0.6$ are shown in Fig. 1.15. The parameters ξ, u_m are determined from (1.61) for each value of the parameter η and then the shear stresses were computed from (1.59) for given values σ_f, E_f etc. The results shown in Fig. 1.15 confirm that if the parameter η is increased then the stress distribution in the region $t > \rho_m$ is shifted to ideally - plastic case. Dependence (1.61) is presented in Fig. 1.16. The influence of the hardening parameter η is stronger for small values of ρ_m (large size of hardening zone). The dependence of the normal critical stresses σ_f on the parameter ρ_m for the fixed values of parameter $(1/\xi) = (u_m / L_c)$ can also be found from (1.61), see Fig. 1.17. As in Fig. 1.16, the influence of the parameter η is stronger for large size of the hardening zone $(1 - \rho_m)$. The distributions of the shear stresses over the nanotubes length for different values of the hardening zone are shown in Fig. 1.18. The maximal value of the shear stress, as in the case of the linear deformation law, is attained at the nanotube end $x = L_c$.

Finally, we will use the similar approach for the case of the bilinear deformation law with the elastic and softening branches.

The equations of the deformation law for the cases of the elastic deformation and the softening state can be written as follows

$$\tau_i(x) = \begin{cases} \kappa_1 u(x), & 0 < u(x) \leq u_m \\ \tau_2 - \kappa_2 u(x), & u_m < u(x) \end{cases} \tag{1.63}$$

where

$$\kappa_1 = \frac{G_1}{H}, \quad \kappa_2 = \frac{G_2}{H}, \quad \tau_2 = u_m \left(\kappa_1 + \kappa_2\right) \tag{1.64}$$

For deformation law (1.63), boundary conditions (1.33) and additional conditions (1.58) the shear stresses along the nanotube axis can be written as follows

$$\tau_i(t) = \begin{cases} G_1 \dfrac{u_m}{H} \dfrac{\cosh(\lambda_1 t)}{\cosh(\lambda_1 \rho_m)}, & 0 \leq t \leq \rho_m \\[4mm] G_2 \dfrac{u_m}{H} \dfrac{\eta \cos\left[\lambda_2 (t-1)\right] - \dfrac{\xi \sigma_f}{E_f \lambda_2} \sin\left[\lambda_2 (t - \rho_m)\right]}{\cos\left[\lambda_2 (\rho_m - 1)\right]}, & \rho_m < t \leq 1 \end{cases} \tag{1.65}$$

Similarly to (1.60)-(1.61), the parameter of the deformation law u_m can be obtain from the condition of stresses continuity

$$\frac{1}{\xi} = \frac{\dfrac{\sigma_f}{E_f \lambda_2}}{\sqrt{\eta} \tanh(\lambda_1 \rho_m) \cos\left[\lambda_2 (\rho_m - 1)\right] - \eta \sin\left[\lambda_2 (\rho_m - 1)\right]} \tag{1.66}$$

and then we can repeat all steps of calculations, as in the previous case.

The following parameters of the model were used for the calculation of the results shown in Figs 1.19-1.22

$$\eta = \frac{G_1}{G_2} = 0.444,\ 0.667,\ 1.,\ 2.,\ 4.;\quad \mu_1 = 1.0 \cdot 10^{-4} \tag{1.67}$$

The distributions of the shear stresses along the nanotube axis for the fixed value of $\rho_m = 0.6$ are shown in fig. 1.19. The parameters ξ, u_m are determined from (1.66) for each value of the parameter η and then the shear stresses were computed from (1.65) for given values σ_f, E_f, etc. The dependence (1.66) is presented in Fig. 1.20. The influence of the softening parameter η is rather strong for the whole range of values ρ_m. The dependence of the normal critical stresses σ_f on the parameter ρ_m for the fixed values of parameter $(1/\xi) = (u_m / L_c)$ can also be found from (1.36), see Fig. 1.21. As in Fig. 1.20, the influence of the parameter η is rather strong for the whole range of the softening zone size $(1 - \rho_m)$. The distributions of the shear stresses over the nanotubes length for different values of the softening zone size are shown in Fig. 1.22. The maximal value of the shear stresses is occurred at the point of the deformation law changing ρ_m and the value of shear stress at this point is determined by the stiffness of the elastic deformation law.

1.4. SUMMARY

1) During the reported period we proposed a mechanical model of the interface adhesion of polymer matrix and nanotubes accounting for the dependencies of the shear stresses between matrix and nanotube versus the main physical-mechanical parameters of the nanocomposite material;

2) The parametric analysis of the influence of the model parameters on the nanotubes and the interface layer stresses states was performed;

3) The asymptotic cases of the stresses states for a small relative stiffness of the interface layer and a large relative size of the nanotube part were considered and analyzed;

4) The comparison with published experimental data was performed and demonstrated a good agreement;

5) The proposed multi-parametric model can be used for the theoretical analysis of properties of new nanocomposite materials and for analysis of the experimental data.

The following directions of activity seem to be most important within the framework of the given model and the extension of this project:

1) taking into account the compliance and strain of the polymer matrix;

2) analysis of an influence of the molecular structure of the jointed materials on the thickness of the interface layer;

3) consideration of the nanofibers with a scrimp and the nanofibers bundles;

4) analysis of nanofibers compression taking into attention the nanfiber buckling;

5) analysis of an influence of the interactions between the nanofibers, nanoparticles and the interface layer in the polymer matrix on the mechanical properties of nanocomposites;

6) analysis of an influence of the adhesion between matrix and nanofiller on the fracture toughness of nanocomposites.

REFERENCES

Annual Report 2002.

Annual Report 2003.

Intermediate Report 2004.

Frankland, S.J.V., V.M. Harik, 2003. Analysis of carbon nanotube pull-out from a polymer matrix, Surface Science, Surface Science Letters, 525 L103–L108.

Frankland S. J. V., Caglar A., Brenner D. W., and Griebel M., 2002. "Molecular Simulation of the Influence of Chemical Cross-Links on the Shear Strength of Carbon Nanotube-Polymer Interfaces.", Journal of. Physical Chemistry B, 106, 3046.

Kelly A., Tyson W.R., 1965. Tensile properties of fibre-reinforced metals: copper/tungsten and copper/molybdenum, J. Mech. Phys. Solids, 13, pp. 329-350.

Kroner, E., 1958. Berechnung der Elastischen Konstanten des Vielkristalls aus den Konstanten der Einkristalls. Z.Phys. 151, 504.

Lau K.T., 2003. Interfacial bonding characteristics of nanotube/polymer composites, Chemical Physics Letters, 370, pp. 399-405.

Riccardi A. and F. Montheillet, 1999. A generalized self-consistent method for solids containing randomly oriented spheroidal inclusions. Acta Mechanica, 133, 39-56.

Roscoe, R.A., 1973. Isotropic composites with elastic and viscoelastic phases: General bounds for the moduli and solutions for special geometries. Rheol. Acta, 12, 404-411.

Salganik R.L., 1973. Mechanics of Bodies with Many Cracks Izv.AN SSSR, Mech. Tv. Tela, No.4, 149-158, (In Russian. Engl. transl. - Mechanics of Solids)

Ustinov, K.B., 2002. Some particular cases of determining the effective elastic characteristics of the media with isolated inclusions. Preprint IPM RAN N715, 50 p. (In Russian).

Ustinov, K.B., 2003. On determining the effective characteristics of elastic two phases media. The case of spheroid inclusions. To be published (In Russian).

Wagner H.D., 2002. Nanotube-polymer adhesion: a mechanical approach, Chemical Physics Letters, 361, pp. 57-61.

Walpole, L.J., 1969. On the overall elastic moduli of composite materials, Journal of Mechanics and Physics of Solids, 17, 235-251.

Wong M. et al., 2003. Physical interaction at carbon nanotube-polymer interface, Polymer, vol. 44, pp. 7757-7764.

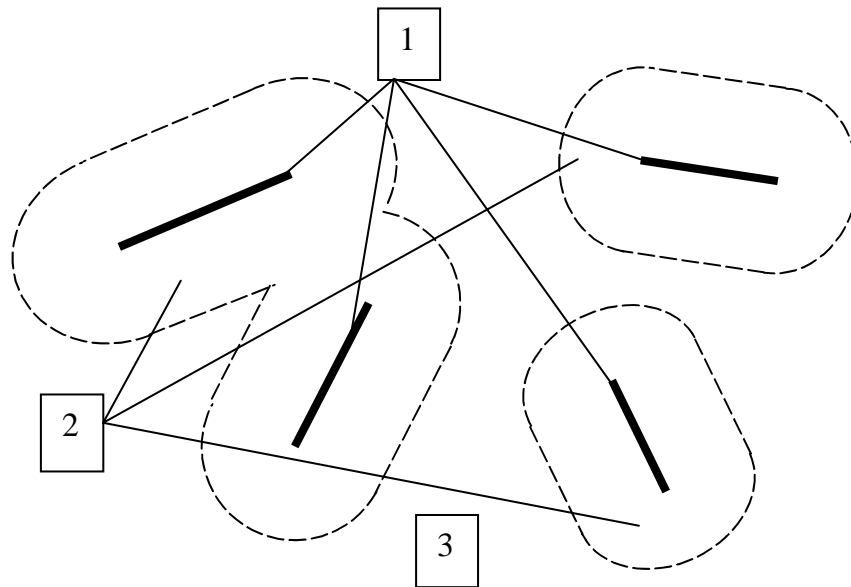Figure 1.1. The composite. 1 – nanoinclusion; 2 –intermediate phase; 3 – matrix.
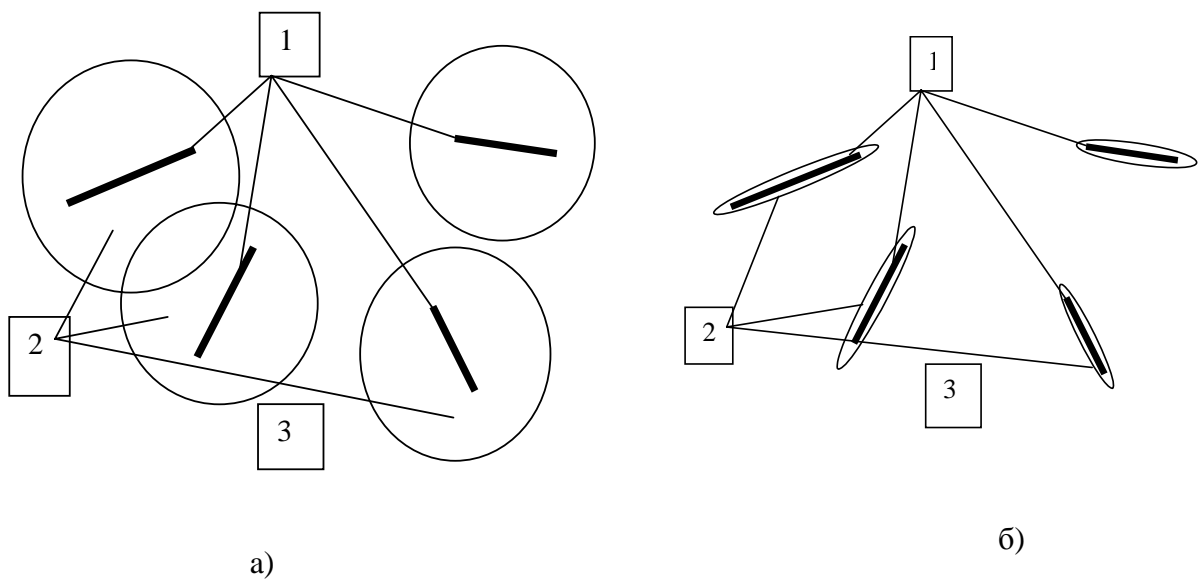

a)

б)

Figure 1.2. Model of the composite. 1 – nanoinclusion; 2 –intermediate phase; 3 – matrix.
a) thick intermediate layer: b) thin intermediate layer.
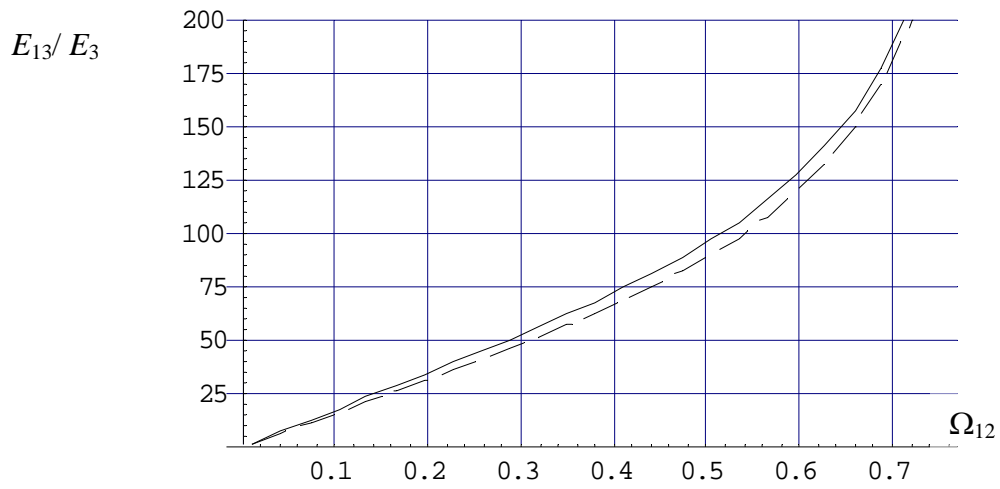
Figure 1.3. Relative Young's modulus of the intermediate layer as a function of the relative concentration of nonoplates in the material of the intermediate phase. Solid line corresponds to Poisson's ratio of the intermediate phase equal to 0.25, dashed line does to 0.45.
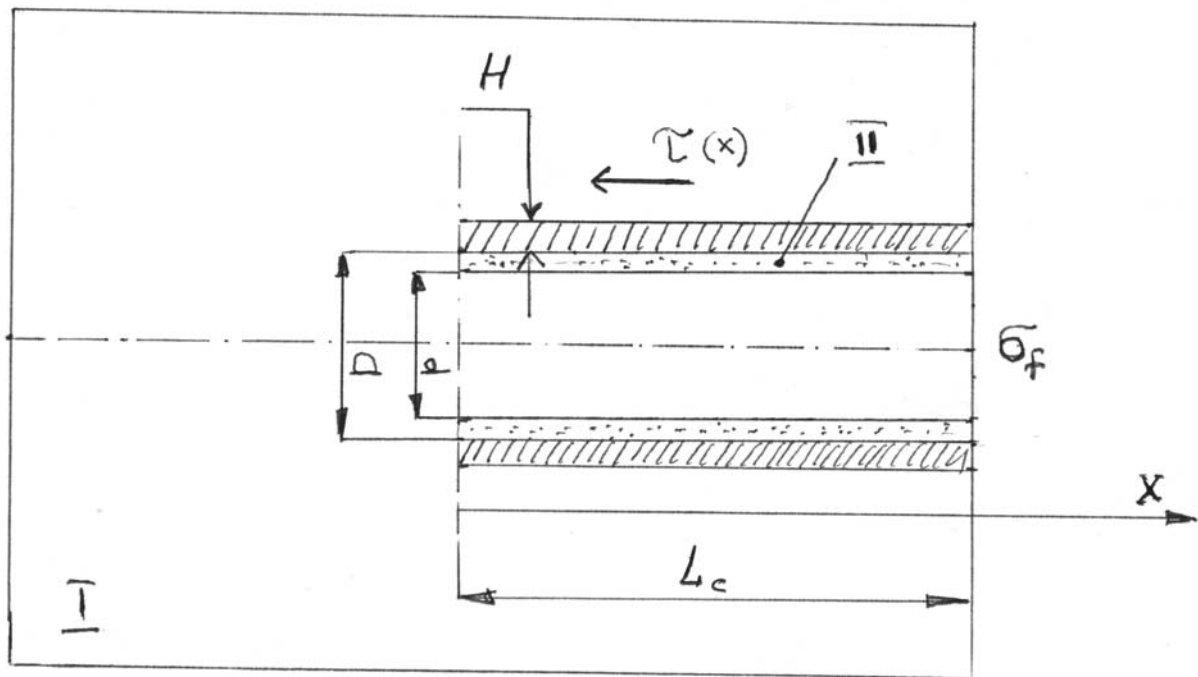
Fig. 1.4 Nanotube (II) embedded in a polymer matrix (I) under the action of the external normal stress σ_f . H is the interface layer thickness.
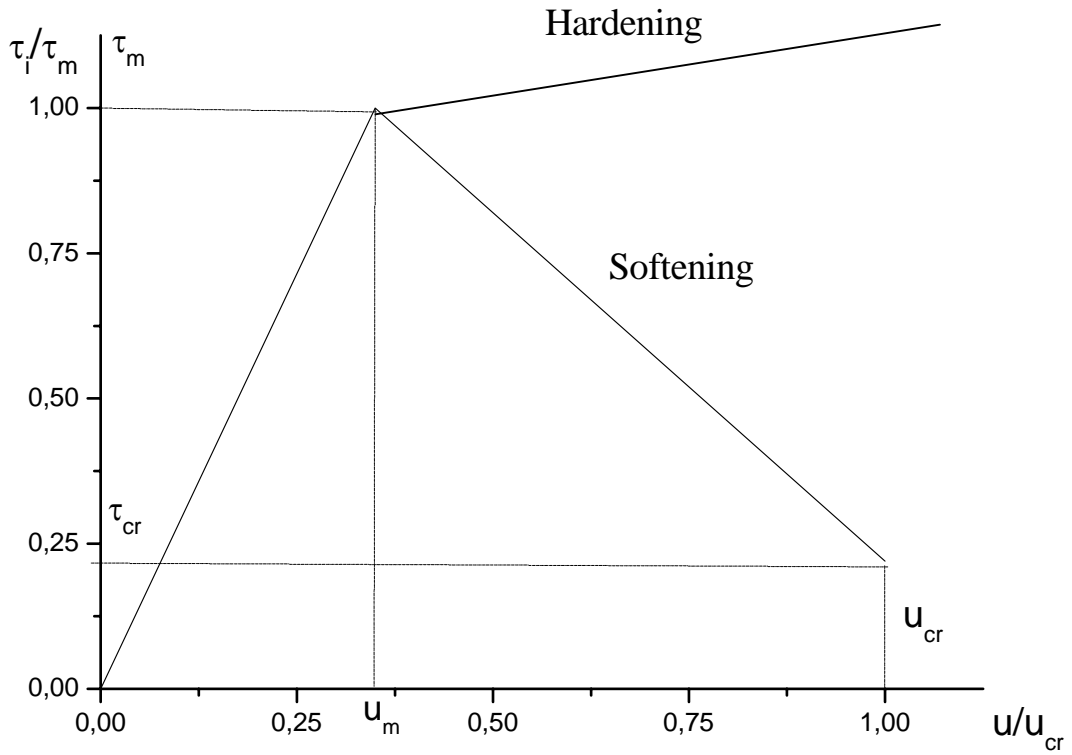
Fig. 1.5. Bilinear shear stress-displacement law for the interface layer
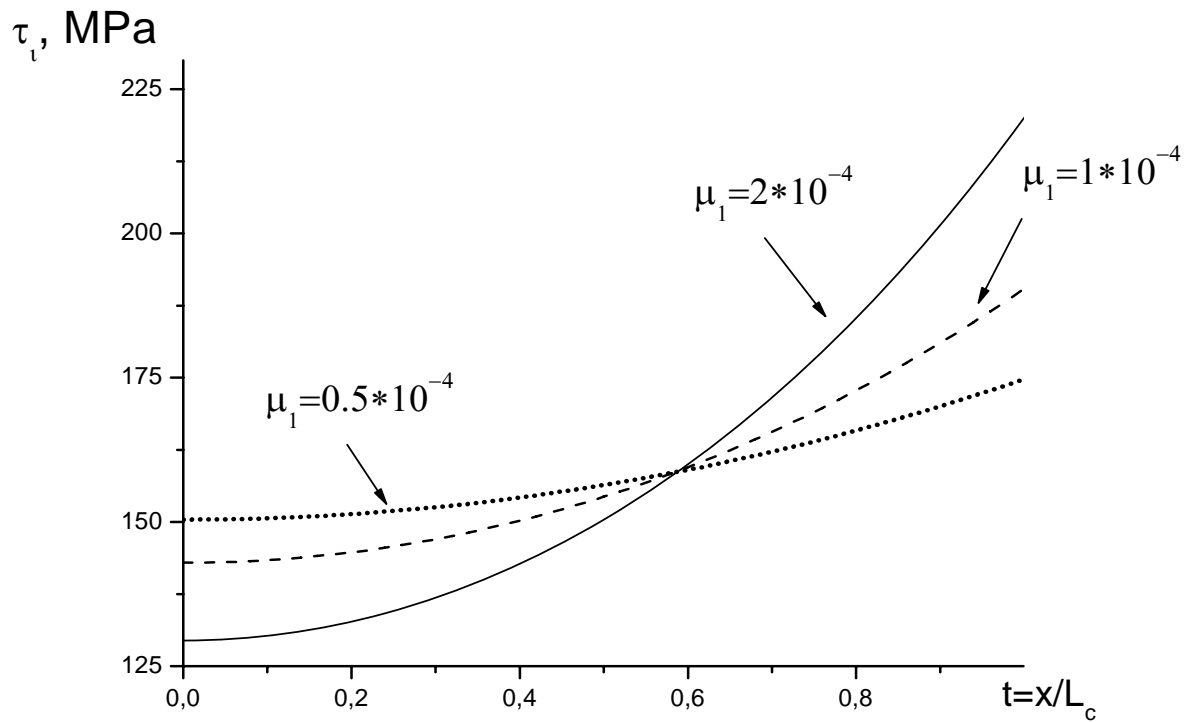
Fig. 1.6. Distribution of the shear stresses over the nanotube length for different values of the relative stiffness of the interface layer, μ_1
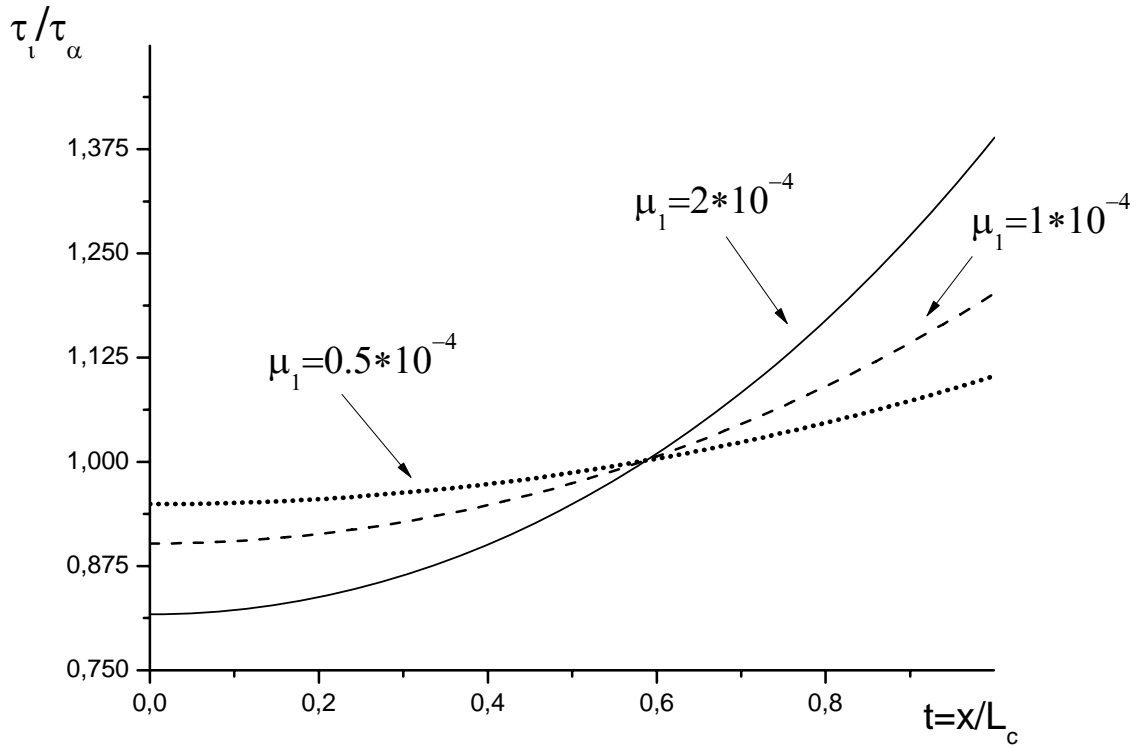
Fig. 1.7.
Distributions of the relative shear stresses along nanotube axis for different values of the relative stiffness of the interface law, μ_1
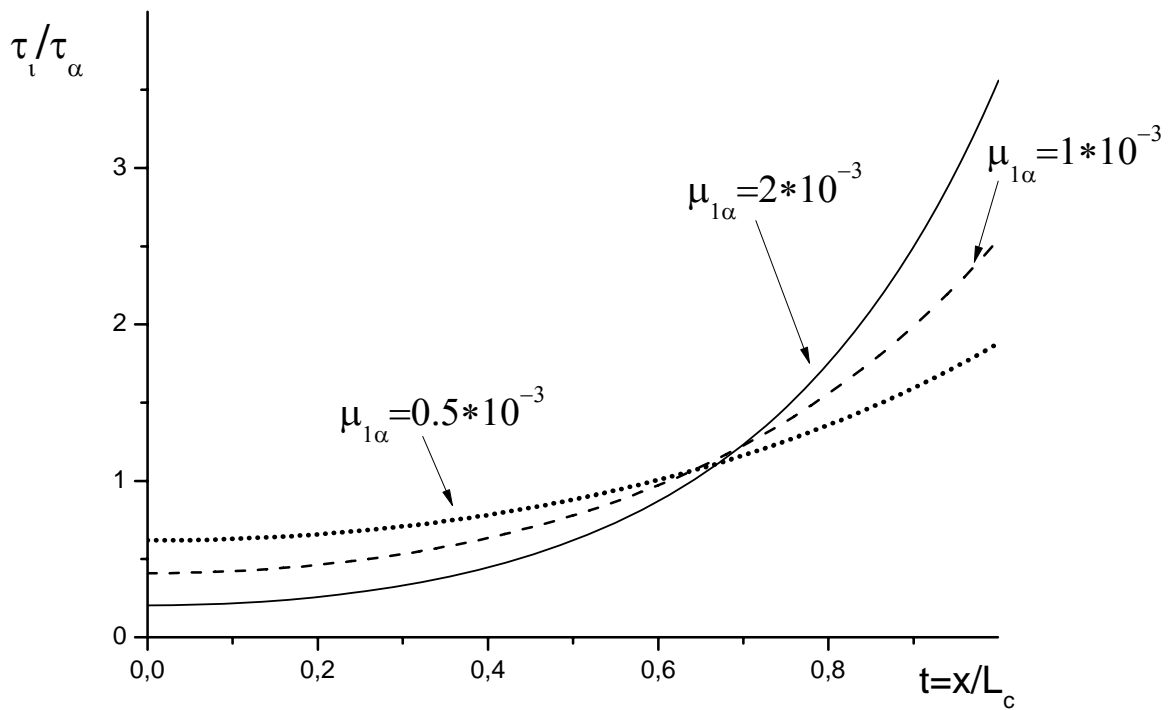
Fig. 1.8. Distributions of the relative shear stress along nanotube axis for different values of the relative stiffness of the interface law, $\mu_{1\alpha} = 10\mu_1$
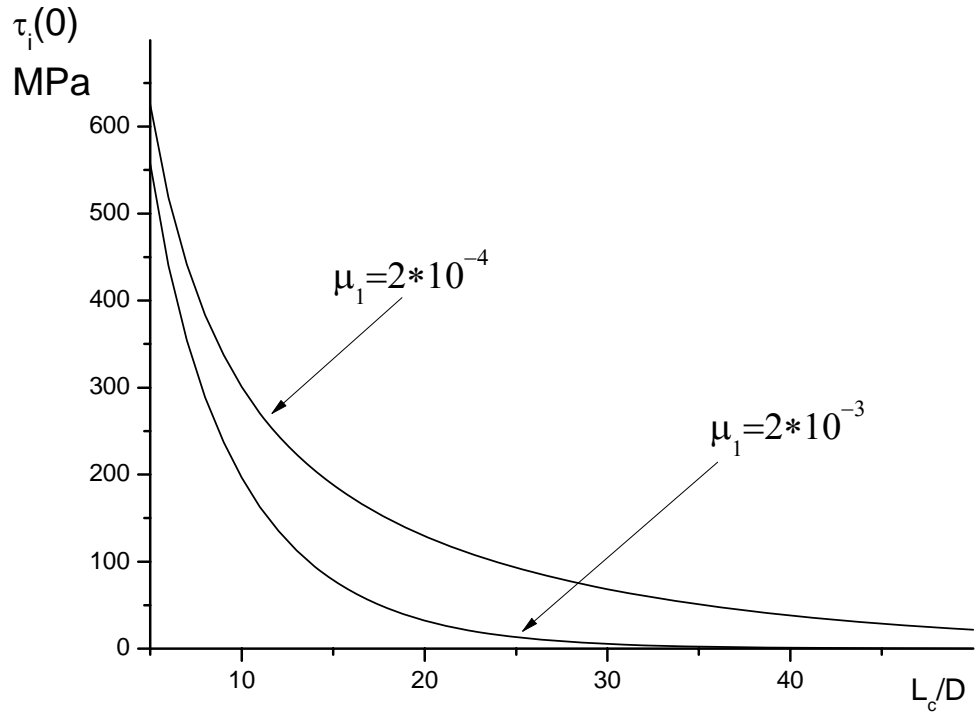
Fig. 1.9. Dependencies of the shear stresses at the breaking zone vs. nanotube length for different values of the relative stiffness of the interface layer, μ_1
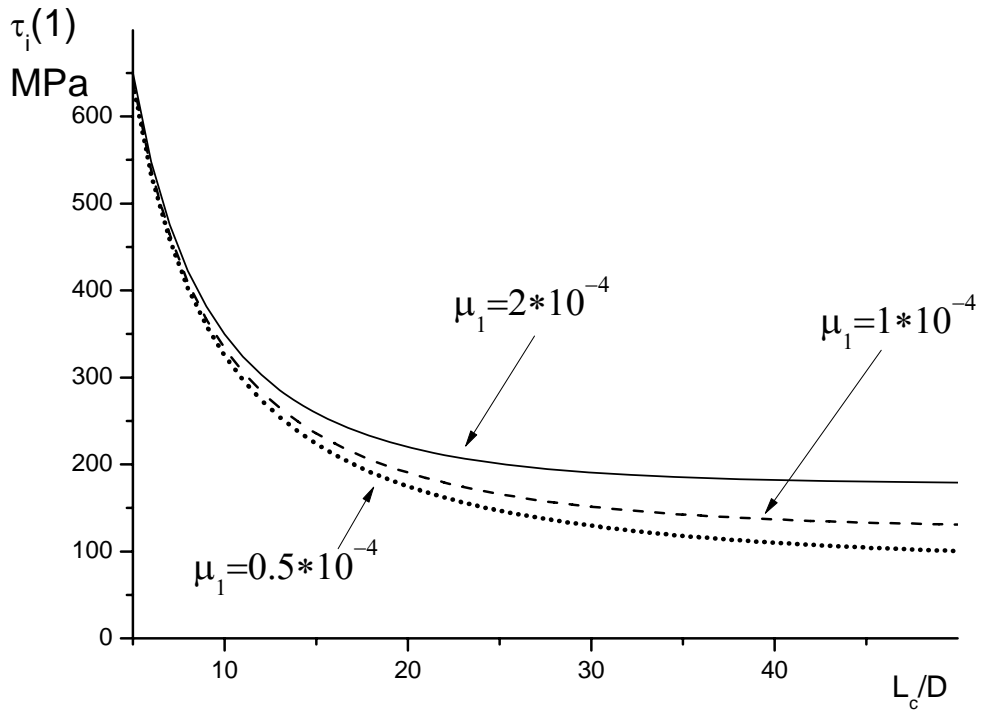
Fig. 1.10. Dependencies of the shear stresses at the loading zone vs. nanotube length for different values of the relative stiffness of the interface layer, μ_1

24
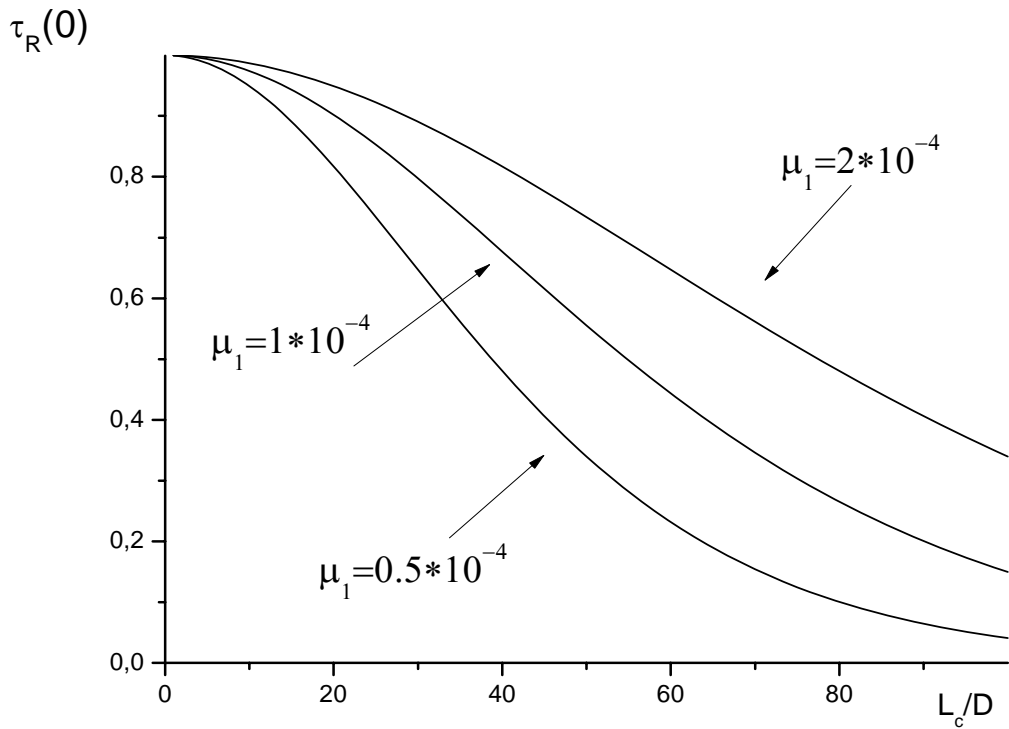
Fig. 1.11. Dependencies of the SCCF in the breaking zone vs. nanotube length for different values of the relative stiffness of the interface layer, μ_1
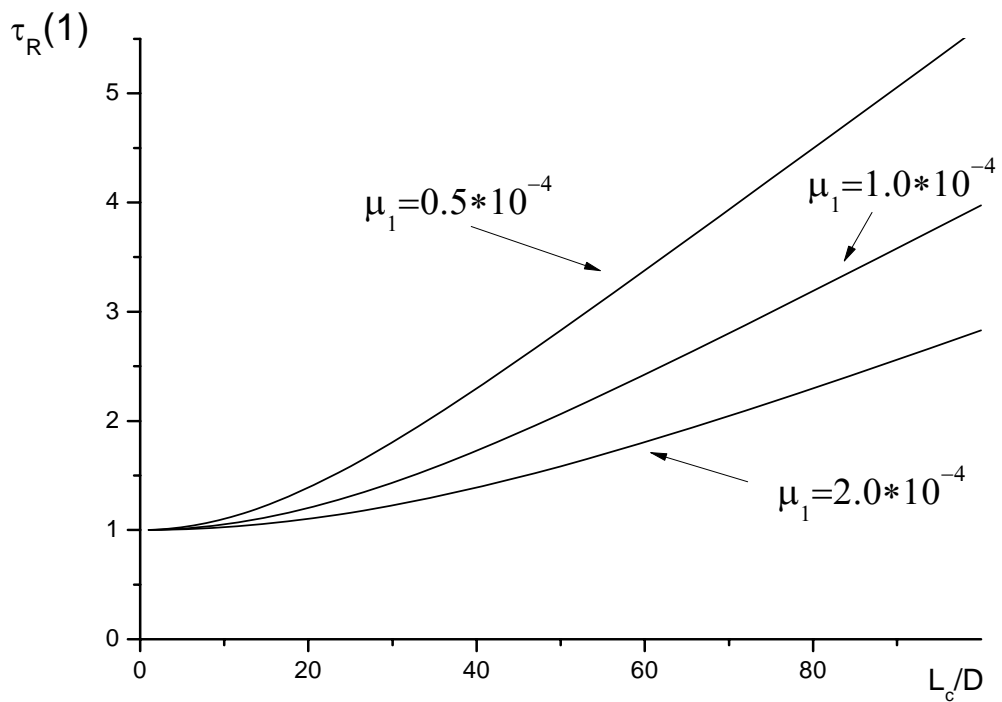
Fig. 1.12. Dependencies of the SCCF in the loading zone vs. nanotube length for different values of the relative stiffness of the interface layer, μ_1
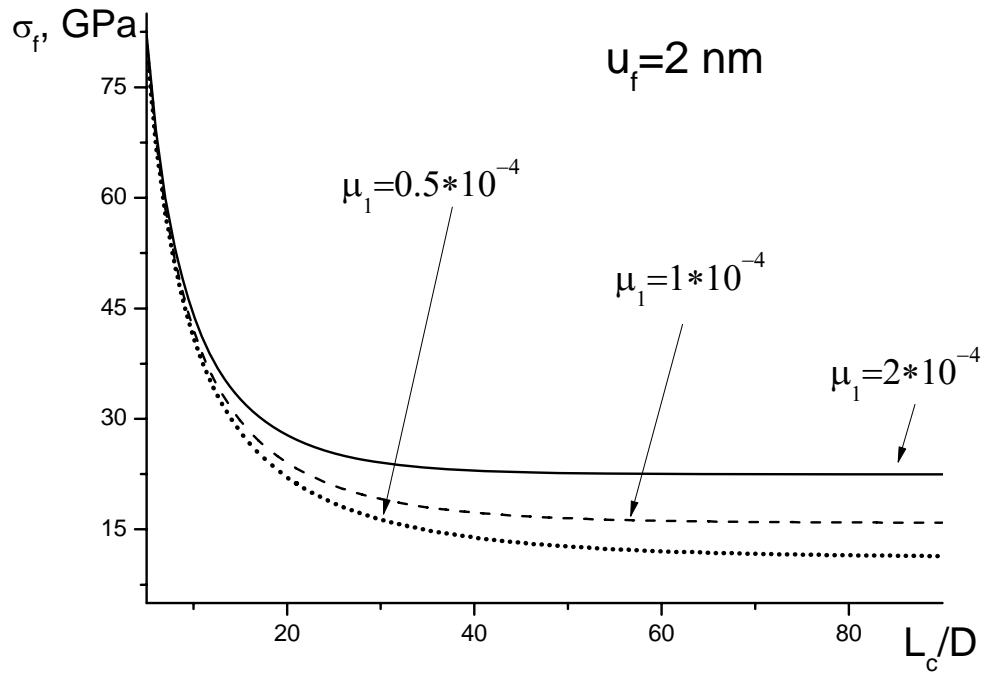
Fig. 1.13. Dependencies of the normal critical stresses vs. nanotube length for different values of the relative stiffness of the interface layer, μ_1
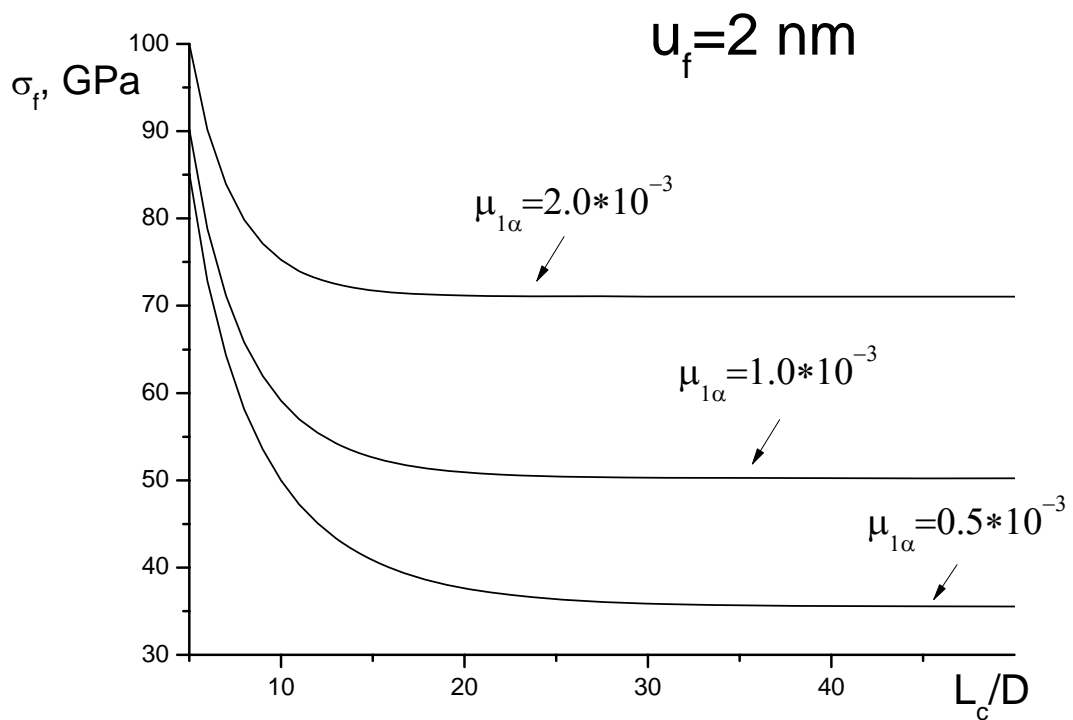
Fig. 1.14. Dependencies of the normal critical stresses vs. nanotube length for different values of the relative stiffness of the interface layer, $\mu_{1\alpha}$
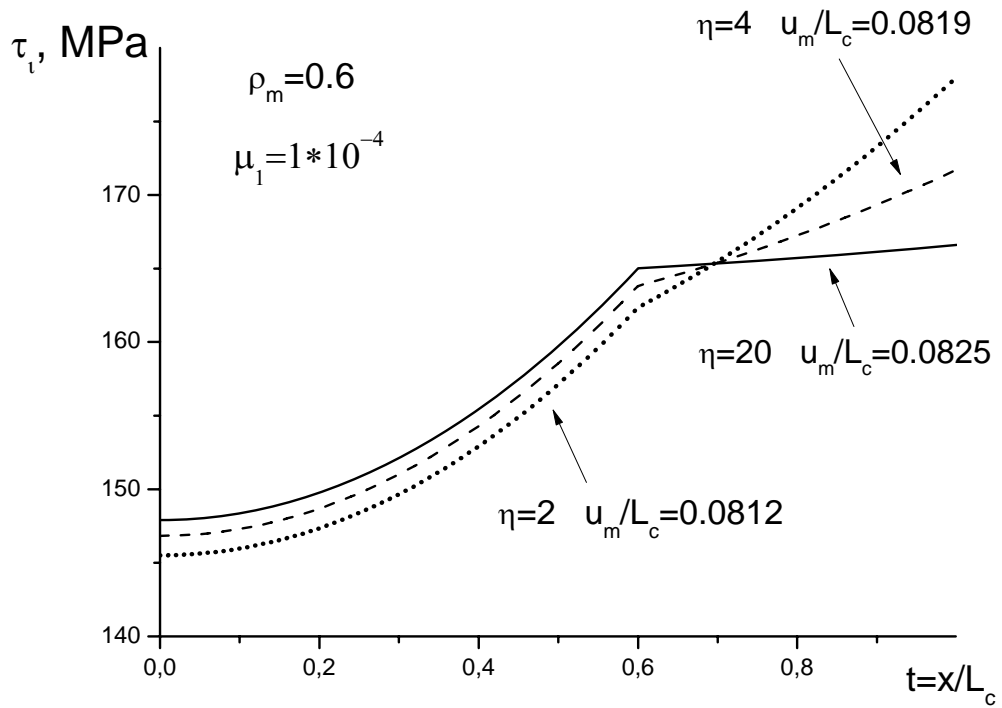
Fig. 1.15. Distributions of the shear stresses over the nanotube length for different values of the hardening parameter, η
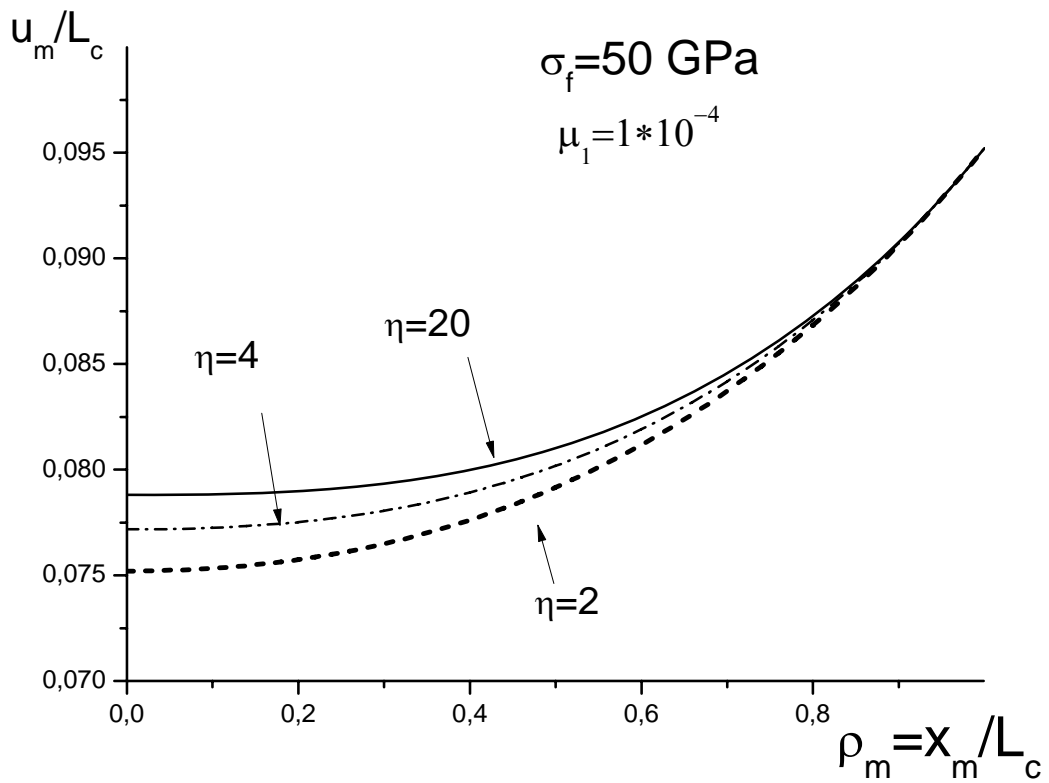
Fig. 1.16. Dependencies of the deformation law parameter u_m vs. the length of the elastic deformation zone for different values of the hardening parameter, η
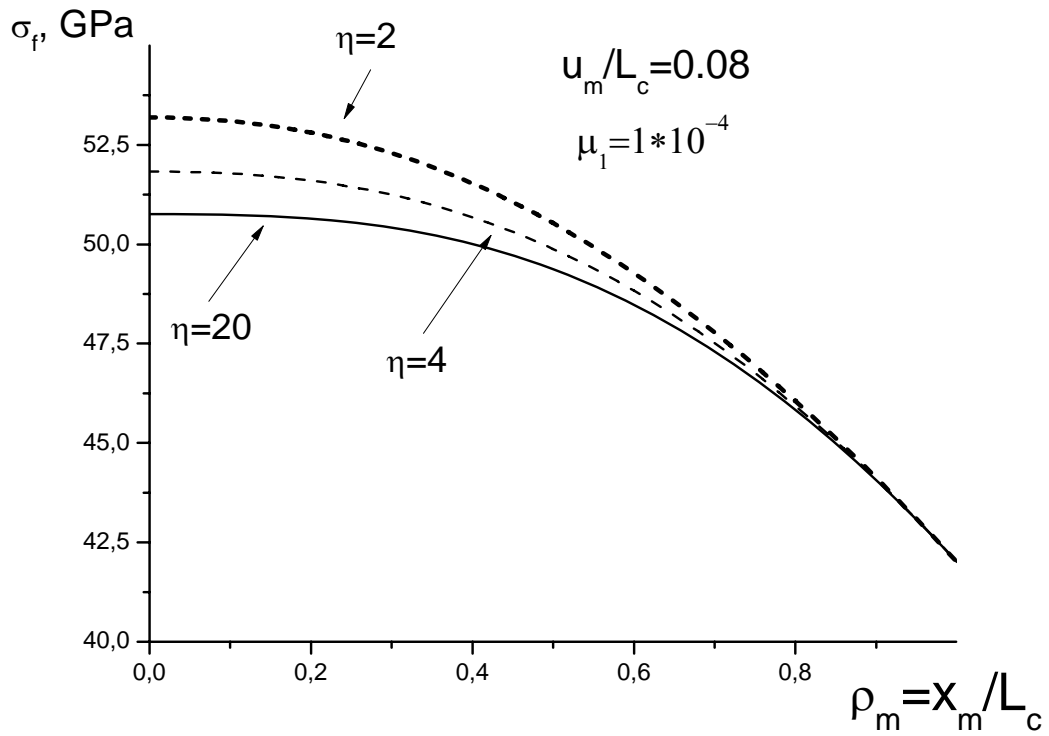
Fig. 1.17. Dependencies of the normal critical stresses vs. the length of the elastic zone size, for different values of the hardening parameter, η
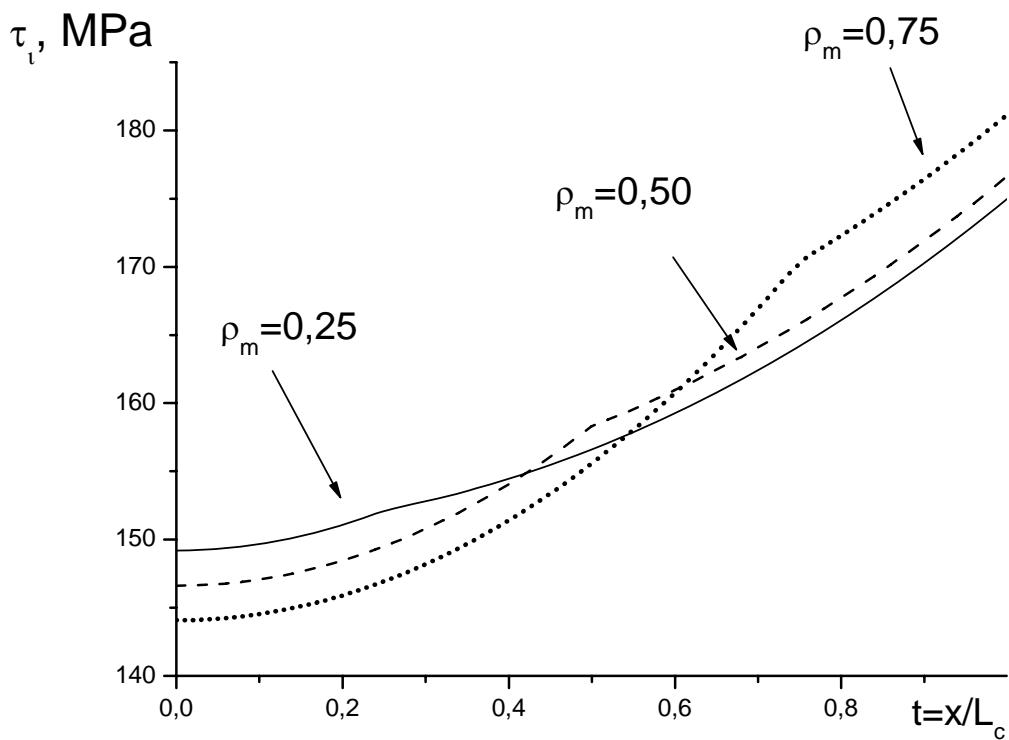
Fig. 1.18. Distributions of the shear stresses over the nanotube length, for different length of the elastic zone size ρ_m, $\mu_1 = 10^{-4}$, $\eta = 2$
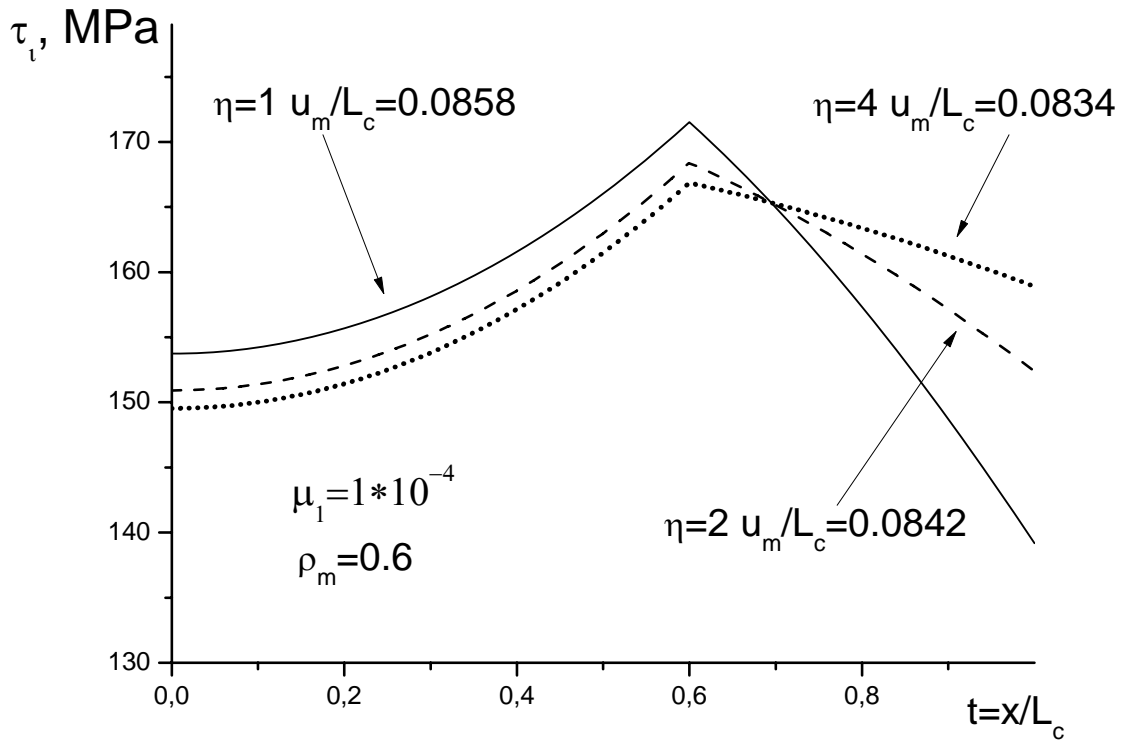
Fig. 1.19. Distributions of the shear stresses over the nanotube length for different values of the hardening parameter, η
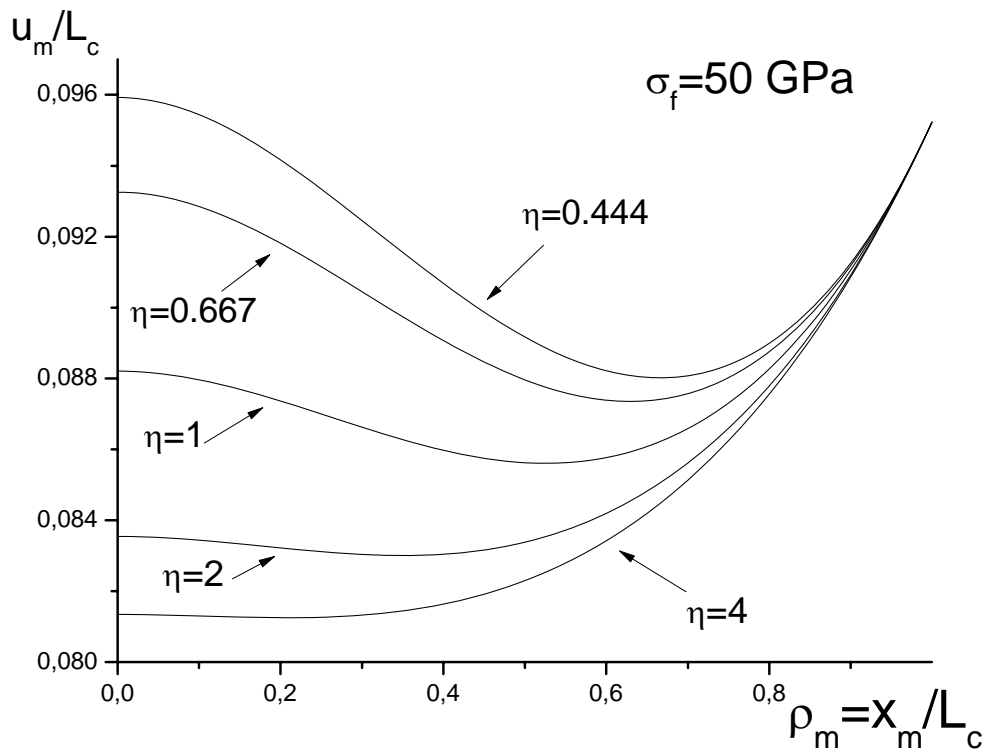
Fig. 1.20. Dependencies of the deformation law parameter u_m vs. the length of the elastic deformation zone for different values of the softening parameter, η
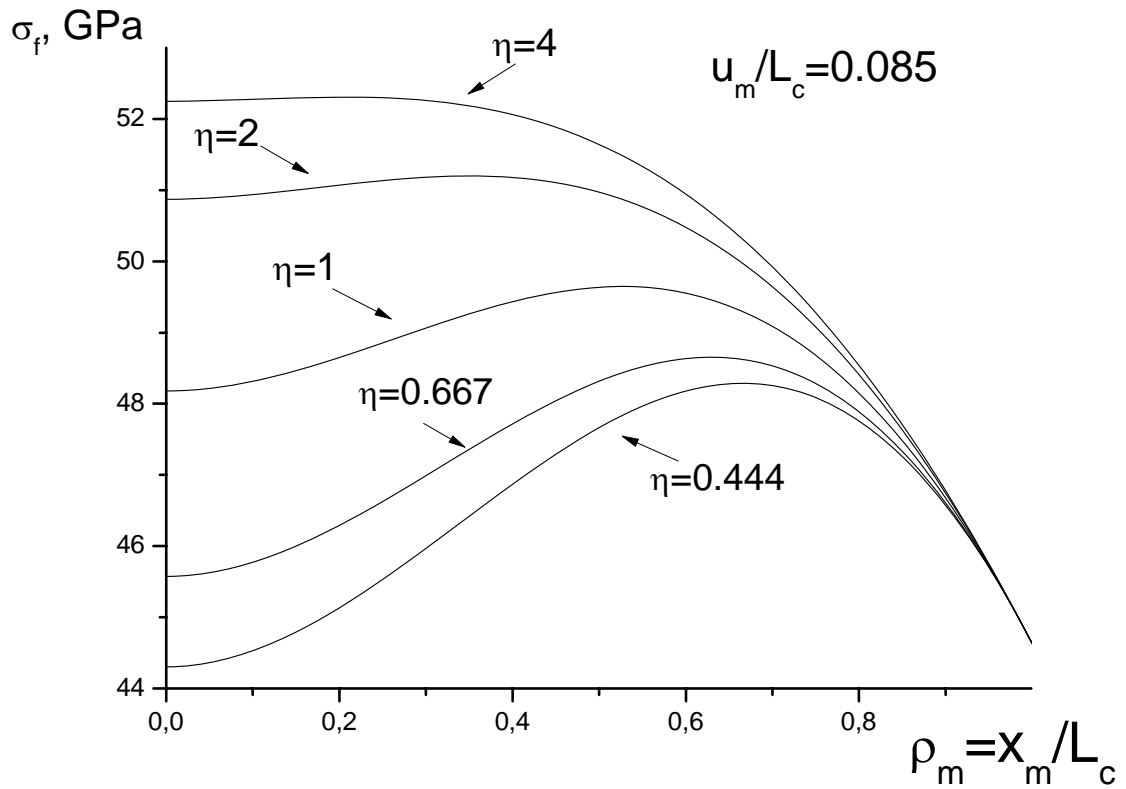
Fig. 1.21. Dependencies of the normal critical stresses vs. the length of the elastic zone size, for different values of the softening parameter, η

Fig. 1.22. Distributions of the shear stresses over the nanotube length, for different length of the elastic zone size ρ_m, $\mu_1 = 10^{-4}$, softening, $\eta = 2$

2. SIMULATION OF THE CONTINUUM BEHAVIOR WITH INTERNAL DEGREE OF FREEDOMS. GENERAL THEORY OF DEFECTS IN CONTINUOUS MEDIA

A new general theory of defects in continuous media is introduced. The general mechanisms of generation and healing of defects are established. The kinematic description of continuum media with defects is presented. The definiti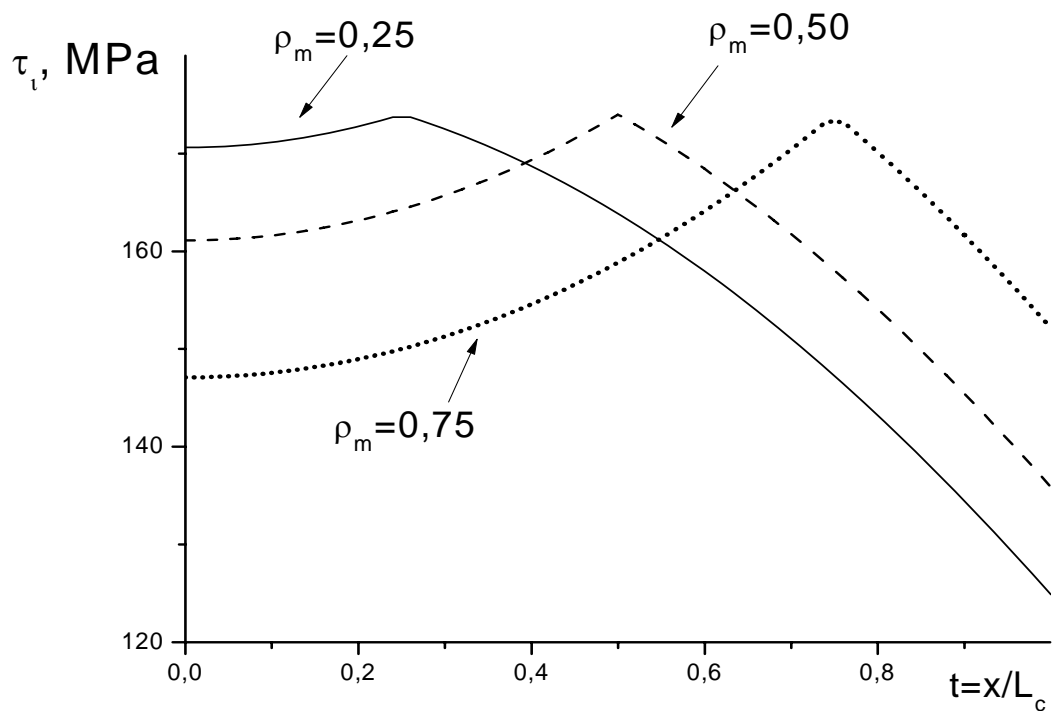on of defects of different levels is given, and the classification of continuous media with defects is introduced. The hierarchic structure of the theory of defects is discussed. It is shown that all the known types of defects are naturally included in the presented classification of defects. A new broad class of defects of new types is established and interpreted. It is shown that the existence of new classes of defects is directly connected with some known theoretical and experimental data on the possibility of generation of such defects as dislocations and disclinations. In particular, it is shown that the generation of dislocations is necessarily connected with the existence of disclinations. The formal class of defects being a source of disclinations is specified. A formal generalization of classification of defects is developed to include the defects of any finite level. The development of consistent theory of defects is very important from both, fundamental and applied viewpoints. The potential applications include, in particular, the modeling of dispersed composite materials, porous media, dynamics of surface effects, crackling, cavitation and turbulence.

INTRODUCTION

Recent advances in mechanics of continuous media with defects are closely related to the developments in our views on strength and plasticity of solids with local disturbances contributing to their overall behavior. Considerable achievements in creation of new technologies and materials are tied to the success in experimental and theoretical studies of the atomic structure, properties and behavior of defects, such as dislocations, disclinations, point defects, inclusions and interfaces. From one side, the language of the theory of defects is sufficiently universal means of interaction between the researchers working in mechanics, physics and material science. It allows describing from the common ground the variety of the different scale physical processes in the deformable media. From the other side, it is also known that in many cases the defects are being formed already at the processing stage for a number of new promising nano- and noncristallic materials like, for example, amorphous crystallic composites, nanocomposites, quasi-crystallic, nano-quasi-cristallic and some other materials [Gutkin (2000)]. These inherited defects affect the overall operational properties of these materials. That is the reason why the theory of defects became so important topic in the modern research and gained the considerable development. Many practically important phenomenological models in theory of defects have been significantly revised in the recent studies.

Different types of defects are introduced and analyzed in [Nabarro F.R.(1967), Kroner E., (1962,1982)]. The achievements in the continuum theory of defects, see e.g., [Kroner E. (1982), De Wit R.(1960,1973), Kadic, A., and Edelen (1983)], proved to be very important for the further studies of plastic deformation and for modeling of media on account of scale effects of different levels. The development of continuum models of defects beyond the classical elasticity appears to be very important for the description not only limited to the short-range interactions typical for the interaction of defects, but also for the modeling of size-dependent effects in elasticity and plasticity. Recently these models were developed in the framework of the gradient elasticity [Gutkin (2000) Aifantis E.C.,(1994,1999)] and gradient plasticity [Fleck, N.A., and Hutchinson, J.W.(1993, 1997,2001); Gao, H., Huang, Y., Nix, W.D., and Hutchinson, J.W., (1999)]. It has been shown that the gradient theories are quite effective in the analysis of the media at the nano- and micro-levels.

The kinematics of defects is a basis in development of phenomenological continuum models in the theory of defects. Firstly, the kinematics of defects (inconsistencies) is the most important element in application of the variational methods for the description of the higher order energetically consistent continuum gradient models, see [Fleck, N.A., and Hutchinson, J.W.(1993, 1997,2001); Gao, H., Huang, Y., Nix, W.D., and Hutchinson, J.W., (1999); Mindlin R.D (1964)]. Indeed, the kinematics of defects allows to establish a set of arguments for the correct formulation of the variation of energy functional. Secondly, the kinematic analysis allows to establish the relation between the different types of defects and to analyze the reasons and conditions for their generation and disappearance [Kroner E., (1962,1960); De Wit R(1960,1973);) Aifantis E.C.,(1`994,1999); Fleck, N.A., and Hutchinson, J.W.(1993, 1997,2001); Gao, H., Huang, Y., Nix, W.D., and Hutchinson, J.W., (1999)].

The possibility of generation (or birth) and disappearance (or healing) of the defects of such two levels as dislocations and disclinations in the continuous media has been established theoretically and experimentally, see e.g., [Kadic, A., and Edelen D.G.B., (1983); Likhachev, V.A., Volkov A.E., and Shudegov V.E., (1986)]. It has been also shown experimentally that the dislocations on disclinations can be borne and disappear. We are not familiar at the present time with experimental studies that would establish the sources of disclinations with the similar clarity. Nevertheless it is possible to state that the fact of generation and disappearance of disclinations has been demonstrated experimentally, and therefore the existence of sources of disclinations has been established.

In the present paper we introduce a new general kinematic theory of defects in continuous media. And we establish the general mechanisms of existence of defects, their generation (or birth) and disappearance (or healing).

The significance of the present work is, in particular, in discovering the interconnection between the developed kinematic models for the continuous media with defects and their role in the hierarchy of multi-scale modeling.

The outline of the paper is as follows. In Section 2, the Cauchy continuous media with and without defects and the scalar potential are introduced and discussed. In Section 3, the Papkovich-Cosserat media are defined, the vector potential and vector field of defects are analyzed. The Saint-Venant continuous media with and without defects, tensor potential and tensor field of defects are introduced and investigated in the Section 4. The N-th level media models and tensor potential of N-th rank are defined and considered in the Section 5. That is followed by the classification of the fields of defects developed in the Section 6. Section 7 provides the conclusions for the present study.

2.1. THE CAUCHY CONTINUOUS MEDIA MODEL. SCALAR POTENTIAL

2.1.1. Defectless Cauchy Medium

Let us denote the continuous vector of displacements in the domain V by $R_i(M)$. And let us establish the conditions under which displacement vector R_i can be represented as a gradient of a scalar function $D^0(M)$, i.e.,

$$R_i = \frac{\partial D^0}{\partial x_i} \ .$$
(2.1)

For an arbitrary point M_0 and a variable point M in the domain V, the scalar potential in Eq. (2.1) is determined in terms of the displacement vector R_i in the following way:

$$D^0(M) = D^0(M_0) + \int_{M_0}^{M} R_i dy_i$$
(2.2)

The condition of unique determination of the scalar function D^0 by means of the displacement vector R_i in arbitrary point M of the medium under study is equivalent to the condition of independence of the contour integral in Eq. (2.2) from the integration path:

$$\frac{\partial R_i}{\partial x_j} \Im_{ijk} = 0,$$ (2.3)

where $\Im_{ijk}$ is the permutation symbol.

Note that the vector of curls ω_k is defined by the formula

$$\omega_k = -\frac{1}{2} \frac{\partial R_i}{\partial x_j} \Im_{ijk}$$
.

Therefore, the necessary and sufficient condition of existence of the scalar function $D^0(M)$ in Eq. (2.2) can be interpreted as a condition of absence of curls ω_k:

$$\omega_k = 0.$$ (2.4)

Eq. (2.4) defines the "defectless Cauchy continuous medium" as such a medium in which curls are absent and the displacement field has a scalar potential.

It is well known that for a formal mathematical description of a continuous medium in the framework of a variational approach [Fleck, N.A., and Hutchinson, J.W., (2001), Mindlin R.D. (1964)] it is sufficient to define a list of continuous arguments. For the defectless Cauchy medium the scalar potential $D^0(M)$ can be chosen as a generalized coordinate. Therefore the defectless Cauchy medium is a model with one degree of freedom.

2.1.2. *Cauchy Continuous Medium with Defects*

As it was established above, the displacement field in the defectless Cauchy medium is defined as a gradient of a scalar field $D^0(M)$; the contour integral in Eq. (2.2) does not depend on the integration path; and vector of curls is zero. In other words, the displacement vector in the defectless Cauchy medium can be defined as a general solution of the homogeneous equation (2.3). That represents a formal property of the defectless Cauchy medium, that is equivalent to the absence of curls.

On the contrary to that, the Cauchy continuous medium with the field of defects is characterized by a presence of non-zero curls:

$$\frac{\partial R_i}{\partial x_j} \Im_{ijk} = -2\omega_k.$$ (2.5)

And in this case, the general solution of Eq. (2.5) for the displacement field will consist of two components:

$$R_i = \frac{\partial D^0}{\partial x_i} + D_i^1,$$ (2.6)

where

$$\frac{\partial D_i^1}{\partial x_j} \Im_{ijk} = -2\omega_k.$$ (2.7)

The first component in Eq. (2.6) is a general solution of the homogeneous equation (2.3), and it is the integrable part of displacements. The second component in Eq. (2.6) is a particular solution of Eq. (2.5), or Eq. (2.7). And therefore it defines a part of displacements that is related to the defectness of medium. Function D_i^1 unlike of function $\dfrac{\partial D^0}{\partial x_i}$, is non-integrable since the integrability condition for this function is not satisfied.

The following formal definition for the potential of displacement field can be given:

$$D = D^0 + D^1 \tag{2.8}$$

Function $D(M)$ in Eq. (2.8) defines the scalar field in the Cauchy medium. It is represented as a sum of $D^0(M)$ and some other scalar function $D^1(M)$ that is determined from the particular solution of the Eq. (2.7) $D_i^1(M)$ as follows:

$$D^1 = \int\limits_{M_0}^{M_x} D_i^1 dy_i \; . \tag{2.9}$$

Scalar field $D^1(M)$ in Eq. (2.8) defines a field of discontinuities (or jumps) of potential of displacement field, and it is determined from the non-integrable part of displacements D_i^1. Contour integral in Eq. (2.9) depends on the integration path. By definition, its value at any point M_o, $J^1(M_0) = \oint D_i^1 dy_i$ depends on a trajectory of integration.

The scalar function $D^1(M)$ is not differentiable in the common sense, otherwise it would satisfy the homogeneous equation (2.3). The generalized derivative of the function $D^1(M)$ can be formally defined as follows:

$$\frac{\partial D^1}{\partial x_i} = D_i^1 \; .$$

Let as define now the Cauchy continuous medium with defects as such that the curls $(-2\omega_k)$ are the sources of defects $D^1(M)$. Under the defects in the Cauchy model we will call the discontinuities of the scalar potential of displacement field. Such defects are defining the continuous field D_i^1 on which the field of defects J^1 is constructed.

The major feature of the above model of medium with defects is that there is no generation of new defects of the above-indicated type. In other words, the source of curls $\omega_k = -\dfrac{1}{2}\dfrac{\partial D_i^1}{\partial x_j}\Im_{ijk}$ is absent. The following differential law of conservation takes place:

$$\frac{\partial(-2\omega_k)}{\partial x_k} = 0$$

This law can be represented in the integral form:

$$\oiint \omega_k n_k dF = 0$$

Later expression demonstrates the absence of generation of defects in the considered representative volume of the medium. Let us note that for the Cauchy medium with defects the generalized coordinates are continuous functions

$D^0(M)$ and $D_i^1(M)$. They can serve as the arguments of the corresponding functional. Therefore, the Cauchy medium with defects is a model with four degrees of freedom. In this case, the gradients of the generalized coordinates $\dfrac{\partial D^0}{\partial x_i}$ and $\dfrac{\partial D_i^1}{\partial x_j}$ are the generalized velocities of the corresponding kinematic state. It can be also observed that in the particular case when $D^0 = 0$, the Cauchy medium model coincides with the classical model of theory of elasticity, in which the generalized coordinates in the variational description are the components of the displacement vector $R_i \equiv D_i^1$, since $D^0(M) \equiv 0$.

2.2. THE PAPKOVICH - COSSERAT CONTINUOUS MEDIA MODEL. VECTOR POTENTIAL, VECTOR FIELD OF DEFECTS

2.2.1 Defectless Papkovich Medium

Consider a continuous medium with a non-symmetrical distortion tensor $d^0{}_{in}$ defined as a gradient of some continuous vector field r_i^0

$$d^0{}_{ij} = \frac{\partial r_i^0}{\partial x_j} \ .$$
(2.10)

It is well known that a tensor of a second rank $d^0{}_{in}$ can be resolved as follows:

$$d^0{}_{in} = \gamma^0{}_{in} + \frac{1}{3}\theta^0 \delta_{in} - \omega^0{}_k \Im_{ink} \ ,$$

where term $\gamma^0{}_{in} + \dfrac{1}{3}\theta^0 \delta_{in}$ defines a symmetrical part of the tensor $d^0{}_{in}$, and the term $\omega^0{}_k \Im_{ink}$ defines its anti-symmetric part; $\gamma^0{}_{in}$ is a deviator tensor or deviatoric strain; $\dfrac{1}{3}\theta^0 \delta_{in}$ is a spherical tensor; and θ^0 is an amplitude of the spherical tensor.

Consider now the homogeneous Papkovich equations that represent the existence conditions for the curvilinear integral in definition of the displacement vector

$$(d^0{}_{in})_{,m} \Im_{nmj} = 0 \ .$$
(2.11)

Eq. (2.11) is the existence criterion for the vector potential of the distortion tensor $d^0{}_{in} = \gamma^0{}_{in} + \dfrac{1}{3}\theta^0 \delta_{in} - \omega^0{}_k \Im_{ink}$. This vector potential r_i^0 is the displacement vector. There is a full analogy here with the case of scalar potential for the displacement vector R_i in the defectless Cauchy continuous medium.

We will define a defectless Papkovich medium as a medium with a continuous vector potential of the distortion tensor of deformation. In the defectless Papkovich medium the displacement vector is continuous and the distortion tensor $d^0{}_{in}$ is a general solution of the homogeneous equation (11). That corresponds to the case of absence of defects – dislocations. In the general case, the defectless Papkovich medium is the Cauchy medium with a continuous

displacement vector. Similarly to the Cauchy medium, the scalar defects are present here since the continuous displacement vector contains both the integrable part $\dfrac{\partial D^0}{\partial x_i}$, as well as a continuous but non-integrable in the sense of Eq. (2.2) part (D_i^1):

$$r_i^0 = \frac{\partial D^0}{\partial x_i} + D_i^1$$

In particular, in the case $D^0 \equiv 0$, the defectless Papkovich medium model coincides with the model of classical theory of elasticity. In this case the displacement vector is continuous, but generally non-integrable in the sense of Eq. (2.2), i.e., the scalar potential for the displacement field does not exist. In the more special particular case $D_i^1 = 0$ the defectless Papkovich medium is completely defectless since both, the dislocations (the vector defects) and the scalar defects are absent in this case.

2.2.2 Papkovich-Cosserat Continuous Medium with Defects

In the defectless homogeneous Papkovich medium the distortion tensor is integrable since it can be determined from the Eq. (2.10) by means of integration over the displacement vector, and the integrability conditions (2.11) are fulfilled. On the contrary to that, for the Papkovich-Cosserat medium with defects, the distortion tensor of deformation d_{ij} can be represented in the general case as a sum of two parts: the integrable part (d_{ij}^0), and the non-integrable part (D_{ij}^2),

$$d_{ij} = d_{ij}^0 + D_{ij}^2 \ . \tag{2.12}$$

where $\quad d_{ij}^0 = \gamma^0{}_{ij} + \dfrac{1}{3}\theta^0 \delta_{ij} - \omega^0{}_k \Im_{ijk} \ .$

Note that Eq. (2.12) is analogous to the Eq. (2.6) written for the Cauchy medium displacement vector.

Following the common procedure let us consider now the non-homogeneous Papkovich equations

$$(d_{in})_{,m} \Im_{nmj} = (\gamma_{in} + \frac{1}{3}\theta\delta_{in} - \omega_k \Im_{ink})_{,m} \Im_{nmj} = \Xi_{ij} \ . \tag{2.13}$$

Here $(d_{in})_{,m} = (\gamma_{in} + \dfrac{1}{3}\theta\delta_{in} - \omega_k \Im_{ink})_{,m}$ is the general tensor filed of curvatures of the model under consideration.

On account of relations (2.11) and (2.12), Eq. (2.13) yields

$$(D_{in}^2)_{,m} \Im_{nmj} = \Xi_{ij} \tag{2.14}$$

The continuous tensor of "inconsistencies" Ξ_{ij} defines the non-homogeneity of the Papkovich relations. The following differential conservation law is valid for this tensor:

$$\frac{\partial \Xi_{ij}}{\partial x_j} = 0 \ .$$

In order to prove that, we will first apply the divergence operator to the left and right sides of equation (2.13)

$$\frac{\partial}{\partial x_j}(\frac{\partial d_{in}}{\partial x_m}\Im_{nmj}) = \frac{\partial \Xi_{ij}}{\partial x_j}$$

In the left-hand side of this expression we have $\frac{\partial}{\partial x_j}\left(\frac{\partial d_{in}}{\partial x_m}\Im_{nmj}\right) = \frac{\partial^2 d_{in}}{\partial x_j \partial x_m}\Im_{nmj}$. Evidently, the term $\frac{\partial^2 d_{in}}{\partial x_j \partial x_m}$ is

symmetrical tensor with respect to indexes j and m. From the other side, by definition the permutation symbol $\Im_{nmj}$ is

anti-symmetric tensor for the same pair of indexes. Therefore the convolution of tensors $\frac{\partial^2 d_{in}}{\partial x_j \partial x_m}$ and $\Im_{nmj}$ in indexes

j and m is equal to zero, which proves the above conservation law.

The solution of the above non-homogeneous Papkovich equation (2.13) with respect to γ_{ij}, ω_k and θ can be

represented as a sum of the following general solution of the homogeneous Papkovich equation for γ_{ij}^0, ω_k^0, θ^0 :

$$\gamma_{ij}^0 = \frac{1}{2}\frac{\partial r_i^0}{\partial x_j} + \frac{1}{2}\frac{\partial r_j^0}{\partial x_i} - \frac{1}{3}\frac{\partial r_k^0}{\partial x_k}\delta_{ij}, \quad \omega_k^0 = -\frac{1}{2}\frac{\partial r_i^0}{\partial x_j}\Im_{ijk}, \quad \theta^0 = \frac{\partial r_k^0}{\partial x_k},$$

and the partial solution of the non-homogeneous Papkovich equation (2.13) denoted by γ_{ij}^Ξ, ω_k^Ξ and θ^Ξ. As a result,

we can write

$$\gamma_{ij} = \gamma_{ij}^0 + \gamma_{ij}^\Xi = (\frac{1}{2}\frac{\partial r_i^0}{\partial x_j} + \frac{1}{2}\frac{\partial r_j^0}{\partial x_i} - \frac{1}{2}\frac{\partial r_k^0}{\partial x_k}\delta_{ij}) + \gamma_{ij}^\Xi,$$

$$\omega_k = \omega_k^0 + \omega_k^\Xi = (-\frac{1}{2}\frac{\partial r_i^0}{\partial x_j}\Im_{ijk}) + \omega_k^\Xi$$

$$\theta = \theta^0 + \theta^\Xi = (\frac{\partial r_k^0}{\partial x_k}) + \theta^\Xi$$

and

$$d_{ij} = d_{ij}^0 + d_{ij}^\Xi, \qquad d_{ij}^\Xi = \gamma_{in}^\Xi + \frac{1}{3}\theta^\Xi\delta_{in} - \omega_k^\Xi\Im_{ink}.$$

The partial solutions of non-homogeneous Papkovich equation with respect to distortion tensor d_{ij}^Ξ, or with respect to

γ_{ij}^Ξ, ω_k^Ξ и θ^Ξ, which is the same, can be considered as the degrees of freedom that are independent of displacements.

For the full analogy with the earlier considered case, the distortion tensor $d_{ij}^\Xi \equiv D_{ij}^2 = \gamma_{in}^\Xi + \frac{1}{3}\theta^\Xi\delta_{in} - \omega_k^\Xi\Im_{ink}$ can be

considered as "generalized displacements"("plastic distortion" [De Wit R., (1973)]. Since the "inconsistencies" tensor

Ξ_{ij} is related to the "generalized displacements" through the following relations:

$$\Xi_{ij} = (\gamma_{in}^\Xi + \frac{1}{3}\theta^\Xi\delta_{in} - \omega_k^\Xi\Im_{ink})_{,m}\Im_{nmj} \qquad\qquad (2.15)$$

it can be interpreted as the tensor of "generalized strains" for these "generalized displacements".

Using the Cosserat terminology, we can call $\omega_k^0 = -\dfrac{1}{2}\dfrac{\partial r_i^0}{\partial x_j}\mathcal{I}_{ijk}$ as the restricted curl, and ω_k^Ξ - as a free curl or spin

("plastic curl" [De Wit R., (1973)]). Analogously we will call γ_{ij}^0 and θ^0 as restricted strains and γ_{ij}^Ξ, θ^Ξ as the free strains.

Eqs. (2.11) - (2.15) describe the kinematics of continuous media with defects of a dislocation type. These relations lead to the following conclusions:

1. The fields of free strains and spins cannot be uniform because in that case $\Xi_{ij} = 0$.

2. The fields of spins have the sources.

Indeed, we can show by making use of Eq. (2.15) that the field of spins is not a vorticity field. By applying convolution of left and right sides of Eq. (2.15) with δ_{ij} we obtain

$$\frac{\partial \omega_k^\Xi}{\partial x_k} = -\frac{1}{2}\Xi_{kk} \neq 0.$$

At the same time, the following equality takes place for the vortex fields with the vector of curls ω_k^0:

$$\frac{\partial \omega_k^0}{\partial x_k} = 0.$$

Let us call the models of continuous media with vector potential as the Papkovich-Cosserat media. The kinematics of such media has the following structure:

• The displacement field R_i represents a superposition of the following two fields: the continuous field r_i^0 and the field of displacement jumps or discontinuities D_i^2, i.e.,

$$D_i = r_i^0 + D_i^2 = (\frac{\partial D^0}{\partial x_i} + D_i^1) + D_i^2; \quad D_i^2 = \int_{M_0}^{M} D_{ij}^2 dy_j,$$

$$(D_{ij}^2 = \gamma_{ij}^\Xi + \frac{1}{3}\theta^\Xi \delta_{ij} - \omega_k^\Xi \mathcal{I}_{ijk}).$$

The classical displacements R_i are determined by the continuous part only, and they can be represented as follows: $R_i \equiv r_i^0$, $r_i^0 = \dfrac{\partial D^0}{\partial x_i} + D_i^1$.

Unlike of the continuous displacement field R_i, the vector field D_i defines the complete displacement field with account of dislocations (jumps). The defective displacements D_i are the sum of the classical displacements R_i, ($R_i \equiv r_i^0$) and the dislocations D_i^2.

- The field of displacement jumps D_i^2 can be expressed in terms of fields of free strains and spins by means of the following relation (analogous to the Chesaro formula):

$$D_i^2 = \int\limits_{M_0}^{M} D_{ij}^2 dy_j = \int\limits_{M_0}^{M_x} (\gamma_{ij}^{\Xi} + \frac{1}{3}\theta^{\Xi}\delta_{ij} - \omega_k^{\Xi}\Im_{ijk})dy_j \, ;$$

- Tensor of "inconsistencies" of displacements Ξ_{ij} is the tensor of dislocations, see [De Wit R., (1973)].

- The following differential conservation law takes place for the dislocation tensor:

$$\frac{\partial \Xi_{ij}}{\partial x_j} = 0 \, .$$

- This conservation law can be represented in the integral form as follows:

$$\iiint \frac{\partial \Xi_{ij}}{\partial x_j} dV = \oiint \Xi_{ij} n_j dF = 0$$

- The flux of tensor Ξ_{ij} through the plane of planar contour can be chosen as a measure of defects (dislocations) [4-6]:

$$\iint\limits_{+} \Xi_{ij} n_j dF = n_j \iint\limits_{0} \Xi_{ij} dF \, ,$$

where F is a closed surface stretched over the planar contour.

In other words, the flux of tensor Ξ_{ij} through the arbitrary surface stretched over the chosen planar contour is invariant. Therefore, it can be chosen as a measure of dislocations.

It is important to note that one of major features of the Papkovich-Cosserat continuous media is that it is not possible to describe the birth or disappearance of dislocations in the framework of these media models because $\oiint \Xi_{ij} n_j dF = 0$. Therefore, the defects associated with the conserved dislocation tensor Ξ_{ij} cannot be born or disappear, [Kroner E(1982), De Wit R., (1973)].

There are two levels of defects in the Papkovich-Cosserat media. The defects of the first rank are related to the conserved dislocations and they are defined by the formula

$$D_i^2 = \int\limits_{M_0}^{M} D_{ij}^2 dy_j$$

The zero-rank defects are associated with the two types of scalar defects. First type is related to the conserved scalar defects defined by a scalar field (2.9), $D^1 = \int\limits_{M_0}^{M} D_i^1 dy_i$, see the Cauchy media. The second type is related to such scalar defects that have the conserved dislocations as their sources. These later scalar defects are described by the field

$D^2 = \int\limits_{M_0}^{M} D_i^2 dy_i$, where $D_i^2 = \int\limits_{M_0}^{M} D_{ij}^2 dy_j$. They, evidently can be born or can disappear because as it was shown

earlier, the fields of spins have the sources, $\dfrac{\partial \omega_k}{\partial x_k} = \dfrac{\partial \omega_k^0}{\partial x_k} + \dfrac{\partial \omega_k^\Xi}{\partial x_k} = \dfrac{\partial \omega_k^\Xi}{\partial x_k} \neq 0$.

Note that under the generalized defects we mean the discontinuous part of the considered kinematic characteristics of the medium. The corresponding field is called the defectness field.

In the general case of the Papkovich-Cosserat media the defectness fields of different ranks (scalar, vector and tensor) are defined by the following relations:

- Defectness field of a zero-rank (scalar):

$$D = (D^0) + D^1 + D^2, \quad D^1 = \int\limits_{M_0}^{M_x} D_i^1 dy_i, \quad D^2 = \int\limits_{M_0}^{M_x} D_i^2 dy_i, \quad D_i^2 = \int\limits_{M_0}^{M_x} D_{ij}^2 dy_j;$$

- Defectness field of a first-rank (vector):

$$D_i = (\dfrac{\partial D^0}{\partial x_i} + D_i^1) + D_i^2, \quad D_i^2 = \int\limits_{M_0}^{M_x} D_{ij}^2 dy_j;$$

- A tensor characteristic of the Papkovich-Cosserat media is the tensor field

$$D_{ij} = \dfrac{\partial}{\partial x_j}(\dfrac{\partial D^0}{\partial x_i} + D_i^1) + D_{ij}^2, \quad D_{ij} \equiv d_{ij}, \quad (D_{ij}^2 = d_{ij}^\Xi = \gamma_{ij}^\Xi + \dfrac{1}{3}\theta^\Xi \delta_{ij} - \omega_k^\Xi \Im_{ijk}),$$

here d_{ij} is a distortion tensor in the Papkovich media.

However, the tensor field D_{ij} is not a defectness field of a second rank since it does not contain a discontinuous

part. First component in the above expression for D_{ij} is a continuous and integrable part of the tensor field,

$$d_{ij}^0 = \dfrac{\partial}{\partial x_j}(\dfrac{\partial D^0}{\partial x_i} + D_i^1), \quad (d_{ij}^0)_{,m} \Im_{nmj} = 0.$$

The second component D_{ij}^2 in the above expression is a continuous non-integrable part, see Eq. (2.14). It should be

noted for a comparison that among the characteristics of the Cauchy medium, apart of a scalar field of defects

$D = D^0 + D^1$ (where D^1 is a discontinuous component), is also a vector field $D_i = \dfrac{\partial D^0}{\partial x_i} + D_i^1$ that is not a

defectness field.

The Papkovich-Cosserat media allow two different types of the sources of defects:

1. The sources of a second rank (sources of dislocations) T_{ij}^2 are defined by a tensor $T_{ij} \equiv T_{ij}^2 = \Xi_{ij}$

$$T_{ij} \equiv T_{ij}^2 = \dfrac{\partial D_{in}^2}{\partial x_m}\Im_{nmj} = \dfrac{\partial(\gamma_{in}^\Xi + \dfrac{1}{3}\theta^\Xi \delta_{in} - \omega_k^\Xi \Im_{ink})}{\partial x_m}\Im_{nmj}.$$

2. The sources of a first rank (sources of the scalar defects) T_i are defined by the spins, i.e., by a vector which can be obtained through the convolution of the total tensor of deformations D_{nm} with the tensor $\Im_{nmj}$ in indexes n and m:

$$T_i \equiv T_i^1 = (\frac{\partial}{\partial x_m}(R_n) + D_{nm}^2)\Im_{nmi}, \quad (R_i \equiv r_i^0, \quad r_i^0 = \frac{\partial D^0}{\partial x_i} + D_i^1)$$

Since $\dfrac{\partial}{\partial x_m}(\dfrac{\partial D^0}{\partial x_n})\Im_{nmi} \equiv 0$, we get

$$T_i = (T_i)_1 + (T_i)_2 = \frac{\partial D_n^1}{\partial x_m}\Im_{nmi} + D_{nm}^2\Im_{nmi},$$

$$(T_i)_1 = \frac{\partial D_n^1}{\partial x_m}\Im_{nmi} = \frac{\partial R_n}{\partial x_m}\Im_{nmi}, \quad (T_i)_2 = D_{nm}^2\Im_{nmi} = -2\omega_i^{\Xi}.$$

The sources of defects $(T_i)_1$ are related only to the conserved scalar defects D^1, since the vector of restricted curls $(T_i)_1 = \dfrac{\partial R_n}{\partial x_m}\Im_{nmi}$ in the general case is not zero, see the Cauchy media. These sources of defects satisfy the conservation condition:

$$div((T_i)_1) = \frac{\partial(T_i)_1}{\partial x_i} = \frac{\partial}{\partial x_i}(\frac{\partial R_n}{\partial x_m}\Im_{nmi}) = 0.$$

For the sources of defects $(T_i)_2$ the conservation condition is not satisfied:

$$\frac{\partial(T_i)_2}{\partial x_i} = \frac{\partial D_{nm}^2}{\partial x_i}\Im_{nmi} = T_{ii} \neq 0, \quad (T_{ij} \equiv T_{ij}^2 = \Xi_{ij}, \quad \frac{\partial \omega_k^{\Xi}}{\partial x_k} = -\frac{1}{2}\Xi_{kk} \neq 0).$$

Therefore, these sources of the scalar defects can be born and can disappear.

2.3. THE SAINT-VENANT CONTINUOUS MEDIA MODEL. TENSOR POTENTIAL, TENSOR FIELD OF DEFECTS.

In order to construct the models that will allow the birth and disappearance of dislocations, it is necessary to develop the kinematic continuous media models of a higher order. We will call them the Saint-Venant continuous media.

2.3.1. Defectless Saint-Venant Medium

Let us introduce the curvatures: $\gamma_{ijn} = \dfrac{\partial \gamma_{ij}}{\partial x_k}$, $\theta_j = \dfrac{\partial \theta}{\partial x_j}$, $\omega_{ij} = \dfrac{\partial \omega_i}{\partial x_j}$. These tensors formally define a tensor of curvatures of a third order, [Fleck, N.A., and Hutchinson, J.W.(1993, 1997,2001); Gao, H., Huang, Y., Nix, W.D., and Hutchinson, J.W., (1999); Mindlin R.D (1964], $D_{ijn}(\omega_{in}, \theta_n, \gamma_{ijn})$, which is a derivative of the distortion tensor, i.e.,

$$(d_{in})_{,j} = D_{ijn} \ , \qquad d_{ij} = d_{ij}(M_0) + \int_{M_0}^{M} D_{ijn} dx_n \qquad\qquad (2.16)$$

Here d_{in} is the distortion tensor, and $D_{ijn} = \gamma_{ijn} + \frac{1}{3}\theta_n \delta_{ij} - \omega_{qn} \Im_{ijq}$, also $\gamma_{ijn} = \gamma_{jin}$, $\gamma_{kkn} = 0$.

Following the common procedure let us consider the conditions of integrability for the distortion tensor

$$\frac{\partial D_{ijn}}{\partial x_m} \Im_{nmk} = 0 \qquad\qquad (2.17)$$

Eq. (2.17) represents the existence conditions for the contour integral (or integrability conditions) in the definition of distortion tensor d_{in} in terms of tensor of curvatures D_{ijn}. Let us call relations (2.17) as the generalized Saint-Venant relations. The integrability conditions represent the existence criterion for the tensor potential of the tensor of curvatures $D_{ijn} = (d_{in})_{,j}$. The role of this tensor potential of a second rank is played by the distortion tensor d_{in}. There is a full analogy here with the case of scalar potential for the vector R_i (the above Cauchy continuous media model) as well as with the case of vector potential for the distortion tensor (the above Papkovich-Cosserat continuous media model).

Let us now prove that Eq. (2.17) is a generalization of the well-known Saint Venant's compatibility equations. First we will rewrite the Eq. (2.17) as follows:

$$\frac{\partial(\gamma_{ijn} + \frac{1}{3}\theta_n\delta_{ij} - \omega_{qn}\Im_{ijq})}{\partial x_m}\Im_{nmk} = \frac{\partial\gamma_{ijn}}{\partial x_m}\Im_{nmk} + \frac{\partial\frac{1}{3}\theta_n\delta_{ij}}{\partial x_m}\Im_{nmk} - \frac{\partial\omega_{qn}\Im_{ijq}}{\partial x_m}\Im_{nmk} = 0 \qquad (2.18)$$

Allocate in the tensor equation (2.18) the anti-symmetric in indexes i, j part. Since first two terms are symmetric in these indexes, we get

$$\frac{\partial\omega_{qn}\Im_{ijq}}{\partial x_m}\Im_{nmk} = 0$$

This equation represents an existence condition for the vector potential ω_i for curvatures ω_{ij}, ($\omega_{ij} = \frac{\partial\omega_i}{\partial x_j}$).

From the other side, we know that the integrability, and therefore the existence conditions of the vector of spins is given by Saint-Venant's equations. The above equation coincides with the known Saint-Venant's equations if $\frac{\partial\omega_i}{\partial x_j}$ is expressed in terms of the derivatives of the components of tensor of deformations. Consequently, Eq. (2.17) contains the Saint-Venant equations as a particular case.

It is easy to obtain the following generalized Saint-Venant's equation (i.e., the compatibility equation) for curvatures θ_n, from the Eq. (2.18) by means of symmetrization and allocation of the spherical part in indexes i,j:

$$\frac{\partial \theta_n}{\partial x_m} \Im_{nmk} = 0,$$

as well as the generalized Saint-Venant's equation for the curvatures γ_{ijn}

$$\frac{\partial \gamma_{ijn}}{\partial x_m} \Im_{nmk} = 0.$$

The above generalized compatibility equations are new. They probably fell out of attention of researchers in earlier studies because in the framework of the classical theory there was no need to define the deformations γ_{ij} and θ in terms of the curvatures γ_{ijn}, θ_j. The generalized compatibility equations represent the existence conditions for the potentials γ_{ij} and θ for the corresponding curvatures $\gamma_{ijn} = \dfrac{\partial \gamma_{ij}}{\partial x_n}$, $\theta_j = \dfrac{\partial \theta}{\partial x_j}$. We will call the media under study as the Saint-Venant continuous media precisely because the generalized Saint-Venant's equations (2.17) lay the basis for the analysis of their kinematics. In the defectless Saint-Venant media the tensor of curvatures D_{ijn} is integrable in the sense of Eq. (2.16). The distortion tensor d_{ij} can be determined uniquely from D_{ijn}, since the integrability conditions (2.17) for D_{ijn} are fulfilled. In the defectless Saint-Venant's media the distortion tensor d_{in} is continuous and the tensor of curvatures D_{ijn} is a general solution of the homogeneous equation (2.17).

Note that in the defectless Saint-Venant media the generalized disclinations are absent. In these media, similarly to the Papkovich-Cosserat media with defects, only the conserved dislocations D_i^2 can be present (the defects of a first rank), as well as two types of scalar defects D^1 and D^2; D^1 being the conserved scalar defects, and D^2 - the scalar defects that can be born and disappear on the conserved dislocations D_i^2.

2.3.2. Saint-Venant Continuous Medium with Defects – Generalized Disclinations

In the general case when the integrability conditions (2.17) are not fulfilled, the following non-homogeneous equation takes place:

$$\frac{\partial D_{ijn}}{\partial x_m} \Im_{nmk} = \Omega_{ijk} \tag{2.19}$$

Here Ω_{ijk} is the continuous tensor of "inconsistencies" given by the relation

$$\Omega_{ijk} = \Gamma_{ijk} + \frac{1}{3}\Theta_k \delta_{ij} - \Omega_{qk}\Im_{ijq} \tag{2.20}$$

Tensor Ω_{ijk} is a reason of non-homogeneity of the generalized Saint-Venant conditions (2.19).

Alternating and balancing Eqs. (2.19) and (2.20) with respect to the first two subscripts, we obtain

$$\frac{\partial \omega_{in}}{\partial x_m} \Im_{nmj} = \Omega_{ij}, \qquad (2.21)$$

$$\frac{\partial \theta_n}{\partial x_m} \Im_{nmj} = \Theta_j, \qquad (2.22)$$

$$\frac{\partial \gamma_{ijn}}{\partial x_m} \Im_{nmk} = \Gamma_{ijk} \qquad (2.23)$$

By continuing and generalizing the common algorithm we can assume that the curvature fields are integrable or non-integrable depending on equality or non-equality to zero of the corresponding tensors of "inconsistencies" Ω_{ij}, Θ_j and Γ_{ijk}. Let us assume that the tensors of "inconsistencies" [De Wit R(1973)] Ω_{ij}, Θ_j and Γ_{ijk} are not equal to zero. By the virtue of Eq. (2.20) these tensors satisfy the following differential conservation laws:

$$\frac{\partial \Omega_{ij}}{\partial x_j} = 0, \qquad \frac{\partial \Theta_j}{\partial x_j} = 0, \qquad \frac{\partial \Gamma_{ijk}}{\partial x_k} = 0$$

The fields of full curls can be divided into two parts: continuous part and a part of jumps or discontinuities (spins),

$$\omega_i = (-\frac{1}{2}\frac{\partial r_n^0}{\partial x_m} \Im_{nmi} + \omega_i^\Xi) + \omega_i^\Omega$$

$$\omega_{ij} = (-\frac{1}{2}\frac{\partial^2 r_n^0}{\partial x_j \partial x_m} \Im_{nmi} + \frac{\partial \omega_i^\Xi}{\partial x_j} + \omega_{ij}^\Omega)$$

Here $\omega_{ij}^{\Omega 0} = -\frac{1}{2}\frac{\partial^2 r_n^0}{\partial x_j \partial x_m} \Im_{nmi} + \frac{\partial \omega_i^\Xi}{\partial x_j}$ can be interpreted as the general solution of the homogeneous Saint-Venant's equation (2.21)

$$\frac{\partial \omega_{in}^{\Omega 0}}{\partial x_m} \Im_{nmj} = 0,$$

and field of jumps ω_{ij}^Ω, that can be interpreted as a partial solution of the non-homogeneous Saint-Venant's equation (2.21)

$$\frac{\partial \omega_{in}^\Omega}{\partial x_m} \Im_{nmj} = \Omega_{ij} (= -\frac{1}{2}\Omega_{nmj} \Im_{nmj}).$$

Analogously the strain fields can be also divided into two parts: continuous part and a part of jumps or discontinuities,

$$\theta = (\frac{\partial r_k^0}{\partial x_k} + \theta^\Xi) + \theta^\Omega, \quad \theta_j = (\frac{\partial^2 r_k^0}{\partial x_j \partial x_k} + \frac{\partial \theta^\Xi}{\partial x_j} + \theta_j^\Omega)$$

and

$$\gamma_{ij} = \left(\frac{1}{2}\frac{\partial r_i^0}{\partial x_j} + \frac{1}{2}\frac{\partial r_j^0}{\partial x_i} - \frac{1}{2}\frac{\partial r_k^0}{\partial x_k}\delta_{ij} + \gamma_{ij}^{\Xi}\right) + \gamma_{ij}^{\Omega}$$

$$\gamma_{ijk} = \left(\frac{1}{2}\frac{\partial^2 r_i^0}{\partial x_k \partial x_j} + \frac{1}{2}\frac{\partial^2 r_j^0}{\partial x_k \partial x_i} - \frac{1}{2}\frac{\partial^2 r_q^0}{\partial x_k \partial x_q}\delta_{ij} + \frac{\partial \gamma_{ij}^{\Xi}}{\partial x_k} + \gamma_{ijk}^{\Omega}\right)$$

Here $\theta_i^{\Omega 0} = \frac{\partial^2 r_k^0}{\partial x_j \partial x_k} + \frac{\partial \theta^{\Xi}}{\partial x_j}$ is the general solution of the homogeneous equation (2.22)

$$\frac{\partial \theta_n^{\Omega 0}}{\partial x_m}\Im_{nmj} = 0,$$

and field of jumps θ_i^{Ω} is a partial solution of the non-homogeneous equation (2.22)

$$\frac{\partial \theta_n^{\Omega}}{\partial x_m}\Im_{nmj} = \Theta_j (= \Omega_{nmj}\delta_{nm}).$$

Correspondingly, $\gamma_{ijk}^{\Omega 0} = \frac{1}{2}\frac{\partial^2 r_i^0}{\partial x_k \partial x_j} + \frac{1}{2}\frac{\partial^2 r_j^0}{\partial x_k \partial x_i} - \frac{1}{2}\frac{\partial^2 r_q^0}{\partial x_k \partial x_q}\delta_{ij} + \frac{\partial \gamma_{ij}^{\Xi}}{\partial x_k}$ can be interpreted as the general solution of

the homogeneous equation (2.23)

$$\frac{\partial \gamma_{ijn}^{\Omega 0}}{\partial x_m}\Im_{nmk} = 0,$$

and field of jumps γ_{ijk}^{Ω} can be interpreted as a partial solution of the non-homogeneous Eq. (2.23)

$$\frac{\partial \gamma_{ijn}^{\Omega}}{\partial x_m}\Im_{nmk} = \Gamma_{ijk} \left(= \frac{1}{2}\Omega_{ijk} + \frac{1}{2}\Omega_{ijk} - \frac{1}{3}\Omega_{nmk}\delta_{ij}\right).$$

As a result, the particular solution of the Eq. (2.19): D_{ijk}^3 can be determined:

$$\frac{\partial D_{ijn}^3}{\partial x_m}\Im_{nmk} = \Omega_{ijk}, \qquad D_{ijk}^3 = \gamma_{ijk}^{\Omega} + \frac{1}{3}\theta_k^{\Omega}\delta_{ij} - \omega_{qk}^{\Omega}\Im_{ijq}.$$

Note that in the Saint-Venant media it is possible to define a tensor field of a third rank:

$$D_{ijk} = \frac{\partial d_{ij}^0}{\partial x_k} + D_{ijk}^3 = \frac{\partial^2 r_i^0}{\partial x_k \partial x_j} + \frac{\partial d_{ij}^{\Xi}}{\partial x_k} + D_{ijk}^3 = \left[\frac{\partial^2}{\partial x_k \partial x_j}\left(\frac{\partial D_i^0}{\partial x_i} + D_i^1\right) + \frac{\partial D_{ij}^2}{\partial x_k}\right] + D_{ijk}^3 =$$

$$= \frac{\partial}{\partial x_k}\left[\frac{\partial}{\partial x_j}\left(\frac{\partial D_i^0}{\partial x_i} + D_i^1\right) + D_{ij}^2\right] + D_{ijk}^3, \qquad D_{ijk} \equiv (d_{ik})_{,j}, \qquad (D_{ij}^2 = d_{ij}^{\Xi} = \gamma_{ij}^{\Xi} + \frac{1}{3}\theta^{\Xi}\delta_{ij} - \omega_k^{\Xi}\Im_{ijk},$$

$$D_{ijk}^3 = \gamma_{ijk}^{\Omega} + \frac{1}{3}\theta_k^{\Omega}\delta_{ij} - \omega_{qk}^{\Omega}\Im_{ijq}).$$

Let us call the defectness field such a field that contains not only a continuous part but also a field of defects. Tensor field D_{ijk} is not a defectness field, similarly to the fact that tensor field of a second rank D_{ij} is not a defectness field in the Papkovich-Cosserat media of a lower level.

The defective fields of different ranks (scalar, vector and tensor) in the Saint-Venant media are defined by the following relations:

- Defectness field of a zero rank (scalar):

$$D = (D^0) + D^1 + D^2 + D^3,$$

$$D^1 = \int_{M_0}^{M_x} D_i^1 dy_i, \quad D^2 = \int_{M_0}^{M_x} D_i^2 dy_i, \quad D_i^2 = \int_{M_0}^{M_x} D_{ij}^2 dy_j,$$

$$D^3 = \int_{M_0}^{M_x} D_i^3 dy_i, \quad D_i^3 = \int_{M_0}^{M_x} D_{ij}^3 dy_j, \quad D_{ij}^3 = \int_{M_0}^{M_x} D_{ijk}^3 dy_k;$$

- Defectness field of a first rank (vector):

$$D_i = (\frac{\partial D^0}{\partial x_i} + D_i^1) + D_i^2 + D_i^3,$$

Defectness field of a first rank defines the general defectness field of displacements that includes all types of dislocations:

$$R_i = (r_i^0) + R_i^\Xi + R_i^\Omega, \quad D_i^2 \equiv R_i^\Xi = \int_M^M D_{ij}^2 dx_j, \quad D_i^3 \equiv R_i^\Omega = \int (\int D_{ijk}^3 dx_k) dx_j;$$

- Defectness field of a second rank

$$D_{ij} = \frac{\partial}{\partial x_j}(\frac{\partial D^0}{\partial x_i} + D_i^1) + D_{ij}^2 + D_{ij}^3.$$

In the scalar defectness field D the defects are defined by D^1, D^2, D^3; in the vector field D_i – by D_i^2, D_i^3. In the tensor defectness field D_{ij} the defects are defined by D_{ij}^3. There is a full analogy here with the case of Papkovich-Cosserat media.

The continuous parts in the right-hand sides of the defectness fields of the first and second ranks are shown in the brackets:

$$\begin{cases} \omega_k = (-\frac{1}{2}\frac{\partial r_i^0}{\partial x_j}\Im_{ijk} + \omega_k^\Xi) + \omega_k^\Omega \\ \theta = (\frac{\partial r_k^0}{\partial x_k} + \theta^\Xi) + \theta^\Omega \\ \gamma_{ij} = (\frac{1}{2}\frac{\partial r_i^0}{\partial x_j} + \frac{1}{2}\frac{\partial r_j^0}{\partial x_i} - \frac{1}{3}\frac{\partial r_k^0}{\partial x_k}\delta_{ij} + \gamma_{ij}^\Xi) + \gamma_{ij}^\Omega \end{cases}$$

$$\begin{cases} \omega_{ij} = -\dfrac{1}{2}\dfrac{\partial^2 r_n^0}{\partial x_j \partial x_m}\Im_{nmi} + \dfrac{\partial \omega_i^{\Xi}}{\partial x_j} + \omega_{ij}^{\Omega} \\[3mm] \theta_j = \dfrac{\partial^2 r_k^0}{\partial x_j \partial x_k} + \dfrac{\partial \theta^{\Xi}}{\partial x_j} + \theta_j^{\Omega} \\[3mm] \gamma_{ijk} = \dfrac{1}{2}\dfrac{\partial^2 r_i^0}{\partial x_k \partial x_j} + \dfrac{1}{2}\dfrac{\partial^2 r_j^0}{\partial x_k \partial x_i} - \dfrac{1}{2}\dfrac{\partial^2 r_q^0}{\partial x_k \partial x_q}\delta_{ij} + \dfrac{\partial \gamma_{ij}^{\Xi}}{\partial x_k} + \gamma_{ijk}^{\Omega} \end{cases}$$

Let us analyse now the sources of dislocations in the Saint-Venant medium. The sorces of dislocations are defined by the anti-symmetric part of the general tensor of curvatures (defectness tensor field) similarly to Eq. (2.5) for the Cauchy media and Eq. (2.13) for the Papkovich-Cosserat media. Then

$$(d_{in}),_m \Im_{nmj} = D_{inm}\Im_{nmj} = \gamma_{inm}\Im_{nmj} + \frac{1}{3}\theta_n\Im_{imj} - \omega_{km}\Im_{ink}\Im_{nmj} = \Xi_{ij} \qquad (2.24)$$

Note that the meaning of the density of dislocations Ξ_{ij} in the Eq. (2.24) differs in the general case from the meaning of the density of dislocations in the Papkovich-Cosserat medium, Eq. (2.14). Equality (2.24) allows to establish a structure of the density of dislocations in the Saint-Venant medium. We have

$$D_{ijk}\Im_{jkq} = \Im_{jkq}\frac{\partial}{\partial x_k}[\frac{\partial}{\partial x_j}(\frac{\partial D_i^0}{\partial x_i} + D_i^1) + D_{ij}^2] + D_{ijk}^3\Im_{jkq} = \frac{\partial D_{ij}^2}{\partial x_k}\Im_{jkq} + D_{ijk}^3\Im_{jkq},$$

$$D_{ij}^2 = d_{ij}^{\Xi} = \gamma_{ij}^{\Xi} + \frac{1}{3}\theta^{\Xi}\delta_{ij} - \omega_k^{\Xi}\Im_{ijk}, \qquad D_{ijk}^3 = \gamma_{ijk}^{\Omega} + \frac{1}{3}\theta_k^{\Omega}\delta_{ij} - \omega_{qk}^{\Omega}\Im_{ijq}.$$

Therefore, the quantity Ξ_{ij} from (2.24) can be written as

$$\Xi_{im} = \frac{\partial}{\partial x_n}(\gamma_{ij}^{\Xi} + \frac{1}{3}\theta^{\Xi}\delta_{ij} - \omega_k^{\Xi}\Im_{ijk})\Im_{jnm} + (\gamma_{ijn}^{\Omega} + \frac{1}{3}\theta_n^{\Omega}\delta_{ij} - \omega_{kn}^{\Omega}\Im_{ijk})\Im_{jnm} = \Xi_{im}^2 + \Xi_{im}^3,$$

where $\quad \Xi_{iq}^2 = \dfrac{\partial D_{ij}^2}{\partial x_k}\Im_{jkq}, \quad \Xi_{iq}^2 = D_{ijk}^3\Im_{jkq}.$

First component in the above equality for the density of dislocations Ξ_{iq} defines the conserved vector field of defects – dislocations, and it coincides with the density of dislocations in the Papkovich-Cosserat medium. The second component Ξ_{iq}^3 is related to the defects of a higher level, i.e., disclinations. This component of the density of dislocations defines the defects that can be born or disappear on the disclinations.

In order to use the unified notation for sources of defects (similarly to the Papkovich-Cosserat media case) we will adopt the following notation:

$$\Omega_{ijk} \equiv T_{ijk} = T_{ijk}^3,$$

$$\Xi_{ij} = \Xi_{ij}^2 + \Xi_{ij}^3 \equiv T_{ij} = (T_{ij})_2 + (T_{ij})_3$$

$$-2(\omega_i^0 + \omega_i^\Xi + \omega_i^\Omega) = T_i = (T_i)_1 + (T_i)_2 + (T_i)_3.$$

The above relation (2.24) represents the existence condition for the dislocations. Correspondingly, the right-hand sides of the Eq. (2.24) are the sources of dislocations. Therefore by means of nine non-homogeneous Papkovich equations we can express nine components of the tensor of curvatures ω_{ij} in terms of dislocation tensor Ξ_{ij}, vector θ_m and the remaining curvatures γ_{inm}:

$$\omega_{ji} = \Xi_{ij} - \frac{1}{2}\Xi_{kk}\delta_{ij} - \gamma_{inm}\Im_{nmj} - \frac{1}{3}\theta_m\Im_{imj}.$$

The existence conditions for jumps (or discontinuities) in full curls ω_i will follow from the generalized Saint-Venant's equations:

$$\frac{\partial \omega_{in}}{\partial x_m}\Im_{nmj} = \Omega_{ij}$$

or

$$\frac{\partial}{\partial x_m}[\Xi_{ni} - \frac{1}{2}\Xi_{kk}\delta_{ni} - \gamma_{npq}\Im_{pqi} - \frac{1}{3}\theta_k\Im_{nki}]\Im_{nmj} = \Omega_{ij} \qquad (2.25)$$

The existence conditions for jumps or discontinuities in the free change of volume after excluding the curvature tensor θ_k by means of Eq. (2.25) and on account of the generalized Saint Venant equations lead to the generalization of the differential conservation law for dislocations. Indeed, let us express explicitly the curvatures related to the free change of volume from (2.25)

$$\frac{1}{3}\frac{\partial \theta_j}{\partial x_i} = (\Omega_{ij} - \frac{1}{2}\Omega_{kk}\delta_{ij}) - \frac{\partial \Xi_{pk}}{\partial x_q}(\delta_{ki}\Im_{pqj} - \frac{1}{2}\delta_{ij}\Im_{pqk} - \frac{1}{2}\delta_{pk}\Im_{iqj}) +$$

$$+ \frac{\partial \gamma_{npq}}{\partial x_m}(\Im_{pqi}\Im_{nmj} - \frac{1}{2}\Im_{pqk}\Im_{nmk}\delta_{ij})$$

Substitute the obtained expressions for $\dfrac{\partial \theta_j}{\partial x_i}$ into the existence conditions for jumps (or discontinuities) in the free change of volume

$$\frac{\partial \theta_n}{\partial x_m}\Im_{nmj} = \Theta_j.$$

We obtain the following chain of equalities, making use of the equality (2.24):

$$\frac{1}{3}\frac{\partial \theta_j}{\partial x_i}\Im_{ji\mu} = \frac{1}{3}\Theta_\mu = \Omega_{ij}\Im_{ji\mu} - \frac{\partial \Xi_{pk}}{\partial x_q}(\Im_{pqj}\Im_{jk\mu} - \delta_{pk}\delta_{q\mu}) + \frac{\partial \gamma_{npq}}{\partial x_m}\Im_{pqi}\Im_{nmj}\Im_{ji\mu} =$$

$$= \Omega_{ij}\Im_{ji\mu} - \frac{\partial \Xi_{pk}}{\partial x_q}(\delta_{pk}\delta_{q\mu} - \delta_{p\mu}\delta_{qk} - \delta_{pk}\delta_{q\mu}) + \frac{\partial \gamma_{npq}}{\partial x_m}(\delta_{p\mu}\delta_{qj} - \delta_{pj}\delta_{q\mu})\Im_{nmj} =$$

$$= \Omega_{ij}\Im_{ji\mu} + \frac{\partial \Xi_{\mu k}}{\partial x_k} + \frac{\partial \gamma_{n\mu j}}{\partial x_m}\Im_{nmj} - \frac{\partial \gamma_{nj\mu}}{\partial x_m}\Im_{nmj} = \Omega_{ij}\Im_{ji\mu} + \frac{\partial \Xi_{\mu k}}{\partial x_k} - \Gamma_{n\mu n}$$

By moving the divergence of the dislocation tensor to the left-hand side, we will finally arrive to the following equation:

$$\frac{\partial \Xi_{\mu k}}{\partial x_k} = \Gamma_{n\mu n} + \frac{1}{3}\Theta_\mu - \Omega_{ij}\Im_{ji\mu} = \Omega_{\mu kk} \tag{2.26}$$

Eq. (2.26) transforms into the conservation law for the dislocation tensor in the Papkovich-Cosserat media model in the case of zero right-hand side, i.e., $\frac{1}{3}\Theta_\mu - \Omega_{ij}\Im_{ji\mu} + \Gamma_{n\mu n} = 0$. For non-zero right-hand side this equation will describe the birth and disappearance of dislocations.

Eq. (2.26) can be represented as follows using the above introduced notation:

$$\frac{\partial T_{jk}}{\partial x_k} = T_{jkk}, \quad (\Xi_{ij} \equiv T_{ij}, \quad \Omega_{ijk} \equiv T_{ijk}).$$

We will interpret the field of jumps ω_i^Ω (the Frank vector field) as a vector field of disclinations, and we will call the tensor of "inconsistencies" Ω_{ij} as the tensor of disclinations, following De Wit [6]. Note that unlike of classical view, the dislocations can be borne and disappear even in the absence of disclinations, i.e., $\Omega_{ij} = 0$, if we will take into account existence of two new classes of defects defined by the "inconsistencies" tensors Θ_μ and $\Gamma_{n\mu n}$. These tensors like the disclinations are equally possible sources of dislocations. And the defects defined by these tensors play the same role as the disclinations play in birth and disappearance of dislocations.

Let us call the scalar field of jumps in the change of volume θ^Ω as pores, and the vector of "inconsistecy" of free change of volume Θ_j as vectors of cavitation. We will also call the tensor field of jumps in deviator γ_{ij}^Ω as the field of twinning, and the "inconsistencies" tensor Γ_{ijk} as a tensor of twinning.

The Saint-Venant continuous media are described in the general case by forty degrees of freedom: D^0 r_i^0, ω_k^Ξ, θ^Ξ, γ_{ij}^Ξ, ω_{ij}^Ω, θ_j^Ω, and γ_{ijk}^Ω. They allow a three-level system of defects. The zero level of defects includes three types of defects: D^1, D^2, D^3. The first level of defects corresponds to dislocations that may be conserved, as well as they may be borne or disappear. The second level of defects corresponds to the non-conservable disclinations, cavitations and twinnings. The set of the Saint-Venant media contains in itself the sub-sets of the Papkovich-Cosserat media as well as the Cauchy media. The Papkovich-Cosserat media are described by thirteen degrees of freedom: D^0 r_i^0, ω_k^Ξ, θ^Ξ, and γ_{ij}^Ξ. And the classical Cauchy media are described by only three degrees of freedom r_i^0.

The following models can be constructed in the framework of the Saint-Venant kinematic continuous media model as the particular cases:

- Media with "turbulence" described by fifteen degrees of freedom r_i^0, ω_k^Ξ, and ω_{ij}^Ω, in which the spins ω_k^Ξ are conserved but the spins ω_k^Ω may be borne or disappear;

- "cavitational" media described by seven degrees of freedom r_i^0, θ^Ξ, and θ_j^Ω, in which the pores θ^Ξ are conserved but the pores θ^Ω may be borne or disappear;

- media with twinning described by twenty-three degrees of freedom r_i^0, γ_{ij}^Ξ, and γ_{ijk}^Ω, in which the free shifts γ_{ij}^Ξ are conserved but the free distortions γ_{ij}^Ω may be borne or disappear, like it happens for example in the processes of crystallization or polymerization.

2.4. THE *N*-TH LEVEL CONTINUOUS MEDIA MODEL. TENSOR POTENTIAL OF *N*-TH RANK.

In this section we develop the kinematic model for defects of (*N-1*)-th level. For this purpose, we define the conserved tensor of "inconsistencies" $T_{...\rho}^N \equiv T_{...\rho}$ of (N)-th rank from the equation

$$\frac{\partial T_{...\rho}^N}{\partial x_\rho} = 0 \tag{2.27}$$

where ρ is a last N-st subscript of the tensor of "inconsistencies". Then the field of multi-strains $D_{...n}$ of *N*-th rank will be defined as a general solution of the conservation equation (2.27)

$$T_{...\rho}^N = \frac{\partial D_{...n}}{\partial x_m} \Im_{nm\rho}, \quad (T_{...\rho}^N \equiv T_{...\rho}) \tag{2.28}$$

Representing the solution of this non-homogeneous equation of compatibility as a sum of the general solution $\dfrac{\partial D_{...}}{\partial x_n}$ of the homogeneous equation (2.27) ($\dfrac{\partial D_{...n}^N}{\partial x_m} \Im_{nm\rho} = 0$) and a particular solution $D_{...n}^N$ of the non-homogeneous Eq. (2.28) we obtain

$$D_{...n} = \frac{\partial D_{...}}{\partial x_n} + D_{...n}^N \tag{2.29}$$

Here tensor $D_{...}$ of (N-1)-st rank can be interpreted as a tensor potential for some tensor of *N*-th rank. Let us call this tensor $\dfrac{\partial D_{...}}{\partial x_n}$ as a tensor of restricted (integrable) multi-deformation; and the tensor $D_{...n}^N$ we will call a tensor of a

free (non-integrable) multi-deformation. From the other side, $D_{...}$ can be considered as a continuous part of the field of multi-displacements. By representing the field of multi-displacements in the form analogous to the field of multi-strains we can write for the tensor of multi- displacement:

$$D_{..k} = \frac{\partial D_{..}^{N-2}}{\partial x_k} + D_{..k}^{N-1} \tag{2.30}$$

Therefore the tensor of multi-displacements is represented as a sum of integrable $\dfrac{\partial D_{..}^{N-2}}{\partial x_k}$ and non-integrable $D_{..k}^{N-1}$ components. Then, with the account of Eqs. (2.29) and (2.30) we can write

$$D_{..kn} = \frac{\partial}{\partial x_n}(\frac{\partial D_{..}^{N-2}}{\partial x_k} + D_{..k}^{N-1}) + D_{..kn}^{N}, \quad D_{...n} \equiv D_{..kn}, \quad D_{...n}^{N} \equiv D_{..kn}^{N} \tag{2.31}$$

Here k is a last but one subscript of the defectness field $D_{..kn}$ of N-th rank or it is a last subscript of the defectness field $D_{..k}$ of $(N$-1)-st rank.

The complete field of multi-displacements $D_{..k}$ (defectness filed) can be determined from the Eq. (2.31) by means of the generalized Chesaro formulae in the form of sum of a continuous component of multi-displacements $(\dfrac{\partial D_{..}^{N-2}}{\partial x_k} + D_{..k}^{N-1})$ and a field of multi-dislocations $D_{..k}^{N}$ (defects of $(N$-1)-st rank)

$$D_{..k} = (\frac{\partial D_{..}^{N-2}}{\partial x_k} + D_{..k}^{N-1}) + D_{..k}^{N}$$

$$D_{..k}^{N} = \int_{M_0}^{M_x} D_{..kn}^{N} dy_n.$$

That leads to the formal definition of the "inconsistencies" tensor of a last but one level $T_{..q}^{N}$ of $(N$-1)-st rank

$$\frac{\partial D_{..k}}{\partial x_n}\Im_{knq} = \frac{\partial^2 D_{..}^{N-2}}{\partial x_n \partial x_k}\Im_{knq} + \frac{\partial D_{..k}^{N-1}}{\partial x_n}\Im_{knq} + D_{..kn}^{N}\Im_{knq} = \frac{\partial D_{..k}^{N-1}}{\partial x_n}\Im_{knq} + D_{..kn}^{N}\Im_{knq} = T_{..q}$$

or

$$\frac{\partial D_{..k}}{\partial x_n}\Im_{knq} = T_{..q}.$$

The law of birth and disappearance of sources of defects of the last but one level takes the following form:

$$\frac{\partial T_{..q}}{\partial x_q} = \frac{\partial}{\partial x_q}(\frac{\partial D_{..k}^{N-1}}{\partial x_n} \Im_{knq} + D_{..kn}^{N} \Im_{knq}) = \frac{\partial D_{..kn}^{N}}{\partial x_q} \Im_{nqk} = T_{..kk}$$

In result

$$\frac{\partial T_{..q}}{\partial x_q} = T_{..kk} \qquad\qquad (2.32)$$

Here $T_{..kk}$ is a tensor of (N-1)-nd rank, since it is formed by the convolution in last two indexes of the corresponding tensor of N-th rank, compare with the Saint-Venant media case. Tensor $T_{..kk}$ defines the sources of defects of (N-1)-nd rank. After N iterations of this algorithm we will arrive to the field of milti-displacements of the zero rank, i.e., to the scalar field D. That will be the natural conclusion of the algorithm.

Note in conclusion that the above-described algorithm can be considered as a realisation of the mathematical induction in the construction of the geometrical theory of defects of N-th rank.

2.5. CLASSIFICATION OF THE FIELDS OF DEFECTS

The above introduced algorithm of the kinematic analysis of the fields of defects allows us to introduce the following general classification of kinematic models for continuum media with defects. This classification is in a good agreement with the available experimental data.

1. The facts of generation and healing of defects of up to the second level have been validated, namely:

   - zero level defects with the tensor of "inconsistencies" $T_i = -2\omega_i$ (turbulence as a defect of the potential state of the continuous medium);

   - first level defects with the tensor of "inconsistencies" $T_{ij} = \varXi_{ij}$ (dislocations); and

   - second level defects with the tensor of "inconsistencies" $T_{ijk} = \varOmega_{ijk}$ (generalized disclinations – "classical" disclinations, cavitation, twinning).

   Indeed, turbulence is a well studied phenomenon. And the defects of dislocations and disclinations are well established experimentally. In the present paper we have offered the explanation for the processes of generation and healing of defects. And we established the interrelation between these processes.

2. After we established that the processes of generation and healing of disclinations take place, in accordance with the present study we should acknowledge the existence of defects of third level with the conserved tensor of "inconsistencies" $T_{ijnm} = \varTheta_{ijnm}$. And therefore it is necessary to take them into account. Otherwise the generalized disclinations could not be born or disappear.

3. The model of continuous media of N-th level with defects has the following kinematic structure:

   - The defectness fields up to the N-th rank inclusive are determined as follows:

$$D = (D^0) + D^1 + D^2 + D^3 + D^4 + ...$$

$$D_i = (\frac{\partial D^0}{\partial x_i} + D_i^1) + D_i^2 + D_i^3 + D_i^4 + ...$$

$$D_{ij} = (\frac{\partial^2 D^0}{\partial x_j \partial x_i} + \frac{\partial D_i^1}{\partial x_j} + D_{ij}^2) + D_{ij}^3 + D_{ij}^4 + ...$$

$$D_{ijk} = (\frac{\partial^3 D^0}{\partial x_k \partial x_j \partial x_i} + \frac{\partial^2 D_i^1}{\partial x_k \partial x_j} + \frac{\partial D_{ij}^2}{\partial x_k} + D_{ijk}^3) + D_{ijk}^4 + ...$$

$$D_{ijks} = (\frac{\partial^4 D^0}{\partial x_s \partial x_k \partial x_j \partial x_i} + \frac{\partial^3 D_i^1}{\partial x_s \partial x_k \partial x_j} + \frac{\partial^2 D_{ij}^2}{\partial x_s \partial x_k} + \frac{\partial D_{ijk}^3}{\partial x_s} + D_{ijks}^4) + ...$$

where all the expressions in brackets represent the continuous parts of fields.

- The discontinuous fields of defects are defined by the following equalities:

$$D^1 = \int_{M_0}^{M_x} D_i^1 dy_i, \qquad D^2 = \int_{M_0}^{M_x} D_i^2 dy_i, \qquad D^3 = \int_{M_0}^{M_x} D_i^3 dy_i, \qquad D^4 = \int_{M_0}^{M_x} D_i^4 dy_i, ...$$

$$D_i^2 = \int_{M_0}^{M_x} D_{ij}^2 dy_j, \qquad D_i^3 = \int_{M_0}^{M_x} D_{ij}^3 dy_j, \qquad D_i^4 = \int_{M_0}^{M_x} D_{ij}^4 dy_j, ...$$

$$D_{ij}^3 = \int_{M_0}^{M_x} D_{ijk}^3 dy_k, \qquad D_{ij}^4 = \int_{M_0}^{M_x} D_{ijk}^4 dy_k, ...$$

$$D_{ijk}^4 = \int_{M_0}^{M_x} D_{ijks}^4 dy_s, \quad ...$$

…………………

In development of the mathematical models of continuous media with defects the above continuous fields D^0, D_i^1, D_{ij}^2, D_{ijk}^3, D_{ijks}^4, … , as well as their derivatives can serve as the arguments of the corresponding functionals or the corresponding variational equations.

- The sources of defects of *N*-th rank satisfy Eqs. (2.28), (2.32). In particular, if we assume that the defects of fourth rank are conserved then the sources of defects (tensor of "inconsistencies") will satisfy the following relations:

$$T_{ijkq} = \frac{\partial D_{ijkn}}{\partial x_m} \Im_{nmq} = \frac{\partial D_{ijkn}^3}{\partial x_m} \Im_{nmq}, \qquad\qquad \frac{\partial T_{ijkq}}{\partial x_q} = 0$$

$$T_{ijk} = \frac{\partial D_{ijn}}{\partial x_m} \Im_{nmk} = \frac{\partial D_{ijn}^2}{\partial x_m} \Im_{nmk} + D_{ijnm}^3 \Im_{nmk}, \qquad\qquad \frac{\partial T_{ijk}}{\partial x_k} = T_{ijnn}$$

$$T_{ij} = \frac{\partial D_{in}}{\partial x_m} \Im_{nmj} = \frac{\partial D^1_{in}}{\partial x_m} \Im_{nmj} + D^2_{inm} \Im_{nmj} + D^3_{inm} \Im_{nmj}, \qquad \frac{\partial T_{ij}}{\partial x_j} = T_{inn}$$

$$T_i = \frac{\partial D_n}{\partial x_m} \Im_{nmi} = \frac{\partial D^0_n}{\partial x_m} \Im_{nmi} + D^1_{nm} \Im_{nmi} + D^2_{nm} \Im_{nmi} + D^3_{nm} \Im_{nmi}, \qquad \frac{\partial T_i}{\partial x_i} = T_{nn}$$

4. The above-introduced classification indicates on the following connection between the processes of birth and disappearance of defects of different levels:

$$\frac{\partial T_i}{\partial x_i} = T_{ii} , \qquad\qquad \frac{\partial(-2\omega_i)}{\partial x_i} = \Xi_{ii} ,$$

$$\frac{\partial T_{ij}}{\partial x_j} = T_{ijj} , \qquad\qquad \frac{\partial \Xi_{ij}}{\partial x_j} = \Omega_{ijj} ,$$

$$\frac{\partial T_{ijk}}{\partial x_k} = T_{ijkk} , \qquad\qquad \frac{\partial \Omega_{ijk}}{\partial x_k} = \Theta_{ijkk} ,$$

$$\frac{\partial T_{ijkq}}{\partial x_q} = 0 (= T_{ijkqq}) , \qquad\qquad \frac{\partial \Theta_{ijkq}}{\partial x_q} = 0 .$$

One of major properties of defects in the general hierarchy is that the defects of N-th rank are the only possible sources or discharges for the defects of $(N+1)$-st rank.

2.6. CONCLUSIONS

It is shown in the present paper that the defects of all known types can be described in the framework of the presently developed theory (or classification) of defects.

1. Within this unified classification the models of continuous media that allow presence of potential of displacements are interpreted as models of continuous media free of defects (the Cauchy continuous media). The defects of zero rank are the discontinuities (jumps) in the potential of displacements. The source of defects of zero level is the vector of curls (the tensor of first rank).

2. In the framework of the introduced unified classification of defects dislocations are defects of the first rank (the Papkovich-Cosserat continuous media). These media allow a two-level system of defects, the scalar defects D^1, D^2 and the dislocations D^2_i. And in this case the dislocations are the conserved defects, i.e. they cannot be born or disappear. The source of dislocations is a tensor of second rank.

3. It is shown that the second level models (the Saint-Venant continuous media) have a complex structure. They incorporate three types of defects. The source of defects in this case is a tensor of a third rank. The following structure of defects of the second level is established:

- Disclinations can be attributed to the classical defects. The source of disclinations is the scew-symmetric part of tensor of a third rank $(T_{ijk} - T_{jik})$ - the anti-symmetric tensor in first two indexes i, j. The disclinations are defects related to discontinuities (jumps) in the field of curls;

- Classification allows to predict the existence of two other types of defects in the continuous media of the second level. Their sources are determined through the symmetrical part of tensor of a third rank $(T_{ijk} + T_{jik})$ - the symmetric tensor in first two indexes i, j. First of them describes the discontinuities (jumps) in the change of volume, it is defined as a vector of "cavitation" T_{kkj}. Second type of these new defects of second rank describes the discontinuities (jumps) in the components of deviatoric part of strain tensor. The source of defects of a second type is a tensor of a third rank. It is defined as a tensor of "twinning", $\frac{1}{2}T_{ijk} + \frac{1}{2}T_{jik} - \frac{1}{3}T_{qqk}\delta_{ij}$.

We called the defects of second level as the generalized disclinations.

4. The possibility of existence of defects of higher than second level is established. The necessity of existence of defects of third level is defined by the condition of generation of defects of the second level. The source of these defects is a tensor of forth rank, and they have a complex hierarchy within the their own class.

5. The classification of defects is generalized for the defects of any finite level. It is shown that the existence of defects of N-th level is necessarily determined by a possibility of generation of defects of (N-1)-st level.

6. The introduced classification allows to desribe the set of arguments of a functional in developing the mathematical continuous media models of a various complexity by means of the variational method:

- In mathematical formulation of the Cauchy continuum media model the main kinematic variables in defining the Lagrangian of this model are the sufficient times differentiable fields D^0 and D_i^1.

- In mathematical formulation of the Papkovich-Cosserat continuum media models the main kinematic variables in defining the Lagrangian of these models are D^0, D_i^1, D_{ij}^2. The set of the Papkovich-Cosserat media are described in the general case by thirteen degrees of freedom, i.e., by the continuous fields $r_i^0 = (\frac{\partial D^0}{\partial x_i} + D_i^1)$, D_{ij}^2, or otherwise ω_k^Ξ, θ^Ξ, and γ_{ij}^Ξ. The set of the Papkovich-Cosserat media contains in itself the sub-sets of the "classical" Cosserat media with six degrees of freedom r_i^0, ω_k^Ξ, as well as the media with "porosity" with only four degrees of freedom r_i^0, θ^Ξ, and the media with "twinning" with eight degrees of freedom r_i^0, γ_{ij}^Ξ, and finally the classical (Cauchy) media with three degrees of freedom r_i^0.

- In mathematical formulation of the Saint-Venant continuous media models it is necessary to keep in mind that in the general case these models are described by forty degrees of freedom, D^0, D_i^1, D_{ij}^2, D_{ijk}^3. Without account of the scalar defects, these media models allow a two-level system of defects. The first level of defects corresponds to dislocations that may be conserved, as well as they may be borne or disappear. The second level

of defects corresponds to the conservable disclinations, cavitation and twinning. The set of Saint-Venant's continuous media contains in itself the sub-sets of the Papkovich-Cosserat media with twelve degrees of freedom r_i^0, ω_k^Ξ, θ^Ξ, γ_{ij}^Ξ, as well as the classical (Cauchy) media with three degrees of freedom r_i^0.

6. The choice of certain type of kinematic structure of the continuous medium with defects is determined by a requirement to describe certain physical properties of medium under study. For example, the models constructed on the basis of the Cauchy media principally cannot be used for developing a theory of fine dispersed composite materials. Indeed, the fine dispersed inclusions can be treated as dislocations in the parent phase or in the matrix. The same is true for the poorly degased matrix. In this case the gas bubbles can be treated as vacancies. Such dislocations cannot be born or disappear. Therefore the theory of fine dispersed composite materials can be developed only on the basis of the model of continuum media with defects of the first level with conserved dislocations. If the phase transitions take place in the continuous medium then they can be connected with the birth of defects – dislocations in the parent phase. It is wrong to attempt to develop such a medium model on the basis of the Papkovich-Cosserat continuous media. As a minimum, the required model in such case will be the Saint-Venant continuous media model with the generatable dislocations and conserved disclinations.

2.7. FORMULATION OF THE MODEL FOR CONTINUUMS WITH AN ADDITIONAL KINEMATICS DEGREE OF FREEDOM. (SIMULATION OF COMPOSITES AS A HETEROGENEOUS CONTINUUM WITH A FIELD OF DEFECTS (FILLERS).

The correct medium models with the microstructure (by the Mindlin's definition) investigated in this part of work. These mediums are defined by both the restricted and free deformations and generalize the known models of Mindlin, Cosserat and Aero-Kuvshinsky. Correctness of the model formulating is established by using the kinematical variational principle based on consecutive formal description of the mediums kinematics, formulating of the kinematical connections for the mediums with different complexity and composition of corresponding strain energy with using the Lagrangian coefficients procedure. The set of constitutive equations is determined and the corresponding boundary problem statement is formulated. It's demonstrated, that concerned medium models are not only model the scale effects, but also are the base for description of rather wide spectrum of the adhesion interactions. In this work the principal attention is focused on analysis of the physical part of the model. For the first time the interpretation of all the physical characteristics is given, which are described the non-classical effects, as well as description of adhesion mechanical parameters is given.

In the works [Lurie S.A., Belov P.A., 2003,] the classification of medium models with different defect fields was suggested. The medium model concerned in this part of work according to offered classification is the model with conserved dislocations [Lurie S.A., Belov P.A.,. 2003]. Applied variants of this model permitted to explain a number of known non-classical effects in mechanics of materials. So in [Lurie S, Belov P, Volkov-Bogorodsky D, Tuchkova N, 2003; Lurie S., Belov P., Tuchkova N, 2004.] it's shown, that they successfully model the effect changing of mechanical properties of nanocomposites associated with changing of the sizes of the reinforcing elements under the constant volume concentration. In [Lurie S, Belov P, 2000, Bodunov A, Belov P, Lurie S,2002; Lurie S, Belov P, Volkov-Bogorodsky D, 2002] there are the scale effects modeled in thin films, mechanics of materials, connected with cohesion interactions, the description of the non-singular cracks with zero opening angle is given. This case actually determines a formal mathematical substantiation of the Barenblatt's hypothesis about existence of the cohesion field.

In this work there the general variant of mediums with conserved dislocations is developing. These case generalizes known models of Mindlin R.D., Tiersten H.F., 1962, Tupin R.A., 1964, Cosserat E., Cosserat F., 1909., an and etc.] The variational formulation of models on base of "kinematical" variational principle is used. The kinematical variational principle is stated in [Obrzcov I.F. Lurie S.A., Belov P.A.1997, Lurie S. Belov P., 2000.P.1 Lurie S.A. Obraztsov I.F. end etc. , 2000; Lurie S, Belov P, Volkov-Bogorodsky D, 2002].

It's shown that the spectrum of the internal interactions is completely determined by a system of the kinematical connections, which are realized in the medium. Therefore, on the stage of the model composition the kinematical restrictions of the medium model are investigated at first. These restrictions s make possible to formulate of the kinematical connections in the context of the principle of virtual displacements. We'll emphasize, for example, that in the framework of classical theory of elasticity the kinematics is completely determined by the symmetrical Cauchy's correlations. In the moment medium models with the constrained torsion the kinematics is set by the totality of the Cauchy's correlations and expressions which are determine the derivatives of a vector of the rotational displacements (crookedness) with vector of displacements [Lurie S, Belov P, Volkov-Bogorodsky D, 2002; Mindlin R.D., Tiersten H.F., 1962; Lurie S, Belov P, 2000] and so on. At the second stage a list of arguments of the strain energy (for the reversible processes) and Lagrangian [Lurie S, Belov P, 2000] is established. The general form of the constitutive equations corresponding to the general form of strain energy is presented and analyzed. It lets to incorporate some simplifications, connected with an account of known experimental data's. As a result the variational formulating of the boundary problem is determined. At that the whole spectrum of the concordant boundary conditions is established.

2.7.1. The kinematical model. We'll write down the known correlations for the displacement vector R_i, which are founded from the asymmetrical Cauchy's correlations through the formal integration:

$$R_i = R_i^0 + \int_{M_0}^{M_x} (\gamma_{in} + \frac{1}{3}\theta\delta_{in} - \omega_k \Im_{ink})dx_n \tag{2.33}$$

Here γ_{in} -tensor strain deviator, θ -cubic strain, ω_k -vector of elastic rotation (pseudovector).

We'll start the description of kinematical models of the non-classical mediums from the analysis of the Papkovich's homogeneous equations which are the existent conditions of the curvilinear integral in the determination of the displacement vector (1.1.):

$$\frac{\partial(\gamma_{in} + \frac{1}{3}\theta\delta_{in} - \omega_k \Im_{ink})}{\partial x_m} \Im_{nmj} = 0 \tag{2.34}$$

The Papkovich's homogeneous equations (1.2.) are able to be interpreted as an existent condition of the vector potential (2.33) R_i. Consequently, on applying (2.34) the displacement vector R_i is the vector potential for the distortion tensor d_{ij}^0:

$$d_{ij}^0 = \gamma_{in} + \frac{1}{3}\theta\delta_{in} - \omega_k \Im_{ink} = \frac{\partial R_i}{\partial x_n} \tag{2.35}$$

We'll draw attention, that differential form $dR_i = d_{ij}^0 dx_j$ is a total differential.

Now let's consider the Papkovich's inhomogeneous equations:

$$\frac{\partial(\gamma_{in} + \frac{1}{3}\theta\delta_{in} - \omega_k \Im_{ink})}{\partial x_m}\Im_{nmj} = \Xi_{ij} \qquad (2.36)$$

Here the quantity Ξ_{ij} determines an incompatibility of displacements. Let's emphasize that in (2.36) Ξ_{ij} - is second-rank pseudotensor, so as its sign changes when replacing the right-hand triple of orts to the left-hand one. In this case one can formally incorporate the displacement vector as a difference of the two infinitely near point's displacements using an expression $dD_i = d_{ij}dx_j$. But there, however, the linear differential form dD_i already is not the total differential and the presented equation for the displacements D_i is nonintegrable.

We'll assert that a displacement field of defects is determined by the vector D_i. The continuous tensor of the "incompatibilities" of displacements Ξ_{ij} is being a tensor of dislocations [De Wit R., 1960.] and obey the differential conservation law:

$$\frac{\partial \Xi_{ij}}{\partial x_j} = 0 .$$

The solution of the Papkovich's inhomogeneous equations (2.36) one can represent as a sum of solution of the Papkovich's homogeneous equation d_{ij}^0 and partial solution of Papkovich's inhomogeneous equations d_{ij}^{Ξ}:

$$d_{ij} = d_{ij}^0 + d_{ij}^{\Xi}$$

The solution of the Papkovich's homogeneous equation (2.34) one can write down through the dislocations in form of asymmetric Cauchy's correlations: $d_{ij}^0 = \dfrac{\partial R_i}{\partial x_j}$. Let's present the asymmetric tensor d_{ij}^0 as decomposition on tensor deviator γ_{ij}^0, spherical tensor $\theta^0 \delta_{ij}$ and antisymmetric tensor $-\omega^0{}_k \Im_{ijk}$. In one's turn we'll represent the antisymmetric tensor as the pseudovector of rotation ω_k^0:

$$d_{ij}^0 = \gamma_{ij}^0 + \frac{1}{3}\theta^0 \delta_{ij} - \omega^0{}_k \Im_{ijk} , \qquad (2.37)$$

где $\gamma_{ij}^0 = \dfrac{1}{2}\dfrac{\partial R_i}{\partial x_j} + \dfrac{1}{2}\dfrac{\partial R_j}{\partial x_i} - \dfrac{1}{3}\dfrac{\partial R_k}{\partial x_k}\delta_{ij} , \qquad \omega_k^0 = -\dfrac{1}{2}\dfrac{\partial R_i}{\partial x_j}\Im_{ijk} , \qquad \theta^0 = \dfrac{\partial R_k}{\partial x_k}$

For the partial solution of the Papkovich's inhomogeneous equation (2.36) there is no continuous vector potential, i.e. it can't be presented in the form of (2.35). One can only write for it the following symmetrized representation:

$$d_{ij}^{\Xi} = \gamma_{in}^{\Xi} + \frac{1}{3}\theta^{\Xi}\delta_{in} - \omega_k^{\Xi}\Im_{ink}$$

It's obvious, that along with d_{ij}^{Ξ} one can concern the values γ_{ij}^{Ξ}, ω_k^{Ξ} and θ^{Ξ} as the generalized displacements. General solution of the Papkovich's inhomogeneous equation (2.36) can be written down in the symmetrized form:

$$d_{ij} = d_{ij}^0 + d_{ij}^{\Xi} = \gamma_{ij} + \frac{1}{3}\theta\delta_{ij} - \omega_k \Im_{ijk}$$

here $\gamma_{ij} = \gamma_{ij}^0 + \gamma_{ij}^{\Xi} = \frac{1}{2}\frac{\partial R_i}{\partial x_j} + \frac{1}{2}\frac{\partial R_j}{\partial x_i} - \frac{1}{3}\frac{\partial R_k}{\partial x_k}\delta_{ij} + \gamma_{ij}^{\Xi}$,

$$\omega_k = \omega_k^0 + \omega_k^{\Xi} = -\frac{1}{2}\frac{\partial R_i}{\partial x_j}\Im_{ijk} + \omega_k^{\Xi}, \qquad\qquad \theta = \theta^0 + \theta^{\Xi} = \frac{\partial R_k}{\partial x_k} + \theta^{\Xi}$$

Using the terminology of the Cosserat medium kinematics, we shall term the $\omega_k^0 = -\frac{1}{2}\frac{\partial R_i}{\partial x_j}\Im_{ijk}$ as a constrained

rotation, and ω_k^{Ξ} - a free rotation or spin. In a similar we'll term the γ_{ij}^0, and θ^0 - as the constrained deformations, and

γ_{ij}^{Ξ}, and θ^{Ξ} - as the free deformations . Consequently, let's coin the definitions of the tensors of free d_{ij}^{Ξ} and

constrained d_{ij}^0 distortion. The kinematics of the mediums with the defects of dislocation type is described by the

generalized Papkovich's correlations (2.36) and Cauchy's correlations for the constrained distortion (2.37). We shall

name such medium models as Papkovich's mediums or the first rank defect mediums. The kinematics of such mediums

has the following structure:

1. The defect displacement field D_i is representing the superposition of two fields – a continuous field $D_i^1 \equiv R_i$

    (of displacements R_i) and the displacement discontinuity fields D_i^2 (of dislocations):

2. The displacement discontinuity fields D_i^2 (dislocation) is integrally expressed through the fields of free

    deformations and spins with using a formulas, which are similar to Cesaro's formulas:

$$D_i^2 = \int_{M_0}^{M_x} (\gamma_{ij}^{\Xi} + \frac{1}{3}\theta^{\Xi}\delta_{ij} - \omega_k^{\Xi}\Im_{ijk})dy_j$$

However, in against the Cesaro's formulas, the integrand isn't satisfying the integrability conditions, i.e. the curvilinear

integral depends on an integration trajectory, it means, that the vector field D_i^2 is not being continuous. At that one can

determine three sorts of dislocations ($(D_i^2)_\gamma$, $(D_i^2)_\theta$, $(D_i^2)_\omega$):

$$D_i^2 = \int_{M_0}^{M_x} (\gamma_{ij}^{\Xi} + \frac{1}{3}\theta^{\Xi}\delta_{ij} - \omega_k^{\Xi}\Im_{ijk})dy_j = (\int_{M_0}^{M_x} \gamma_{ij}^{\Xi} dy_j) + (\frac{1}{3}\int_{M_0}^{M_x} \theta^{\Xi} dy_i) + (-\int_{M_0}^{M_x} \omega_k^{\Xi}\Im_{ijk}dy_j) =$$
$$= (D_i^2)_\gamma + (D_i^2)_\theta + (D_i^2)_\omega$$

(2.39)

3. There are the Cauchy's correlations hold true, generalized on the defect mediums with dislocations, which are
    named the first rank mediums:

$$d_{ij} = \frac{\partial D_i}{\partial x_j} = \frac{\partial D_i^1}{\partial x_j} + \frac{\partial D_i^2}{\partial x_j} = \frac{\partial R_i}{\partial x_j} + d_{ij}^{\Xi}$$

4. The displacement incompatibility tensor Ξ_{ij} is the tensor of dislocations [De Wit R., 1970] :

$$\Xi_{ij} = \frac{\partial d_{in}^{\Xi}}{\partial x_m} \Im_{nmj} = \frac{\partial(\gamma_{in}^{\Xi} + \frac{1}{3}\theta^{\Xi}\delta_{in} - \omega_k^{\Xi}\Im_{ink})}{\partial x_m} \Im_{nmj}$$

At that one can determine tree types of dislocation tensor, which are connected consequently with γ_{ij}^{Ξ}, ω_k^{Ξ} and θ^{Ξ}:

$$\Xi_{ij} = \frac{\partial(\gamma_{in}^{\Xi} + \frac{1}{3}\theta^{\Xi}\delta_{in} - \omega_k^{\Xi}\Im_{ink})}{\partial x_m} \Im_{nmj} = \frac{\partial \gamma_{in}^{\Xi}}{\partial x_m}\Im_{nmj} + \frac{1}{3}\frac{\partial \theta^{\Xi}}{\partial x_m}\Im_{imj} - \frac{\partial \omega_k^{\Xi}}{\partial x_m}\Im_{nki}\Im_{nmj} = \tag{2.40}$$

$$= (\Xi_{ij})_\gamma + (\Xi_{ij})_\theta + (\Xi_{ij})_\omega$$

The quantities $(\Xi_{ij})_\gamma$, $(\Xi_{ij})_\theta$ and $(\Xi_{ij})_\omega$ in decomposition (2.40) are being the sources of consequently three types of dislocations: γ - dislocations, θ - dislocations и ω - dislocations.

5. The differential conservation law of dislocation takes place. It is following from the definition of the dislocation tensor:

$$\frac{\partial \Xi_{ij}}{\partial x_j} = 0$$

6. The integral analogue of conservation deformation law obviously, has the following presentation:

$$\iiint \frac{\partial \Xi_{ij}}{\partial x_j} dV = \oiint \Xi_{ij} n_j dF = 0$$

Le us notice, that as a measure of injury (dislocations) one can choose a tensor flux Ξ_{ij} through a plane in which the chosen flat contour lies.

$$\iint_F \Xi_{ij} n_j dF = n_j \iint_0 \Xi_{ij} dF$$

Here F - is an arbitrary surface, spanned on the flat contour. In other words, the tensor flux Ξ_{ij} through any surface, spanned on the chosen flat contour is the same.

From the adduced analysis follows, that the concept of defect of the continuum is complex and can be determined with using a complex of tensor objects. For the dislocations such complexes of objects are:

- pseudotensor of incompatibilities Ξ_{ij},

- the second rank tensor of free distortion d_{ij}^{Ξ},

- vector (first rank tensor) of the discontinued dislocations D_i^2.

It is possible to refer here corresponding Burgers's vector which can be received from (2.39) by combining an initial M_0 and endpoint M_x of a flat trajectory of integration (n_n - is a constant normal vector to a plane of the integration trajectory):

$$b_i = \int_{M_0}^{M_x} d_{ij}^{\Xi} dx_j \equiv \oint d_{ij}^{\Xi} dx_j = \oint d_{ij}^{\Xi} s_j ds = \oint d_{ij}^{\Xi} v_m n_n \Im_{jmn} ds =$$

$$= \iint \frac{\partial d_{ij}^{\Xi} n_n}{\partial x_m} \Im_{jmn} dF = \iint \frac{\partial d_{ij}^{\Xi}}{\partial x_m} \Im_{jmn} n_n dF = \iint \Xi_{in} n_n dF = n_n \iint \Xi_{in} dF$$

where s_j -is an unit vector, being tangent to a flat contour, n_n - the vector of the unit normal to a plane of a trajectory, and the vectors s_j, v_m, n_n form the three orts, connected with the current point of a contour.

Kinematical analysis of the model allows establishing the total set of generalized coordinates and velocities, being necessary for formulating of functional and concordant variational medium model equation. In a considered case, for the Papkovich's medium with system of conserved defects - dislocations the generalized coordinates are the continuous quantities R_i d_{ij}^{Ξ}, and it is necessary to consider corresponding tensor quantities d_{ij}^0 Ξ_{ij} as a "velocities".

We shall note also, that as a result of the made kinematical analysis, in essence, a new natural classification of dislocations, is offered. In work [De Wit R., 1970] the classification of dislocations based on invariant determination of glide dislocations $b_i v_i = v_i \oint d_{ij}^{\Xi} s_j ds$, $b_i n_i = n_i \oint d_{ij}^{\Xi} s_j ds$ and separation dislocations $b_i s_i = s_i \oint d_{ij}^{\Xi} s_j ds$, as corresponding projections of Burgers's vector has been offered. Let's note, that such classification does not describe power independence of the allocated types of dislocations. We offer other classification which eliminates this lack. We shall write down expression for the Burgers's vector:

$$b_i = \oint (\gamma_{ij}^{\Xi} + \frac{1}{3}\theta^{\Xi}\delta_{ij} - \omega_k^{\Xi}\Im_{ijk})s_j ds = \oint \gamma_{ij}^{\Xi} s_j ds + \frac{1}{3}\oint \theta^{\Xi} s_i ds - \oint \omega_k^{\Xi}\Im_{ijk} s_j ds =$$

$$= (b_i)_\gamma + (b_i)_\theta + (b_i)_\omega$$

Consequently, according to offered classification we'll term $\gamma -$ as the dislocations the of quantities $\gamma_{ij}^{\Xi} s_j$; $\theta -$ the dislocations of quantity $\theta^{\Xi} s_i$ and accordingly $\omega -$ the dislocations of the $\omega_k^{\Xi}\Im_{ijk} s_j$. In future it will be shown, that the potential free distortion energy $\mu^{22}\gamma_{ij}^{\Xi}\gamma_{ij}^{\Xi}$, scope change $\frac{(2\mu^{22} + 3\lambda^{22})}{6}\theta^{\Xi}\theta^{\Xi}$ and torsion $\chi^{22}\omega_k^{\Xi}\omega_k^{\Xi}$ haven't cross terms. That's why the potential energies of coined types of dislocations are additive, they can exist being separate and independent from the other sorts of dislocations.

2.7.2. A variational formulating of model.

In the works [Obrzcov I.F. Lurie S.A., Belov P.A.1997, Lurie S. Belov P., 2000.P.1 Lurie S.A. Obraztsov I.F. end etc. , 2000; Lurie S, Belov P, Volkov-Bogorodsky D, 2002] the kinematical variational method of modeling is formulated. In concordance with it the kinematical connections of the medium are determinated, the virtual action of internal forces is postulated as a virtual action of reaction force factors on the kinematical connections peculiar to the medium. This action is presented as a linear form of variations of its arguments. This form can be integrated for the conservative mediums. As a result the strain energy is determined. For the linear mediums the strain energy is being the quadratic form of one's arguments.

For the mediums with conserved dislocations such kinematical connections are the Papkovich's inhomogeneous equations in use to free distortion, and Papkovich's homogeneous equations for the constrained distortion. The last ones can be integrated in the general form. The Cauchy's asymmetrical correlations are the solution of the Papkovich's homogeneous equations for the constrained distortion. Thus, according to the kinematical variational principle the virtual action of the internal forces one should present in the following form:

$$\overline{\delta U} = \iiint [\sigma_{ij}\delta(d_{ij}^0 - \frac{\partial R_i}{\partial x_j}) + m_{ij}\delta(\Xi_{ij} - \frac{\partial d_{in}^{\Xi}}{\partial x_m}\Im_{nmj})]dV . \qquad (2.41)$$

Here $\overline{\delta U}$ - the virtual action which in general representation is the linear form of its argument's variations and is optional integrated (for the mediums with dissipation see [Lurie S., Belov P. 2001]; σ_{ij} and m_{ij} - are a tensors of a Lagrange multipliers, which in physical meaning are the reaction force factors, providing a fulfillment of the respective kinematical connections.

Let's present $\overline{\delta U}$ in (2.41) as the linear form of one's argument's variations. Using the integration by parts we'll get the following expression in the items, including the derivatives:

$$\overline{\delta U} = \iiint [\sigma_{ij}\delta d_{ij}^0 + \frac{\partial \sigma_{ij}}{\partial x_j}\delta R_i + m_{ij}\delta\Xi_{ij} + \frac{\partial m_{ij}}{\partial x_m}\Im_{nmj}\delta d_{in}^{\Xi}]dV +$$

$$+ \oiint [-\sigma_{ij}n_j\delta R_i - m_{ij}n_m\Im_{nmj}\delta d_{in}^{\Xi}]dF \qquad (2.42)$$

We'll content oneself with considering the mediums without the dissipation of energy. Then such potential U exists, (potential energy), that the virtual action $\overline{\delta U}$ in (2.42) is being the variation of this potential:

$$\overline{\delta U} = \delta U , U = \iiint U_V dV + \oiint U_F dF , U_V = U_V(d_{ij}^0;d_{ij}^{\Xi};\Xi_{ij};R_i), U_F = U_F(d_{ij}^{\Xi};R_i) .$$

In future it will be demonstrated, that for the considered generalized medium model with scale effects be not conflicted in the particular case with classical theory and known experimental data's, the displacement vector must be lacking in the lists of arguments for the density of strain energy. Hence, we offer:

$$U = \iiint U_V dV + \oiint U_F dF , U_V = U_V(d_{ij}^0;d_{ij}^{\Xi};\Xi_{ij}), U_F = U_F(d_{ij}^{\Xi}) \qquad (2.43)$$

Taking into account the list of arguments in (2.43) and evaluate the variation δU in the volume, we'll obviously obtain:

$$\sigma_{ij} = \frac{\partial U_V}{\partial d_{ij}^0},   m_{ij} = \frac{\partial U_V}{\partial \Xi_{ij}},   p_{in} = \frac{\partial m_{ij}}{\partial x_m}\Im_{nmj} = \frac{\partial U_V}{\partial d_{ij}^{\Xi}},   M_{ij} = \frac{\partial U_F}{\partial d_{ij}^{\Xi}} = A_{ijnm}d_{nm}^{\Xi} \qquad (2.44)$$

One should interpret the formulas (2.44) as a generalized Green's formulas for the volume and surface force factors. These correlations make possible to express the Lagrangian and find the respective Euler's equations:

$$\delta L = \iiint [(\frac{\partial \sigma_{ij}}{\partial x_j} + X_i)\delta R_i^0 - (\frac{\partial m_{in}^{\Xi}}{\partial x_m}\Im_{nmj} + p_{ij})\delta d_{ij}^{\Xi}]dV +$$

$$+ \oiint [(Y_i - \sigma_{ij}n_j)\delta R_i^0 - (M_{in} + m_{ij}n_m\Im_{nmj})\delta d_{ik}^{\Xi}(\delta_{kn} - n_k n_n)]dF = 0 \qquad (2.45)$$

62

2.7.3. Constitutive Equations. Physical interpretation of the generalized elastic constants.

Let's consider again the densities of potential energy in the volume and on the surface. Contenting oneself with considering of physically liner mediums. Then U_V is determinated as the quadratic form of one's arguments:

$$
\begin{aligned}
2U_V &= 2U_V(d_{ij}^0; d_{ij}^\Xi; \Xi_{ij}; R_i) = \\
&= C_{ijnm}^{11} d_{ij}^0 d_{nm}^0 + 2C_{ijnm}^{12} d_{ij}^0 d_{nm}^\Xi + C_{ijnm}^{22} d_{ij}^\Xi d_{nm}^\Xi + C_{ijnm}^{33} \Xi_{ij} \Xi_{nm}
\end{aligned}
\tag{2.46}
$$

When finding (2.46) the following quite substantiated simplifications were incorporated:

1. A coefficient in the quadratic item at the displacements $C_{ij} R_i R_j$ is offered to be equal to zero in the quadratic form for the density of potential energy. Otherwise an operator of equilibrium equations would have presentation of Helmholtz equations that excludes the existence of homogeneous modes of deformation.

2. The coefficients at all the rest bilinear components, which includes the displacement vector are also assumed zero. Otherwise, when the quadratic in displacements items $C_{ij} R_i R_j$ are lacking, the cubic density of the strain energy wouldn't be positive defined.

The structure of the Young modulus tensors C_{ijnm}^{pq} in (2.46) is determined by theirs decomposition on isotropic 4th rank tensors, constructed as a multiplication of a pair of Kronekker tensors with all the possible index permutations:

$$
C_{ijnm}^{pq} = C_1^{pq} \delta_{ij} \delta_{nm} + C_2^{pq} \delta_{in} \delta_{jm} + C_3^{pq} \delta_{im} \delta_{jn}
\tag{2.47}
$$

To interpret physically founded structures of the modulus tensors, we'll consider the corresponding parts of potential energies. Let's take a look at the cubic density of the strain energy $C_{ijnm}^{11} d_{ij}^0 d_{nm}^0$, connected with the tensor of constrained distortion invariants $d_{ij}^0 = \dfrac{\partial R_i}{\partial x_j}$. Let's represent every kinematical factor being the second rank tensor (pseudotensor for the dislocations) as the tensor decomposition on the deviator, spherical and antisymmetric parts:

$$
d_{ij}^0 = (\frac{1}{2}d_{ij}^0 + \frac{1}{2}d_{ji}^0 - \frac{1}{3}d_{kk}^0 \delta_{ij}) + \frac{1}{3}d_{kk}^0 \delta_{ij} + (\frac{1}{2}d_{ij}^0 - \frac{1}{2}d_{ji}^0) = \gamma_{ij}^0 + \frac{1}{3}\theta^0 \delta_{ij} + \omega_{ij}^0
\tag{2.48}
$$

where $\omega_{ij}^0 = -\omega_k^0 \Im_{ijk}$

Then, taking into account (2.48) we'll find:

$$
\begin{aligned}
C_{ijnm}^{11} d_{ij}^0 d_{nm}^0 &= [C_1^{11}\delta_{ij}\delta_{nm} + C_2^{11}\delta_{in}\delta_{jm} + C_3^{11}\delta_{im}\delta_{jn}]d_{ij}^0 d_{nm}^0 = \\
&= (C_2^{11} + C_3^{11})\gamma_{nm}^0 \gamma_{nm}^0 + (3C_1^{11} + C_2^{11} + C_3^{11})\frac{1}{3}\theta^0 \theta^0 + (C_2^{11} - C_3^{11})\omega_{nm}^0 \omega_{nm}^0
\end{aligned}
\tag{2.49}
$$

The first item in (2.49) determines the distortion energy

$(C_2^{11} + C_3^{11})(\frac{1}{2}\frac{\partial R_i}{\partial x_j} + \frac{1}{2}\frac{\partial R_j}{\partial x_i} - \frac{1}{3}\frac{\partial R_k}{\partial x_k}\delta_{ij})(\frac{1}{2}\frac{\partial R_i}{\partial x_j} + \frac{1}{2}\frac{\partial R_j}{\partial x_i} - \frac{1}{3}\frac{\partial R_q}{\partial x_q}\delta_{ij})$, therefore we'll term the corresponding multipliers as a shear modulus for the constrained distortion.

The reasoning are completely similar for the rest items presenting in the cubic density of potential energy expression $2C_{ijnm}^{12}d_{ij}^{0}d_{nm}^{\Xi}$, $C_{ijnm}^{22}d_{ij}^{\Xi}d_{nm}^{\Xi}$, $C_{ijnm}^{33}\Xi_{ij}\Xi_{nm}$. It is obvious that the analogues of the shear modulus μ^{pq} for the deviators of all corresponding kinematical factors are embedded similarly:

$$(C_2^{pq}+C_3^{pq})=2\mu^{pq} \qquad (2.50)$$

The second item in (2.49) determines a potential energy of the volume change $(3C_1^{11}+C_2^{11}+C_3^{11})\dfrac{1}{3}\dfrac{\partial R_k}{\partial x_k}\dfrac{\partial R_q}{\partial x_q}$, so we'll term the corresponding multipliers as the cubic impaction modulus for the constrained distortion. In the same way the cubic impaction modules $2\mu^{pq}+3\lambda^{pq}$ are embedded for the spherical tensors of all the rest kinematical factors:

$$(3C_1^{pq}+C_2^{pq}+C_3^{pq})=K^{pq}=2\mu^{pq}+3\lambda^{pq} \qquad (2.51)$$

The third item in (2.49) represents the torsion potential energy $(C_2^{11}-C_3^{11})(\dfrac{1}{2}\dfrac{\partial R_i}{\partial x_j}-\dfrac{1}{2}\dfrac{\partial R_j}{\partial x_i})(\dfrac{1}{2}\dfrac{\partial R_i}{\partial x_j}-\dfrac{1}{2}\dfrac{\partial R_j}{\partial x_i})$, determines the asymmetry in a stress tensor and has no classical analogues. Therefore we'll term the corresponding multipliers as third Lame coefficient for the constrained distortion (d_{ij}^{0}). In the same way the analogues of the third Lame coefficient χ^{pq} for the corresponding invariants of other kinematical factors are embedded.

$$(C_2^{pq}-C_3^{pq})=2\chi^{pq} \qquad (2.52)$$

Solving the equations set (2.50)-(2.52) in regard to coefficients C_j^{pq}, $j=1,2,3$ and taking into account (2.42), we'll get:

$$C_{ijnm}^{pq}=\lambda^{pq}\delta_{ij}\delta_{nm}+(\mu^{pq}+\chi^{pq})\delta_{in}\delta_{jm}+(\mu^{pq}-\chi^{pq})\delta_{im}\delta_{jn}, \quad C_{ijnm}^{pq}=C_{ijnm}^{qp} \qquad (2.53)$$

We can finally write down the following expression for the density of the potential energy U_V:

$$2U_V=[\mu^{11}(\gamma_{nm}^0\gamma_{nm}^0)+\mu^{12}(\gamma_{nm}^0\gamma_{nm}^{\Xi})+\mu^{22}(\gamma_{nm}^{\Xi}\gamma_{nm}^{\Xi})]+$$

$$+\frac{1}{3}[(2\mu^{11}+3\lambda^{11})\theta^0\theta^0+(2\mu^{12}+3\lambda^{12})\theta^0\theta^{\Xi}+(2\mu^{11}+3\lambda^{11})\theta^{\Xi}\theta^{\Xi}]+$$

$$+2[\chi^{11}\omega_{nm}^0\omega_{nm}^0+\chi^{12}\omega_{nm}^0\omega_{nm}^{\Xi}+\chi^{22}\omega_{nm}^{\Xi}\omega_{nm}^{\Xi}]+$$

$$+C_{ijnm}^{33}\Xi_{ij}\Xi_{nm}$$

Let's note that a part of the density of the potential energy, which is connected with the dislocation tensor, $C_{ijnm}^{33}\Xi_{ij}\Xi_{nm}$ determines rapidly changeable local part of the potential energy of dislocations. The remaining part of strain energy's density is slow variable and can be founded as the sum of potential energies of three types of dislocations: γ - dislocations, θ - dislocations and ω - dislocations. Hence, the slow variable part of the strain energy doesn't contain any cross term from the stated types of dislocations and being the additive form relative to free distortion components. Let's note that it is the integral characteristics that are used to estimate the damage of mediums.

That's why in such problems, probably, one can neglect local rapidly variable part of energy for the rough estimate. At that the additivity really takes place in the density of the potential energy decomposition in relation to free distortion components.

In the general case the cubic density of the potential energy contains no cross terms corresponding to free distortion (γ_{nm}^{Ξ}), volume change (θ^{Ξ}) and torsion ω_k^{Ξ} at small-scale values of the constants C_{ijnm}^{33}, corresponding to the scale effects (theirs dimension differs from the Young modulus into square of length). This circumstance has been used as a substantiation of the correctness in relation to new classification of different types of dislocations.

We'll present the generalized Hooke's equations (2.44) for the volume force factors in the following form:

$$\sigma_{ij} = C_{ijnm}^{11} \frac{\partial R_n}{\partial x_m} + C_{ijnm}^{12} d_{nm}^{\Xi}, \quad p_{ij} = C_{ijnm}^{21} \frac{\partial R_n}{\partial x_m} + C_{ijnm}^{22} d_{nm}^{\Xi}, \quad m_{ij} = C_{ijnm}^{33} \Xi_{nm} \qquad (2.54)$$

Let's emphasize that generalized impulses $\sigma_{ij}, p_{ij}, m_{ij}$ in (2.53) are not only depending on generalized velocities $\frac{\partial R_n}{\partial x_m}$, Ξ_{ij}, but also on generalized coordinates d_{ij}^{Ξ}. In this connection it is possible to give different interpretations of the "non-classical" components in generalized Hooke's law (2.54). In the one hand one can redefine the stress tensor, excluding the items in the right parts which are containing the free distortions d_{ij}^{Ξ}. Then the combination $(C_{pqij}^{22} \sigma_{ij} - C_{pqij}^{12} p_{ij})$ can be determined as the generalized stress tensor. Then the other linear independent combination $(C_{pqij}^{21} \sigma_{ij} - C_{pqij}^{11} p_{ij})$ will have the physical meaning of the generalized Winkler foundation on the generalized displacements d_{ij}^{Ξ}.

At another interpretation of the constitutive equations one should acknowledge, that along with stress tensor σ_{ij} in such mediums the additional force factors called the "dislocation" stresses p_{ij} take place. This second variant is being more traditional and more preferable. We'll adduce the following reasons. Let's consider that $C_{ijnm}^{12} = 0$. As will be shown in future, in this case the general boundary problem disintegrates on boundary problem in relation to displacements R_i and on boundary problem in relation to free distortion d_{ij}^{Ξ}. At that the boundary problem concerning to displacements at the additional consideration $\chi^{11} = 0$ (theory of elasticity with the symmetrical stress tensor) coincides with the classical theory of elasticity. Then the force factor σ_{ij} assumes the mean of classical stresses. Accordingly the force factor p_{ij} assumes the mean of Winkler reaction in the couple stress equilibrium equations. At $C_{ijnm}^{12} \neq 0$ the mutual perturbance of a classical displacement field and pure dislocation conditions occurs. The cross terms of the Hooke's law equations for the σ_{ij} and p_{ij} express these perturbances. The same reasons give the algorithm of solving the general boundary problem using the method of successive approximations.

In the case of surface density of potential energy the situation is more difficult. For the smooth surface the natural preferential direction - surface normal is always exists. The equations of the Hooke's law for the internal force factors on the surface must be transversely isotropic and, as a result the kinematical factors, connected with the surface normal and a tangential plane, will appear in these equations of the Hooke's law disparately.

Let's analyze the surface density of the strain energy more explicit. We'll consider the expression of surface part of the virtual action. The first item in it is completely accords to the classical presentation. This one appears as a result of integration in parts of the expression $\iiint [\sigma_{ij}\delta(\frac{\partial R_i}{\partial x_j})]dV$ in the equality (2.41). The second item in the expression of surface part of the virtual action (2.42), (2.43) is being non-classical and is indebted to kinematical variational principle of the model evolving with its appearance. This item is connected with the surface energy of adhesion U_F. Let's consider this item more explicit:

$$-\oiint m_{ij}n_m \mathfrak{Э}_{nmj}\delta d_{in}^\Xi dF = -\oiint m_{ij}n_q \mathfrak{Э}_{pqj}\delta[d_{nm}^\Xi(\delta_{in}-n_in_n)+d_{nm}^\Xi n_in_n](\delta_{pm}-n_pn_m)dF - $$
$$-\oiint m_{ij}n_q \mathfrak{Э}_{pqj}\delta[d_{nm}^\Xi(\delta_{in}-n_in_n)+d_{nm}^\Xi n_in_n]n_mn_p dF \qquad (2.55)$$

Let' emphasize, that $n_pn_q\mathfrak{Э}_{pqj}=0$ is like a convolution of the symmetrical tensor n_pn_q with the antisymmetric pseudotensor $\mathfrak{Э}_{pqj}$. Hence, the action of the couple stresses (2.55) on surface of a body performs not on all nine components of the free distortion tensor d_{in}^Ξ, but only on six of them $d_{im}^\Xi(\delta_{pm}-n_pn_m)$:

$$-\oiint m_{ij}n_m \mathfrak{Э}_{nmj}\delta d_{in}^\Xi dF = -\oiint m_{ij}n_q \mathfrak{Э}_{pqj}\delta d_{im}^\Xi(\delta_{pm}-n_pn_m)dF \qquad (2.56)$$

In the general case the density of the strain energy (potential energy of adhesion) on the surface of the body has the following expression:

$$U_F = \frac{1}{2}[A_{ijnm}d_{nm}^\Xi d_{ij}^\Xi] \qquad (2.57)$$

The generalized equations of the law on surface are set by correlations (2.44). Let's notice, that the density of the potential energy is not depends on dislocation vector. Otherwise, the variational setting would result in systematic corrections in the static boundary conditions of the classical solution that conflicts with available experimental data.

It is important to notice, that correlations (2.56) allow specifying the list of arguments in the density of the surface potential energy in (2.57). This specified list of arguments is now determined with six «plain» components of the free distortion tensor $d_{im}^\Xi(\delta_{pm}-n_pn_m)$: $U_F = U_F(d_{ik}^\Xi(\delta_{kj}-n_kn_j))$. As a result, the whole correct variational setting of the boundary problem (2.45) acquires the following final appearance:

$$\delta L = \iiint [(\frac{\partial \sigma_{ij}}{\partial x_j}+X_i)\delta R_i^0 - (\frac{\partial m_{in}^\Xi}{\partial x_m}\mathfrak{Э}_{nmj}+p_{ij})\delta d_{ij}^\Xi]dV +$$
$$+\oiint [(Y_i - \sigma_{ij}n_j)\delta R_i^0 - (M_{in}+m_{ij}n_m \mathfrak{Э}_{nmj})\delta d_{ik}^\Xi(\delta_{kn}-n_kn_n)]dF = 0 \qquad (2.58)$$

This implies, that for the investigated medium model in every ordinary point of the surface here there is nine boundary conditions. The analysis of the determinative equations and the boundary problems at all makes possible to demonstrate that general order of the determinative equations in relation to components of the displacement vector and the potentials for the components of the free distortion is equal to eighteen. Hence, the mathematical setting of the investigated model is being concordant, because nine boundary conditions for the boundary problem of eighteenth order there are.

The structure of the adhesion modulus tensor A_{ijnm} is determined by its decomposition on the fourth rank tensors, constructed as all the possible multiplications of pairs of the "plain" Kronekker's tensors and the tensors, founded with using the product of the unit normal vectors of $n_i n_j$ type, with all the possible permutations of indexes. Besides let's take into account, that the adhesion potential energy must be not dependent on the components of the free distortion vector with the last index, coinciding with index of the unit normal to surface vector. Only in this case the classical natural boundary conditions for the stresses stay fixed on the surface of a body. This fact doesn't carry any contradiction in a special case when turning to the classical medium model and is being in good agreement with the numerous experimental data.

One can make sure that in such case the general structure of the adhesion modulus tensor has the appearance:

$$A_{ijnm} = [A_1 (\delta_{ij} - n_i n_j)(\delta_{nm} - n_n n_m) + A_3 n_i n_n (\delta_{jm} - n_j n_m) +$$
$$+ (A_2 + A_4)(\delta_{in} - n_i n_n)(\delta_{jm} - n_j n_m) + (A_2 - A_4)(\delta_{im} - n_i n_m)(\delta_{jn} - n_j n_n)] \tag{2.59}$$

Here A_i - are some constants.

Let's consider the density of the strain energy on the surface and give the physical interpretation of the adhesion components of the strain energy, taking into account the correlations (2.56), (2.59). The surface potential energy will have the appearance of a quadratic function of only the following components of free distortion - $d_{ik}^{\Xi}(\delta_{jk} - n_j n_k)$. This circumstance is important when developing the concordant theory and will be concerned in future.

Let's present the free distortion as the tensor decomposition on the "plain" deviator:

$$^2\gamma_{ij} = \frac{1}{2} d_{nm}^{\Xi}(\delta_{in} - n_i n_n)(\delta_{jm} - n_j n_m) + \frac{1}{2} d_{nm}^{\Xi}(\delta_{jn} - n_j n_n)(\delta_{im} - n_i n_m) -$$
$$- \frac{1}{2} d_{nm}^{\Xi}(\delta_{ij} - n_i n_j)(\delta_{nm} - n_n n_m)$$
,

the "plain" spherical tensor:

$$^2\theta = d_{nm}^{\Xi}(\delta_{nm} - n_n n_m)$$

the "plain" antisymmetric tensor:

$$^2\omega_{ij} = \frac{1}{2} d_{nm}^{\Xi}(\delta_{in} - n_i n_n)(\delta_{jm} - n_j n_m) - \frac{1}{2} d_{nm}^{\Xi}(\delta_{jn} - n_j n_n)(\delta_{im} - n_i n_m)$$

and the "plain" vector of angular displacement of the surface at the one's bend:

$$^2\alpha_i = d_{nm}^{\Xi} n_n (\delta_{mi} - n_m n_i)$$

Here the upper index "2" emphasizes the fact of the corresponding free distortion tensor components are evaluated on the surface of the body. As a result we'll get:

$$d_{ik}^{\Xi}(\delta_{jk} - n_j n_k) = {}^2\gamma_{ij} + \frac{1}{2}{}^2\theta(\delta_{ij} - n_i n_j) + {}^2\omega_{ij} + {}^2\alpha_j n_i \tag{2.60}$$

Taking into account (2.59), one can certain, that free distortion tensor on the surface, presented as the decomposition (2.60) converts to the canonical form:

$$2U_F = A_{ijnm}d_{ij}^{\Xi}d_{nm}^{\Xi} = (A_1 + A_2)({}^2\theta^2\theta) + 2A_2({}^2\gamma_{ij}{}^2\gamma_{ij}) + 2A_4({}^2\omega_{ij}{}^2\omega_{ij}) + A_3({}^2\alpha_k{}^2\alpha_k) \tag{2.61}$$

Comparing the first three items in (2.61) with the corresponding items of the cubic potential energy in the plain statement, one can draw an analogy between the Lame's coefficients and the adhesion modules.

We'll enter the following natural definitions:

- a modulus A_2 is an adhesion analogue of the shear modulus $A_2 = \mu^F$;

- a modulus A_1 is an adhesion analogue of the second Lame's coefficient $A_2 = \lambda^F$;

- a modulus A_4 is an adhesion analogue of the third Lame's coefficient $A_4 = \chi^F$;

- a modulus $A_3 = \delta^F$ is an adhesion analogue of the Winkler rigidity of an "internal substrate" of the surface producing the reaction moment proportional to free rotational displacements of the elements of the surface centerline (the near-surface layer) in two orthogonal directions.

Accordingly the first item in the potential energy (2.61) is being the energy of change a "plain volume" – the surface. That's why we'll term this energy as energy of a surface tension. A theory of the surface tension is rather well known beyond the frameworks of the mechanics of continua as the autonomous empirical theory. Thus, one can assert that the surface tension is being a particular effect of the evolving theory.

The second and the third items in (2.61) determine correspondingly the distortion energy and the energy of the torsion in the plane being tangent to the surface. In respect to the identification of the adhesion physical constants one can realize joint account of the distortion and torsion energies in the frameworks of the test problems modeling a friction of two half-spaces with ideally smooth surface of contact. In one's capacity of the first test problem for which only the distortion energy realizes the problem of the pulling of a fiber out from a loaded matrix can be offered. Owing to axial symmetry of this problem the surface of the fiber doesn't feel the torsion deformations. The solution of such problem establishes the connection between a static friction coefficient and the adhesion modulus. In respect to the second problem an anti-plain contact problem can be considered. For this problem, apparently along with the torsion the distortion of the contact surface is taking place. The solution of the similar problems gives the fundamental possibility to realize a corresponding experiments and determine the corresponding adhesion modules $A_2 = \mu^F$ and $A_4 = \chi^F$.

The fourth item determines the energy of a surface bend, being the energy of deformation of the "internal Winkler springs". As the test problem here there is a problem of medium's behavior being under the pressure in the faces of the gap between two half-spaces with ideally smooth surface can be applied. The using of the adhesion model here allows

to model two effects. The first of them is effect of existence of a medium surface meniscus. The second one is connected with an average elongation of the medium in the gap, which is founded with the help of the non-classical model and the similar result, founded using the classical solution in respect to the physical phenomenon of capillarity.

2.7.4. **The fundamental role of the cross tensor of modules.**

Let's consider again the constitutive equations (2.44), (2.54) and offer in them $C_{ijnm}^{12} = 0$. Then we'll get:

$$\sigma_{ij} = C_{ijnm}^{11} \frac{\partial R_n}{\partial x_m}, \quad p_{ij} = C_{ijnm}^{22} d_{nm}^{\Xi}, \quad m_{ij} = C_{ijpq}^{33} \Xi_{pq} \tag{2.62}$$

It's easy to see, that in this case the general boundary problem decomposes in two independent boundary problems. With account of (2.54), (2.62) we'll get the separate problem for the displacement vector:

$$\iiint (C_{ijnm}^{11} \frac{\partial^2 R_n}{\partial x_j \partial x_m} + P_i^V) \delta R_i dV + \oiint (P_i^F - C_{ijnm}^{11} n_j \frac{\partial R_n}{\partial x_m}) \delta R_i dF = 0 \tag{2.63}$$

The problem of the free distortion tensor is also formulated separately:

$$\iiint [C_{ijnm}^{22} d_{nm}^{\Xi} - (C_{inpq}^{33} \Im_{nmj} \Im_{srq}) \frac{\partial^2 d_{ps}^{\Xi}}{\partial x_m \partial x_r}] \delta d_{ij}^{\Xi} dV - \oiint [A_{ijnm} d_{nm}^{\Xi} - (C_{inpq}^{33} \Im_{nmj} \Im_{srq}) n_m \frac{\partial d_{ps}^{\Xi}}{\partial x_r}] \delta d_{ij}^{\Xi} dF = 0$$

Hence, the boundary problem it relation to the free distortion vector components in this case is being homogeneous. It corresponds to the absence of dislocations. As a result, at $C_{ijnm}^{12} = 0$ the model is reduced to the model of an intact medium. At the same time the heterogeneous subsystem of the equations of force equilibrium (at $\chi^{11} = 0$) and the boundary problem (2.63) as a whole coincides with the boundary problem of the classical theory of elasticity. Presented arguments allow giving the following natural interpretations to the modules of elasticity $\mu^{11}, 2\mu^{11} + \lambda^{11}, \chi^{11}$:

- μ^{11} is the shear modulus of the medium being not damaged with the γ - dislocations, $\mu^{11} = G$;

- $2\mu^{11} + 3\lambda^{11} = K$ is the modulus of cubic pressure of a medium being not damaged with the θ - dislocations. Here the Young modulus is determined by formula: $2\mu^{11} + \lambda^{11} = E$;

- value χ^{11} can be interpreted as a "torsion modulus" of the medium which is being not damaged with ω - dislocations $\chi^{11} = \chi$.

Let's further consider equations founded from the variational equation (2.45), (2.58). To find the general equilibrium equations expressed in displacements one should set the multipliers at variations of displacements and at variations of free distortion tensor components equal to zero. The first equation group we'll term as the equations of force equilibrium. Correspondingly, the second equation group (second rank tensor equation) we'll term the moment balance equations. The set of generalize equilibrium equations can be presented in the form of kinematical variables R_i, d_{ij}^{Ξ} using the generalized equations of the Hooke's law (2.54). From this equation set the subsystem of

equations is singled out. This subsystem generalizes the equilibrium equations of Lame in classical theory of elasticity and expressed through the displacement vector R_i :

$$E_1 \frac{\partial^2 R_k}{\partial x_i \partial x_k} + P_i^V - l_E^2 E_2 \Delta \frac{\partial^2 R_k}{\partial x_i \partial x_k} - l_E^2 \frac{\partial^2 P_k^V}{\partial x_i \partial x_k} +$$

$$+ G_1 (\Delta R_i - \frac{\partial^2 R_k}{\partial x_i \partial x_k}) - l_G^2 G_2 (\Delta R_i - \frac{\partial^2 R_k}{\partial x_i \partial x_k}) - l_G^2 (\Delta P_i^V - \frac{\partial^2 P_k^V}{\partial x_i \partial x_k}) = 0$$

Here the following designations are used:

$$E_1 = \frac{4(\mu^{11}\mu^{22} - \mu^{12}\mu^{12})}{3\mu^{22}} + \frac{[(2\mu^{11} + 3\lambda^{11})(2\mu^{22} + 3\lambda^{22}) - (2\mu^{12} + 3\lambda^{12})^2]}{3(2\mu^{22} + 3\lambda^{22})},$$

$$E_2 = \frac{[(2\mu^{11} + \lambda^{11})(2\mu^{22} + \lambda^{22}) - (2\mu^{12} + \lambda^{12})^2]}{(2\mu^{22} + \lambda^{22})},$$

(2.64)

and

$$G_1 = \frac{(\mu^{11}\mu^{22} - \mu^{12}\mu^{12})}{\mu^{22}} + \frac{(\chi^{111}\chi^{22} - \chi^{12}\chi^{12})}{\chi^{22}},$$

$$G_2 = \frac{[(\mu^{11} + \chi^{11})(\mu^{22} + \chi^{22}) - (\mu^{12} + \chi^{12})^2]}{(\mu^{22} + \chi^{22})},$$

(2.65)

$$l_E^2 = \frac{\chi^{33}(2\mu^{22} + \lambda^{22})}{\mu^{22}(2\mu^{22} + 3\lambda^{22})}, \quad l_G^2 = \frac{(\mu^{33} + \chi^{33})(\mu^{22} + \chi^{22})}{4\mu^{22}\chi^{22}},$$

Where values E_1 and G_1 , obviously, can be treated as modules of elasticity of the damaged medium; parameters l_G^2 , l_E^2 are scale characteristics of medium, they have dimension of a square of length.

Directly from correlations (2.64), (2.65) the following inequalities ensue:

$$(2\mu^{11} + \lambda^{11}) - E_1 = \frac{4\mu^{12}\mu^{12}}{3\mu^{22}} + \frac{(2\mu^{12} + 3\lambda^{12})^2}{3(2\mu^{22} + 3\lambda^{22})} > 0$$

$$(\mu^{11} + \chi^{11}) - G_1 = \frac{\mu^{12}\mu^{12}}{\mu^{22}} + \frac{\chi^{12}\chi^{12}}{\chi^{22}} > 0$$

(2.66)

Correlations (2.64) - (2.66) are rather important. They specify a fundamental role cross tensor of modules. Moreover, the equations (2.64), (2.65) establish exact connection between modules of elasticity of the intact medium: $(2\mu^{11} + \lambda^{11})$ and $(\mu^{11} + \chi^{11})$ and modules of elasticity of the damaged medium: E_1 и G_1

From inequalities (2.66) follows, that the modules of damaged medium are always less than Young modules of the intact medium. Equality is possible only when $\mu^{12} = 0$, $\lambda^{12} = 0$ ($C_{ijnm}^{12} = 0$) and medium with conserved dislocations degenerates in the intact classical medium (at $\chi^{11} = 0$).

In summary we shall note the following important circumstance. Dimension of modules $\mu^{33}, \lambda^{33}, \chi^{33}$ differs from the one of modules $\mu^{11}, \lambda^{11}, \chi^{11}$, $\mu^{12}, \lambda^{12}, \chi^{12}$ and $\mu^{22}, \lambda^{22}, \chi^{22}$ on dimension of a square of length. Thus, the account of the contribution of invariants of dislocation pseudotensor $C^{33}_{ijnm}\Xi_{nm}\Xi_{ij}$ in expression of potential energy with inevitability results in scale effects in volume. We shall note, that dimension of adhesive modules also differs from volumetric modules on dimension of length. Thus, the account of an adhesive component in expression for potential energy results in modeling scale effects on a surface.

The submitted generalized model of mechanics of continua as a whole is theoretical model in which a surface tension, static friction bodies with ideally smooth surface of contact, the meniscus, wettability and capillarity are modeled as special effects within the framework of unified continual description. All these special effects are united by one signature they are the scale effects in continuums.

2.7.5. Conclusions.

In work, on a basis of variational kinematical principle [Lurie S, Belov P, Volkov-Bogorodsky D, Tuchkova N, 2003; Lurie S., Belov P., Tuchkova N. 2004; Lurie S, Belov P, 2000; Lurie S, Belov P, 1998] the full and correct model of mediums with conserved dislocations is given. The special attention is given to the analysis of kinematical correlations for at the variational description kinematics of medium completely determines the system of internal interactions in volume and on the surface of the considered body. On the basis of the carried out kinematical analysis the new classification of the dislocations is offered. This classification allows describe three types of dislocations: γ - dislocations, θ - dislocations, ω dislocations.

This classification, in the first, gives new kinematical interpretation of dislocations as reflects connection of dislocations with distortion- γ, with change of volume θ (porosity) and with twisting ω (curls or spins). The offered classification actually allows predicting of the special cases of dislocations when in the medium only one or two types of dislocations dominate. So, for example, in the medium with the distributed defects the dislocations generated only by free rotational displacements ω_k^{Ξ} can be dominating. Then as the special case of the general model we receive a "classical" variant of Cosserat mediums model where $\gamma_{ij}^{\Xi} = 0$ and $\theta^{\Xi} = 0$, and free distortion tensor is determined by a correlation $d_{ij}^{\Xi} = -\omega_k^{\Xi}\Im_{ijk}$. The porous medium also can be considered as a special case of the general model. In the porous medium dominate the dislocations generated only by free volume change θ^{Ξ}. Then for the porous medium with four degrees of freedom R_i, θ^{Ξ} we have $\omega_k^{\Xi} = 0$ and $\gamma_{ij}^{\Xi} = 0$ and $d_{ij}^{\Xi} = \frac{1}{3}\theta^{\Xi}\delta_{ij}$. At last, medium concerns to special models with one dominating type of dislocations with eight degrees of freedom R_i γ_{ij}^{Ξ}. The dislocations generated only by free distortion γ_{ij}^{Ξ} here dominate. It is obvious, that thus $d_{ij}^{\Xi} = \gamma_{ij}^{\Xi}$. Similarly it is possible to predict presence of mediums with two types of dislocations. In works [Lurie S, Belov P, Volkov-Bogorodsky D, Tuchkova N, 2003; Lurie S., Belov P., Tuchkova N. 2004; Lurie S, Belov P, Volkov-Bogorodsky D, 2002], the model of such medium has been considered. There the dislocations generated by free distortion γ_{ij}^{Ξ} were neglected. On its basis it is constructed a continual variant of the theory of interphase interactions [Lurie S, Belov P, Volkov-Bogorodsky D, Tuchkova N, 2003;

Lurie S., Belov P., Tuchkova N., 2004]. This theory has allowed modeling and explaining known scale effects in mechanics of fine-dyspersated composites, determined by cohesive and adhesive local interactions. The classification offered in the presented work allows to consider also one more special case of mediums, where it is possible to neglect either θ^{Ξ} (not porous mediums) or ω_k^{Ξ} (spinless mediums). As far as it is known to authors, such mediums were not investigated yet.

Second, the offered classification is proved and from the physical point of view as shows physical meaning of various types of dislocations. So, it is proved, that the specified types of dislocations: γ - dislocations, θ - dislocations, ω - dislocations give corresponding, mutually independent components in the basic, slow variable part of density of strain energy. These shares of potential energy have no cross terms. Thus, additivity in decomposition of slow variable part of strain energy density concerning three various types of dislocations takes place. Thus, presence of a nonclassical, not local component of the potential energy connected to defects - dislocations is rather unexpected for gradient models, which is the model of mediums with system of the distributed dislocations.

Use in the given work of the consecutive variational approach and the detailed analysis of boundary conditions, has enabled to formulate the consistent and coordinated boundary problem for mediums with conserved dislocations with nine boundary conditions in each nonexceptional point of a surface. It speaks that at the consecutive variational formulation of a problem, the coordination of mathematical statement is always achieved. The order of the problem is actually determined by amount of independent boundary conditions at variational statement. We shall remind that in the most consecutive theory of mediums with Mindlin's microstructures [Mindlin R.D., Tiersten H.F. 1962], the boundary problem contains twelve boundary conditions that do not correspond to the general order of the resolving equations. Apparently, it is connected by that in work [Mindlin R.D., Tiersten H.F. 1962], the properties of surface density of the potential energy has not been established, corresponding to adhesive interactions and the analysis of work of these surface interactions has not been given.

At last, it is necessary to note, that within the framework of the offered model the spectrum of scale effects in volume and on a surface is taken into account. Really, the account of invariants of the dislocation pseudotensor $C_{ijnm}^{33}\Xi_{nm}\Xi_{ij}$ in terms of potential energy with inevitability results in scale effects in volume. On the other hand, the account of energy of adhesion in expression of potential energy results in modeling the scale effects on the surface, as dimension of tensor *A* differs from dimension of the Young modules. Apparently, the submitted generalized model of mechanics of continua is the first correct theoretical model, in which various special scale effects (cohesion interactions, a surface tension and so forth) in volume and on a surface are modeled within the framework of unified continual description.

2.7.6. Test problems for definition of the physical constants. Algorithms.

(The mechanical effective properties of composites).

In this section the connection between physical parameters of the model and structural parameters of the material is established on the base of the strict and correct mathematical statement.

The test problems allowing to define all spectrum of modules of elasticity are established. Thus, formulas for definition of characteristics of a researched material both damaged, and the non-damaged mediums are established. In essence, algorithms of definition of all spectrum of physical constants for mediums with fields of defects - dislocations (the filled composites, porous environments), taking into account scale effects are offered.

The filled composites are treated as defective mediums in which materials of matrixes and inclusions are defective mediums. This fact allows to construct models of the inclusions and a matrix in view of scale effects. Interactions of such scale effects for inclusions and matrixes results to spatial structures formation, which are treated as an interphase layer. In result, geometrical and mechanical properties of an interphase layer are completely defined (determined) by characteristics (classical and non classical) of the contacting phases (Chapter 3).

Limiting cases are become very important when the sizes of inclusions become commensurable with the sizes of nuclear structures are represented. Then inclusions can be treated as a dislocations of replacement, and pores and nano-cracks as vacancies. In this case characteristics of the mediums with kept defects - dislocations determine the effective properties of nano-composites (mediums).

Let's consider the moment equilibrium equations and moment boundary conditions in a case when adhesion can be neglected. Integrating them accordingly on the volume and the surface, we shall receive the following integrated equations:

$$\iiint (p_{ij} - \frac{\partial m_{in}}{\partial x_m} \Im_{nmj}) dV + \oiint m_{in} n_m \Im_{nmj} dF = 0$$

Let's use the Gauss's theorem. Then we establish nine integral equations that can be treated as generalized global equilibrium equations for "pure" moments.

$$\iiint p_{ij} dV = 0 \tag{2.67}$$

We can use the constitutive equations of the model (2.54), (2.62). Substituting their in (2.67) we find:

$$\iiint p_{ij} dV = \iiint (-C^{21}_{ijnm} \frac{\partial R_n}{\partial x_m} + C^{22}_{ijnm} d^{\Xi}_{nm}) dV =$$

$$= -\iiint C^{21}_{ijnm} \frac{\partial R_n}{\partial x_m} dV + \iiint C^{22}_{ijnm} d^{\Xi}_{nm} dV =$$

$$= -C^{21}_{ijnm} \iiint \frac{\partial R_n}{\partial x_m} dV + C^{22}_{ijnm} \iiint d^{\Xi}_{nm} dV = 0$$

By definition, global deformation characteristics of the defectness mediums damaged with kept dislocations are the following integrals:

$$\iiint (d_{ij} - \frac{\partial R_i}{\partial x_j} - d^{\Xi}_{ij}) dV = 0$$

$$\iiint \frac{\partial R_i}{\partial x_j} dV + \iiint d^{\Xi}_{ij} dV = \iiint d_{ij} dV \tag{2.68}$$

Considering equations (2.67) and (2.68) as system of eighteen algebraic equations, we can write its solution respect to required integrals:

$$\iiint \frac{\partial R_i}{\partial x_j} dV + \iiint d^{\Xi}_{ij} dV = \iiint d_{ij} dV$$

$$- C^{21}_{ijnm} \iiint \frac{\partial R_n}{\partial x_m} dV + C^{22}_{ijnm} \iiint d^{\Xi}_{nm} dV = 0$$

For presentation we shall divide this tensor system into the equations concerning spherical, deviatorical and antisymmetric part separately. Then for a scalar part we can get:

$$\iiint \frac{\partial R_k}{\partial x_k} dV + \iiint \theta^{\Xi} dV = \iiint d_{kk} dV$$

$$- (2\mu^{12} + 3\lambda^{12}) \iiint \frac{\partial R_k}{\partial x_k} dV + (2\mu^{22} + 3\lambda^{22}) \iiint \theta^{\Xi} dV = 0 \tag{2.69}$$

For deviatorical part we can get:

$$\iiint (\frac{1}{2}\frac{\partial R_i}{\partial x_j} + \frac{1}{2}\frac{\partial R_j}{\partial x_i} - \frac{1}{3}\frac{\partial R_k}{\partial x_k}\delta_{ij})dV + \iiint \gamma_{ij}^{\Xi} dV = \iiint (\frac{1}{2}d_{ij} + \frac{1}{2}d_{ij} - \frac{1}{3}d_{kk}\delta_{ij})dV$$

$$-\mu^{12}\iiint (\frac{1}{2}\frac{\partial R_i}{\partial x_j} + \frac{1}{2}\frac{\partial R_j}{\partial x_i} - \frac{1}{3}\frac{\partial R_k}{\partial x_k}\delta_{ij})dV + \mu^{22}\iiint \gamma_{ij}^{\Xi} dV = 0$$

(2.70)

For antisymmetric part:

$$\iiint (-\frac{1}{2}\frac{\partial R_i}{\partial x_j}\Im_{ijk})dV + \iiint \omega_k^{\Xi} dV = \iiint(-\frac{1}{2}d_{ij}\Im_{ijk})dV$$

$$-\chi^{12}\iiint (-\frac{1}{2}\frac{\partial R_i}{\partial x_j}\Im_{ijk})dV + \chi^{22}\iiint \omega_k^{\Xi} dV = 0$$

(2.71)

Accordingly, solutions of these systems look like:

$$\begin{cases} \iiint \dfrac{\partial R_k}{\partial x_k}dV = \dfrac{(2\mu^{22} + 3\lambda^{22})}{(2\mu^{22} + 3\lambda^{22}) + (2\mu^{12} + 3\lambda^{12})}\iiint d_{kk}dV \\ \\ \iiint \theta^{\Xi}dV = \dfrac{(2\mu^{12} + 3\lambda^{12})}{(2\mu^{22} + 3\lambda^{22}) + (2\mu^{12} + 3\lambda^{12})}\iiint d_{kk}dV \end{cases}$$

(2.72)

$$\begin{cases} \iiint (\dfrac{1}{2}\dfrac{\partial R_i}{\partial x_j} + \dfrac{1}{2}\dfrac{\partial R_j}{\partial x_i} - \dfrac{1}{3}\dfrac{\partial R_k}{\partial x_k}\delta_{ij})dV = \dfrac{\mu^{22}}{\mu^{22} + \mu^{12}}\iiint(\dfrac{1}{2}d_{ij} + \dfrac{1}{2}d_{ij} - \dfrac{1}{3}d_{kk}\delta_{ij})dV \\ \\ \iiint \gamma_{ij}^{\Xi}dV = \dfrac{\mu^{12}}{\mu^{22} + \mu^{12}}\iiint(\dfrac{1}{2}d_{ij} + \dfrac{1}{2}d_{ij} - \dfrac{1}{3}d_{kk}\delta_{ij})dV \end{cases}$$

(2.73)

$$\begin{cases} \iiint (-\dfrac{1}{2}\dfrac{\partial R_i}{\partial x_j}\Im_{ijk})dV = \dfrac{\chi^{22}}{\chi^{22} + \chi^{12}}\iiint(-\dfrac{1}{2}d_{ij}\Im_{ijk})dV \\ \\ \iiint \omega_k^{\Xi}dV = \dfrac{\chi^{12}}{\chi^{22} + \chi^{12}}\iiint(-\dfrac{1}{2}d_{ij}\Im_{ijk})dV \end{cases}$$

(2.74)

For the further reasonings we will use the example of the scalar part. Similar reasonings will give result for deviatorical and antisymmetric parts.

Integral deformational characteristic $\iiint d_{kk}dV$ defines the changing of volume of the mediums damaged by the conserved dislocations. The changing of volume of the mediums damaged is θ^{Ξ}. Then, the following equation takes place:

$$\iiint d_{kk}dV = \Delta V$$

here ΔV is common changing of volume, associated with changing of external load $\Delta P = \iiint P_i^V x_i dV + \oiint P_i^F x_i dF$. Let,s introduce the parameter:

$$f_\theta = \frac{(2\mu^{12} + 3\lambda^{12})}{(2\mu^{22} + 3\lambda^{22}) + (2\mu^{12} + 3\lambda^{12})}$$

(2.75)

Then, the solution of (2.72) can be written as:

74

$$\begin{cases} \iiint \dfrac{\partial R_k}{\partial x_k}\,dV = (1-f_\theta)\Delta V \\[2mm] \iiint \theta^{\varXi}\,dV = f_\theta\,\Delta V \end{cases}$$

Parameter f_θ defines the properties of the mediums due to modulus $\mu^{12}, \mu^{22}, \lambda^{12}, \lambda^{22}$. This parameter does not depend from loads and changing's of externals. Thus, we can write:

$$\begin{cases} \iiint \dfrac{\partial R_k}{\partial x_k}\,dV = \Delta[(1-f_\theta)V] \\[2mm] \iiint \theta^{\varXi}\,dV = \Delta[f_\theta V] \end{cases}$$

Let's introduce the treatment for parameter $f_\theta V$ as volume part of the mediums damaged by θ - dislocations.

On the other hand the parameter $(1-f_\theta)V$ can be treat as volume part of the medium, which is not damaged by the θ - dislocations. Then parameter f_θ, can be treat as volume part of the θ - dislocations. One is connected with non-classical physical characteristics by the relation (2.75).

Similar reasonings enter relative volume fractions and two other types of dislocations.

Аналогичными рассуждениями вводятся относительные объёмные доли и двух других типов дислокаций:

$$f_\gamma = \frac{\mu^{12}}{\mu^{22} + \mu^{12}} \tag{2.76}$$

$$f_\omega = \frac{\chi^{12}}{\chi^{22} + \chi^{12}} \tag{2.77}$$

Thus, six relations (2.62) - (2.64), and (2.75) - (2.77) between experimentally definable parameters and the formal parameters of the mediums entered into the theories of the pseudocontinuum with kept dislocation are established.

Equations (2.75) - (2.77) can form a basis for experimental definition of a part of the nonclassical modules which are included in tensor C^{12}. As example, f_θ can be determined experimentally as the volumetric part of pores or inclusions. This value also can be found on the known data of the volumetric part of inclusions.

Test problems

Let's consider the moment equations of balance, moment boundary conditions in absence of adhesion and the equation of Hooke's law. We shall express free distortion through derivatives from the moments and displacements:

$$\sigma_{ij} = C^{11}_{ijnm}\frac{\partial R_n}{\partial x_m} - C^{12}_{ijnm}d^{\varXi}_{nm}, \quad p_{ij} = -C^{21}_{ijnm}\frac{\partial R_n}{\partial x_m} + C^{22}_{ijnm}d^{\varXi}_{nm}, \quad m_{ij} = C^{33}_{ijnm}\varXi_{nm} = (C^{33}_{ijnm}\Im_{srm})\frac{\partial d^{\varXi}_{ns}}{\partial x_r}$$

With the help of the equations of balance dislocation pressure can be expressed through a rotor of the moments. Using Hooke's law, we shall find the following:

$$d^{\varXi}_{pq} = C^{-22}_{pqrs}C^{21}_{rsnm}\frac{\partial R_n}{\partial x_m} + C^{-22}_{pqrs}\frac{\partial m_{ra}}{\partial x_b}\Im_{abs}$$

$$\sigma_{ij} = [C^{11}_{ijnm} - C^{12}_{ijpq}C^{-22}_{pqrs}C^{21}_{rsnm}]\frac{\partial R_n}{\partial x_m} - C^{12}_{ijpq}C^{-22}_{pqrs}\frac{\partial m_{ra}}{\partial x_b}\Im_{abs} \tag{2.78}$$

Let's take into account the relations:

75

$$\iiint \sigma_{ij} dV = \iiint P_i^V x_j dV + \oiint P_i^F x_j dF$$

$$\iiint \frac{\partial m_{ra}}{\partial x_b} \Im_{abs} dV = \oiint m_{ra} n_b \Im_{abs} dF = 0$$

(2.79)

So, according to the (2.74), (2.75) we will receive the following:

$$[C_{ijnm}^{11} - C_{ijpq}^{12} C_{pqrs}^{-22} C_{rsnm}^{21}] \iiint \frac{\partial R_n}{\partial x_m} dV = \iiint P_i^V x_j dV + \oiint P_i^F x_j dF$$

(2.80)

If $C_{ijpq}^{12} = 0$, the formulas (2.80) are give the solutions of the test problems for the definition of modules of elasticity for the mediums intact with the appropriate dislocations.

If $C_{ijpq}^{12} \neq 0$, the formulas (2.80) are give the decisions of the problems for the definition of modules damage by the appropriate dispositions:

$$[C_{ijnm}^{11} - C_{ijpq}^{12} C_{pqrs}^{-22} C_{rsnm}^{21}] \oiint R_n n_m dF = \iiint P_i^V x_j dV + \oiint P_i^F x_j dF$$

(2.81)

The relation (2.81) is the tensor equation of the second rank containing 9 linear equations be relative 9 component of isotropic tensors of "damaged" modules C^{11}, C^{12}, C^{22}. Thus, these relations essentially allow to determine all modules of dimension of classical modules. From here drop out (by virtue of the equations (2.80) modules determining local effects. At integrated estimations (2.81) local characteristics can not be determined. Except for the modules determining global characteristics is of two groups of modules, determining scale effects - local characteristics. They should be defined from local test problems. The dislocation volumetric characteristics which are included in the tensor C33 can be determined by a direct method under characteristics of the mechanics of destruction (see Report 4, Annual Report, first year) or, by the indirect route under characteristics of interphase layers (under integrated characteristics of composites (Report 8, Annual Report, second year)). The second group of the modules determining local characteristics is adhesive modules. These characteristics can be defined, for example with use of effects of a superficial tension, a meniscus and capillarity (for liquid phases), and also with use of experiments with friction of rest.

2.8. THE KLAPEIRON'S THEOREM

The Klapeiron's Theorem is the fundamental theorem of any model of the solid medium. This theorem allows to link the potential energy and the work of the external forces in accurate solution of the appropriate boundary-value problem.

2.8.1. The Klapeiron's Theorem for one body with active surface

Let's show that the Klapeiron's Theorem take place for the generalized model of the medium with the Lagrangian:

$$L = A - \frac{1}{2} \iiint [C_{ijnm}^{11} \frac{\partial R_n}{\partial x_m} \frac{\partial R_i}{\partial x_j} + 2C_{ijnm}^{12} \frac{\partial R_n}{\partial x_m} d_{ij}^{\Xi} + C_{ijnm}^{22} d_{nm}^{\Xi} d_{ij}^{\Xi} + C_{ijnm}^{33} \Xi_{nm} \Xi_{ij}] dV -$$

$$- \frac{1}{2} \oiint A_{ijnm} d_{nm}^{\Xi} d_{ij}^{\Xi} dF$$

For this purpose we shall calculate the value of the Lagrangian in the stationary point (if the all equations and boundary conditions were satisfied) in view of the physical relations (2.53),(2.63). The following sequence of equality takes place:

$$L = A - \frac{1}{2}\iiint [C_{ijnm}^{11}\frac{\partial R_n}{\partial x_m}\frac{\partial R_i}{\partial x_j} + 2C_{ijnm}^{12}\frac{\partial R_n}{\partial x_m}d_{ij}^{\Xi} + C_{ijnm}^{22}d_{nm}^{\Xi}d_{ij}^{\Xi} + C_{ijnm}^{33}\Xi_{nm}\Xi_{ij}]dV -$$

$$-\frac{1}{2}\oiint A_{ijnm}d_{nm}^{\Xi}d_{ij}^{\Xi}dF =$$

$$= A - \frac{1}{2}\iiint [(C_{ijnm}^{11}\frac{\partial R_i}{\partial x_j} + C_{ijnm}^{12}d_{ij}^{\Xi})\frac{\partial R_n}{\partial x_m} + (C_{ijnm}^{12}\frac{\partial R_n}{\partial x_m} + C_{ijnm}^{22}d_{nm}^{\Xi})d_{ij}^{\Xi} + (C_{iqnm}^{33}\Xi_{nm}\Im_{qjk})\frac{\partial d_{ij}^{\Xi}}{\partial x_k}]dV$$

$$-\frac{1}{2}\oiint A_{ijnm}d_{nm}^{\Xi}d_{ij}^{\Xi}dF =$$

$$= A - \frac{1}{2}\iiint [\sigma_{ij}\frac{\partial R_i}{\partial x_j} + p_{ij}d_{ij}^{\Xi} + m_{ijk}\frac{\partial d_{ij}^{\Xi}}{\partial x_k}]dV - \frac{1}{2}\oiint A_{ijnm}d_{nm}^{\Xi}d_{ij}^{\Xi}dF =$$

$$= A - \frac{1}{2}\iiint [-\frac{\partial \sigma_{ij}}{\partial x_j}R_i + (p_{ij} - \frac{\partial m_{ijk}}{\partial x_k})d_{ij}^{\Xi}]dV - \frac{1}{2}\oiint [\sigma_{ij}n_jR_i + (m_{ijk}n_k + A_{ijnm}d_{nm}^{\Xi})d_{ij}^{\Xi}]dF =$$

$$= A - \frac{1}{2}\iiint P_i^V R_i dV - \frac{1}{2}\oiint P_i^F R_i dF = A - \frac{1}{2}A = \frac{1}{2}A$$

From here we receive the following formulation of the Klapeiron's theorem for a body with an active surface: "Potential energy of a body with an active surface is equal to half of work of external forces ":

$$\frac{1}{2}A = U_V + U_F$$

Let's note, that in spite of a "classical" kind of this theorem, the structure and the contents of potential energy have completely other contents. First, the volumetric part of potential energy contains nonclassical composed, dependent on components the tensor of free distortion and the tensor dispositions:

$$U_V = \frac{1}{2}\iiint C_{ijnm}^{11}\frac{\partial R_n}{\partial x_m}\frac{\partial R_i}{\partial x_j}dV + \frac{1}{2}\iiint [2C_{ijnm}^{12}\frac{\partial R_n}{\partial x_m}d_{ij}^{\Xi} + C_{ijnm}^{22}d_{nm}^{\Xi}d_{ij}^{\Xi} + C_{ijnm}^{33}\Xi_{nm}\Xi_{ij}]dV$$

Second, the "classical" member in a volumetric part of potential energy it is calculated on displacements which satisfy with other, than classical, to the equations of balance.

Thirdly, the potential energy as a additional item contains superficial potential energy. This part of potential energy is not equal to zero for an adhesion-active surface.

2.8.2 Dupre's equation

Let adhesive interaction between two bodies take place. Dupre's equation defines the connection between work of external forces on system of two bodies with adhesive interaction contact, the potential energies these bodies and the energy of their adhesive interaction. Thus, Dupre's equation is the mathematical formulation of Klapeyron's theorem for this system of bodies.

On a free surface from kinematic connections the kinematic variables in nonclassical boundary conditions are any. Possible work of resulting force factors on the appropriate kinematic variables on a surface transform to zero then when all appropriate force multipliers become to zero. For brevity we shall enter true tensor of moment pressure of the third rank through pseudotensor of moment pressure of the second rank:

$$m_{ijk} = m_{in} \Theta_{njk}$$

Thus nonclassical boundary conditions get the following kind:

$$m_{ijk} n_k + A_{ijnm} d_{nm}^{\Xi} = 0$$

Let's define the tensor of adhesive flexibility A_{pqij}^-**, as the solution of the following linear algebraic system:**

$$A_{pqij}^- A_{ijnm} = \delta_{pn}(\delta_{qm} - n_q n_m)$$

Solving this system, we shall receive expression for components tensor of adhesive flexibility through adhesive modules.

Clapeyron's theorem for a compound body with active surfaces.

Lagrangian for this body has the following kind.

$$L = L^{(1)} + L^{(2)}$$

$$L = \{ \iiint_{V_1} P_i^{(V_1)} R_i^{(1)} dV + \iint_{F_1} P_i^{(F_1)} R_i^{(1)} dF -$$

$$-\frac{1}{2} \iiint_{V_1} (C_{ijnm}^{11} \frac{\partial R_n}{\partial x_m} \frac{\partial R_i}{\partial x_j} + 2 C_{ijnm}^{12} \frac{\partial R_n}{\partial x_m} d_{ij}^{\Xi} + C_{ijnm}^{22} d_{nm}^{\Xi} d_{ij}^{\Xi} + C_{ijnm}^{33} \Xi_{nm} \Xi_{ij})^{(1)} dV$$

$$-\frac{1}{2} \oiint_{F_1} A_{ijnm}^{(1)} d_{nm}^{(1)} d_{ij}^{(1)} dF \} +$$

$$+\{ \iiint_{V_2} P_i^{(V_2)} R_i^{(2)} dV + \iint_{F_2} P_i^{(F_2)} R_i^{(2)} dF -$$

$$-\frac{1}{2} \iiint_{V_2} (C_{ijnm}^{11} \frac{\partial R_n}{\partial x_m} \frac{\partial R_i}{\partial x_j} + 2 C_{ijnm}^{12} \frac{\partial R_n}{\partial x_m} d_{ij}^{\Xi} + C_{ijnm}^{22} d_{nm}^{\Xi} d_{ij}^{\Xi} + C_{ijnm}^{33} \Xi_{nm} \Xi_{ij})^{(2)} dV$$

$$-\frac{1}{2} \oiint_{F_2} A_{ijnm}^{(2)} d_{nm}^{(2)} d_{ij}^{(2)} dF \} -$$

$$-\iint_{C} (A_{ijnm}^{(1)} - A_{ijnm}^{(2)}) d_{ij} d_{nm} dF$$

where upper indexes ($P_i^{(V_1)}$, $R_i^{(1)}$, $P_i^{(F_1)}$, $R_i^{(1)}$ and so on) show the attributes of contacting bodies.

In the last equation it is taken into account, that on a surface of contact C free distortions of first and second body are equal:

$$d_{nm}^{(1)} = d_{nm}^{(2)} = d_{nm}.$$

Let kinematic variables of the first and second body satisfy to the appropriate equations of balance and boundary conditions then it is possible to write down:

$$L = \{ \frac{1}{2} \iiint_{V_2} P_i^{V_2} R_i^2 dV + \iint_{F_2} P_i^{F_2} R_i^2 dF - \frac{1}{2} \iiint_{V_2} [(\frac{\partial \sigma_{ij}^2}{\partial x_j} R_i^2 + \sigma_{ij}^2 \frac{\partial R_i^2}{\partial x_j}) + p_{ij}^2 d_{ij}^{\Xi} + m_{ij}^2 \frac{\partial d_{in}^2}{\partial x_m} \Theta_{nmj}] dV$$

$$-\frac{1}{2} \oiint_{F_2} A_{ijnm}^2 d_{nm}^2 d_{ij}^2 dF \} -$$

$$-\iint_{C} (A_{ijnm}^1 - A_{ijnm}^2) d_{ij} d_{nm} dF$$

Let's transform last two parts of energy equation in a volumetric part:

$$L^{(1)} = \{\frac{1}{2}\iiint\limits_{V_1} P_i^{V_1} R_i^1 dV + \iint\limits_{F_1} P_i^{F_1} R_i^1 dF - \frac{1}{2}\iiint\limits_{V_1} [(\frac{\partial \sigma_{ij}^1}{\partial x_j} R_i^1 + \sigma_{ij}^1 \frac{\partial R_i^1}{\partial x_j}) + p_{ij}^1 d_{ij}^1 + m_{ij}^1 \frac{\partial d_{in}^1}{\partial x_m}\Im_{nmj}]dV$$

$$-\frac{1}{2}\oiint\limits_{F_1} A_{ijnm}^1 d_{nm}^1 d_{ij}^1 dF\} +$$

$$\iiint\limits_{V_1} [p_{ij}^1 d_{ij}^1 + m_{ij}^1 \frac{\partial d_{in}^1}{\partial x_m}\Im_{nmj}]dV = \iiint\limits_{V_1} [p_{ij}^1 d_{ij}^1 + m_{ij}^1 \Im_{nmj}\frac{\partial d_{in}^1}{\partial x_m}]dV = \iiint\limits_{V_1} [p_{ij}^1 d_{ij}^1 - m_{ijm}^1 \frac{\partial d_{in}^1}{\partial x_m}]dV =$$

$$= \iiint\limits_{V_1} [-\frac{\partial m_{ijm}^1}{\partial x_m}d_{ij}^1 - m_{ijm}^1 \frac{\partial d_{in}^1}{\partial x_m}]dV = -\iiint\limits_{V_1} \frac{\partial(m_{ijm}^1 d_{ij}^1)}{\partial x_m}dV =$$

$$= -\iint\limits_{F_1} m_{ijm}^1 n_m^1 d_{ij}^1 dF - \iint\limits_{C} m_{ijm}^1 n_m^1 d_{ij}^1 dF$$

Similar calculations can be made and for the second body. In view of the received results it is possible to write:

$$L = \{\frac{1}{2}\iiint\limits_{V_1} P_i^{V_1} R_i^1 dV + \iint\limits_{F_1} (P_i^{F_1} - \frac{1}{2}\sigma_{ij}^1 n_j^1)R_i^1 dF - \frac{1}{2}\oiint\limits_{F_1} (m_{ijm}^1 n_m^1 + A_{ijnm}^1 d_{nm}^1)d_{ij}^1 dF\} -$$

$$-\frac{1}{2}\iint\limits_{C} \sigma_{ij}^1 n_j^1 R_i^1 dF - \frac{1}{2}\iint\limits_{C} m_{ijm}^1 n_m^1 d_{ij}^1 dF +$$

$$+\{\frac{1}{2}\iiint\limits_{V_2} P_i^{V_2} R_i^2 dV + \iint\limits_{F_2} (P_i^{F_2} - \frac{1}{2}\sigma_{ij}^2 n_j^2)R_i^2 dF - \frac{1}{2}\oiint\limits_{F_2} (m_{ijm}^2 n_m^2 + A_{ijnm}^2 d_{nm}^2)d_{ij}^2 dF\} -$$

$$-\frac{1}{2}\iint\limits_{C} \sigma_{ij}^2 n_j^2 R_i^2 dF - \frac{1}{2}\iint\limits_{C} m_{ijm}^2 n_m^2 d_{ij}^2 dF$$

If for each body nonclassical boundary conditions on free from contact of a part of a surface of both bodies are satisfied then last items in braces are equal to zero. Accordingly, the second items will give half of work of external superficial forces if classical boundary conditions on that part of a surface which does not participate in adhesive interaction of bodies are satisfied. Then the expression for Lagrangian becomes simpler and takes the form:

$$L = \{\frac{1}{2}\iiint\limits_{V_1} P_i^{V_1} R_i^1 dV + \frac{1}{2}\iint\limits_{F_1} P_i^{F_1} R_i^1 dF\} + \{\frac{1}{2}\iiint\limits_{V_2} P_i^{V_2} R_i^2 dV + \frac{1}{2}\iint\limits_{F_2} P_i^{F_2} R_i^2 dF\} -$$

$$-\frac{1}{2}\iint\limits_{C} \sigma_{ij}^1 n_j^1 R_i^1 dF - \frac{1}{2}\iint\limits_{C} m_{ijm}^1 n_m^1 d_{ij}^1 dF - \frac{1}{2}\iint\limits_{C} \sigma_{ij}^2 n_j^2 R_i^2 dF - \frac{1}{2}\iint\limits_{C} m_{ijm}^2 n_m^2 d_{ij}^2 dF$$

In view of that $n_m^1 = -n_m^2 = n_m$, that if on a surface of contact C kinematic and static variables of the first and second body satisfy to conditions of contact precisely, last four composed are mutually destroyed. In result stationary value of Lagrangian is received:

$$L = \frac{1}{2}\iiint\limits_{V_1} P_i^{V_1} R_i^1 dV + \frac{1}{2}\iint\limits_{F_1} P_i^{F_1} R_i^1 dF + \frac{1}{2}\iiint\limits_{V_2} P_i^{V_2} R_i^2 dV + \frac{1}{2}\iint\limits_{F_2} P_i^{F_2} R_i^2 dF = A^1 + A^2$$

Thus, Klapeyron's theorem for composed bodies is proved: "The stationary value of Lagrangian of system of two bodies with adhesion interaction is equal half of work of external forces enclosed to this system"

With the help of this theorem possible to prove the «Dupre's theorem». For this purpose it is necessary to substitute in expression of Lagrangian of systems its stationary value:

$$L = L^1 + L^2, \qquad L = (A^1 - U^1) + (A^2 - U^2), \qquad \frac{1}{2}(A^1 + A^2) = (A^1 - U^1) + (A^2 - U^2)$$

$$U^1 + U^2 = \frac{1}{2}(A^1 + A^2)$$

Here $U^{(1)}$ and $U^{(2)}$ potential energy of interative bodies.

It is possible to write down the following equality

$$U^1 + U^2 = U_0^{\ 1} + U_0^{\ 2} - U^{12},$$

U^{12} - is the energy of adhesion interaction of contacting bodies, $U_0^{\ 1}, U_0^{\ 2}$ - are the potential energies of isolated bodies.

The values U^{12}, $U_0^{\ 1}, U_0^{\ 2}$, A^1, A^2 can be calculated on the basis of the solution of the appropriate boundary problems and can be written through parameters of the model.

Proved «Dupre's theorem» can help to define in the direct experimental way the energy of adhesive interaction of the bodies on the basis of Young's equation. We shall remind, that Young's equation connects an angle of a meniscus (experimentally measured parameter) to superficial energy of interaction.

2.9. ASYMPTOTIC INTEGRATION OF THE BOUNDARY PROBLEM.

The asymptotic consideration of the boundary problem is rather perspective tool of the approached decomposition the common boundary problem on a classical boundary problem and some amendment to it, connected with defectiveness of medium.

The "kinematic" variation principle and analysis of the kinematic structure of the theory of the medium with kept dislocations have resulted in the following boundary problem:

$$\delta L = \iiint \left[\left(\frac{\partial \sigma_{ij}}{\partial x_j} + P_i^V \right) \delta R_i + \left(p_{ij} - \frac{\partial m_{in}}{\partial x_m} \mathfrak{I}_{nmj} \right) \delta d_{ij}^\Xi \right] dV +$$

$$+ \oiint \left[(P_i^F - \sigma_{ij} n_j) \delta R_i - (A_{ijnm} d_{nm}^\Xi - m_{in} n_m \mathfrak{I}_{nmj}) \delta d_{ij}^\Xi \right] dF = 0$$

Thus the generalized equations of Hook's law take place:

$$\sigma_{ij} = C_{ijnm}^{11} \frac{\partial R_n}{\partial x_m} + C_{ijnm}^{12} d_{nm}^\Xi, \quad p_{ij} = C_{ijnm}^{21} \frac{\partial R_n}{\partial x_m} + C_{ijnm}^{22} d_{nm}^\Xi, \quad m_{ij} = C_{ijnm}^{33} \Xi_{nm},$$

where the tensors of the modules of elasticity in volume of a body are determined by equality:

$$C_{ijnm}^{11} = \lambda^{11} \delta_{ij} \delta_{nm} + (\mu^{11} + \chi^{11}) \delta_{in} \delta_{jm} + (\mu^{11} - \chi^{11}) \delta_{im} \delta_{jn}$$

$$C_{ijnm}^{12} = \lambda^{12} \delta_{ij} \delta_{nm} + (\mu^{12} + \chi^{12}) \delta_{in} \delta_{jm} + (\mu^{12} - \chi^{12}) \delta_{im} \delta_{jn} = C_{ijnm}^{21}$$

$$C_{ijnm}^{22} = \lambda^{22} \delta_{ij} \delta_{nm} + (\mu^{22} + \chi^{22}) \delta_{in} \delta_{jm} + (\mu^{22} - \chi^{22}) \delta_{im} \delta_{jn}$$

$$C_{ijnm}^{33} = \lambda^{33} \delta_{ij} \delta_{nm} + (\mu^{33} + \chi^{33}) \delta_{in} \delta_{jm} + (\mu^{33} - \chi^{33}) \delta_{im} \delta_{jn}$$

and the tensor of the modules of adhesion on the body surface give the following general view:

$$A_{ijnm} = \lambda^F (\delta_{ij} - n_i n_j)(\delta_{nm} - n_n n_m) + \delta^F n_i n_n (\delta_{jm} - n_j n_m) +$$
$$+ (\mu^F + \chi^F)(\delta_{in} - n_i n_n)(\delta_{jm} - n_j n_m) + (\mu^F - \chi^F)(\delta_{im} - n_i n_m)(\delta_{jn} - n_j n_n)$$

Let's remind, that on the basis of results of the previous unit (Section 2.7 of the present Report) at $C_{ijnm}^{12} = 0$ the decision of a regional problem becomes:

$$R_i = R_i^0, \quad d_{ij}^\Xi = 0$$

Let's enter into consideration some norms of the tensor modules: $\left\| C_{ijnm}^{11} \right\|$, $\left\| C_{ijnm}^{12} \right\|$ and $\left\| C_{ijnm}^{22} \right\|$. If the ratio of the norms of the tensors $\left\| C_{ijnm}^{11} \right\|$ and $\left\| C_{ijnm}^{22} \right\|$ is about "one", and the ratio $\dfrac{\left\| C_{ijnm}^{12} \right\|}{\left\| C_{ijnm}^{11} \right\|} = \delta$ is small, then this parameter δ can be used in the construction of the asymptotic decomposition.

The parameter δ we will name small parameter of the defectness.

$$\delta = \frac{\left\| C_{ijnm}^{12} \right\|}{\left\| C_{ijnm}^{11} \right\|}$$

Let's give the determination of the geometry size of the body l as the specific relative fraction of superficial

$$l = \frac{V}{F}$$

Let's define also small parameter of multiscale-effects ε with the help of a ratio:

$$\frac{C_{ijnm}^{33}}{\left\| C_{ijnm}^{11} \right\|} \frac{1}{l^2} = \frac{C_{ijnm}^{33}}{\left\| C_{ijnm}^{33} \right\|} \frac{\left\| C_{ijnm}^{33} \right\|}{\left\| C_{ijnm}^{11} \right\| l^2} = \overline{C}_{ijnm}^{33} \frac{\left\| C_{ijnm}^{33} \right\|}{\left\| C_{ijnm}^{11} \right\| l^2} = \overline{C}_{ijnm}^{33} \varepsilon^2, \qquad \varepsilon = \frac{1}{l}\sqrt{\frac{\left\| C_{ijnm}^{33} \right\|}{\left\| C_{ijnm}^{11} \right\|}}$$

Accordingly, we shall enter definition for small parameter of adhesive effects a:

$$\frac{A_{ijnm}}{\left\| C_{ijnm}^{11} \right\|} \frac{1}{l} = \frac{A_{ijnm}}{\left\| A_{ijnm} \right\|} \frac{\left\| A_{ijnm} \right\|}{\left\| C_{ijnm}^{11} \right\| l} = \overline{A}_{ijnm} \frac{\left\| A_{ijnm} \right\|}{\left\| C_{ijnm}^{11} \right\| l} = \overline{A}_{ijnm} a, \qquad a = \frac{\left\| A_{ijnm} \right\|}{\left\| C_{ijnm}^{11} \right\| l}$$

If $C_{ijnm}^{12} \neq 0$, we will find the decision in the following form:

$$R_i = R_i^N \delta^N$$
$$d_{ij}^\Xi = d_{ij}^M \delta^M$$

In result, the common boundary problem is breaks up into the two independent boundary problems: the boundary problem for the vector of displacement, which will define the basic asymptotic process and the boundary problem for the tensor of the free distortion, which will define the auxiliary asymptotic process.

The basic asymptotic process

This case is take place when the asymptotic process is determined by the small parameter of the defectness δ.

Let's give definition of the normalized loadings $\overline{P}_i^V, \overline{P}_i^F$ and normalized tensors of the modules $\overline{C}_{ijnm}^{11}, \overline{C}_{ijnm}^{12}, \overline{C}_{ijnm}^{22}$

$$\frac{P_i^V}{\left\| C_{ijnm}^{11} \right\|} = \overline{P}_i^V, \quad \frac{P_i^F}{\left\| C_{ijnm}^{11} \right\|} = \overline{P}_i^F, \quad \frac{C_{ijnm}^{11}}{\left\| C_{ijnm}^{11} \right\|} = \overline{C}_{ijnm}^{11}, \quad \frac{C_{ijnm}^{12}}{\left\| C_{ijnm}^{11} \right\|} = \frac{C_{ijnm}^{12}}{\left\| C_{ijnm}^{12} \right\|} \frac{\left\| C_{ijnm}^{12} \right\|}{\left\| C_{ijnm}^{11} \right\|} = \overline{C}_{ijnm}^{12} \frac{\left\| C_{ijnm}^{12} \right\|}{\left\| C_{ijnm}^{11} \right\|} = \overline{C}_{ijnm}^{12} \delta$$

$$\frac{C_{ijnm}^{22}}{\left\|C_{ijnm}^{11}\right\|} = \frac{C_{ijnm}^{22}}{\left\|C_{ijnm}^{22}\right\|} \frac{\left\|C_{ijnm}^{22}\right\|}{\left\|C_{ijnm}^{11}\right\|} = \overline{C}_{ijnm}^{22}$$

Then the variational equation can be resulted in a kind:

$$\iiint (\overline{C}_{ijnm}^{11} \frac{\partial^2 R_n}{\partial x_j \partial x_m} + \overline{C}_{ijnm}^{12} \delta \frac{\partial d_{nm}}{\partial x_j} + \overline{P}_i^V) \delta R_i dV + \oiint (\overline{P}_i^F - \overline{C}_{ijnm}^{11} n_j \frac{\partial R_n}{\partial x_m} - \overline{C}_{ijnm}^{12} \delta n_j d_{nm}) \delta R_i dF =$$

$$= \iiint (\overline{C}_{ijnm}^{11} \delta^N \frac{\partial^2 R_n^N}{\partial x_j \partial x_m} + \overline{C}_{ijnm}^{12} \delta^{M+1} \frac{\partial d_{nm}^M}{\partial x_j} + \overline{P}_i^V) \delta R_i dV +$$

$$+ \oiint (\overline{P}_i^F - \overline{C}_{ijnm}^{11} n_j \delta^N \frac{\partial R_n^N}{\partial x_m} - \overline{C}_{ijnm}^{12} n_j \delta^{M+1} d_{nm}^M) \delta R_i dF =$$

$$= \iiint (\overline{C}_{ijnm}^{11} \delta^N \frac{\partial^2 R_n^N}{\partial x_j \partial x_m} + \overline{C}_{ijnm}^{12} \delta^N \frac{\partial d_{nm}^{N-1}}{\partial x_j} + \overline{P}_i^V) \delta R_i dV +$$

$$+ \oiint (\overline{P}_i^F - \overline{C}_{ijnm}^{11} n_j \delta^N \frac{\partial R_n^N}{\partial x_m} - \overline{C}_{ijnm}^{12} n_j \delta^N d_{nm}^{N-1}) \delta R_i dF =$$

$$= \delta^N \{ \iiint (\overline{C}_{ijnm}^{11} \frac{\partial^2 R_n^N}{\partial x_j \partial x_m} + P_i^{VN}) \delta R_i dV + \oiint (P_i^{FN} - \overline{C}_{ijnm}^{11} n_j \frac{\partial R_n^N}{\partial x_m}) \delta R_i dF \} = 0 \qquad (2.82)$$

$$P_i^{VN} = \begin{cases} \overline{P}_i^V & npu \quad N = 0 \\ \overline{C}_{ijnm}^{12} \dfrac{\partial d_{nm}^{N-1}}{\partial x_j} & npu \quad N > 0 \end{cases} \qquad (2.83)$$

$$P_i^{FN} = \begin{cases} \overline{P}_i^F & npu \quad N = 0 \\ -\overline{C}_{ijnm}^{12} n_j d_{nm}^{N-1} & npu \quad N > 0 \end{cases} \qquad (2.84)$$

The auxiliary asymptotic process

In auxiliary iteration process there are two additional small parameters: parameter of multyscale-effects ε and parameter of adhesive effects a. We shall define with their help of the normalized tensors of modules of adhesion $\overline{A}_{ijnm}$ and modules of dislocation $\overline{C}_{ijnm}^{33}$.

The definition of the normalized tensors of modules of adhesion $\overline{A}_{ijnm}$: $\overline{A}_{ijnm} = \dfrac{A_{ijnm}}{\left\|A_{ijnm}\right\|}$

The definition of the normalized tensors of modules of dislocation $\overline{C}_{ijnm}^{33}$: $\overline{C}_{ijnm}^{33} = \dfrac{C_{ijnm}^{33}}{\left\|C_{ijnm}^{33}\right\|}$

In view of the entered definitions we have the following equation

$$\iiint (\overline{C}_{ijnm}^{22} d_{nm}^{\Xi} + \overline{C}_{ijnm}^{12} \delta \frac{\partial R_n}{\partial x_m} - \overline{C}_{inpq}^{33} \varepsilon^2 \frac{\partial^2 d_{pr}^{\Xi}}{\partial \overline{x}_m \partial \overline{x}_s} \Im_{rsq} \Im_{nmj}) \delta d_{ij}^{\Xi} dV -$$

$$- l \oiint (\overline{A}_{ijnm} a d_{nm}^{\Xi} - \overline{C}_{inpq}^{33} \varepsilon^2 n_m \Im_{nmj} \frac{\partial d_{pr}^{\Xi}}{\partial \overline{x}_s} \Im_{rsq}) \delta d_{ij}^{\Xi} dF = 0 \qquad (2.85)$$

Case, when small parameters of one order, i.e. $\varepsilon \sim \delta$ **and** $a \sim \delta$

Then, auxiliary iterative process (2.85) can be formulated as:

$$\iiint (\overline{C}_{ijnm}^{22} \delta^M d_{nm}^M + \overline{C}_{ijnm}^{12} \delta^{N+1} \frac{\partial R_n^N}{\partial x_m} - \overline{C}_{inpq}^{33} \delta^{M+2} \frac{\partial^2 d_{pr}^M}{\partial x_m \partial x_s} \Im_{rsq} \Im_{nmj}) \delta d_{ij}^{\Xi} dV -$$

$$- l \oiint (\overline{A}_{ijnm} \delta^{M+1} d_{nm}^M - \overline{C}_{inpq}^{33} n_m \Im_{nmj} \delta^{M+2} \frac{\partial d_{pr}^M}{\partial x_s} \Im_{rsq}) \delta d_{ij}^{\Xi} dF =$$

$$= \delta^N \{ \iiint (\overline{C}_{ijnm}^{22} d_{nm}^N + p_{ij}^N) \delta d_{ij}^{\Xi} dV - l \oiint (\overline{A}_{ijnm} d_{nm}^{N-1} - M_{ij}^N) \delta d_{ij}^{\Xi} dF \} = 0 \qquad (2.86)$$

If thus $\varepsilon \leq \delta$ and $a \leq \delta$ auxiliary process degenerates in algebraic connection between components free and constrained distortion.

Otherwise auxiliary iterative process as a regional problem takes place only then when at least one of parameters ε or a exceeds parameter of defectness δ :

1. small parameter of multyscale-effects ε more than small parameter of defectness δ : $\varepsilon > \delta$

2. small parameter of adhesive interactions a more than small parameter of defectness δ : $a > \delta$

Here we are interested with a case when the boundary problem concerning free distortion degenerates in algebraic. If this special case takes place, non-uniform generalized equations for moments (2.86) concerning free distortion degenerate in the algebraic equations. With the help of these algebraic equations components of the free distortion are excluded from system of the equations (2.82- (2.84):

$$p_{pq}^N = \begin{cases} 0 & npu \quad N = 0 \\ \overline{C}_{pqsr}^{12} \dfrac{\partial R_s^{N-1}}{\partial x_r} & npu \quad N > 0 \end{cases}$$

$$d_{nm}^{N-1} = -\overline{C}_{nmpq}^{-22} \overline{C}_{pqsr}^{12} \frac{\partial R_s^{N-2}}{\partial x_r}$$

Work of resulting force factors (last composed in (2.86)) which defines nonclassical boundary conditions is asymptotic neglible small. I.e. this work is equal to zero in asymptotic sense. Thus, the decision of the equations of the theory of mediums with kept dispositions in this case is reduced to a sequence of decisions of the classical theory of elasticity with the effective loadings dependent on even number of approximation.

$$P_i^{VN} = \begin{cases} \overline{P}_i^V & npu \quad N = 0 \\ -\overline{C}_{ijnm}^{12} \overline{C}_{nmpq}^{-22} \overline{C}_{pqsr}^{12} \dfrac{\partial^2 R_s^{N-2}}{\partial x_j \partial x_r} & npu \quad N > 0 \end{cases}$$

$$P_i^{FN} = \begin{cases} \overline{P}_i^F & npu \quad N = 0 \\[2mm] \overline{C}_{ijnm}^{12} n_j \overline{C}_{nmpq}^{-22} \overline{C}_{pqsr}^{12} \dfrac{\partial R_s^{N-2}}{\partial x_r} & npu \quad N > 0 \end{cases}$$

Case when the small parameter a is more the than others.

Assume that $a > \delta$ and $a > \varepsilon$. Let's also present $a = \delta^{\log_\delta a} > \delta$ and $\varepsilon = \delta^{\log_\delta \varepsilon} \le \delta$, then the variation equation for the auxiliary iterative process is possible to present in form:

$$\iiint (\overline{C}_{ijnm}^{22} \delta^N d_{nm}^N + \overline{C}_{ijnm}^{12} \delta^{M+1} \frac{\partial R_n^M}{\partial x_m} - \overline{C}_{inpq}^{33} \varepsilon^2 \delta^K \frac{\partial^2 d_{pr}^K}{\partial \overline{x}_m \partial \overline{x}_s} \Im_{rsq} \Im_{nmj}) \delta d_{ij}^\Xi dV - $$

$$- l \oiint (\overline{A}_{ijnm} \delta^{n+\log_\delta a} d_{nm}^n - \overline{C}_{inpq}^{33} \delta^{m+2\log_\delta \varepsilon} n_m \Im_{nmj} \frac{\partial d_{pr}^m}{\partial \overline{x}_s} \Im_{rsq}) \delta d_{ij}^\Xi dF = 0$$

Let's determine, at what n both m adhesive and multyscale-composed are essential.

$$\delta^{n+\log_\delta a} = \delta^N \qquad\qquad \delta^{m+2\log_\delta \varepsilon} = \delta^N$$

$$n = N - \log_\delta a \qquad\qquad m = N - 2\log_\delta \varepsilon$$

as $a > \delta$, then the numerical value of a parameter is equally $-\log_\delta a > 0$.

At such situation the asymptotic process is divergent. Thus, a problem follows to reformulate concerning the maximal small parameter. The similar situation will take place and for a case, when $\varepsilon > \delta$.

All these variants demand separate additional researches.

Method of the reduced loadings.

The free distortion it is determined from system of the algebraic equations and looks like:

$$d_{pq}^N = \begin{cases} 0 & npu \quad N = 0 \\[2mm] -\overline{C}_{pqij}^{-22} \overline{C}_{ijnm}^{12} \dfrac{\partial R_n^{N-1}}{\partial x_m} + \overline{C}_{pqij}^{-22} \overline{C}_{inpq}^{33} \dfrac{\partial^2 d_{pr}^{N-2}}{\partial x_m \partial x_s} \Im_{rsq} \Im_{nmj} & npu \quad N > 0 \end{cases}$$

If in last expression for free distortion to neglect local scale effects

$$d_{pq}^N = \begin{cases} 0 & if \quad N = 0 \\[2mm] -\overline{C}_{pqij}^{-22} \overline{C}_{ijnm}^{12} \dfrac{\partial R_n^{N-1}}{\partial x_m} & for \quad N > 0 \end{cases}$$

On the basis of the constructed ratio (2.82) - (2.84) the algorithm of the account of damage of material in the basic intense condition further is offered. This algorithm can be used for the account of damage (development of porosity and so on), in about of the ends of cracks; damage of material in zones of concentrators of pressure; damage of zone of plasticity connected to development in the mechanics of destructions (see works on gradient of plasticity [Hatchinson , 1997; Fleck, Hatchinson, 2001 and so on]. On the other hand the developed method of the reduced loadings can be considered as theoretically proved way of the account of development of damage in the filled composites and anisotropic composite materials under various conditions of loading. Certainly, for this purpose it is required to give

generalization stated before results on anisotropic mediums that is connected only to some technical difficulties connected to increase of quantity independent component of tensors of modules C_{ijnm}^{pq} and A_{ijnm}.

Algorithm:

1) $N = 0$. As consequence, thus $d_{pq}^0 = 0$.

Displacement to zero approximation R_i^0 is determined on known loadings as the decision of a classical regional problem:

$$\{ \iiint (C_{ijnm}^{11} \frac{\partial^2 R_n^0}{\partial x_j \partial x_m} + P_i^{V0}) \delta R_i dV + \iint (P_i^{F0} - C_{ijnm}^{11} n_j \frac{\partial R_n^0}{\partial x_m}) \delta R_i dF \} = 0$$

2. $N = 1$. It is determined of the free distortion as a first approximation d_{pq}^1

$$d_{pq}^1 = -C_{pqij}^{-22} \overline{C}_{ijnm}^{12} \frac{\partial R_n^0}{\partial x_m}, \quad (d_{pq}^0 = 0)$$

3. The reduced loadings in the basic process for definition of displacements of the first approximation are determined:

$$P_i^{V1} = \overline{C}_{ijnm}^{12} \frac{\partial d_{nm}^{1-1}}{\partial x_j} = 0, \quad P_i^{F1} = 0$$

4. There are displacements for the first approximation: $R_i^1 = 0$

5. It is determined of the free distortion for the second approximation $d_{pq}^2 = 0$

6. The reduced loadings in the basic process for definition of displacements for the second approximation are determined:

$$P_i^{V2} = \overline{C}_{ijnm}^{12} \frac{\partial d_{nm}^1}{\partial x_j}, \quad P_i^{F2} = -\overline{C}_{ijnm}^{12} n_j d_{nm}^1$$

7. There are displacements for the second approximation as the decision of the following regional problemof the classical theory of elasticity:

$$\iiint (C_{ijnm}^{11} \frac{\partial^2 R_n^2}{\partial x_j \partial x_m} + P_i^{V2}) \delta R_i dV + \iint (P_i^{F2} - C_{ijnm}^{11} n_j \frac{\partial R_n^2}{\partial x_m}) \delta R_i dF \} = 0,$$

$$P_i^{V2} = \overline{C}_{ijnm}^{12} \frac{\partial d_{nm}^1}{\partial x_j}, \quad P_i^{F2} = -\overline{C}_{ijnm}^{12} n_j d_{nm}^1$$

Further for realization of algorithm points 1-4 for definition d_{pq}^3, P_i^{V3} P_i^{F3}, R_i^3 etc repeat.

The common decision of a problem with the account of damage is in the form of decomposition:

$$R_i = \sum_{N=0}^{S} R_i^N \delta^N, \quad \left\| C_{ijnm}^{12} \right\| = \delta$$

As a whole constructed so the decision depends on two parameters μ^{12}, λ^{12} and two parameters μ^{22}, λ^{22} (if to accept, that $\chi^{pq} = 0$). Thus the following conditions should be observed: $\varepsilon \leq \delta$ and $a \leq \delta$. Generally all these parameters should be found as a result of data processing experimental researches of a material, for example, curves describing process of dependence of degradation of mechanical properties from parameter of process (amplitude of loading at quasi-static loading or numbers of cycles loading etc.).

If we are limited to the basic process on parameter δ we a priori should assume that inequalities $\varepsilon \leq \delta$ and $a \leq \delta$ are carried out. Generally speaking, these assumptions should be checked up by experimental way.

CONCLUSIONS

1. It is shown in the present part that the defects of all known types can be described in the framework of the presently developed theory (or classification) of defects. The choice of certain type of kinematic structure of the continuous medium with defects is determined by a requirement to describe certain physical properties of medium under study. For example, the models constructed on the basis of the Cauchy media principally cannot be used for developing a theory of fine dispersed composite materials. Indeed, the fine dispersed inclusions can be treated as dislocations in the parent phase or in the matrix. The same is true for the poorly degased matrix. In this case the gas bubbles can be treated as vacancies. Such dislocations cannot be born or disappear. Therefore the theory of fine dispersed composite materials can be developed only on the basis of the model of continuum media with defects of the first level with conserved dislocations. If the phase transitions take place in the continuous medium then they can be connected with the birth of defects – dislocations in the parent phase. It is wrong to attempt to develop such a medium model on the basis of the Papkovich-Cosserat continuous media. As a minimum, the required model in such case will be the Saint-Venant continuous media model with the generatable dislocations and conserved disclinations.

2. On a basis of variational kinematical principle the full and correct model of mediums with conserved dislocations is given. The special attention is given to the analysis of kinematical correlations for at the variational description kinematics of medium completely determines the system of internal interactions in volume and on the surface of the considered body. On the basis of the carried out kinematical analysis the new classification of the dislocations is offered. This classification allows describe three types of dislocations: γ - dislocations, θ - dislocations, ω dislocations.

This classification, in the first, gives new kinematical interpretation of dislocations as reflects connection of dislocations with distortion-γ, with change of volume θ (porosity) and with twisting ω (curls or spins). The offered classification actually allows predicting of the special cases of dislocations when in the medium only one or two types of dislocations dominate. So, for example, in the medium with the distributed defects the dislocations generated only by free rotational displacements ω_k^{Ξ} can be dominating.

The porous medium also can be considered as a special case of the general model. In the porous medium dominate the dislocations generated only by free volume change θ^{Ξ}.

At last, medium concerns to special models with one dominating type of dislocations with eight degrees of freedom R_i, γ_{ij}^Ξ . The dislocations generated only by free distortion γ_{ij}^Ξ here dominate. It is obvious, that thus $d_{ij}^\Xi = \gamma_{ij}^\Xi$. Similarly it is possible to predict presence of mediums with two types of dislocations.

In works [Lurie S, Belov P, Volkov-Bogorodsky D, Tuchkova N, 2003; Lurie S., Belov P., Tuchkova N. 2004; Lurie S, Belov P, Volkov-Bogorodsky D, 2002], the model of such medium has been considered. There the dislocations generated by free distortion γ_{ij}^Ξ were neglected. On its basis it is constructed a continual variant of the theory of interphase interactions [Lurie S, Belov P, Volkov-Bogorodsky D, Tuchkova N, 2003; Lurie S., Belov P., Tuchkova N., 2004]. This theory has allowed modeling and explaining known scale effects in mechanics of fine-dyspersated composites, determined by cohesive and adhesive local interactions. The classification offered in the presented part of work allows to consider also one more special case of mediums, where it is possible to neglect either θ^Ξ (not porous mediums) or ω_k^Ξ (spinless mediums). As far as it is known to authors, such mediums were not investigated yet.

The offered classification is proved and from the physical point of view as shows physical meaning of various types of dislocations. So, it is proved, that the specified types of dislocations: γ - dislocations, θ - dislocations, ω - dislocations give corresponding, mutually independent components in the basic, slow variable part of density of strain energy. These shares of potential energy have no cross terms. Thus, presence of a nonclassical, not local component of the potential energy connected to defects - dislocations is rather unexpected for gradient models, which is the model of mediums with system of the distributed dislocations.

Use in the given work of the consecutive variational approach and the detailed analysis of boundary conditions, has enabled to formulate the consistent and coordinated boundary problem for mediums with conserved dislocations with nine boundary conditions in each nonexceptional point of a surface. It speaks that at the consecutive variational formulation of a problem, the coordination of mathematical statement is always achieved.

At last, it is necessary to note, that within the framework of the offered model the spectrum of scale effects in volume and on a surface is taken into account. Really, the account of invariants of the dislocation pseudotensor $C_{ijnm}^{33} \Xi_{nm} \Xi_{ij}$ in terms of potential energy with inevitability results in scale effects in volume. On the other hand, the account of energy of adhesion in expression of potential energy results in modeling the scale effects on the surface, as dimension of tensor *A* differs from dimension of the Young modules. Apparently, the submitted generalized model of mechanics of continua is the first correct theoretical model, in which various special scale effects (cohesion interactions, a surface tension and so forth) in volume and on a surface are modeled within the framework of unified continual description.

The Klapeiron's and Dupre's theorems were proved. The Klapeiron's Theorem is the fundamental theorem of any model of the solid medium. This theorem allows to connect the potential energy and the work of the external forces in accurate solution for the appropriate boundary-value problem. Dupre's equation defines the connection between of the work of external forces for system of two bodies with adhesive interaction contact, the potential energies of these

bodies and the energy of their adhesive interaction. Thus, Dupre's equation is the mathematical formulation of Klapeyron's theorem for this system of bodies. Using «Dupre's theorem» we can to define in the direct experimental way the energy of adhesive interaction of bodies on the basis of Young's equation.

3.	The algorithm of the account of damage of material in the basic intense condition further is offered. This algorithm can be used for the account of damage (development of porosity and so on), in about of the ends of cracks; damage of material in zones of concentrators of pressure; damage of zone of plasticity connected to development in the mechanics of destructions. On the other hand the developed method of the reduced loadings can be considered as theoretically proved way of the account of development of damage in the filled composites and anisotropic composite materials under various conditions of loading.

REFERENCES

Annual Report 2002.

Annual Report 2003.

Intermediate Report 2004

Aifantis E.C., Gradient effects at the macro, micro and nano scales. *J. Mech. Behav. Mater.,* Vol. 5 No. 3, pp. 335-353, 1994.

Aifantis E.C., Strain gradient interpretation of size effects. *Int. J. Fracture,* 95, pp. 299-314, 1999.

Belov P., Lurie S., Bodunov A., and etc. On modeling of scale effects in thin structures //Mechanics of composite materials and structures. 2002, v.8. N4. p.78-88

Cosserat E., Cosserat F., Theore des corps deformables, Paris, Hermann. 1909.

De Wit R., The Continual Theory of the Stationary Dislocations. *Solid State Physics*, Vol. 10, 249 p., N. Y., 1960.

De Wit R., Theory of dislocations: continuous and discrete disclinations in isotropic elasticity, *J. of Research of the National Bureau of Standards*, 77A, No. 3, pp. 359-368, 1973.

Fleck, N.A., and Hutchinson, J.W., A phenomenological theory for strain gradient effects in plasticity. *J. Mech. Phys. Solids*, 41, pp. 1825-1857, 1993.

Fleck, N.A., and Hutchinson, J.W., A reformulation of strain gradient plasticity. *J. Mech. Phys. Solids*, 49, pp. 2245-2271, 2001.

Fleck, N.A., and Hutchinson, J.W., Strain gradient plasticity. *Advanced in Applied Mechanics*, 33. pp 295-361, 1997.

Gao, H., Huang, Y., Nix, W.D., and Hutchinson, J.W., Mechanism-based strain gradient plasticity – I. Theory. *J. Mech. Phys. Solids*, 47, pp. 1239-1263, 1999.

Gutkin M.Yu., Nanoscopics of dislocations and disclinations in gradient elasticity. *Reviews of Advanced in Materials Science*, Vol.1, No.1, pp. 27-60, 2000.

Kadic, A., and Edelen D.G.B., *A Gauge Theory of Dislocations and Disclinations*. Lect. Notes in Physics, Springer, Berlin-Heidelberg, Vol. 174, 168 p., 1983.

Kroner E., Dislocations and Continuum Mechanics. *Appl. Mech. Rev.,* 15, pp. 599-606, 1962.

Kroner E., *Gauge Field Theories of Defects in Solids.* Stuttgart: Max-Plank Inst., 1982.

Likhachev, V.A., Volkov A.E., and Shudegov V.E., *Continuum Theory of Defects,* Leningrad State Univ. Publ., Leningrad, 228 p., 1986, in Russian.

Lurie S, Belov P, Volkov-Bogorodsky D, Multiscale Modeling in the Mechanics of Materials: Cohesion, Interfacial Interactions, Inclusions and Defects.//In book Analysis and Simulation of Multifield Problems, Springer, 2003; 12 p. 101-110.

Lurie S, Belov P, Volkov-Bogorodsky D, Tuchkova N, Nanomechanical Modeling of the Nanostructures and Dispersed Composites, Int. J. Comp Mater Scs 2003; 28(3-4):529-539

Lurie S. Belov P. Mathematical models of the mechanics of solids and physical fields. Scientific publication of Computing Centre RAS.2000.P.151

Lurie S., Belov P. Variation Model of Nonholonomic Mediums // Mechanics of composite materials and structures. ,2001, т.7, N 2, p. 157-166.

Lurie S., Belov P., Tuchkova N. The Application of the multiscale models for description of the dispersed composites// Int. Journal "Computational Materials Science" A., 2004, 36(2):145-152.

Lurie S.A. Belov P.A., Babeshko A.V. and ets. Multiscale modeling in the solid mechanics// Mechanics of composite materials and structures. 2002, v.8. N1, p. 71-82

Lurie S.A. Obraztsov I.F. end etc. On the new Cohesion Field Model in Solid // News High School, North - Caucasian Region, vol.3, 2000 (devoted to the eight-decade of academician Vorovich I.I. Russian Academy of Sciences), 110-118 p.

Lurie S.A., Belov P.A. Solid Mechanics Deformation Model and analogies in Field Theory// Mechanics of Solids, p.157-166. - Allerton Press, Mehanika tverdogo tela, Inc. 1998., No 3. P. 157-166

Mindlin R.D. Micro-structure in linear elasticity, Arch. Ration. Mech. And Analysis, 1, 51-78 (1964)

Mindlin R.D., Tiersten H.F. Effects of the couple-stress in linear elasticity, Arch. Ration. Mech. And Analysis, 11, 415-448 (1962)

Nabarro F.R.N., *Theory of Crystal Dislocations*. Oxford Univ. Press, Oxford, 1967.

Obraztsov I.F. Lurie S.A. Belov.P.A. On the Generalized Expansions in Applied Theory of Elasticity and Some its Application to Composite Structures // Mechanics of Composite Materials and Design, 1997, № 3, с. 62-79.,.

Toupin R.A., Theories of elasticity with couple-stress, Arch. Ration. Mech. And Analysis, 2, 85-112 (1964)

3. THE THEORY OF INTERPHASE LAYER

Introduction

Recently, in the papers [Lurie S, Belov P, Volkov-Bogorodsky D, Tuchkova N, 2003; Lurie S, Belov P, Volkov-Bogorodsky D, Springer, 2003], the generalized continuum model with kept dislocations was developed. The mathematical statement of the model was given. This statement may be considered as the generalization of the Cosserat theory of pseudo-continuums. Generally, the model presented allows to describe local-cohesion interactions[Lurie S, Belov P, Volkov-Bogorodsky D, Tuchkova N, 2003] and superficial effects[Lurie S, Belov P, Volkov-Bogorodsky D, Springer, 2003].

On base of the continual theory of medium with kept defects the simplest variant of the cohesion interactions and superficial effects model is constructed. This model, represents nonclassical generalization of the theory of elasticity, and takes into account the "main", most essential contribution of scale effects from the point of view offered by authors of the common classification of models with scale effects [Lurie S.A., Belov P.A., Babeshko A.V., Yanovskii Y.G., 2002].

Analytical estimations of properties of a biphase material near boundaries of the phases, taking into account nonclassical effects are given. Geometrical and mechanical properties of the cohesion interphase layer were received by the formal way. The interphase layer basic properties are specified.

In result, formal theoretical bases of the cohesion-adhesive model of an interphase layer are constructed.
In the given section on the basis of the previous researches the theory of an interphase layer is formulated. The description of the interphase layer theory and some main applications include the following moments:
- the formal mathematical statement,
- the physical constitutive equations,
- the identification problem of the parameters determining nonclassical effects,
- the qualitative analysis of the theory-analytical estimations of properties of an interphase layer,
- the qualitative analysis of the theory-estimation of an interphase layer influence on the effective characteristics of a composite,
- some application for quantum mechanical approaches,
- numerical modeling of the stress state of the cell with inclusions and some notes about specific averaging procedures for filled composites,
- previously results of the generalized Eshelby problem

3.1. THE FORMAL MATHEMATICAL STATEMENT FOR INTERPHASE LAYER THEORY. BASED EQUATIONS.

The interphase layer theory allows to study the specific local interactions which determining features of the properties of contacting phases and material as whole:
1. cohesion fields and the internal interactions associated to them.
interfacial adhesive interactions
The marked types of interactions are characterized by essential localness, small area of interaction, concentrate about defects, borders, interfaces.
The following requirements were formulated for correct nonclassical:
The models have to describe the behavior of the deformed media taking into accounts the scale effects (among the physical parameters of the models there should be the constants of various dimensions).
The total deformation energy has to depend not only on the volumetric density of energy, but also on the surface density of deformation energy which could not to be reduced to some volumetric deformation energy. The surface effects and scale effects are determined by the phase interfaces.
The deformation models have to be consistent and correct.

The generalized models of deformation taking into accounts the scale effects may not contradict the classical models, and have to include them as a limiting case.

Further on the basis of variant of the defects (dislocations) preserving continuum theory, with use of system of additional assumptions the particular variant of moment cohesion model the appropriate superficial phenomena was offered. In the report (Technical Report 01.04.03 – 30.04.03) the reasonable set of the specified system of additional simplifications was given.

General mathematical statement is formulated. This mathematical statement is completely determined by following equation for the Lagrange functional and the following variational equation:

$$\delta L = 0,$$

$$L = A - \frac{1}{2}\iiint \left[2\mu\gamma_{ij}\,\gamma_{ij} + (\frac{2\mu}{3}+\lambda)\theta^2 + 8\frac{\mu^2}{C}\xi_{ij}\,\xi_{ij} + \frac{(2\mu+\lambda)^2}{C}\theta_i\,\theta_i\right]dV \qquad (3.1)$$

$$-\frac{1}{2}\oiint [D_{ij}\dot{R}_i\dot{R}_j]dF$$

where

$$\theta_i = \frac{\partial\theta}{\partial x_i} = \frac{\partial^2 R_j}{\partial x_i \partial x_j}, \quad \xi_{ij} = \frac{1}{2}\frac{\partial\omega_i}{\partial x_j}+\frac{1}{2}\frac{\partial\omega_j}{\partial x_i} = -\frac{1}{4}\frac{\partial^2 R_n}{\partial x_j \partial x_m}\Im_{nmi} - \frac{1}{4}\frac{\partial^2 R_n}{\partial x_i \partial x_m}\Im_{nmj}$$

and $D_{ij} = A\,n_i n_j + B\,(\delta_{ij} - n_i n_j)$

Here, R_i are the components of the displacement vector, γ_{ij} and θ are the components of the deviator of strain and spherical deformation tensor, ω_k are the components of the rotation vector, $\dot{R}_i$ is normal derivation of the displacement vector on the surface; $\Im_{ijk}$ is the Levi-Civita tensor, δ_{ij} is the Kronecker delta, $\omega_k = -\frac{1}{2}\frac{\partial R_i}{\partial x_j}\Im_{ijk}$,

n_i is the normal vector to surface, $\frac{\partial\omega_i}{\partial x_j} = \xi_{ij} + \frac{1}{3}\xi\delta_{ij} - \xi_k\Im_{ijk}$, $\frac{\partial\theta}{\partial x_j} = \theta_j$, μ,λ are the Lame coefficient, and

C is the physical constant that determine the cohesion interactions.

It is worth emphasizing that the cohesion interaction model proposed contains only one new physical constant C as compared to the classical theory of elasticity. This constant has the dimension that differ from the dimensions of the Lame coefficients, and differ from them on a square of length. In the work [Lurie S., Belov P., Volkov-Bogorodsky D., Tuchkova N., 2003; Lurie S., Belov P., Volkov-Bogorodsky D., 2003], it was shown that the constant C in (3.1) is related to conventional parameters of the fracture mechanics for a brittle material. In the given work, material mechanical and geometrical characteristics of an interphase layer will be defined with the help of this constant model for each of phases in a composite.

Coefficient B is responsible for the surface effects at each point of the surface within the tangential plane. The coefficient A is responsible for the interaction normal to the surface. Both of coefficients in (3.1)correspond to the interactions of adhesion type. In any event the surface effects describe the local effects, which are concentrated near the domain boundaries.

Constitutive equations

Within the framework of the submitted statement the constitutive equations of model are specified. Let's write the constitutive equations:

Stresses fields are defined by classical equations: $\sigma_{ij} = \frac{\partial U_V}{\partial(\partial R_i^0/\partial x_j)} = 2\mu\gamma_{ij} + (\frac{2\mu}{3}+\lambda)\theta\delta_{ij}$

and moment stresses:

$$m_{ij} = \frac{\partial U_V}{\partial \Xi_{ij}} = 8\frac{\mu^2}{C}\xi_{ij} + \frac{(2\mu+\lambda)^2}{C}\theta_k \Im_{ijk} \tag{3.2a}$$

On any plane with a normal n_i the vector of forces can be determined

$$T_i = \{2\mu\gamma_{ij} + (\frac{2\mu}{3}+\lambda)\theta\delta_{ij} + l_0^2[2\mu\Delta\omega_n\Im_{ijn} - \frac{(2\mu+\lambda)^2}{\mu}\Delta\theta\delta_{ij}]\}n_j +$$

$$+ l_0^2(\delta_{qj} - n_q n_j)\frac{\partial}{\partial x_q}[-2\mu(\frac{\partial\omega_k}{\partial x_p} + \frac{\partial\omega_p}{\partial x_k})n_p\Im_{ijk} + \frac{(2\mu+\lambda)^2}{\mu}\frac{\partial\theta}{\partial x_k}n_k\delta_{ij}] \tag{3.2b}$$

and moment vector

$$M_i = l_0^2[-2\mu(n_m n_j\Im_{ijn} + n_n n_j\Im_{ijm})\frac{\partial\omega_n}{\partial x_m} + \frac{(2\mu+\lambda)^2}{\mu}\frac{\partial\theta}{\partial x_k}n_k n_i] \tag{3.2c}$$

On a vector T_i it is possible to establish the effective normal stresses in a direction of a normal n_p and effective shear stresses in the appropriate tangent plane. Normal a component looks like: $\tilde{\sigma}_{ii} = T_i n_i$, two components of tangent components of stresses are equal: $\tilde{\sigma}_{ij} = T_i(\delta_{ij} - n_i n_j)$, $\quad n_j((\delta_{ij} - n_i n_j) = 0$.

Correct boundary problem

Integration by parts allows constructing a correct boundary problem, which gives mathematical statement in moment adhesive-cohesion model: The variation statement of this model leads to the following mathematical formulation of the problem:

$$\iiint\{L_{ij}[-\frac{l_0^2}{\mu}L_{ij}(..) + \delta_{jk}(..)]R_k + P_i^V\}\delta R_i dV + \iint\left[(M_i - D_{ij}\dot{R}_j)\delta\frac{\partial R_i}{\partial x_q}n_q dF + (P_i^F - T_i)\delta R_i\right]dF = 0, \tag{3.3}$$

on any plane with a normal n_i on the boundary surface the vector of forces T_i is determined

$$T_i = \{2\mu\gamma_{ij} + (\frac{2\mu}{3}+\lambda)\theta\delta_{ij} + l_0^2[2\mu\Delta\omega_n\Im_{ijn} - \frac{(2\mu+\lambda)^2}{\mu}\Delta\theta\delta_{ij}]\}n_j + l_0^2(\delta_{qj} - n_q n_j)\frac{\partial}{\partial x_q}[-2\mu(\frac{\partial\omega_k}{\partial x_p} + \frac{\partial\omega_p}{\partial x_k})n_p\Im_{ijk} + \frac{(2\mu+\lambda)^2}{\mu}\frac{\partial\theta}{\partial x_k}n_k\delta_{ij}]$$

and moment vector $\quad M_i = l_0^2[-2\mu(n_m n_j\Im_{ijn} + n_n n_j\Im_{ijm})\frac{\partial\omega_n}{\partial x_m} + \frac{(2\mu+\lambda)^2}{\mu}\frac{\partial\theta}{\partial x_k}n_k n_i]$.

Here Δ is the Laplace operator, $l_0^2 = \frac{\mu}{C}$, R_i are components of the displacement vector, γ_{ij} and θ are the components of the deviator of strain and spherical deformation tensor, ω_k are the components of the rotation vector, $\Im_{ijk}$ is the Levi-Civita tensor, δ_{ij} is the Kronecker delta, μ, λ are the Lame coefficient, C is the physical constant that determine the cohesion interactions (Annual Report 2002,2003), P_i^V is the vector of density of the external loads over the body volume, P_i^F is the vector of density of the surface load, F is the boundary surface and $L_{ij}(...)$ is the operator of the classical theory of elasticity, that is, $L_{ij}(...) = \mu\Delta(...)\delta_{ij} + (\mu+\lambda)\frac{\partial^2(...)}{\partial x_i \partial x_j}$,

$D_{ij}\dot{R}_i\dot{R}_j = A\ n_i n_j\dot{R}_i\dot{R}_j + B\ (\delta_{ij} - n_i n_j)\dot{R}_i\dot{R}_j$ is energy, which associated with changing of defectiveness of a surface of contact because modified a surface.

New physical constants A and B determine the surface effects associated with the normal to the surface of the body, and the superficial effects in the tangent plane respectively. Note that the ideal adhesive interactions influences only for a local state and does not change classical boundary conditions.

To understand the physical sense let's define displacement of cohesion field. Let's name a vector of the cohesion displacement the following vector:

$$u_i = -\frac{1}{C}L_{ij}(R_j) = -\frac{1}{C}[(2\mu+\lambda)\frac{\partial^2 R_j}{\partial x_i \partial x_j} + \mu(\delta_{ij}\Delta R_j - \frac{\partial^2 R_j}{\partial x_i \partial x_j})] \tag{3.4}$$

Using (3.2) we receive the equations for a vector function u_i (3.3):

$$(2\mu+\lambda)\frac{\partial^2 u_j}{\partial x_i \partial x_j} + \mu(\Delta u_i - \frac{\partial^2 u_j}{\partial x_i \partial x_j}) - Cu_i + P_i^V = 0 \tag{3.5}$$

or $\quad H_{ij}(u_j) + P_i^V = 0$, where $H_{ij}(...) = L_{ij}(...) - C(...)\delta_{ij}$

Similarly we shall enter definition of a vector of classical displacements U_i. In the equation (3.3) it is possible to change a sequence of action of operators. Then we shall receive the following definition of a vector U_i:

$$U_i = [-\frac{1}{C}L_{ij}(...) + (...)\delta_{ij}]R_j = -\frac{(2\mu+\lambda)}{C}\frac{\partial^2 R_k}{\partial x_j \partial x_k} - \frac{\mu}{C}(\Delta R_j - \frac{\partial^2 R_k}{\partial x_j \partial x_k}) + R_j \tag{3.6}$$

Obviously, the vector U_i is satisfies to the classical equations of balance:

$$(2\mu+\lambda)\frac{\partial^2 U_j}{\partial x_i \partial x_j} + \mu(\Delta U_i - \frac{\partial^2 U_j}{\partial x_i \partial x_j}) + P_i^V = 0$$

Taking into account definitions (3.6) for U_i and definitions (3.4) for u_i the general solution of the equations (3.3) it is possible to present as the following decomposition:

$$R_i = U_i - u_i \tag{3.7}$$

Thus, the boundary value problem (3.3) represents the couple boundary value problem for the classical solution and the solution for cohesion fields model. The boundary value problem generally is not divided.

The formulas (3.3)-(3.6) show the structure of solution in framework of the model with scale effects.

3.1.1. Particular models.

Let us consider the formal two and one-dimensional statements of the boundary problems.

Two dimensional problem

Projections of the load to the ort Z_i vanish: $P_i^V Z_i = 0$ and $P_i^F Z_i = 0$. Similarly, projections of the displacement to the ort Z_i vanish: $R_j Z_j = 0$: $r_i = R_j(\delta_{ij} - Z_i Z_j) \implies r_i Z_i = 0$. The displacement vector r_i is the function of two coordinates, i.e. it is independent of z, $z = x_j Z_j$: $\frac{\partial r_i}{\partial x_j}Z_j = 0$. Hence, the volumetric strain and the rotation vector are

$$\theta = \frac{\partial r_p}{\partial x_q}(\delta_{pq} - Z_p Z_q) \qquad \omega_k = \omega Z_k, \quad \omega = -\frac{1}{2}\frac{\partial r_p}{\partial x_q}Z_s \Im_{pqs}$$

Thus, it is assumed that the displacement vector is determined in plane area Ω with the boundary G. Variational equation (3.3) is reduced to: $R_i = r_s s_i + r_n n_i$

$$\iint\limits_{\Omega} [[-\frac{1}{C}L_{ij}(...) + (...)\delta_{ij}]L_{jk}(r_k) + P_i^V]\delta r_i dxdy -$$

$$-\oint [\frac{\mu^2}{C}(\ddot{r}_s - \frac{\partial \dot{r}_n}{\partial s}) + B\,\dot{r}_s]\delta \dot{r}_s ds - \oint [\frac{(2\mu+\lambda)^2}{C}(\ddot{r}_n + \frac{\partial \dot{r}_s}{\partial s}) + A\,\dot{r}_n]\delta \dot{r}_n ds +$$

$$+ \oint\limits_{G(n_i Z_i = 0)} \{P_s^F - [\mu \dot{r}_s + \mu \frac{\partial r_n}{\partial s} - \frac{\mu^2}{C}\nabla^2(\dot{r}_s - \frac{\partial r_n}{\partial s})] + \frac{(2\mu+\lambda)^2}{C}(\frac{\partial^2 \dot{r}_s}{\partial s^2} + \frac{\partial \ddot{r}_n}{\partial s})\}\delta r_s dF +$$

$$+ \oint\limits_{G(n_i Z_i = 0)} \{P_n^F - [(2\mu+\lambda)\dot{r}_n + \lambda \frac{\partial r_s}{\partial s} - \frac{(2\mu+\lambda)^2}{C}\nabla^2(\frac{\partial r_s}{\partial s} + \dot{r}_n)] - \frac{\mu^2}{C}(\frac{\partial \ddot{r}_s}{\partial s} - \frac{\partial^2 \dot{r}_n}{\partial s^2})\}\delta r_n dF = 0$$

(3.8)

In the last equation the contour integrals (the second line) are equal to zero when the considered plane area G has no angular points.

In particular case the problem is reduced to the boundary value problem with respect to a scalar function, determined within the Ω with the boundary G. The scalar component of displacement may be three-dimensional, two-dimensional and one-dimensional function of coordinates. Two variants will be considered: two-dimensional and one-dimensional cases.

One dimensional problem

Let us consider the formal one-dimensional statement of the problem. Projections of the load to the orts Y_i and Z_i vanish: $P_i^V Y_i = P_i^V Z_i = 0$ and $P_i^F Y_i = P_i^F Z_i = 0$. The displacement vector is collinear to X_i axis: $R_i = rX_i$, $R_j Y_j = R_j Z_j = 0$. The single projection r of vector R_i does not depend on coordinates y and z: $y = x_j Y_j$ и $z = x_j Z_j$ $\frac{\partial r}{\partial x_j}(\delta_{ij} - X_i X_j) = 0$.

Then the variational equation is reduced to

$$\int\limits_0^l [EF(r'' - \frac{E}{C}r'''') + (P_i^V X_i)]\delta r dx + [EF(-\frac{E}{C})\ddot{r} - A_2 \dot{r} - A_1 r]\delta \dot{r}\,\Big|_{x=0}^{x=l} +$$

$$+ [(P_i^F X_i) - EF(\dot{r} - \frac{E}{C}\ddot{r}) - Ar - A_1 \dot{r}]\delta r\,\Big|_{x=0}^{x=l} = 0$$

(3.9)

The equations (3.3), (3.8), (3.9) give the full mathematical 3-D, 2-D and 1-D statements for the models that allow to describe the deformation of the mediums taking into account cohesion types interactions and surface effects.

The statement (3.9) is base for receiving of the analytical solutions and for analytical estimations of the mechanical properties of the interphase layer.

3.2. SOME QUALITATIVE ANALYSIS OF RESULTS.
EQUIVALENT TREATMENTS OF THE INTERPHASE LAYER.

The purpose of our consideration is the approached estimations of properties of the non-homogeneous continuums, based on consecutive and strict theoretical positions.

For an explanation of phenomenons of scale effects in mechanics of materials authors of the report proposed to use the simplest variant of the correct and variation-coordinated model. For the greater clearness it was used the simplified, one-dimensional statement of the problem, allowing to receive the analytical solution of a problem within the framework of nonclassical model (Annual Report 2003, Annual Report 2004). It allowed clearing physical sense of scale effects to specify a range of change of known parameters of a material at which scale effects can be shown in the form of mechanical effects, nonconventional from the point of view of the classical description.

To describe the interphase layer properties let's remind the main stages of preliminary composite structure investigations. The compound of biphase strictures were considered. One dimension consideration was used as basis. The following parameters of phases were taken into account: a) the length of the first phase is ($x_0 \le x < x_1$), physical parameters of first phase are determined by Joung's moduli E_M and the cohesion moduli C_M, b) the length of the second phase is ($x_1 < x \le x_2$), physical parameters of second phase are determined by Young's moduli E_D and the cohesion moduli C_D. The line $x = x_1$ is contact of phases. The compound fragment was loaded with the tension on the edges $x = x_0$ and $x = x_2$. The following steps was done:

-The equilibrium equations were solved for each fragment separately. The exact common solution for compound fragment was found.

-Potential energy of a compound fragment can be calculated using exact solutions for fragments and contact problem as whole.

-Comparing this potential energy of a compound fragment with potential energy of the equivalent homogeneous fragment of material allow to find the effective mechanical properties for the compound of biphase strictures in framework of the multiscale research.

The direct calculation of the potential energy of a compound fragment gives:

$$\Theta = \frac{\sigma^2 F}{2}\left[\frac{[(x_1 - x_0) - x_f]}{E^M} + \frac{[(x_2 - x_1) + x_f]}{E^D}\right]$$
(3.10)

Using equation (3.9) we can write the following equation

$$\frac{l}{E_0} = \frac{(l_M - x_f)}{E^M} + \frac{(l_D + x_f)}{E^D}$$
(3.10a)

where $l = (x_2 - x_o)$ are the full length of a compound fragment, $l_M = (x_1 - x_0)$, $l_D = (x_2 - x_1)$, E_0 is moduli of elasticity of an equivalent homogeneous fragment, $l_M^0 = (x_1 - x_0)$ is the length of the individual element of the first phase (matrix) in the considered combined element; $l_D^0 = (x_2 - x_1)$ is the length of the individual element of the second phase (inclusion) in the considered combined element. The equation (3.10a) models a compound cell as a certain biphase material with the modified volumes of phases, due to the account of a boundary interphase layer. Natural reduction interphase a cohesion layer to mechanical characteristics of two phases takes place.

Effective length of interphase layer x_f

It is interesting to note, that definition of thickness of an interphase layer is connected to size x_f. The given thickness of an interphase layer accordingly to properties of a matrix and inclusion, is equal x_f and occupies a part of volume of a "weak" material of a matrix, adding a part of effective volume of a rigid phase of inclusion. Having in view of, that the generalized characteristic x_f, it is easy to specify connection of the received result with results of modelling on model of an effective field (effective matrix) Mori and Tanaka (Mori and Tanaka, 1973) and models of an effective continuum (Hershey, 1954; Hill, 1962, 1965; Budiansky, 1965; Budiansky and O'Connell, 1976; O'Connell and Budiansky, 1974).

The formula for energy of deformation of a considered fragment can be written in the other view

$$\Theta = \frac{\sigma^2 F}{2}\left[\frac{l_1}{E_1} + \frac{l_2}{E_2} + \frac{l_f}{E_f}\right]$$
(3.11)

where $l_1 + l_2 + l_f = l$, $l_1 = (x_1 - x_0) - x_M$, $l_2 = (x_2 - x_1) - x_D$, $l_f = x_M + x_D$,

$E_1 = E^M$, $E_2 = E^D$, E_f - the moduli of elasticity of "an interphase layer"

$x_M = (1 - e^{-2a_M(x_1-x_0)})/a_M(1 + e^{-2a_M(x_1-x_0)})$, $x_D = (1 - e^{-2a_D(x_2-x_1)})/a_D(1 + e^{-2a_D(x_2-x_1)})$,

Let's notice, that the formula (3.11) allows to find the average moduli of elasticity of an equivalent homogeneous fragment through characteristics of phases:

$$E_0 = (x_2 - x_0) \left[\frac{l_1}{E_1} + \frac{l_2}{E_2} + \frac{l_3}{E_f} \right]^{-1}$$

(3.12)

Equality (3.12) shows, that the offered model naturally enters definition of the fictitious interphase layer connected with by cohesion interactions, located about border of contact of phases. As consequence, energy of interaction corresponds to a compound cell from three phases which in the given modelling problem are averaged under Reuss's scheme. Thus the general length of a compound fragment is kept constant that the part of an interphase layer x_M lays in a matrix, and other part x_D - in inclusion. Hence, the layer of a matrix in length $l_1 = (x_1 - x_0) - x_M$ has the moduli equal to the moduli of a matrix $E_1 = E^M$. The layer of inclusion in length $l_2 = (x_2 - x_1) - x_D$ has the moduli equal to the moduli of inclusion $E_2 = E^D$. The third phase is interphase layer in length $l_3 = x_M + x_D$. Its moduli is determined by the mechanical and geometrical parameters of a matrix and inclusion and adhesion properties.

Notes about adhesion interactions.

Let's give sone notes about adhesion interactions. Within the frame of the conducted according to the project investigations, a model of "cohesion" interphase layer accounting for the scale effect was suggested (Annual Report, 2003). Initially the model was related to the local interaction of cohesion type. The relation of the model with the cohesion field is explained by the fact that the solution found for the crack of normal opening corresponds to the cohesion field in the vicinity of the crack tip, and the unique constant of the model may be expressed in terms of parameters of fracture mechanics. Besides, it was shown (Annual Report, 2003, Section 2.6) that the suggested model yields the natural description of the additional layer localized in the vicinities of the interphase boundaries while determining the effective stiffness of non-uniform fragment. Hence, the suggested variant of the "multiscale" model of deformation of the multiphase media may be reasonably considered as a model of the interphase layer.

On the first stage the model of the "moment cohesion", which mathematical statement is given in previously Section, does not account for the surface effects. This model describes only the local character of interaction of cohesion fields of the phases in the contact zones. Therefore, we will call this model (modeling mechanical parameters of the layer) "pure cohesion" model of the interphase layer. On the second stage (Technical Report, 01.04.03-30.09.03; Annual Report, 2004) both the for the surface effects and cohesion local effects were taken into account in framework of multiscale model of the " interphase layer.

Let's make some remarks concerning adhesive effects based on the results of the Intermediate Technical Report 01.04.03-30.09.03, Annual Technical Report 2004).We established early that superficial effects are described with aid of additional coefficients in the expression in the superficial density of energy of deformation. These coefficients according to its physical nature have to be related to adhesion restrains. We received (Intermediate Technical Report 01.04.03-30.09.03, Annual Technical Report 2004) that the part of potential energy corresponded by the superficial effects can be written as $D_{ij} \dot{R}_i \dot{R}_j = A \, n_i n_j \dot{R}_i \dot{R}_j + B \, (\delta_{ij} - n_i n_j) \dot{R}_i \dot{R}_j$ in the square-law form for superficial density of energy of deformation. It is important to notice, that the account of such superficial interactions formally results in change only "nonclassical" boundary conditions. Really, the new physical constants D_{ij} determining properties of a surface, enter into expression for variation Lagrange only at a variation of a normal derivative from displacements. Thus, the account of ideal adhesive interactions influences only for a local state and does not change classical boundary conditions. Other words the principle of localness nonclassical part of solution takes place.

Let's notice, that if the surface is somehow modified then properties of a surface at the contact of phases also can be taken into account with the help items of type $D_{ij} \dot{R}_i \dot{R}_j$ in superficial density of energy of deformation. However

thus factors D_{ij} are not connected with cohesion characteristics of phases and can vary over a wide range. We can treat the superficial density of deformation energy $D_{ij}\dot{R}_i\dot{R}_j$ as energy, which associated with changing of defectiveness of a surface of contact because modified a surface. Thus, if parities $A^M - A^D < 0$ for pair a matrix (M) - inclusion (D) the superficial interactions connected to the account $D_{ij}\dot{R}_i\dot{R}_j$ result in reduction of rigidity of phases contact (defectiveness) are carried out. On the contrary, if for pair a matrix- inclusion takes place an inequality $A^M - A^D > 0$ the increase of rigidity of contact of phases as a whole takes place. The similar situation takes place with constants B. Note that to rigidity with the top index "M", correspond to a soft phase, and with an index "D" - rigid.   More common the qualitative analysis of the interfacial potential energy and physical sense all set of physical constants associated with adhesion interactions was done in the Chapter 2 of the present Report.

Estimation of the average Young elastic modulus and shear modulus of the interphase layer

The following approximate analytical formulas take place for estimation of the average Young elastic modulus and shear modulus of the interphase layer(Annual Report, 2003, Section 2.6; Technical Report, 01.04.03-30.09.03 Section 2.2.):

$$E_f = \frac{(E_M x_M + E_D x_D + A^M - A^D)}{(x_M + x_D)} = \frac{(E_M x_M + E_D x_D)}{(x_M + x_D)}[1 + \frac{(A^M - A^D)}{(E_M x_M + E_D x_D)}]$$

(3.13)

where $x_M = \dfrac{(1 - e^{-2a_M(x_1 - x_0)})}{a_M(1 + e^{-2a_M(x_1 - x_0)})}$, $\quad x_D = \dfrac{(1 - e^{-2a_D(x_2 - x_1)})}{a_D(1 + e^{-2a_D(x_2 - x_1)})}$, $a_M = \sqrt{\dfrac{C_M}{E^M}}$ $\quad a_D = \sqrt{\dfrac{C_D}{E^D}}$

Analytical estimation for the shear elastic modulus of the interphase layer:

$$G_f = \frac{(G^D y_D + G^M y_M + B_M - B_D)}{(y_D + y_M)} = \frac{(G^D y_D + G^M y_M)}{(y_D + y_M)}[1 + \frac{(B_M - B_D)}{(G^D y_D + G^M y_M)}],$$

(3.14)

were $y_M = \dfrac{(1 - e^{-2b_M(x_1 - x_0)})}{b_M(1 + e^{-2b_M(x_1 - x_0)})}$, $\quad y_D = \dfrac{(1 - e^{-2b_D(x_2 - x_1)})}{b_D(1 + e^{-2b_D(x_2 - x_1)})}$, $b_M = \sqrt{\dfrac{C_M}{G^M}}$ $\quad b_D = \sqrt{\dfrac{C_D}{G^D}}$

where $l_M^0 = (x_1 - x_0)$ is the length of the individual element of the first phase (matrix) in the considered combined element; $l_D^0 = (x_2 - x_1)$ is the length of the individual element of the second phase (inclusion) in the considered combined element The first phase ($x_0 \le x < x_1$) of the fragment is determined by Young's modulus E_M and cohesion modulus C_M, the second phase ($x_1 < x \le x_2$) does by Young's modulus E_D and cohesion modulus C_D, G^M, G^D are shear moduli of the first and second phases the fragment, constants $A^M - A^D$ and $B^M - B^D$ describe the adhesion properties of the contact intherphase layer. In the whole, the mentioned relations for the elastic moduli of the interphase "cohesion" layer are determined in terms of the elastic moduli of the phases and two additional "cohesion" constants.

Let's put, that the stresses of phases are constant in a vicinity of border of phases. Then, the modulus of elasticity varies under the same law as deformation. Assume for simplified that $A^M - A^D = 0$. Then on the basis of the received solution we can receive that flexibility of a matrix $E_M^{-1}(x)$ is monotonously reduced at approach border of contact of phases, and the flexibility of inclusion $E_D^{-1}(x)$ is monotonously increased near border of contact of phases:

$$E_M^1(x) = [\frac{1}{E_M} - (\frac{1}{E_M} - \frac{1}{E_f})\frac{cha_M x}{cha_M x_1}]^{-1}, \quad E_D^1(x) = [\frac{1}{E_D} + (\frac{1}{E_f} - \frac{1}{E_D})\frac{cha_D(x_2 - x)}{cha_D(x_2 - x_1)}]^{-1}$$

So, we propose the new treatment of the interphase layer. Interphase layer is intermediate layer in the contact zone where modulus of the elasticity is not constant. Modulus of the elasticity of intermediate layer changes continuously from modulus of inclusion to modulus of matrix as exponential function.

Characteristic of effective length of an interphase layer.

The effective characteristic length of the interphase layer x_f also changes due to account of the local adhesion effect to normal of the surface. This length x_f rises when $A^M > A^D$ and diminishes when $A^M < A^D$ (defect of bound interactions).

$$x_f = \frac{(E_D - E_M)x_M x_D}{(E_M x_M + E_D x_D)}[1 + \frac{E_M E_D (x_M + x_D)^2}{x_M x_D (E_D - E_M)^2} \frac{\dfrac{(A^M - A^D)}{(E_M x_M + E_D x_D)}}{(1 + \dfrac{(A^M - A^D)}{(E_M x_M + E_D x_D)})}] \qquad (3.15)$$

The similar equations we can find for estimation of the characteristic length y_f of the interphase layer in the tangent direction on the surface

$$y_f = \frac{y_D y_M (G^D - G^M)}{(G^D y_D + G^M y_M)}[1 + \frac{G^M G^D (x_M + x_D)^2}{x_M x_D (G^D - G^M)^2} \frac{\dfrac{(B^M - B^D)}{(G^M x_M + G^D x_D)}}{(1 + \dfrac{(B^M - B^D)}{(G^M x_M + G^D x_D)})}] \qquad (3.16)$$

Note that x_f, y_f in (3.15),(3.16) have dimensional length, and define the effective thickness of an interphase layers for tension and shear on border of two phases, matrix – inclusion.

Equivalent treatments of the interphase layer.

The publications devoted to the study of effective characteristics of composites may be conventionally subdivided into three groups: the method of effective inclusions, the method of effective matrix, and the method based on the hypothesis of three phases. Let us now demonstrate that the model of inter-phase layer proposed in this work include all the three methods mentioned as its consequence. Let us consider one-dimensional statement for a two-phase structure. In this case, in accordance to the classical theory for a two-phase fragment, we can use the Reuss formula for determination of effective properties of a composite. In the case of two-phase material, the modification of this formula based on some additional hypotheses (the method of effective inclusions, the method of effective matrix) is in contrast with the theory of elasticity. The theory of cohesion layer is a non-classic generalization of the theory of elasticity.

Consider the relationship for generalized rigidity (3.10a) (the generalization of the Reuss formula) and rewrite it as follows:

$$\frac{l}{E} = \frac{(l_M - x_f)}{E^M} + \frac{(l_D + x_f)}{E^D}, \quad x_M = a_M^{-1}th(a_M l_M / N), \quad x_M = a_D^{-1}th(a_D l_D / N), \quad l = l_D + l_M,$$

$$x_f = x_D x_M (E^D - E^M)(E^D x_D + E^M x_M)^{-1}, \quad E_f = (E^D x_D + E^M x_M)(x_D + x_M)^{-1}$$

The model of effective matrix, the model of effective inclusion, and the model of three phases can be obtained as a consequence of this formula. In accordance with the model of effective matrix, we get the following values of effective rigidity: $\frac{l}{E} = \frac{l_M}{E_*^M} + \frac{l_D}{E^D}$; here, the effective modulus of the matrix E_*^M can be calculated from the

relationship $\frac{1}{E_*^M} = \frac{1}{E^M} - (\frac{1}{E^M} - \frac{1}{E^D})\frac{2x_f}{l_M}$. In accordance with the model of effective inclusion, the modulus of

a composite can be determined by the formula $\frac{l}{E} = \frac{l_M}{E^M} + \frac{l_D}{E_*^D}$ and the effective modulus of inclusion E_*^D can

be determined by the formula $\frac{1}{E_*^D} = \frac{1}{E^D} - (\frac{1}{E^M} - \frac{1}{E^D})\frac{2x_f}{l_D}$. In accordance with the model of three phases, the

modulus of a composite can be determined by the formula $\frac{l}{E} = \frac{l_M^*}{E^M} + \frac{l_D^*}{E^D} + \frac{l_f}{E_f}$, where the properties of

the phases are determined by the moduli E^M, E^D, and E_f, respectively, and the lengths of the phases are

$l_M^* = l_M - x_M$, $l_D^* = l_D - x_D$, and $l_f = (x_M + x_D)$.

Thus, using the model of inter-phase layer, we have an opportunity to provide some grounding in theory for the hypotheses discussed earlier.

3.3. ANALYTICAL ESTIMATIONS OF THE INTERPHASE LAYER PROPERTIES

Further to estimate the contribution of cohesion interactions at calculation of integrated characteristics, we will formulate some results of the analysis for solution of the cohesion type model from the point of view of taken into account scale effects. For simplicity we will consider the case of the pure cohesion type interactions and will assume that constants A, and B associated with adhesive properties are equal to zero, $A = B = 0$. The analysis is based on the comparing of the lengths of different phases with the length of the cohesion type interaction for which of the phases. The analysis of the equations (3.13)-(3.16) allows to establish the following **estimations:**

1. Some initial estimations of an interphase layer

1. 1. *Effective length of a matrix $l_1 = (x_1 - x_0) - x_M$ strictly more zero ($a_M(x_1 - x_0) > 0$).*

$$l_1 = (x_1 - x_0) - x_M > 0$$

Consequence: the cohesion field of a matrix lays inside a matrix $(x_1 - x_0) > x_M > 0$.

1.2. *Effective length of inclusion $l_2 = (x_2 - x_1) - x_D$ strictly more zero ($a_D(x_2 - x_1) > 0$).*

$$l_2 = (x_2 - x_1) - x_D > 0$$

Consequence: the cohesion field of inclusion lays inside inclusion $(x_2 - x_1) > x_D > 0$.

1.3. *The moduli of an interphase layer lays in an interval $E^M \le E_f \le E^D$.*

Really, as values x_M and x_D are *strictly more zero*, then

$$E_f = \frac{(E^D x_D + E^M x_M)}{(x_D + x_M)} = E^D - (E^D - E^M)\frac{x_M}{(x_D + x_M)} \le E^D$$

$$E_f = \frac{(E^D x_D + E^M x_M)}{(x_D + x_M)} = E^M + (E^D - E^M)\frac{x_D}{(x_D + x_M)} \ge E^M$$

In case of a homogeneous fragment $E_f = E^D = E^M$.

2. Estimation of characteristics of an interphase layer E_f and x_f.

2.1. *The sizes of phases considerably exceed lengths of cohesion interactions, $a_M(x_1 - x_0) \gg 1$ and $a_D(x_2 - x_1) \gg 1$.*

*The following **micro-mechanical** description of an interphase layer are valid:*

$$E_f = \frac{[E^D a_M + E^M a_D]}{[a_D + a_M]} \qquad x_f = \frac{(E^D - E^M)}{[E^D a_M + E^M a_D]}$$

For classical model it is necessary to accept $a^D \to \infty$, $a^M \to \infty$. *Hence, the interphase layer is absent,* $x_f \to 0$.

2.2. *The size of inclusion less appropriate of cohesion zones: and* $a_D(x_2 - x_1) \ll 1$, *small concentration of inclusions:* $a_M(x_1 - x_0) \gg 1$.

*Variant **of the nano-mechanical** description of an interphase layer at small concentration **of nano-inclusions** (properties of inclusion it is determined it by a cohesion field)*

$$E_f = \frac{[E^D \frac{1}{(x_1 - x_0)} + E^M a_D]}{[a_D + \frac{1}{(x_1 - x_0)}]} \qquad x_f = \frac{(E^D - E^M)}{[E^D \frac{1}{(x_1 - x_0)} + E^M a_D]}$$

2.3. *Ultrahigh concentration* $a_M(x_1 - x_0) \ll 1$ *of the big inclusions* $a_D(x_2 - x_1) \gg 1$

Micro-nano-mechanical the description of an interphase layer (interaction of a matrix is defined it by a cohesion field)

$$E_f = \frac{[E^D a_M + E^M \frac{1}{(x_2 - x_1)}]}{[\frac{1}{(x_2 - x_1)} + a_M]} \qquad x_f = \frac{(E^D - E^M)}{[E^D a_M + E^M \frac{1}{(x_2 - x_1)}]}$$

2.4. *Ultrahigh concentration **of nano-inclusions**:* $a_M(x_1 - x_0) \ll 1$ *and* $a_D(x_2 - x_1) \ll 1$

*The full **nano-mechanical** **description** of an interphase layer **for high - filled composite with nano-inclusions.***
a) The moduli of an interphase layer is with the help of the classical circuit of averaging by Foyght:
Really, from formulas (3.14), (3.16) we have

$$E_f = \frac{[E^D \frac{1}{(x_1 - x_0)} + E^M \frac{1}{(x_2 - x_1)}]}{[\frac{1}{(x_2 - x_1)} + \frac{1}{(x_1 - x_0)}]} = E^D f + E^M (1 - f), \quad x_f = \frac{(E^D - E^M)}{[E^D \frac{1}{(x_1 - x_0)} + E^M \frac{1}{(x_2 - x_1)}]}$$

3. Estimations of parameters of an individual equivalent homogeneous fragment

3.1. *The sizes of phases considerably exceed lengths of cohesion interactions,* $a_M(x_1 - x_0) \gg 1$ *and* $a_D(x_2 - x_1) \gg 1$.

Then the circuit of averaging by Reuss is fair.

$$E_0 = \frac{1}{\{\frac{(1-f)}{E^M} + \frac{f}{E^D}\}}$$

3.2. *The size of inclusion less appropriate of cohesion zones:* $a_M(x_1 - x_0) \gg 1$ *and* $a_D(x_2 - x_1) \ll 1$

Then we receive variant of nonclassical model (with the effective moduli of inclusions) with small concentration of inclusions.

$$E_0 = \frac{1}{\{\frac{(1-f)}{E^M} + \frac{f}{E_f}\}}$$

3.3. *High concentration of the big inclusions:* $a_M(x_1 - x_0) \ll 1$ *and* $a_D(x_2 - x_1) \gg 1$

The variant of nonclassical model (with the effective moduli of a matrix), but with the classical scheme of averaging by Reuss takes place.

$$E_0 = \frac{1}{\{\frac{f}{E^D} + \frac{(1-f)}{E_f}\}}$$

3.4. *High concentration of small inclusions:* $a_M(x_1 - x_0) \ll 1$ *and* $a_D(x_2 - x_1) \ll 1$

The homogeneous environment is described by the effective moduli of an interphase layer

$$E_0 = E_f$$

Note that on the base of received results it is easy to establish the equations, which allow to estimate the properties of fragment from three different phases and so on. Then we can get some generalized of the last formulas in item **3.4.** that allow to estimate properties of the ceramics.

3.4. SOME APPLICATIONS AND NEW PARTICULAR RESULTS.

In this section we marked some particular results, that are new in the theoretical sense and fundamental results.

3.4.1 Modeling of the cohesion field near top of the crack of the normal opening. (Nonsingular crack). Estimation of a physical constant C.

Nonsingular solution for crack (model task).

Let's consider problem about the crack of the normal opening within the framework of double plane statement. Consider a model problem of the crack of the normal opening in the frame of the doubled plane state, i.e. suppose that among two components of the displacement vector only component $v(x, y) \equiv U_2(x, y)$ remains nonzero (see statement in Annual Report for 2003 and (2.7) in Annual Report for 2004). The expansion of a solution of the cohesion field model as the sum of solutions of the harmonic equation and Helmholtz's equation is used. Let's remind, that classical stress is understood as expression obtained after an operation of an operator of stress on a classical part of displacement U. Similarly, the cohesion stress is the expression obtained by an operation of an operator of stresses (see section) on cohesion displacement u is understood. If to express classical and cohesion transition through complete displacement r it is easy to establish following. The equality to zero simultaneously classical and cohesion stress on boundaries of the crack reduces in precise sufficing of boundary conditions for couple model of cohesion field.

The following solution was obtained for the crack of the normal opening as a non-singular solution at $r \to 0$:

$$\frac{\partial v}{\partial y} = [\ \sqrt{\frac{2}{\pi}\left(\frac{\mu}{C}\right)^{1/2}} K_\alpha\left(r\sqrt{\frac{C}{\mu}}\right) - r^{-\alpha}\ ]\sin(\alpha\varphi) \tag{3.17}$$

where $\alpha = 1/2$, $r = \sqrt{\frac{\mu}{(2\mu + \lambda)}y^2 + x^2}$

For $r \to \infty$ solution (!.1) behaves as the classical one, because McDonald's function decays as an exponent. The figure shows the qualitative strain distribution at the crack tip with respect to parameter C.
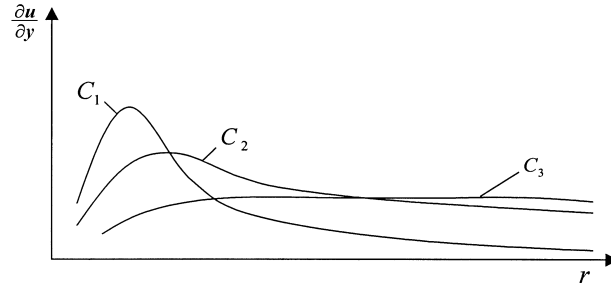
Fig.3.1. Strain distribution at the crack tip for various C ($C_1 > C_2 > C_3$)

Summary. A variant of variational algorithm to construct models on the base of the introduced kinematics constrains is suggested. As an example, the simplest medium model accounting for both volume and surface scale effects has been constructed. It has been shown that in the frame of this model, the cohesion field, similar to Barenblatt's one (Barenblatt,1962) is described in the natural way.

The next section concerns the identification problem respect to additional physical constant C.

Estimation of a physical constant C.

Solution allow to give same simplified estimations for new physical constant of the model C. We will use the asymptotic solution near end of a crack. Aaccording to a solution (!.17) we can write

$$\sigma = \sigma_a \frac{1 - e^{-ar}}{(ar)^{\frac{1}{2}}} \sin(\frac{\varphi}{2}), \quad a^2 = \frac{C}{E}, \quad E \text{-is modulus of elasticity} \tag{3.18}$$

Let's define distance r_0, on which stress as the function r accepts a maximum value. A requirement

$$\frac{\partial \sigma}{\partial (ar)} = 0$$

gives the following equation for definition ar_0:

$$e^{ar_0} = 1 + 2ar_0$$

It is easy to show, that last equation has the unique natural root:

$$q = ar_0 = 1,256431$$

Hence, we can write:

$$C = q^2 \frac{E}{r_0^2} = 1,578619 \frac{E}{r_0^2}$$

Let's define displacements $v(r,\varphi)$. We have: $v(r,\varphi) = v(r,0) + \int_0^\varphi \frac{\sigma(r,\varphi)}{E} r d\varphi$. Substituting in this equation

expression for stresses we can find:

$$v(r,\varphi) = -2 \frac{\sigma_a}{aE} (1 - e^{-ar})(ar)^{\frac{1}{2}} Cos(\frac{\varphi}{2})$$

Let's find the connection between amplitudes of the displacements and stresses in a point where the stresses reach a maximum value. The magnitude of transverse displacements in this point we can define as magnitude of the crack open displacement. We can write

$$v(r_0,0) = -2 \frac{\sigma_a}{aE} (1 - e^{-ar_0})(ar_0)^{\frac{1}{2}} = -\delta_a,$$

where δ_a is the crack open displacement.

For amplitude of the stresses we can receive the following equation:

$$\sigma_a = E \frac{a\delta_a (1+2q)}{4q^{\frac{3}{2}}} = 0,623581 Ea\delta_a$$

Let us consider equation (3.18). Assuming that maximum of stresses is reached in the point $r = r_0, \varphi = \pi$, we can find:

$$\sigma_a = \sigma_{max} \frac{(1+2q)}{2q^{1/2}} = 1,566974 \sigma_{max}$$

Taking into accjunt the previous equation we can write

$$\sigma_{max} = 0,397952 E a \delta_a$$

Assume that crack open displacement δ_a reach to critical value δ_c, when stresses σ_{max} reach to magnitude of theoretical strength σ_c. Thus, we can introduce the definition of the critical value of crack open displacement:

$$\delta_c = \frac{\sigma_c / E}{0,397952\, a}$$

Then, we can write:

$$a^2 = \frac{C}{E} = \left(\frac{\sigma_c / E}{0,397952}\right)^2 \frac{1}{\delta_c^2}$$

Let's find estimation σ_c / E, which can be received on the base of analysis interaction between two layers of atoms. The character of interatomic interaction can be shown on the dependence stress-interatomic layer fig 3.2.
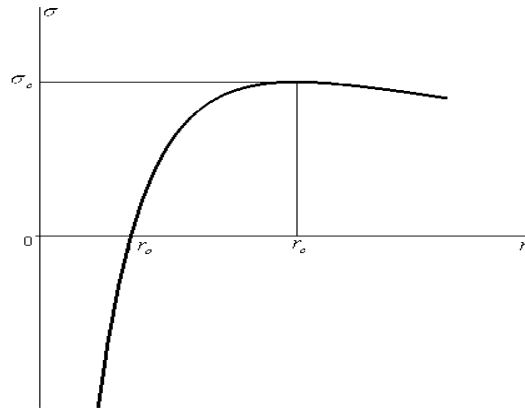
fig 3.2.

Let's approximate this dependence on the interval $(r_o, +\infty)$, with the aid trigonometric function:

$$\sigma = \begin{cases} \sigma_c \sin \dfrac{\pi}{2} \dfrac{r-r_o}{r_c - r_o} & npu \quad 0 < \dfrac{r-r_o}{r_c - r_o} < 1 \quad (r_o < r < r_c) \\ 0 & npu \quad \dfrac{r-r_o}{r_o} \geq 1 \end{cases}$$

or

$$\sigma = \begin{cases} \sigma_c \sin \dfrac{\pi}{2} \dfrac{\left(\dfrac{r-r_o}{r_o}\right)}{\left(\dfrac{r_c - r_o}{r_o}\right)} & npu \quad 0 < \dfrac{r-r_o}{r_c - r_o} < 1 \quad (r_o < r < r_c) \\ 0 & npu \quad \dfrac{r-r_o}{r_o} \geq 1 \end{cases}$$

Let's interpret value $(r - r_o)/r_o$ as tensile strain ε and $E = \left. \dfrac{d\sigma}{d\varepsilon} \right|_{\varepsilon=0}$.

We will call σ_c as ultimate theoretic strength. Experimental dates show that destruction of materials has place for stresses less then $0.1\sigma_c$.

We can find the following equation

$$\sigma_c = \frac{2\varepsilon_c}{\pi} E, \quad \text{or} \quad \frac{\sigma_c}{E} = \frac{2\varepsilon_c}{\pi}$$

here $\left(r_c - r_o\right)/r_o = \varepsilon_c$ is ultimate deformation.

Using of the last equation leads to the following formula for constant C :

$$C = \left(\frac{2\varepsilon_c/\pi}{0,397952}\right)^2 \frac{E}{\delta_c^2} = 2,55917 \frac{\varepsilon_c^2 E}{\delta_c^2}$$

It is possible to define the value r_0 (the length of Barenblat's zone (Barenblatt, 1962.) through the critical value of crack open displacement δ_c :

$$r_0 = 3,141588\delta_c$$

At last, the additional modulus C can be defined through specific surface energy γ. Taking into account the famous definition for value γ we can get:

$$2\gamma = \sigma_c \delta_c = \frac{2\varepsilon_c}{\pi} E \delta_c$$

In result, we have the following equation:

$$C = 0,25857 \frac{\varepsilon_c^4 E^3}{\gamma^2}$$

Thus, we established that new physical constant of the model C is determined through based constants of fracture mechanics:

$$C = 25,2580 \frac{\varepsilon_c^2 E}{r_0^2}; \quad (\text{ magnitude of the Barenblatt's zone - } r_0)$$

$$C = 2,55917 \frac{\varepsilon_c^2 E}{\delta_c^2}; \quad (\text{critical value of crack open displacement - } \delta_c) \qquad (3.19)$$

$$C = 0,25857 \frac{\varepsilon_c^4 E^3}{\gamma^2}; \quad (\text{specific surface energy } \gamma)$$

$$C = 1,03428 \frac{\varepsilon_c^4 E^5}{K_{1C}^4}, \quad \text{when } \left(1 - v^2\right) \sim 1; \quad (K_{1C} \text{ -is stress intensity factor , } v \text{ is Poisons coefficient})$$

So, formulas (3.19) give approximated estimation of the constant of the "momental cohesion model" with the aid of the famous parameters of the fracture mechanics. Other words we received some solution of the identification problem respect to the physical constant C.

3.1. Table of the material properties and constant C

Materials	Ultimate stresses σ	ν, Poisons coefficient	E, Γna	G, $\Gamma\Pi a$	ε_c, %	$\alpha, 10^{-6}$ $^0C^{-1}$ for temperature 20-100 C^0 100-200 C^0 200-300 C^0	K_{1C}, $M\Pi a \cdot M^{1/2}$	C, $\Pi a / M^2$	l_0, 10^{-6} M
Steel									
Steel 3	7860	0,33	210	77	5-8	13,3	96-110	$0,204\cdot10^{21}$ – $1,80\cdot10^{21}$	32,11-107,92
Steel 20	7860	0,33	210	77	5-8	13,3	124-170	$7,318\cdot10^{21}$- $31,61\cdot10^{21}$	53,57-257,75
Alloyed steel 30ХГСН2А	7770	0,26	195	77	8	10,6 11,2 13,0	250-300	$14,74\cdot10^{21}$ – $30,58\cdot10^{21}$	252,53-363,64
Alloyed steel 40ХСН2МА	7810	0,26	195	77	10	11,2 12,7 13,5 14,2	180-210	$1,499\cdot10^{21}$ – $2,778\cdot10^{21}$	83,78-114,04
Alloyed steel H18K9M5T	8000	0,3	190-218	70-72	5-14	11,2	115-180	$1,12\cdot10^{21}$ – $15,21\cdot10^{21}$	13,96-353,00
Steel for cryogenic structures 07Х16Н6	8000	0,3	207-221	79	20-23	10,5	105-138	$1,73\cdot10^{21}$ – $12,55\cdot10^{21}$	4,20-10,93
aluminum alloy									
aluminum alloy, D16	2800	0,34	72	27	10-19	22,9	26,7	$0,394\cdot10^{21}$- $5,132\cdot10^{21}$	3,75-13,52
В95	2850		72	26,5	12	22,9	51,0	$6,134\cdot10^{21}$	34,26
АК4-1	2800		72	27	6-8	20,8 23,0	23	$0,293\cdot10^{21}$- $9,27\cdot10^{21}$	15,67-27,87
1420	2470		75		9-10	22,2	21,3	$0,782\cdot10^{21}$- $1,192\cdot10^{21}$	7,93-9,79

В93пч	2840		72		7-9	22,0 23,9	26,7-37,8	$0,258 \cdot 10^{21}$ – $2,351 \cdot 10^{21}$	16,69-55,31
В95пч	2850		72		12	22,0 23,9	34,7-40,9	$0,148 \cdot 10^{21}$ – $0,286 \cdot 10^{21}$	15,86-22,03
В96Ц1	2890		72		8	22,0 23,9	26,7	$0,161 \cdot 10^{21}$	21,13
Titanium steels									
ВТ3-1	4500	0,35-0,38	115	39,2	14-21	8,6 9,8 10,9	55-67	$0,369 \cdot 10^{21}$ – $4,42 \cdot 10^{21}$	5,1-17,03
ВТ-6	4430		115		10-13	8,4 8,7 10,0	80,5-90,0	$0,141 \cdot 10^{21}$ – $3,17 \cdot 10^{21}$	28,51-60,22
ВТ-9			118		8-14	8,3 8,6 8,7	80,0-81,5	$0,222 \cdot 10^{21}$ – $2,197 \cdot 10^{21}$	23,06-73,29
ВТ-22	4600		110		10	8,0 8,2 8,4	69,5	$7,139 \cdot 10^{21}$	39,25
ceramics									
ceramics $ZrO_2 + MgO$	3700-4300	0,3	172			0,58	5,9		
ceramics $Y_3Al_5O_{12}$							8,7		
ceramics Y_2O_3							2,5		
ceramics $ZrO_2 + Y_2O_3$	5900-6090		172				11-18		
Nonmetallic materials									
soda-lime glass	2400-2580		74-95		0,01		1,7		
plexiglass							2,9		
acrylic resi	1110-1210		1,88				4,5		

3.4.2. About Generalized Eshelby Solution

In framework of a work under project the generalized Eshelby solution was construct based on the model which takes into account the local scale effects. Let's remind that Eshelby received[Eshelby J.D., 1957] the following equation

$$\varepsilon_{ij}^{c}(P) = \hat{S}_{ijpq}(P)\,\varepsilon_{pq}^{(0)}$$

which allow to connect the field of restricted deformation in inclusion ε^{c} and the field of "free from stresses deformation" $\varepsilon^{(0)}$, with the aid of classical matrix $\hat{S}_{ijpq}$ (Eshelby matrix). Here ε^{c} is deformation of the embedded inclusion together with matrix under homogeneous loading of matrix with inclusions (by stresses on the infinity).

In compliance with the fundamental Eshelby's method the effective mechanical properties of composite λ^{eff} (the matrix with inclusion of any shape) can be found using the Eshelby's matrix

$$\lambda^{eff} = \lambda^{0} + \lambda^{0}K\Omega \qquad K = \left(\lambda^{0} + \Delta\lambda S\right)^{-1}\Delta\lambda = \left(\Delta\lambda^{-1}\lambda^{0} + S\right)^{-1} \tag{3.20}$$

or

$$\lambda^{eff} = \lambda^{0} + T\Delta\lambda\,\Omega \qquad T = \lambda^{0}\left(\lambda^{0} + \Delta\lambda S\right)^{-1} = \left(I + \Delta\lambda S\lambda^{0^{-1}}\right)^{-1} \tag{3.21}$$

Here λ^{0} is tensor of moduli of elasticity for the matrix without inclusion, and $\Delta\lambda$ is matrix of jumps of moduli of the elasticity between inclusion and matrix.

In our work we received the generalized of the Eshelby's solution. The generalized matrix has the following view

$$\hat{S}_{ijpq}(P) = \tilde{S}_{ijpq}(P) - S_{ijpq}(P)` \tag{3.22}$$

where

$$\tilde{S}_{ijpq}(P) = \tilde{T}_{ijkl}(P)\,C_{klpq}, \qquad \tilde{T}_{ijkl}(P) = -\frac{\delta_{li}\,\tilde{\varphi}_{,kj}(P) + \delta_{lj}\,\tilde{\varphi}_{,ki}(P)}{8\pi\mu} + \frac{\tilde{\psi}_{,ijkl}(P)}{16\pi\mu\,(1-\nu)}, \tag{3.23}$$

$$\tilde{\varphi}(P) = \int_{G}\frac{dP'}{|P - P'|}, \qquad \tilde{\psi}(P) = \int_{G}|P - P'|\,dP'; \tag{3.24}$$

$$S_{ijpq}(P) = T_{ijkl}(P)\,C_{klpq}, \qquad T_{ijkl}(P) = -\frac{\delta_{li}\,\varphi_{,kj}(P) + \delta_{lj}\,\varphi_{,ki}(P)}{8\pi\mu} + \frac{\psi_{,ijkl}(P)}{4\pi C}, \tag{3.25}$$

$$\varphi(P) = \varphi(P,\kappa_{2}) = \int_{G}\frac{e^{-\kappa_{2}|P-P'|}}{|P - P'|}\,dP', \qquad \psi(P) = \varphi(P,\kappa_{2}) - \varphi(P,\kappa_{1}). \tag{3.26}$$

the functions $\varphi(P)$ also $\psi(P)$ are like volumetric integrals generalizing Newton potential on Helmholtz equation, $\kappa_{1} = \sqrt{C/2\mu + \lambda}\;\;\kappa_{2} = \sqrt{C/\mu}$.

This solution was established with the help of Ostrogradsky-Gauss theorem using the following expansion for common vector of displacement: $\vec{R} = \vec{U} - \vec{u}\;\;\vec{U} = \vec{R} - \frac{1}{C}L(\vec{R})\;\;\vec{u} = -\frac{1}{C}L(\vec{R})$.

The following equation was used for vector of displacements $\vec{u}_{j}(P,P')$, caused by the point force applied in a point P' (generalization of the fundamental solution of a classical problem of the elasticity theory (Somilliana tensor)):

$$\vec{u}_{j}(P,P') = \{u_{ij}\}, \quad u_{ij}(P,P') = \frac{1}{4\pi\mu}\frac{\delta_{ij}}{|P-P'|}e^{-\kappa_{2}|P-P'|} - \frac{1}{4\pi}\frac{\partial^{2}}{\partial x_{i}\partial x_{j}}\left(\frac{1}{|P-P'|}\frac{e^{-\kappa_{1}|P-P'|} - e^{-\kappa_{2}|P-P'|}}{C}\right)$$

here P' is a point of the action of point force, δ_{ij} – Croneker symbol, $\kappa_{1} = \sqrt{C/2\mu + \lambda}\;\;\kappa_{2} = \sqrt{C/\mu}$. In

extreme case $C \to 0$ the solution above transforms in classical Somilliana tensor [Christensen R.M. 1979.]. ralizing Newton potential on Helmholtz equation:

The matrix (3.23), (3.24) corresponds to the classical solution and coincides with a matrix received by Eshelby in the work [Eshelby J.D., 1957], and the matrix (3.25), (3.26) corresponds to the cohesion field and is the modification to the Eshelby solution, caused by the work of a surface layer in considered model of spatial moment cohesion.

Explicit analytical formulas (3.23), (3.24) define behavior of the constructed solution in a matrix and in a inclusion. Eshelby has been investigated in detail the behavior of a classical part of the solution, which has asymptotic on infinity as A/r^2. He in particular has shown that the solution is homogeneous inside inclusion of ellipsoid form, and also has calculated through elliptic functions values of elements of a matrix, which is in this case a constant inside inclusion.

Also the solution (3.20) has a similar behavior. It is exponentially tends to zero on infinity and weakly varying near some constant value inside inclusion. Formulas (3.25)- (3.26) can be used for averaging a composite material within the framework of spatial model of moment cohesion.

We can formulate shortly the advantages of a technique, based on the equations(3.20)- (3.26):

1. Almost analytical relations which are convenient for the numerical analysis

2. Common algorithm of definition of the effective characteristics of Composites which was developed by Mura 1982 remains the same

3. This technique allows to consider both small volume fractions of inclusions, and finite volume fractions of inclusions (a differential method)

4. The technique is remained in force for inclusions of the any form and any orientation

5. Only three additional constants completely describe characteristics of an inter-phase layer (C, A, B)

3.4.3. A meniscus as multiscale effect.

Assume that the element of the medium is deformed between two rigid plates. The length of the element is $2l$. The distance between plates is $2h$. At the edges of element ($x = \pm l$) the constant tension stresses are applied. Friction between plates and an element of medium is absent. The problem about a meniscus is considered. We assume in this problem that displacement field is defined by the longitudinal component of displacement $r(x, y)$ in direct of axis x only: $R_i = rX_i$

The solution of this problem is interesting from the point of view of studying of the role of adhesion in effect of formation of a meniscus. The problem about a meniscus can be used for statement of experiment with definition of adhesive parameter. The differential equilibrium equation has the following view:

$$\frac{G}{C}\overline{\nabla}^2\overline{\nabla}^2 r + \overline{\nabla}^2 r + q = 0, \text{ where } \overline{\nabla}^2(...) = s^2\frac{\partial^2(...)}{\partial x^2} + \frac{\partial^2(...)}{\partial y^2}, \quad s^2 = \frac{E^M}{G^M}$$

The boundary conditions is:

$$E[\dot{r}(l, y) - \frac{G}{C}\overline{\nabla}^2\dot{r}(l, y)] = \frac{P}{2h} \qquad\qquad G[\dot{r}(x, h) - \frac{G}{C}\overline{\nabla}^2\dot{r}(x, h)] = 0$$

for $x = \pm l$: $\qquad\qquad$ and for $y = \pm h$:

$$A\,\dot{r}(l, y) + \frac{E^2}{C}\ddot{r}(l, y) = 0 \qquad\qquad B\,\dot{r}(x, h) + \frac{G^2}{C}\ddot{r}(x, h) = 0$$

Coefficients A, B are defined the adhesive effects concerning tension - compression and shear.

It is convenient to use the following expansion of the total displacement on the "cohesion" and "classical" displacements:

$$r = U - u, \quad U = r - \frac{G}{C}\overline{\nabla}^2 r, \quad u = -\frac{G}{C}\overline{\nabla}^2 r$$

Then, for simplified cases the boundary problem can be formulate as two independent problems. The first problem is the "classical" problem:

$$\overline{\nabla}^2 U = 0, \quad E\dot{U}(l, y) = \frac{P}{2h}, \quad G\dot{U}(x,h) = 0.$$

The second problem is the boundary problem of the cohesion field:

$$G\overline{\nabla}^2 u - Cu = 0,$$

and boundary conditions: $E\dot{u}(l, y) + Au(l, y) = \dfrac{P}{2h}, \quad G\dot{u}(x,h) + Bu(x,h) = 0, \quad A = \dfrac{E^2}{A_2} \quad B = \dfrac{G^2}{B_2}$

Variational statement was formulated in the Technical Itermediate Report 2004(for 10 quarter). We found approximate solution using the Ritz's method using expansions of boundary problems mention above. Let's take the approximate functions as fundamental solutions of classical and "cohesion type" boundary problems in framework of the Ritz's method. Results of solution of the model problems ($A = 0, \quad E/G = 10, \quad C/G = 10$) we on the can see figure 3.3. The solid line (*parameter* $q \geq 0$) and dotted line (*parameter* $q \leq 0$) show the distribution of the relative angle of wettability ($G(\partial u / \partial y), \quad u$ *is displacement alone axis x*) for variable of the parameter of shear adhesion properties $q = \dfrac{Bh}{G}$ (h is width of capillary)
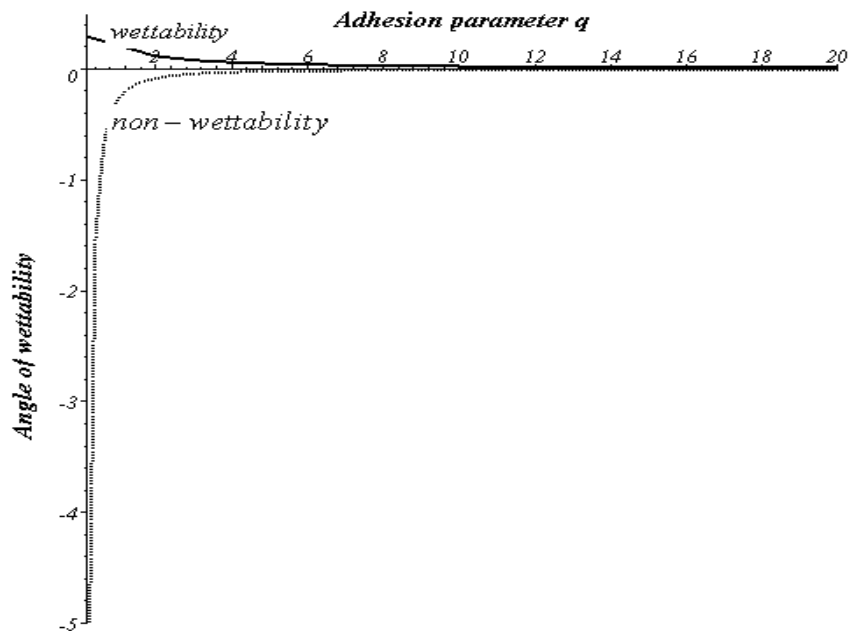
Figure 3.3.

So, we can see results of modeling of wettability (*parameter* $q \geq 0$) and non-wettability effects (*parameter* $q \leq 0$).

The qualitative analysis of the offered approximated solution allows to describe the effect of a meniscus of a liquid on the border "liquid - capillary". The angle of the meniscus can be both positive, and negative depending on the adhesive module of pair "liquid - capillary".

3.4.4 On the concept of quantum-mechanical modeling

Let's present the brief summary of results received in the previous report (Annual report 2004, Intermediate Report for 10 Quarter) within the framework of quantum-mechanical modeling. We shall try to formulate some conclusions also.

Let the potential of atom interaction is $U(r)$. Here r - is distance from the center of atom up to some point in which is placed the sampling body, taking up from the atom some attractive (repulsive) force σ:

$$\sigma(r) = U'(r).$$

Characteristics of the material properties constructed on the chosen class of potentials, are reduced to the following:

1. The "Equilibrium" distance r_0 between two identical atoms is determined as distance on which force of interaction is equal to zero:

$$\sigma(r_0) = U'(r_0) = 0$$

2. The "Limiting" distance r_c between two identical atoms is determined as distance on which force of interaction is maximal:

$$\sigma'(r_c) = U''(r_c) = 0$$

3. The modulus of elasticity E and deformation ε is determined as follows:

$$E = r_0 U''(r_0), \qquad \varepsilon(r) = \frac{(r - r_0)}{r_0}$$

4. Breaking point σ_c and ultimate strain ε_c is determined as follows:

$$\sigma_c = U'(r_c), \quad \varepsilon_c = \varepsilon(r_c) = \frac{(r_c - r_0)}{r_0} = \varepsilon_c \text{ And } \quad r_c = r_0(1 + \varepsilon_c)$$

Thus, any potential which has one local minimum and one backoff point basically is suitable for the description of interaction of pair atoms.

5. Potentials define the nonlinear dependences for constitutive equations:

$$\sigma(\varepsilon) = E(\varepsilon)\varepsilon, \qquad \sigma_c = E(\varepsilon_c)\varepsilon_c$$

So, the following relations can be found

$$\left(\frac{\sigma}{\sigma_c}\right) = \frac{E_0 \varepsilon_c}{\sigma_c}\left(\frac{E(\varepsilon)}{E_0}\left(\frac{\varepsilon}{\varepsilon_c}\right)\right), \qquad \text{or} \qquad \left(\frac{\sigma}{\sigma_c}\right) = \left(\frac{E_0 \varepsilon_c}{\sigma_c}\right)\left[\left(\frac{E(\varepsilon)}{E_0}\right)\left(\frac{\varepsilon}{\varepsilon_c}\right)\right]$$

Thus, we can use parameter $q = \dfrac{\sigma_c}{E_0 \varepsilon_c}$, which is the dimensionless parameter of the modelled medium. It may be that this factor is individual for every medium.

6. At last $h = U_c - U_0$ is additional macroparameter of medium, which can be treated as depths of a potential pit which size can be connected with energy of destruction or temperature of fusion (or other phase transition).

Thus, it is possible to determine five macroparameters of modeled medias r_0, r_c, E, σ_c, h.

In the previous report it was offered four base macroparameters of medium

The analysis of various potentials is reduced to the analysis of conformity between parameters of potentials and macroparameters of medium.

Brief analysis of potencials

We propose to use the method of continuum mechanics. The brief analysis of the set up concept of the one-dimensional case (the Annual report for 2004) shows:

1) The classical theory of elasticity cannot describe behaviour of nanostructures as determines elastic properties of medium in only one parameter E. In this theory there is no description of scale effects, there is no characteristic scale r_0 - equilibrium distance.

2) The theory of mediums with kept dislocations (see the classification given in section 2.1. of the present report) can describe properties of nanostructures only about a point of equilibrium position. It determines elastic properties of medium with half set of necessary parameters: C, E. These parameters can be connected with parameters of the chosen potential r_0, E. However the theory of mediums with kept dislocations (Papkovich-Cosserat mediums) basically cannot to model a microcrack nucleation in a vicinity of breaking point destruction.

3) The Saint-Venant theory of the medium basically is minimally complete theory, which takes into account all necessary properties of a material. Really, it contains three groups of parameters of the different dimension distinguished on an even degree of length. They can be connected with corresponding modules of elasticity and strength.

Here brief description of potentials is given within the framework of the suggested concept. It was used the determination of formal properties of the researched medium $r_0, r_c, E, \sigma_c, U_0, U_c$, which is reduced to two groups of ratios:

$$U(r_0) = U_0 \qquad U'(r_0) = 0, \qquad U''(r_0) = \frac{E}{r_0}$$

and $\qquad U(r_c) = U_c \qquad U'(r_c) = \sigma_c, \qquad U''(r_c) = 0$

The first group concerns to behaviour of a material about a point of equilibrium position r_0 (parameters r_0, E, U_0). The second group concerns to behaviour of a material in about a point of limiting state r_c (parameters r_c, σ_c, U_c).

Potentials

1. Morse's Potential. Morse's potential contains four formal parameters A_1, A_2, a_1, a_2 and looks like:

$$U(r) = A_1 e^{-a_1 r} + A_2 e^{-a_2 r}$$

According to the conception of the modelled medium the four macroparameters r_0, r_c, E, σ_c are expressed through four parameters of the modelling potential A_1, A_2, a_1, a_2. Thus, macroparameters of medium are independent. In this respect Morse's potential is quite coordinated and has sufficient number of internal parameters. However one more parameter of medium h is dependent with specified in four parameters r_0, r_c, E, σ_c of medium. This fact can be related to disadvantages of Morse's potential. Besides potentials of this class are non-singular and **contradict to principle of indetermining**.

The remark . Morse's potential was used in [6](P. Zhang, Y. Huang, P.H. Geubelle, P.A. Klein, K.C. Hwang, 2002 and P. Zhang, Y. Huang, H Gao, R.c. Hwang, 2002) for modelling of the Young module of single-wall nanotubes. The following potential was used:

$$U(r) = \frac{D^e}{S-1}[e^{-\beta\sqrt{2S}(r-R^e)} - Se^{-\beta\sqrt{\frac{2}{S}}(r-R^e)}]$$

The calculations which have been lead for values of parameters of potential, the data in (P. Zhang, Y. Huang, P.H. Geubelle, P.A. Klein, K.C. Hwang, 2002) shows, that limiting deformation achieves 35.75 %. On the other hand relation of the module of elasticity E_0 to the limiting stresses σ_c is equal approximately 7.62. Such relation is typical of rigid materials with small limiting deformation. In the mentioned works [6,7] it is underlined that fact, that limiting deformations can achieve great values ε_c (more than 50 %). We account that the nanotube as macro-object, probably, has rather small limiting deformations.

2. Lennarda-Johnson's potential.

Lennarda-Johnson's potential also has been considered earlier. It contains only two formal parameters and looks like: $U(r) = A_1 r^{-6} + A_2 r^{-12}$.

It was established that Lenarda-Johnson's potential is not well. In result, macroparameters of modelled mediums cannot be independent. After obvious calculations it is possible to receive the following relations for macroparameters of medium at use of Lenarda-Johnson's potential*:*

$$r_c = r_0 \sqrt[6]{\frac{13}{7}} = 1,108683417968720 r_0, \quad \varepsilon_c = \sqrt[6]{\frac{13}{7}} - 1 = 0,108683417968720,$$

111

$$\sigma_c = \frac{1}{6}[(\frac{r_c}{r_0})^{-7} - (\frac{r_c}{r_0})^{-13}]E_0 = 0,037359734683399E_0, \quad q = \frac{\sigma_c}{E_0\varepsilon_c} = 0,343748249564168.$$

$$U_c - U_0 = T_f = \frac{1}{72}[1-(\frac{r_c}{r_0})^{-6}]^2 Er_0 = 0,002958579881657 Er_0,$$

The simplicity and singular properties concern to advantages of Lenarda-Johnson's potential.

3. *Papkovich's Potentials.*

The new Papkovich's Potentials has been offered based on the our investigations (Lurie S, Belov P, Volkov-Bogorodsky D, Tuchkova N. 2003; Lurie S, Belov P, Volkov-Bogorodsky D, 2003) Papkovich's Potential has

three formal parameters $a \ A_1, A_2$ and looks like: $U(r) = A_1\frac{1}{r} + A_2\frac{e^{-ar}}{r}$. Note, that for Papkovich's

potential macro-parameter of the limit strength σ_c connects rigidly with Young's modulus E for the Papkovich's potential. Thus using Papkovich's potential we can realize the prognosis of the macro-properties of the continuum. On the other hand using the macro-properties of the continuum we can find the parameters of the Papkovich's potential(r_0, r_c, E are known).

The Papkovich's potential has the singularity in the zero point($r \to 0$). In this sense Papkovich's potential is better then Morse's potential.

4. *The combined potential.*

In the given section the new potential, which combines positive properties of the Morse's potential and Lennarda-Johnson's potential, is offered. Let's consider a linear combination of the Morse's potential and Lennarda-Johnson's potential. We shall take into account their advantage properties and we shall write the following equations for definition of the model parameters:

$$U(r) = A_0[-\frac{1}{a_1}e^{-a_1\frac{r-r_0}{r_c-r_0}} + \frac{1}{a_2}e^{-a_2\frac{r-r_0}{r_c-r_0}}] + A_3[-2(\frac{r}{r_0})^{-6} + (\frac{r}{r_0})^{-12}]$$

The system of four parameters of potential A_0, A_3, a_1, a_2 can be found from four macroparameters of the modelled mediums r_c, σ_c, E_0, T

Conclusions. The offered new potential has the following advantages:

-This potential is singular;

-The combined potential takes into account and cohesion interactions and van der Waals interactions;

-This potential has enough number of the internal parameters which provide the common form of potential and allow to consider the macroparameters of medium as independent.

-Its weakness is the following: using the combined potential we must solve the nonlinear equations to find the parameters of potential from the macroparameters of the medium.

Comparing of the potencials.

Let's compare the dependences $\overline{\sigma} = F(\overline{\varepsilon})$ or $\sigma/\sigma_c = F(\varepsilon/\varepsilon_c)$ for the Lennarda-Johnson's potential,

Morse's Potencial and Papkovich's Potentials.
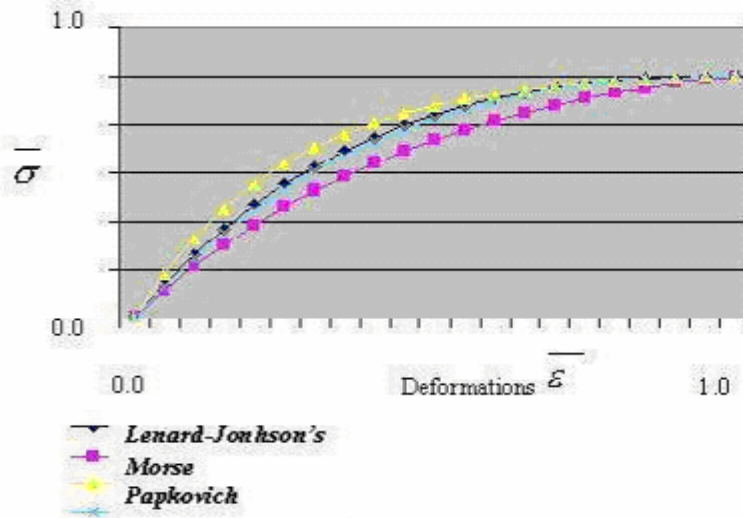
Fig. 3.3.

Results of comparison of the curves resulted on figure 3.3 show, that compared potentials are actually equivalent at modelling classical modules of elasticity of the mediums. Moreover, it is possible to show, that we can consider the various potentials as equivalent potentials for calculation of effective Young modules of the researched objects if we can provide equality of characteristics ε_c, σ_c. Note that as was reported the ultimate deformations respected to different potential are differ because considered potentials are not common enough and don't allow modeled the ultimate characteristics independently. We must take into account this fact. Using the equation we can conclude that parameter $q = \dfrac{E_0 \varepsilon_c}{\sigma_c}$ is almost the same for mention above potentials. Then we can receive the approximate estimation of the stiffness (Young modulus) for Morse's potential and Lennarda-Johnson's potential. Let's consider Morse's potential $U(r) = \dfrac{D^e}{S-1}[e^{-\beta\sqrt{2S}(r-R^e)} - Se^{-\beta\sqrt{\frac{2}{S}}(r-R^e)}]$. We will use the values of parameters of potential, the data in [P. Zhang, Y. Huang, P.H. Geubelle, P.A. Klein, K.C. Hwang, 2002]: $D^e = 6.325eV$, $S = 1.29$, $\beta = 15nm^{-1}$, $R^e = 0.1315nm$, $r_0 = 0.1315nm$. Taking into account Conception it can be found that $E_0 = 2r_0 D^{(e)}\beta^2$. Then we have $E_0 \approx 374eV / nm$ and $\varepsilon_c \approx 35.75\%$.

Assume now that ultimate stresse σ_c is the same for Morse's potential and Lennarda-Johnson's potential. Then we can find $(E_0\varepsilon_c)_{Len\_J} = (E_0\varepsilon_c)_{Morse}$. Taking into account that $(\varepsilon_c)_{Len\_J} \approx 0.1$, and $(E_0\varepsilon_c)_{Morse} \approx 0.36$ we can establish that

$(E_0)_{Len\_J} = \dfrac{(\varepsilon_c)_{Morse}}{(\varepsilon_c)_{Len\_J}}(E_0)_{Morse}$ or $(E_0)_{Len\_J} \approx 3.6(E_0)_{Morse} \approx 1346\,EV / nm$

Effective modulus of elasticity for nanostructure
On the preliminary report (Intermediate Technical Report (2004), quarter 10) the procedure of the determination of the strain energy, which is taking into account interatomic interactions was proposed.

On the base of this procedure the effective modulus of elasticity for nanostructure can be calculated. Let us consider the fragment of carbon nanotubes(see Figure 3.4b). The beam elements in such structure has two type elements with length equal to r_0 and with length equal $r_0\sqrt{3}$.

The modulus of rods of different lengths essentially differ due to nonlinear character of atomic interaction. Modulus of rods with length equal to r_0 are calculated according to the offered concept of potentials using the following formulas $E_0 = U''(r_0)r_0$. Note, that for the rods with length equal to $r_0\sqrt{3}$ we can not use the analogies formulas $E_{\sqrt{3}} = U''(r_0\sqrt{3})r_0\sqrt{3}$. Really let's consider Morse's potential and Lennarda-Johnson's potential. Figure show the distribution of the relative stresses (to ultimate stresses) from deformation. So, to receive the rigidity of the rods with length equal to $r_0\sqrt{3}$ we must take the secant moduli from the dependences Figure 3.4b.
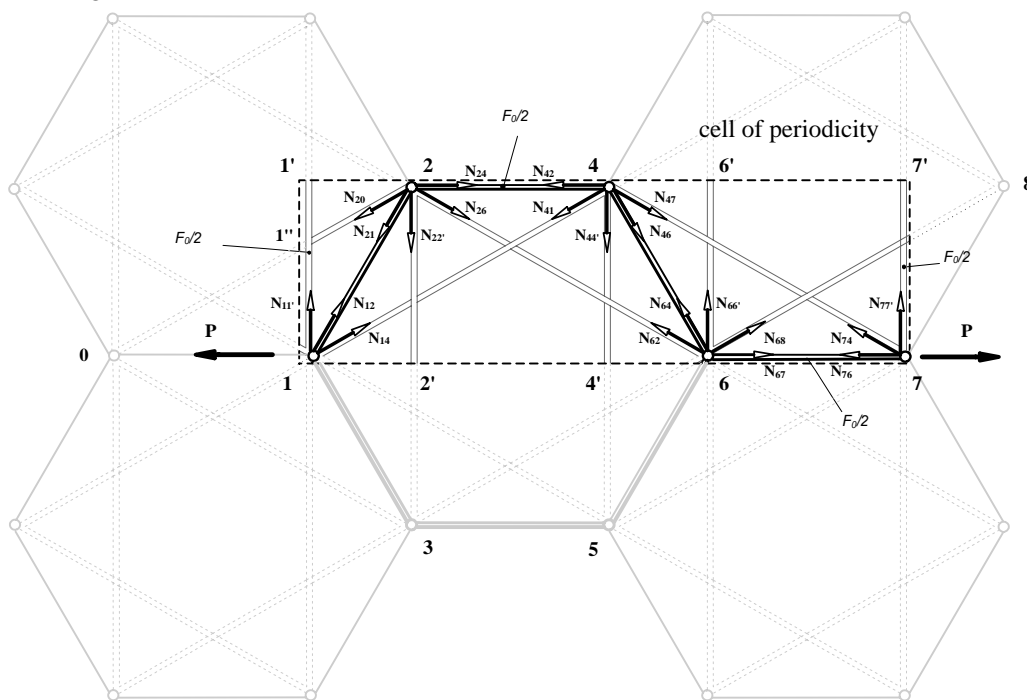
Figure 3.4 a

Figure 3.4b

114
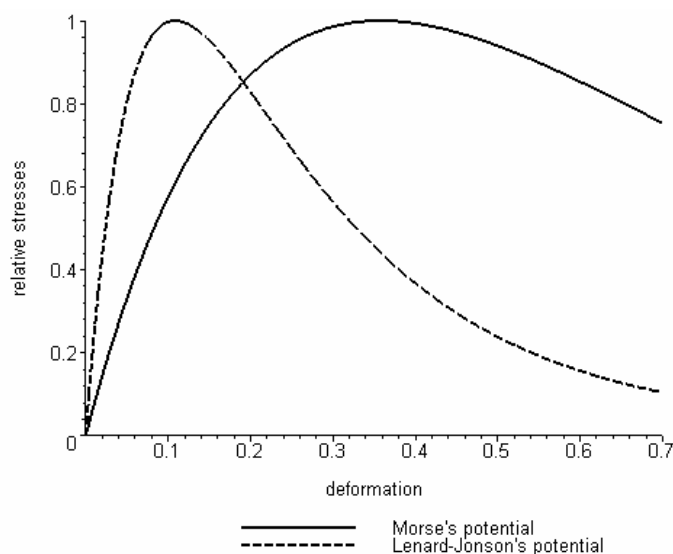
Let's will use the one dimension simplified model for estimation of the effective rigidity of the nanotube. Then, we can establish effective rigidity for the equivalent fragment with the length equal $3\,r_0$:

$$E_{eff} = \frac{3\sqrt{3}}{2\sqrt{3}+1} E_{r_0}$$

This value is upper bound for the rigidity of the nanotube. To find the value of the modulus we mast take into aacount the width of the elementary atomic layer $\delta \approx 0{,}335nm$ [Zhang P., Huang Y., Geubelle P.H., Klein P.A., Hwang K.C. 2002].

If you want to make more exact calculations we can specify the calculating scheme. For more full account of interactions it is offered to consider atomic structure in the cell as generally statically indeterminate truss. Then to findthe rigidity of the rods with length equal to $r_0\sqrt{3}$ we must take the secant moduli from the dependences Figure 3.4b.

Conclusions.

Preliminary conclusions are reduced to the following:

1. The various potentials can be used for modelling of the properties of a concrete material (it can be achieve using the appropriate choice of parameters of potential). Equivalence of potentials DON'T takes place for definition integral characteristics (STIFFNESS) in a vicinity of a "equilibrium" condition.

2. Using of the potentials with small number of the parameters is equivalent to the assumption of the some correlation between strength both limiting deformation and Young module.

3. The strength macroparameters of the mediums can be connected to additional parameters, such as temperatures of phase transitions. It is important to generalize the conception on a dynamic case. In the considered cases of modelling it was considered, that kinetic energy of the particles is small in comparison with potential energy of their interaction.

In conclusion we shall note, that significant interest represents the analysis of connections between macroparameters of the concrete materials, which can be done using the known tabulared data for one-nuclear materials (metals). Comparison of these dates with theoretical equations will allow estimating area of applicability of the potentials.

3.5. DEVELOPMENT OF NUMERICAL METHODS FOR MODELLING MEDIA WITH INCLUSIONS.

In this part are presented results on asymptotic homogenization of system of the moment cohesion equations and the formula for effective characteristics of composite materials with the periodic microstructure taking into account local effects near boundary of microinclusions. Also are presented the summary of results on development of algorithm of block analytical-numerical method for spatial moment cohesion problems and some numerical results confirming a correctness of the algorithm.

3.5.1. Homogenization of the system of the equations of moment cohesion.

Let's give in brief the basic results on asymptotic homogenization of the system of the fourth order equations of the moment cohesion with periodic fast oscillating coefficients [Bakhvalov N.S., Panasenko G.P. 1989; Bensoussan A, Lions JL, Papanicolau G. 1978] that corresponds to a technique of definition of effective characteristics of media with periodic microinclusions (of the spheroidal form) with the account of local effects near the interphase layer.

The technique of homogenization is based on a method of "many scales" according to which parallel with slow variables x are entered fast variables $\zeta = \varepsilon^{-1} x$, and system of the equations of moment cohesion rewrites in the form:

$$-\frac{1}{\varepsilon^{-2}C} L\, L_C(\zeta; \vec{R}) + \vec{F}(x) = 0, \qquad L_C(\zeta; \vec{R}) \equiv \frac{\partial}{\partial x_k}\left(A_{kj}(\zeta)\frac{\partial \vec{R}}{\partial x_j}\right) - \varepsilon^{-2} C(\zeta)\vec{R} = 0, \qquad (3.27)$$

$$\zeta = \varepsilon^{-1} x, \quad x = (x_1, x_2, x_3),$$

where ε is the typical size of microinclusions (see Fig. 3.4), $A_{kj}(\zeta)$ are piecewise-constant matrix of Lame factors in a media-matrix and in periodically located microinclusions, $A_{kjpq}(\zeta) = \lambda(\zeta)\delta_{pq}\delta_{kj} + 2\mu(\zeta)\delta_{kp}\delta_{jq}$, $C(\zeta)$ is a parameter of the cohesion field, determined by the width l_0 of an interphase layer, $C(\zeta) = \mu(\zeta)/l_0^2$; $\mu(\zeta) = \mu_m$, $\lambda(\zeta) = \lambda_m$ in a matrix $\mu(\zeta) = \mu_f$, $\lambda(\zeta) = \lambda_f$ in inclusion.

$$\leftarrow \varepsilon \rightarrow$$
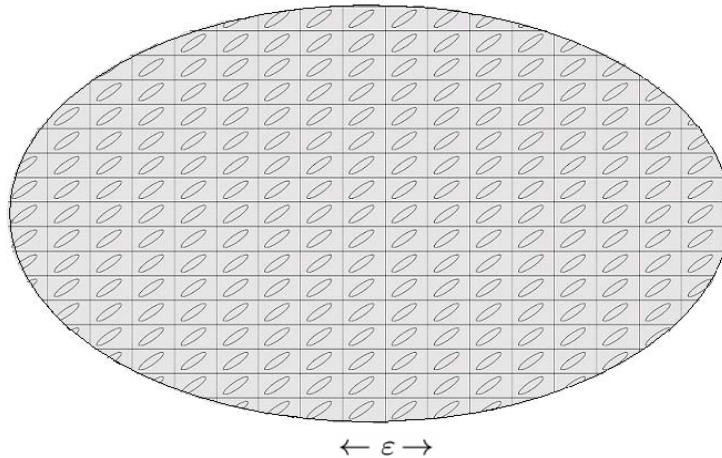
Fig. 3.4.

Asymptotic decomposition for the solution of (3.27) is searched as formal asymptotic expansions on degrees of geometrical parameter ε, which is the period of repeated microinclusions:

$$\vec{R}(x,\zeta) = \sum_{l \geq 0} \sum_{i=(i_1 \ldots i_l)} \varepsilon^l \, N_i(\zeta) \, D^i \vec{V}(x), \tag{3.28}$$

here $\vec{V}(x)$ is the solution of averaging operator (slow function), $N_i(\zeta)$ are the matrix functions being consecutive solutions of a chain of problems on a cell of periodicity with inclusion (fast functions, periodic with the period 1), i is multiindex, $D^i \vec{V}(x)$ are every possible derivatives of the order l on slow variables.

In decomposition (3.28) slow and fast variables are divided. Matrix functions $N_i(\zeta)$ describe local behaviour of the solution near microinclusions, the vector function $\vec{V}(x)$ describes global behaviour of the solution and corresponds to homogenized media with constant factors.

The equations for $N_i(\zeta)$ and the average equation for $\vec{V}(x)$ are received after substitution (3.28) in (3.27), applications of the formula of differentiation of the composite function dependent on slow and fast variables,

$$D_x f(x,\zeta) = \frac{\partial f}{\partial x} + \varepsilon^{-1} \frac{\partial f}{\partial \zeta} \;,$$

and equating of members with identical degrees ε^l in transformed formal asymptotic expansion to zero.

The most important are two first members in decomposition (3.28):

$$\vec{R}(x,\zeta) \approx \vec{V}(x) + \varepsilon \, N_l(\zeta) \frac{\partial \vec{V}(x)}{\partial x_l}, \qquad \hat{A}_{kj} \frac{\partial^2 \vec{V}(x)}{\partial x_k \, \partial x_j} + \vec{F}(x) = 0, \tag{3.29}$$

where $\hat{A}_{kj}$ are the constant matrix factors corresponding to the homogenized elastic media (generally anisotropic), calculated through periodic matrix functions $N_l(\zeta)$ on the formula of averaging on a cell of periodicity G (see [Bakhvalov N.S., Panasenko G.P. 1989]):

$$\hat{A}_{kj} = \left\langle A_{kj}(\zeta) + A_{kl}(\zeta) \frac{\partial N_j(\zeta)}{\partial \zeta_l} + A_{kl}(\zeta) \frac{\partial H_j(\zeta)}{\partial \zeta_l} \right\rangle, \tag{3.30}$$

$$H_j = -\frac{1}{C} L(N_j), \qquad \langle f(\zeta) \rangle = \frac{1}{\mathrm{mes}(G)} \int_G f(\zeta) \, d\zeta . \tag{3.31}$$

Asymptotic approximation (3.29) describes in the first order on ε strain-stress state of the considered heterogeneous media with periodic microinclusions with the account of local effects. Matrix functions of fast variables $N_l(\zeta)$ are defined by the equations on a cell of periodicity (Fig. 3.2) with a contact conjugate condition on surface of inclusion:

$$L \, L_C \left(N_l + \zeta_l \, E \right) = 0, \qquad [N_l] = \left[\frac{\partial N_l}{\partial n} \right] = \left[M_{(n)}(N_l) \right] = \left[P(N_l + \zeta_l \, E) \right] = 0, \tag{3.32}$$

where E is a unit matrix, $\vec{n}$ is a vector of an external normal to a surface of inclusion. The auxiliary problem (3.32) is reduced to a homogeneous problem of moment cohesion on a cell of periodicity with inclusion and with conditions of periodic jump along directions x, y or z.

In the formula for homogenized factors (3.30) matrix function $H_j(\zeta)$ represents a cohesion component of the general field of displacements, and function $N_j(\zeta) + H_j(\zeta)$ is a classical component of the general field of

displacements. Thus, the formula of averaging in a problem of moment cohesion coincides with the classical formula of averaging in the theory of elasticity, but a classical component of the general field of displacements in problems of moment cohesion will differ from displacements in the classical theory of elasticity because of action of a cohesion field caused by presence of an interphase layer.
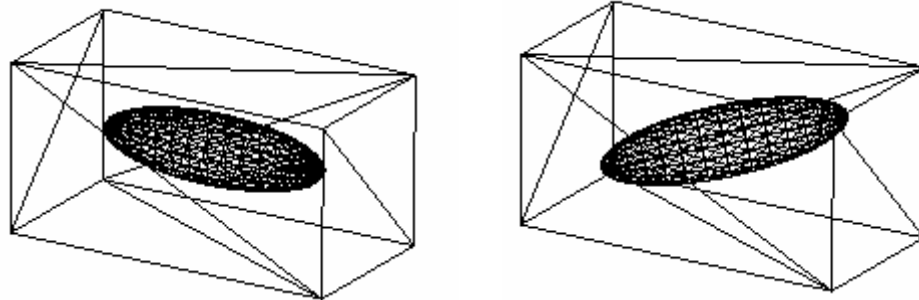
Fig. 3.5.

Thus, the problem (3.32) is the basic in the theory of asymptotic homogenization of system of the equations of moment cohesion, and development of effective numerical-analytical methods is of interest for the solving of these problems. Also is of interest development of effective numerical methods for calculation of averaging characteristics (3.30), (3.31) of periodic media with microinclusions with account of local effects. For previous period within the framework of these tasks just development of such method for a problem (3.32) was carried out on the basis of a block analytic-numerical method of multipoles [Vlasov V.I., Volkov D.B. 1995; Vlasov V.I., Volkov D.B. 1996; Vlasov V.I., Volkov-Bogorodsky D.B ; Volkov-Bogorodsky D.B. 2000; Volkov-Bogorodsky D.B. 2001].

The problem (3.32) can be considered also as independent on a homogenization method problem of testing of a sample of a composite material with inclusions under special loading conditions.

Energy of strain-stress state of cell G in a problem of spatial moment cohesion determined through components of strain tensor of displacements $\varepsilon_{ij}(\vec{R})$ and a vector of elastic rotations $\vec{\omega} = 1/2 \, rot \, \vec{R}$ in the following kind:

$$E(\vec{R}) = \frac{1}{2}\int_G \left[2\mu\,\varepsilon_{ij}\,\varepsilon_{ij} + \lambda\,\theta^2 + 8\frac{\mu^2}{C}\xi_{ij}\,\xi_{ij} + \frac{(2\mu+\lambda)^2}{C}\theta_i\theta_i \right] dV \,,$$

where

$$\theta_i = \frac{\partial \theta}{\partial \zeta_i}\,, \qquad \theta = \theta(\vec{R}) = \varepsilon_{ii}\,, \qquad \varepsilon_{ij} = \frac{1}{2}\left(\frac{\partial R_i}{\partial \zeta_j} + \frac{\partial R_j}{\partial \zeta_i} \right)\,, \qquad \xi_{ij} = \frac{1}{2}\left(\frac{\partial \omega_i}{\partial \zeta_j} + \frac{\partial \omega_j}{\partial \zeta_i} \right)\,.$$

On the boundary between two phases both components of the general field of displacements interact among themselves in such a manner that satisfied four conditions:

$$\left[\vec{R} \right] = \left[\frac{\partial \vec{R}}{\partial n} \right] = \left[\vec{M}_{(n)}(\vec{R}) \right] = \left[\vec{P}(\vec{R}) \right] = 0 \,,$$

where

$$\vec{P}(\vec{R}) = \vec{p}(\vec{U}) + \frac{\partial \vec{M}_{(s)}(\vec{R})}{\partial s} + \frac{\partial \vec{M}_{(\tau)}(\vec{R})}{\partial \tau}\,, \qquad \vec{p}(\vec{U}) = A_{kj}\frac{\partial \vec{U}}{\partial \zeta_j}\,n_k \,,$$

$\vec{p}(\vec{U})$ are classical forces on a surface of inclusion from a classical component of the general field of displacements, $\vec{s}$ and $\vec{\tau}$ are two orthogonal directions in a tangent plane on a surface of inclusion,

118

$$M_{i(n)}(\vec{R}) = \frac{(2\mu + \lambda)^2}{C} \frac{\partial \theta(\vec{R})}{\partial \zeta_m} n_m n_i - \frac{2\mu^2}{C} \frac{\partial \omega_k(\vec{R})}{\partial \zeta_m} (n_m n_j \Im_{ijk} + n_k n_j \Im_{ijm}),$$

where $\{\Im_{ijk}\}$ is Somilliana tensor, accepting value ± 1, depending on even or odd permutation of indexes $\{ijk\}$.

3.5.2. The summary of results.

The basic stages in development of a block analytic-numerical method of nultipoles for the problems of moment cohesion were stated during performance of a work and reflected in the previous reports. We shall result in brief the summary of the basic results.

It was performed several general schemes of a block method of multipoles, and in a final variant it has been reserved as the most convenient scheme of dividing initial domain "in a joint" for construction system of blocks. This scheme assumes dividing of initial domain $\bar{G} = \cup \, \bar{B}_k$ into system of the blocks $\{B_k\}$ crossed among themselves only on the boundary: $B_k \cap B_l = \varnothing \; k \neq l$. These blocks are simply connected subdomains of G inside which the solution of homogeneous Helmholtz equation is searched as expansions

$$\Phi(P) = \sum_{n=0}^{\infty} \sum_{m=0}^{n} \left[a_{nm} \Phi_n^m (P - P_0) + b_{nm} \bar{\Phi}_n^m (P - P_0) \right] \tag{3.33}$$

on system of special functions Φ_n^m (see [5]), similar to the polynomials having singularities in infinity point:

$$\Phi_n^m(P) = \sum_{p=0}^{\left[\frac{n-m}{2}\right]} \frac{I_{m+p}(\kappa r)}{p!} \left(\frac{r}{2\kappa} \right)^p e^{im\varphi} \frac{d^{2p}}{d\,z^{2p}} \left(A_m z^{n-m} \right), \qquad A_m = (2/\kappa)^m \, m!, \tag{3.34}$$

where $I_m(t)$ are modified Bessel functions of the first kind [Bateman H., Erdelyi A. 1973] $r e^{i\varphi} = x + i\,y$.

For block structure is used dividing spatial area on tetrahedral blocks (see an example on Fig. 3.6):
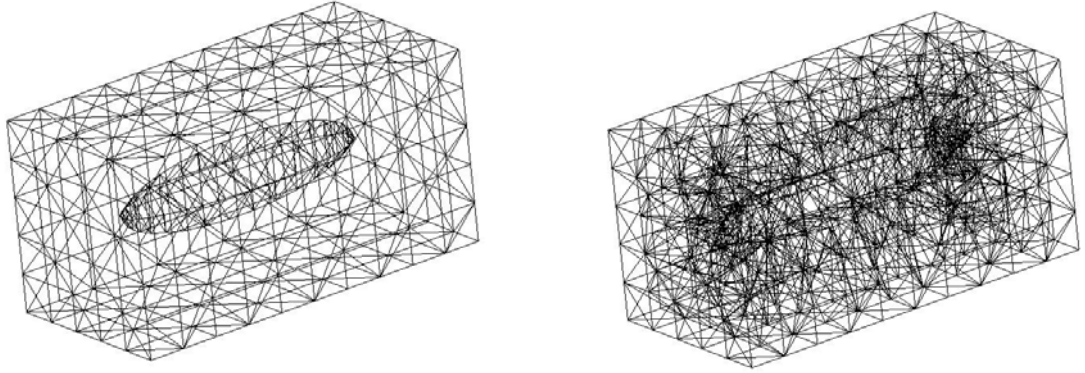
Fig. 3.6.

At that curvature of spheroidal inclusion is taken into account, i.e. tetrahedral blocks adjoining to boundary of inclusion are replaced during solution of the problem with curvilinear tetrahedrons.

For plane domains is used splitting of computation area into system of elementary triangles or quadrangles, without presentation of strict requirements on their form and the size (see Fig. 3.7). Thus curvature of inclusions also is taken into account.
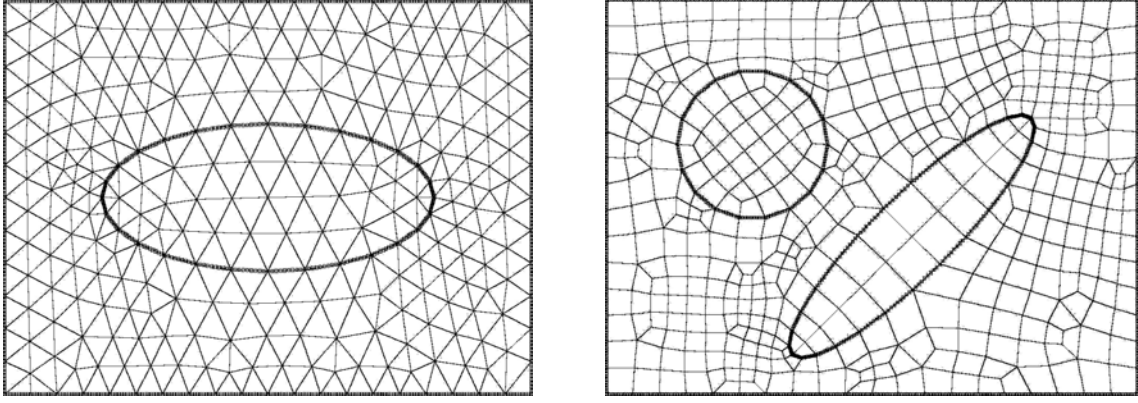
Fig. 3.7.

Every elementary tetrahedron, triangle or a quadrangle is used as the separate block B_k in a block analytical-numerical method of multipoles.

Connection between the general displacements and the auxiliary potentials satisfying Laplace or Helmholtz equations is established by means of general Neuber-Papkovich type representation.

It has been proved that the field of the displacements, submitting to the non-uniform equation $L_C(\vec{u}) = \vec{F}$, can be uniquely represented through two coordinated among themselves vector potentials, satisfying to Helmholtz equation:

$$\nabla^2 \vec{f}(P) - \frac{C}{\mu} \vec{f}(P) = \vec{F}(P),$$ (3.35)

$$\nabla^2 \vec{f}^*(P) - \frac{C}{2\mu + \lambda} \vec{f}^*(P) = \vec{F}(P).$$ (3.36)

We will name these potentials coordinated in some point P_0 inside domain of representation of displacements if in this point coincide any derivatives on variables $w = x + i\, y$ and z:

$$\frac{\partial^n \vec{f}(P_0)}{\partial w^m \partial z^{n-m}} = \frac{\partial^n \vec{f}^*(P_0)}{\partial w^m \partial z^{n-m}}, \qquad \frac{\partial}{\partial w} = \frac{1}{2}\left(\frac{\partial}{\partial x} - i \frac{\partial}{\partial y} \right), \qquad 0 \le m \le n.$$ (3.37)

The condition (3.11) uniquely defines potential $\vec{f}^*$ through potential $\vec{f}$ (or vice versa).

Theorem 1. _Any solution of the cohesion field equation_ $L_C(\vec{u}) = \vec{F}$ _can be uniquely represented as_

$$\vec{u}(P) = \frac{1}{\mu} \vec{f}(P) + \frac{1}{C} \nabla \operatorname{div}\left[\vec{f}^*(P) - \vec{f}(P) \right]$$ (3.38)

through two vector potentials $\vec{f}$ _and_ $\vec{f}^*$, _satisfying Helmholtz equation (3.35), (3.36), and coordinated among themselves by a condition (3.37)._

From conditions (3.37) in particular follows, that $\vec{f}^*(P) \to \vec{f}(P)$ at $C \to 0$; it can be show, that for solution of the homogeneous equation $L_C(\vec{u}) = 0$ the following property is carried out

$$\operatorname{div}\left[\frac{\vec{f}^*(P) - \vec{f}(P)}{C} \right] \to \frac{\vec{r}\, \vec{f}(P)}{4(1-\nu)}, \qquad C \to 0.$$

Thus, from representation (3.38) at $C \to 0$ follows representation for a classical component $\vec{U}(P)$ of the general field of the displacements, satisfying to the homogeneous equation of classical theory of elasticity $L(\vec{U}) = 0$. It is so-called Neuber-Papkovich representation [Novazki V. 1975] for displacements in the static theory of elasticity:

120

$$\vec{U}(P) = \frac{1}{\mu}\vec{f}_0(P) - \frac{1}{4\mu\,(1-\nu)}\nabla\left[\vec{r}\,\vec{f}_0(P)\right],$$

where $\vec{r} = (x,\,y,\,z)$ is a radius-vector to the point P from the beginning of coordinates, $\vec{f}_0$ is a harmonious vector, $\vec{r}\,\vec{f}_0$ is a scalar product of two vectors.

Thus, the solution of the homogeneous equation of spatial moment cohesion is reduced to a finding of the vector potentials satisfying Laplace or Helmholtz equations. These potentials are used in a block analytical-numerical method and are represented as decomposition (3.33), (3.34).

The representation (3.33), (3.34) is analogue of Taylor series for solution of the equation (3.35) or (3.36), because it strong satisfies to Helmholtz equation, and its corfficirnts can be calculated with the help of differentiation on variables z and $w = x + i\,y$.

Theorem 2. *Any solution of the equation (3.35) can be represented in some vicinity of a point $P_0 \in G$ as convergent series (3.33 (3.34), and coefficients a_{nm} and b_{nm} are calculated with the help of differentiation of the solution Φ in a point P_0:*

$$a_{nm} = \frac{1}{m!\,(n-m)!}\frac{\partial^n\Phi(P)}{\partial w^m\,\partial z^{n-m}}, \qquad b_{nm} = \frac{1}{m!\,(n-m)!}\frac{\partial^n\Phi(P)}{\partial \overline{w}^m\,\partial z^{n-m}}, \qquad b_{n0} = 0.$$

Theorems 1 and 2 are theoretical basis of a block method of multipoles in application to the solution of a problem (3.32). As basic system of functions the system of multipoles (3.34) can be applied. From the theorem 2 follows completeness of this system of functions.

Conjunction of local representations in blocks and the satisfaction to conditions (3.32) on boundary of inclusion was carried out by means of system of functional of the least squares method simultaneously sewing functions and its normal derivatives on boundary between blocks. The condition of functional minimization is realized as block system of the equations for a finding of unknown coefficients in decomposition (3.33).

Periodic conditions for a problem (3.32) represent a special kind of loading, corresponding to a uniform stretching of a sample in the certain direction, for example in direction of an axis x:

$$\vec{u}\,(x+L,\,y,\,z) = \vec{u}\,(x,\,y,\,z) + \vec{e}_x, \quad \vec{u}\,(x,\,y+H,\,z) = \vec{u}\,(x,\,y,\,z), \quad \vec{u}\,(x,\,y,\,z+W) = \vec{u}\,(x,\,y,\,z), \qquad (3.39)$$

where L, H and W are accordingly the sizes of a parallelepiped in a direction x, y and z, $\vec{e}_x$ is basis vector of axes x. To the boundary conditions (3.39) the following functional of square-law residual are correspondent for local solutions in blocks:

$$\left\|\vec{U}_k^+ - \vec{U}_j^- - \vec{e}_x\right\|^2_{L_2(S_k)} + \left\|\vec{u}_k^+ - \vec{u}_j^-\right\|^2_{L_2(S_k)} + \sum_l\left\|\frac{\partial\vec{U}_k}{\partial n} - \frac{\partial\vec{U}_l}{\partial n}\right\|^2_{L_2(S_{kl})} + \sum_l\left\|\frac{\partial\vec{u}_k}{\partial n} - \frac{\partial\vec{u}_l}{\partial n}\right\|^2_{L_2(S_{kl})} = \min,$$

$$\left\|\frac{\partial\vec{U}_j^+}{\partial n} - \frac{\partial\vec{U}_k^-}{\partial n}\right\|^2_{L_2(S_j)} + \left\|\frac{\partial\vec{u}_j^+}{\partial n} - \frac{\partial\vec{u}_k^-}{\partial n}\right\|^2_{L_2(S_j)} + \sum_l\left\|\vec{U}_k - \vec{U}_l\right\|^2_{L_2(S_{kl})} + \sum_l\left\|\vec{u}_k - \vec{u}_l\right\|^2_{L_2(S_{kl})} = \min;$$

here S_k and S_j are parallel boundaries of blocks B_k and B_j, connected among themselves by a condition of parallel transposition along a coordinate axis x; $\vec{U}_k^+$, $\vec{u}_k^+$ and $\vec{U}_j^-$, $\vec{u}_j^-$ are corresponding values of local functions on boundaries S_k and S_j. It is supposed, that in case of periodic loading block system of all sample meets the requirement,

that the parallel sides of a parallelepiped are divided by boundary blocks so, that to each element S_k will be corresponding a parallel element S_j.

Minimization of all functiomal system results in block system of the linear equations for a finding of unknown coefficients in the solution:

$$A_k \vec{X}_k + \sum_l T_{kl} \vec{X}_l = \vec{H}_k, \qquad k = 1, 2, \ldots N. \tag{3.40}$$

For the solution of system of the equations (3.40) it was applied two methods – direct and iterative. The first is block realization of a Gauss elimination method with the direct inversing on each step of exception of a diagonal matrix A_k with the help of Gauss-Jordan method with a full pivoting. The second method is the iterative scheme of GMRES with preconditioning, constructed by the incomplete triangular decomposition ILUT.

Calculation of residual norm for required magnitude in functional was carried out by means of Gaussian quadratures of the high order adapted for a curvilinear surface of spheroidal inclusions.

3.5.3. Another systems of basic functions.

Besides system of multipoles (3.34) it can be used other systems of basic functions. Below deduction of parametrical family of multipoles for the solution of Helmholtz equation is given. This family contains as a special case system (3.34) and can be used instead (3.34) for achieving more quality of approximation. This result was not included in the previous reports.

The system is entered on the basis of the analysis of initial Helmholtz equation in complex variables $w = x + i\,y$, $\bar{w} = x - i\,y$ and z:

$$\nabla^2 \Phi - \kappa^2 \Phi = 4 \frac{\partial^2 \Phi}{\partial w \, \partial \bar{w}} + \frac{\partial^2 \Phi}{\partial z^2} - \kappa^2 \Phi = 0. \tag{3.41}$$

The system of multipoles is entered with the help of separation of complex variables w, $\bar{w}$ and z:

$$\Phi(P) = \Phi(w, \bar{w}, z) = \sum_p \phi_p(w, \bar{w}) \, U_p(z). \tag{3.42}$$

Substitution (3.42) in (3.41) allows to group members of turning out formal series as follows:

$$\nabla^2 \Phi(P) - \kappa^2 \Phi(P) = \sum_p \left\{ \left(4 \frac{\partial^2 \phi_p(w, \bar{w})}{\partial w \partial \bar{w}} - \kappa_1^2 \phi_p(w, \bar{w}) \right) U_p(z) + \phi_p(w, \bar{w}) \left(U_p''(z) - \kappa_2^2 U_p(z) \right) \right\}.$$

In this representation the free constant κ^2 in the equation is replaced with the sum of two any constants $\kappa^2 = \kappa_1^2 + \kappa_2^2$. The first term in the received sum corresponds to a case when exponentially decreasing members communicate with a plane, orthogonal to the chosen direction. The second term corresponds to a case exponentially decreasing members communicate directly with the chosen direction (i.e. with an axis z).

Let's assume the following:

1) $U_0(z)$ is any function;

2) $\phi_0(w, \bar{w})$ is the decision of plane Helmholtz equation,

$$4 \frac{\partial^2 \phi_0(w, \bar{w})}{\partial w \partial \bar{w}} - \kappa_1^2 \phi_0(w, \bar{w}) = 0;$$

3) all other members satisfy to conditions:

$$\left(4 \frac{\partial^2 \phi_p(w, \bar{w})}{\partial w \partial \bar{w}} - \kappa_1^2 \phi_p(w, \bar{w}) \right) U_p(z) + \phi_{p-1}(w, \bar{w}) \left(U_{p-1}''(z) - \kappa_2^2 U_{p-1}(z) \right) = 0.$$

Then members of series (3.42) take to zero after a regrouping, and the common solution of Helmholtz equation is received as formal series (3.42) with two sequences of unknown functions $\phi_p(w, \overline{w})$ and $U_p(z)$ connected among themselves the recurrent correlations which are obraining as a result of performance of above formulated conditions:

$$4\frac{\partial^2 \phi_p(w, \overline{w})}{\partial w \partial \overline{w}} - \kappa_1^2 \phi_p(w, \overline{w}) - \phi_{p-1}(w, \overline{w}) = 0, \qquad (3.43)$$

$$U_p^{''}(z) - \kappa_2^2 U_p(z) + U_{p+1}(z) = 0. \qquad (3.44)$$

A formal series (3.42) – (3.44) represents some class of the common solutions of the equation (3.41), parametrically dependent on parameter κ_1, and based on continuation of solution of Helmholtz equation from a plane on all space along an axis z; function $U_0(z)$ sets a way of such continuation.

The concrete type of the common solution (3.42) is defined by additional reasons. An origin point for the equations (3.43), (3.44) is any function $U_0(z)$ and the solution of plane equation $\phi_0(w, \overline{w})$. We put $\phi_0(w, \overline{w})$ in the form:

$$\phi_0(w, \overline{w}) = w^\mu F_\mu(\kappa_1^2 \, w \overline{w}), \qquad (3.45)$$

$$F_\mu(t) = \sum_{k=0}^{\infty} \frac{t^k}{4^k \, k! \, (\mu+1)_k}, \qquad (3.46)$$

where $(a)_k = a(a+1)\ldots(a+k-1)$ is Pokhgammer symbol [Bateman H., Erdelyi A. 1973]. This is the elementary solution of plane Helmholtz equation in the cylindrical coordinates, similar to power function w^μ (which we name a plane multipole of Laplace equation), and it is expressed through modified Bessel function:

$$\phi_0(w, \overline{w}) = \phi_0(r, \varphi) = A_\mu I_\mu(\kappa_1 r) \, e^{i\mu\varphi}, \qquad A_\mu = \frac{2^{\mu/2}(\mu+1)!}{\kappa_1^\mu}.$$

All other functions $\phi_p(w, \overline{w})$ of the recurrent equation (3.43) also can be expressed through (3.46):

$$\phi_p(w, \overline{w}) = \phi_p^{(\mu)}(w, \overline{w}) = \frac{(-1)^p w^{\mu+p} \overline{w}^p}{4^p \, p! \, (\mu+1)_p} F_{\mu+p}(\kappa_1^2 \, w \overline{w}). \qquad (3.47)$$

Recurrent system of the equations (3.44) is resolved as $U_p(z) = u_p(z) e^{-\kappa_2 z}$, where $u_p(z)$ are polynomials of a decreasing degree connected by recurrent correlations:

$$U_p(z) = u_p(z) e^{-\kappa_2 z}, \qquad u_{p+1}(z) = u_p^{''}(z) - 2\kappa_2 u_p'(z). \qquad (3.48)$$

The choice of the remaining unknown function $u_0(z)$ is connected with definition of the common solution (3.42) – (3.44) in a limiting case $\kappa = 0$. If we believe $u_0(z) = z^{\nu-\mu}$ at the whole non-negative $\nu - \mu$, the system of functions (3.42) – (3.44) at $\kappa_{1,2} \to 0$ transforms in system of spherical functions, i.e. in system of electrostatic multipoles [Morse P.M., Feshbach H. 1953].

Thus, we have obtained (at the whole non-negative $\nu - \mu$) required system of functions:

$$\Phi(P) = \Phi_\nu^\mu(P, \kappa_1, \kappa_2) = \sum_{p=0}^{\nu-\mu} \frac{(-1)^p w^{\mu+p} \overline{w}^p}{4^p \, p! \, (\mu+1)_p} F_{\mu+p}(\kappa_1^2 \, w \overline{w}) \, u_p(z) e^{-\kappa_2 z}, \qquad (3.49)$$

$$u_{p+1}(z) = u_p^{''}(z) - 2\kappa_2 u_p'(z), \qquad u_0(z) = z^{\nu-\mu}, \qquad \nu - \mu = k \geq 0. \qquad (3.50)$$

At $\kappa_{1,2} \to 0$ representation (3.49), (3.50) transforms (at the whole non-negative ν и μ) in representation for system of the normalized spherical functions $B_\mu R^\nu P_\nu^{-\mu}(\cos\theta)\, e^{i\mu\varphi}$, where $B_\mu = 2^{-\mu}/\Gamma(\mu+1)$, Γ is Euler's function, $R = \sqrt{x^2 + y^2 + z^2}$.

Directly differentiating (3.49) and taking into account a relationship $F_\mu'(t) = -F_{\mu+1}(t)/4(\mu+1)$, it is easy to make sure of differential recurrent correlations:

$$\frac{\partial\,\Phi_\nu^\mu}{\partial z} = (\nu-\mu)\,\Phi_{\nu-1}^\mu - \kappa_2\Phi_\nu^\mu \;, \qquad \frac{\partial\,\Phi_\nu^\mu}{\partial z} = (\nu-\mu)\,\Phi_{\nu-1}^\mu, \qquad \mu\neq 0, \tag{3.51}$$

$$\frac{\partial\,\Phi_\nu^\mu}{\partial\,\overline{w}} = -\frac{(\nu-\mu)(\nu-\mu-1)\Phi_{\nu-1}^{\mu+1} - \kappa_1^2\,\Phi_{\nu+1}^{\mu+1} - 2(\nu-\mu)\kappa_2\Phi_\nu^{\mu+1}}{4(\mu+1)}, \tag{3.52}$$

Correlations (3.51) – (3.52) allow analytically differentiating of local representations of solution (3.33).

3.5.4. Three-dimensional, plane and double plane problems of moment cohesion.

Because the initial model is enough difficult object, it is a spatial system of the equations of 4-th order, and then debugging of a method was carried out on more simple models. It is possible to form hierarchy of these models, consistently simplifying initial model. They are spatial model of moment cohesion, plane model and so-called double plane model of moment cohesion.

It is necessary to note, that, despite of simplifications, all these models are of interest for research of properties of composite materials with local effects, and can be practically applied for calculation of effective characteristics of materials with microinclusions.

The initial spatial model is represented by the vector equation

$$-\frac{1}{C}L\,L_C(\vec{R}) + \vec{F} = 0, \quad L_C(\vec{R}) = \mu\nabla^2\vec{R} + (\mu+\lambda)\nabla\,\mathrm{div}\,\vec{R} - C\,\vec{R}, \tag{3.53}$$

with junction conditions on a surface of inclusion

$$\left[\vec{R}\right] = \left[\frac{\partial\,\vec{R}}{\partial n}\right] = \left[\vec{M}_{(n)}(\vec{R})\right] = \left[\vec{p}\,(\vec{U}) + \frac{\partial\vec{M}_{(s)}(\vec{R})}{\partial s} + \frac{\partial\vec{M}_{(\tau)}(\vec{R})}{\partial\tau}\right] = 0. \tag{3.54}$$

The plane model is represented by a projection of spatial model in 2D. Formally it corresponds to conditions: $R_z = 0$, $\partial/\partial z = 0$. The equation in 2D has the same form (3.53) as well as in 3D, but junction conditions (3.54) become simpler:

$$\left[\vec{R}\right] = \left[\frac{\partial\,\vec{R}}{\partial n}\right] = \left[\vec{M}_{(n)}(\vec{R})\right] = \left[\vec{p}\,(\vec{U})\right] = 0; \tag{3.55}$$

into a last component are entered only surface forces of a classical component of the general field of displacements.

It follows from the formula of representation the cohesion moments which becomes simpler in 2D as follows:

$$\vec{M}_{(n)}(\vec{R}) = \left\{M_{(n)},\, -M_{(s)}\right\}, \qquad \vec{M}_{(s)}(\vec{R}) = \left\{M_{(s)},\, M_{(n)}\right\},$$

$$M_{(n)} = M_{11}(\vec{R})\,n_x + M_{12}(\vec{R})\,n_y, \qquad M_{(s)} = -M_{11}(\vec{R})\,n_y + M_{12}(\vec{R})\,n_x,$$

$$M_{11}(\vec{R}) = \frac{(2\mu+\lambda)^2}{C}\frac{\partial\,\theta(\vec{R})}{\partial n}, \qquad M_{12}(\vec{R}) = -\frac{2\mu^2}{C}\frac{\partial\,\omega_3(\vec{R})}{\partial n}.$$

The continuity of each component $\left[M_{(n)}(\vec{R})\right] = \left[M_{(s)}(\vec{R})\right] = 0$ or $\left[M_{(11)}(\vec{R})\right] = \left[M_{(12)}(\vec{R})\right] = 0$ follows from conditions of a continuity of the cohesion moments $\vec{M}_{(n)}(\vec{R})$, and the continuity of tangent derivatives on a smooth part of a contour

follows from here. Thus, in a plane case jump of tangent derivatives of the cohesion moments can be rejected, and on a surface of smooth inclusion work only classical forces $\vec{p}\,(\vec{U})$.

The double plane problem assumes the approximate description of a plane problem due to rejection of one components of a vector of displacements: $R_y = 0$. Boundary conditions (3.29) are satisfied approximately (in the first order of accuracy). In result we receive one equation of 4-th about remaining component $R = R_x$:

$$-\frac{1}{C}L\,L_C\,R = 0, \qquad L = L_C\big|_{C=0}, \quad L_C = (2\mu+\lambda)\frac{\partial^2}{\partial x^2} + \mu\frac{\partial^2}{\partial y^2} - C. \tag{3.56}$$

Thus the problem breaks up to two independent problems for a classical field of displacement U ($\square U = 0$) and for cohesion field u ($L_C\,u = 0$), in composition forming full displacement $R = U - u$. On boundary of inclusion the approximate junction conditions are set:

$$[U] = [u] = 0, \quad \left[\mu\frac{\partial U}{\partial n} + (\mu+\lambda)\frac{\partial U}{\partial x}\,n_x\right] = 0, \quad \left[\frac{\partial u}{\partial n} - \frac{\partial U}{\partial n}\right] = 0.$$

The transformation of coordinates $\Phi(x,\ y) = \Phi(\sqrt{2\mu+\lambda}\ \tilde{x},\ \sqrt{\mu}\ \tilde{y}) = \tilde{\Phi}(\tilde{x},\ \tilde{y})$ is applied to a double plane problem instead of representation (3.38), which reduce the equation (3.56) to Helmholtz equation $\nabla^2\tilde{\Phi} - C\,\tilde{\Phi} = 0$.

All these problems of moment cohesion have been consistently realized by a block analytical-numerical method. Below is represented results of testing of a spatial problem of moment cohesion for a homogeneous spatial beam with the sizes $L = 1$, $H = 2$ and $W = 1$ (see fig. 3.8), subject to a uniaxial tension along the axis y:

$$L\,L_C(\vec{R}) = 0, \quad \frac{\partial\vec{R}(P')}{\partial n} = 0, \quad \vec{M}_{(n)}(\vec{R}) = 0, \qquad P' \in S^{(\pm x)} \cup S^{(\pm y)}\ ,$$

$$\vec{R}(P') = 0, \quad \frac{\partial\vec{R}(P')}{\partial n} = 0, \quad P' \in S^{(-y)}, \quad \vec{R}(P') = \vec{e}_2, \quad \frac{\partial\vec{R}(P')}{\partial n} = 0\ , \quad P' \in S^{(+y)};$$

here $S^{(-y)}$ and $S^{(+y)}$ accordingly the bottom and top face of a beam. The beam has been divided on 10 tetrahedral blocks as it is shown on fig. 3.8. The problem in the formulated statement has the analytical solution:

$$R_2(y) = \frac{1}{2}\left[1 + \frac{(y-H/2)\kappa(e^{H\kappa} - e^{-H\kappa}) - (1-e^{-H\kappa})e^{\kappa y} - (1-e^{H\kappa})e^{-\kappa y}}{2 - (1-H\kappa/2)e^{H\kappa} - (1+H\kappa/2)e^{-H\kappa}}\right], \qquad \kappa = \frac{C}{2\mu+\lambda}.$$

On fig. 3.9 the picture of convergence of a block method of multipoles is submitted at $N \to \infty$; displacement and its derivative along an axis y are submitted at $N = 1, 2, 3, 4, 5, 7$. At $N = 7$ the numerical solution practically coincides with the analytical solution, the relative error together with the first order derivatives is equal 10^{-4}.
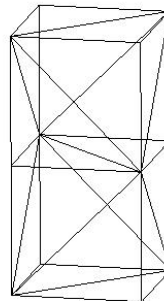
Рис. 3.8
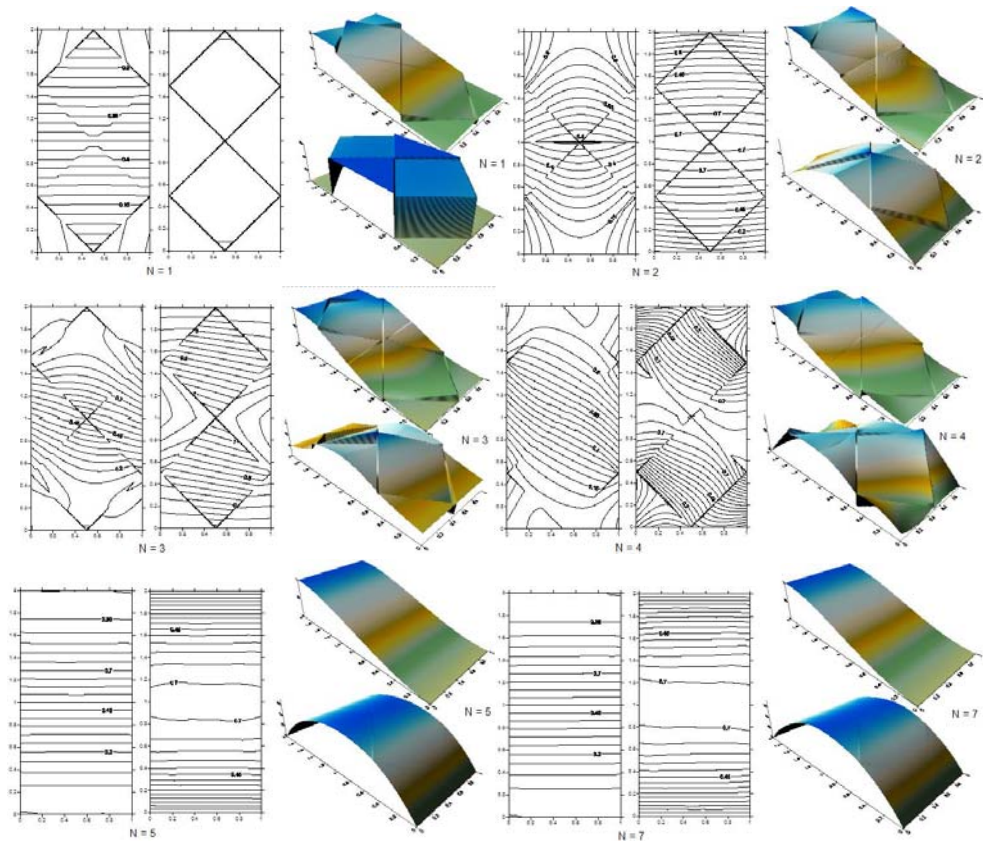
Рис. 3.9.

Other numerical results have been submitted in the previous reports. In the annual report for 2002 numerical results for a double plane problem were submitted. Some new numerical results for a plane problem of moment cohesion are presented below.

3.5.5. Examples of numerical calculations.

It is represented below comparative calculations by a block analytical-numerical method of a plane moment cohesion problem on a rectangular cell $L \times H$ with inclusion of elliptic (or, in particular, circular) form. It is of interest research of influence of a cohesion field determined by parameter $c_0 = C/\mu = l_0^{-2}$ on distribution of tension and density of energy in a matrix and inclusion, and also comparison of a strain-stress state and distributions of energy in a cell for moment and for the classical problem, it is formally corresponds to a limiting process $c_0 \to \infty$. The classical problem has been realized separately with the help of a block method of multipoles.

On Fig. 3.10 distribution of density of energy in a cell is represented at different value of cohesion parameter ($c_0 = 100,\ 1000,\ \infty$) for inclusion of the circular form with the radius $R = 0.4$, located in the center of a rectangular matrix with the sizes $L = 2\ H = 1.2$. It was assumed that in matrix $\mu_m = 1$, $\nu_m = 0.3$, in inclusion $\mu_f = 2$, $\nu_f = 0.3$:
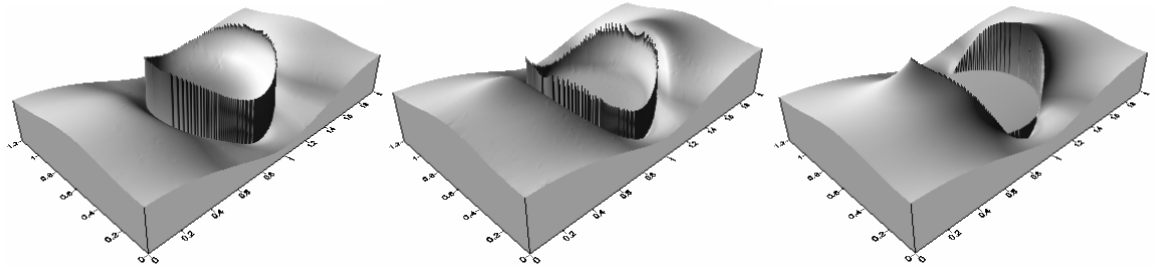
Fig. 3.10.

Redistribution of energy between a matrix and inclusion is well visible. For a classical problem energy is concentrated basically in a matrix, for a modelling problem of plane moment cohesion energy is redistributed in inclusion.

On Fig. 3.11 distribution components $\sigma_{xx}(\vec{R})$ and $\sigma_{yy}(\vec{R})$ of classical stress tensor is presented at the same values of cohesion parameter $c_0 = 100, \ 1000, \ \infty$:
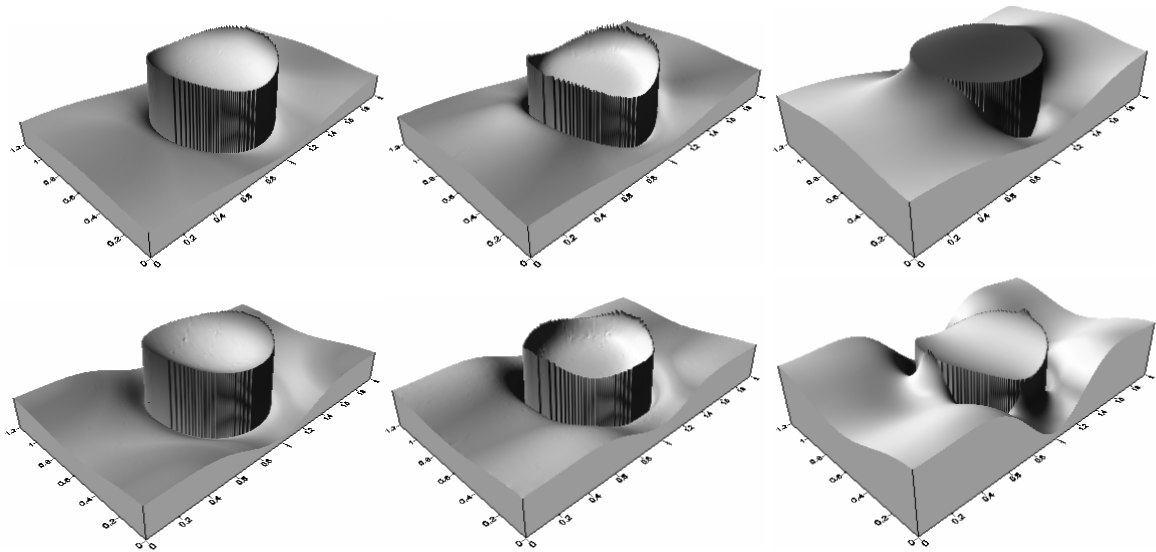
Fig. 3.11.

Here is observed the unloading of a matrix at reduction of parameter c_0 (i.e. at increasing width of an interphase layer l_0).

And at last, on Fig. 3.12 is represented distribution of the periodic function $N_{1x}(P) = R_x(P) - x$, having high significance in the asymptotic theory of homogenization (3.29), (3.30), and function of cubic dilatation $\theta(\vec{R})$ at the same values of cohesion parameter:

127
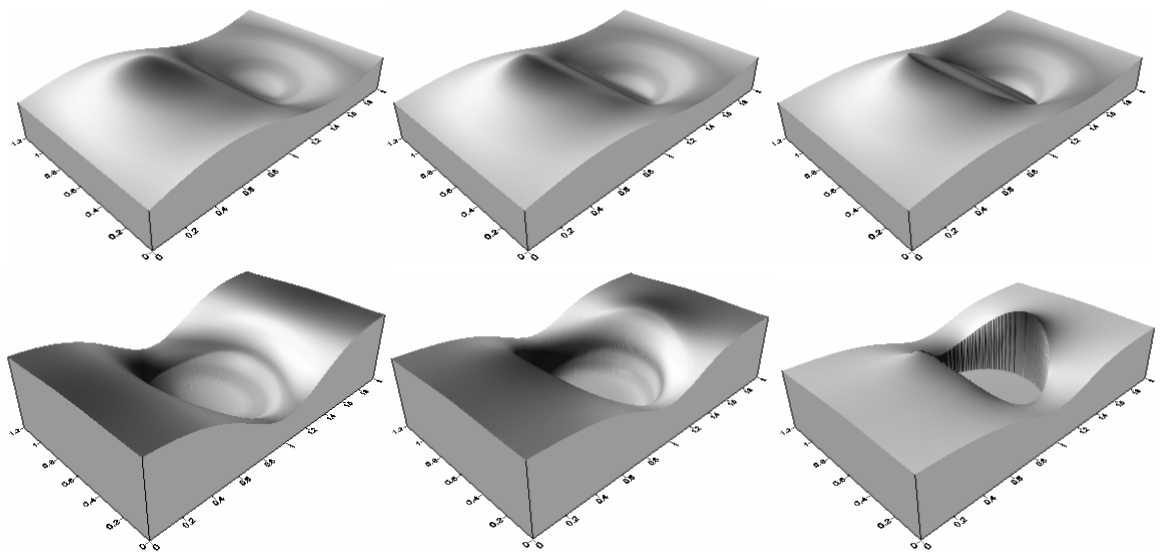
Fig. 3.12.

Changing of width of an interphase layer and effect of smoothing of the solution is well visible at increasing portion of cohesion field (i.e. at reduction c_0).

On Fig. 3.13 – 3.16 picture of changing of function $N_{1x}(P)$ (Fig. 3.13), density of energy (Fig. 3.14), components of stress tensor $\sigma_{xx}(\vec{R})$ (Fig. 3.15) and cubic dilatation $\theta(\vec{R})$ (Fig. 3.16) are presented at various value of cohesion parameter $c_0 = \infty,\ 1000,\ 100$ on a middle line $\{0 < x < 2,\ y = 0.6\}$:
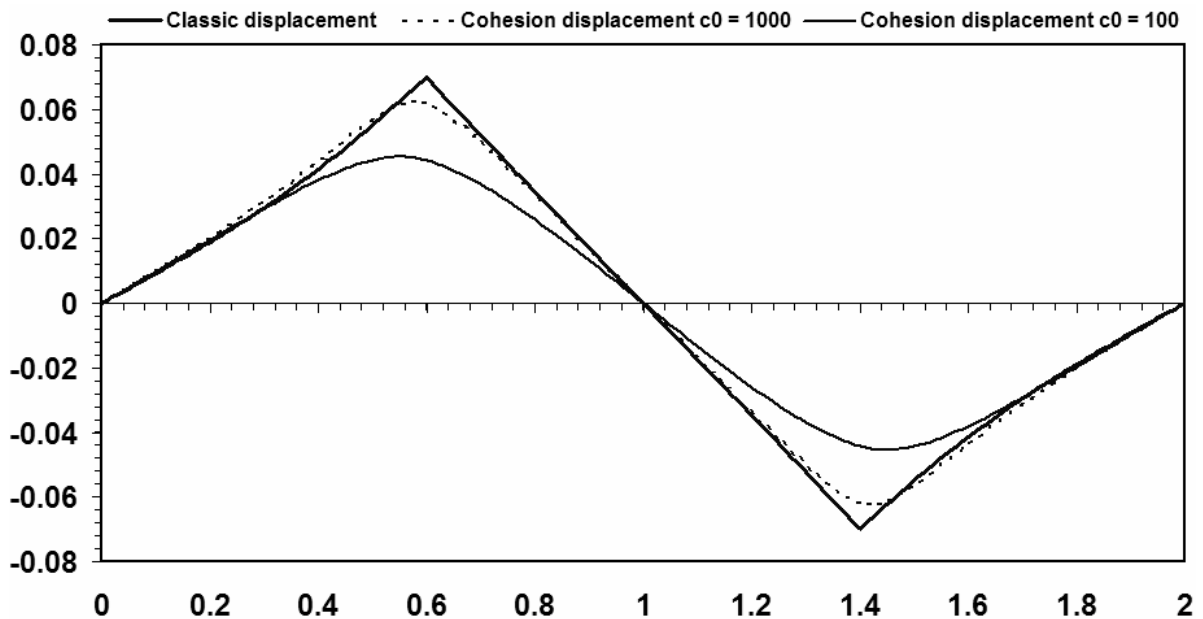
Fig. 3.13.

Fig. 3.14.

Fig. 3.15.

129
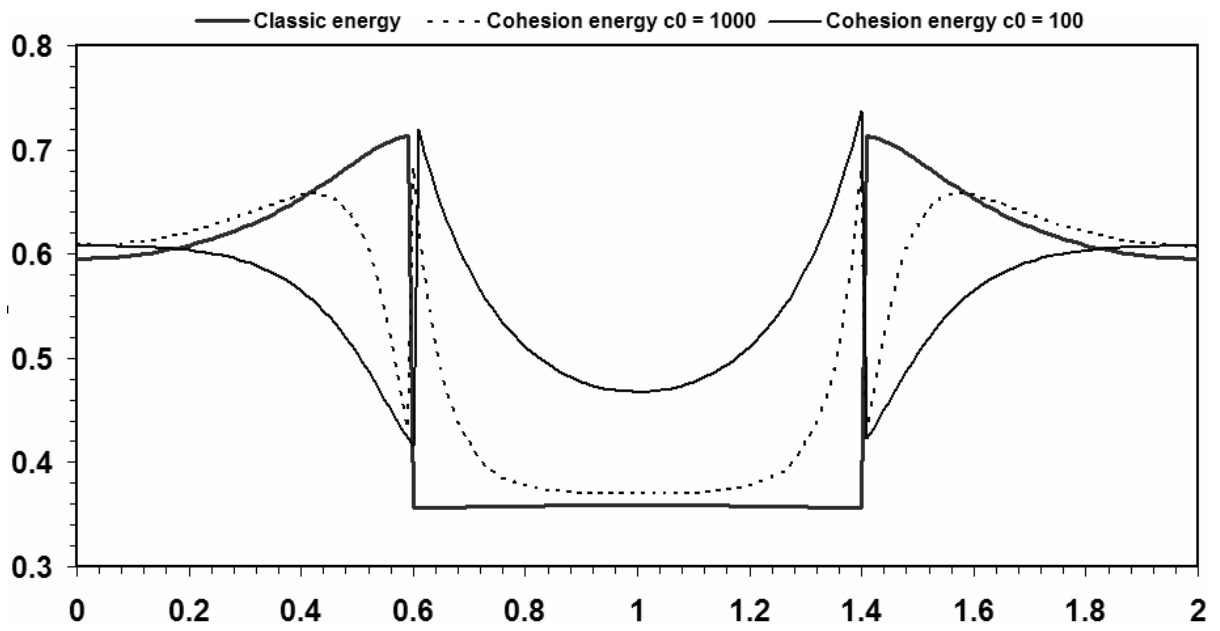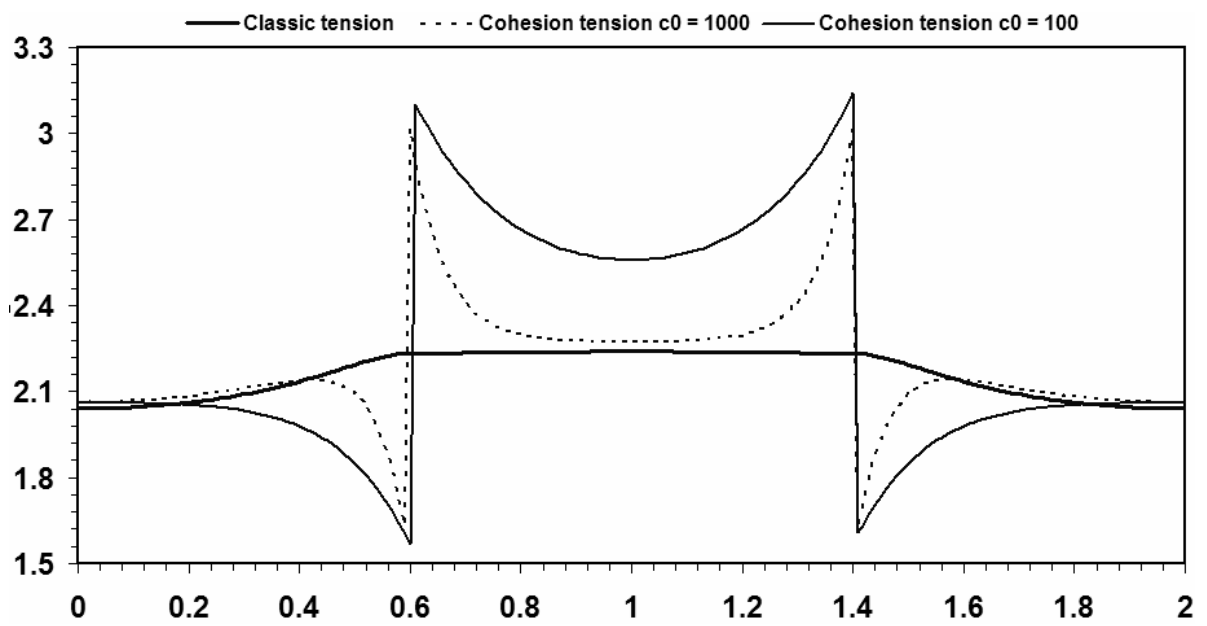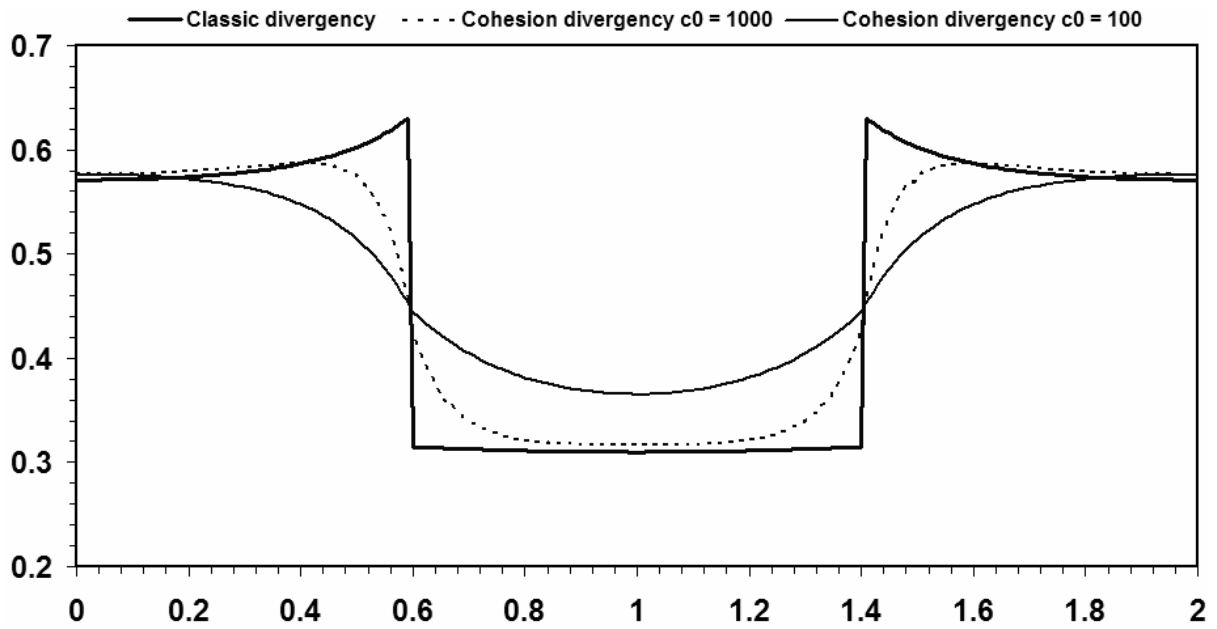
Fig. 3.16.

On Fig. 3.17 the picture of changing of a relative part of energy in inclusion E_f in relation to energy in a matrix E_m (i.e. factor of energy accommodation $\eta = E_f/E_m$) for the same model is represented at a variation of parameter $c_0 = 100 - 1000$:
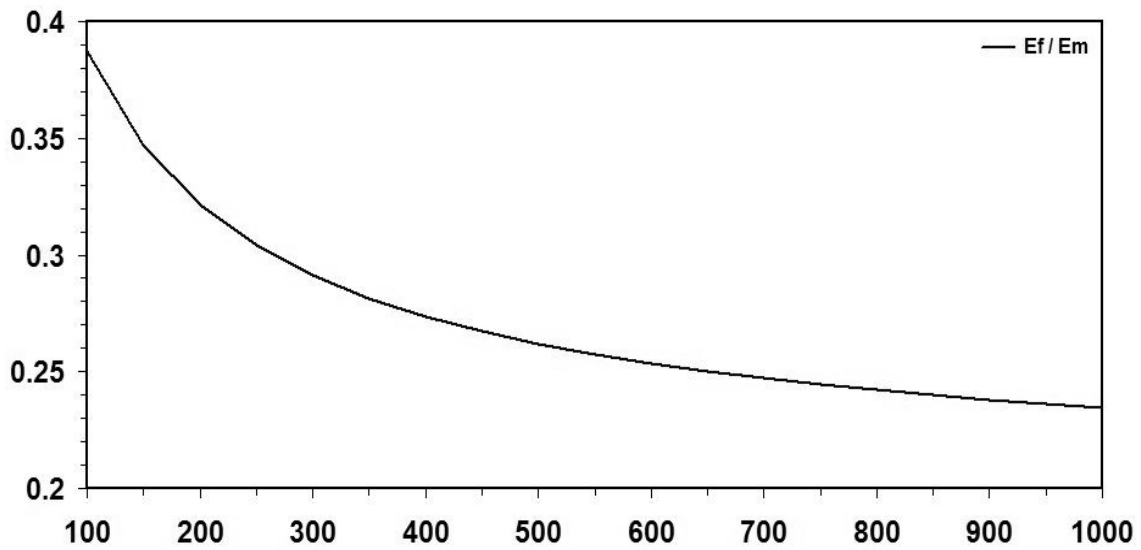
Fig. 3.17.

On Fig. 3.18 changing of energy accommodation for inclusion of ellipsoidal form with semi-axis $a = 0.2 - 0.8$ and $b = 0.2 - 0.5$ is represented at a variation of geometrical parameters of inclusion. On the right half of picture change a is submitted at fixed $b = 0.2$, and on the left half of picture changes b at fixed $a = 0.2$:
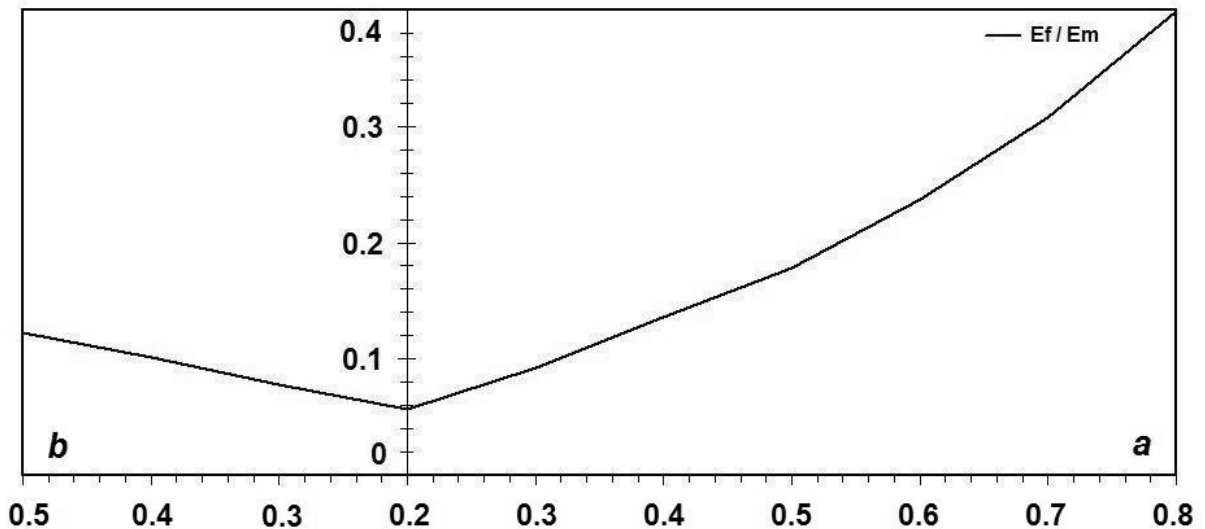
Fig. 3.18.

For plane model of moment cohesion comparative research of distribution of density of energy and of tension tensor components have been carried out also at turn of inclusion inside a cell that is important for calculation of effective characteristics of materials with random distribution of inclusions. Results are similar already presented in the annual report for 2002 for a double plane problem.

3.5.6. Features of the current realization of algorithm.

Unfortunately, the current realization of a block analytic-numerical algorithm encounters some numerical difficulties connected to instability of the calculation. At some unsuccessful choice of norm of junction functional during the calculation arises, apparently, singular or close to singular block matrix resulting in loss of calculation. This feature of algorithm demands more attentive studying of this phenomenon and modification of algorithm of the solution of the block system of equations due to introduction in stages of algorithm singular decomposition of elements of a block matrix, in particular QR-decomposition. This feature is temporal technical difficulty, and is overcome now due to a variation of calculating parameters (a degree of used multipoles, parameters of norm of junction functional, geometrical elements of block structure), that is inconvenient for practical realization. At correct selection of parameters we receive actually analytical solution of a problem.

3.5.7. Perspectives on the future.

The algorithm of a block method of multipoles can be applied to more complex models of an interphase layer including not only cohesion, but also adhesion effects, and also to the coupled problems including thermal and electromagnetic processes. After working off of algorithm of a block method of multipoles, on its base special form functions for considered models of moment cohesion and adhesions can be constructed with the purpose of their application in a traditional final elements method.

3.6. THE DETERMINATION OF THE MATHEMATICAL MODEL PARAMETERS BASED ON EXPERIMENTAL DATA.

In the Annual Report for 2004 the identification problem was solved on the base of the experimental dates [Miva M, 1978]. The solution of the problem of identification allowed us to get the values of the model parameters for the inter-phase layer a_D and a_M. It was established that $a_M < a_D$ for the both types of composite materials. Taking into consideration that the parameters a_D^{-1} and a_M^{-1} have the dimensions of length and, in fact, determine the length of the inter-phase cohesive layer in the matrix and in the inclusion, we can see that the values of these parameters obtained are in good agreement with the physical sense of the inter-phase layer. The inter-phase layer is generated in the each of phases in the neighborhood of the contacting zone; at that, the depth of the inter-phase layer in the matrix (the phase with smaller rigidity) is greater as compared to the depth of the inter-phase layer in the inclusion (the phase with greater rigidity). All set cohesion and adhesion type parameters were found based on the one-dimensional statement.

Here we consider more common problem. Dealing with problem to enforce model results to fit datasets and to identify physical parameters ("data assimilation problem") we assume that we have experimental data. The experimental data are set of K points with coordinates $\left(E^e\right)_1$, $\left(E^e\right)_2$, ... , $\left(E^e\right)_K$. Here the letter E denote specific energy (it is equivalent to the Young's modulus) of composite material. Each point corresponds to the composite. The matrixes of all these composites manufactured of the same material. The material of fraction is also the same.

The considered composites are differed by the sizes of fragments particles, their shapes, locations, concentration. Fig. 3.19 shows the meshes of a matrix of composite (parallelepiped) with blob from filling agent (dark ellipsoids).
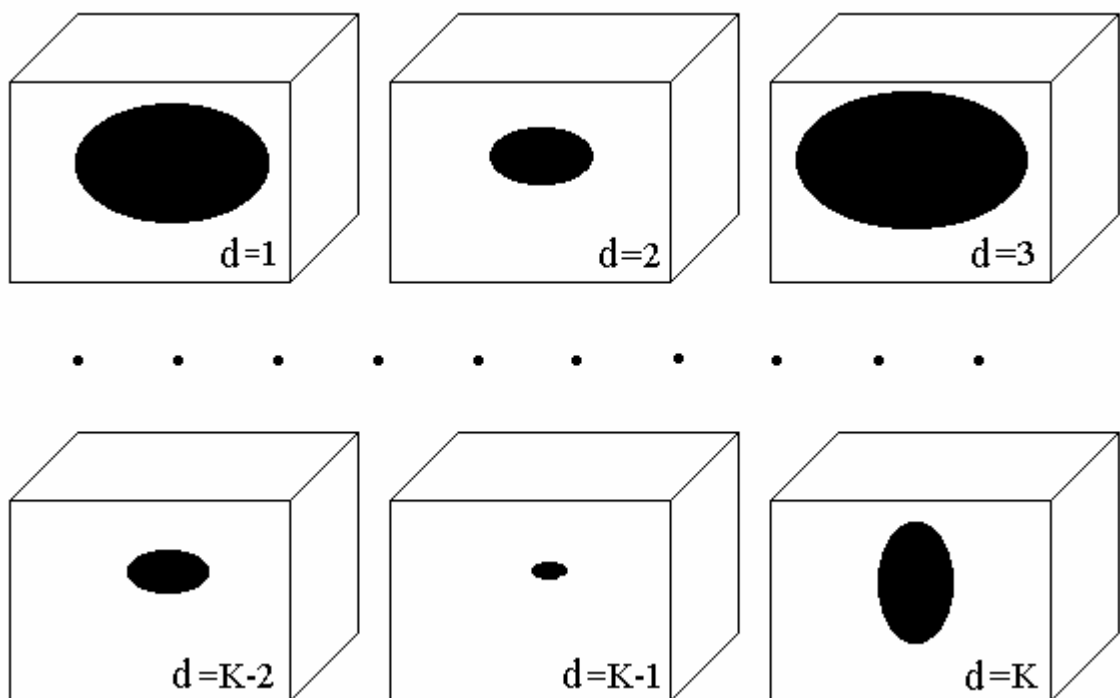
Fig. 3.19

The problem of identification of mathematical model parameter is formulated as follows: to find the parameters in such a way, that the "distance" between experimental set of points with coordinates $\left(E^e\right)_1$, $\left(E^e\right)_2$, ... , $\left(E^e\right)_K$ and theoretical set of points to be minimum. As the "distance" between experimental set of points and theoretical set of points next cost function was chosen

$$\Phi = \sum_{d=1}^{K} \frac{1}{K} \cdot \left[E_d^t - E_d^e\right]^2 , \tag{3.57}$$

where E_1^t, E_2^t, ... , E_K^t is the theoretical set of points obtained with the help of selected model at some (given) set of parameters.

The proposed algorithm of the solution of the problem of identification of model parameters we shall illustrate on an example of one-parameter three-dimensional model.

To calculate the theoretical values E_d^t of specific energy of d-th composite material within the framework of this model the obtained earlier relation will be utilized

$$E_d^t = \frac{1}{2} \iiint\limits_{G_d} \left[2\mu\varepsilon_{ij}\varepsilon_{ij} + \lambda\theta^2 + 8\frac{\mu^2}{C}\xi_{ij}\xi_{ij} + \frac{(2\mu+\lambda)^2}{C}\theta_i\theta_i \right] dV \tag{3.58}$$

In (3.58) region G_d is represented by join of region $\left(G_d\right)_m$ of a matrix and region $\left(G_d\right)_f$ of fullerene; parameters μ and λ in the matrix and in the fullerene are different; $R_i(x, y, z)$ - component of displacement vector;

$$\varepsilon_{ij} = \frac{1}{2}\left(\frac{\partial R_i}{\partial x_j} + \frac{\partial R_j}{\partial x_i}\right); \ \theta = \theta(\overline{R}) = \sum_{i=1}^{3}\varepsilon_{ii} \ ; \ \theta_i = \frac{\partial \theta}{\partial x_i}; \ \overline{\omega} = \frac{1}{2}rot\,\overline{R} \ ; \ \xi_{ij} = \frac{1}{2}\left(\frac{\partial \omega_i}{\partial x_j} + \frac{\partial \omega_j}{\partial x_i}\right).$$

In (3.58) and everywhere below on each of recurring subscripts the summation in limits from 1 up to 3 is supposed.

The displacement field $R_i(x, y, z)$ is defined from the solution of a following boundary value problem (here subscript d, pointing conformity to an d-th composite, is pulled down).

In region G_m the fulfilling of an equation is required

$$A_i^{(m)} \equiv -(2\mu_m + \lambda_m)\frac{\partial \theta^{(m)}}{\partial x_i} - 2\mu_m\frac{\partial \omega_q^{(m)}}{\partial x_p}\Xi_{qpi} + 2\frac{\mu_m^2}{C}\Delta\frac{\partial \omega_q^{(m)}}{\partial x_p}\Xi_{qpi} + \frac{(2\mu_m + \lambda)^2}{C}\Delta\frac{\partial \theta^{(m)}}{\partial x_i} = 0.$$

In region G_f the relation should be fair

$$A_i^{(f)} \equiv -(2\mu_f + \lambda_f)\frac{\partial \theta^{(f)}}{\partial x_i} - 2\mu_f\frac{\partial \omega_q^{(f)}}{\partial x_p}\Xi_{qpi} + 2\frac{\mu_f^2}{C}\Delta\frac{\partial \omega_q^{(f)}}{\partial x_p}\Xi_{qpi} + \frac{(2\mu_f + \lambda)^2}{C}\Delta\frac{\partial \theta^{(f)}}{\partial x_i} = 0.$$

On a surface Γ being demarcation of fullerene and the matrix, should be equal among themselves to functions $R_i^{(m)}(x, y, z)$ and $R_i^{(f)}(x, y, z)$, functions $\frac{\partial R_i^{(m)}}{\partial n}$ and $\frac{\partial R_i^{(f)}}{\partial n}$, functions $M_i^{(m)}$ and $M_i^{(f)}$, and also functions $P_i^{(m)}$ and $P_i^{(f)}$, where,

$$M_i^{(m)} \equiv -2\frac{\mu_m^2}{C}(n_p n_j \Xi_{ijq} + n_q n_j \Xi_{ijp})\frac{\partial \omega_q^{(m)}}{\partial x_p} + \frac{(2\mu_m + \lambda_m)^2}{C}\frac{\partial \theta^{(m)}}{\partial x_t}n_t n_i ,$$

$$M_i^{(f)} \equiv -2\frac{\mu_f^2}{C}(n_p n_j \Xi_{ijq} + n_q n_j \Xi_{ijp})\frac{\partial \omega_q^{(f)}}{\partial x_p} + \frac{(2\mu_f + \lambda_f)^2}{C}\frac{\partial \theta^{(f)}}{\partial x_t}n_t n_i ,$$

$$P_i^{(m)} \equiv \left[2\mu_m \varepsilon_{ij}^{(m)}{}_{ij} + \lambda\theta^{(m)}\delta_{ij} - \frac{(2\mu_m + \lambda_m)^2}{C}\delta_{ij}\Delta\theta^{(m)} + 2\frac{\mu_m^2}{C}\Xi_{ijr}\Delta\omega_r^{(m)} \right] n_j -$$

$$-(\delta_{kj} - n_k n_j)\frac{\partial}{\partial x_k}\left[-2\frac{\mu_m^2}{C}n_t \Xi_{ijp}\left(\frac{\partial\omega_p^{(m)}}{\partial x_t} + \frac{\partial\omega_t^{(m)}}{\partial x_p} \right) + \frac{(2\mu_m + \lambda_m)^2}{C}\delta_{ij}\frac{\partial\theta^{(m)}}{\partial n} \right],$$

$$P_i^{(f)} \equiv \left[2\mu_f \varepsilon_{ij}^{(f)} + \lambda_f \theta^{(f)}\delta_{ij} - \frac{(2\mu_f + \lambda_f)^2}{C}\delta_{ij}\Delta\theta^{(f)} + 2\frac{\mu_f^2}{C}\Xi_{ijr}\Delta\omega_r^{(f)} \right] n_j -$$

$$-(\delta_{kj} - n_k n_j)\frac{\partial}{\partial x_k}\left[-2\frac{\mu_f^2}{C}n_t \Xi_{ijp}\left(\frac{\partial\omega_p^{(f)}}{\partial x_t} + \frac{\partial\omega_t^{(f)}}{\partial x_p} \right) + \frac{(2\mu_f + \lambda_f)^2}{C}\delta_{ij}\frac{\partial\theta^{(f)}}{\partial n} \right],$$

and the vector $\bar{n} = \|n_1, n_2, n_3\|^T$ - the vector of a normal to a surface in the given point.

On the edges $ADHE$ and $BCGF$ of parallelepiped $ABCDEFGH$ see fig. 3.20) the values of displacement vector $\bar{R}^{(m)}$ and its normal derivatives $\dfrac{\partial\bar{R}^{(m)}}{\partial n}$ are prescribed, and $\dfrac{\partial\bar{R}^{(m)}}{\partial n} = \bar{0}$.

As to remaining edges, it is required, that on them the relations $M_i^{(m)} = 0$ and $P_i^{(m)} = 0$ ($i = 1, 2, 3$) should be fair.
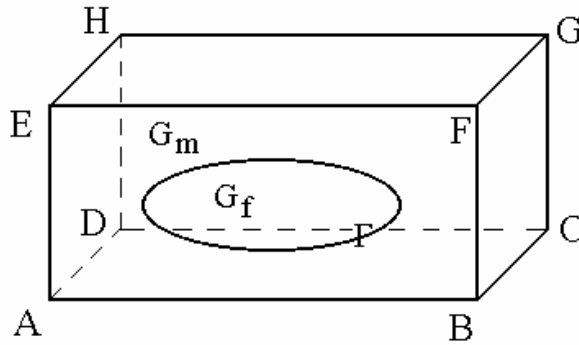
Fig. 3.20

As the parameter of considered model the magnitude of C is selected. The cost function $\Phi(C)$ from (3.57) depends on magnitude of parameter C as explicitly (through a relation (3.58)), and implicitly (through a function $R_i(x, y, z)$).

The differential of the function $\Phi(C)$ (variation) is determined as follows:

$$\delta\Phi = \sum_{d=1}^{K}\frac{1}{K}2\left(E_d^t - E_d^e\right)\delta E_d^t . \tag{3.59}$$

As to a variation δE_d^t of a function (3.59), applicable variation of parameter C, the methods of a calculus of variations are applied to its calculus [1]. After carrying out the rather complicated calculations it is possible to receive next form of the first variation of a functional (3.58):

$$\delta E_d^t = \frac{1}{2}\iiint\limits_{G_d}\left[-\left(8\frac{\mu^2}{C^2}\xi_{ij}\xi_{ij} + \frac{(2\mu + \lambda)^2}{C^2}\theta_i\theta_i \right)\delta C \right]dV +$$

$$= \frac{1}{2}\iiint\limits_{G_d^{(m)}}\left[-\left(8\frac{\mu^2}{C^2}\xi_{ij}^{(m)}\xi_{ij}^{(m)} + \frac{(2\mu + \lambda)^2}{C^2}\theta_i^{(m)}\theta_i^{(m)} \right)\delta C \right]dV +$$

134

$$+\frac{1}{2}\iiint_{G_d^{(f)}}\left[-\left(8\frac{\mu^2}{C^2}\xi_{ij}^{(f)}\xi_{ij}^{(f)}+\frac{(2\mu+\lambda)^2}{C^2}\theta_i^{(f)}\theta_i^{(f)}\right)\delta C\right]dV+$$

$$+\iiint_{G_d^{(m)}}\left(\overline{A}^{(m)},\delta\overline{R}^{(m)}\right)dV+\oint_{S_d^{(m)}}(\overline{B}^{(m)},\delta\overline{R}^{(m)})dS+\oint_{S_d^{(m)}}(\overline{D}^{(m)},\delta\left(\frac{\partial\overline{R}^{(m)}}{\partial n}\right))dS+$$

$$+\iiint_{G_d^{(f)}}\left(\overline{A}^{(f)},\delta\overline{R}^{(f)}\right)dV+\oint_{\Gamma}(\overline{P}^{(m)}-\overline{P}^{(f)},\delta\overline{R})dS+\oint_{\Gamma}(\overline{M}^{(m)}-\overline{M}^{(f)},\delta\left(\frac{\partial\overline{R}}{\partial n}\right))dS.$$

Allowing, that the displacement fields $\overline{R}^{(m)}$ and $\overline{R}^{(f)}$ are defined from the solution of the formulated above boundary value problem, the first variation of a functional (3.58) can be recorded so:

$$\delta E_d^t=\frac{1}{2}\iiint_{G_d^{(m)}}\left[-\left(8\frac{\mu^2}{C^2}\xi_{ij}^{(m)}\xi_{ij}^{(m)}+\frac{(2\mu+\lambda)^2}{C^2}\theta_i^{(m)}\theta_i^{(m)}\right)\delta C\right]dV+$$

$$+\frac{1}{2}\iiint_{G_d^{(f)}}\left[-\left(8\frac{\mu^2}{C^2}\xi_{ij}^{(f)}\xi_{ij}^{(f)}+\frac{(2\mu+\lambda)^2}{C^2}\theta_i^{(f)}\theta_i^{(f)}\right)\delta C\right]dV. \tag{3.60}$$

Now, having computed with the help of relations (3.59), (3.60) the differential of the cost function $\Phi(C)$, it is possible to apply any gradient method [2] (for example, method of conjugate gradients) for minimization of the cost function and for definition of parameter C of model in common 3D case.

If the number of parameters of model is insignificant, it is possible to take advantage of more simple straight method of calculus of a gradient of a cost function $\Phi(C)$ with the help of formula

$$\frac{d\Phi(C)}{dC}\approx\frac{\Phi(C+\Delta C)-\Phi(C)}{\Delta C} \tag{3.61}$$

and again to apply a gradient method.

3.6.1. Numerical experiments.

The numerical experiments were carried out for different mathematical models. Here the results of some experiments for a rectangular cell within the framework of full statement for a plane problem of moment cohesion (i.e. in the assumption, that the displacement vector has two coordinates and there is no dependence on z-coordinate) are presented. The calculations on definition of specific energy of a composite were carried out with the help of the described above block analytical-numerical method of multipoles.

As the model parameters the cohesive parameters $\overline{C}$ were selected: C_m for a matrix and C_f for fullerene. The cost function $\Phi(C_m,C_f)$ from (3.57) depends on values of these parameters C_m and C_f.

For debugging the parameter identification algorithm the set from several "experimental" points was used. The described above algorithm of the solution of the straight problem at fixed values of cohesive parameters arguments C_m and C_f was applied to their receiving.

All reduced below results are obtained for the composite on the basis of epoxy ($E_m=3.41$ GigaPa) with fullerene from glass shot ($E_f=87.5$ GigaPa). The inclusions for all "experimental" points were selected in the shape of a sphere, and radius of a sphere varied. All lengths are indicated in a

dimensionless form. The half of length of a rectangular cell is selected as a unit of length. The specific energy of a composite is referred to μ_m, and required parameters C_m and C_f to μ_m and μ_f accordingly.

The gradient of a cost function was evaluated with the help of a straight method (3.61).

In the table the radiuses of spheres, coefficient of volumetric filling up and specific energy of a composite are indicated.

The number of «experimental» Point	1	2	3	4a	4b
The radius of sphere-inclusion	0.20	0.25	0.30	0.4	0.4
Coefficient of volumetric filling up	0.0524	0.0818	0.1178	0.2094	0.2094
Specific energy of a composite	1.23204	1.30111	1.39425	1.58925	1.71573

3.6.1.1. Experiment 1.

For an "experimental" point with number 4a (radius of sphere - inclusion is equal 0.4) the study of dependence of specific energy of a composite upon cohesive parameters C_m and C_f was carried out. The results of these studies are introduced on fig. 3.21, where the dependence of specific energy of a composite upon a cohesive parameter C_f of fullerene is figured at a fixed value of cohesive parameter C_m of a matrix. The digits near curves indicate a value of cohesive parameter C_m of a matrix, at which one this curve is constructed. Analysis of the results of calculations, introduced on fig. 3.21, allows to draw a conclusion about monotonic dependence of specific energy of a composite upon on cohesive parameters C_m and C_f.

3.6.1.2. Experiment 2.

For an "experimental" point with number 4b (radius of sphere - inclusion is equal 0.4) the specific energy of a composite was set $E_a^e = 1.58925$. The problem consists in definition of such parameters of model C_m and C_f, at which one the idealized (made with the aid of model) value of specific energy of a composite would coincide with given. For this purpose the required parameters also varied in following limits: $C_m \subset [100,1000]$, $C_f \subset [100,1000]$. At everyone values C_m and C_f a value of a function

$$\Phi(C_m, C_f) = [E_a^t - E_a^e]^2, \tag{3.62}$$

also was evaluated. The minimum of this function should be found.

The method of conjugate gradients was applied to looking up of a minimum of a function (3.62). It was found that the cost function (3.62) receives a minimum value at $C_m = C_f = 500$ (this point on fig. 3.21 and in the table is marked by the character a). On fig. 3.22 the cross-section of a surface

$\Phi = \Phi(C_m, C_f)$ by a plane $C_m = 500$ is introduced, and on fig. 5 the cross-section of a surface $\Phi = \Phi(C_m, C_f)$ by a plain $C_f = 500$ is introduced. The figures 4, 5 demonstrate that the cost function has at the found values of parameters of model the brightly expressed minimum.

3.6.1.3. Experiment 3.

This experiment differs from previous only by set value of specific energy of a composite $E_b^e = 1.71573$ ("experimental" dot 4b). It was found that the cost function

$$\Phi(C_m, C_f) = \left[E_b^t - E_b^e \right]^2 ,$$

(3.63)

receives a minimum value at $C_m = C_f = 200$ (point b on fig. 3.21 and in the table). On fig. 3.24 the cross-section of a surface $\Phi = \Phi(C_m, C_f)$ by a plain $C_m = 200$ is presented, and on fig. 3.25 the cross-section of a surface $\Phi = \Phi(C_m, C_f)$ by a plain $C_f = 200$ is presented. The brightly expressed minimum of a cost function is here too observed at the received values of parameters of model.

3.6.1.4. Experiment 4.
In this experiment as "experimental" points the points labeled in the table by 1, 2 and 3 were selected. Here problem consists in definition of such model parameters C_m and C_f, at which one obtained theoretically values of specific energy for each composite would coincide with the given. The required parameters C_m and C_f also varied in the same limits: $C_m \subset [100, 1000]$, $C_f \subset [100, 1000]$. At everyone values of C_m and C_f a value of a function

$$\Phi(C_m, C_f) = \sum_{d=1}^{3} \frac{1}{3} \cdot \left[E_d^t - E_d^e \right]^2 ,$$

(3.64)

also was evaluated. The minimum of function (3.64) should be found.

A conjugate gradients method was also applied to looking up of a minimum of a function (3ю348). It was found that the cost function (3.64) receives a minimum value at $C_m = 300$ and $C_f = 450$. In this experiment also it was revealed, that the cost function Φ has at the retrieved values of model parameters the brightly expressed minimum.

3.6.2. Conclusion.

The held calculations have shown, that the proposed algorithm of identifying the model parameters allows to retrieve cohesive parameters C_m and C_f with a high accuracy.

Fig. 3.21

Fig.3.22

138

Fig. 3.23

Fig. 3.24

139
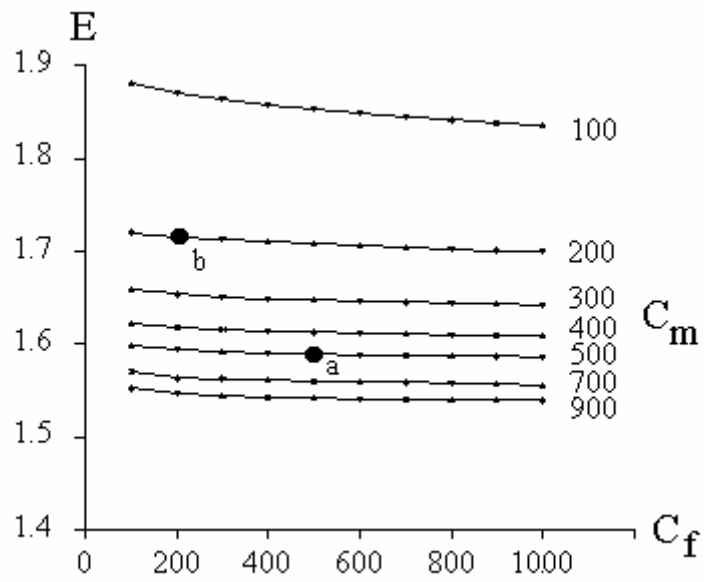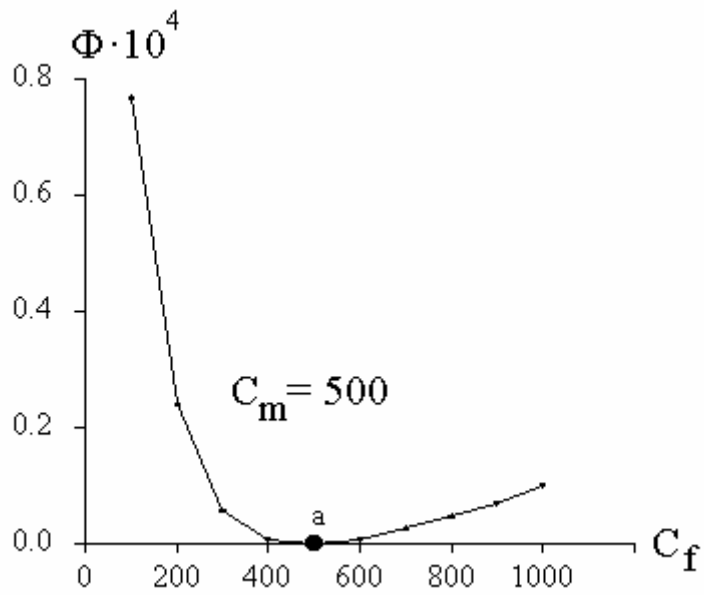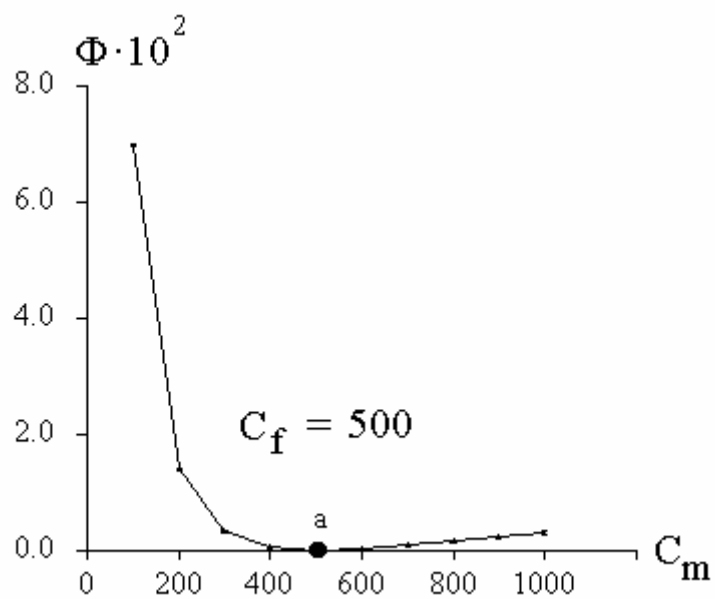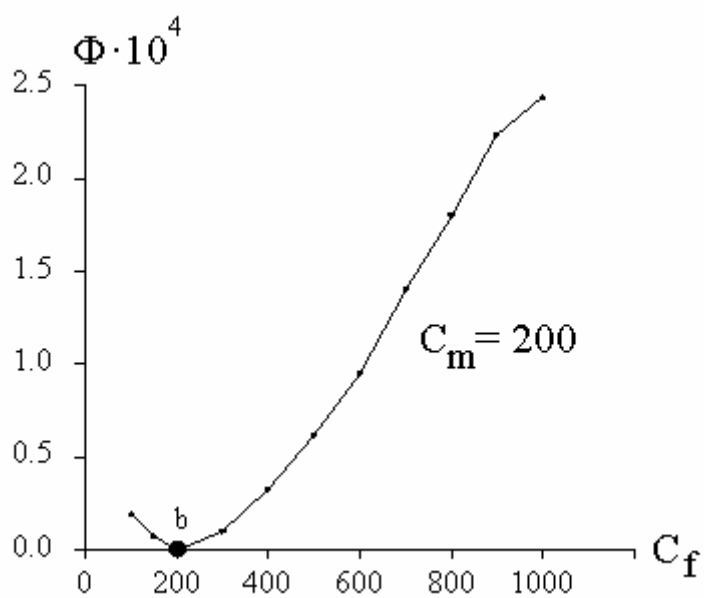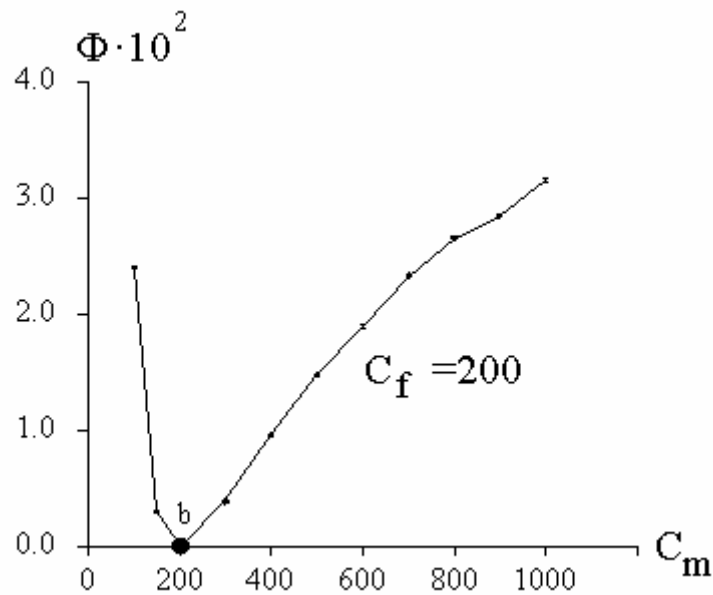
Fig. 3.25

Results

The investigations were carried out to apply the developed technique on main model. In the main model the displacement vector has already two components. The system of partial differential equations for the components is essentially more complicated. The conditions for these components on the boundary between matrix material and reinforcing material become noticeably complicated. The model was allowed to have has some parameters. For the main model the expression permitting to determine a precise value of a variation of a coast functional, cased by a variation of parameters is obtained. This expression depends both on movement vector and auxiliary functions (Lagrangian multiplicities). The Lagrangian multiplicities are determined from the solution of a so-called "conjugate" boundary value problem, the equations and boundary conditions for which one are obtained in the paper. The investigation both "conjugate" problem and main problem is held. The conclusion is made that the proposed algorithm is correct in more complicated case.

REFERENCE

Bakhvalov N.S., Panasenko G.P. 1989. Homogenization of processes in periodic media. Kluwer, Dordrecht/Boston/ London, 1989.

Barenblatt G.I. 1962. Mathematical Theory of Equilibrium Cracks in Brittle Fracture, *Advances in Applied Mechanics*, **7**, Academic Press.
Bateman H., Erdelyi A. 1973. Higher transcendental functions. (**1-3**). NY: Mc. Graw-Hill Book Company. 1973.

Belov P., Lurie S. 2002. On modeling of scale effects in thin structures. Mech Composite Mater and Struct 2002;8:78-88.

Bensoussan A, Lions JL, Papanicolau G. 1978. Asymptotic analysis for periodic structures. Amsterdam, 1978.

Bodunov A., Belov P., Lurie S. 2002. Scale effects in the thin films. J of Composite Mater and Struct VIMI 2002;2:33-40.

Budiansky B. 1965. On the elastic moduli of some heterogeneous materials. J Mech Phys Solids 1965;13:223-227.

Christensen R.M. 1979. Mechanics of composite materials. , J. Wiley& Sons. Inc

Eshelby J.D. 1957. "The determination of the elastic field of an ellipsoidal inclusion and related problems". *Proc.Roy.Soc.Lond*.

Gao H., Huang Y., Nix W.D., Hutvhinson J.W. 1999. Mechanism-based strain gradient plasticity-I. Theory. J of the Mech and Solids 1999;47:1239-1263.

Grachov N.I., Evtushenko Y.G. 1980. A library of programs for solving optimal control problems. J Comp Math and Math Physics 1980;19:99-119.

Lurie S., Belov P., Volkov-Bogorodsky D. 2003. Multiscale Modeling in the Mechanics of Materials: Cohesion, Interfacial Interactions, Inclusions and Defects. In: Wendland LW, editor. Analysis and Simulation of Multifield Problems, Springer, 2003; 12 p. 101-110.

Lurie S., Belov P., Volkov-Bogorodsky D., Tuchkova N. 2003. Nanomechanical Modeling of the Nanostructures and Dispersed Composites, Int J Comp Mater Scs 2003; 28(3-4):529-539

Lurie S., Belov P. 2000. Mathematical models of the mechanics of solids and physical fields. *Scientific publication of Computing Centre* RAS. 2000.P.151

Miva M, and etc. 1978. Influence of the diameters of particles on the modulus of elasticity of reinforced polymers, Kobunshi Ronbunshu. 1978; 35(2):125-129.

Mori T, Tanaka K. 1973. Average stress in matrix and average elastic energy of materials with misfitting inclusions. Acta Metallurgica 1973;21:571-574.

Morozov N.F. 1984. Mathematical questions of the theory of elasticity. *Science Publ.* (in Russian)

Morse P.M., Feshbach H. 1953. Methods of Theoretical Physics. (**1-2**). McGraw-Hill, New-York, Toronto, London, 1953.

Mura T. 1982. Micromechanics of defects in solids. Martinus Nijhoff Publishers, 1982

Nemat-Nasser.S., Iwakuma T., Hejazi M. 1982. On composite with periodic structure. Mech Mater 1982;1(3):239-267.

Novazki V. 1975. Theory of Elasticity. Moscow, *Nauka publishers*, 1975 (In Russian).

Nunan K.C., Keller J.B. 1984. Effective elasticity tensor of a periodic composite. J. Mech and Phys Of Solids 1984;32(4) 259-280.

Odegard G.M., Gates T.S., Nicolson L.M. and Wise K. 2002. Equivalent-continuum modeling with application to carbon nanotubes. 2002; NASA, TM-2002-211454.

Odegard G.M., Gates T.S., Wise K., Park C., Siochi E.J. 2002. Constitutive modeling of nanotube-reinforced polymer composites 2002; NASA/ CR-20020211760

Odegard G.M., Gates T.S. 2002. Constitutive modeling of nanotube/polymer composites with various nanotube orientation. In Proceedings Annual Conf on Experimental and Appl Mech, June, Milwaukee, WI, 2002.

Reuss A. 1929. Math. Und Mech., 9, 1, 49-58 , 1929

Riccardi A., Montheillet F. 1999. A generalized self-consistent method for solids containing randomly oriented spheroidal inclusions. Acta Mechanica, 1999;133:39-56.

Sangini A.S., Lu W. 1987. Elastic coefficients of composites containing spherical inclusions in a periodic array. J. Mech and Phys. Of Solids. 1987;35(1):1-21.

Thostenson E.T., Ren Z., Chou T.W. 2001. Advances in the science and technology of carbon nanotubes and their composites: a review. Composites Science and Technology 2001;61:1899-1912

Tibbetts G.G., McHugh J.J. 1999. Mechanical properties of vapor-grown carbon fiber composites with thermoplastic matrices. J of Mater Res 1999;14:2871-2880

Tucker III C.L., Liang E. 1999. Stiffness Predictions for Unidirectional Short-Fiber Composites: Review and Evaluation, Composites Science and Technology. 1999;59:655-671.

Vlasov V.I., Volkov D.B. 1995. The multipole method for Poisson equation in regions with rounded corners, *Comp. Maths Math. Phys.* , **35**, 6 , 687-707.

Vlasov V.I., Volkov D.B. 1996. Analytic-numerical method for solving the Poisson equation in domains with rounded corners *ZAMM*. **76**, Suppl. 1. P. 573-574.

Vlasov V.I., Volkov-Bogorodsky D.B. 1998, Block multipole method for boundary value problems in complex-shaped domains // *ZAMM*. **78**, Suppl. 3, 1111-1112.

Volkov-Bogorodsky D.B. 2000. Development block analytical-numerical method for problems in mechanic and acoustic, *Proceedings of the conference* "Composite materials". M.: IAM RAN, 2000. 44-56 (In Russian).

Volkov-Bogorodsky D.B. 2001. On construction of harmonic maps of spatial domains by the block analytical-numerical method. *Proc. of the minisymposium "Grid generation: New trends and applications in real-world simulations"* in the Int. conf. "Optimization of finite-element approximations, splines and wavelets" (St.-Petersburg, 25-29 June 2001). Moscow: *Computing Centre RAS*, 2001, 129-143.

Wakashima K., Otsuka M., Umekawa S. 1974. Thermal expansion of heterogeneous solids containing align ellipsoidal inclusions, J Compos Mater 1974;8:391-404.

Zhang P., Huang Y., Geubelle P.H., Klein P.A., Hwang K.C. 2002. The elastic modulus of single-wall carbon nanotubes: a continuum analysis incorporating interatomic potentials. Int J of Solids and Structures, 2002;39:3893-3906.

4. DEVELOPMENT OF MOLECULAR MODELS OF INTERPHASE LAYERS FOR REINFORCEMENT COMPOSITES BY DIRECT NUMERICAL MODELING.

4.1. INVESTIGATION OF STRUCTURAL AND MICROMECHANICAL CHARACTERISTICS OF COMPOSITE "POLYMER - TECHNICAL CARBON" AT THE PHASE BORDER BY MONTE-CARLO METHOD

4.1.1. Investigation of molecular mobility at interphase layer of microcluster n-$C_{100}H_{202}$ and graphite.

By Monte-Carlo method (Allen M.P., Tildesley D.J., 1987) (procedure of Metropolis, (Metropolis N.A., Rosenbluth A.W., Rosenbluth M.N., Teller A.H., Teller E., 1953)) for canonic NVT ensemble using an unorthodox algorithm (Teplukhin A.V., 2004) the systems with contain two-ply fragment of graphite with size equal 60x61x6,8Å (2856 carbon atoms) and 48 molecules of n-alkane (n-$C_{100}H_{202}$) at temperature 450K (melt of polyethylene) have been investigated. Components of system (17352 atoms) have occupied the elementary cubic cell (rib~66 Å). Initial configuration of system has been made by replication of molecule n-$C_{100}H_{202}$ (see fig.4.1) 4,2 and 6 times along coordinate axis (x,y,z accordingly). General view of elementary cell before we start to model shows in fig.4.2.
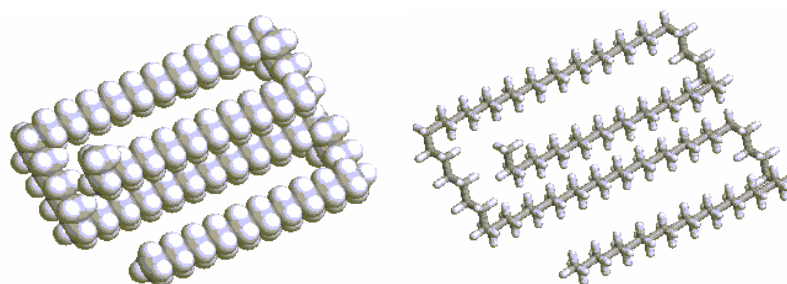
Figure 4.1: n-$C_{100}H_{202}$ molecule in initial configuration (volumetric and carcass models, white color are hydrogen atoms, gray color are carbon atoms).
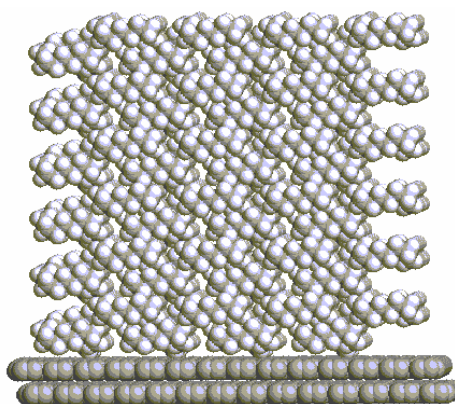
Figure 4.2: General outlook of elementary cell of system before modeling.

Alteration of internal energy during computational experiment has calculate using atom-atomic potential functions (Poltev V.I., Shulyupina N.V., 1986) for values of intermolecular interactions and parameters of

AMBER data-base (Weiner S.J., Kollman P.A., Nguyen D.T., Case D.A., 1986) for values of self molecular interactions (energy of deformation of valent bonds and angles, torsion potentials). Calculations of structural and dynamic characteristics model system have been made by means of parallel computational technologies (Teplukhin A.V., 2004) on supercomputer MVC 5000 BM (Moscow).

After accomplishment of $2 \cdot 10^6$ tests (for each of CH_2 or CH_3- group) by method of Monte-Carlo it is proved, that mass of alcanes adopted in compact form (see fig.4.3) which shows the higher local density in compare with the initial configuration (see fig.4.2).
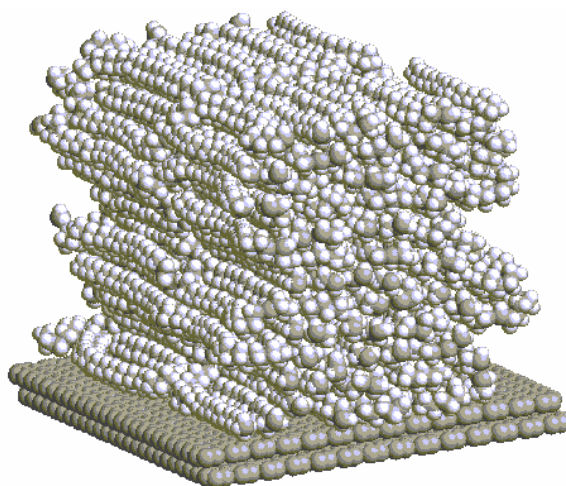
Figure 4.3: General view of elementary cell of the system after relaxation at 450K.

Hydrocarbon chains have maintained predominantly collinear collocation and formed wide area with dense hexagonal package (as it can see for crystals of normal paraffin at temperatures close to melt temperature (Kitaygorodsky A.I., 1971)).

Section of model cell by cross to chains flatness one can see in fig.4.4. Increase of local density happened because of decrease the size of sample in normal direction to graphite surface. This process, has leaded to crack of material in flatness which is normal to graphite surface direction and initialized evolution of cracks in flatness which are parallel to graphite (see fig.4.5). As it can see from fig.4.4 some defects in molecular package forego a propagation of cracks.
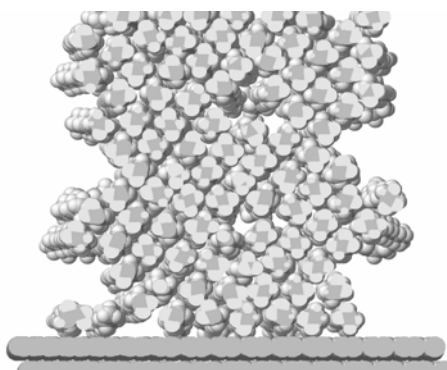
Figure 4.4: Section of elementary cell of the system after relaxation at 450K.

a)   b)
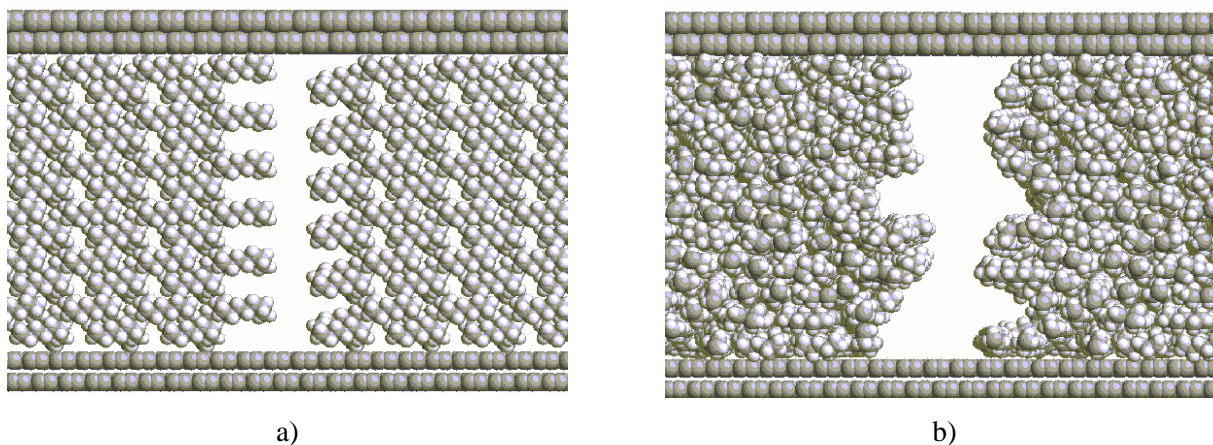
Figure 4.5: Cracks propagation into the material at an initial (a) and a final (b) stages of relaxation.

Dependence of local density CH_2 or CH_3- groups (ns) on distance to graphite surface has complex character (see fig.4.6). So, close to graphite surface a polymer layer is characterized by the high value of density (the first and the last peaks on the curve). It is explained by low potential energy of atomic groups, which are kept with graphite by means of Van-der-Waals constant. Further, it is possible to observe the area of quasi-crystalline (hexagonal) phase (3-4 peaks) and area (~12Å) with defects.
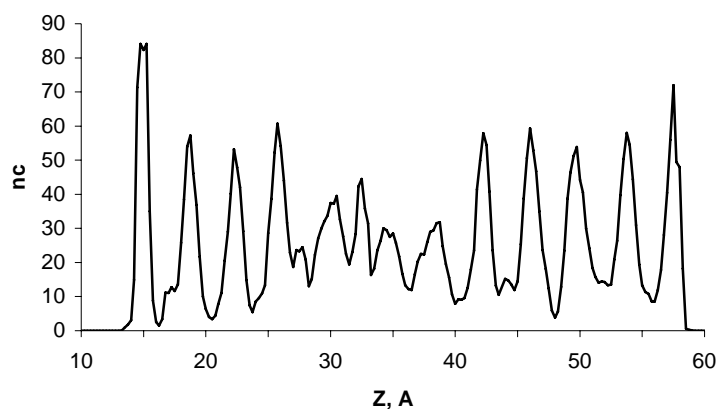
Figure 4.6: Alteration of local density CH_2 or CH_3- groups (***nc*** in relative units) along a normal to graphite surface direction.

In order to calculate a dependence of motion of CH_2 or CH_3- groups of n-alcanes on distance to graphite surface the space of cell, we model, was rubricate on layers with thickness 0.5Å (around Z-coordinate) parallel to graphite flatness (XY-flatness). As a measure of mobility CH_2 or CH_3- groups we chosen the value of mean square displacement of center mass of carbon atoms during 5000 steps of Metropolis procedure. Mobility into layer (z, z+0.5) has calculated as a mean arithmetical of molecular mobility of molecules inside a given layer when we started to calculate. In order to enhance a reliability of results, the calculations have made in two series by 10 pairs of launching (the first one with calculation of mobility, but the second one without). Above method let us to decrease a discrepancy of data up to 20%.

In fig.4.7 one can see the dependence of mobility CH_2 or CH_3- groups (D_t) and its lateral (D_l) and normal (D_n) components on distance to graphite surface, calculated at temperature 450K.
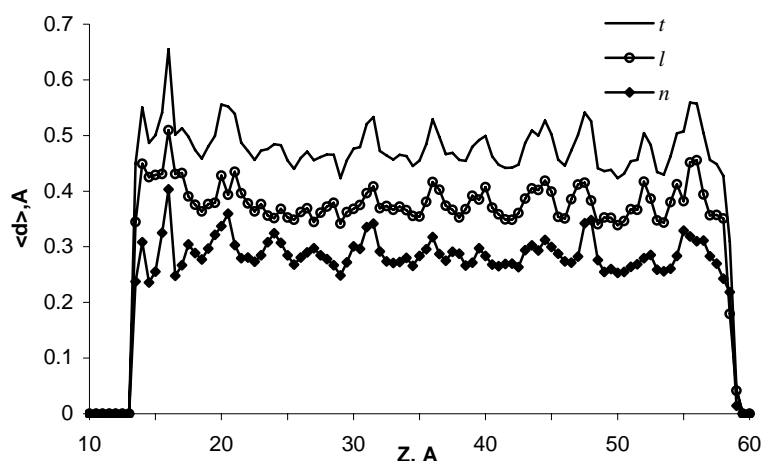
Figure 4.7: Dependence of mobility of CH_2 and CH_3- groups for n-alcanes (d_t) along a normal to graphite surface (Z-coordinate) at 450K, d_l and d_n are lateral and normal components.

Unfortunately, the accuracy calculations of mobility in above batch of experiments was insufficient for observation of specific effects. One can to note small deceleration of mobility into the layer of immediate contact of polymer with graphite (area of the first and the last maximum in fig.4.7).

4.1.2. Investigation of shear elasticity for molecules of n-$C_{100}H_{202}$ on the graphite surface by Monte-Carlo method.

A system contained two layers fragment of graphite 60x61x6.8 A^3 size (2856 carbon atoms) and 48 molecules of n-alcane (n-$C_{100}H_{202}$) at 300K has been investigated. The components of system (17352 atoms) occupied an elementary cubic cell (rib size is 66A).

As initial configuration of system it was taken the last configuration of the system, which has been describe in previous part of work (see part 4.1.1.). All calculations have been made in parallel algorithmic procedures.

Shear deformation for fragment of system under study is realized by keeping some periodic border conditions superimposed on the model cell, as it follows below.

1. The potential energy E_0 has calculated for initial configuration of alcane chains: after its precursory relaxation at 300K.

2. The particles of over and under contact layers for CH_2 or CH_3- groups, which have located inside the monomolecular layer of upper surface of cell or within Van-der-Waals contact with graphite surface have fixed.

146

3. Each particle (atoms of graphite belong to caudal contact layer) is dislocated in parallel to graphite surface (for example, along the coordinate axis X; axis Z coincides with direction which is perpendicular to graphite surface). Value and direction of displacement of particles is qualified by value of its z-coordinate

$$\Delta x = \begin{cases} s \dfrac{z - d/2}{(d/2)}, z \ge d/2 \\ s \dfrac{d/2 - z}{(d/2)}, z < d/2 \end{cases},$$

here d is the distance between middle surfaces of contact layer, and s=0.1A is the maximum value of displacement for one step of deformation.

4. After that the relaxation of system under consideration at 300K arises. Standard procedure of Metropolis is employed only to particles which did not get at contact groups (~10 tests of Monte-Carlo method for each CH_2 or CH_3-groups).

5. It is calculated the potential energy of system after regular shear and relaxation E. Shear stress of a system during deformation one can evaluate as P=(E-E_0)/V, where V is the volume of cell. Value (relative) deformation at this moment is $\gamma = (2s \cdot m)/d$, where m is the quantity of performed cycles of shear. Value of shear elastic modulus is: G=P/γ.

6. If m<M_{max} we have to overpass to 3-d stage of modeling, otherwise we have to stop the calculations. M_{max} is the maximum quantity of cycles by shear (in our calculations M_{max}=100).

Initial and final configurations of system under shear deformation for two mutually perpendicular directions represent in figs.4.8 and 4.9.
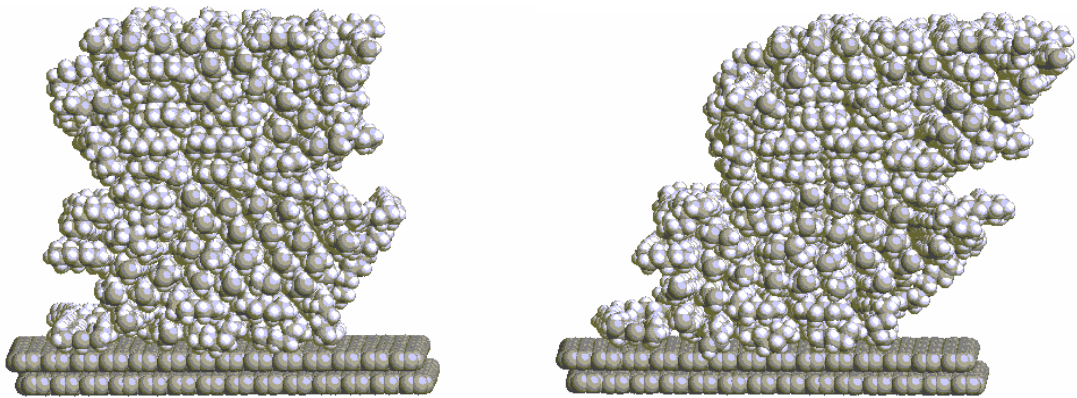
Figure 4.8: Shear in X direction, which is normal to basic mass of alcane chains.
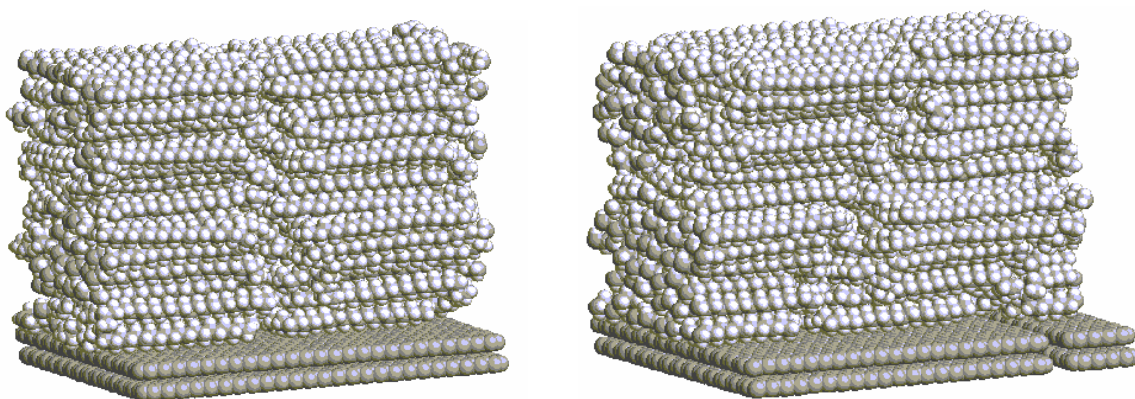
Figure 4.9: Shear in Y direction along basic mass of alcane chains.

Alteration of elastic modulus during the shear deformation one can see in fig.10 (G_x and G_y, Pa) for two mutually perpendicular direction of shear (γ, in relative units). In our opinion so sizable anisotropy of shear modulus is explained by energetic disadvantageous increasing of lateral surface of crack (see part 4.1.1.) at deformation in X-direction (fig.4.8). Decreasing of G_x value during the final stage of deformation has been induced by temporary shortening above surface in connection with "healing" one of microcracks.
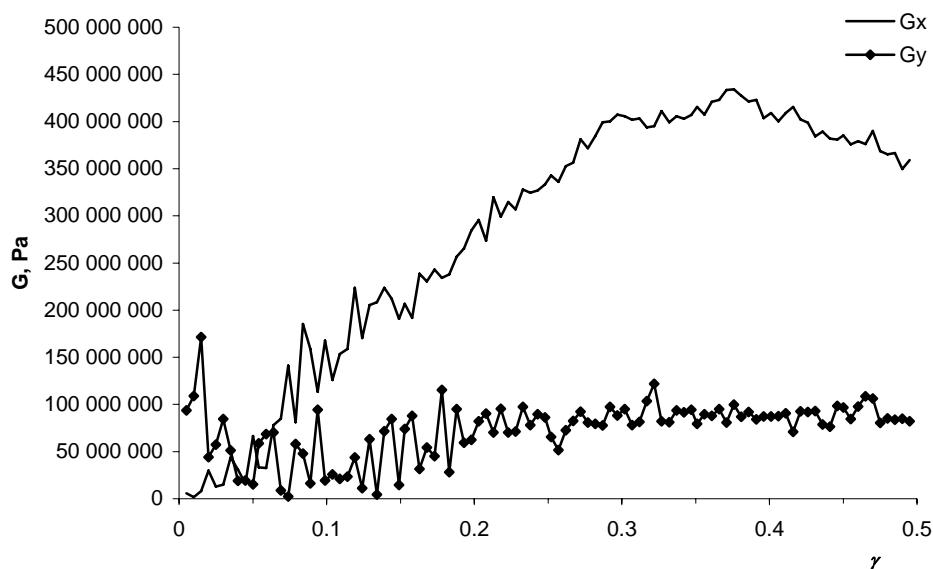
Figure 4.10: Dependence of elastic modulus (G, Pa) of value of shear deformation γ (relative units) at temperature 300K for two mutually perpendicular directions (see figs.4.8 and 4.9 for details).

One can note, that asymptotic values 80 and 430 MPa for shear elastic modulus of interphase layer of the system «n-$C_{100}H_{202}$ - graphite», are in precise corresponding with known from literature data (Koshkin N.I., Shirkevich M.G., 1976).

4.2. QUANTUM MECHANICAL INVESTIGATION OF STRUCTURE AND MECHANICAL PROPERTIES OF NANOCOMPOSITE INTERFACES

This part is devoted to direct computational quantum mechanical investigation of the microstructure and microscopical mechanical characteristics of complex nanocomposites consisting from polymer matrix and highly dispersed fillers. Chemical structure of nanocomposite components, microscopic aspect of the process of deformation and friction at the composite interface caused by both mechanical stresses and adsorption is discussed in the mechanochemical modelling in a framework of a cluster approach in which approximations of microscopical deformation and friction are realized.

4.2.1. General task of investigation. Development of computational approach.

Microstructure and mechanical characteristics of nanostructured materials or composites is now a topic of wide and advanced investigations. It is well known that highly developed and complex interface between fillers and matrix of these materials is mainly responsible for their unique properties that accounts for increasing application of nanocomposites in technology and industry. And now it is evident that nanostructured materials require a lot of time and money consumptions for manufacturing, they are highly difficult for experimental characterization and analytical testing. Therefore theoretical investigations of composites take on special significance. Computational modelling allows to study the microscopical structure and mechanical properties of nanoparticles and interfaces of nanocomposites, it gets possible to predict some important properties of nanomaterials and to perform computational selection of nanocomposites with necessary and preset characteristics.

The most of theoretical approaches, which are used now for investigation of composites, use the solid state principles, i.e. an approach in which material is considered as continuum. Properties and deformation of composites are described here by means of finite elements where molecular structure of materials is not taken into account. Nevertheless there are the natural limits of finite division of materials into elements, which are atoms and molecules bearing information about their chemical properties. Therefore it looks highly perspective to study the structure and mechanical properties of nanocomposites using theoretical atom-level approaches which can be joined in a complex hierarchy system combining quantum mechanics, molecular dynamics and Monte Carlo, mesoscopic molecular mechanics and molecule-engineering design. Such a hierarchical system represents complementary and interconnected approaches and quantum mechanics can be considered as the first and important step in the theoretical study of microstructure and mechanical properties of composites.

4.2.1.1. Quantum mechanical method.

Since bulk of time-consuming calculations of complex clusters were conducted, the originally elaborated semiempirical method PM3 was applied (Stewart J.J.P., 1989), which was modified specially for calculating large molecular systems.

This method was realized within the original package CLUSTER1, which does not concede to *ab initio* approaches in accuracy of calculations, however considerably gain in speed of calculations. The applied method

is intended for calculation of base structural and energetic characteristics of nanosized molecular systems in the basic electron state.

4.2.1.2. Parallel calculations.

Since in work it was necessary to perform a lot of calculations of large molecular systems (up to several hundreds atoms) corresponding to successive steps of deformation with full optimization of space structure of molecular systems parallel calculations was realized within package NANOPACK exploiting fast semiempirical quantum mechanical calculations. Calculation in a parallel mode was conducted on supercomputers in the interdepartmental supercomputer center of the Russian Academy of Science. Calculation in a parallel mode using NANOPACK package allowed carrying out the direct quantum mechanical calculations of molecular systems of the real nanoscale size with reasonable computational time.

4.2.1.3. Cluster approach.

Computational experiment was realized in cluster approach in which some part of polymer-filler interface was considered as model cluster consisting of up to some hundreds atoms and being up to several tens of nanometers in diameter. Quantum mechanical modelling consisted in preliminary construction and QM optimization of cluster models of composite components with various chemical structures. Than on the base of these models a complex cluster representing the adsorption complex of these components can be received and optimised in QM approach. Calculated binding enthalpy in this cluster energetically characterized strength of intermolecular interactions in the interface of composite components. Earlier it has been shown (E.Nikitina, 2001), that such cluster approach within QM modelling yields reliable results at definition of microscopical structure and energetic characteristics of a big number of composite interfaces.

4.2.1.4. Modelling of molecular system deformation. Mechanochemical internal coordinate approach.

Deformation of polymer-filler interface and internal friction at this interface has been investigated in quantum mechanical study in a framework of co-ordinate of microscopical deformation and friction approximations.

Computational mechanochemical experiment, which was applied for the analysis of the microscopic characteristics of deformation of molecular systems, was organised by analogy to macroscopic mechanical experiment in a mode of active loading. Firstly the microscopic models of both polymer and high-dispersed filler particle as well as the model of their complex, suitable for the quantum-chemical study of the mechanical properties of the composite interface is constructed and optimised in QM approach. Than, mechanochemical internal coordinate of deformation (MIC) is chosen, which change allows describing a required sequence of deformation states of the molecular system under study. Coordinate of internal deformation is determined by two groups of atoms, which set surfaces of the application of deformation force, as well as direction and kind of deformation. The computational experiment consists in sequential step-by-step deformation of molecular system starting from a stable initial state up to the bond break along the MIC. The full space optimisation of the molecular system is carried out within the framework of quantum-chemical calculation on each step of

deformation. Atoms determining MIC are excluded from the process of optimisation. Force of deformation of the molecular system is determined as a gradient of total energy of the system on MIC.

4.2.1.5. Modelling of molecular system friction. Microscopic friction coordinate approach.

Computational experiment, which was applied for the analysis of the characteristics of microscopic friction in the interface of nanocomposite was organised quite similar in the modelling peculiarities to the described above MIC approach.

Such study can be carried out within the framework of approach of microscopic friction coordinate (MFC) realized in the present work. In the case of MFC modelling microscopic coordinate of friction is set by two groups of atoms in a system of two molecules determining a direction and a plane of friction. The position of the first particle is fixed by exception of some its atoms from a process of optimisation. The computational experiment consists in sequential step-by-step moving of the second particle from an initial state along the surface of the first molecule corresponding MFC. Full space optimisation of the atoms, which do not determine MFC, is carried out on each step. Determining MFC atoms are excluded from the process of optimisation. The microscopic force of friction is calculated as a gradient of energy of system on MFC.

4.2.2. Results of computational experiments and discussion.

4.2.2.1. Internal microscopic friction in a matrix of rubber and in its adsorption complex with a particle of graphite carbon filler.

The microscopic energy and force characteristics of friction of two chain segments of unsaturated organic polymer have been simulated within the framework of MFC approach. These chain segments were modelled by two molecules of heptane. Fully optimised starting structure of a complex, consisting from two heptane molecules were designed is presented in fig.4.11. The received characteristics were compared with similar ones calculated for intermolecular friction of segment of unsaturated organic polymer along the surface of carbon filler in their adsorption complex. Polymer chain segment was modelled also by heptane molecule and the surface of a carbon particle was simulated by sp^2-carbon cluster with graphite structure. Fully optimized structure of corresponding adsorption is shown in fig.4.12. Introduction of microscopic friction coordinate and the sequential steps of intermolecular friction are presented in fig.4.13 and fig.4.14 for the first and the second systems respectively.
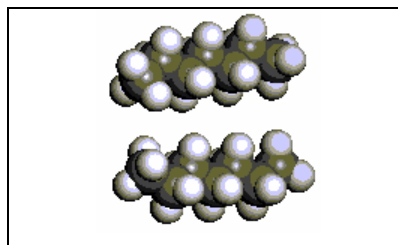
Figure 4.11: Optimised structure of adsorption complex, consisting of two heptane molecules.
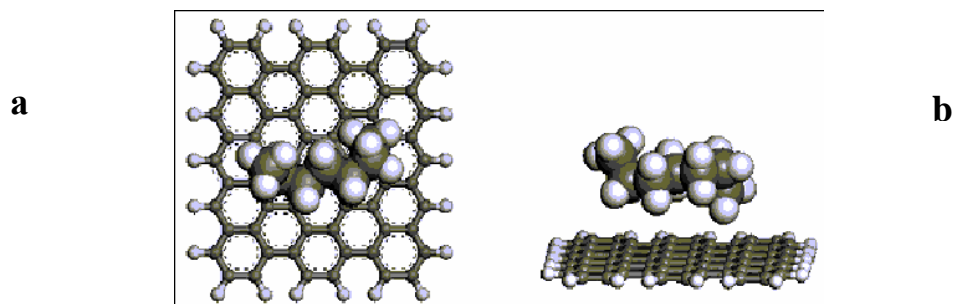
Figure 4.12: Optimized structure of adsorption complex, consisting of heptane molecule and sp^2-carbon cluster with graphite structure. (a - top view, b - side view).
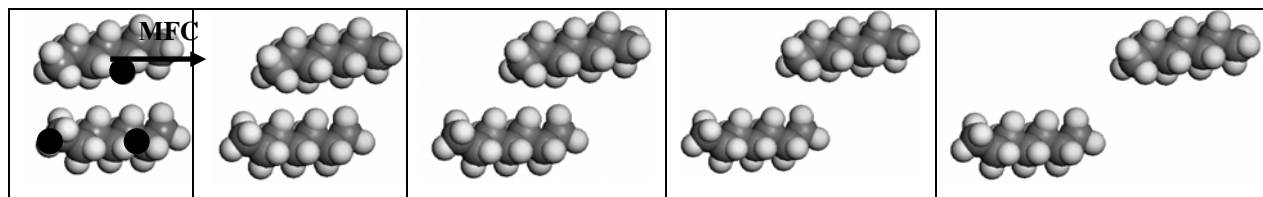
Figure 4.13: Introduction of microscopic friction coordinate (MFC) and sequential steps of intermolecular friction of two molecules heptane.
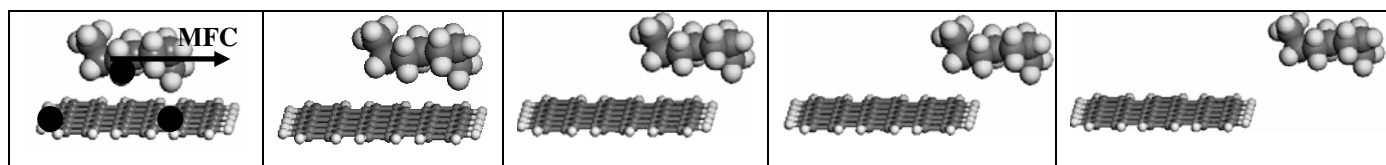
Figure 4.14: Introduction of microscopic friction coordinate (MFC) and sequential steps of intermolecular friction of molecule heptane along the surface of carbon cluster.

The energy and force characteristics obtained within quantum-chemical modelling of microscopic intermolecular friction of two chain segments of unsaturated organic polymer molecules as well as corresponding characteristics received for the friction of the latter chain along the surface of graphite carbon particle are presented in fig.4.15 and fig.4.16 respectively.
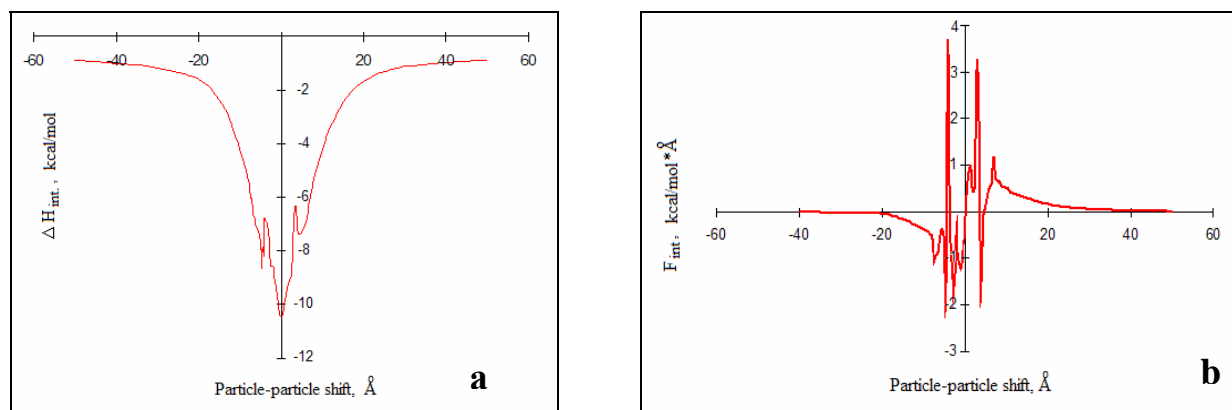
Figure 4.15: Energy (a) and force (b) characteristics of microscopic intermolecular friction in the system of two heptane molecules.
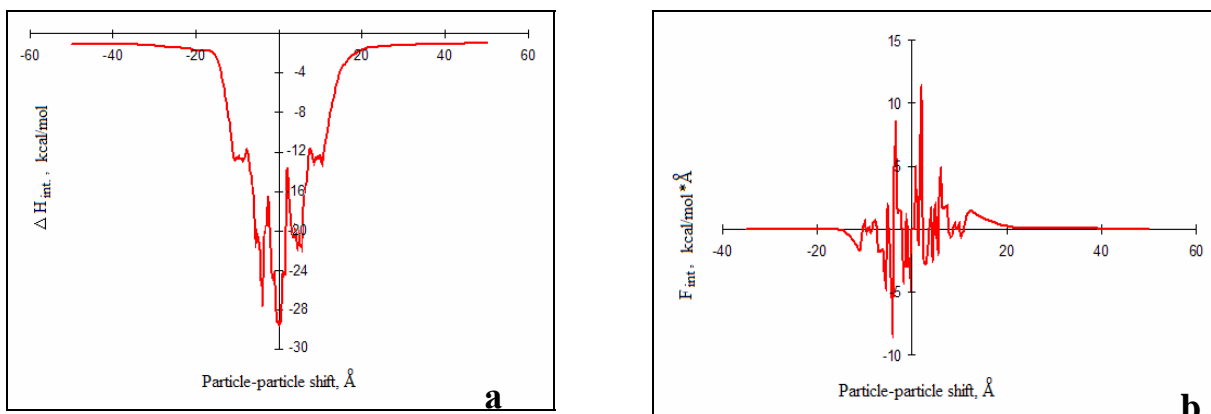
Figure 4.16: Energy (a) and force (b) characteristics of microscopic intermolecular friction in the system of heptane molecule and carbon cluster with graphite structure.

In the course of the modelling it was obtained that the force of "shift deformation" (or of intermolecular friction) for the system of polymer - polymer is equalled approximately 4 kcal/mol*A, and the similar force characteristic for the system of polymer - carbon particle is equalled approximately 10-12 kcal/mol*A. At the same time the value of destroying force for a polymeric chain is equal approximately 80-100 kcal/mol*A for individual polymer, and at about 2 times less for polymeric chain being in a contact with filler surface (see discussed above results).

Thus cohesion strengthening of organic polymer chains on the surface of carbon fillers was revealed in a framework of quantum-chemical study. Maximal force of tearing off polymer particle adsorbed on carbon surface was found approximately 3 times higher than for polymer in a polymeric matrix. Owing to rather weak however quite sufficient for immobilization of polymeric chain segments on the carbon surface Van-der-Waals forces, around carbon filler particle some condensed layer of rubber is formed with the lowered mobility of chain segments which most likely is responsible for strengthening of organic polymers by filling them with high dispersed carbon.

4.2.2.2. Enthalpy of adsorption in adsorption complex of rubber - carbon filler with nonterminated regular structure.

Based on the abovementioned results the study was carried dedicated to an investigation of the structure of carbon surface, which can supply the best strengthening effect for the rubber composites.

It was taken into account in the study that the microscopical mechanism of the strengthening of the organic rubber composites by filling them with high dispersed carbon can occur due to immobilization of organic polymer chains on the surface of carbon particles. So in the current study the investigation of the correlation of structure the carbon particle surface with corresponding effect of composite strengthening was fulfilled in the framework of QM modeling.

It was found experimentally, that the surface of the technical carbon represents the partially or fully destroyed structure of graphite. Defects of the lattice caused by the thermal treatment lead to the absence of short range ordering. Such partially defected high dispersed carbon represents high abilities as strengthening filler for organic composites. But it was obtained, that properties of technical carbon as the strengthening agent

can become worse after long-term thermal treatment. So it is important to study the connection of the structure of the carbon surface with it's affinity as filler of composites.

For the study of the connection of structure the carbon particle surface with corresponding effect of composite strengthening in the framework of quantum-chemical modeling there were constructed and fully optimized four models of the technical carbon, containing 299 atoms each. These models represent different possible structures of carbon particle surfaces (see fig.4.17,a-d).
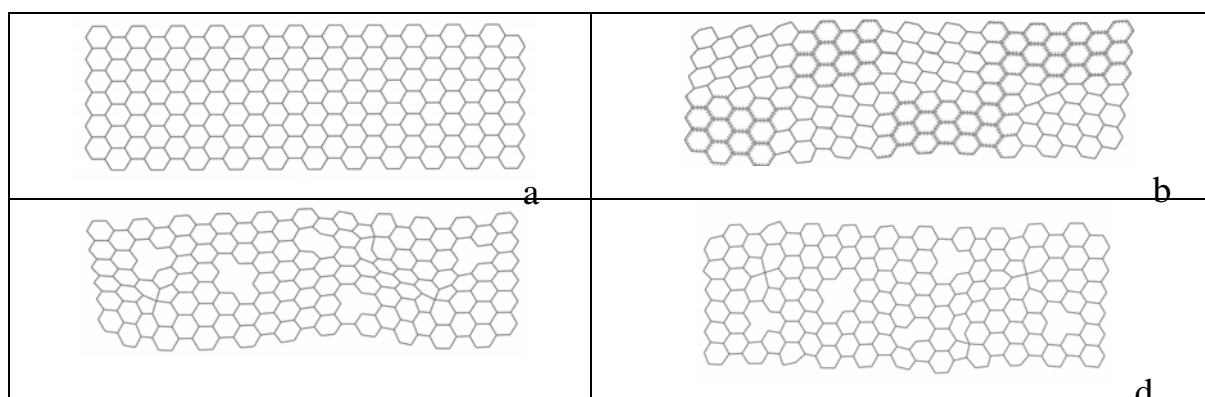
Figure 4.17: Optimized structures of different models of the carbon surfaces (a:C1, b: C2, c: C3, d: C4, (see text, top view).

Model of the carbon surface with regular graphite structure (C1) is represented in fig.4.17,a. The model with sp^2- and sp^3- carbon in the regular arrangement (C2) is presented in fig.4.17,b. The model, keeping as graphite sp^2- carbon, but with non-regular arrangement (with different holes in the structure) (C3) is presented in fig.4.17,c. The model in which carbon exists both in sp^2- and sp^3- hybridizations and in non-regular arrangement (with different holes in the structure) (C3) is presented in fig.4.17,d.

Adsorption complexes of the model organic polymer $H-(CH_2)_n-H$, where n=25 on these four carbon model surfaces was calculated. Fully optimized structures of the corresponding adsorption complexes are presented in fig.4.18,a-d.

Enthalpy of adsorption calculated for one monomer unit $-CH_2-$ for all models are shown in the diagram, see fig.4.19. Forces of the shift deformation for the movement of the segment of organic polymer along the carbon surface for 1 A, i.e. forces of microscopical friction of polymer chain along the carbon surface were calculated for all models under study. These forces are represented in fig.4.21.
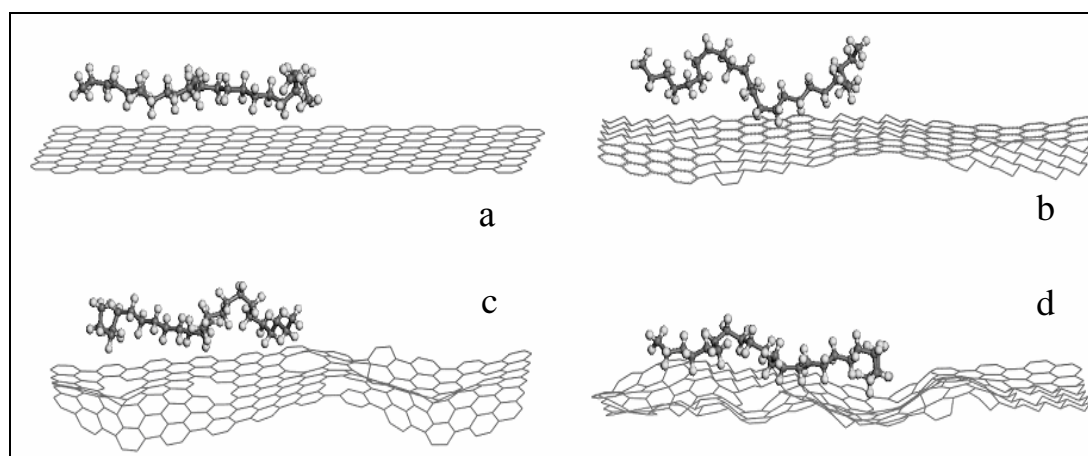
Figure 4.18: Optimized structures of different models of adsorption complexes of the organic polymer segment
H-$(CH_2)_n$-H, n=25 with carbon surfaces (a:C1, b: C2, c: C3, d: C4, (see text, side view).
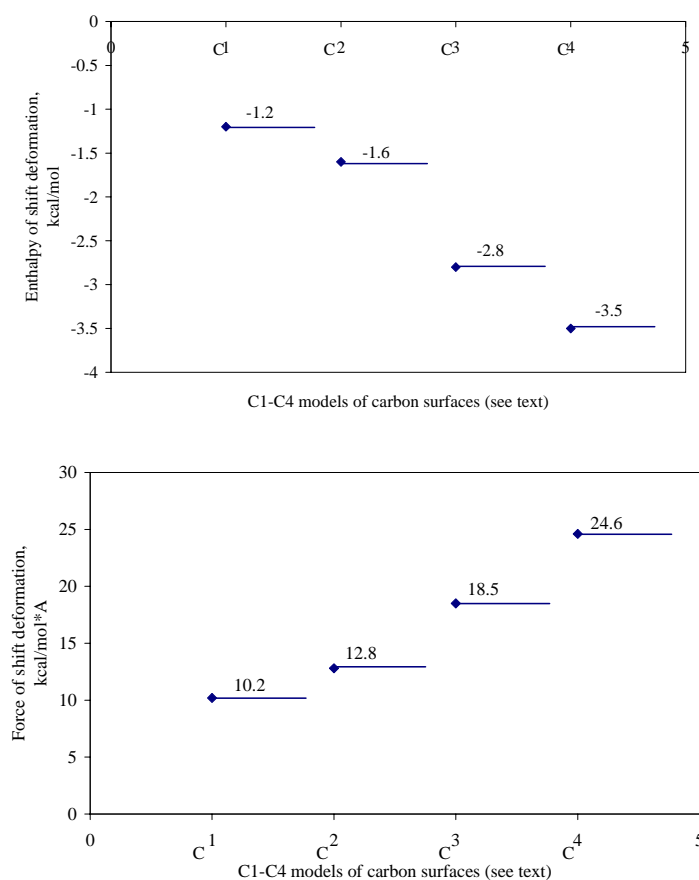
Figure 4.19: Enthalpy of adsorption (a) of the segment of organic polymer H-$(CH_2)_n$-H, n=25, calculated for one monomer unit -CH_2- and forces of the shift deformation (b) for its movement along the carbon surfaces C1, C2, C3, C4.

As it is seen from the results the enthalpy of binding of one monomer unit -CH_2- with carbon surfaces decreases in the row: C1>C2>C3>C4, so thus the less energetic favorable contact was obtained for adsorption complex of polymer –graphite surface (C1), and the most energetic favorable contact was obtained for adsorption complex of polymer –surface (C4), with carbon in sp^2/sp^3-hybridization with non regular defected surface, containing some holes. Calculated forces of microscopical friction confirm the previous state. Thus the force of shift deformation is minimal for microscopical friction of the segment of polymer chain along the regular graphite surface (C1), and maximal for the case of the most defected surface (C4), being at about 2.5 times higher. The first results, presented in this stage show the abilities of such kind of computational modeling, and in the further study it is interesting to make more detailed ranking of carbon particles with accordance to defection structure of their surfaces and in some computer selection obtain structure of carbon particles, revealing the best effect of strengthening for organic composites.

4.2.2.3. Shift deformations in adsorption complex of rubber with nonterminated carbon fillers.

Microscopic force characteristics obtained for friction of polymer chains were compared with the analogical results of the modelling of microscopical friction of the segment of organic polymer $H-(CH_2)_n-H$, where n=25 along carbon surfaces C1-C4.

Structure of intermolecular complex of two interacted segments of organic polymer corresponded to two different steps of particle-particle shifting optimised in QM approach and the introduced microscopic friction coordinate (MFC) are presented in fig.4.20. Stepwise shifting from the equilibrium state was carried out for 60 steps of shifting with value of one step equal 0.5 A. The dependence of force of particle-particle shifting on the value of shifting is presented in fig.4.21.
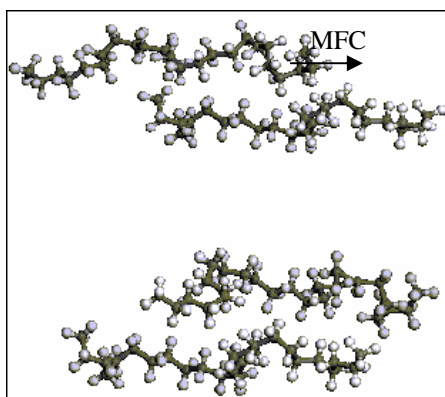
Figure 4.20: Microscopic friction coordinate (MFC) and two steps of shifting in the system of two segments of organic polymer $H-(CH_2)_n-H$, where n=25.

Obtained data was compared to results of similar calculation for microscopical shift of the same segment of organic polymer $H-(CH2)_n-H$ for n=25 along the surfaces of model carbon particles C1-C4 described above. Step-by-step shift was modelled for 130 steps with size of latter equal 0.5A.

Calculated dependences of shift force on size of shift for all investigated molecular complexes are presented in figs.4.22-4.25. Diagrams evidently show "friction at atomic level". Maximums on the curves correspond to the closest atom-atom contacts; minimums correspond to the positions of atoms fare from each other. Maximums shifting forces characterize forces of molecular friction or molecular cohesion polymers and carbon surfaces.
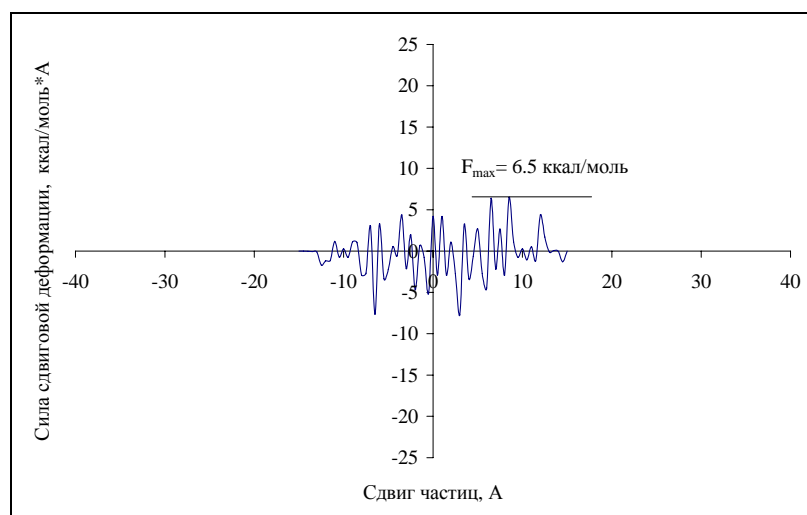
Figure 4.21: Force of shift deformation or molecular friction in the complex of two segments of organic polymer H-(CH$_2$)$_n$-H, where n=25.
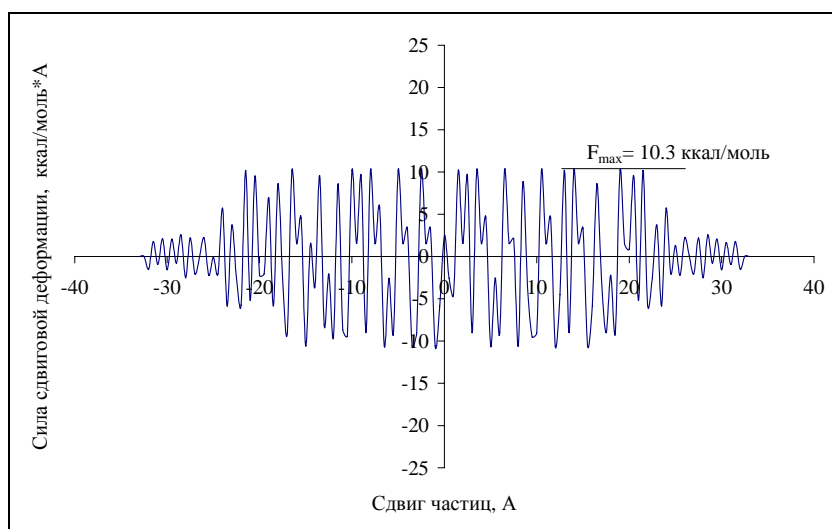
Figure 4.22: Force of shift deformation or molecular friction in the complex of segment of organic polymer H-(CH$_2$)$_n$-H, where n=25 and model of carbon surface C1.
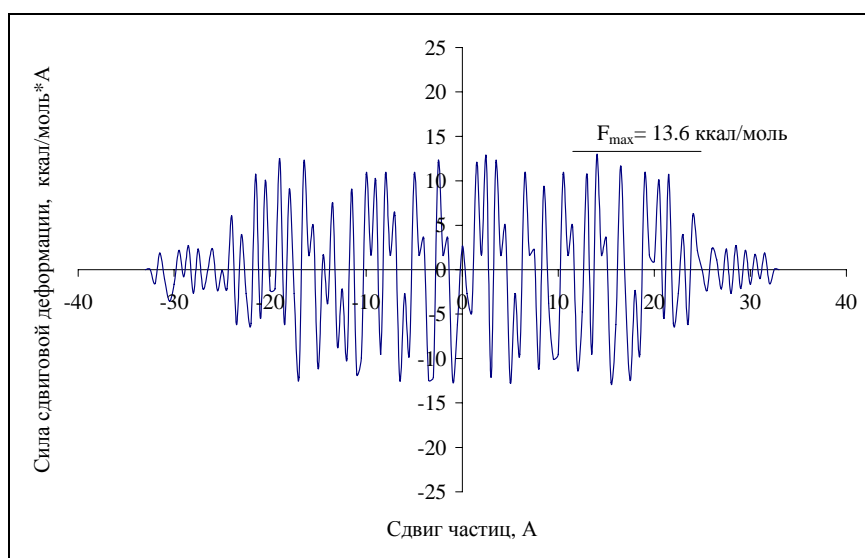
Figure 4.23: Force of shift deformation or molecular friction in the complex of segment of organic polymer H-(CH$_2$)$_n$-H, where n=25 and model of carbon surface C2.
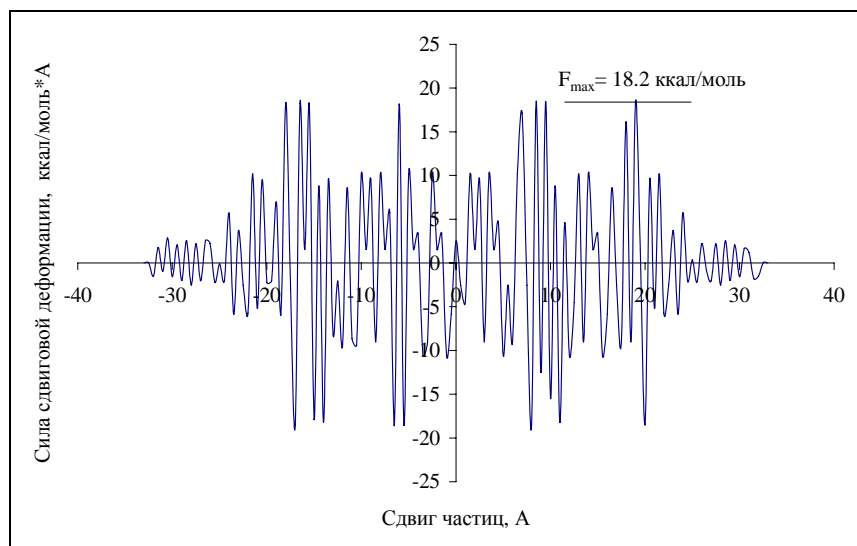
Fig.4.24. Force of shift deformation or molecular friction in the complex of segment of organic polymer H-(CH$_2$)$_n$-H, where n=25 and model of carbon surface C4.
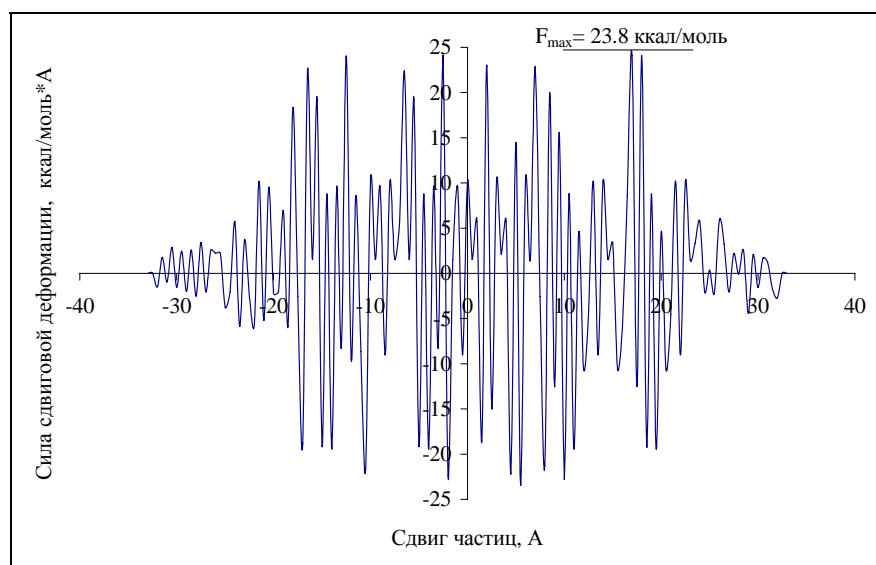
Fig.4.25. Force of shift deformation or molecular friction in the complex of segment of organic polymer H-(CH$_2$)$_n$-H, where n=25 and model of carbon surface C4.

The results revealed that the force of shift deformation or shift friction in polymer matrix is 2-3 times lower, than the same force for molecular friction in the system polymer- surface of carbon particle. This is a reason of immobilisation of polymer chain on the surface of carbon. Moreover, calculations revealed that force of shift friction increases in the row of adsorption complexes with the models: C1<C2<C3<C4, so that the minimal value of shift force was obtained for regular C1 graphite surface and the maximal – for more defective surface C4.

Thus, from the received data it is visible, that the most energetically unfavorable contact is received for the system polymer - graphite surface (C1). The most energetically favourable contact is received for a case of adsorption of polymer on a surface in the sp^2/sp^3-carbon hybridization, having holes and five-ring defects (C4) on which fragment of polymer chain immobilized better, and, hence, which has the best strengthening properties

as filler for rubber composites. Summarizing in should be mentioned, that in the given section the technique offered earlier is tested on an example of calculation of molecular friction in the complex system consisting of organic polymer and carbon filler.

4.2.2.4. Influence of terming of carbon particles by hydrogen on enthalpy of their binding with rubber matrix.

At the current stage termination of these model surfaces by hydrogen atoms was investigated. All structures presented in fig.4.17 have some unsaturated valences, which are located on the atoms on the boundary of aromatic ring system for C-sp^2-structures, or on the atoms in the "hole" defects or on the surface C atoms in sp^3-hybridization. Nonterminated these atoms are very energetically favorable for chemical and adsorption activity. These atoms can be terminated in air or under heat treatment by hydrogen atoms or/and hydroxyls. Chemical activity of these active places is changed after termination; nevertheless these active places also play in essential role in adsorption processes.

Similarly to the research described in section 2.3 adsorption of a segment of organic polymer H-named by hydrogen (CH2) $_n$-H for n=25 has been calculated on H-terminated surfaces C1_H…C4_H. Completely QM optimized structures of corresponding adsorption complexes are presented on fig.4.26,a-d.

Enthalpies of the adsorptions calculated for one monomer unit -CH2- for each these surfaces and force of shift deformation at movement of a segment of organic polymer along a surface on 1A (forces of microscopic friction of polymer above a surface of carbon particle) are presented on fig.4.27,a and b.
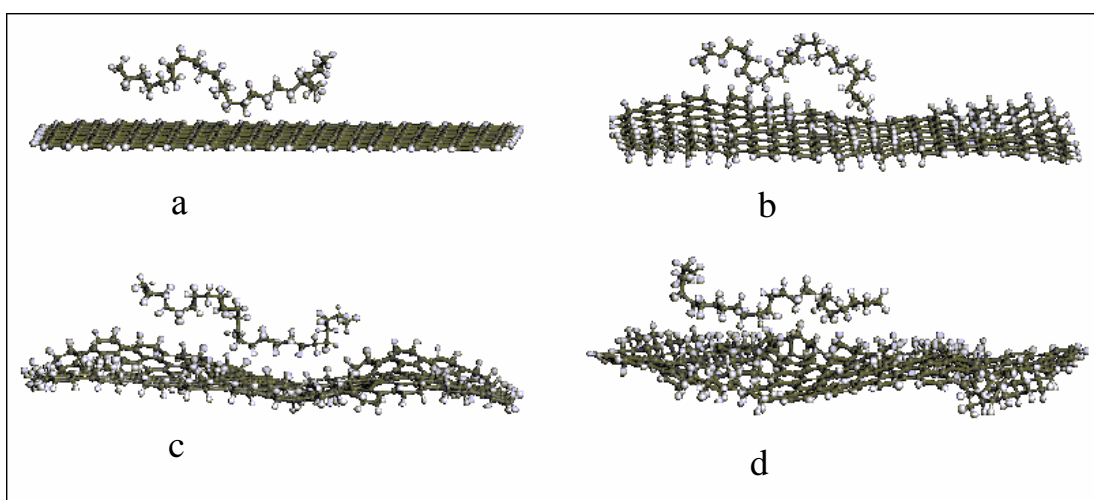
Figure 4.26: Models of adsorption complexes of segment of organic polymer H-(CH2) $_n$-H for n=25 and terminated by hydrogen carbon surfaces: C1_H (a), C2_H (b), C3_H (c), C4_H (d).

It was obtained that enthalpy of binding of one monomer unit -CH$_2$- with the H-modified carbon surfaces decreases in the same number, as for nonterminated carbon surfaces, namely in a row: C1_H> C2_H> C3_H> C4_H. Graphite surface (C1_H) was found as the energetically most-unprofitable contact for system polymer, and the most energetically favourable contact is received for a case of adsorption of polymer on H-terminated surface containing defects with atoms of carbon in sp2/sp3-hybridizations and having different holes in a structure. (C4_H).
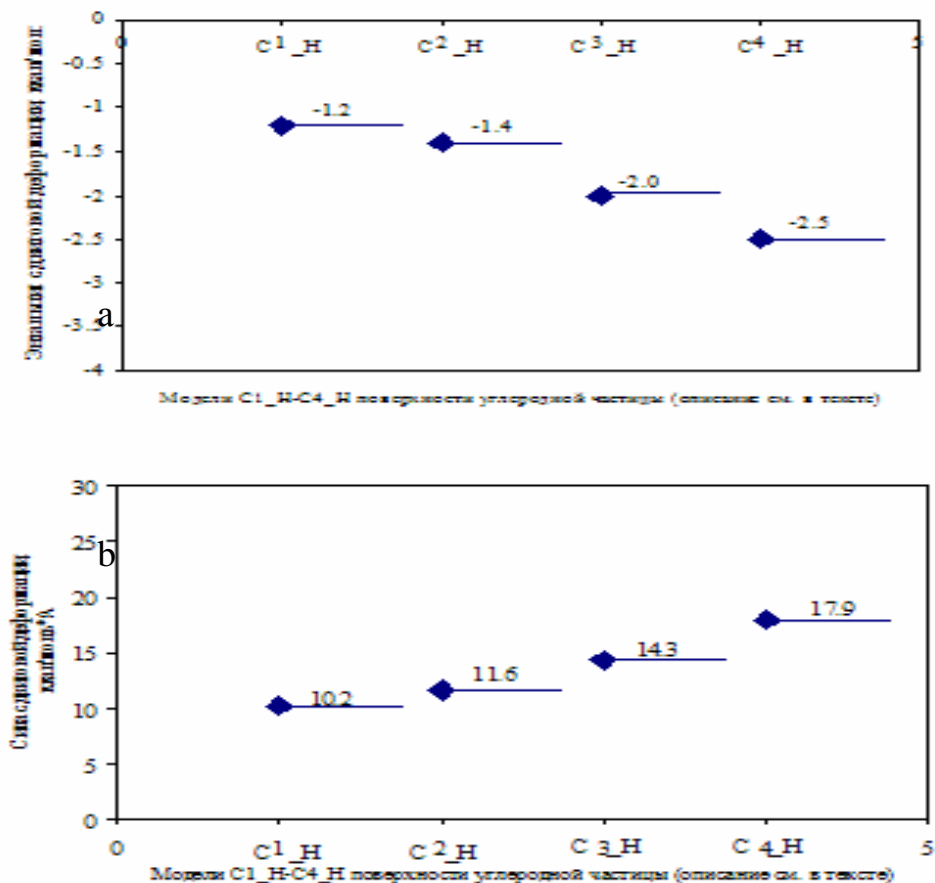
Figure 4.27: Enthalpies of adsorptions (a) of a segment of organic polymer H-(CH2)$_n$-H for n=25 and forces of its shift deformation (b) at movement on 1A, calculated on one monomer unit -CH$_2$- for models C1_H, C2_H, C3_H, C4H of carbon surfaces terminated by hydrogen.

Consideration of the stress diagram of friction for studied surfaces also confirms the received energetic result. Force of shift of microscopic friction is minimal for a case of strictly periodic graphite surface (C1_H). It is worth to mention that for nonterminated and H-terminated models the same result was received. However if to compare the similar nonterminated and terminated defective surfaces force of microscopic friction along the terminated surface makes approximately 0.9-0.7 from force of microscopic friction along not terminated surface. Is of interest in the further during consecutive numerical quantum mechanical experiment to make more detailed ranging a surfaces of carbon particles on number and a kind of defects of a lattice of graphite and kind of its termination., Also by selection in computer design to establish a microscopic structure of a surface of technical carbon, optimum for the best strengthening effect.

4.2.2.5. A structure and adsorption properties of nonterminated and terminated balk particles of amorphous soot.

Balk soot particles was considered both not terminated (clean), and terminated by hydrogen. Adsorption on a surface of such soot particles of water both in an individual state and in a cluster or drop-like state

consisted from several H-bonded water molecules was considered in a course of QM modeling. Also adsorption of model polyethylene oligomer on different (H-terminated and clean) soot model particle surfaces was studied in absence and at the presence of water.

Several microscopic models of technical carbon (amorphous soot) suitable for carrying out of QM calculations of the complex composite interface were constructed. Two carbon clusters with number of atoms 170 and 670 modeled technical carbon. The small particle had diameter ~15 A, and big ~25A. The bulk of particles had a structure of carbon in and *sp3*-configuration, the surface of particles had both C-sp^2, and C-sp^3 a structure, thus, the surface contained both the graphite, and the diamond-like structures disorderly distributed and represented amorphous carbon. Full QM optimization of structure of these model clusters has been performed. Structures received C170 and C670 clusters are presented in fig.4.28.

a

b
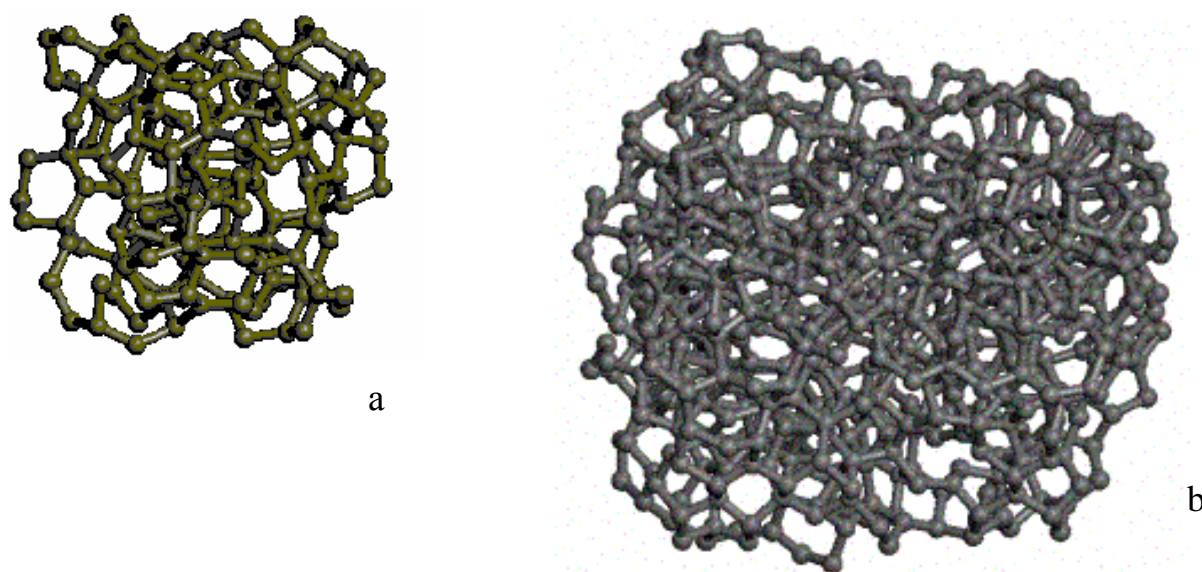
Figure 4.28: Optimized structures of C170 (a) and C670 (b) clusters of amorphous soot with nonterminated surface.

Various variants of surface termination by hydrogen of carbon models were considered (bounding effects). It is known, that amorphous soot, which is used as filler for rubbers, is made in vacuum. In this case its surface can remain nonterminated also interacting with matrix of polymer (rubber) On the other hand, the surface of such particle has exclusive chemical reactivity. At contact to air such surface can be terminated. We have considered termination of a surface of amorphous soot by hydrogen. Quantum mechanical minimization of H-terminated carbon clusters was fulfilled and obtained structures are presented in fig.4.29.
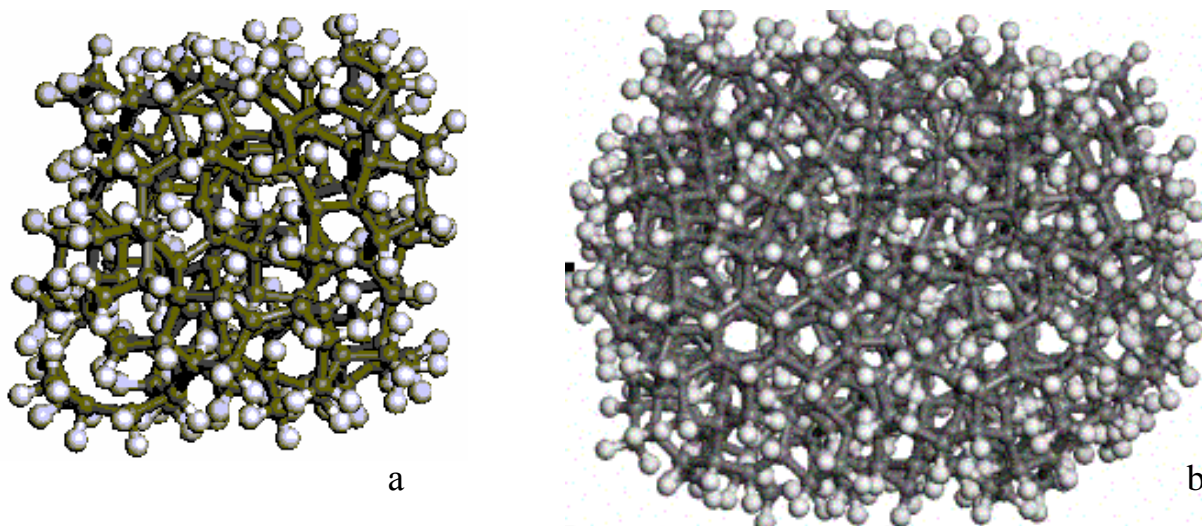
Figure 4.29. Optimized structures of H-C170 (a) and H-C670 (b) clusters of amorphous soot with the surface terminated by hydrogen.

Interaction amorphous soot model cluster C670 with individual water molecules and with the water connected in a complex, i.e. with model drop of water has been considered (see fig.4.30,a and b). Besides interaction of individual molecules of water and a drop of water with the model of H-terminated soot cluster H-C670 has been considered also considered (see fig.4.31,a and b).
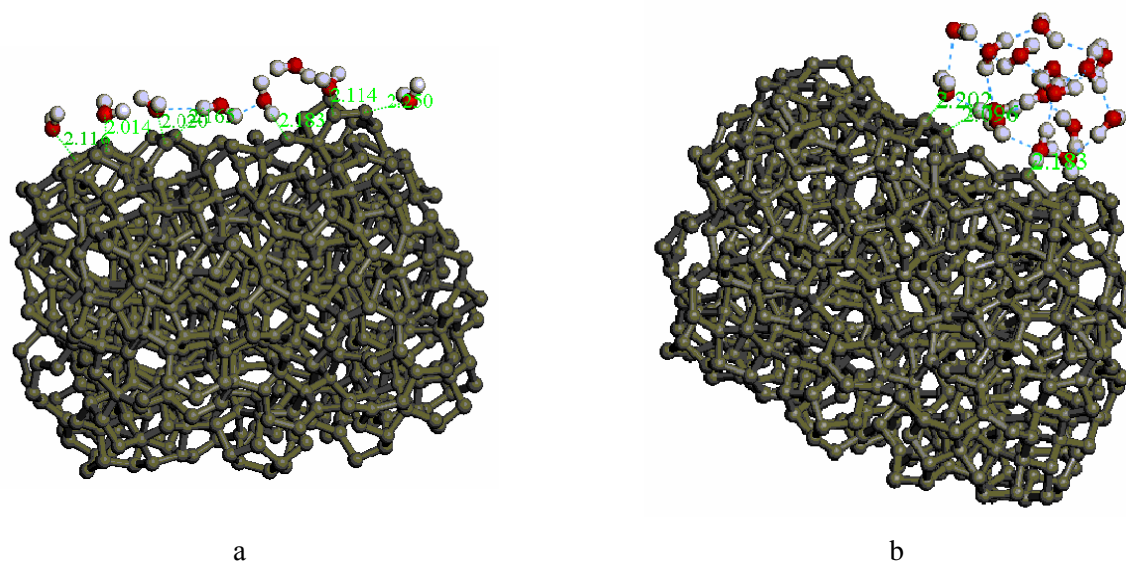
Figure 4.30: Interaction of nonterminated soot particle C670 with individual water molecules (a) and with the H-bonded drop of water (b).

<div style="text-align:center">a   b</div>
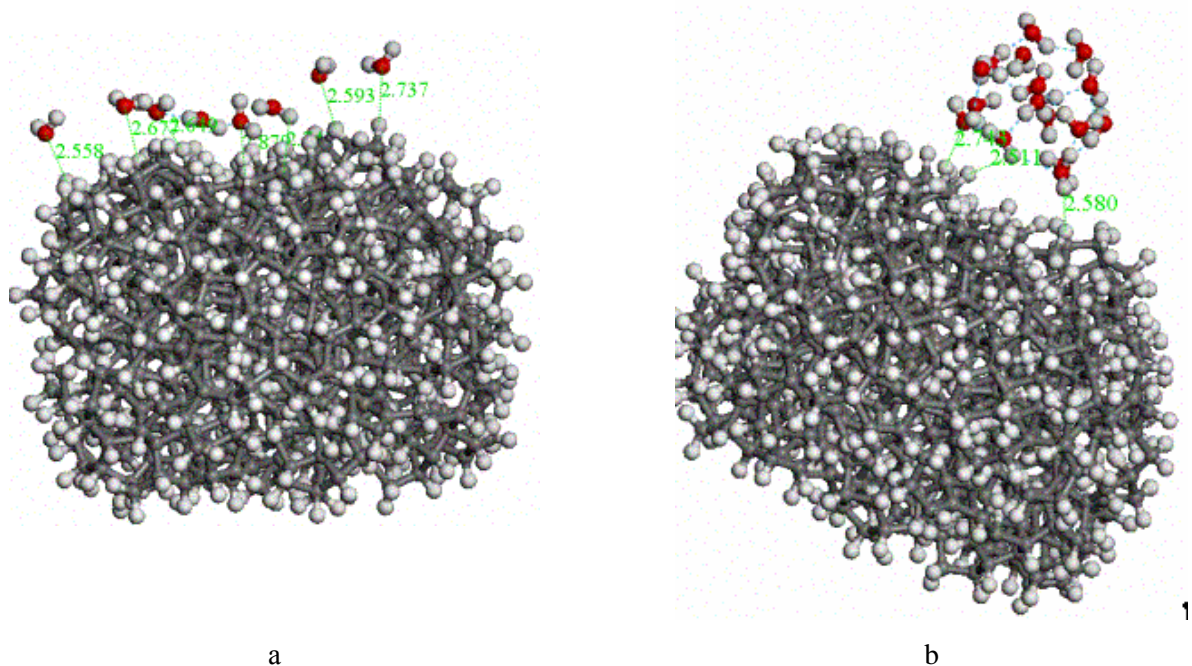
Figure 4.31: Interaction of the soot particle H-C670 terminated by hydrogen with individual water molecules (a) and with the H-bonded drop of water (b).

During quantum mechanical modelling it has been shown, that on nonterminated carbon surface there is an adsorption of individual water molecules which can be characterized as Van-der-Waals one: $R_{C...O}$ =2.0-2.2A, ΔH~2-2.5 kcal/mol (calculated for one water molecule). Much weaker interactions of water molecules occur with nonterminated carbon surface: $R_{H...O}$ =2.5-2.8A, ΔH~1.3-1.5 kcal/mol (calculated for one water molecule).

The H-bonded water drop does not spread on carbon surface, interacting with the latter as a unit. As it has been shown in QM calculations energy of hydrogen bonding OH … O in cluster, consisting of several water molecules is ΔH_{bind}~4 kcal/mol, that is, more, than energy of interaction of water molecule with soot surface, thus, is energetically proved clusterising of H-connected water molecules on soot surface.

Further adsorption of polyethylene oligomer consisting of 16 monomer units - $(CH2)_{n-}$, where n=16, on nonterminated and terminated carbon particles without water and at presence of water was considered. Corresponding structures of QM optimized adsorption complexes I, II, III, IV are presented on fig.4.32-4.33. Enthalpies of binding of polyethylene chain calculated for one monomer unit - (CH_2)- for different complexes I, II, III, IV are presented on fig.4.34. It is visible, that most energetically favourable adsorbing ability represents nonterminated carbon surface in absence of water.
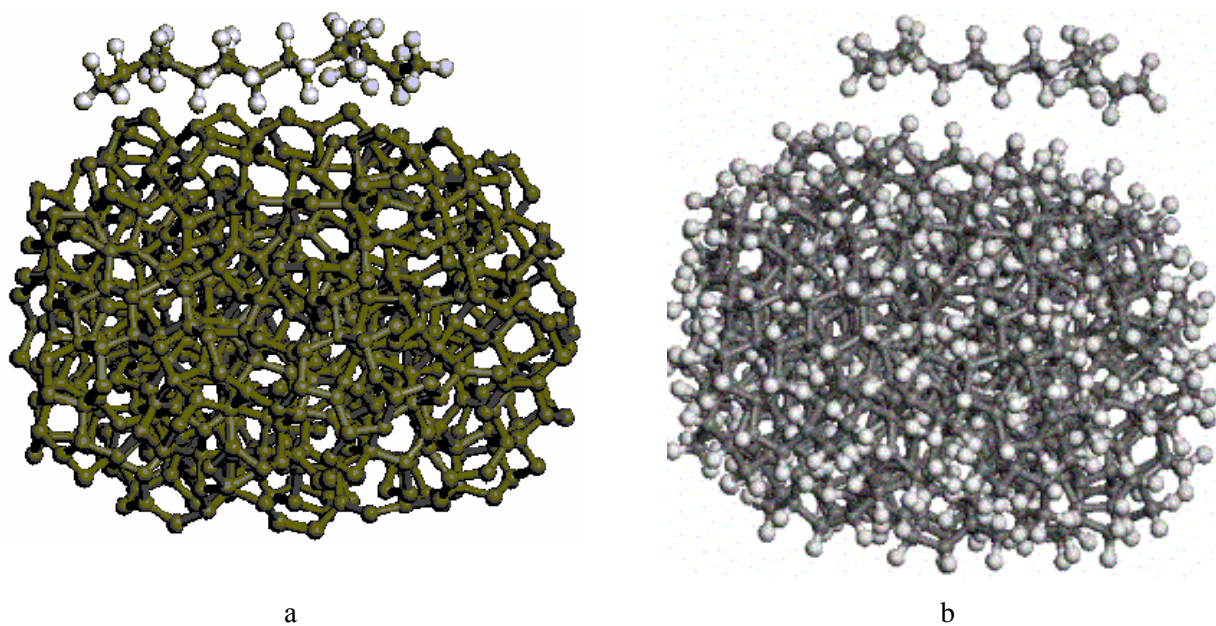
Figure 4.32: Interaction of polyethylene oligomer with nonterminated C670 () and H-terminated H-C670 () soot particles (adsorption complexes I and II, respectively).
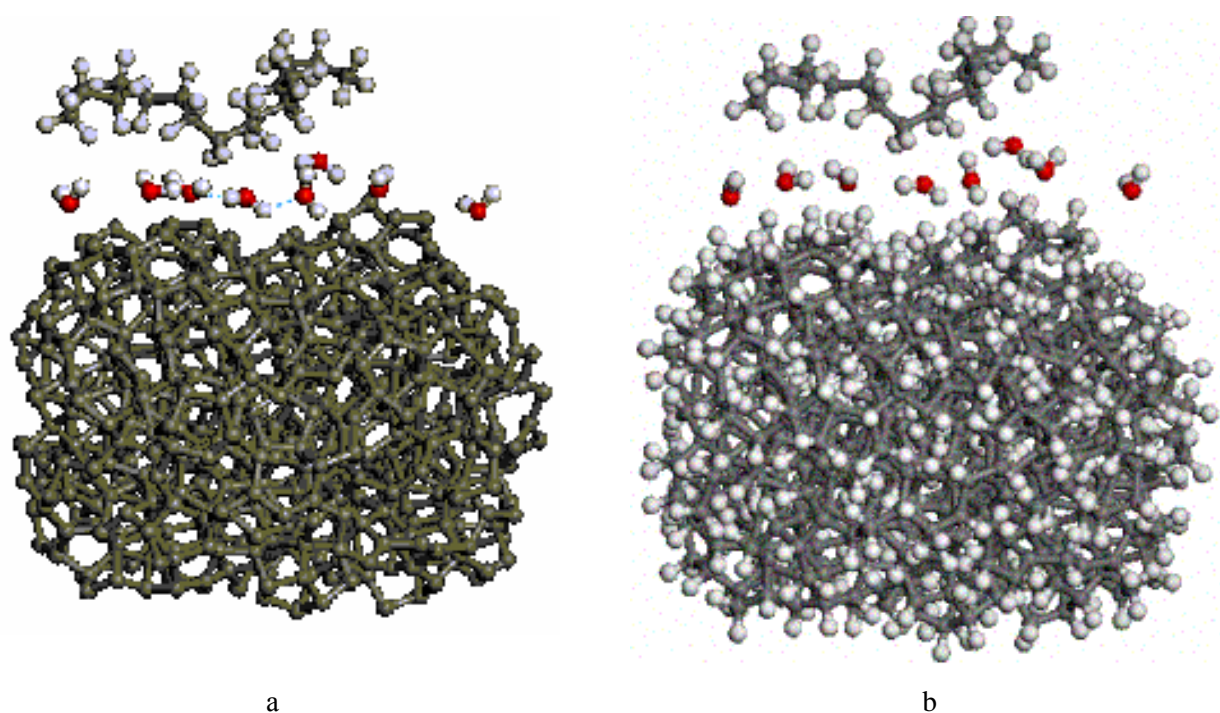
Figure 4.33. Interaction of polyethylene oligomer with nonterminated C670 () and H-terminated H-C670 () soot particles with the presence of water (adsorption complexes I and II, respectively).
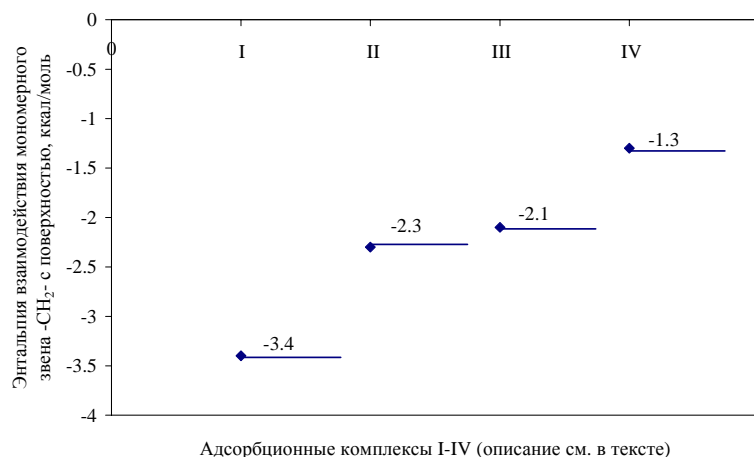
Figure 4.34. Enthalpy of polyethylene binding with soot models calculated for one monomer unit - (CH$_2$) - for different adsorption complexes I, II, III, IV.
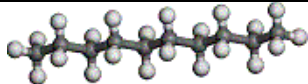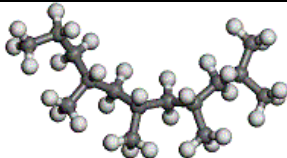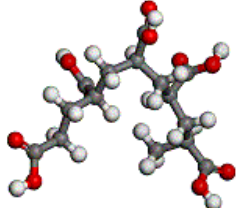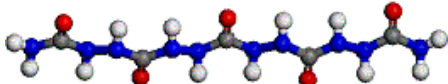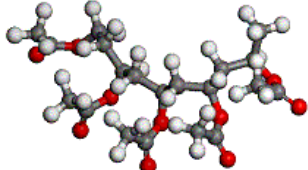
It was obtained that fragment of organic polymer interacts with nonterminated carbon surface at about 1.5 times stronger than with H-terminated carbon surface. Water interlayer between polymer and carbon surface decrees strength of interaction in the system. The reinforcing effect of pure nonterminated carbon fillers is the best.

4.2.2.6. Influence of chemical nature and structure of polymer on strengthening effect of carbon fillers on rubber composite.

The impact of chemical nature of polymer and chemical nature of surface soot modification on the enthalpy of binding and the force of intermoleculat\r shifting (friction) was considered. Carbon model in this study contains 170 atoms of C and has a diameter of ~15 A. The nuclear of this particle had a structure of carbon in and sp^3-configuration, the surface of the particle had both C-sp^3, and C-sp^3 a structure, thus, the surface contained both the graphite, and the diamond-like structures disorderly distributed and represented amorphous carbon. Moreover the same particle, but H-terminated was taken for the modeling also (see structures of these carbon clusters in figs. 4.28,a and 4.29, a). Adsorption of polymers of different chemical and space structure on the surfaces of these soot particles was studied in QM modeling. For this study individual molecules of the oligomers CH$_3$-(R)$_n$-CH$_3$, with n=5 were constructed and optimized in QM. There were considered oligomers with different chemical nature: polyethylene, polypropylene, polyacrylic acid, polurea, and polyvinyl acetate. The description of model oligomers and QM optimized structures of its molecules are presented in Table 4.1.
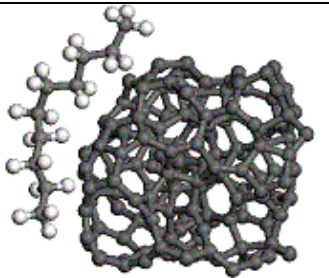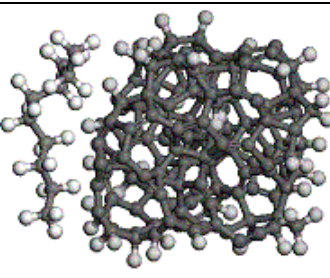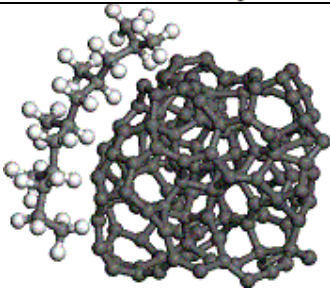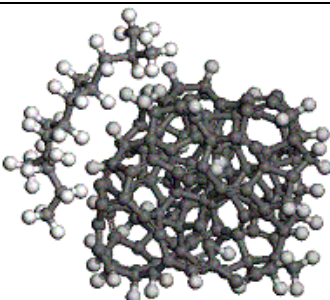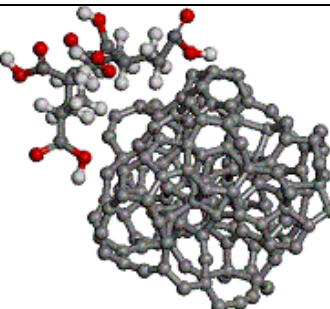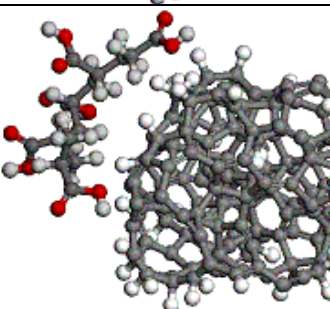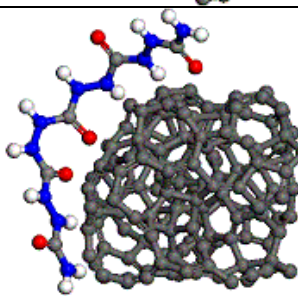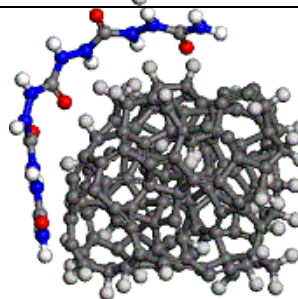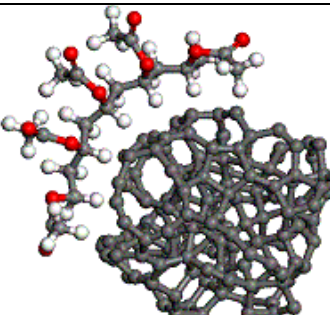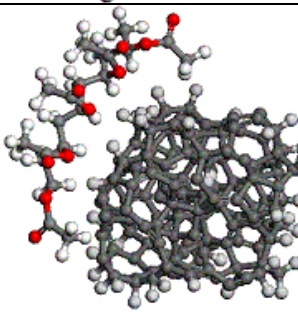
Table 4.1.

The description of model oligomers used in QM modelling of adsorption of polymeric chain fragments on a surface of soot particles.

Fragment of polymer (oligomer):	Structural formula of monomer unit R: $CH3-(R)_n-CH3$, $n=5$	Optimized in QM structure of oligomer
Polyethylene (PE)	$-(CH_2CH_2)-$	
Polypropylene (PP)	$-(CH_2CHCH_3)-$	
Polyacrylic acid (PAA)	$-(CH_2COOHCH_2)-$	
Polurea (PU)	$-(NHNHCO)-$	
Polyvinyl acetate (PVA)	$-(CH_2COC(O)CH_3CH_2)-$	

Adsorption of each of these oligomers was calculated on the surfaces of nonterminated and H-terminated soot particles C170. QM optimized structures of the corresponding adsorption complexes are summarized in Table 4.2.

Table 4.2.

Optimized models of adsorption complexes of polymers with soot particles.

N	Fragment (oligomer,) of polymer:	Adsorption on non-terminated soot surface	Adsorption on H-terminated soot surface
1	Polyethylene (PE)		
2	Polypropylene (PP)		
	Polyacrylic acid (PAA)		
4	Polurea (PU)		
5	Polyvinyl acetate (PVA)		

Binding enthalpies and forces of intermolecular microscopic shifting (with movement of the molecules along each other on 1A) were calculated for each of these complexes (see figs.4.35 and 4.36). For the best

comparing and polymer energetic ranking by binding enthalpy these values were calculated for one monomer unit.
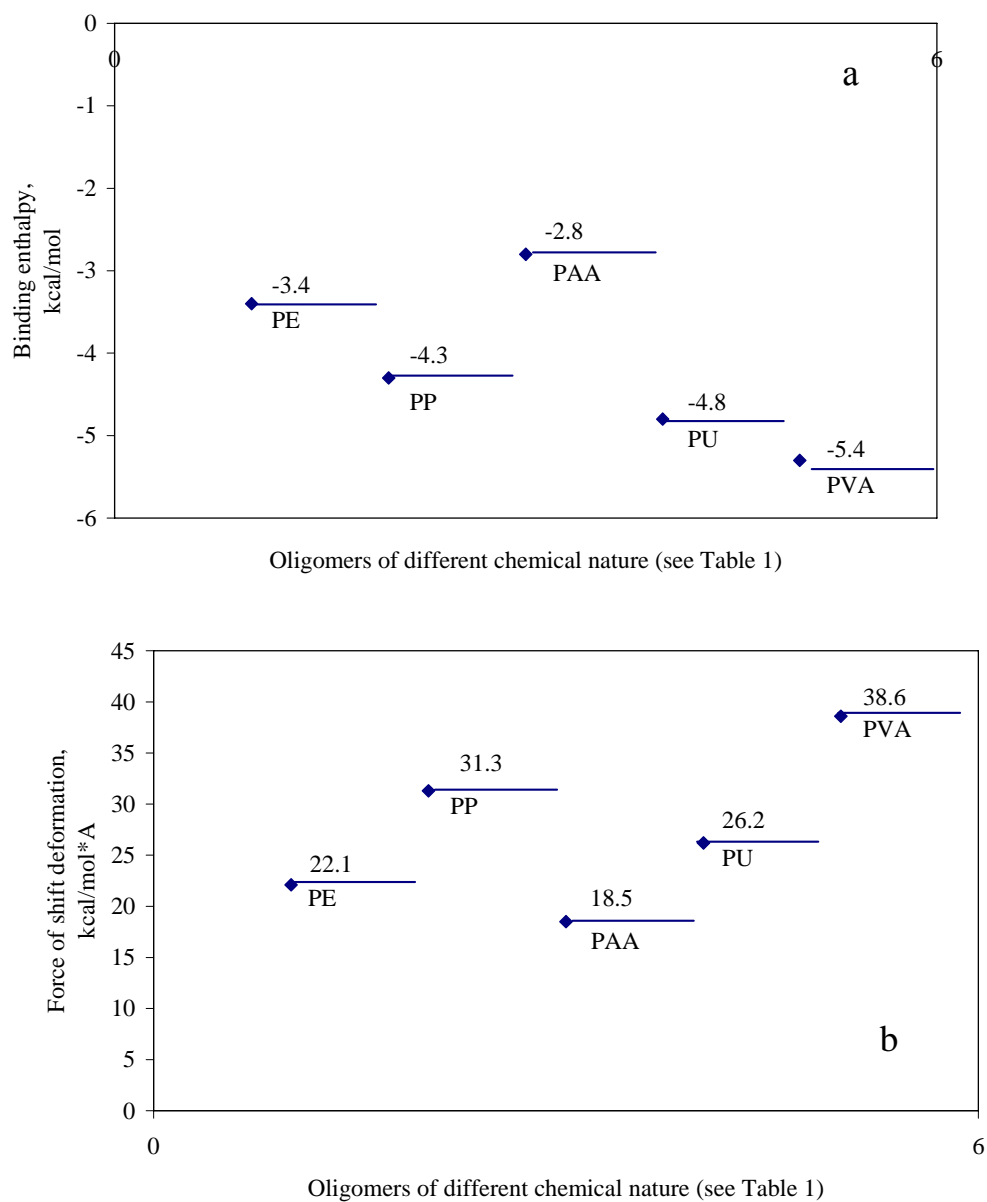
Figure 4.35. Binding enthalpy (a) and force of shift deformation (b) of the segment of organic polymer CH_3-$(R)_n$-CH_3, n =5, calculated for one monomer unit -R- for model soot particle with nonterminated surface.
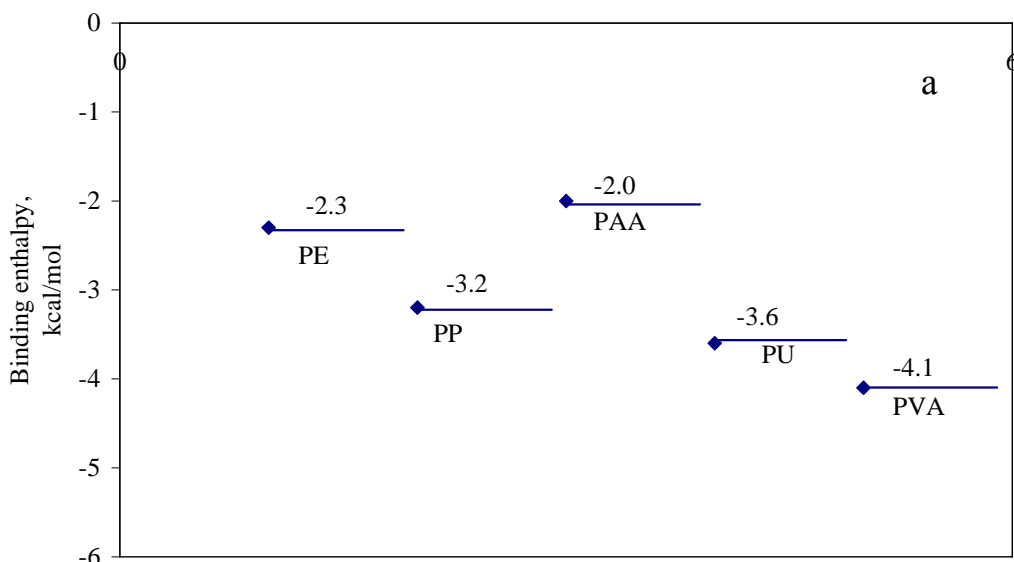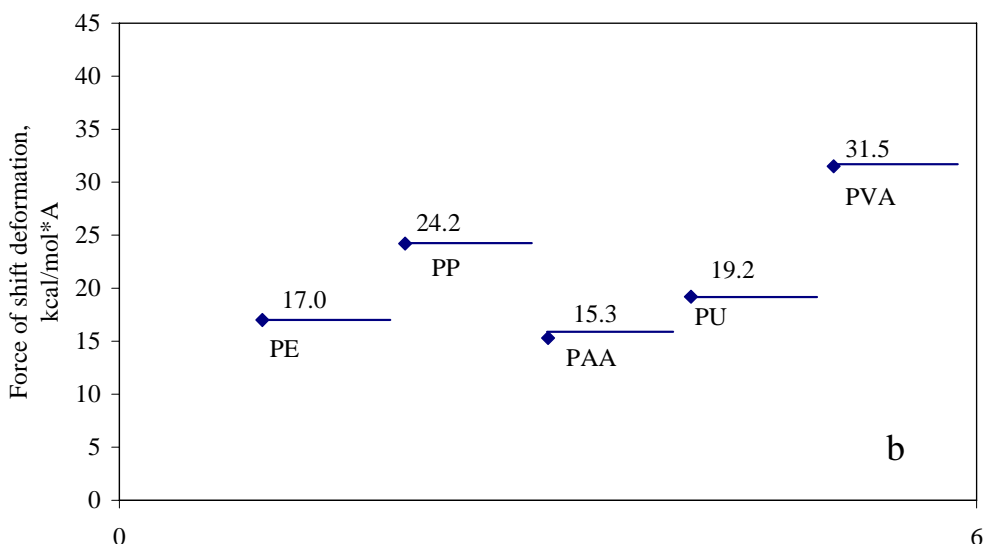
Figure 4.36. Binding enthalpy (a) and force of shift deformation (b) of the segment of organic polymer CH_3-$(R)_n$-CH_3, n=5, calculated for one monomer unit -R- for model soot particle with H-terminated surface.

Some conclusions could be done about impact of chemical nature of the polymer matrix on the interaction of the polymer segments with surface of soot fillers. The binding enthalpy and the force of shifting is determined mainly by square of hydrophobic contact between polymer fragment and surface of soot particle (i.e. by presence and number of CH_2 и CH_3 groups), and by the presence and number of electronegative atoms (O, N) in the polymer structure. Moreover the conformations of the polymer fragment on the interface, namely complementary character of its space structure with structure of soot surface impact also of the polymer adsorption.

It was obtained that binding enthalpy and force of shifting of polypropylene in ~1.5 times higher than the same values obtained for polyethylene. It can be explained with greater square of hydrophobic contact between

polymer fragment and surface of soot particle in the case of polypropylene. In the same time binding enthalpy and force of shifting of polurea in ~1.7 times higher than the same values obtained for polyethylene. Having at about the same surface of interparticle contact molecule of polurea oligomer has N and O electronegative atoms, which play the decisive role in the binding in this case.

The most energetically favorable contact of the oligomers under study was obtained for polyvinyl acetate (~ in 2.0 times higher than for polyethylene), that can be explained by the impact of the two factors described above. This molecule has high square of hydrophobic contacts and also contains electronegative atoms O.

The lack of high adsorption capacity in the case of polyacrylic acid (it also has electronegative atoms O in the structure) can all means be explained by not favorable conformation of this molecule under adsorption on the soot surface, that can follow from not favorable geometry of the corresponding adsorption complex for realization both hydrophilic and hydrophobic contacts. This oligomer revealed small value of binding enthalpy.

Analogical values, obtained for H-terminated soot surface, revealed the same regularity for different kinds of polymers however in a total binding enthalpies and forces of shifting are at about 0.7 times less than for nonterminated surface.

4.2.2.7. Influence of chemical structure of filler surface (particles of carbon) on their aggregation ability.

To study the aggregation of soot particles in the individual state and in the polymer matrix quantum mechanical modeling was performed for interaction of two soot particles. Chemical modification of the soot surface was studied as a factor, which can prevent sintering of the soot filler particles. The impact of chemical modification of soot surface on the binding enthalpy and force shifting was studied in QM approach. Four particles of C170 were constructed as nonterminated, -H, -OH, and -COO⁻ terminated. The latter surfaces were negatively charged. Interaction of two particles of each kind was calculated in QM modeling and obtained complexes are presented in Table 4.3.
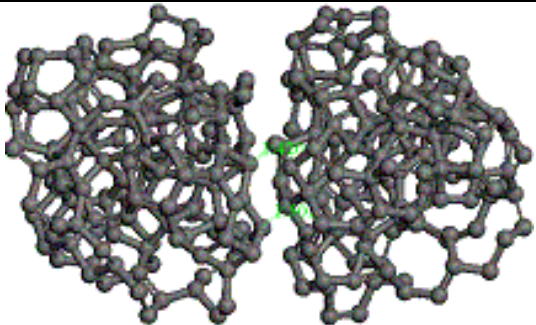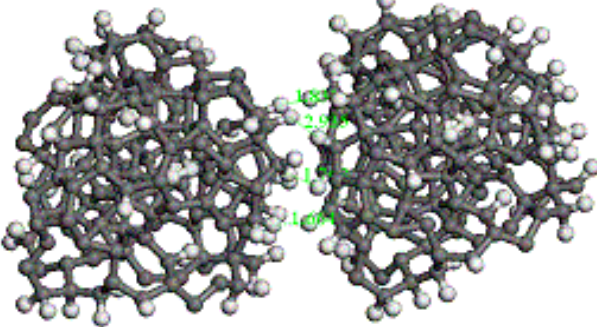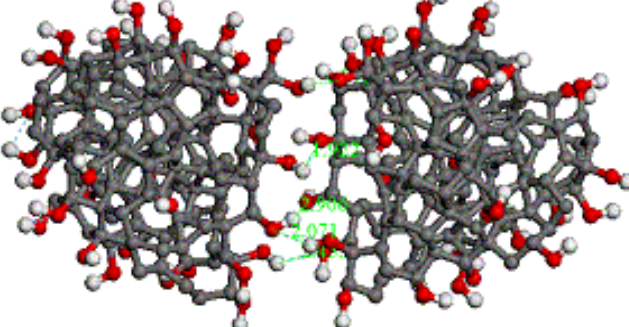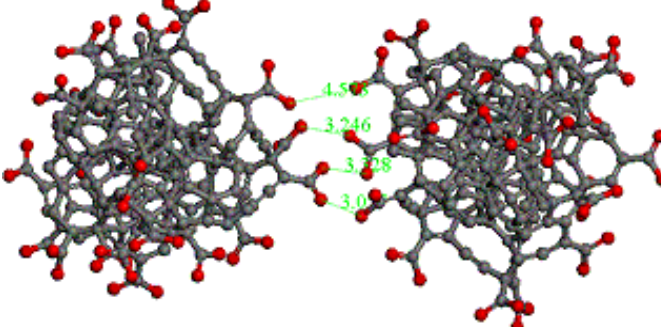
Calculated minimal interparticle distances, binding enthalpies and forces of particle-particle shifting are presented also in this table. The latter two values were calculated for one unit of surface the contact of the two particles (1A) for the convenience of comparison.

As it is seen from the results, presented in the Table 4.3 the strong interaction is observed in the case of interaction of nonterminated carbon surfaces. It leads in some cases to the formation of new covalent bonds C-C between the former soot particles. Thus the initial protoparticles of the amorphous carbon with nonterminated surfaces interact with each other forming larger molecular structures, which can not be easily divided into the initial particles, but which kept in the main details their initial structure.

In the case of carbon particles with H-terminated surfaces much weaker interaction of the particles was obtained. Hydrophobic H…H interactions keep interacted particles at the H…H distances at about 1.6-1.7A. Binding enthalpy and forces of intermolecular shifting are enough for interparticle agglomeration. It is very likely that this kind of agglomeration can be destructed with an impact of adsorption interlayer between soot particles, which can be polymer or water.

Table 4.3.

Optimized models of adsorption complexes of two soot particles.

System	QM optimized structure	Min. distance between particles, A	ΔH bind, kcal/mol	Fsh kcal/mol* A
2 soot particles with non-terminated surface		1.4-1.5	-72.3	103
2 soot particles with H-terminated surface		1.6-1.7	-2.6	19
2 soot particles with OH-terminated surface		1.9-2.0	-4.5	32
2 soot particles with COO⁻-terminated charged surface		3.0-3.2	-0.4	2.5

In the case of interaction of the soot particles, which surfaces are terminated by hydroxyls, interparticle agglomeration is determined by hydrogen bonding between particles. Minimal interparticle distances correspond to the standard hydrogen bonds (1.9-2.0 between H and O atoms participating in H-bond formation). Aggregation or sintering of the soot particles is stronger than in the case of H-terminated soot surfaces, but possible can be destructed in water solution or in the presence of polymer matrix.

In the case of interaction of the carbon particles, which surface is terminated by negatively charged COO⁻ groups, particles are slightly repulsed, and aggregation is not taking place. (The shortest distance between particles is O…O 3.0-3.2, so the surface modification similar studied can prevent soot particles agglomeration if necessary.

4.2.2.8. Aggregation of filler particles (carbon particles) at presence of water molecules and polymer on their surface.
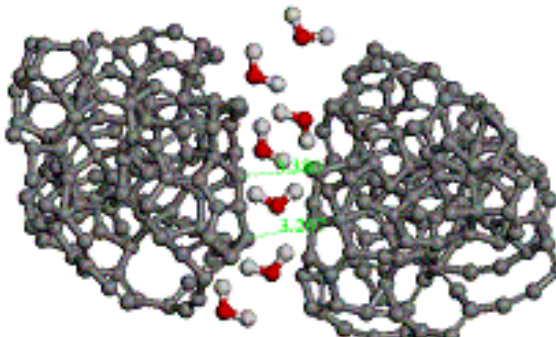
The impact of chemical nature of the particles, which are adsorbed at the interface of two soot particles on their binding enthalpy and force of microscopical friction, was studied. Nonterminated, terminated by H soot surfaces were taken into consideration.
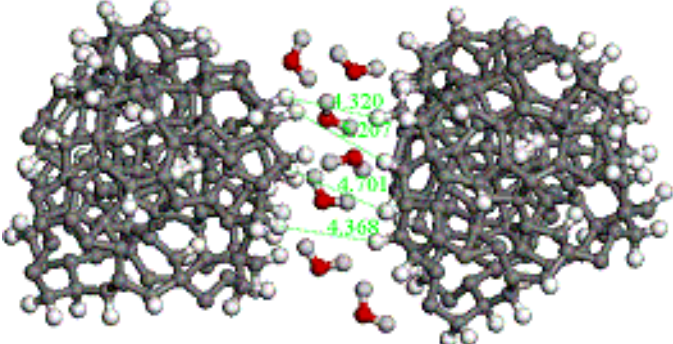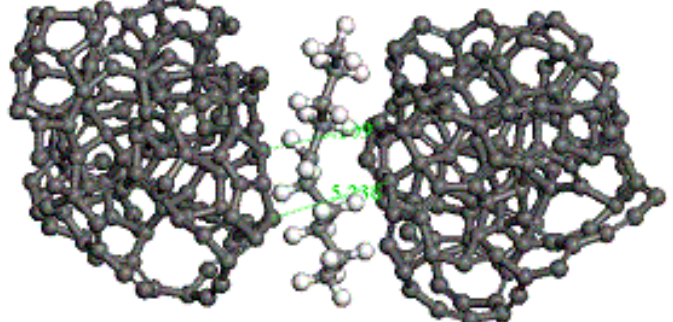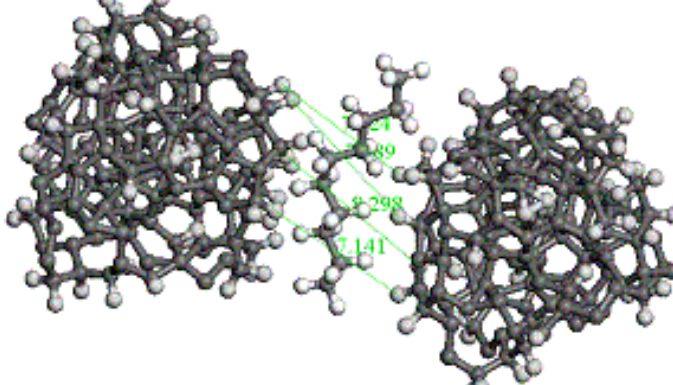
Interaction of two soot particles was studied also in the presence of interparticle molecular layer, consisting of polymer molecules and/or water molecules. Surfaces of the soot particles were examined as nonterminated and terminated by H atoms. QM optimized structures of adsorption complexes obtained in this study are presented in Table 4.4. In this table the results of enthalpy of binding and intermolecular force of shifting are also presented.

As it is seen from the results, aggregation of the soot particles can be prevented by adsorption interlayer of polymer between the soot particles. Adsorption of water in the interparticle interface can be considered as competitive process for polymer adsorption. For the formation of the contact polymer-filler water layer on the soot surface has to be removed. Energetic of these competitive processes is similar, and so for stronger adsorption of the polymer chains on the filler particles modification both polymer molecule and surface of the fillers has to be performed.

Table 4.4.

Optimized models of adsorption complexes of two soot particles with interface interlayer of polymer and water

System	QM optimized structure	Min. distance between particles, A	ΔH bind, kcal/mol	Fsh kcal/mol*A
2 soot particles with non-terminated surface and water interlayer		3.2-3.4	-3.8	22

2 soot particles with H-terminated surface and water interlayer		4.3-4.4	-1.9	13
2 soot particles with non-terminated surface and polymer interlayer		4.7-5.1	-3.3	19
2 soot particles with H-terminated surface and polymer interlayer		7.0-7.2	-2.1	15

4.2.2.9. Investigation of interaction of rubber polymeric molecules with filler particles (technical carbon). Uniaxial deformation and intermolecular friction.

The adsorption complexes of the carbon soot particles with the fragments of the polymer chains with different chemical nature have been studied recently. In the present part two natural rubbers, i.e. polybutadiene and isoprene have been examined in the quantum mechanical level in comparison with polyethylene. The main attention was devoted on the modeling of microscopic mechanical properties of adsorption complexes of these polymers with particles of amorphous carbon.

A cluster model of amorphous carbon designed in the previous step of the study, which contain 170 atoms of carbon being of ~15A in diameter was used in the present study. The surface of this particle was partially terminated by hydrogen atoms.

Adsorption of model polymer chains of two natural rubbers, namely polybutadiene and isoprene as well as of polyethylene was modeled on the surface of this model particle. Model polymer chains represent individual oligomer molecules $CH_3-(R)_n-CH_3$, where n=10. Totally quantum mechanical optimized structures of these oligomers are presented in Table 4.5. Totally quantum mechanical optimized structures of the

corresponding adsorption complexes of these oligomers with model particle of amorphous carbon are collected in Table 6. Among the structures some geometrical, energetic and mechanical characteristics of these adsorption complexes are also presented in Table 4.6.

In this Table 6 minimal distances between oligomer molecule and carbon particle R, enthalpy of binding calculated via one monomer unit of the polymer, maximal force (critical force of the rupture) of uniaxial deformation of the polymer chain Fdeform MAX, and maximal force of the microscopical friction Fsift MAX are presented.

Table 4.5.

Model polymers, for which quantum mechanical modeling was performed.
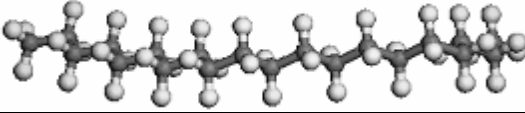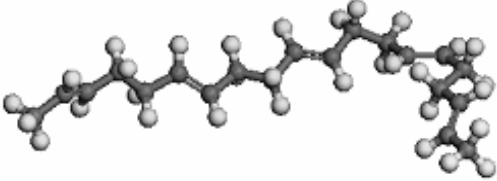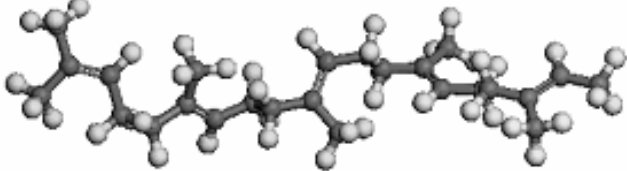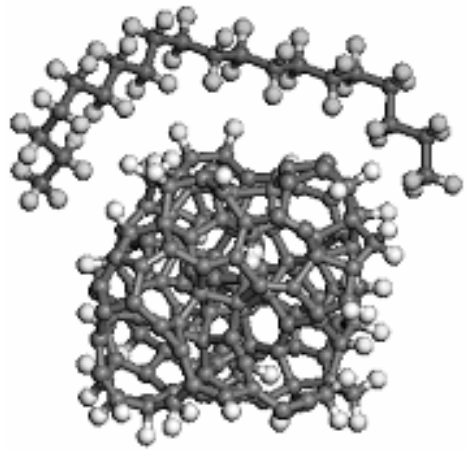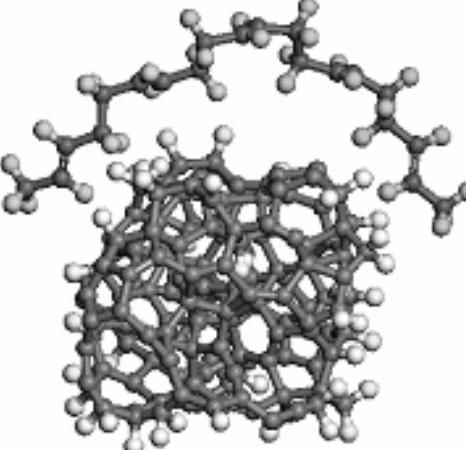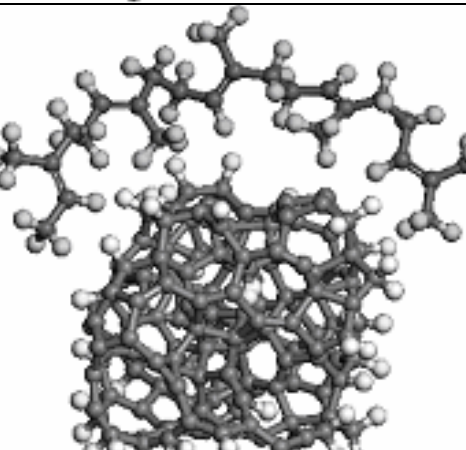
Polymer	Structural formula of monomer unit R: $CH_3-(R)_n-CH_3$, n= 10	Quantum mechanical optimized structure of oligomer
Polyethylene (PE)	$-(CH_2CH_2)-$	
Polybutadiene (PB)	$-(CH_2-CH=CH-CH_2)-$	
Isoprene (I) (para- isomer)	$-(CH_2-C(CH_3)=CH-CH_2)-$	

Table 4.6.

Model adsorption complexes of amorphous carbon particle with oligomers listed in Table 4.6 together with their geometrical, energetic and deformation characteristics, calculated in quantum mechanical approach

Adsorption complex	Optimized structure of the complex	Min distance between particles, R, A	ΔH bind kcal/mol	Fdeform MAX kcal/mol A	Fsift MAX kcal/mol A
Polyethylene (PE) –carbon particle		3.2-3.4	-3.9	120.3	8.3
Polybutadiene (PB) – carbon particle		3.0-2.9	-4.2	114.8	16.1
Isoprene (I) – carbon particle		2.6-2.8	-5.5	103.1	23.9

Two microscopical mechanical characteristics were modeled for each of adsorption complexes under study. Firstly, the dependence of the force of the deformation of the polymer chain on the elongation of the polymer chain was calculated for oligomers in the contact with carbon particle. Uniaxial tension of the polymer chain was considered till the polymer bond rupture. Secondly, force of microscopical friction, i.e. change of

cohesion of the polymer chain with displacement of the polymer chain along the surface of the carbon particle was calculated. Corresponding force curves obtained in this modeling are presented in fig.4.37-4.38.
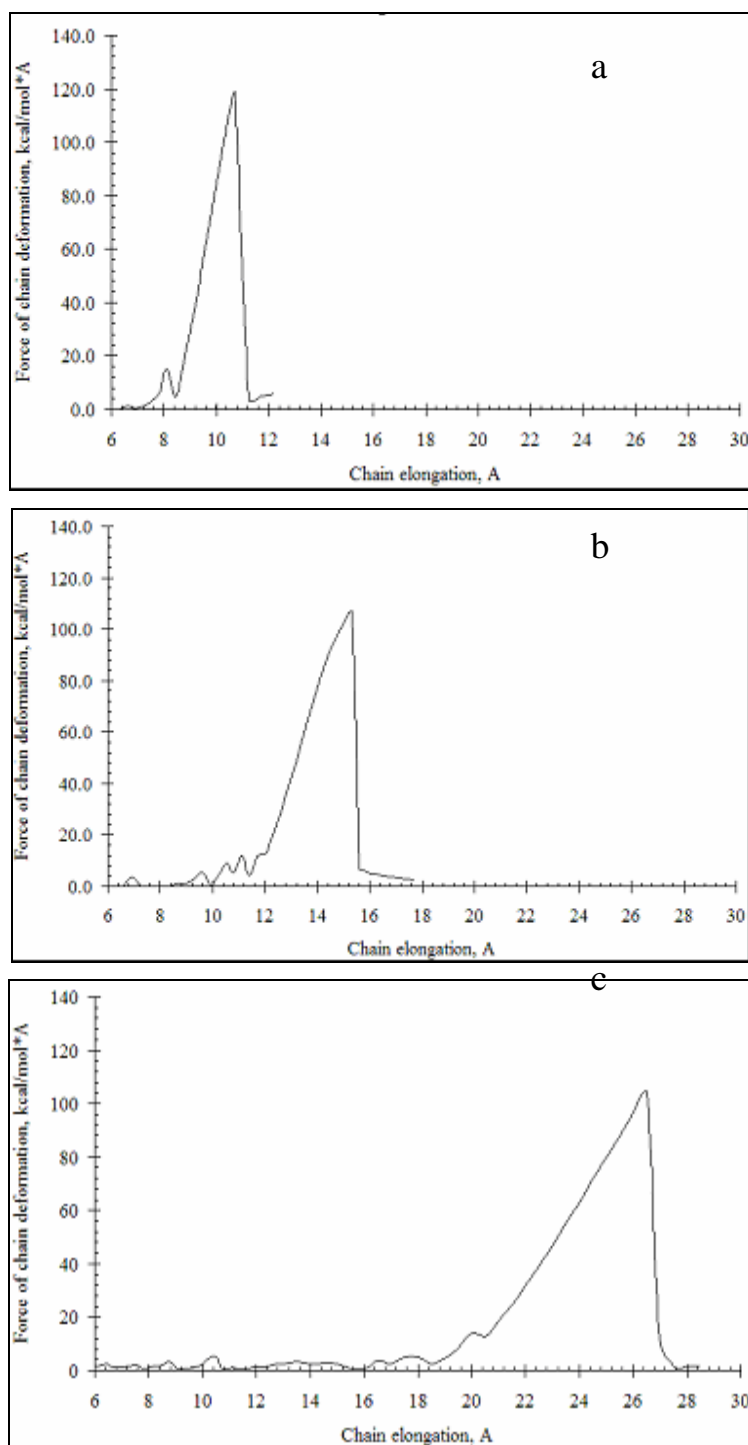
Figure 4.37: Dependence of deformation force on elongation of the polymer chain in the contact with carbon particle for polyethylene (a), polybutadiene (b), and isoprene (c).
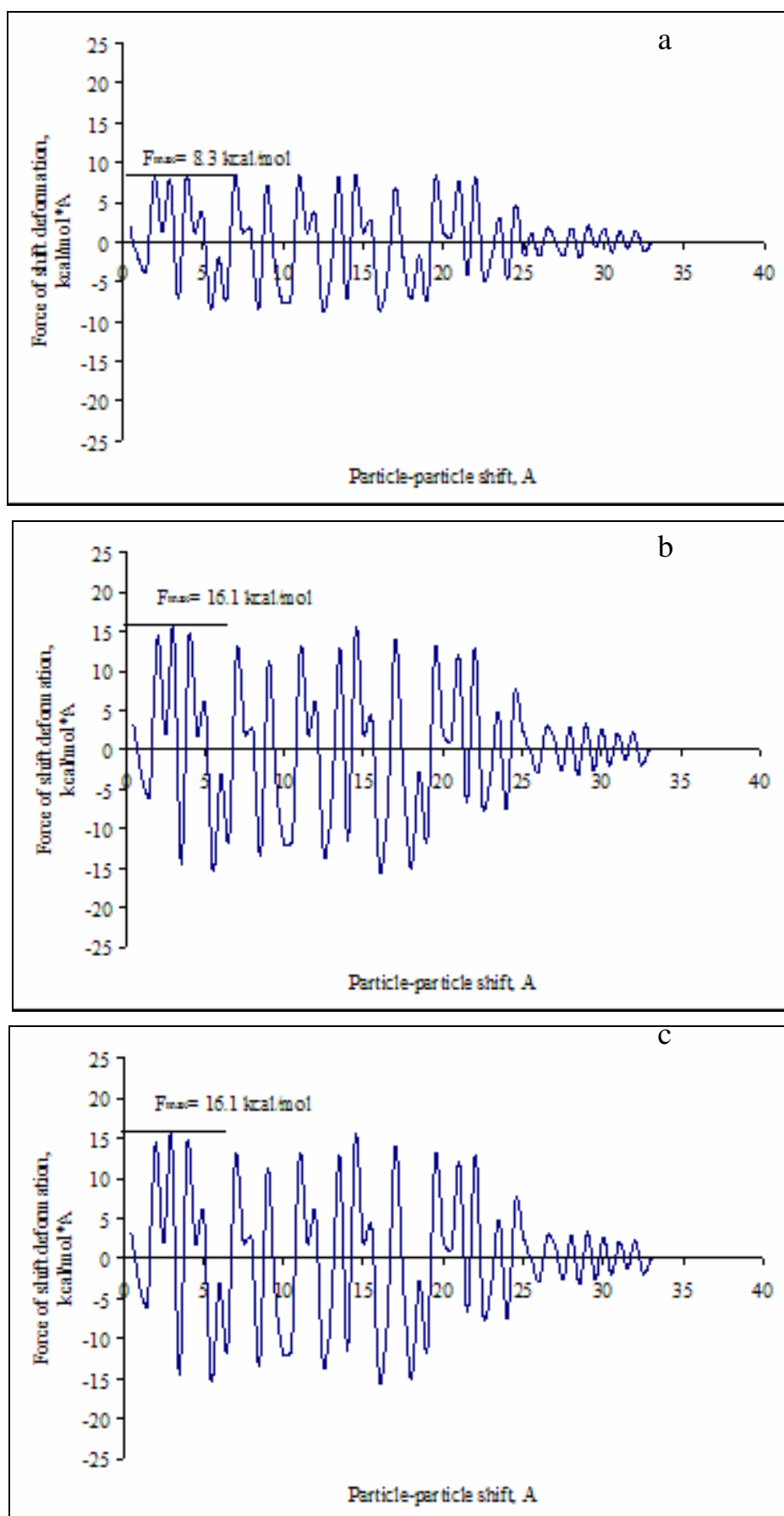
Figure 4.38: Dependence microscopical friction force on the displacement of the polymer chain along carbon particle for polyethylene (a), polybutadiene (b), and isoprene (c).

Some conclusions can be obtained in the course of QM modeling in a framework of microscopic internal coordinate of deformation (MIC) and microscopic friction coordinate (MFC) approaches.

Force curves of uniaxial tension for polyethylene, polybutadiene, and isoprene reveal the similar peculiarities. The first part of each curve of the low elongations corresponds to region of entropic torsional conformation changes of the polymer chain. It presents the low forces of the deformation The second part of each curve represents Hook's or enthalpic region of elongations of the polymer chain. In this part elongation of the valence bonds occurs mainly. This region is characterized by considerable growing up the force of deformation. Maximum value of the deformation force corresponds to the critical force of polymer bond rupture.

In the row of polyethylene, polybutadiene, and isoprene considerably elongating the enthalpic region and decreases the critical force of polymer bond rupture. Thus the growing up the elastic character of the polymer chain in the studied row is revealed. Isoprene shows the most elastic properties corresponding to the obtained force regularities.

Place of the polymer chain rupture occurs in each case in the vicinity of the surface of carbon particle being in the contact with the polymer molecule. The rapture of the polymer chain passes via cyclic transition complex with participation of the carbon surface active groups. Thus the destruction of the polymer chains in filled rubbers occurs mainly, by all mean, in the places of polymer contact with the filler particles.

The best cohesion with carbon particle surface (the highest forces of microscopic friction) was obtained for isoprene molecule representing branchy and flexible chain, and the worst one was found in the case of polyethylene molecule. Hence the best reinforcement can be reported for the combination of isoprene-amorphous carbon and the worth for system polyethylene-amorphous carbon.

Obtained dependences of polymer molecule cohesion with carbon particle surface (or of the highest forces of microscopic friction) are in a good accordance with calculated geometrical and energetic characteristics which confirm the best effectiveness of isoprene-amorphous carbon composite system as filled rubber.

4.2.2.10. Investigation of interaction polyisoprene rubber with ultradispersed fillers of the various nature.

Quantum mechanical modeling of microscopical mechanical properties has been performed for the rubber polymer in a contact with particles of high dispersed fillers of different nature. Thus adsorption of the natural rubber isoprene on particles of technical carbon (amorphous black soot), high dispersed amorphous silica (white soot), fullerene C60, and carbon tube C200 was examined at quantum mechanical level The main attention was devoted to the modeling of microscopical geometrical, energetical and mechanical properties of these adsorption complexes.

Cluster models of the particles of high dispersed fillers used in the study are presented in fig.4.39. Particle of amorphous carbon designed in the previous steps of the study contains 170 atoms of carbon being of ~15 A in diameter. The surface of this particle was partially terminated by hydrogen atoms. Particle of high dispersed amorphous silica contains 220 atoms with Si-O-Si main motive being of ~22x14 A in dimention. The surface of this particle was totally terminated by hydroxyls. Fullerene was presented by particle C60, containing 60 carbon

atoms being of ~7 A in diameter. Particle of carbon tube was modeled by particle C200 of 200 carbon atoms. It was at about 20 A in length and ~8 A in diameter. Surfaces of two latter particles were not terminated, containing aromatic motive of sp2- carbon.

Adsorption of model polymer chain of natural rubber, namely isoprene was modeled on the surface of these model particles. Model polymer chain was represented by individual oligomer molecule CH_3-(CH_2-$C(CH_3)$=CH-CH_2)$_n$-CH_3, where n=10.
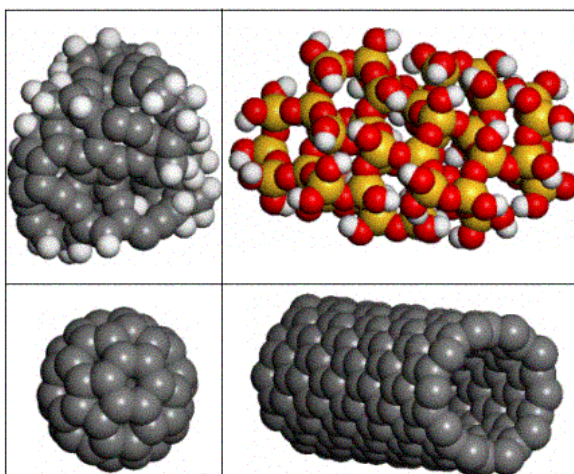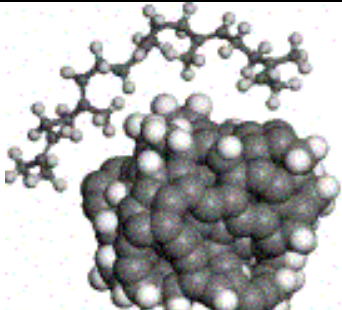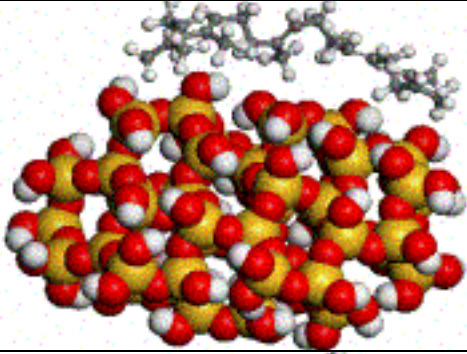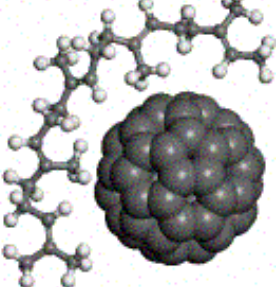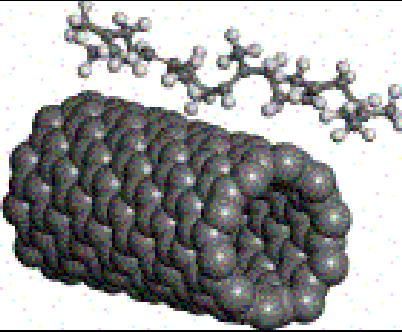

Figure 4.39: Optimized structures of model particles of high dispersed fillers: (a) H-terminated particle of amorphous carbon, (b) OH-terminated particle of high dispersed amorphous silica, (c) fullerene particle C60, and (d) particle of carbon tube C200.

Optimized in quantum mechanical approach structures of corresponding adsorption complexes consisting from polyisoprene oligomer and ultradispersed particles filler of different chemical nature are presented in Table 4.7.

Table 4.7.

Model adsorption complexes of isoprene oligomer with high dispersed fillers of different nature.

Adsorption complex	Optimized structure of the complex	Min distance between particles, R, A	ΔH bind kcal/mol	Fsift MAX kcal/mol A
Isoprene - carbon particle		2.6-2.8	-5.5	23.9

		R	ΔH	Fsift MAX
Isoprene - silica particle		2.2-2.4	-8.1	31.7
Isoprene – fullerene C60 particle		3.0	-3.2	15.4
Isoprene – carbon tube C200 particle		2.8	-3.8	18.1

Among the structures some geometrical, energetical and mechanical characteristics of these adsorption complexes are also presented in Table 1. Minimal distances between oligomer molecule and filler particle R, enthalpy of binding calculated via one monomer unit of the polymer, and maximal force of the microscopical friction Fsift MAX calculated via 1 A of polymer shifting along filler surface are presented in this Table.

In the course of QM modeling some conclusions can be done concerning the impact of chemical nature of the filler particles on the interaction of the polymer segments with surface of fillers. The binding enthalpy and the force of shifting are determined mainly by hydrophobic contacts between polymer fragment and surface of filler particle. Moreover the conformations of the polymer fragment in a contact with filler surface, namely complementary character of its space structure with structure of filler affects also on the polymer adsorption. The best cohesion of isoprene chain with filler particle surface (the highest forces of microscopic friction) was obtained for the system isoprene-silica. A little worth is cohesion of isoprene with carbon black or soot. Such fillers as fullerene and high dispersed carbon tubes represent lower forces of adhesion, being practically similar with a little preference of the latter. Thus quantum mechanical modeling can provide us with information about ranking of filler particles with respect to their chemical nature and structure, and allows making some recommendations concerning surface modification of fillers.

4.2.3. Quantum-mechanical investigation of the interface in natural rubber – clay (montmorillonite) system.

In the present part of quantum mechanical (QM) study there has been investigated the microscopical mechanisms of reinforcement of natural rubber by nanolayered alumosilicates (clays). Such kind of modeling allowed taking into account from the first principles the chemical nature of filler and rubber in characterization of mechanical properties of nanocomposites. An attempt was done to understand of interface morphology and the reasons of improvements of latex microscopical mechanical characteristics after introducing nanolayers of montmorillonite clay into natural rubber (cis-1,4-polyisoprene) on a nano or molecular level. The special attention was devoted to reviewing the ways of surface modification of hydrophilic clay platelets by hydrophobic or organophilic agents for enhancing the adhesion between rubber chains and clay filler surfaces. For this purpose ion exchange of clay interlayer cations (originally metallic ones) by different organic cations was investigated. Possibility and perspectives of application for rubber reinforcement of two fillers of different chemical mature, namely clay and carbon soot in the same time, has been studied also.

4.2.3.1. Quantum-mechanical modeling of polyisoprene and montmorillonite.

Natural rubber is a high molecular weight polymer of isoprene, C_5H_8. with repeating $CH–C(CH_3)=CH–CH_2–$ unit. Cis-1,4-polyisoprene configuration is essential for rubber. The double bond in each repeating unit in the polymer chain is a site of steric isomerism since it can have either a cis or a trans configuration. The polymer chain segments on each carbon atom of the double are located on the same side of the double bond in the cis configuration (II) and on the opposite sides in the trans configuration (III). Cis-1,4-polyisoprene has very low crystallinity and is an excellent elastomer over a considerable temperature range.

The following model was constructed and optimized quantum mechanically for representing the part of rubber (cis-1,4-polyisoprene) chain: $CH_3–[CH–C(CH_3)=CH–CH_2]_n–CH_3$, where n=10. Totally optimized structure of this molecule is presented in the fig.40.
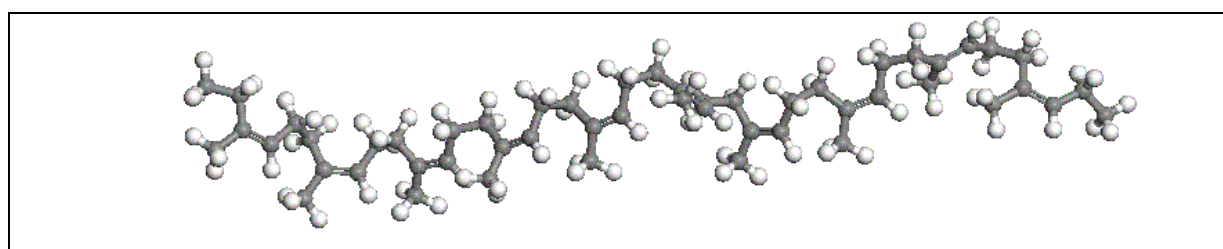

Figure 4.40: Structure of quantum-mechanically optimized of CH_3-$[CH–C(CH_3)=CH–CH_2]_{10}$– CH_3 model of poly-cis-1,4-isoprene.

Natural rubber latex basically consists of a dispersed phase containing rubber particles (poly-cis-1,4-isoprene) and other non-rubber components in minor quantities (filler), and the dispersing medium, water, which contains several organic substances and mineral salts. Mechanical characteristics of latex are mainly depended on nature of fillers.

Montmorillonite clay was selected as the filler in a present study of natural rubber latex composites. Montmorillonites are relatively cheap materials with fine-grained particle and high surface area. In addition,

they are readily dispersed in water (latex) without the aid of dispersing agents and are easily incorporated as a dry or aqueous dispersion without risking the destabilization of the latex.

The crystal structure of the clay itself is most important. Montmorillonite consists of three "layers": an aluminum-containing octahedron layer sandwiched between two silicate layers thus its structure consists of a gibbsite $Al(OH)_3$ layer bonded to a siloxane (S_2O_5) layer. The O^{2-} atoms at the apexes of the silica tetrahedra replaces the OH^- groups of the octahedral layer, and are shared between the layers. This three-layer grouping is referred to as a platelet. The platelets stack in various ways. Electrostatic and weak Van der Waal forces hold successive layers of montmorillonite structure. Consequently, montmorillonite has the ability to undergo extensive interlayer expansion or swelling in a direction perpendicular to the silicate anions. Water is absorbed between the platelets. There is an unsatisfied negative charge on the face of the clay platelet and cations such as Ca^{2+}, Mg^{2+}, and Na^+ are attracted to the spaces between the platelets due to the net negative charge on the "faces" of the platelets. The characteristic expansion of the interlayer structure exposes a large active surface area and permits polymer molecules to enter into the galleries. Separation of clay platelets can occur under certain conditions giving very high aspect ratio filler, which dramatically improves composite properties.

In the present study as a model of clay particle was chosen two montmorillonite platelets each consisting of 232 atoms, which were stacked one above other in parallel manner forming sandwich-like particles. Four water molecules and four Ca^{2+} cations were inserted into platelet interlayer. Totally quantum mechanically optimized structure of this cluster is presented in the fig.4.41. Distance between clay platelets was found as 11.21 A for this model.
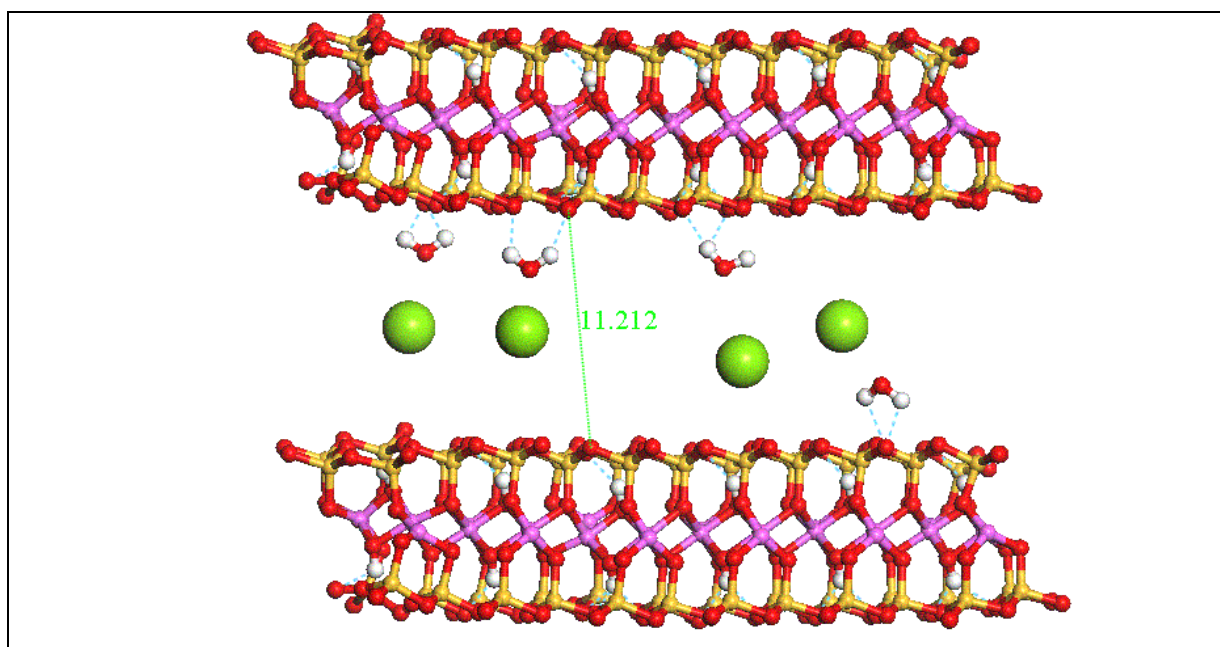
Figure 4.41: Structure of quantum-mechanically optimized cluster of two interacted montmorillonite platelets with 4 calcium cations and 4 water molecules in the interlayer space. Large green spheres represent interlayer calcium cations; system of hydrogen bonding is represented in blue dotted lines. All atoms were allowed to vary during the simulation.

4.2.3.2. Quantum-mechanical investigation of modification of montmorillonite surface.

According to the structure three different types of clay-polymer composites can be distinguished, namely conventional, intercalated, exfoliated composites. When the matrix polymer chains are unable to penetrate between the layers of the silicate particles conventional composites is formed. Intercalated structures are formed when one or more polymer chains intercalate between the layers. Hereby the interlayer spacing is increased but the ordered layer structure of the clay particles is retained. In exfoliated composites the clay particles are completely delaminated and the silicate layers do not show any periodicity in their arrangement.

In general the reinforcing ability of clay is considered to be poor in conventional composites because of its large particle size and low surface activity, although clays have a long tradition as semi-reinforcing fillers and extenders in the plastic industry. Recently, such clays as montmorillonite have attracted a great deal of interest as nanocomposite reinforcements in polymers owing to their intrinsically anisotropic character and swelling capabilities. Because of the clay layer structure and its ability to disperse into nanometer-size platelets, nanometer reinforced materials with unique physical and chemical properties can been obtained. It has been reported in the literature that exfoliated structures are primarily responsible for high mechanical reinforcement, while intercalated and conventional structure play only a minor role (Burnside S.D. and Giannelis E.P., 1995; Alexandre M. and Dubois P., 2000).

In the present study there were examined some factors which support the expansion and delamination of montmorillonite platelets in rubber matrix. These factors make it easy the rubber chain penetration into the clay interlayer zone due to enhancing its interaction with hydrophilic clay surface and provide the formation of exfoliated nanocomposite structure.

The clays are characterized by their ion (e.g. cation) exchange capacities, which can vary widely. One important consequence of the charged nature of the clays is that they are generally highly hydrophilic species and therefore naturally incompatible with a wide range of polymer types. A necessary prerequisite for successful formation of rubber-clay nanocomposites is therefore alteration of the clay polarity to make the clay 'organophilic' to help compatibilize the surface chemistry of the clay and the hydrophobic rubber matrix. Organophilic clay can be produced from normally hydrophilic clay by ion exchange with an organic cation such as an alkylammonium cation. The role of alkylammonium cations in the organo-clay is to lower the surface energy of the inorganic host and to improve it's wetting characteristics with rubber.

The present quantum mechanical modeling reviewed an impact of chemical nature of the interlayer organic cations (a pendant group) on manufacturing and properties of rubber- montmorillonite nanocomposite. The main question ahead of this study was to find *in silico* the way of determining the chemical composition and structure of organic clay interlayer cations that make thermodynamically favorable penetration of polymer chains into the interlayer region and assist in delamination of the clay in rubber matrix.

For this purpose the quantum chemical modeling was fulfilled to reproduce microscopical structure and mechanical properties of the interface in the system of natural rubber (cis-1,4-polyisoprene) and clay (montmorillonite) with the presence of organic cations of different nature.

As the model pendant group for the present study these were taken four organic cations (ammonium ions), namely $CH_3-(CH_2)_7-NH_3^+$, $CH_3-(CH_2)_{17}-NH_3^+$ (octadecylammonium ion), $C_6H_6-CH=CH-(CH_2)_{17}-NH_3^+$

(vinylbenzyl-octadecylammonium ion), CH_3-$(CH_2)_{37}$-NH_3^+ ions. Totally QM optimized structures of these organic cations are presented in the fig.42.

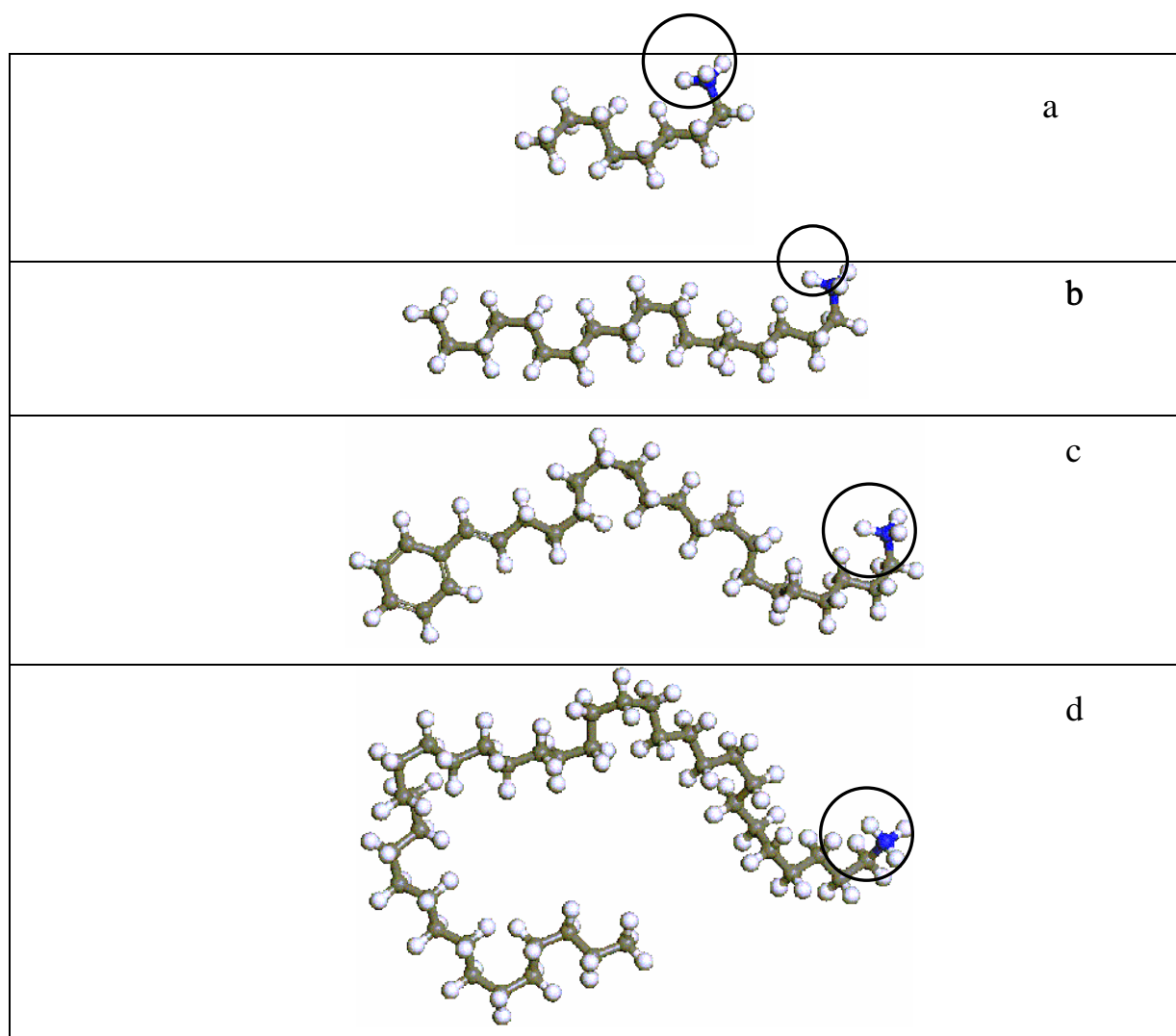Figure 4.42: Structures of quantum-mechanically optimized pendant groups which were studied in rubber-clay system: CH_3-$(CH_2)_7$-NH_3^+ (a), CH_3-$(CH_2)_{17}$-NH_3^+ (b), C_6H_6-CH=CH-$(CH_2)_{17}$-NH_3^+ (c), CH_3-$(CH_2)_{37}$-NH_3^+ (d) ions; -NH_3^+ groups are marked by circles.

Adsorption complexes of model montmorillonite cluster, which is presented in the fig.4.41, with all of these organic cations have been constructed and optimised in quantum mechanical approach with total space optimisation. Corresponding structures are presented in the fig.4.44 together with intermolecular distances between clay platelets.

Two pendant groups of each chemical structure were inserted into the interlayer space between two platelets of clay replacing several calcium ions and water molecules, located primarily in the inter-platelet zone. Each cation is grafted onto clay surface with formation of several H-bonds between H atoms of –NH_3^+ group and O atoms of silica tetrahedra. As it is seen from this figure clay platelets very slightly change their intermolecular distances regarding to the clay model without pendant group (from 11.21 to 11.24 A) remaining parallel manner of orientation of platelets in the case of the smallest organic cation CH_3-$(CH_2)_7$-NH_3^+. Setting CH_3-$(CH_2)_{17}$-NH_3^+ and C_6H_6-CH=CH-$(CH_2)_{17}$-NH_3^+ groups in the zone between platelets leads to some swelling

of clay structure (intermolecular distances are growing up to 14.19 and 15.76 A respectively) and loss parallel orientation of the platelets the effect, which is more remarkable in latter case. Interaction several of long and knot-like CH_3-$(CH_2)_{37}$-NH_3^+ particles with clay leads to remarkable growing up inter-platelet distances and loses parallel orientation of clay platelets.
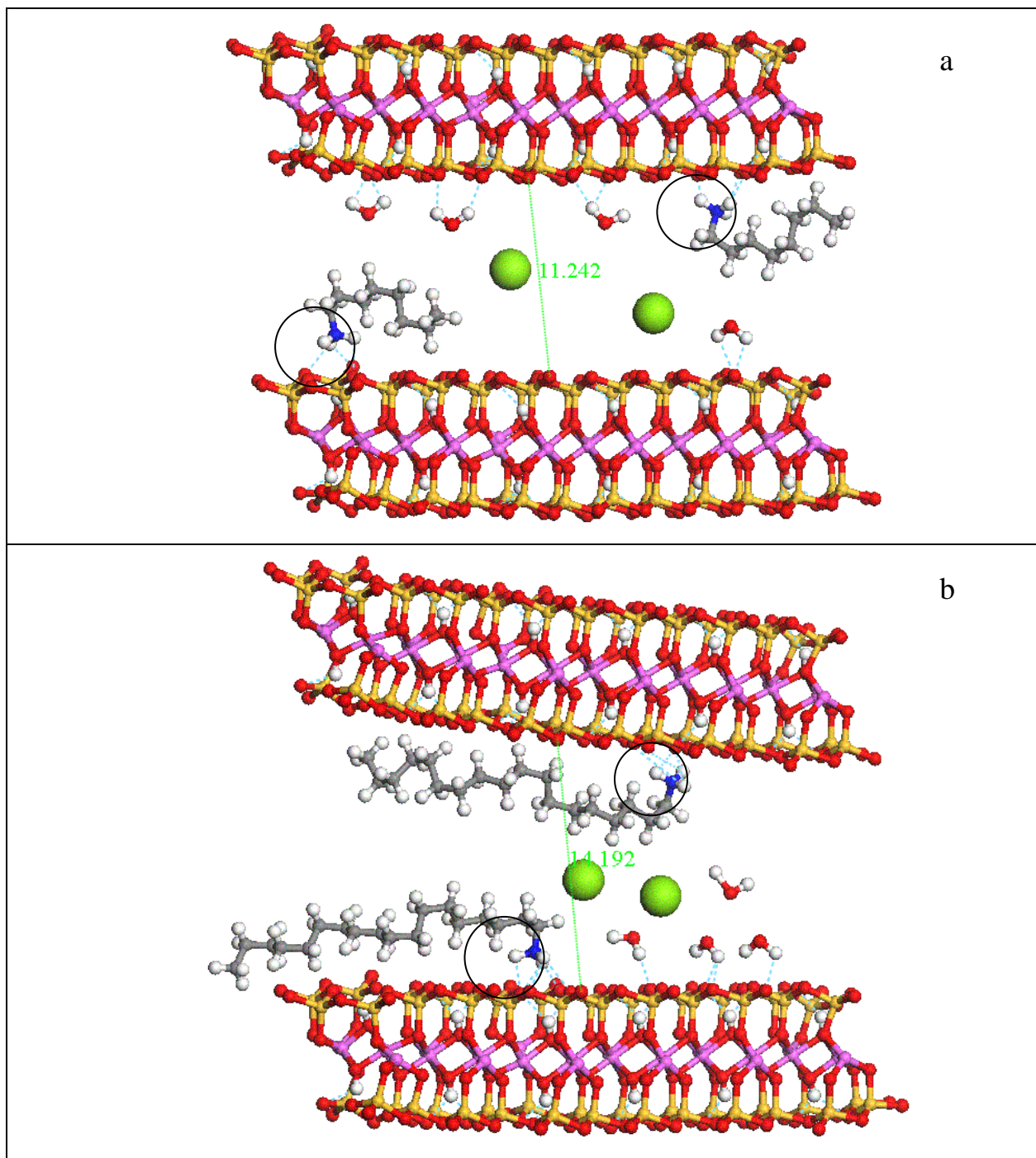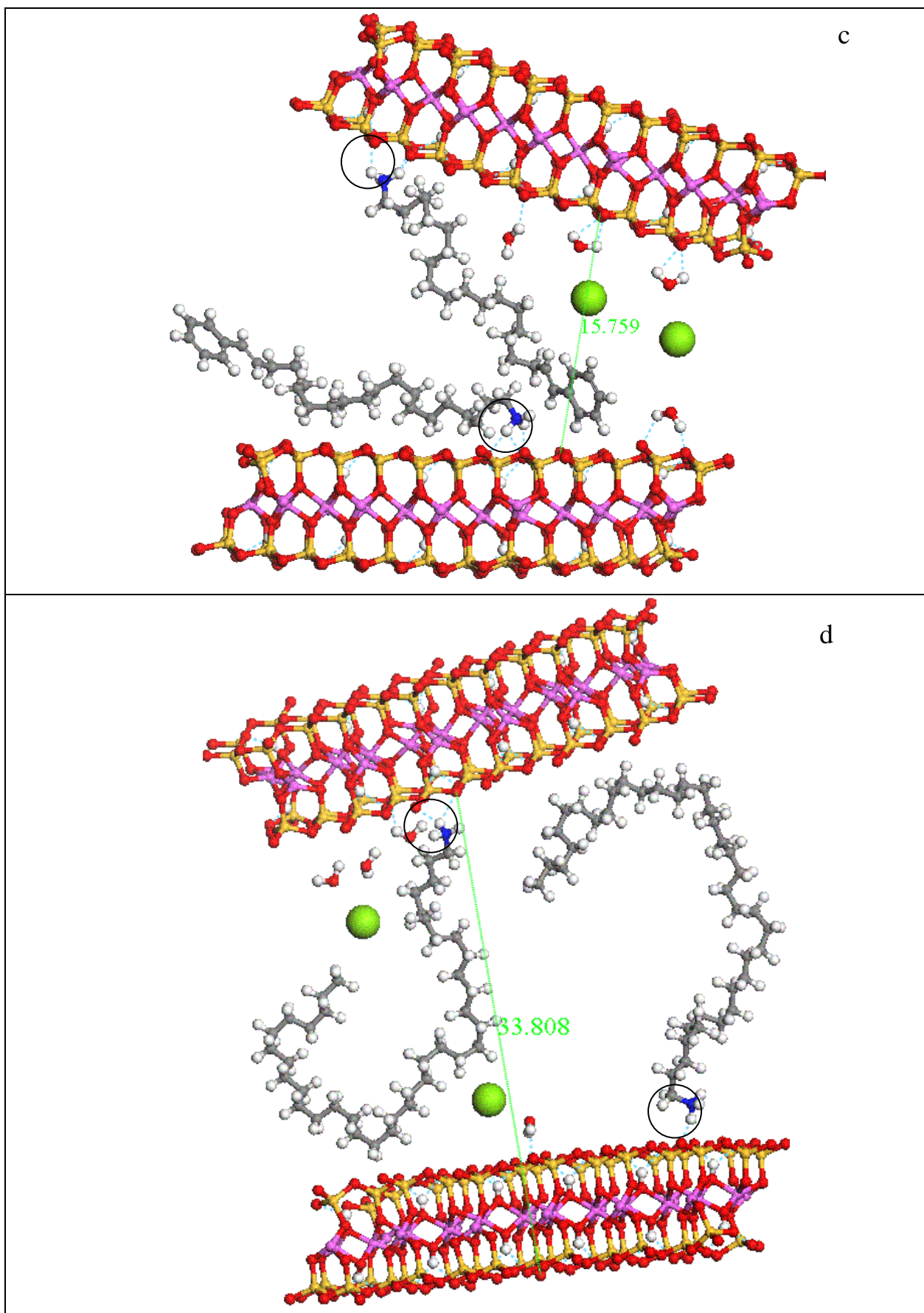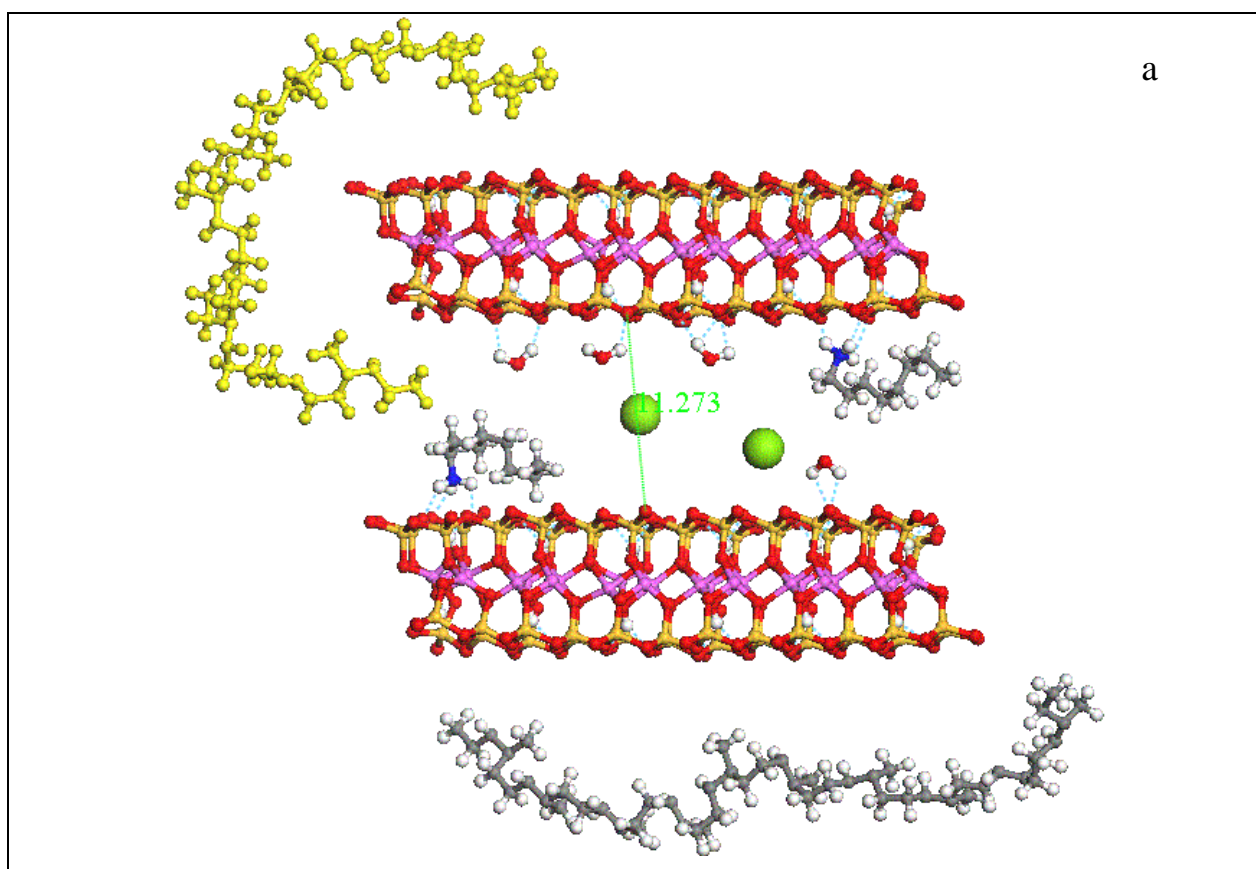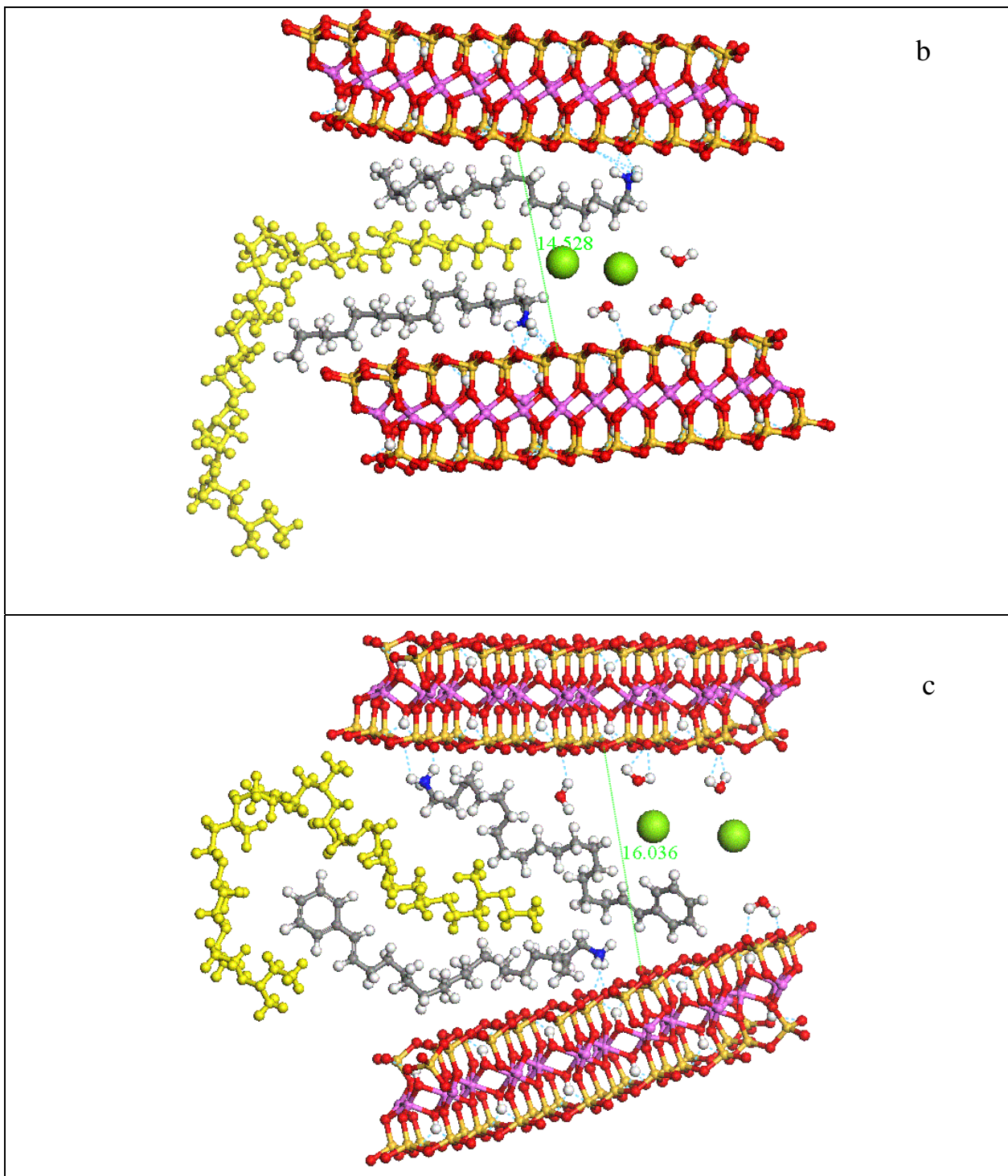
Figure 4.43: QM optimised structures of adsorption complexes of model two-layered cluster and organic cations: $CH_3-(CH_2)_7-NH_3^+$ (a), $CH_3-(CH_2)_{17}-NH_3^+$ (b), $C_6H_6-CH=CH-(CH_2)_{17}-NH_3^+$ (c), $CH_3-(CH_2)_{37}-NH_3^+$ (d)

ions; -NH$_3^+$ groups are marked by circles. Hydrogen bonds in the system are marked by dotted lines. Calcium ions are represented by large spheres.

4.2.3.3. Quantum-mechanical investigation of interaction of polyisoprene and modified montmorillonite.

Interaction of model polyisoprene molecule, which is presented in the fig.4.40 with all organo-clay systems, which were modeled in the previous step of study, was studied in quantum mechanical approach. Microscopic structure, energetic and microscopic force-of-adhesion characteristics were calculated for the model adsorption complexes, presented in the figure 5. These complexes consisted from one or two molecules of cis-1,4- polyisoprene CH_3-[CH–$C(CH_3)$=CH–CH_2]$_n$– CH_3, where n=10, on the one hand, and from two-layered montmorillonite cluster with two ammonium ions and several Ca^{2+} ions and water molecules in the interlayer space of clay on the other hand.

a

b

c
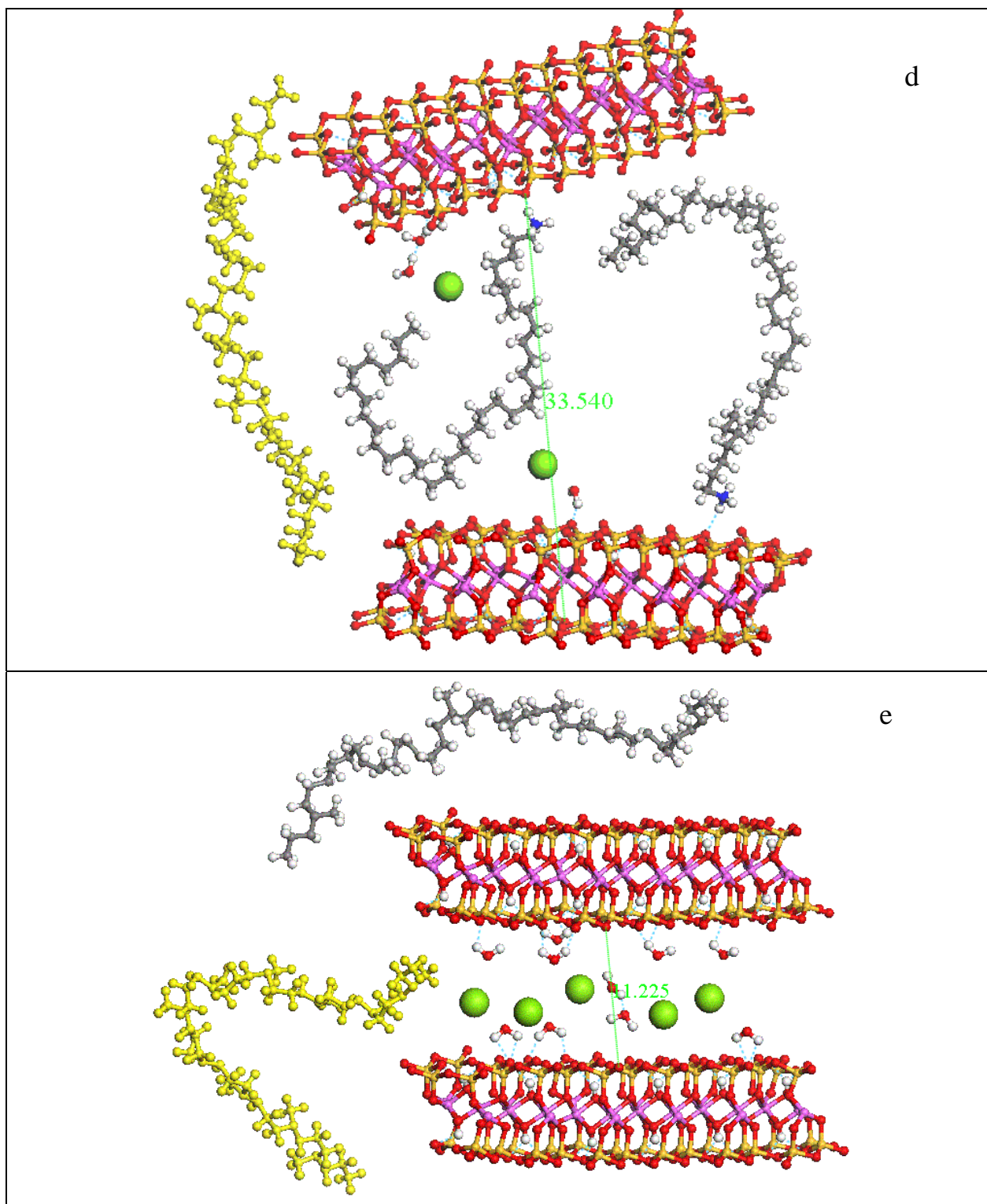
Figure 4.44: Totally optimised structures of adsorption complexes of one or two molecules of cis-1,4-polyisoprene CH_3-[CH–C(CH_3)=CH–CH_2]$_n$– CH_3, where n=10 and of two-layered montmorillonite cluster with two ammonium ions and several Ca^{2+} ions and water molecules in the interlayer space of clay. Rubber molecule is marked by yellow color. The complexes differ by chemical structure of organic cations: CH_3-$(CH_2)_7$-NH_3^+ (a), CH_3-$(CH_2)_{17}$-NH_3^+ (b), C_6H_6-CH=CH-$(CH_2)_{17}$-NH_3^+ (c), CH_3-$(CH_2)_{37}$-NH_3^+ (d). For comparison an analogical system but without pendant ion is presented (e)

The following microscopical energetic and mechanic characteristics were calculated for each of adsorption complexes under study: enthalpy of binding ΔH_{bind} of polyisoprene with organo-clay, i.e. with montmorillonite model together with Ca^{2+} ions, water molecules and together with ammonium ions, which provide 'organophilic' character of clay surface and force of microscopical friction F_{shift}, as characteristic of microscopical friction or change of microscopical cohesion of the rubber chain with displacement of the polymer chain along the surface of montmorillonite particle covered by organic cations and water. Both values were calculated per one polyisoprene monomer unit $-[CH–C(CH_3)=CH–CH_2]_n-$. The obtained results are collected in Table 4.8.

Table 4.8.

Structural, energetic, and force characteristics of polyisoprene-montmorillonite model complexes with different pendent groups in clay inter layer zone

System according to the figure 5	Distance between clay layers, A	Parallel orientation of clay platelets	ΔH_{bind}, kcal/mol	F_{shift}, kcal/mol*A
a	11.27	yes	-1.9	9.6
b	14.53	no	-8.7	33.3
c	16.04	no	-7.9	31.9
d	33.54	no	-1.3	8.7
e	11.23	yes	-1.6	9.1

4.2.3.4. Quantum-mechanical investigation of triple system: natural rubber – amorphous carbon – montmorillonite.

As some short example we present here the additional results in which two-filler system for natural rubber is examined. The idea was to use together carbon black (soot) and natural clay (montmorillonite) for making rubber-based nanocomposites with better mechanical properties.

As filler agent was taken the model, which is presented in the fig.4.45,a, corresponding adsorption complex of this filler component with the same rubber model is presented in the fig.4.45,b.
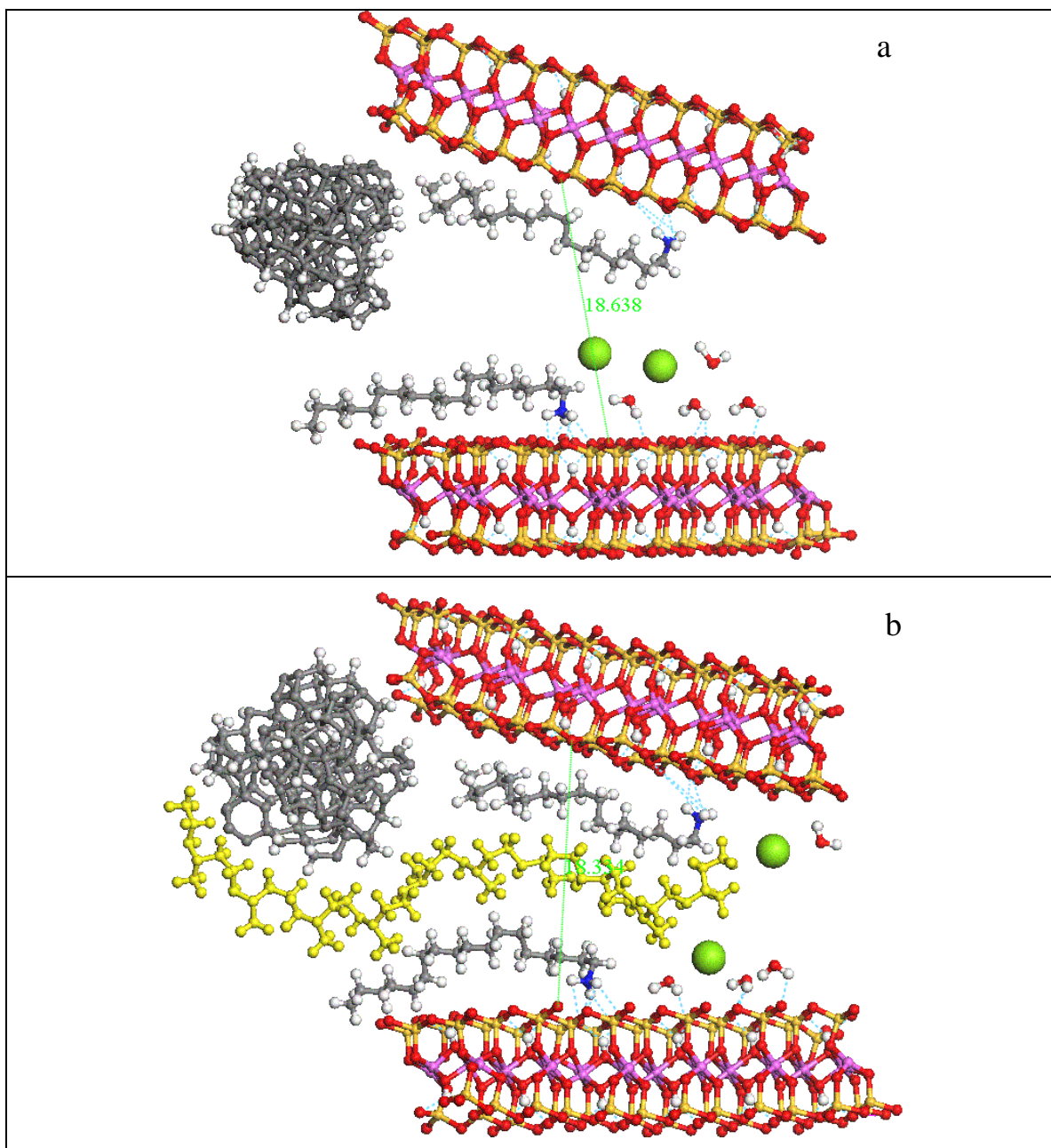
Figure 4.45: Totally optimised structure of adsorption complexes of model two-layered cluster and organic cation CH_3-$(CH_2)_{17}$-NH_3^+, Calcium, water together with soot particle without (a) and with (b) rubber chain.

As it is seen from the structure of rubber-filler complex, obtained after the total optimization in QM, such kind of 'close' interactions can provide unique mechanical properties of nanocomposite. Rubber chain easily penetrate between clay layers with the help of interaction with carbon particle, filler particles delaminated and nanocomposites with exfoliated structure and very strong hydrophobic contacts both with clay and carbon black (calculated ΔH_{bind}, is -12.3 kcal/mol and F_{shift}, is 45,2 kcal/mol*A) can be achieved. Such kind of filler synergism also is an interesting topic for QM modeling in framework of presented approach.

4.3. INVESTIGATION OF A MICROSCOPIC STRUCTURE AND PROPERTIES OF POLYMER - TECHNICAL CARBON COMPOSITE USING MOLECULAR DYNAMIC METHOD

4.3.1. Introduction

The microscopic structure, some energetic characteristics, and also the behaviour in time of polymer - technical carbon composite were considered in the framework of molecular dynamic (MD) approach.

The behaviour of individual chains of polymer matrix in vacuum and water environment has been studied. Molecular models of polymer of a various degree of polymerisation were considered. Conformation possibility for polymer molecule to come to knot-like structure was studied at the lengthening the molecular chain.

Also interaction of filler particle, namely, a model particle of amorphous soot with partially H-terminated surface and structure received in preliminary quantum mechanical modelling, with polymer matrix was investigated. Polythene and polyisoprene was considered as polymer components. Correspondent polymeric components represented one chain of polymer, one layer of polymer matrix and several layers of polymer matrix with flat and parallel each other structure. Filler particle was inserted either above these layers or in-between latter. In the course of the modelling an attempt to establish difference of a microscopic structure of complexes of particles of amorphous carbon with polythene and polyisoprene was done keeping in the mind that only polyisoprene is rubber among considered polymers.

An impact of water, which was considered in MD modeling in explicit (molecular) model, on interactions in system polymer - amorphous carbon was as well investigated. Adsorption complexes consisting of soot particle, some tens molecules of water and (a) one chain, (b) one layer and (c) two layers of polymer were used as the models in this case.

4.3.2. Method of modelling

Calculations in work were fulfilled within the software package on molecular dynamics CHARMM29 which has been received from authors (The CHARMM Development Project, Professor Martin Karplus, Department of Chemistry & Chemical Biology, Harvard University) and it is licensed. This package represents the most developed, fast and theoretically proved on the present moment program on molecular dynamics (Neria E., Fischer S., Karplus M., 1996). This program is based on modern force fields CHARMM22 and MMFF (Merk), which yield correct qualitative and quantitative results (MacKerell A.D., Bashford D., Bellott M., Dunbrack R.L., Evanseck J.D., Field M.J., Fischer S., Gao J., Guo H., Ha S., Joseph-McCarthy D., Kuchnir L., Kuczera K., Lau F.T.K., Mattos C., Michnick S., Ngo T., Nguyen D.T., Prodhom B., Reiher III W.E., Roux B., Schlenkrich M., Smith J.C., Stote R., Straub J., Watanabe M., Wiorkiewicz-Kuczera J., Yin D., Karplus M., 1998). This program includes GBorn (Generalized Born) continuum environment model (Still W.C., Tempczyk A., Hawley R.C. Hendrickson t., 1990) which now also is considered as one of the most theoretically proved models of solvent. In calculations there is an opportunity, if necessary, to place partial charges on atoms of molecular models, receiving them directly from preliminary quantum mechanical calculation that allows improving parameterisation of the method.

The scheme of molecular dynamic calculation of molecular system (one MD start) consists in the following:

1. minimization of the structure, 1000 steps
2. heating of the system up to 300K (3ps, step is 1fs)
3. equilibration for 50ps
4. computation of MD trajectory 600 ps during which molecular system is relaxing. Record of coordinates is performed through everyone 10 steps

Using received trajectory dynamics of system in time is considered. Geometrical and energetic parameters of system are received at the equilibrium in the end of a trajectory. All molecular systems have been calculated in the present work using such scheme.

4.3.3. Molecular dynamic investigation of behaviour of individual polymer chains of various lengths in vacuum and in the water environment

Molecular dynamic (MD) calculations have been performed for polythene oligomers, i.e. for individual model chains of polyethylene with a various degree of polymerization (from 6 up to 100), the number of monomer units of polymer chain increased by one. These calculations were done with MMFF force field both in vacuum and in GBorn continuum model.

Calculations in GBorn continuum environment were fulfilled for molecular systems with MMFF charges, and also with partial charges on atoms of polymer chain received in quantum mechanical calculation by program MOPAC. Necessity of setting additional charges is caused by peculiarity of MMFF force field, in which partial charges on hydrocarbon atoms are accepted equal to zero that often leads to some realistic results. Obtained trajectories allowed calculating the mean distance between ends and corresponding RMSD for each molecule.

An example of polymer conformation received in the end of MD trajectory is presented in the fig.4.46.
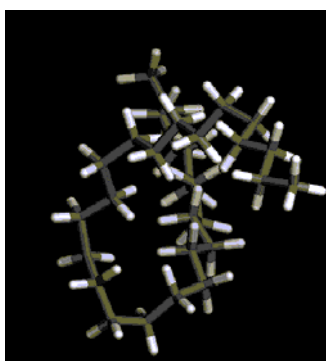

Figure 4.46: Structure of polythene oligomer with 30 monomer units received in the in the end of molecular dynamic trajectory.

It was obtained that there is almost no difference between trajectories in vacuum and in GB for molecules without partial atomic charges. This could be explained with the fact that GB influences only on electrostatic interactions.

Differences were observed for GBorn modelling both with partial atomic charges and without. In the fig.4.47 the dependence of mean distance between the ends of polymer <l> from number of monomer units (-CH$_2$-) n is presented. The polyethylene could be described with freely jointed chain model. This implies that <l> should be proportionally to the square root of n.

For the short chains (number of units n=6-15) this dependence is approximately linear. The visualization of MD trajectory shows that these molecules almost don't experience any conformational changes. Only longer chains move more freely and form balls or knots with polymer properties. This could be also illustrated with dependence of RMSD <l> on n (see the fig.4.48).

Fluctuation in some points could be seen. This could be explained with the fact that during the MD trajectory some long molecules could form balls with the shape, making further motions labored, bothering to change freely distances between the terminal carbon atoms of molecule (keeping it close or distant to each other).
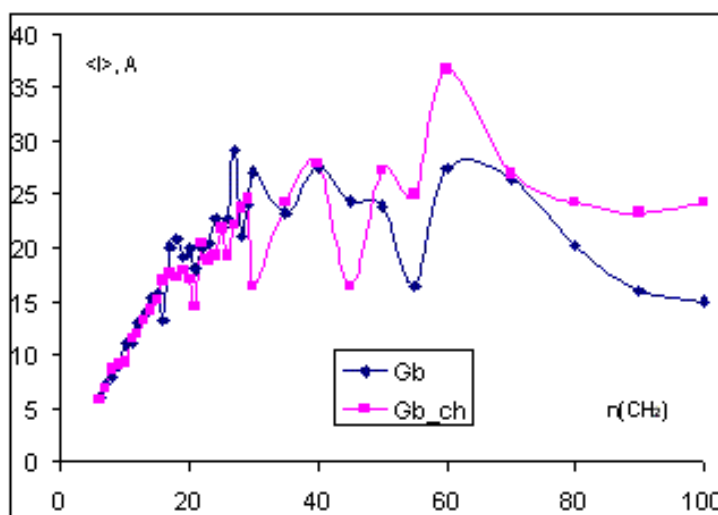
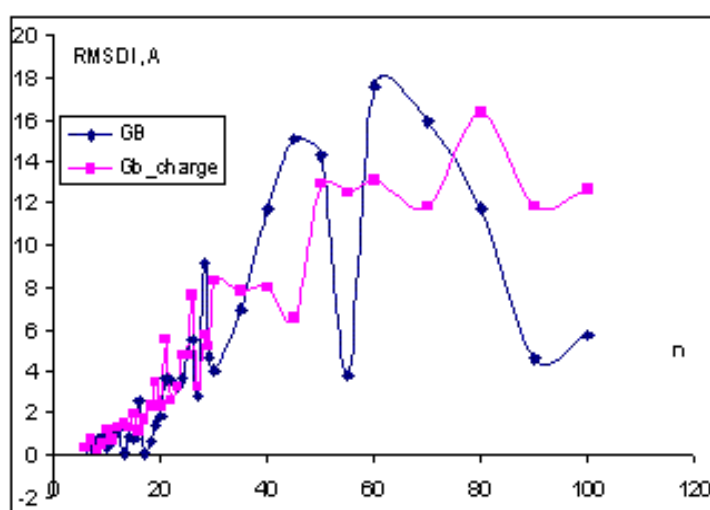Figure 4.47. Dependence of mean distance <l> between polyethylene oligomer molecule ends from number of monomer units n in a molecule.

Figure 4.48. Dependence of root mean square distance (RMSD <l>) between polyethylene oligomer molecule ends from number of monomer units n in a molecule.

194

We have seen that for the longest molecules (C70-C100) the value of <l> lowers and it could be hardly referred to as a fluctuation. This is the representation of the fact, that non-polar molecules are unfavorable in polar solvent (GB model represents a water solvent) and the balls of polymer are being "compressed" to make the surface of contact with solvent less. In this case values of <l> for molecules carrying partial atomic charges are higher than for molecules without atomic charges because they are more polar and hence are favorable in GB solvent. Thus, for reliable modelling of polymeric chains they should be large enough with polymerization degree of the order of several tens.

4.3.4. Molecular dynamic investigation of interaction of an individual polymer chain with amorphous carbon particle

This part is devoted to studying of interaction of amorphous soot particle with one chain of polythene and polyisoprene.

The structure of amorphous carbon particle of was received from quantum mechanical calculation (PM3). It was a cluster of amorphous carbon with sp^3-/sp^2-hybridization, with 170 carbon atoms and partially terminated by hydrogen surface.

Oligomer molecules of polythene and polyisoprene with 50 monomer units were considered as models of chain for both polymers so the molecule of polyethylene contained approximately 300 atoms and polyisoprene ~ 700 atoms. Linear conformations of oligomer molecules were taken as initial structures. Preliminary MD calculations for each of polymer molecules in free state have been performed. Received MD structures of single polymer molecules are presented in the fig.4.49. As it is seen from obtained MD results both molecules polyethylene and polyisoprene achieved complicated ball-like or knot-like structures of polymer chains.
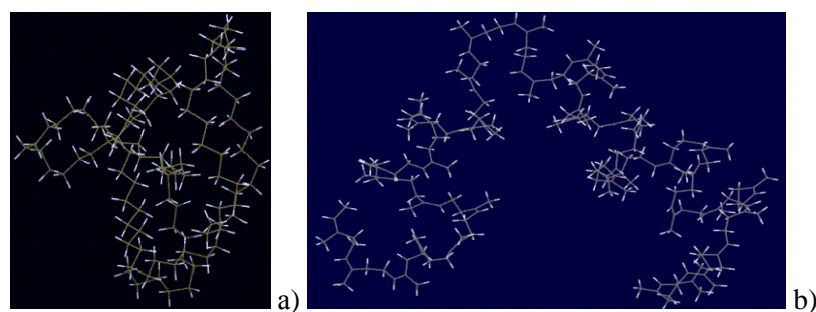

Figure 4.49: MD structures of polymer molecules: (a) polyethylene, (b) polyisoprene.

Adsorption complexes of model soot particle with single polymer chain were also calculated starting from linear configuration of polymer chain. Obtained after MD modeling structures of these complexes are presented in the fig.4.50.
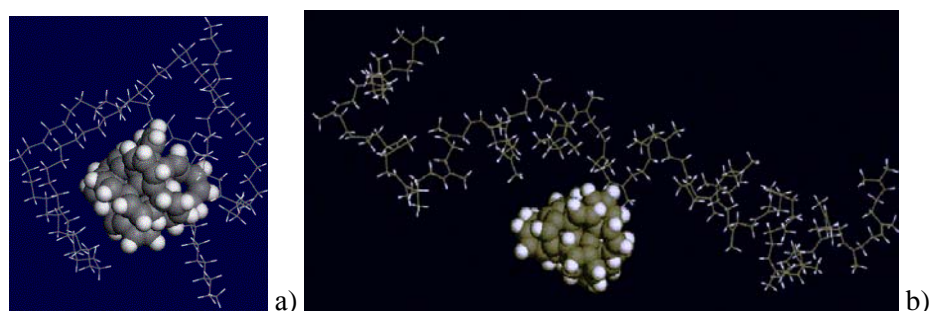
Figure 50: MD structures of adsorption complexes of carbon particle with single polymer molecules: (a) polyethylene, (b) polyisoprene.

It was obtained that received MD structures of adsorption complexes of polyethylene and polyisoprene are distinctly different. If the molecule of polyethylene after various conformational changes is bended into a knot or ball in a contact with carbon particle (also as well as in the case of absence of carbon particle), the molecule of polyisoprene has kept the linear geometry in a greater degree at the presence of carbon particle.

Average intermolecular distances in case of interaction carbon particle and polyisoprene molecule have appeared a little shorter ($R_{H.H}$=2.3-2.5A), than in case of polyethylene ($R_{H.H}$=2.5-2.8A). For more careful investigation of distinctions in interaction of carbon particle with polyethylene and polyisoprene the quantitative calculation of interaction energy of soot particle with these single polymer chains has been lead. Calculated energies of interactions ΔE_{total} at equilibrium part of MD trajectory are presented in fig.4.51.
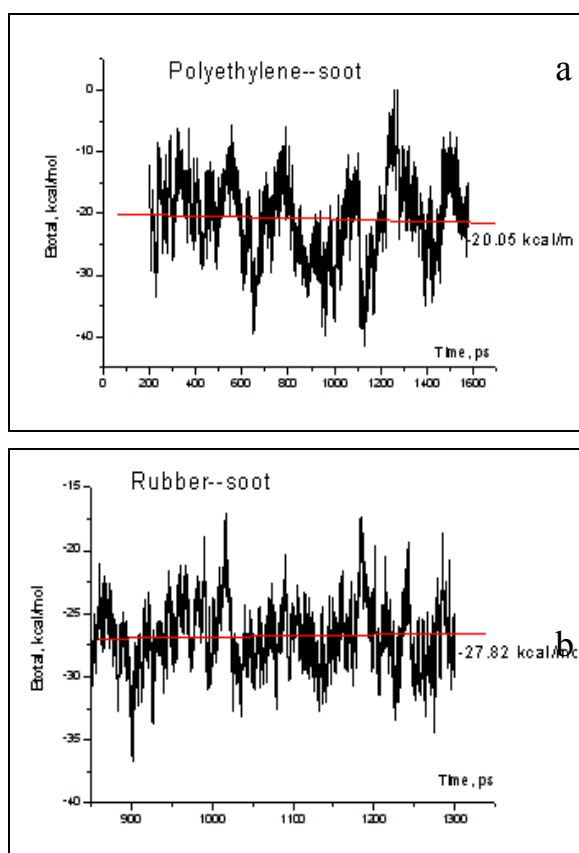

Figure 4.51: Interaction energy of carbon particle with single polymer chain of polyethylene (a) and polyisoprene (b) at equilibrium part of MD trajectory.

As it is seen from the received results it is visible, that interaction of carbon particle with polyisoprene is energetically more favourable, than with polyethylene. Indeed, calculated average value of interaction energy of polymer - carbon particle has appeared equal -20.05 kcal/mol and -27.82 kcal/mol for polyethylene and polyisoprene, respectively.

4.3.5. Molecular dynamic investigation of interaction of polymers layers with amorphous carbon particle.

Interaction of amorphous carbon particle which structure was discussed in the previous part of work, with polymer layers was studied. Polyethylene and polyisoprene have been taken also as polymer component.

As polyethylene component was taken a model represented two layers in parallel orientation having some distance in-between. Each layer was constructed from 10 single molecules of polyethylene chains; each chain contained 50 monomer units. Thus, this model contained at about 6000 atoms. The initial structure of polymer layers has been taken flat. Interaction of carbon particle placed between these two layers of polyethylene was calculated in MD. The structure of the adsorption complex received during MD modelling is presented in the fig.4.52. As it is visible from the figure initial flat structure of polyethylene was not kept in time. Polyethylene component represents amorphous complex knot with soot particle of immersed in it.
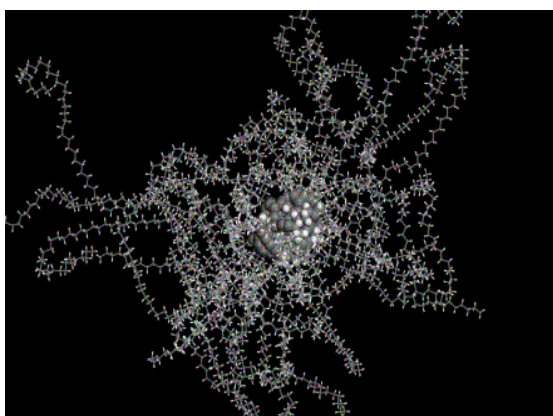

Figure 4.52: MD structure of adsorption complex of carbon particle with two layers of polyethylene/

Some models of layered polyisoprene matrix have been considered. In the beginning the case when the model of a polymer matrix represented one flat layer of polyisoprene chains, consisting from 9 chains was considered. Each chain contained 50 monomer units. MD modelling of such layer without adsorption carbon particle leaded to the structure presented in the fig.4.53. From the received data it is visible, that the layer of polyisoprene chains revealed great strength may be due high intermolecular Van-der-Waals interactions. Indeed, it has a tendency to keep a regular flat structure better than an individual polyisoprene chain and much better than layers of polyethylene chains, which at similar modelling pass very quickly into amorphous state.
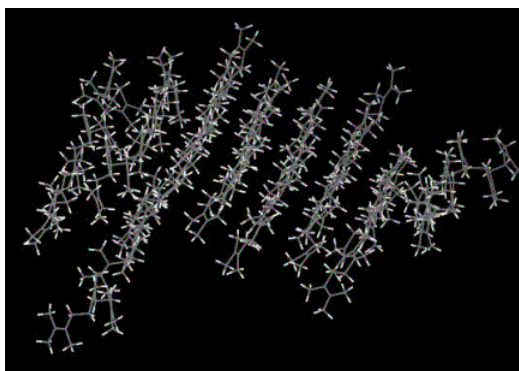
Figure 4.53: MD structure of one polyisoprene layer in absence of contact to carbon particle.

At addition of carbon particle to such flat polyisoprene layer followed by MD calculations an adsorption complex was found, which structure is presented in the fig.4.54. Thus it was received that addition of soot molecule stabilized polyisoprene layer, at which it was not observed tendencies to bending. Polyisoprene layer in this case remained, practically, flat, and did not "envelop" carbon particle. Some fluctuations and bends of polymer chains occurred only on a border of polymer layer were intermolecular interactions with neighbours were not compensated.
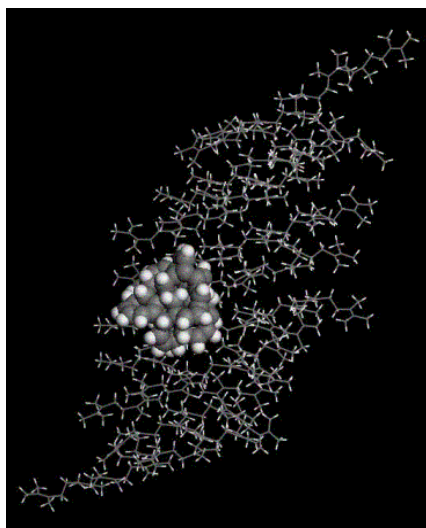

Figure 4.54: MD structure adsorption complex of carbon particle with one polyisoprene.

Further the case when the polymeric matrix represented three parallel layers of closely interacting polyisoprene chains has been considered. The degree of polymerization of each chain was 10; each layer contained 10 parallel chains. MD calculation of such model in a free state has shown, that the structure of polyisoprene layers is very stable and does not undergo some essential changes in time. Polyisoprene revealed nonpolar intermolecular contacts between chains that are strong enough to keep regular structure of a polymer matrix. MD optimized structure these three polyisoprene layers in absence of carbon particle is presented in the fig.4.55.
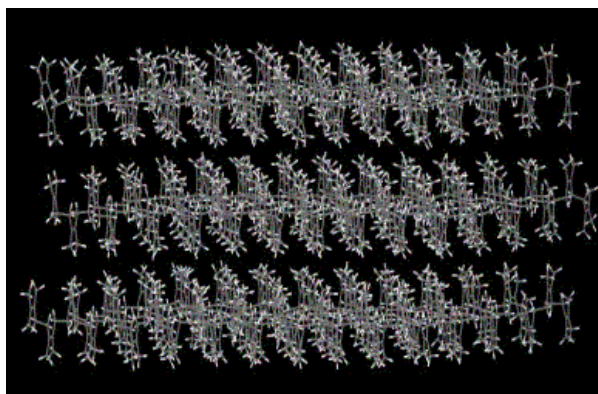
Figure 4.55: MD structure of three interacting polyisoprene layers in absence of contact to carbon particle.

An addition of soot particle to such three polyisoprene layers (the molecule of soot has been placed on a surface of layers) and the further MD optimization did not lead to significant changes in a flat configuration of polyisoprene layers. The structure of corresponding adsorption complex is presented in the fig.4.56.
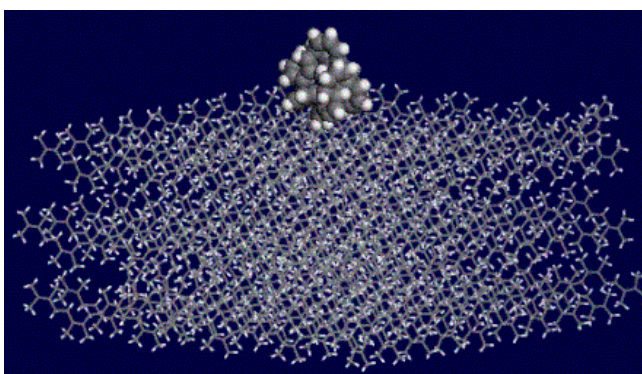

Figure 4.56: MD structure of adsorption complex, in which carbon particle is placed on a surface of three interacting polyisoprene layers.

MD modelling has shown, that adsorption complex of layered polyisoprene and soot particle is very stable, the flat structure of polyisoprene layers is kept better, than that of polyisoprene matrix without filler. The molecule of soot has remained adsorbed on a surface of polymer. Since modelling was spent in vacuum, the environment did not impact on polar interactions.

Besides for polyisoprene matrixes model have been taken two layers of polyisoprene chains, each of which consisted of 9 chains with 50 monomer units. These two layers were located on some distance to each other and had parallel orientation. For this model interaction of carbon particle with polymer layers also was investigated. The carbon particle was located between these layers. MD modelling has been performed for such complex; the received structure is shown in the fig.4.57. From the received data follows, that in this case also the carbon particle rendered stabilizing impact on polyisoprene matrix. Polymer layers at the presence of carbon particle keep flat parallel structure, and only on borders of a layer insignificant bends of polymer chains are.
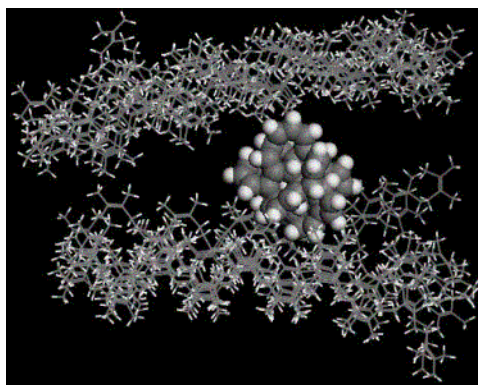
Figure 4.57: MD structure of adsorption complex in which the carbon particle is placed between two polyisoprene layers.

4.3.6. Molecular dynamic investigation of water influence on interaction of polyisoprene with carbon particle

Investigation of water influence on adsorption of soot particle on polyisoprene has been carried out. The systems containing water in explicit (molecular) model can achieve MD relaxation extremely slowly, therefore tong-time 10 nanoseconds MD runs of the systems consisting of carbon particle, several water molecules and polyisoprene component were performed.

In the beginning the case when the single polyisoprene chain interacted with soot particle and several water molecules was considered. Here water molecules were placed in the place-of-contact of filler particle and polymer. An example of MD optimized structure is presented in the fig4.58. If to compare this structure with similar, but received in absence of water molecules (see the fig.4.50), it is seen, that polyisoprene component kept the ordered structure less at presence of water
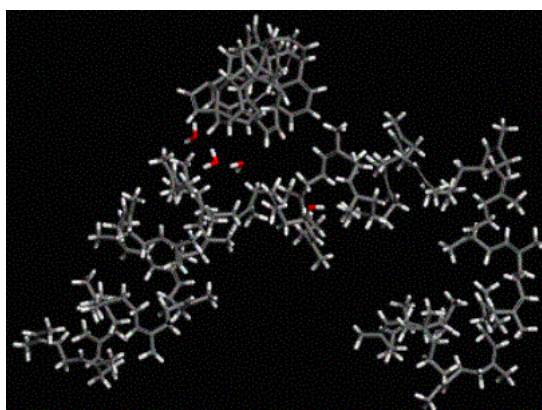

Figure 4.58. MD structure of adsorption complex consisting of carbon particle, polyisoprene chain and four water molecules.

The number of water molecules varied from 1 up to 5. Thus calculation of interaction energy dE_{total}, for all five adsorption complexes containing different quantity of water molecules was performed. Results of MD calculation are presented in the fig.4.59,a-e. In the same figure (4.59,f) the similar calculation received for

system polyisoprene carbon particle without water is presented for comparison. On most lengthening parts of equilibrium dynamics average value of total energy was calculated, and its change with increase in number of water molecules in adsorption complex is presented in the fig.4.60. On the base of received results the conclusion can be drawn up, that water acts on system of polyisoprene matrix - carbon filler as destabilization agent. The structure of polyisoprene layers in adsorption complex with carbon particle re-ordered in the presence of water, and energy of polymer-filler interaction decreased.
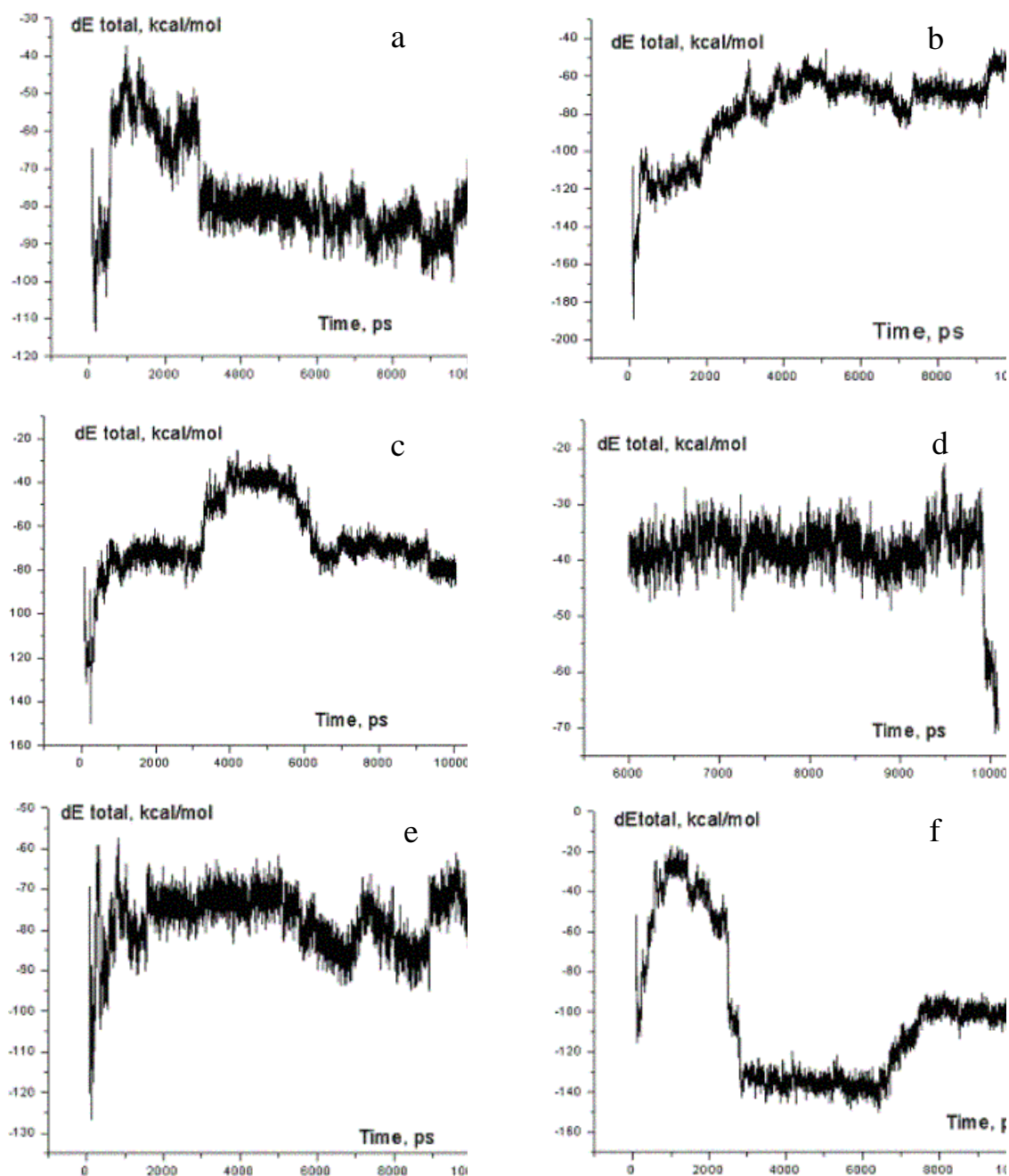

Figure 4.59: Interaction energy of dE_{total} received during MD calculation for five adsorption complexes containing carbon particle, polyisoprene molecule and different number of water molecules: 1 - (a); 2 - (b); 3 - (c); 4 - (d); 5 - (e); (f) - the same system, but in absence of water.
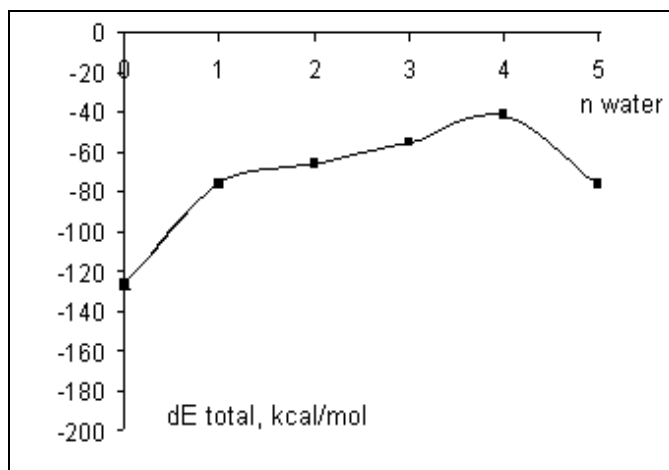
Figure 4.60: Change of average value of total interaction energy in systems of carbon particle - water - polyisoprene at increase in number of water molecules.

The similar conclusion can be made on the base of MD modelling, which was fulfilled for two other models of adsorption complexes of carbon particle and isoprene matrix. The first model represented carbon particle interacting with one flat polyisoprene layer contacting with 20 water molecules. This model is similar to those presented in the fig.4.54 with the difference that water is placed between polymer and filler. The second model consisted of the carbon particle placed between two polyisoprene layers; 40 molecules of water in this model is placed in the field of contact of polymer with filler. This model is similar those presented in the fig.4.57, but at it also contain water layers between polyisoprene and soot. MD structures of these complexes are presented in the figs.4.61 and 4.62.

Results of MD calculations displayed that introduction of water in polyisoprene – soot system destabilized the system. The structure of polymeric layers becomes a little more disordered, average intermolecular distances between carbon particle and polyisoprene grow up from $R_{H..H}$=2.3-2.5A до $R_{H..H}$=2.8-3.3A and calculated interaction energy of polymer-filler complex decreased on 30-40 %.
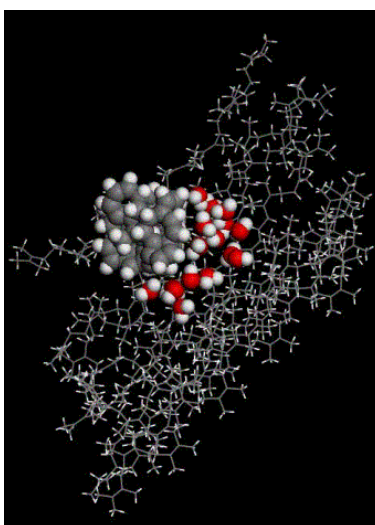

Figure 4.61: MD structure of the complex consisting of carbon particle, polyisoprene layer and an intermediate water layer.
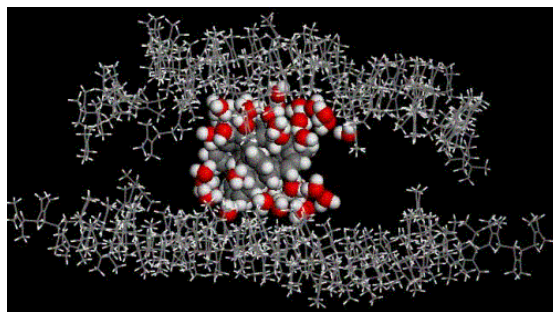
Figure 4.62: MD structure of the complex consisting of carbon particle, two polyisoprene layers and an intermediate water layer.

GENERAL CONCLUSIONS:

1. A new approach to model and investigation of texture and mechanical characteristics of large molecular systems in frame of Monte-Carlo method has been developed. As a base of the method is an unorthodox algorithm allowed to make a classical Metropolis procedure for a few polymer molecules. Algorithm under consideration belongs to class of program which use space decomposition and has high grade of calibration. Energy of intermolecular interactions is calculated by method of atom-atomic potential functions taking into account the electrostatic interactions. Energy of internal molecular interactions (energy of stresses of chemical bonds, valent and torsion angles) calculated on the base of parameter AMBER data-set. Computational experiments with molecular systems keeping up to 10^4-10^6 atoms have been made on computational complexes MVC-1000M and MVC-5000M (Moscow). It was used from 8 up to 729 processors.

2. The structures of model mixtures of n-pentane and carbon microclusters C_{38} (graphite type) as prototype of reinforced polymer composites have been investigated. It was stated, that at distance bigger than Van-der-Waals radius C_{38} (~7A) carbon microclusters construct stacking self-associates keeping up to 18 molecules of C_{38}. Axis of such stacks orient to graphite surface arbitrarily.

3. It was shown the strong dependence the grade of associate of carbons microclusters on form of its surface. So, the particles of amorphous carbon C_{38} form into pentane relatively bulk associates which content about 3-4 particles.

4. Chemical modification of components of mixture influence substantially on structure and mechanical properties of materials under study. So, aquation of carbon microclusters leads to decreasing the middle value of potential energy of particles.

5. It was stated, that nanolayers of water condensate, which happens in moist atmosphere on the carbon surface, can substantially influence on efficiency of interactions the particle of filler with surrounding polymers, and alters the mechanical properties of composite material.

6. We proposed the method and investigated a mobility of polymer molecules close to surface of particle of filler. It was fixed the presence of layer with limited mobility around area of contact "polymer – graphite".

7. It was developed the method of evaluation of shear modulus for composite microcluster during the model by Monte-Carlo method.

8. In the course of the modelling it was obtained that the force of "shift deformation" (or of intermolecular friction) for the system of polymer - polymer is equalled approximately 4 kcal/mol*A, and the similar force characteristic for the system of polymer - carbon particle is equalled approximately 10-12 kcal/mol*A. At the same time the value of destroying force for a polymeric chain is equal approximately 80-100 kcal/mol*A for individual polymer, and at about 2 times less for polymeric chain being in a contact with filler surface (see discussed above results).

Thus cohesion strengthening of organic polymer chains on the surface of carbon fillers was revealed in a framework of quantum-chemical study. Maximal force of tearing off polymer particle adsorbed on carbon surface was found approximately 3 times higher than for polymer in a polymeric matrix. Owing to rather

weak however quite sufficient for immobilization of polymeric chain segments on the carbon surface Van-der-Waals forces, around carbon filler particle some condensed layer of rubber is formed with the lowered mobility of chain segments which most likely is responsible for strengthening of organic polymers by filling them with high dispersed carbon.

9. As it is seen from the results the enthalpy of binding of one monomer unit -CH$_2$- with carbon surfaces decreases in the row: C1>C2>C3>C4, so thus the less energetic favorable contact was obtained for adsorption complex of polymer –graphite surface (C1), and the most energetic favorable contact was obtained for adsorption complex of polymer –surface (C4), with carbon in sp^2/sp^3-hybridization with non regular defected surface, containing some holes. Calculated forces of microscopical friction confirm the previous state. Thus the force of shift deformation is minimal for microscopical friction of the segment of polymer chain along the regular graphite surface (C1), and maximal for the case of the most defected surface (C4), being at about 2.5 times higher. The first results, presented in this stage show the abilities of such kind of computational modeling, and in the further study it is interesting to make more detailed ranking of carbon particles with accordance to defection structure of their surfaces and in some computer selection obtain structure of carbon particles, revealing the best effect of strengthening for organic composites.

10. The results revealed that the force of shift deformation or shift friction in polymer matrix is 2-3 times lower, than the same force for molecular friction in the system polymer- surface of carbon particle. This is a reason of immobilisation of polymer chain on the surface of carbon. Moreover, calculations revealed that force of shift friction increases in the row of adsorption complexes with the models: C1<C2<C3<C4, so that the minimal value of shift force was obtained for regular C1 graphite surface and the maximal – for more defective surface C4.

11. Thus, from the received data it is visible, that the most energetically unfavorable contact is received for the system polymer - graphite surface (C1). The most energetically favourable contact is received for a case of adsorption of polymer on a surface in the *sp^2/sp^3*-carbon hybridization, having holes and five-ring defects (C4) on which fragment of polymer chain immobilized better, and, hence, which has the best strengthening properties as filler for rubber composites. Summarizing in should be mentioned, that in the given section the technique offered earlier is tested on an example of calculation of molecular friction in the complex system consisting of organic polymer and carbon filler.

12. It was obtained that enthalpy of binding of one monomer unit -CH$_2$- with the H-modified carbon surfaces decreases in the same number, as for nonterminated carbon surfaces, namely in a row: C1_H> C2_H> C3_H> C4_H. Graphite surface (C1_H) was found as the energetically most-unprofitable contact for system polymer, and the most energetically favourable contact is received for a case of adsorption of polymer on H-terminated surface containing defects with atoms of carbon in sp2/sp3-hybridizations and having different holes in a structure. (C4_H).

Consideration of the stress diagram of friction for studied surfaces also confirms the received energetic result. Force of shift of microscopic friction is minimal for a case of strictly periodic graphite surface (C1_H). It is worth to mention that for nonterminated and H-terminated models the same result was

received. However if to compare the similar nonterminated and terminated defective surfaces force of microscopic friction along the terminated surface makes approximately 0.9-0.7 from force of microscopic friction along not terminated surface. Is of interest in the further during consecutive numerical quantum mechanical experiment to make more detailed ranging a surfaces of carbon particles on number and a kind of defects of a lattice of graphite and kind of its termination., Also by selection in computer design to establish a microscopic structure of a surface of technical carbon, optimum for the best strengthening effect.

13. During quantum mechanical modelling it has been shown, that on nonterminated carbon surface there is an adsorption of individual water molecules which can be characterized as Van-der-Waals one: $R_{C...O}$ =2.0-2.2A, ΔH~2-2.5 kcal/mol (calculated for one water molecule). Much weaker interactions of water molecules occur with nonterminated carbon surface: $R_{H...O}$ =2.5-2.8A, ΔH~1.3-1.5 kcal/mol (calculated for one water molecule).

The H-bonded water drop does not spread on carbon surface, interacting with the latter as a unit. As it has been shown in QM calculations energy of hydrogen bonding OH … O in cluster, consisting of several water molecules is ΔH_{bind}~4 kcal/mol, that is, more, than energy of interaction of water molecule with soot surface, thus, is energetically proved clusterising of H-connected water molecules on soot surface.

It was obtained that fragment of organic polymer interacts with nonterminated carbon surface at about 1.5 times stronger than with H-terminated carbon surface. Water interlayer between polymer and carbon surface decrees strength of interaction in the system. The reinforcing effect of pure nonterminated carbon fillers is the best.

14. Some conclusions could be done about impact of chemical nature of the polymer matrix on the interaction of the polymer segments with surface of soot fillers. The binding enthalpy and the force of shifting is determined mainly by square of hydrophobic contact between polymer fragment and surface of soot particle (i.e. by presence and number of CH_2 и CH_3 groups), and by the presence and number of electronegative atoms (O, N) in the polymer structure. Moreover the conformations of the polymer fragment on the interface, namely complementary character of its space structure with structure of soot surface impact also of the polymer adsorption.

It was obtained that binding enthalpy and force of shifting of polypropylene in ~ 1.5 times higher than the same values obtained for polyethylene. It can be explained with greater square of hydrophobic contact between polymer fragment and surface of soot particle in the case of polypropylene. In the same time binding enthalpy and force of shifting of polurea in ~ 1.7 times higher than the same values obtained for polyethylene. Having at about the same surface of interparticle contact molecule of polurea oligomer has N and O electronegative atoms, which play the decisive role in the binding in this case.

The most energetically favorable contact of the oligomers under study was obtained for polyvinyl acetate (~ in 2.0 times higher than for polyethylene) that can be explained by the impact of the two factors described above. This molecule has high square of hydrophobic contacts and also contains electronegative atoms O.

The lack of high adsorption capacity in the case of polyacrylic acid (it also has electronegative atoms O in the structure) can all means be explained by not favorable conformation of this molecule under adsorption on the soot surface, that can follow from not favorable geometry of the corresponding adsorption complex for realization both hydrophilic and hydrophobic contacts. This oligomer revealed small value of binding enthalpy.

Analogical values, obtained for H-terminated soot surface, revealed the same regularity for different kinds of polymers however in a total binding enthalpies and forces of shifting are at about 0.7 times less than for nonterminated surface.

15. As it is seen from the results the strong interaction is observed in the case of interaction of nonterminated carbon surfaces. It leads in some cases to the formation of new covalent bonds C-C between the former soot particles. Thus the initial protoparticles of the amorphous carbon with nonterminated surfaces interact with each other forming larger molecular structures, which can not be easily divided into the initial particles, but which kept in the main details their initial structure.

In the case of carbon particles with H-terminated surfaces much weaker interaction of the particles was obtained. Hydrophobic H…H interactions keep interacted particles at the H…H distances at about 1.6-1.7A. Binding enthalpy and forces of intermolecular shifting are enough for interparticle agglomeration. It is very likely that this kind of agglomeration can be destructed with an impact of adsorption interlayer between soot particles, which can be polymer or water.

In the case of interaction of the soot particles, which surfaces are terminated by hydroxyls, interparticle agglomeration is determined by hydrogen bonding between particles. Minimal interparticle distances correspond to the standard hydrogen bonds (1.9-2.0 between H and O atoms participating in H-bond formation). Aggregation or sintering of the soot particles is stronger than in the case of H-terminated soot surfaces, but possible can be destructed in water solution or in the presence of polymer matrix.

In the case of interaction of the carbon particles, which surface is terminated by negatively charged COO^- groups, particles are slightly repulsed, and aggregation is not taking place. (The shortest distance between particles is O…O 3.0-3.2, so the surface modification similar studied can prevent soot particles agglomeration if necessary.

16. As it is seen from the results, aggregation of the soot particles can be prevented by adsorption interlayer of polymer between the soot particles. Adsorption of water in the interparticle interface can be considered as competitive process for polymer adsorption. For the formation of the contact polymer-filler water layer on the soot surface has to be removed. Energetic of these competitive processes is similar, and so for stronger adsorption of the polymer chains on the filler particles modification both polymer molecule and surface of the fillers has to be performed.

17. Some conclusions can be obtained in the course of QM modeling in a framework of microscopic internal coordinate of deformation (MIC) and microscopic friction coordinate (MFC) approaches.

Force curves of uniaxial tension for polyethylene, polybutadiene, and isoprene reveal the similar peculiarities. The first part of each curve of the low elongations corresponds to region of entropic torsional conformation changes of the polymer chain. It presents the low forces of the deformation The second part

of each curve represents Hook's or enthalpic region of elongations of the polymer chain. In this part elongation of the valence bonds occurs mainly. This region is characterized by considerable growing up the force of deformation. Maximum value of the deformation force corresponds to the critical force of polymer bond rupture.

In the row of polyethylene, polybutadiene, and isoprene considerably elongating the enthalpic region and decreases the critical force of polymer bond rupture. Thus the growing up the elastic character of the polymer chain in the studied row is revealed. Isoprene shows the most elastic properties corresponding to the obtained force regularities.

Place of the polymer chain rupture occurs in each case in the vicinity of the surface of carbon particle being in the contact with the polymer molecule. The rapture of the polymer chain passes via cyclic transition complex with participation of the carbon surface active groups. Thus the destruction of the polymer chains in filled rubbers occurs mainly, by all mean, in the places of polymer contact with the filler particles.

The best cohesion with carbon particle surface (the highest forces of microscopic friction) was obtained for isoprene molecule representing branchy and flexible chain, and the worst one was found in the case of polyethylene molecule. Hence the best reinforcement can be reported for the combination of isoprene-amorphous carbon and the worth for system polyethylene-amorphous carbon.

Obtained dependencies of polymer molecule cohesion with carbon particle surface (or of the highest forces of microscopic friction) are in a good accordance with calculated geometrical and energetic characteristics, which confirm the best effectiveness of isoprene-amorphous carbon composite system as filled rubber.

18. In the course of QM modeling some conclusions can be done concerning the impact of chemical nature of the filler particles on the interaction of the polymer segments with surface of fillers. The binding enthalpy and the force of shifting are determined mainly by hydrophobic contacts between polymer fragment and surface of filler particle. Moreover the conformations of the polymer fragment in a contact with filler surface, namely complementary character of its space structure with structure of filler affects also on the polymer adsorption. The best cohesion of isoprene chain with filler particle surface (the highest forces of microscopic friction) was obtained for the system isoprene-silica. A little worth is cohesion of isoprene with carbon black or soot. Such fillers as fullerene and high-dispersed carbon tubes represent lower forces of adhesion, being practically similar with a little preference of the latter. Thus quantum mechanical modeling can provide us with information about ranking of filler particles with respect to their chemical nature and structure, and allows making some recommendations concerning surface modification of fillers.

19. As it is seen from the obtained results enthalpy of binding of rubber chains on a clay surface and force of microscopical friction in this system, which interconnected with cohesion is strongly depended on modification of clay surface by hydrophobic agent (organic cation). If there is not cation exchange in clay interlayer (case e), and surface of latter reveals hydrophilic properties, there is not any expansion or swelling of clay structure in a contact with rubber, since rubber chains practically cannot penetrate between clay platelets, and delamination of clay layers does not observed. In this case rubber and clay can form only conventional, in the best case intercalate composites that do not possess high mechanical and wear capacity. Practically the same result can be obtained if take rather short alkylammonium surface agent for

modification of clay platelets (case a). At application of organic cations with too long chains, these huge molecules can locate between clay platelets filling all filler surface area by some kind of hindered knot. In this case delamination of clay layer could be observed, but immediate contact of rubber chains with clay particles is inconvenienced. In this case also the formation of composites with good mechanical properties is problematic. The best case can be observed if use organic cations with middle-sized chains at about 15-20 monomer units and various modification of uncharged end providing better hydrophobic binding with rubber chains (cases b and c in current study). Such kind of alkylammonium cations promote expansion of clay structure, rubber chain penetration between clay platelets, delamination of clay sandwich-like structure and finally they provide the formation of exfoliated rubber-clay composites where clay platelets are completely delaminated and do not show any periodicity in their arrangement. Taking into account high values of calculated enthalpies of rubber-clay binding and microscopical forces of cohesion it can be proposed that nanocomposites in this case can reveal high mechanical and wear capacities. Thus using computational experiment which is done from the first principles taking into account chemical nature of all components of nanocomposites the goal-seeking search of best 'partners' can be done in silico, some times much faster than in experiment. Of course, experimental verification of the main results has to be done.

20. As it is seen from the structure of rubber-filler complex, obtained after the total optimization in QM, such kind of 'close' interactions can provide unique mechanical properties of nanocomposite. Rubber chain easily penetrate between clay layers with the help of interaction with carbon particle, filler particles delaminated and nanocomposites with exfoliated structure and very strong hydrophobic contacts both with clay and carbon black (calculated H_{bind}, is -12.3 kcal/mol and F_{shift}, is 45,2 kcal/mol*A) can be achieved. Such kind of filler synergism also is an interesting topic for QM modeling in framework of presented approach.

Thus quantum mechanical modeling can provide us with information about interconnection of nanocomposite mechanical characteristics and chemical nature of their components, and allows making some recommendations concerning choosing the fillers, their surface modification and application of combination of different fillers.

21. During molecular dynamic modelling distinction in behaviour of polythene and polyisoprene is revealed at their interaction with carbon fillers. The polyethylene matrix significantly changes the configuration in time and is always turned off in a ball of chains, both in case of contact with carbon filler, and in case of its absence. Systems with polyethylene matrixes, practically, do not keep initial structure and quickly pass in an amorphous condition, being aggregated around of soot filler particle. Polyisoprene chains, on the contrary, in many respects keep initial structure in time and introduction carbon filler in the system strengthens this tendency. Polyisoprene component is stabilized at the presence of carbon filler. This conclusion leads from both structural, and energetic results of MD calculations.

22. Introduction water into system of polyisoprene - carbon destabilizes corresponding adsorption complexes however in this case systems keep enough ordered the structure.

23. During the molecular-dynamic modelling it was shown, there is the discrepancy between behaviour of polyethylene and polyisoprene chains under their interaction with carbon fillers. The polyethylene chains

sharply change their configuration on time and always furls into ball both in case of contact to carbon particles and without. Materials with polyethylene matrix practically do not keep an initial configuration and quickly jump in amorphous condition, aggregated around carbon particle.

Polyisoprene chains, contrariwise, keep initial structure and injection into system of carbon filler deepens this tendency. Polyisoprene's component is stabilized in presence of carbon filler. As structural so energetic results of molecular dynamic calculation testify about.

24. Injection into composite system polyisoprene – carbon filler some water destabilizes appropriate adsorption complexes, but at this case the system keeps the shape of its structure pretty long.

REFERENCES:

1. Allen M.P., Tildesley D.J., Computer simulation of liquids, Oxford University Press, N.Y., 1987.

2. Alexandre M. and Dubois P. Polymer-layered Silicate Nanocomposites: Preparation, Properties and Uses of a New Class of Materials, Mater. Sci. Eng., 2000, v.28, pp.1-63.

3. Burnside S.D. and Giannelis E.P. Synthesis and Properties of NewPoly(dimethylsiloxane) Nanocomposites, Chem. Mater., 1995, v.7, N9, pp.1597-1600 and

4. Generalized Born Equation: Still W.C. Tempczyk A., Hawley R.C. Hendrickson t., J. Am. Chem. Soc. 1990, v.112, pp.6127-6129.

5. Kitaygorodsky A.I. Molecular crystals (in rus.), M., Nauka, 1971, 424 p.

6. Koshkin N.I., Shirkevich M.G. Directory on elementary physics (in rus.), M., Nauka, 1976, 256 p.

7. MacKerell A.D., Bashford D., Bellott M., Dunbrack R.L., Evanseck J.D., Field M.J., Fischer S., Gao J., Guo H., Ha S., Joseph-McCarthy D., Kuchnir L., Kuczera K., Lau F.T.K., Mattos C., Michnick S., Ngo T., Nguyen D.T., Prodhom B., Reiher III W.E., Roux B., Schlenkrich M., Smith J.C., Stote R., Straub J., Watanabe M., Wiorkiewicz-Kuczera J., Yin D., Karplus M. All-Atom Empirical Potential for Molecular Modeling and Dynamics Studies of Proteins, J. Phys. Chem. B, 1998, v.102, pp.3586-3616.

8. Metropolis N.A., Rosenbluth A.W., Rosenbluth M.N., Teller A.H., Teller E., J. Chem. Phys., 1953, v.21, pp.1087-1092.

9. Neria E., Fischer S., Karplus M. Simulation of Activation Free Energies in Molecular Systems, J. Chem. Phys., 1996, v.105, pp.1902-1921.

10. Nikitina E., Computational modelling of surfaces and interfaces of nanoobjects, Composite Mechanics and Design, 2001, v. 7, №3, pp.288-331.

11. Poltev V.I., Shulyupina N.V., J.Biomol.Struct.Dyn., 1986, v.3, pp.739-765.

12. Stewart J.J.P., J. Comput. Chem., 1989, v.10, N2, pp.209-264.

13. Teplukhin A.V., Mathematical modeling (in rus.), 2004, v.16, pp.15-24.

14. Weiner S.J., Kollman P.A., Nguyen D.T., Case D.A., J. Comput. Chem., 1986, v.7, pp.230-252.

15. The CHARMM Development Project, Professor Martin Karplus, Department of Chemistry & Chemical Biology, Harvard University.

5. EXPERIMENTAL INVESTIGATIONS OF STRUCTURE AND RHEOLOGICAL PROPERTIES OF ELASTOMERIC MATERIALS FILLED WITH DISPERSE PARTICLES.

In order to verify the adequacy of above theoretical approximation for prognosis of the mechanical properties of viscoelastic heterogeneous media filled with the active filler the set of experimental tests for model samples were made. We have chosen the samples of natural rubber (SVR-3L type) filled with the different sorts of technical carbon (N220, N660, N339, N330, N550). Technical characteristics of above technical carbons correspond to international standard (ASTM D 1765) and indicate in Table 5.1.

Table 5.1.

Basic characteristics of different types of technical carbon (ASTM D 1765).

Marking of technical carbon	N 339	N 220	N 330	N 550	N 660
Iodine absorption number	90±5	121±5	82±5	43±5	36±5
OBP absorption number	120±5	114±5	102±5	121±5	90±5
CTAB surface area	93±6	111±6	82±6	42±6	36±6
Pour density, pelleted carbon black	345±30	345±30	375±30	360±30	425±30
pH value	6-9	6-9	6-9	6-9	6-9
Heating loss at 105°C, max	0.9	0.9	0.9	0.9	0.9
Ash content, max	1.0	1.0	1.0	1.0	1.0

As it can see from the Table the fillers which we have used for investigation quite differ from each other on physical and chemical properties and first of all on value of specific surface area and therefore on size of particles. This circumstance allows us to prepare the full-scale analysis of an influence just that factor in light of reinforcement mechanism.

One can remind that according to some theoretical prognosis it is having legible quadratic dependence of some mechanical characteristics, viz. elastic moduli, on diameter of the particles of an active filler.

Experiments of this part of work were made on the samples of elastomers (natural rubber) filled with 20, 40 and 60% by mass of technical carbon. All of samples were plastificated by stearin acid.

5.1. MICROSTRUCTURE INVESTIGATIONS.

It is obviously, that different theoretical predictions and prognosis must be supported some experimental verifications. First of all it concerns to direct experimental evaluation of structure and geometrical parameters of particles, aggregates or agglomerates of particles of active fillers as in initial state so inside a medium of polymer matrix.

As it easy to see from the results of molecular modeling (see Part 4 of the present work) inside polymer matrix the particles of active fillers are able to form the aggregates with different configuration. For carbon particles a form of such kind aggregates depends, in particular, on structure of surface of separate particles (see data by Monte-Carlo modeling). From other side, the data of molecular modeling testify about formation interphase layer with specific properties which is located inside a disperse-filled polymer medium.

Above layer consists of molecules of polymer, which are adsorbed on the surface of solid phase and have an limited mobility (as it is typically for polymeric glassy state). At these conditions an effective surface of particles of filler is sharply increased, and simultaneity is increased a part of material with higher strength properties, because, as it is known, a polymer medium in glassy-state condition is characterized by bigger enough elastic moduli.

For experimental tests of structure of microheterogeneous polymer medium some samples of technical carbons (see Table 5.1) and samples of row rubber compounds filled with above sorts of technical carbon have been used.

Microstructure investigations have been made by Dynamic Force Microscope (DSM), (NanoSurfe model, Swiss) and Optical Interference Microscope New View 5000 (Zygo Inc., USA).

In figs.5.1-5.5 one can show the results of microscopic investigations of structure of the carbon particles, which represent in Table 5.1. It is important to note the authors proposed new technology of preparation of samples for microscopic investigations, which allowed to get the necessary grade of detail of surfaces of samples under study.

The structure of graphite particles for samples N220, which have been placed in view of DSM, exhibits in fig.5.1 (a – atop outlook, b – three-dimensional image). One can see, that carbon particles (white peaks) is evenly distributed on the model surface (there is no aggregation).
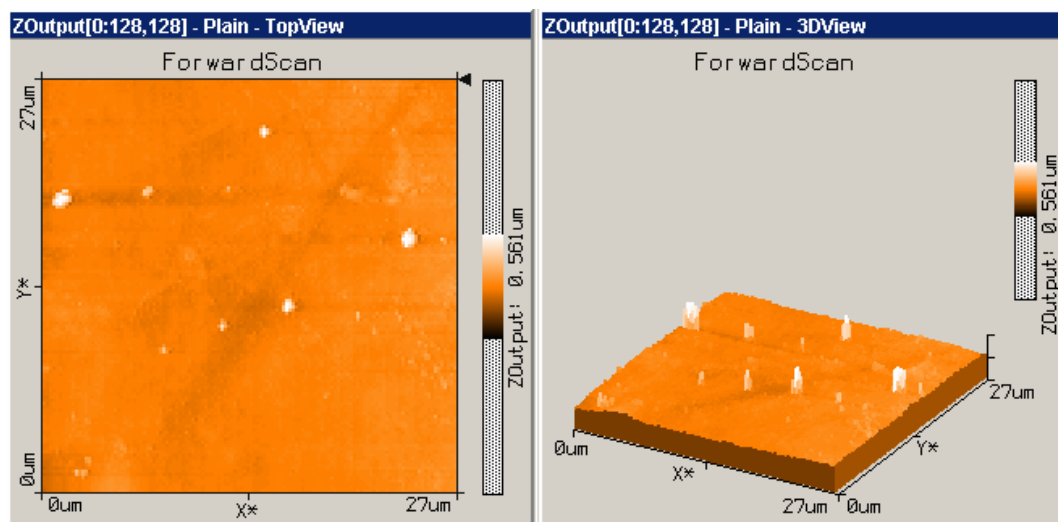

Figure 5.1: Particles of technical carbon (sample N220), debarked on the model surface. Date of DSM: a) atop view, b) three-dimensional image.

In fig.5.2 exhibits an individual carbon particle (sample N220) by magnification about 30 times more, than in fig.5.1. (atop view and three-dimensional image). It is clearly to see a form of particle, one can assign its size (about 220 nm). At fig.5.3 depicts a microscopic structure of carbon sample N330. It is clearly to see a formation of aggregate, consisted of two particles.
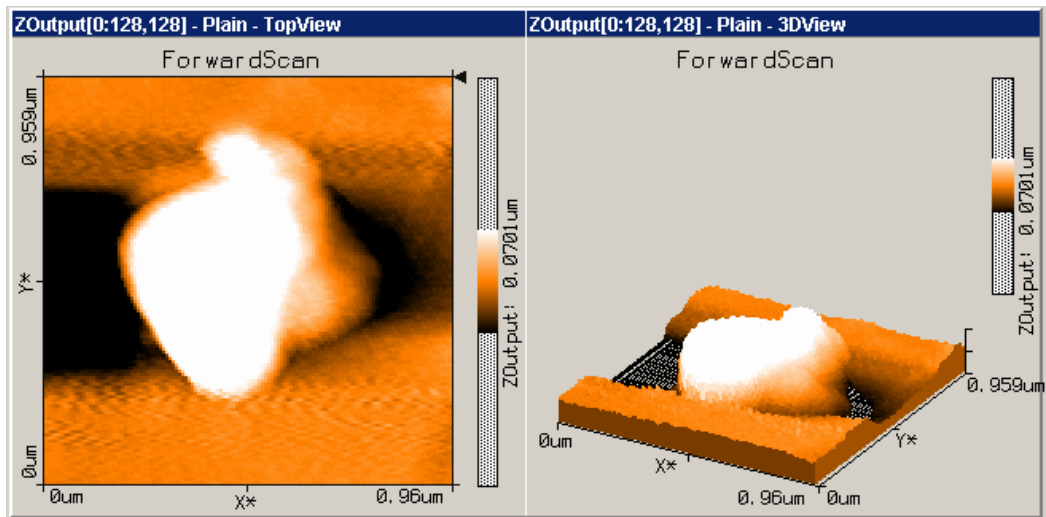
Figure 5.2: The carbon particle (N220), debarked on the model surface. Date of DSM: a) atop view, b) three-dimensional image.
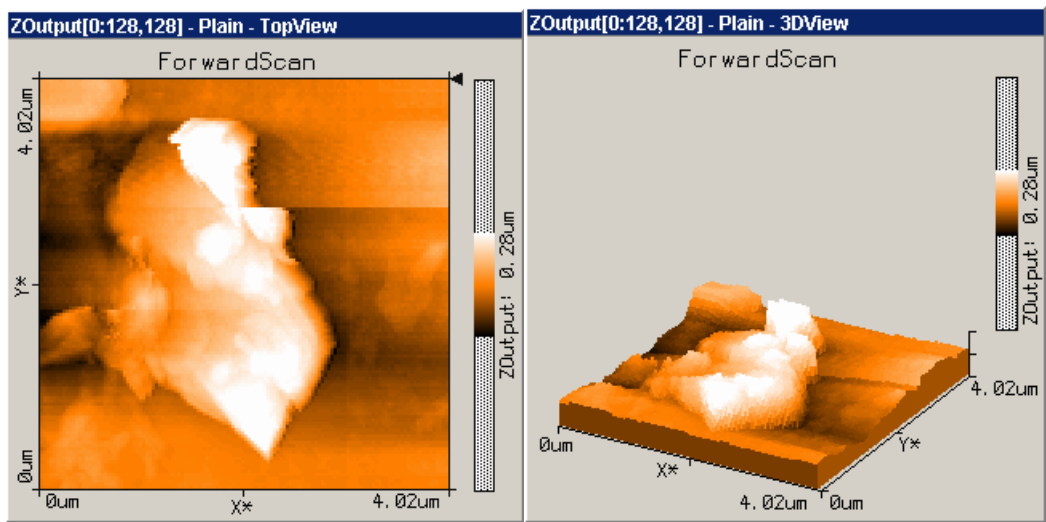

Рис.5.3. The sample of structure of technical carbon (N330): a) atop view, b) three-dimensional image.

In figs.5.4 and 5.5 exhibit the data of microscopic investigations of the samples N550 and N660. One can see, that they look as aggregates of particles, though during the preparation of the samples for microscopic investigations the carbon particles have been treated by ultrasound in order to avoid effect of adhesion.
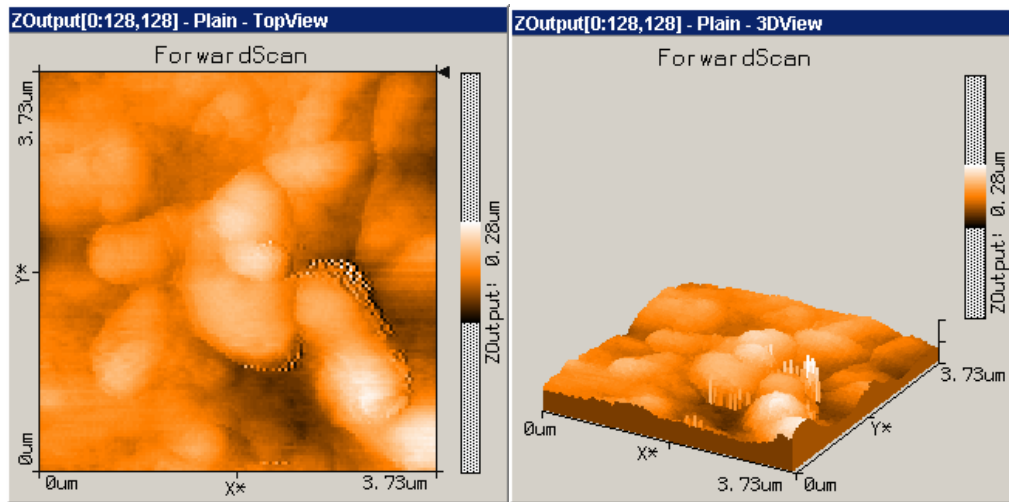
Figure 5.4: The sample of structure of technical carbon (N550): a) atop view, b) three-dimensional image.
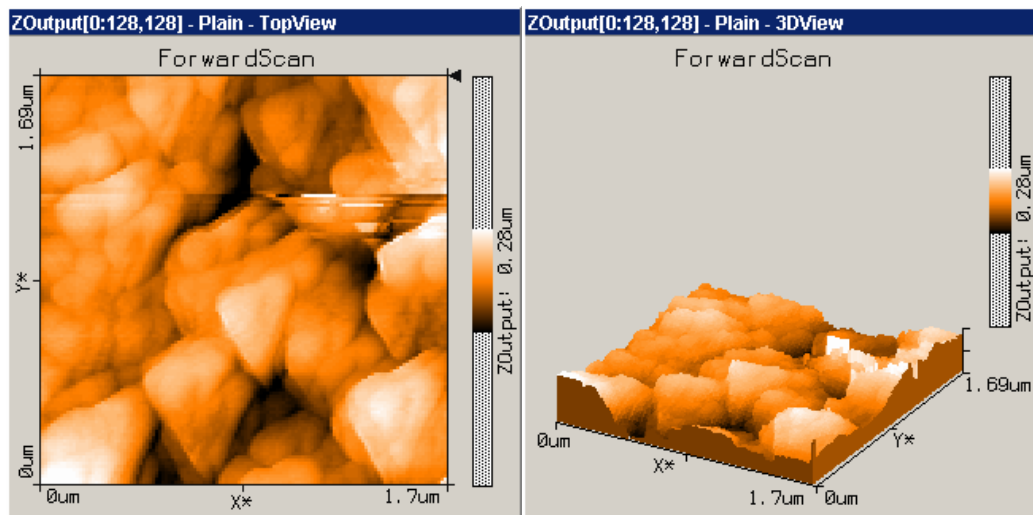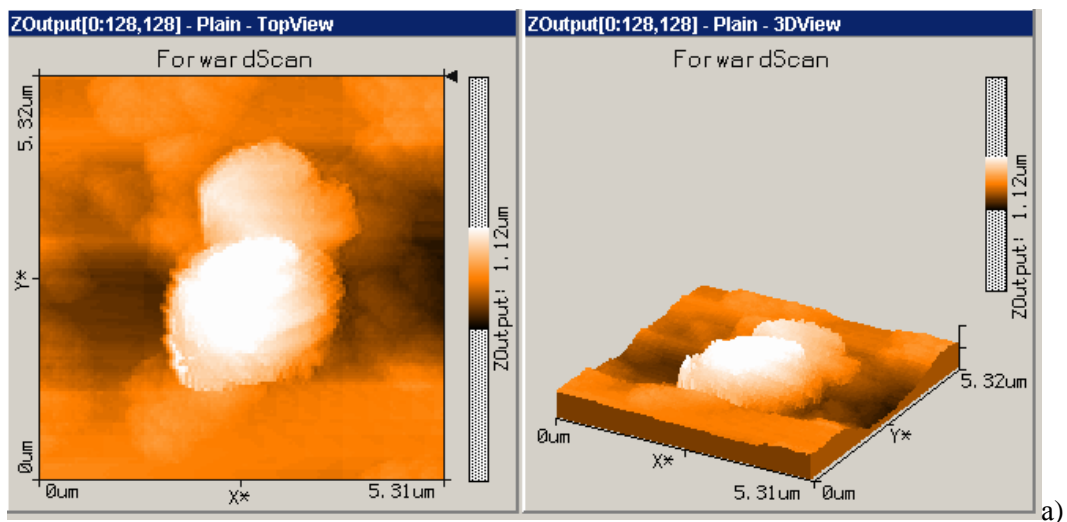

Figure 5.5: The sample of structure of technical carbon (N660): a) atop view, b) three-dimensional image.

In fig.5.6 is shown the data of microscopic investigations of structure for elastomeric compounds, that is, natural rubber and technical carbon N220.
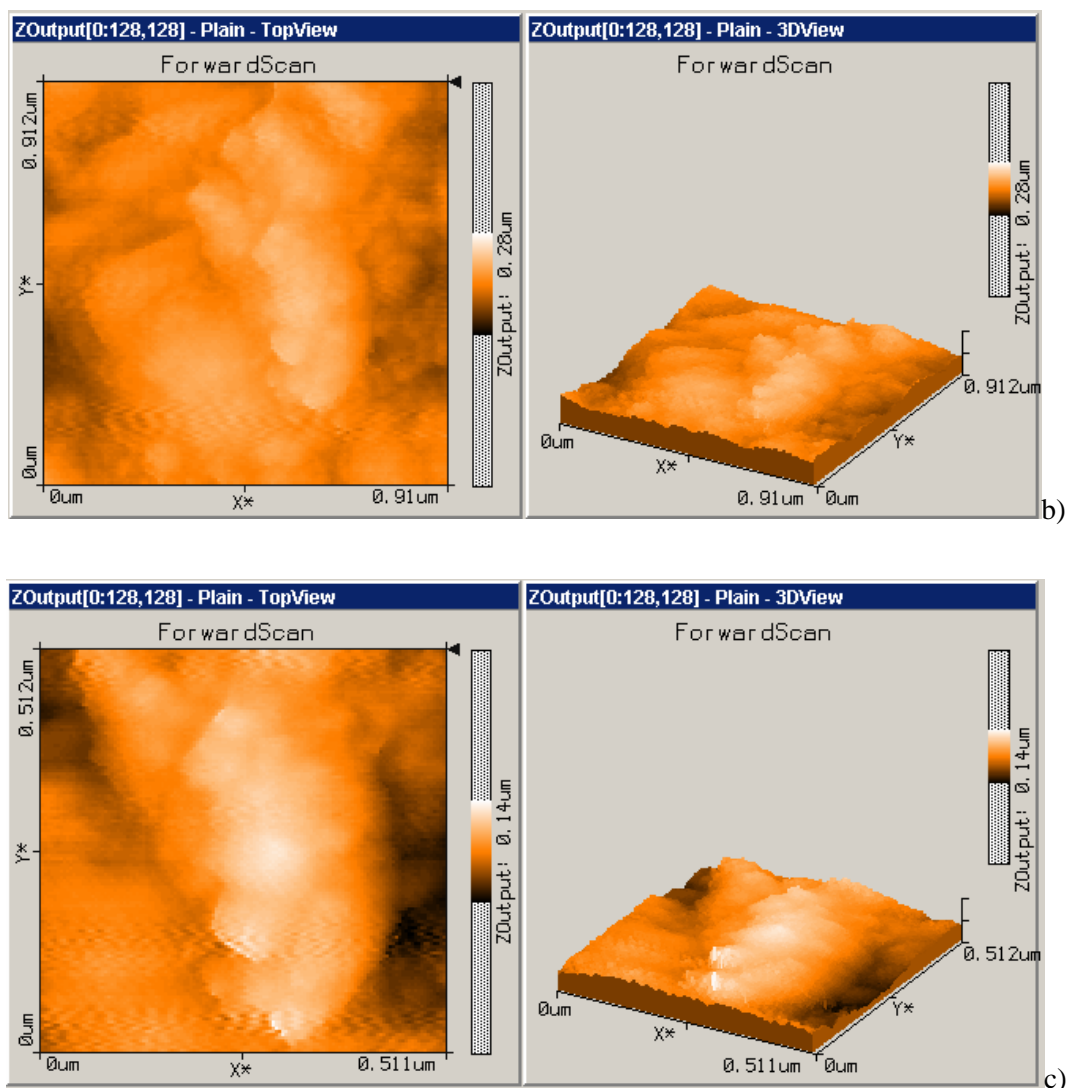

a)

Figure 5.6: Microscopic image of structure of elastomeric compounds consisted of natural rubber and technical carbon N220». a)-c) are the different grade of magnification.

Pictures 5.6 (a-c) concern to the different grade of magnification. One can see from the pictures, that in elastomeric matrix the particles of technical carbon is aggregated (fig.5.6,a). Possibly, it arises by two reasons. Firstly during the mixing (milling) under influence of big stresses goes a convergence of carbon particles and they can incorporate under Van-der-Vaals interactions. Secondly, it is clear, that by interaction of carbon particles with molecules of natural rubber adhesion of molecules on the surface of particles occurs. In this case a formation of coating (film) on the surface of particles arises and under this reason an effective diameter of those increases, practically, in two times (compare fig.5.2 and fig.5.6,c). In this conditions a distance between nearby structures is contacted and adhesion between arises.

One can note, that above situation is agreed with predictions of molecular modeling (method of molecular dynamics) (see figs.4.57, 4.61, Part 4).

As the conclusions of this part of work we can note, that microstructure investigations of geometry of surface foundation of particles of disperse filler and aggregations of those inside elastomeric matrix (by DSM

215

method) give us very useful information for verification of theoretical and model evaluations of parameters of microclusters of composite polymeric structures.

5.2. RHEOLOGICAL INVESTIGATIONS.

Investigations have putted through by means of rheological equipment, RheoStress 150 (Haake Company, Germany, ISO 9001) under periodical deformation mode in wide range of frequencies (10^{-2}-10^2 Hz), under different amplitude of deformation mode (10^{-5}-$0.5 \cdot 10^1$ Hz), under stationary deformation mode, namely – relaxation shear stresses and under different temperatures.

Set of mechanical characteristics has been estimated, that is, the components of the complex dynamical modulus, namely, the storage and loss moduli, tangent of mechanical losses, the complex dynamical viscosity, the relaxation modulus, the compliance.

The results let us to analyze some mechanical and relaxation dependencies for elastomeric composites filled with technical carbons in light of the variation of precise physical and chemical properties of technical carbon and to verify an adequacy of some relations predicted by theory which is developed.

The results we have got (see previous stages of work for 2002, 2003, 2004 years) let us construct and analyze the most important relaxation dependencies of elastomer composites with disperse filler (row rubber mixtures) in connection with alteration of some physico-chemical properties of technical carbon and verified the adequacy of some expressions theoretically predicted before.

One of the problem of fabrication of reinforced rubber composite, as it was seen from results of previous stages of work, is an optimal selection of ingredients for composite compound. In this aim is very perspective ideated the using of nano-size fillers, in particular, montmorillonite as prospective nano-size filler for rubber compound. It is obviously, that problem requires separate investigations. Nevertheless, in Part 4 we have discussed some physico-chemical and micromechanical peculiarities of interaction of montmorillonite with basic components of rubber compound and some methods of possible modification the surface of its in order to prevent an aggregation by injection in elastomeric matrix.

In this part of work it is expediently to discuss some rheological characteristics of elastomeric compounds filled with montmorillonite in order to analyse the possibility of its using. This investigations has been made on samples of natural rubber, containing 20, 40, 60% by volume of montmorillonite. The samples have been prepared according to the same technology as in previous stages of above work (see the work for 2002-2003 years). It was made the rheological characteristics above systems in wide diapason of alteration of frequencies (f), relative amplitude of deformations (γ) by temperature 120°C (see fig.5.7).
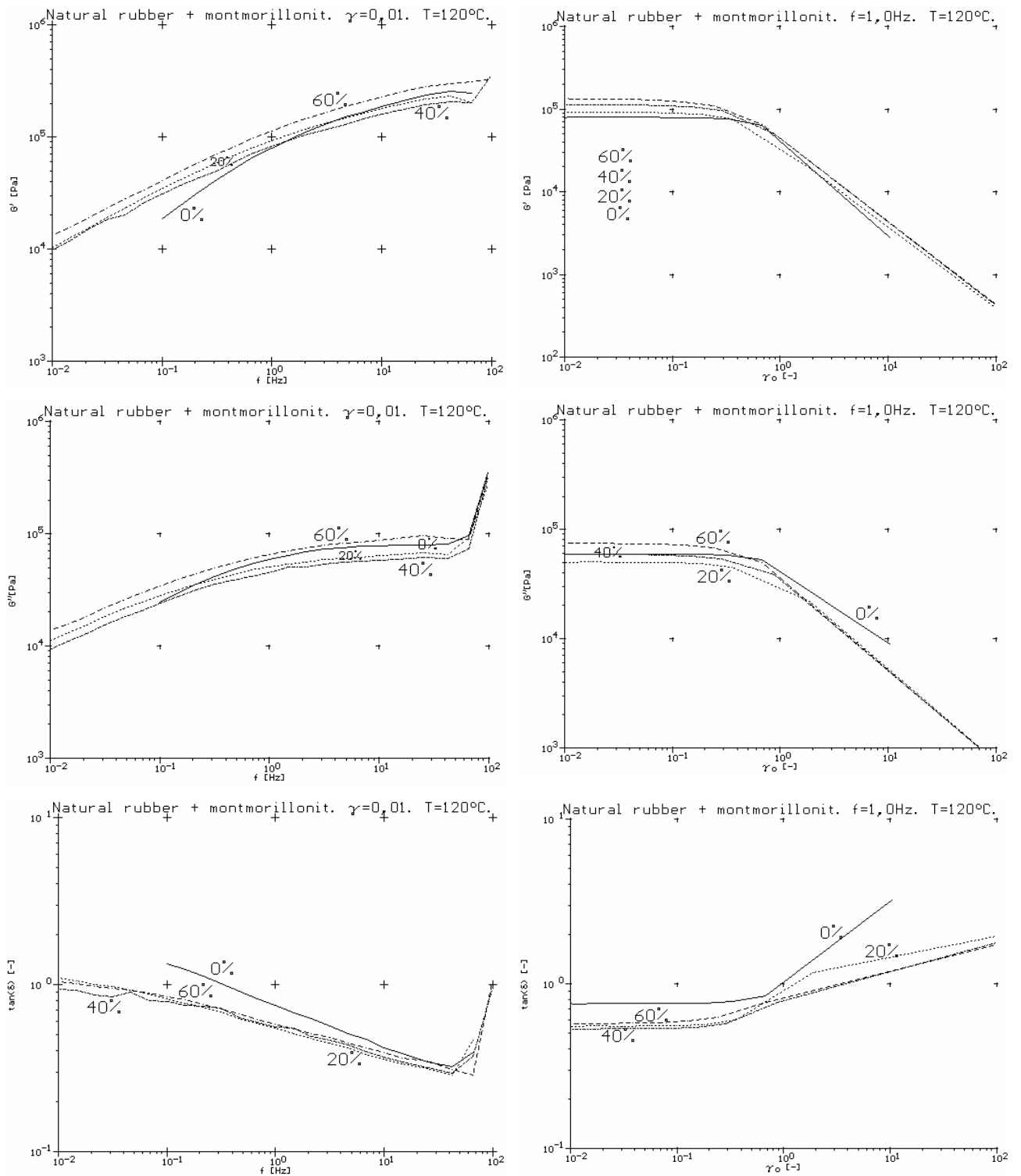
Figure 5.7: Dependencies of rheological characteristics of storage G' and loss G'' moduli and tangent of mechanical losses $tg\delta$ on frequencies f by small relative deformations $\gamma = 0.01$ and on values of γ at constant frequency f=1,0 Гц for sample of natural rubber filled with 20, 40 and 60% by volume montmorillonite. Temperature T=120°C.

As it is easy to see in fig.5.7 the frequency dependencies of rubber mixture containing montmorillonite by small relative deformations ($\gamma = 0.01$), that is, in linear deformation mode, qualitatively very little differ from

the same curve for elastomeric matrix in the region of frequencies 10^0-10^2 Hz. That concerns to dependencies for storage modulus $G'(f)$, loss modulus $G''(f)$ and tangent mechanical losses $tg\delta(f)$. Below 10^0 Hz it is clearly to see a trend of magnification of G' and G'' and decline of $tg\delta$ and it is explained by decreasing of fluidity of filled medium.

Summarize one can note, the general view of behavior of the samples of natural rubber filled with montmorillonite seems as typical for media filled with non-active filler. The dependencies of G', G'' and $tg\delta$ on γ as qualitatively so quantitatively are similar the analogical curves for elastomeric matrix, that is, for natural rubber. Above results is very understable from rheological points of view. They are typical for compounds filled with non-active components.

6. IDENTIFICATION OF PARAMETERS OF MODEL OF VISCOELASTIC MEDIA TAKING INTO ACCOUNT DATA OF EXPERIMENTAL INVESTIGATIONS.

6.1. LINEAR NEURAL NETWORK MODEL FOR VISCOELASTIC MEDIA.

In order to describe a viscoelastic behavior of media under study (prototype of reinforced rubber composite) it was used the system approach based on the neural network model and procedure of its installation as dynamic system.

The structure of coming neural network is assigned of mathematical problem which based on initial information from one side, and seeking solution from another. The common algorithm of neural network is formulated from mathematical setting as it follows:

1. Option of initial configuration of network, for instance, as a monolayer keeping an amount neurons equal the half of total amount of input and output.

2. Model and training of network with evaluation of given mistakes and utilization of complementary neurons and intermediate layers (rule of hierarchy-adaptive models).

3. Elicitation of effect of re-training and correction of network configuration (regularization of algorithm of training).

In detail above schema looks as it follows:

- Designation of figuration of input signal;

- Designation of variety of actual output signal at n moment of time;

- Designation of wishful output signal at n moment of time;

- Designation of mistake of solution at n moment of time (as residual between real and wishful output signal);

- Formulation of function of activation. As the activation function one can state a non-linear function the minimum of which is much less of minimal value of input signal, but maximum is much more than maximal value of this signal;

- Description of structure of neural network;

- Formation of functional of optimization (it is formed from conditions of problem). The most frequently it is used: the functional of minimization of mean-quadratic mistake; the functional of minimization of modulus; the functional of minimization of entropy; the functional of minimization of exponential mistake;

- Option of method for scan of extreme of the functional of optimization. (The most simple and common method is gradient.);

- Option of initial values of weights. (The initial values of weights are usually chosen from the conditions of problem and sort of activation function, by which the activation value for each neural hit into the area of nonlinearity for function of activation, but not into the area of its saturation.)

At the given stage of work it was realized the first stage of synthesis of neural network for given viscoelastic media, namely, matrix of rubber composite (polybutadiene).

The linear integral model Maxwell's type was chosen as training schema for input and wishful output signals by creation of viscoelastic model of media. Above model has been identified at the previous stages of work and some experimental data of the authors have been used. These data were made during the rheological

experiments at the RheoStress-150 (HAAKE, Co.) and look as dependencies of dynamical characteristics, that is, storage G' and loss G'' moduli on experimental frequencies ω.

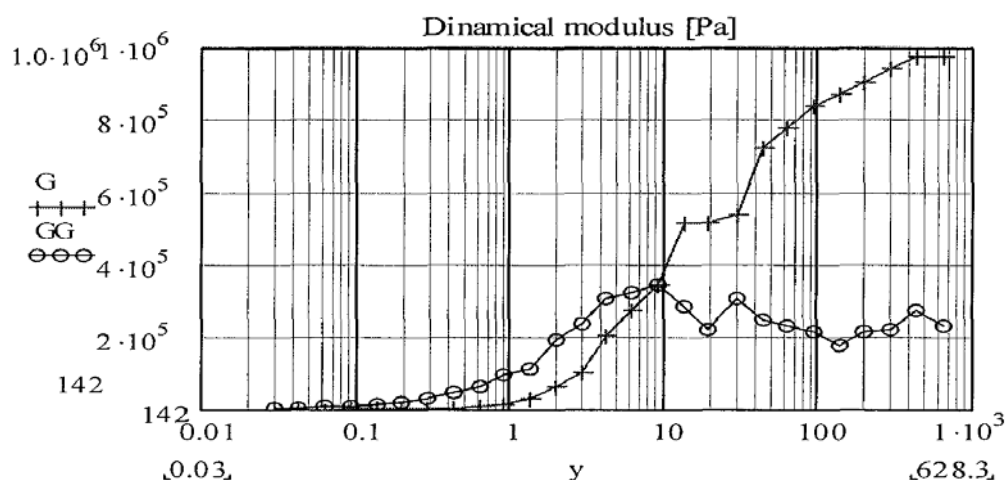In fig.6.1 the graphs of functions $G'(\omega)$ and $G''(\omega)$ are exhibited.

Figure 6.1: Dynamic moduli of storage $G'(\omega)$ and loss $G''(\omega)$. Polybutadiene. T=40°C. Amplitude of deformation $\gamma = 0.005\%$.

Let us take the non-linear model of viscoelastic behavior of given material as integral model with Fredholm's operator of the first kind

$$\sigma(t) = \int_{-\infty}^{t} G(t - \tau)\gamma(\tau)d\tau \tag{6.1}$$

Here $\gamma(\tau)$ is the gradient of deformation rate, $\sigma(\tau)$ is the stress, $G(s)$ is the relaxation modulus. Identification of model (6.1) for description of behavior of above media has been taken at the previous stages of work.

In the fig.6.2 is shown the outlook of input signal as rectangular impulse with amplitude $\gamma = 0.005$, the reaction of which we would like to identify.
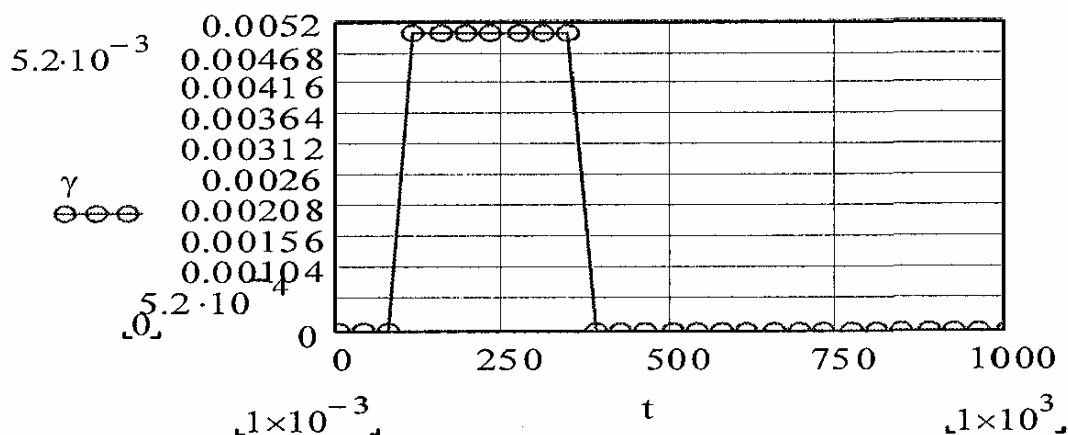

Figure 6.2: The input training signal.

As the wishful output signal let us take function $\sigma(t)$, which is exhibited in fig.6.3.
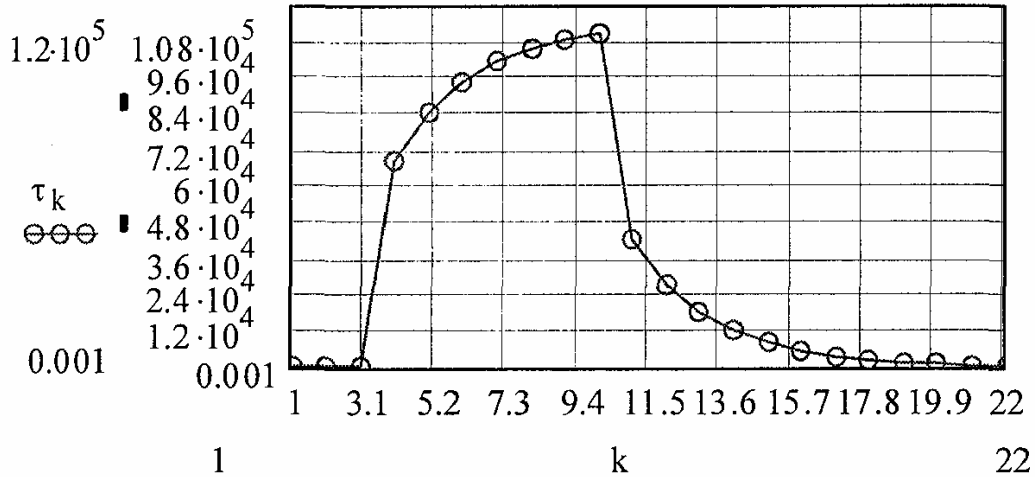
220

Figure 6.3: Dependence $\sigma(t)$ calculated according to expression (1).

Conventionally takes the model (6.1) as real object and neural network of this object must be construct and ground. The initial information for synthesis of network consist in a limited multiplicity of the input and output signals, that is, consists of a priory uncertainty (ill-posed by Hadamard the algorithms of adaptation and training).

6.1.1. Adaptation and training of neural network.

Let us to consider some general conditions, which we can meet during the procedure of synthesis of neural network.

Designation number of layers of network and number of neurons of layer is very important problem. After that it is necessary to fix the values of weights and displacements, which minimize the mistake of solution. It is attained by means of procedure of training of network. By analysis input and output signals, weight and displacements of the networks are installed automatically such a way, that it will be possibly to minimize the discrepancy between wishful signal and output signal. This discrepancy is a mistake of training. Thus, procedure of training we can characterize as process of matching of parameters for the model or phenomena, which is realized by neural network. The mistake of training for given configuration of neural network is calculated by comparison all output values with wishful values. Above discrepancy let us to form so-called function of mistakes, that is, criterion of quality of training. Usually this function is taken a sum of quadrates of mistakes.

Algorithm of training of neural network is similar to algorithm of scan of global extreme of the multi variables function. During the training of network a function of mistakes has to come down.

6.1.2. Construction of linear stationary neural network.

Let us to consider further a procedure of adaptation and training of neural network, which must be used for solution of linear operation.

221

If a real system is linear or closed to linear, that linear neural network can model this system with very small error. Let as further to discuss a problem of synthesis of neural network for stationary model and for non-stationary model.

We will consider a real object (polybutadiene at 40°C) which is deformed in linear area of deformation (small deformation $\gamma = 0.005$). Gradient of given deformations and appropriate response as relaxation of stresses show in figs.6.4 and 6.5.
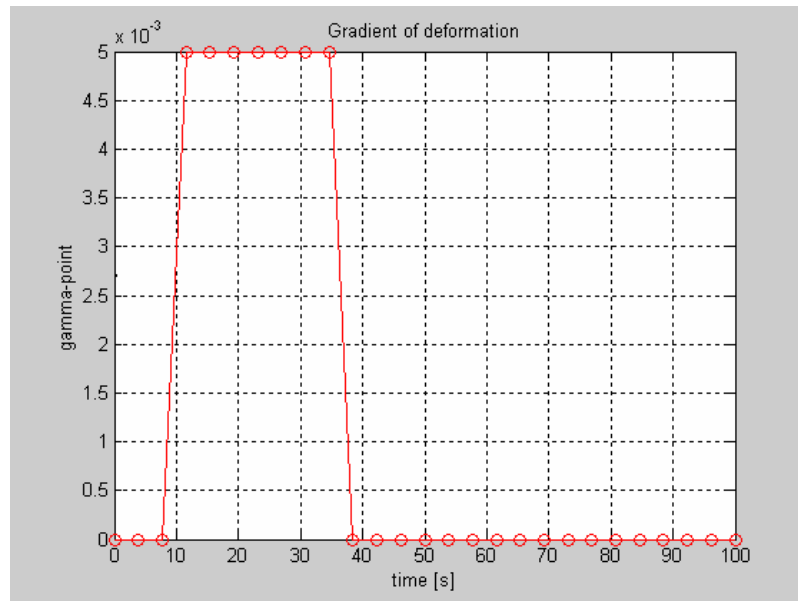

Figure 6.4: Gradient of given deformation. Polybutadiene. T=40°C.
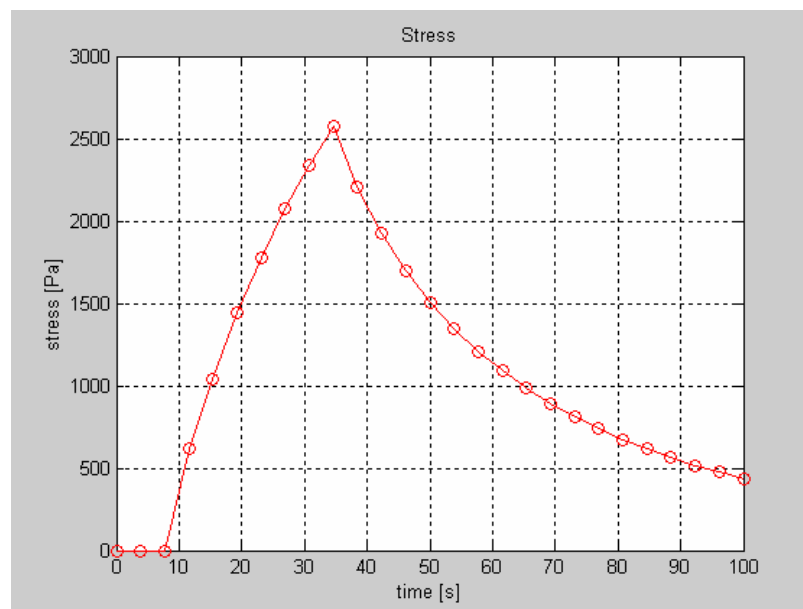

Figure 6.5: Relaxation function. Polybutadiene. T=40°C. $\gamma = 0.005$.

It is required to train a linear neural network so that, it could be describe stress-strain condition of polybutadiene at small deformation. Herewith, what ever additional information besides input and output signal

as strains and stresses could not be allowed. A problem consist in selection of order of network by means of summation the elements of retardation.

In order to construct above neural network firstly the model of 3-d order has trained and qualified the errors of those process. Because the errors of such kind model were bigger than it is allowed, an automatically increasing of complexity by means of extension the elements of retardation and appropriate synaptic connections was happened. After that a bunch of models from 6-th up to 20-th order has been made and tasted. Hierarchy of modes has stopped automatically after approaching to minimal error of training. Herewith the order of models has been limited by 24 numbers of elements of retardation. Note, that further enforced increasing the grade of model above 24-th elements leaded to ill-posed model. The last one is equal to ill-posed by Hadamard's integral model.

In figure 6 exhibits output signal of of 24-th order network and experimental data for real object (polybutadiene) which has been identified by above network in case of identity of input signals. As it can see from figure 6 the output signals coincide.
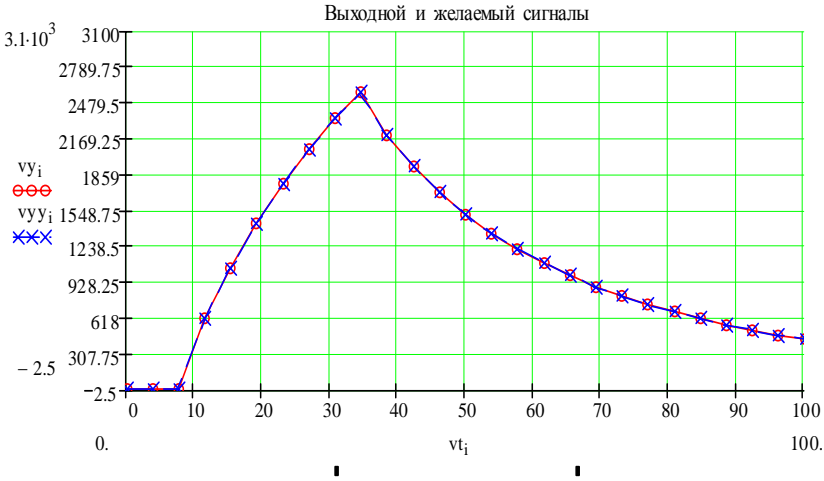

Figure: 6.6. Matching of output (o) and wishful (x) signals for 24-th order neural network.
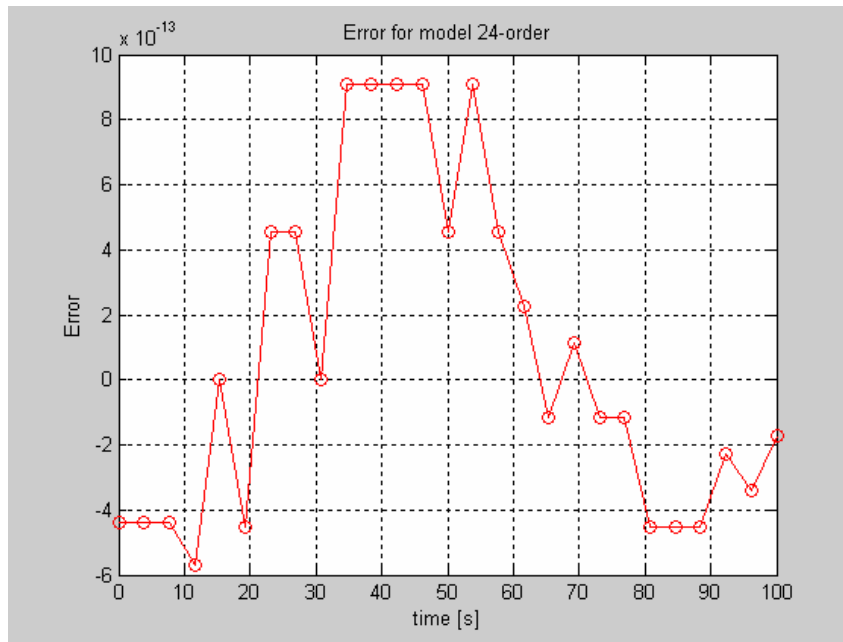
Figure: 6.7. Errors of training for 24-th order neural network.

In fig.6.7 exhibits the graph of errors of training. Thus, to describe a behavior of viscoelastic media at small (linear) deformations one can used the neural network model of 24-th order complexity. The model proposed consists of only one layer of neurons with linear functions of activation and with appropriate number the elements of retardation. It was shown, that above model successfully manages with problem of identification of linear stress–strain conditions such sort of viscoelastic object as polybutadiene. Herewith, there are not required any a priory information about materials functions, relaxation moduli, relaxation spectrums, dynamical moduli, differential or integral equations.

6.2. LINEAR NON-STATIONARY CLASSICAL MODEL.

At previous stages of work, using some experimental data it was stated, that at finite (non-linear) deformations a viscoelastic medium could not described by means of linear integral model which has been proposed for small (linear) deformations. Developing above approach for finite deformations the non-linear model, based on the integral operator Hammerstein's type, has been offered by the authors, and an appropriate algorithm of its identification on the basis of Tikhonov's smooth functional has also been synthesized. Statistical algorithm of identification, which figure a method of regularization for Hammerstein's operator on the base of criteria Byes, we have also constructed. Taking into account a complexity evaluation of function of non-linearity in Hammerstein's operator according to data of traditional real experiments the bit-linear approximation to construct a non-linear model has been proposed. Above model let us to identify the model of viscoelastic behavior up to large values of deformations leaded to alteration of relaxation characteristics by form and by location axis of relaxation times.

It is important, that in above mentioned case it was considered a problem when relaxation modulus of viscoelastic medium depended on tensor gradient deformation only and did not depend on temperature. But, a

224

synthesis of model of viscoelastic medium, when the relaxation modulus is a function of temperature is also important. In both cases it is stated, that relaxation modulus of medium is calculated from relaxation spectrum.

Earlier, we accepted, that non-linear behavior of medium from phenomenological point of view is considered by elements of Maxwell. The last elements have to include the non-linear elastic components. A relaxation spectrum has formed by non-linear tensor function on elastic coefficients of Maxwell's elements, but components of viscosity have been stable. Below we also consider a happening of small deformation, when relaxation spectrum does not depend on tensor of gradient of deformation, but an alteration of temperature changes both the shape and the location about axis of relaxation times of spectrum (because of alteration the coefficients of viscosity in Maxwell's elements). Such case we conditionally will be call as linear non-stationary on time.

Let us shortly to analyze a behavior of linear non-stationary classical model.

We accept, that dynamic moduli of storage $G'(\omega, T_k)$ and losses $G''(\omega, T_k)$ by $k = 1,..., N$ have been evaluated by constant temperature T_k and frequencies ω (Ferry J.D., 1980). Using the experimental data, it is easy to evaluate the relaxation spectra h, using the solution for ill-posed by Hadamard equations (6.2) and procedure of regularization (Yanovsky Yu.G., Basistov Yu.A. and Siginer D.A., 1996).

$$G'(\omega, T_k) = \int_0^\infty h'(s, T_k) \frac{\omega^2 s^2}{1 + \omega^2 s^2} \mathrm{d}(\ln s)$$

$$G''(\omega, T_k) = \int_0^\infty h''(s, T_k) \frac{\omega s}{1 + \omega^2 s^2} \mathrm{d}(\ln s), \quad k = 1,..., N \tag{6.2}$$

$$h(s, T_k) = \mu h'(s, T_k) + (1 - \mu) h''(s, T_k), \quad \mu \in (0,1) \tag{6.3}$$

Coefficient μ depends an vicinity of experimental and calculated moduli, s is the relaxation time. Using (6.3) it is easy to calculate the complex of relaxation moduli

$$G(t_k, T_k) = \int_0^\infty h(s, T_k) \exp\left\{-\frac{t_k}{s}\right\} \mathrm{d}(\ln s), \quad t_k \in [u_k, u_{k+1}) \quad by \quad T = T_k \tag{6.4}$$

Non-stationary relaxation modulus one can qualify as

$$G(t) = \sum_{k=1}^{N} G(t_k, T_k), \quad t \in [u_1, \ u_N] \tag{6.5}$$

Above non-stationary relaxation modulus begets non-stationary linear classical model in according to equation

$$\boldsymbol{\tau}(x,t) = \int_{-\infty}^{t} G(t-s) \frac{\alpha \mathbf{D}\mathbf{C}_t^{-1}(\mathbf{x},s)/\mathbf{D}s}{(\alpha-3) + \beta I + (1-\beta) II} \mathrm{d}s \tag{6.6}$$

where $I = tr\mathbf{C}_t^{-1}$, $II = tr\mathbf{C}_t$, $\alpha > 0$, $0 \le \beta \le 1$, $\mathbf{C}_t = \mathbf{F}_t^T \mathbf{F}_t = \mathbf{C}_t^T$ is the tensor of Cauchy-Green and matrix of Yakobi.

Let us further to debate reaction of non-stationary model (6.6) on consistency of input impulses (gradient of deformations) as dependence, which represents in fig.6.8.
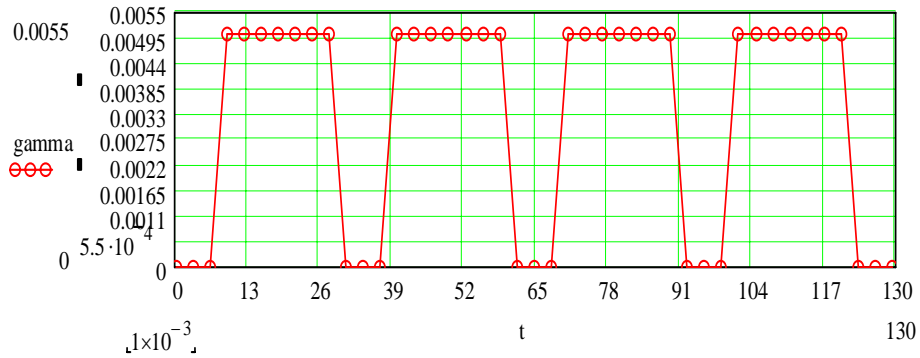
Figure 6.8: Consistency of impulses the gradient of deformations.

Reaction of non-stationary model (6.6) exhibits as a sequence of graphs the relaxation of stresses, herewith each relaxation curve characterizes the same object at different temperature. This reaction shows in fig.6.9.
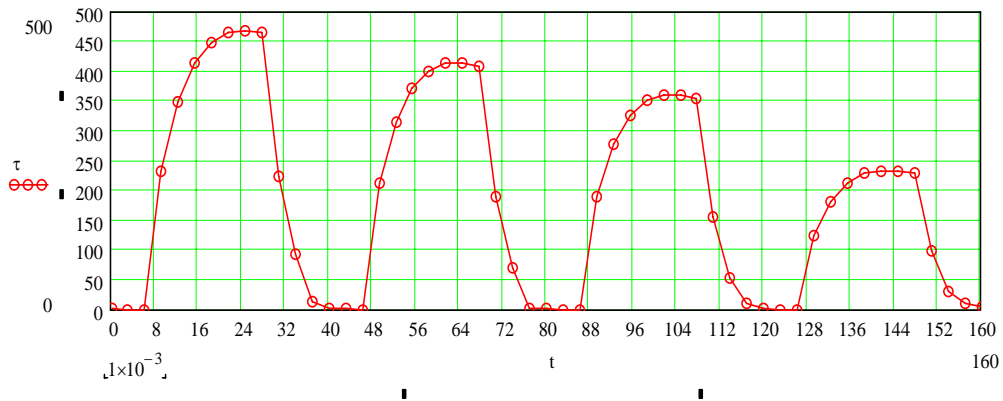

Figure 6.9: Relaxation function of linear non-stationary model.

From fig.6.9 one can see in order to realize the linear non-stationary model it is necessary to get some additional information about interval of temperature, where consistency of stationary models approximates non-stationary model. In a certain sense it is the bit-stationary approximation of non-stationary model. An absence or a limitation additionally information leads to uncertainty, which influence on accuracy of solution of equation (6.2).

Above drawback of integral models with kernel, which based on relaxation spectrum, enforce us to reqruit some new models for control of dynamic processes, in particular, neural networks because of the high-operation and fitness to parallel calculations of those. Such sort of models able solve the problems of control to dynamic objects without algorithmization of process. They can be used for procedure of training and adaptation of model.

6.3. LINEAR NON-STATIONARY NEURAL NETWORK MODEL.

Above we already discussed stationary non-linear neural network model of viscoelastic media. Let us to consider further a problem of synthesis of neural network model for linear non-stationary object, when the object can change its characteristics during the time. To synthesis a neural network let us to accept, that real object contents next recurrent expressions

$$y(n) = 0.5\,y(n-1) + r(n), \quad 0 \le n \le 800,$$
$$0.9y(n) = 0.6\,y(n-1) + r(n), \quad 801 \le n \le 1200.$$

(6.7)

Let us to accept, that input signal of that object is equal $r(t) = \sin\big(8\sin(4t)t\big)$ with time of quantum 0.005 second on the length [0,6] seconds. Graph of this signal shows in fig.6.10.
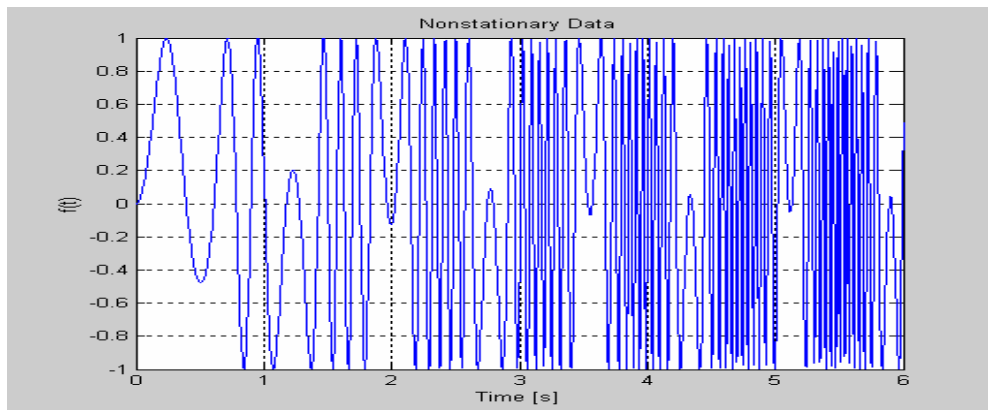

Figure 6.10: Training input signal.

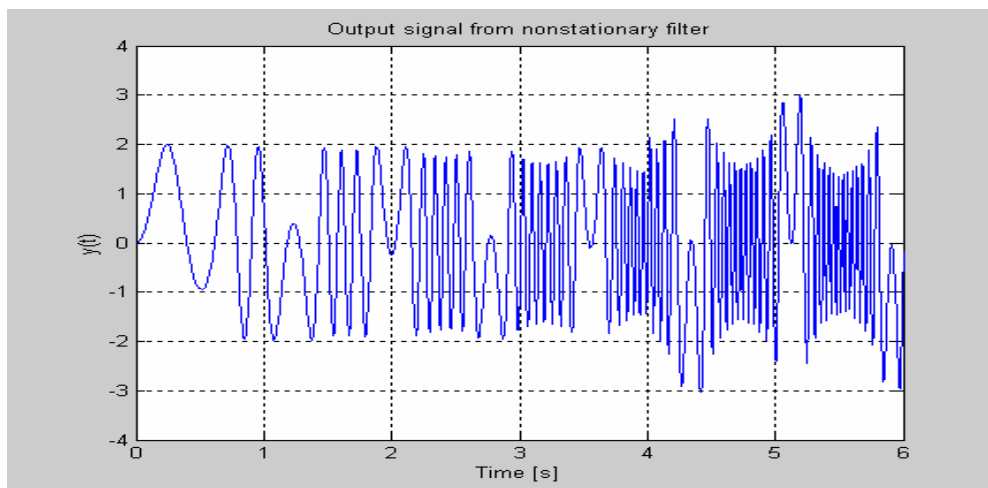Output signal of non-stationary model (6.6) exhibit in fig.6.11.

Figure 6.11: Output signal of non-stationary model (6.7).

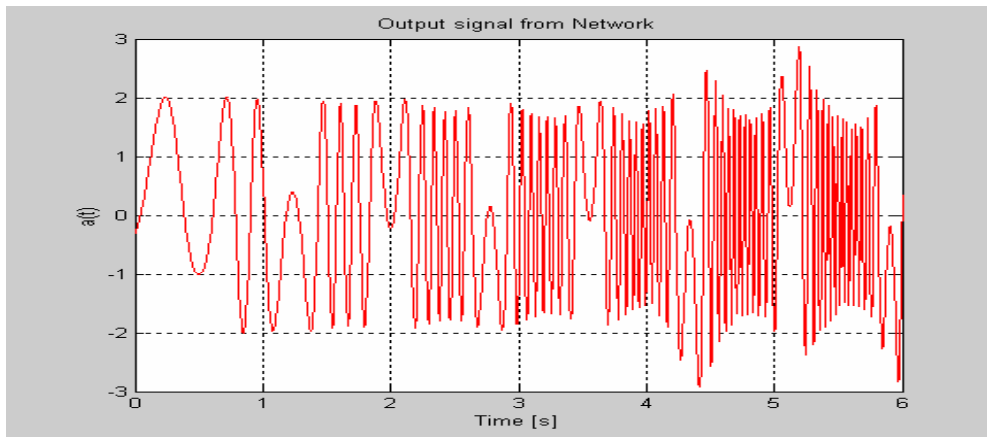Output signal of neural network one can see in fig.6.12.

Figure 6.12: Output signal of neural network.

From comparison figs.6.11 and 6.12 it is evidently that graphs of signals coincide. It indicates, that network has successfully installed on wishful non-stationary signal from outlet of model (6.7).

A structural schema, which has been synthesized for above problem exhibit in fig.6.13.
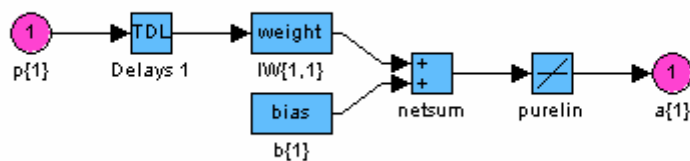
Figure 6.13: Structural schema synthesized neural network.

Weight and displacement after adaptation of network takes values IW{1,1}=[0.4926, 2.3787], b{1}=[-0.3100].

From fig.6.13 it follows the network does not content a consistence of stationary models for non-stationary signal and, unlike (6.7), deputizes unique display «input-output», which has been realized by expression

$$a(n) = 0.4926 \, r(n) + 2.3787 \, r(n-1) - 0.3100.$$

Below, in fig.6.14, we exhibit the function of mistakes as residual values of output and wishful signal for each time.

Figure 6.14: Function the mistakes of training of neural network.

From fig.6.14 it follows, that neural network more precisely reproduces the first stationary model (6.7), working at tim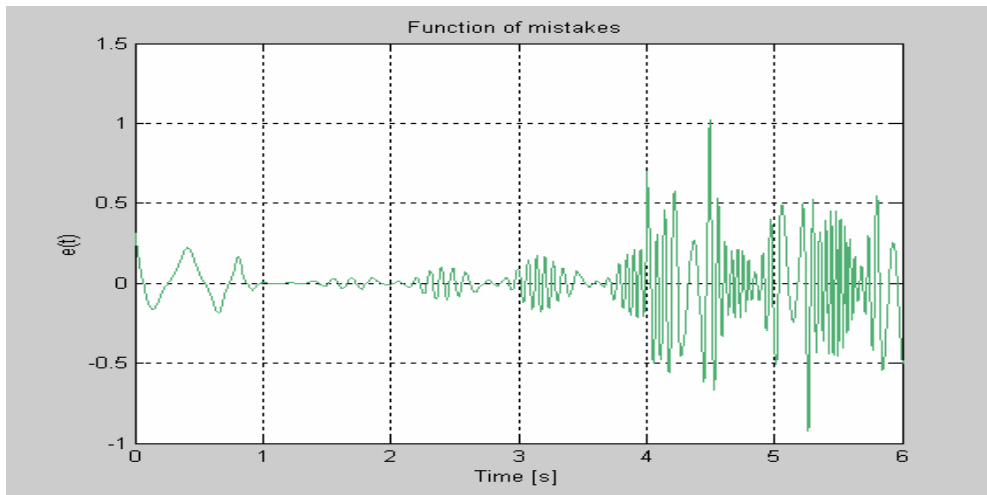e interval [0,4] seconds. The second stationary model (6.7), working in diapason [4,6] seconds is much worse reproduced by network. On the whole, workability of linear non-stationary network model one can state as satisfactory.

6.4. USING THE NON-STATIONARY NEURAL NETWORK MODEL FOR DESCRIPTION OF BEHAVIOR OF VISCOELASTIC MEDIUM.

As a training material for neural network model let us take the figs.6.8 and 6.9, which have been calculated by classical linear non-stationary model according to data made by Rheometre Rheostress 150 (HAAKE) as dynamic storage $G'(\omega)$ and losses $G''(\omega)$ moduli.

In fig.6.15 let us to show the structural schemes of synthesized network analysis of which will be made below:
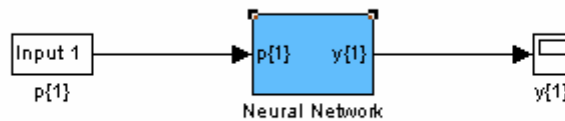
Figure 6.15a: General structural schema of network.
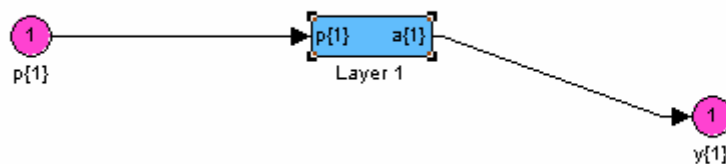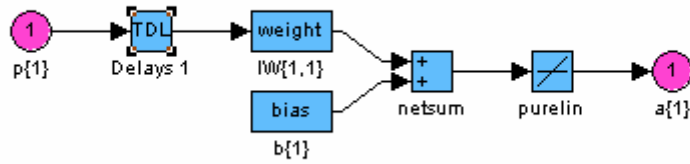
Figure 6.15b: Structural schema of neural layer and neural network.
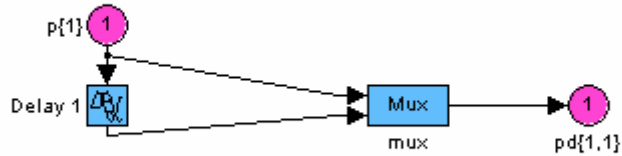
Figure 6.15c: Structural schema of weight summation with one element of retardation.

After training an output signal has been synthesized by network (fig.6.15) (see fig6.16 (x)). Therein displays also a dependence (o), made on the base of non-stationary model.
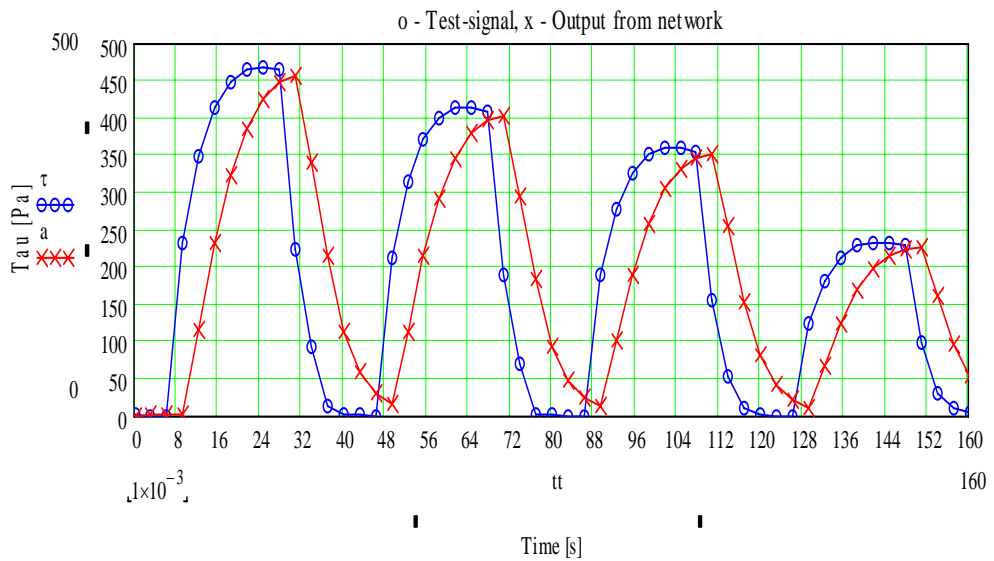
Figure 6.16: Wishful (o) and extradited (x) signals of neural network, which stores one element of retardation.

From matching signals it is easy to see a retardation around time signals from outcome of network with respect of wishful signal, that stipulates the big enough mistake of training in equable metrics (see fig.6.17).
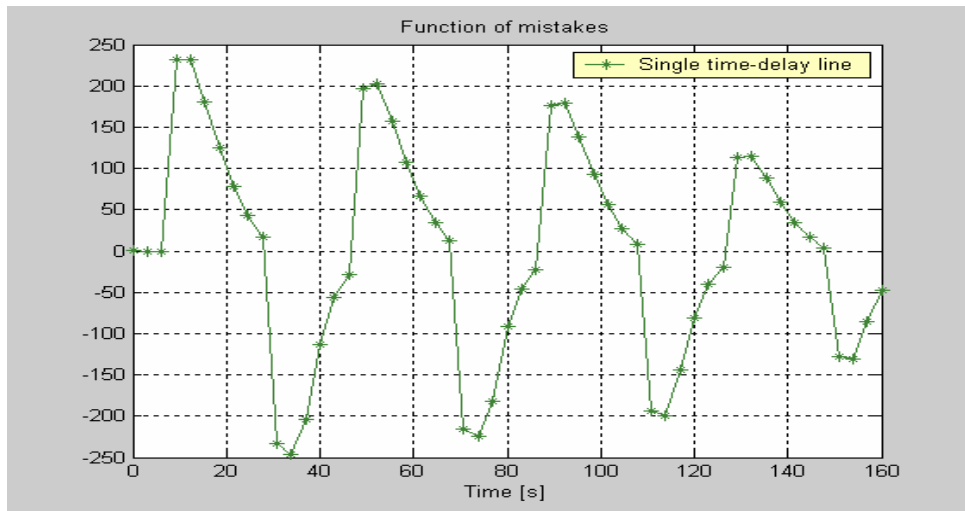
Figure 6.17: Function of mistake of training in equable metrics for network with one element of retardation.

In fig.6.18 represents the structural scheme of retardation with 12-th elements, but in fig.6.19 represents the function of mistake.
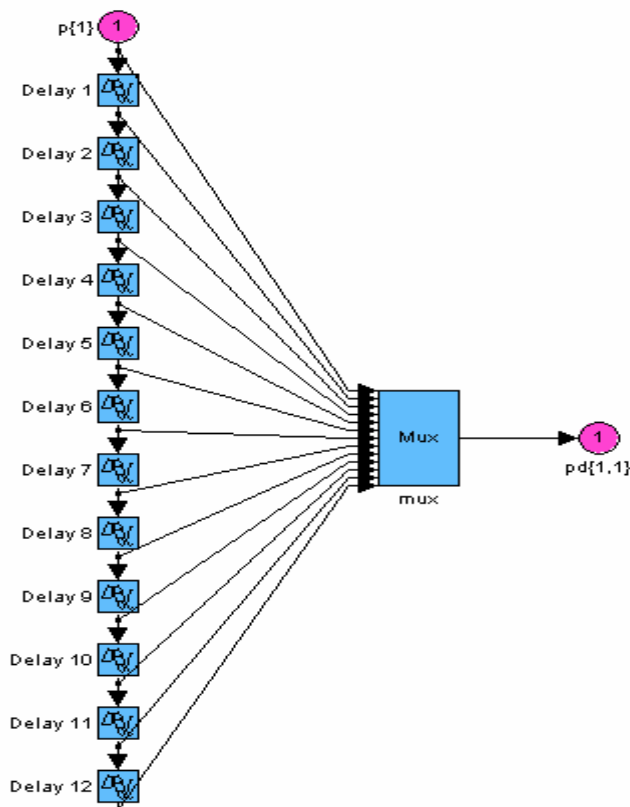
Figure 6.18: Block of weight summation of network with 12-th elements of retardation.
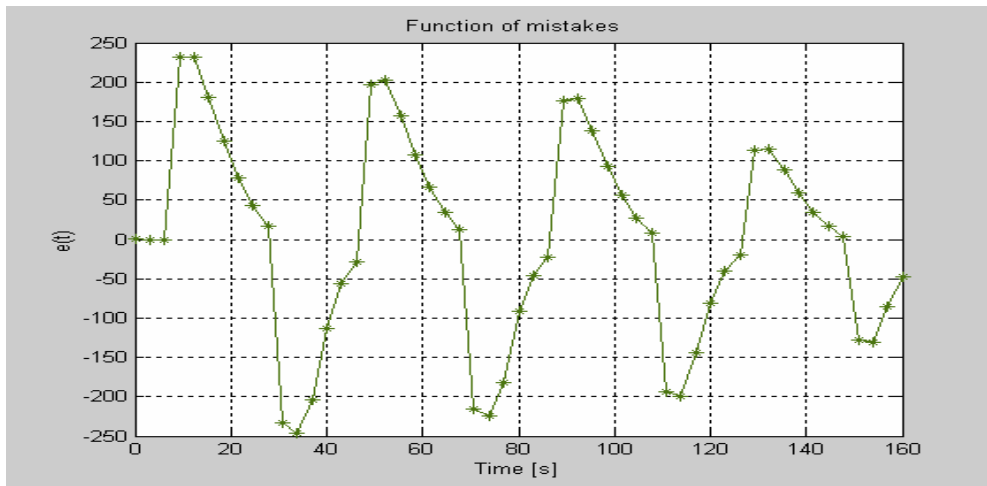
Figure 6.19: Function of mistakes the network with 12-th elements of retardation in equable metrics.

It is easy to see from figs.6.17 and 6.19, that function the mistakes of training of network does not change. Accordingly output signal of network did not change.
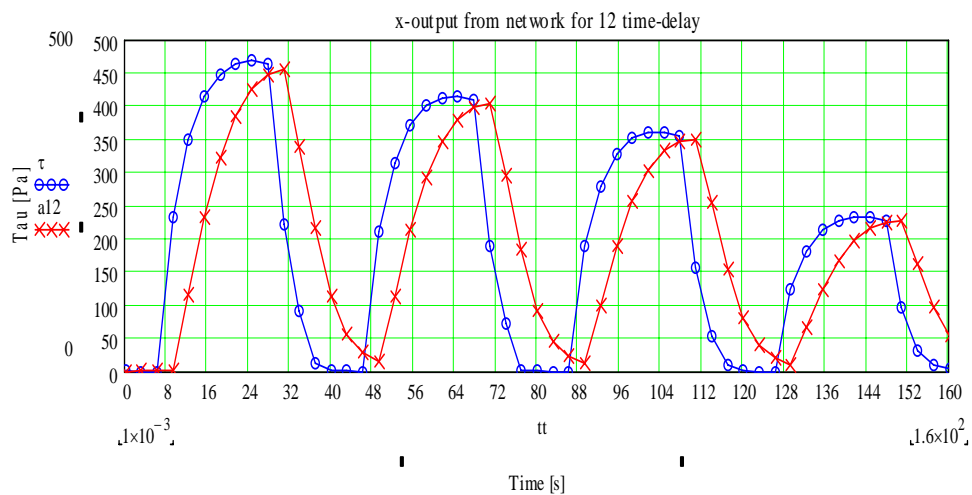
Figure 6.20: Wishful (o) and extradited (x) signals of neural network with 12-th elements of retardation.

From matching graphs in figs.6.16 and 6.20 it follows, that increasing of number of elements of retardation in structure of neural network does not influence on accuracy of its operation. One can mark, that in above test problem, exhibited for modeling of two stationary filters, such retardation in signals did not observe. One can propose, that it is necessary to increase a dimensions of vectors in experimental data. Because the ability of experimental equipment is limited, we made a solution to increase a number of points of observation in experiments by means of interpolation of data. It was made the increasing dimensions of vectors of data up to 800. Above expanded data one can see in figs.6.21 and 6.22.
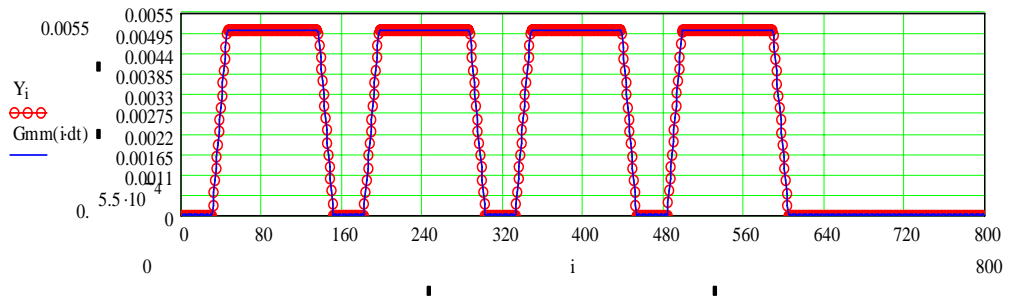
Figure 6.21: Expanded interpolated input signal (gradient of deformation).
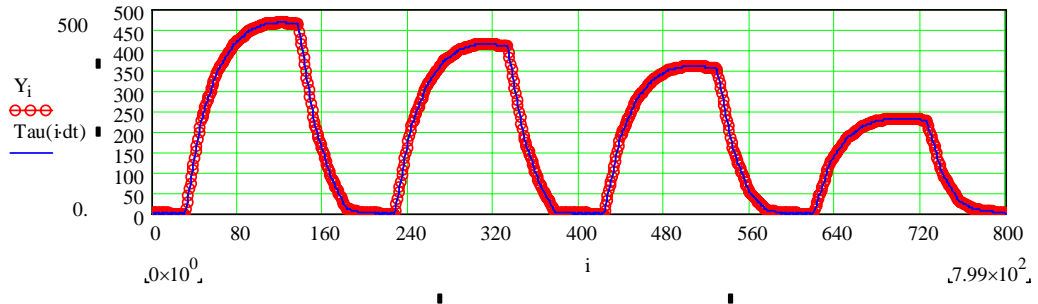
Figure 6.22: Expanded interpolated wishful signal (stresses).

Output signal of neural network for expanded by dint of interpolation experimental data represent in fig.6.23.
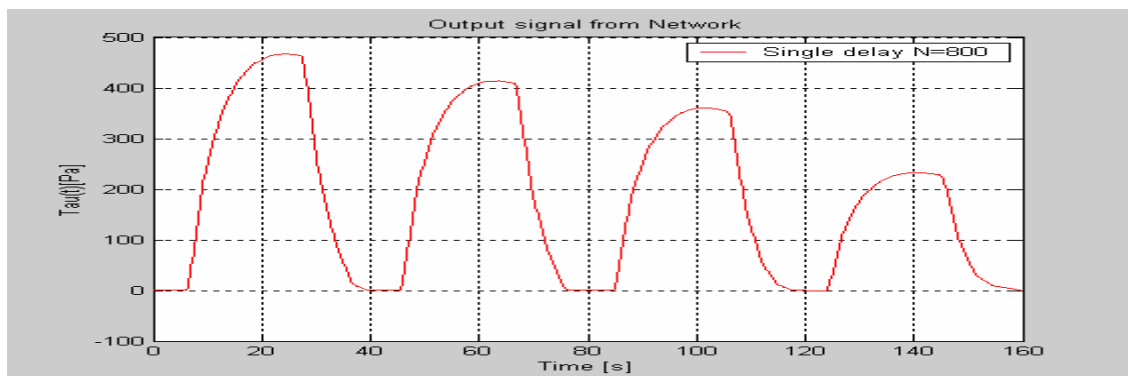
Figure 6.23: Output signal of neural network model with one element of retardation by expanded dimensions of vectors of data.

From fig.6.23 one can see, that retardation of output signal, we observed earlier, with respect to wishful signal has disappeared. The network is fairly well reproduces non-stationary model even by one element of time retardation. Function of errors above network exhibits in fig.6.24.
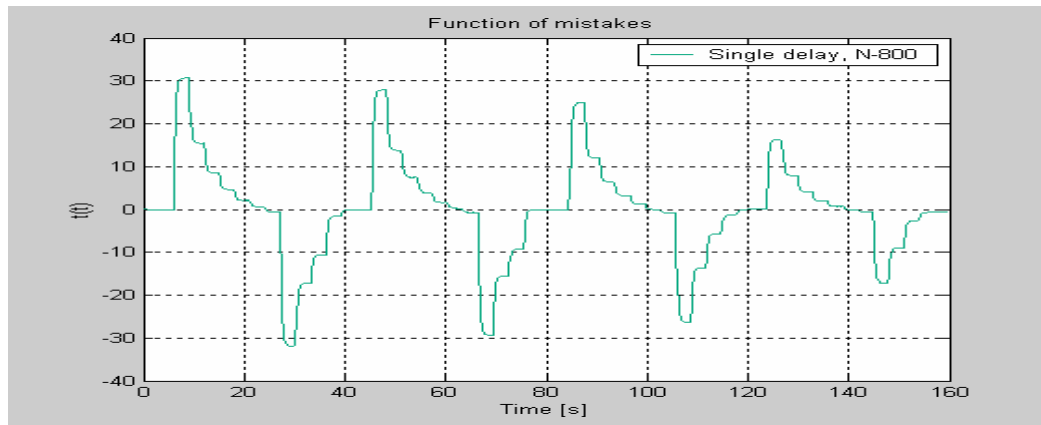
Figure 6.24: Function of errors of network with expanded experimental data.

From matching of figs.6.24 and 6.19 one can conclude, that errors in fig.6.24 practically one order less.

6.5. CONCLUSIONS.

1. Classical non-stationary model of behavior of viscoelastic media is constructed on the base of integral or differential equations, depending on parameters non-stationary (for example such parameter as temperature). Non-stationary model step by step switches available stationary model, in dependence on appropriate intervals of values of parameters of non-stationary.

2. Neural non-stationary network model does not require an entering of additional parameter of non-stationary and, therefore continuously reproduce a wishful non-stationary signal. The model does not synthesized as a set of stationary models, which depend on parameter of non-stationary, and it is the main advantage of the model.

3. Neural network model is simple enough both in the constructive and in the algorithmically performance in compare with classical case. It has the bigger mobility and let us to use the parallel calculations.

4. Synthesis and analysis of neural work model to describe the behavior of viscoelastic media shows, that to accomplishment of required accuracy of work for neural network without using the feedback (small mistake of training), it is necessary an interpolation of experimental data in order to expand a dimension of vectors.

REFERENCIES.

1. Ferry J.D., Viscoelastic Properties of Polymers. Wiley: New York, 1980, 641 p.

2. Yanovsky Yu.G.,Basistov Yu.A. and Siginer D.A., Linear Inverse Problems in Viscoelastic Continua and a Minimax Method for Fredholm Equation of the First Kind. Int. J. Engng Sci., v.34, N11, pp. 1221-1245, 1996.

7. PERSPECTIVE OF THE FURTHER RESEARCHES WITH USE OF THE RESULTS RECEIVED IN WORK UNDER PROJECT. OFFERS OF VARIANTS OF THE FURTHER RESEARCHES

In this section the further directions of researches are briefly formulated. These researches can be received on the basis of the perspective preliminary theoretical workings received within the framework of the project. Certainly, these theoretical workings did not showed all in reports under the project as their subjects is beyond problems formulated in the Work Plan of project.

The following directions of researches are offered to our colleagues from the USA as the formulation of concrete themes of researches at the further colaboration. After a choice of concrete directions of the further researches the detailed description of corresponding stages of researches and the plan of works can be formulatedd.

As a result it is possible to formulate and briefly describe the following directions of probable researches which realization is guaranteed by both theoretical reserve and available base for experimental researches.

7.1. STUDYING OF THE MECHANICAL PROPERTIES OF NANOCOMPOSITES

It is suggested to continue the study of the mechanical properties of nanocomposite in the following directions:

1. To continue studying the influence of the intermediate phase to the effective properties of the composite. Such a phase may appear during polymerization process in the form of thin or thick shells surrounding nano-particles. The study was commenced during the project and a method of estimation the influence of the intermediate phase properties was suggested, based on consequent consideration of contribution of the inclusions and intermediate phase into the effective properties. It is suggested to develop this approach to account for anisotropy effects and various types of space distribution.

2. To study the influence of the area of contact between the matrix and inclusions. Researches on this and previous point may help to understand such processes as intercolation and exfoliation and their influences to the effective mechanical properties of the composite.

3. To study the influence of the matrix anisotropy and to obtain a solution for effective elastic properties of composite with anisotropic matrix (at least for some important particular cases of anisotropy). For the last years, a lot of attention has been devoted to the problem of influence of inclusions of various shapes to the effective properties of composites with *isotropic* matrices. At the same time much less attention has been given to consideration the anisotropic matrices. This is mainly due to the fact that the latter case need much more complicated calculations involved, such that the general analytical solution for this case in the closed form is still unknown. Meanwhile, to obtain such a such a solution, at least for some important particular cases of matrix anisotropy, would be of great interest due to:
    -   such a solution is of importance itself;
    -   for calculating effective elastic properties of composite even on the base of isotropic matrix such methods as self consistent method and differential self consistent method involve solutions for an inclusion in the anisotropic matrix.

4. In the applied relation researches connected with development of numerical - analytical design procedures of effective nanocomposites characteristics are perspective on the basis of method Eshelby (1957,1961) and exact Eshelby type solution, Mura (1982), Kovalenko and Salganik (1977) method with account of scale effects - local interactions of adhesion-cohesion type. These techniques allow generalizing effective design procedures in case of nanocomposites, taking into account adhesive

interactions and local interactions of cohesion type correctly. Use of well fulfilled differential scheme to such modified method will allow using it for enough big concentration of the inclusions up to 20-30 %.

Here it is foreseen two stages. The first is connected with receiving of generalized Eshelby matrix not only for a case of local effects of cohesion type (this solution is submitted in reports under the project), but also on more general case which is taking into account a full spectrum of adhesion-cohesion local effects. This, fundamental problem by present time is actually solved. The second stage is connected with solution of the identification problem of three model parameters which being in charge of cohesive and adhesive interactions on the basis of the solution received with the help of generalized matrix Eshelby (the analytical solution) and with use of optimum control methods (a method of the conjugate gradients, automatic differentiation, etc.). Use of special numerical quadratures for effective calculation a component of Eshelby matrix in spatial statement for inclusions of special forms can be supposed.

5. The next direction is connected to studying thermodynamic properties (heat conductivity, thermal capacities, coefficient of temperature expansion, damping factor and so forth) of the damaged mediums on the basis of four-dimensional model [Belov P.A, Lurie S.A. About Model of the Heat Transfer in the Dynamically Deformable Mediums // Mechanics of composite materials and structures. ,2000, т.6, N 3, c. 436-444;   Lurie S.A, Belov P.A, Kalamkarov A. New Fenomena of the Heat and Mass Transfer for Dynamically Deformable Mediums // Book of Abstract of Annual Meeting GAMM 2001, ETH Zurich, 2001, February 12-15, p.84;   Lurie S., Belov P. Variation Model of Nonholonomic Mediums // Mechanics of composite materials and structures. ,2001, т.6, N 3, p. 436-444.]. The studying of diffusion processes on the basis of analogy to thermodynamic processes (heat conductivity) is supposed. Bases of such research are medium models with scale effects and their generalization on nonconservative mediums.

7.2. ADHESION INTERACTIONS

1. The following directions of activity seem to be most important within the framework of the model of polymer-nanotube adhesion and the extension of this project:

   1) taking into account the compliance and strain of the polymer matrix;
   2) analysis of an influence of the molecular structure of the jointed materials on the thickness of the interface layer;
   3) consideration of the nanofibers with a scrimp and the nanofibers bundles;
   4) analysis of nanofibers compression taking into attention the nanfiber buckling;
   5) analysis of an influence of the interactions between the nanofibers, nanoparticles and the interface layer in the polymer matrix on the mechanical properties of nanocomposites;
   6) analysis of an influence of the adhesion between matrix and nanofiller on the fracture toughness of nanocomposites.
   7) development of techniques of an estimation of adhesive properties using the correct solution of problems of identification of adhesive parameters on the base of experimental tests fro macromechanical characteristics of a composite, and by realization of direct tests of adhesive properties of materials (measurement of corners of a meniscus, use of effect capillarity and definition of the friction factors)
   8)   The further studying of superficial properties is possible in the following directions:

       1. Development of the nonlinear theory of adhesion for studying conglutination mechanisms, agglutination and so forth also managements of them. Adhesion as processes of buckling failure (consequence - adhesive strength)

2. ` Research of the physical phenomena (for example absorption, filtrations and so forth) which can be modeled as special effects of the constructed medium model with conserved dislocations. Management of superficial properties. Designing of filters, chemical reactors, cleaning devices and so forth. Development of porous medium models, designing of porous elements (porous membranes and so forth).

7.3. MODELLING OF THE DAMAGE ACCUMULATION AND OTHER APPENDICES

1. Correct procedure of account of the damage accumulation based on the general model of mediums with conserved defects (the Annual report 2005) represents also practical interest. We offer the direction of researches where the new correct way of the account of dislocation damage as on mechanical characteristics of a material as a whole also on its durability in real conditions will be fulfilled.

   This procedure is based on strong asymptotic approach and takes into account local scale effects peculiar to development of failure in the material.

   Developed asymptotic procedure provides constructions of the basic asymptotic process and local processes in parallel.

   -The basic asymptotic process allows to receive estimations for integrated characteristics of effective modules of elasticity, to take into account an accumulated damage in a material due to concentration of various type dislocations (in the Final report it is specified all possible types of dislocations, is given their classification) in a vicinity of generalized heterogeneities (top of crack, contact zones of different phases and so forth). For this purpose within the framework of any numerical algorithm of the solution of a direct problem of the theory of elasticity the iterative scheme of loadings recalculation with the account of failure can be used. (see the final report)

   -Local asymptotic processes will allow establishing parameters of failure and character of damage distribution (damage redistributions). Besides, local asymptotic processes will allow estimating the damage influence on local distribution of stresses, for example, in contact zones in the phases. It is especially important for damage strength estimation of composite materials with nanoinclusions. As the special case the failure determined by special type of dislocations - porosity is modeled.

   Let's note, that preliminary researches at modeling of zone of plasticity (as damage zones), in vicinities of the top of cracks and its evolution depending on load conditions, variability of a field of the stresses caused by concentrators of stresses, showed the good results.

   Thus, it's offered the direction of researches where the new correct way of the dislocation damage account as on rigid characteristics of a material as a whole, also on its strength in real conditions will be fulfilled.

2. Generalization on a dynamic case of the theory of defects is one of the important directions of the further researches. Creation of a theoretical basis is of interest for studying of nonclassical properties of the damaged medium and nanocomposites using the resonant methods. For this purpose it is necessary to formulate a variant of geometrical theory of defects for four-dimensional space when time is equal in rights coordinate, instead of model parameter. This direction already develops; some results are stated in works:

   1. Lurie S., Belov P. About Model of the Heat Transfer in the Dynamically Deformable Mediums // Mechanics of composite materials and structures. ,2000, т.6, N 3, с. 436-444;
   2. Lurie S.A, Belov P.A, Kalamkarov A. New Fenomena of the Heat and Mass Transfer for Dynamically Deformable Mediums // Book of Abstract of Annual Meeting GAMM 2001, ETH Zurich, 2001, February 12-15, p.84;
   3. Lurie S., Belov P. Variation Model of Nonholonomic Mediums // Mechanics of composite materials and structures. ,2001, т.6, N 3, p. 436-444.

3. Studying of defects dynamics in continua in view of limited speed of interactions distribution ofvarious types also is represented and being rather perspective. The created theoretical base, numerical - analytical methods of the solution and scientific workings will allow to study here <relativistic> effects in defective mediums. The interesting practical results can be received from studying of abnormal effects in heterogeneous materials with nanostructures, connected with limited speeds such as shock waves, Reley's waves and so forth and also their interaction with structure of a material. Significant interest represents the studying of essentially located packages of sound waves (phonons) and their interaction with nanostructures. This research is connected to use of resonant methods, with development of new methods of nondestructive check when by results of interaction generated phonons with structural parameters it is possible to study properties of materials.

4. Within the framework of the same approach on the basis of multiparametric models of the
defectness mediums it is offered to develop a technique of the specified estimation and design of the dissipative characteristics of viscoelastic materials. For this purpose, first of all it is necessary to receive within the framework of a kinematic variational principle the generalized equations of Navier-Stoks type (generalization of the equilibrium equations on a viscoelastic case) and corresponding generalizations of the moment equilibrium equations, of which analogues does not exist for the viscoelastic medium.

5. Research of the medium(materials and structure) behaviour under loading of the physical fields with high changeability on the coordinates within the framework of models of the high order (taking into account scale effects) is more correct than in view of the classical theory. Additional terms, according to more full description of external influences, enter both into the equations of balance, and in boundary conditions. These terms contain components of gradients of higher order in comparison with classical model. Thus, using of the classical models for the description is high-gradient actions results to "smoothing" of such actions and, in result, in loss of the essential effects connected to the big changeability of acting physical fields. So, for example, at research temperature loading with the high changeability it is shown, that the model of the mediums, which is taking into account scale effects, contains in the equation of balance derivatives up to the third order from a field of temperatures, and in boundary conditions up to the second order. In result, it is shown, that in case of temperature fields with low amplitudes, but high gradients the new effects bringing significant amendments in distribution of syresses take place. Value of the stresses can differ more than on the order in comparison with the values received on classical model.

   The explanation of the effect of superficial cracking for the ceramics under surface coatings is given in case rigidity of a covering exceeds rigidity of ceramics. So, development of researches connected with studying of the materials and structures under loading of the physical fields with high changeability , will allow to receive methods of calculation and designing for the nanocomposites, thin films, protective coatings and so forth, These researches will allow to give techniques of the account of high gradients of external actions on the fields of stresses, to offer the recommendation to technological processes.

6. The algorithm of a block method of multifields can be applied to more complex models of an interphase layer, which include not only cohesion and adhesion effects, but also the associated problems including thermal and electromagnetic processes. On the basis of generalized formula Neiber-Papcovich numerical modelling of processes in composite materials can be considered in view of acoustic interactions.
   Specific finite elements can be constructed on the basis of algorithm of a block method of multifields with the purpose of their application in a traditional method of finite elements.

7.4. MOLECULAR MODELING

The next evolution of the work is proposed in two main directions: scientific – fundamental branch and engineering branch.

1. In fundamental direction:

a. It will be develop the methods and algorithms of molecular modeling (quantum mechanics (QM), molecular dynamic (MD) and Monte-Carlo (MK)) to calculations complex heterogeneous systems consisted of polymeric macromolecules and combination of active fillers for amount of particles under computational calculations above 10^6 (nano- and mezo- levels);

b. It will be expand the three-dimensional object-oriented approach of finite elements method with automatic generation of network to modeling of stress-strain conditions for representative elements of structure of heterogeneous media (perspective composites), consisted of polymeric matrix, combination of active fillers and supplements and interphase layers (micro- level);

c. It will be elaborate the new methods of identifications, that is, theoretical description of non-linear viscoelastic behavior of heterogeneous media, consisted of polymers and active ingredients for control the rheological behavior under processing, in particular, on the basis of neural network approach;

d. An experimental verification of above fundamental results (see a-c) will be made on the basis of contemporary scientific equipment; particularly, atomic-force and tunnel scanning microscopy optical three-dimensional interferometric microscopy, set of rheological tools, stress-strain apparatus, etc.

2. In engineering direction it is important:

a. Studying of dependence of structure, energetic, mechanical properties of nanocomposites consisting of polymer and ultradisperse filler, on the chemical nature and structure, modification of a surface, the size, quantity of interacting particles of filler and polymer. Studying the influence of water on the state of the interface of a complex composite. Studying of ways of formation of composites with in advance set properties. Studying of ways of filler introduction into a polymeric matrix for reproduction of demanded properties of composites. Computer selection of nanocomposite components.

b. Construction of corresponding molecular models of nanocomposite components and their adsorption complexes, quantum mechanical minimization of space structure of these complexes, calculations of microscopic deformation characteristics in microscopic coordinate of deformation and microscopic coordinate of friction approximations. Calculation of microscopic Young's moduli, stress-strain curves, microscopic coefficients of adhesion.

c. A polymeric matrix: rubbers, resins, thermoplastics. Fillers: amorphous technical carbon, carbon particles with a defective surface, various carbon particles with modified surface, fullerenes, carbon tubes, white soot (ultradisperse silicate) and its modified hydrophobic forms, natural clay, in particular, monmorillonite and any combinations two or several fillers.

d. Connection with MD and MK modeling. Construction and optimization in QM approach of initial models for use in MD and MK. Calculation of enthalpic component of interaction energy of particles with the subsequent calculation of entropic component in MD or MK. Calculation of special force fields for fragments of nanocomposite components for introduction of QM-corrected parameters into MD and MK calculation. QM/MM the approach in which the part of system (up to several hundreds atoms i.e. at about area of contact of particles) is modeled more strictly in QM the approach, and other part (up to several thousand atoms of an environment) in faster MM approach. The account of influence of solvent and environment on interaction and mechanical properties of nanocomposite components in explicit (molecular) and implicit (continuum) models.

GENERAL RESULTS

The following results were obtained:

1. On the base of the classical Eshelby's approach the effective solutions for determining effective properties of the composites formed by the elastic matrix and isolated inclusions have been obtained in the closed form. The solutions have been presented both in tensor and matrix forms.

2. A number of important particular cases, for which asymptotical representations are possible, have been pointed out: flat inclusions (nano-plates), and needle-like inclusions (nano-tubes). The combined influence of the shape and relative stiffness of inclusions has been investigated; it has been shown that the presence of two parameters (the ratio of maximal an minimal dimensions of the inclusion and relative stiffness of inclusions) leads to non-uniform limit transition, which restricts the area of applicability of known classical asymptotical formulae. The areas of applicability of asymptotical formulae have been obtained (appears to be for the first time).

3. The influence of anisotropy of the inclusions to the effective composite properties has been investigated (Final Report, 2003). It has been shown that the main influence is due to some particular combinations of elastic parameters of inclusions, and these combinations have been pointed out.

4. The influence of the orientation of inclusions in space have been investigated both for isotropic and anisotropic inclusions. For the composites on the base of nano-tubes three types of space distribution have been considered: random, aligned and transverse (all inclusions lay in parallel planes). The solution for last case appears to be obtained for the first time.

5. The nonlinear influence of concentration has been accounted for with the help of differential self-consistent method and the method of effective field (Mori-Tanaka).

6. The obtained results were compared with the results known from the literature. The obtained results appear to be important as it are, as well as an useful tool for constructing more advanced models such as three-phases models, accounting for the presence of an intermediate layer between the matrix and inclusions.

7. An algorithm for approximate calculating the effective characteristics of three phase composite material formed by the matrix, nano-tubes (or disk-like nano-particles) and surrounding them regions of the third phase is suggested.

8. For the three-phase composite the following problems have been formulated. First, knowing mechanical and geometrical properties of all phases to calculate the effective properties of the composite (the direct problem). Second, knowing elastic properties of the matrix and the composite, to estimate the properties of the Intermediate phase and/or the inclusions (inverse problem).

9. Variants of solutions of both direct and inverse problems have been suggested. Examples of solving both direct and inverse problems have been presented.

10. The algorithm for calculating the effective characteristics of three phase composite material formed by the matrix, nano-tubes (or disk-like nano-particles) and surrounding them regions of the third phase is developed. Variants of both direct and inverse problems are considered for both thick and thin intermediate layer.

11. In the frame of the approach the effects caused by anisotropy are accounted. An example of solving inverse problem has been presented: estimation of the properties of intermediate layer.

12. During the reported period we proposed a mechanical model of the interface adhesion of polymer matrix and nanotubes accounting for the dependencies of the shear stresses between matrix and nanotube versus the main physical-mechanical parameters of the nanocomposite material.

13. The parametric analysis of the influence of the model parameters on the nanotubes and the interface layer stresses states was performed. The asymptotic cases of the stresses states for a small relative stiffness of the interface layer and a large relative size of the nanotube part were considered and analyzed. The comparison with published experimental data was performed and demonstrated a good agreement.

14. The proposed multi-parametric model can be used for the theoretical analysis of properties of new nanocomposite materials and for analysis of the experimental data.

15. On the basis of the previous researches the consistent and correct theory of interphase layer is formulated. The model is supposed to be a basis for construction of more complex models for nanomechanics. The description of the interphase layer theory and some main applications include the following moments: -the formal mathematical statement,- the physical constitutive equations, - the identification problem of the parameters determining nonclassical effects, -the qualitative analysis of the theory-analytical estimations of properties of an interphase layer, -the qualitative analysis of the theory-estimation of an interphase layer influence on the effective characteristics of a composite, -some application for quantum mechanical approaches, -numerical modeling of the stress state of the cell with inclusions and some notes about specific averaging procedures for filled composites, - previously results of the generalized Eshelby problem.

16. The particular examples are considered:

    -The approximated analytical dependences of the properties of interphase layer in a composite near the border between an inclusion and matrix on the characteristics of cohesion and adhesion fields of phases are established and approximate analytical estimations of Young's and shear moduli of the interphase layer are given.

    -The model problem for nonsingular crack in be-plane 2-D statement was investigated. The hypothesis of existence of local stress fields near a crack tip has received the formal substantiation. The new physical constant C (cohesion field) was identified form the parameters of the fracture mechanics (critical crack disclosing ,δ_k, within the Barenblatt's zone of length, r_0, and specific superficial energy, γ) is established.

17. The solution of the meniscus problems is given, which is interesting for determining the role of the surface effects (adhesion) for the known effect of meniscus forming. This solution may be used for formulation of the experiment aiming at determining the adhesion parameter.

18. Composite materials are considered taking into account the theory of interphase layer (local cohesion and adhesion effects). The account of these local effects allows to model effect of strengthening of the filled composite materials.

19. Approximate analytical estimations of Young's modulus of the composite materials taking into account the local cohesion and adhesion effects are established which show the good agreement with the experimental dates for all diapason of the sizes if inclusions and volume fractures.

20. An analytical representation is received for the constrained deformation of an inclusion of arbitrary shape in an infinite matrix. Eshelby matrix connecting deformations inside a cell and homogeneous deformations at infinity is obtained. Here, we received new fundamental result. From Eshelby matrix for a considered class of problems of interphase layer the classical Eshelby matrix and additional component corresponding to influence of a cohesion surface layer on rigidity of a cell are picked out. The received formulas are base for effective technical of calculating of average properties a composite material within the framework of model of moment cohesion.

21. A variant of the consecutive concept of the quantum-mechanical description of materials was formulated. The suggested concept allows connecting macro- and micro-characteristics of materials with parameters of potentials used for modelling continuum environments as ensemble of the particles connected by special character of interactions. The different types of potentials are considered within the framework of the suggested research. Their analysis is given.

22. There were developed several approaches for an estimation of the homogenized properties of heterogeneous media with complex microstructure, described by problems of spatial moment cohesion, allowing to receive effective characteristics of composite materials, and also to simulate a picture of strain-stress state in a micro cell with inclusion of the any form with account of action of local cohesion and adhesion fields of displacements. On the basis of procedure of asymptotic homogenization of composite materials with a periodic microstructure it was received the formula for effective characteristics of composite materials with account of the local effects. This formula is based on the solution of spatial problems of moment cohesion in a periodic cell with special conditions of periodic jump for which the block method of multipoles has been developed.

23. With the help of a block method of multipoles distribution of energy density and components of stress tensor in micro cell with inclusion is simulated at variation of cohesion field parameters and of inclusion orientation inside a cell that has significance for quality evaluation of influence of cohesion fields and for calculation of effective characteristics of materials with random distribution of inclusions.

24. The algorithm of the solution of a problem of model parameters identification has been developed according to experimental researches for the general three-dimensional case. The series of the calculations has been made. These calculations have shown, that the offered algorithm of model parameters identification allows restoring cohesion parameters with high accuracy. The following results was received for the identification problem of model parameters according to experimental researches:- The problem of model parameters identification using the data of experimental researches has been formulated. Setting of this variational problem allowing choosing from allowable set of model parameters such set, at which some criterion function accepts the minimal value; - Among a set of criterion functions has been chosen what is the most suitable for a considered identification problem; -The problem of one-dimensional "moment cohesion" model parameters identification has been solved with use of available experimental data. - The algorithm of the solution of mathematical model parameters identification problem has been developed in a case double-plane moment cohesion model. The expression was received, allowing receiving exact value of a variation of criterion functional, caused by a variation of parameter. -The algorithm of the solution of a problem of model parameters identification has been developed according to experimental researches for the general three-dimensional case. -The series of the calculations has been made. These calculations have shown, that the offered algorithm of model parameters identification allows restoring cohesion parameters with high accuracy. The problem of the model parameters identification on the base of the experimental data (Minoru Miva, 1978)is solved in the frame of the simplified model. It is shown, that micromechanical modeling gives the good description of a composite as a whole. The effect of rigidity increase of a composite with reduction of diameter of particles is modeled.

25. A new general kinematic theory of defects in continuous media the general mechanisms of existence of defects, their generation (or birth) and disappearance (or healing) were establish the general mechanisms of existence of defects, their generation (or birth) and disappearance (or healing). We

establish the general mechanisms of existence of defects, their generation (or birth) and disappearance (or healing). The significance of the present work is, in particular, in discovering the interconnection between the developed kinematic models for the continuous media with defects and their role in the hierarchy of multi-scale modeling.

26. The full and correct model of mediums with conserved dislocations is given the new classification of the dislocations is offered, which gives the additivity in decomposition of slow- changing part of strain energy density concerning with three various types of dislocations takes place.

It was prove the existence of nonclassical, non-local component of the potential energy associated with defects – dislocations that is very unexpected for gradient models, which is the model of mediums with system of the distributed dislocations.

27. It was obtained the generalized model of mechanics of continua as a whole that is theoretical model in which a surface tension, static friction bodies with ideally smooth surface of contact, the meniscus, wettability and capillarity are modeled as special effects within the framework of unified continual description. For the first time strictly proved physical treatment of all generalized modules of elasticity both in volume of the researched mediums and on its surface is given. Ways of definition new physical constant are offered to the generalized model appropriate as damage accumulation of a material and also to local scale effects of the cohesion and adhesive type on the basis of a sequence of test tests. Within the framework of the offered model the spectrum of scale effects in volume and on a surface is taken into account. Apparently, the submitted generalized model of mechanics of continua is the first correct theoretical model, in which various special scale effects (cohesion interactions, a surface tension and so forth) in volume and on a surface are modeled within the framework of unified continual description.

28. The Klapeiron's and Dupre's theorems were proved for the pseudocontinuum model with scale effects of the cohesion and adhesion types. The Klapeiron's allows to connect the potential energy and the work of the external forces in accurate solution for the appropriate boundary-value problem. «Dupre's theorem» can help to define in the direct experimental way the energy of adhesive interaction of bodies on the basis of Young's equation.

29. The algorithm of the damage accumulation estimation (development of porosity and so on), was proposed on the base strong generalized model of the mediums with reserved dislocation. This algorithm for the account of damage accumulation (development of porosity and so on), near the ends of cracks; damage of material in zones of concentrators of stresses; damage of zone of plasticity connected to development in the mechanics of destructions was proposed on the base strong generalized model of the mediums with reserved dislocation. The asymptotic method of the reduced loadings was proposed, as theoretically proved way of the account of the damage accumulation in the filled composites and anisotropic composite materials under various conditions of loading.

30. Theory of reinforcement of rubber composites is elaborated on the basis of multiscale hierarchical model and approach, which consider rubber composite as heterogeneous multicomponent medium, description the properties of which is necessary make taking into account the physico-chemical and micromechanical peculiarities of its components and using the different structural scales of detalization: from nano-, mezo- up to micro- and macro.

31. For nano- and mezo-description of structural and mechanical properties of above composites the unorthodox algorithms have been developed by the authors. On the base of above algorithms in parallel regimes of calculations by supercomputer some computational experiments (methods of Monte-Carlo, molecular dynamics, quantum mechanics) have been made. Representative volumes of

medium under consideration have kept up to 10^6 atoms and molecules, that corresponds to microclusters of real composite's structures.

32. By dint of above methods the general peculiarities of formation the microstructure of polymeric composites, consisted of different polymeric matrixes (the thermoplastics, the elastomers, the thermoreactoplastics) and the active fillers (black and white soot, fullerens, nanotubes, montmorillonite), terminated by different chemical groups have been elaborated. Separately it was investigated an influence of molecular water inside a microcluster on the micromechanical behavior of above media.

33. It was stated, that the results of molecular modeling signify as a base for creation of optimal structural formula of the expected perspective composites. A variation of component's content, physical and chemical properties of the ingredients let us a consciously aim the requisite micromechanical properties of mesoscopic microclusters, that is, the representative elements of composite's structure.

34. A correctness of atomic-molecular computational model under study is verified by means of nano- and microstructure experiments. The methods of dynamic force and tunnel-scanning microscopy and optical interference microscopy have been used. Some important geometrical parameters and sizes of nano- and mezoscopic formations for aggregates and agglomerates of particles of fillers, length of interphase layers, parameters of polymeric matrix and other concomitant structures, which are formed inside a heterogeneous composite's media during the preparation of row rubber compounds, have been elaborated.

35. To describe a macromechanical (rheological) properties of heterogeneous medium in viscoelastic state (available for processing into articles) some constitutive rheological equations have been proposed. In order to construct above constitutive equations the unorthodox integral models of viscoelastic media have been used and a method of theoretical and experimental identification the civility of those have also been developed. In particular, it was shown the availability of neural network models for identification of viscoelastic and relaxation properties of composite's polymer media.

36. Viscoelastic properties of model elastomeric compounds on the base of natural rubber filled with different sorts of disperse particles (black and white soot, montmorillonite) have been tested in wide range of regimes and parameters of deformations and temperatures by rheological equipment. The most important relaxation parameters of viscoelastic heterogeneous medium, which governs a macrorheological behavior of above medium by deformation (processing) have been calculated and systematized.

37. To estimate the efficient (average) macrocharacteristics of strength properties of heterogeneous media (rubber composites, particularly) a new method have been proposed. Above stage of work logically finalizes the multiscale hierarchical description of behavior of reinforcement rubber composite at the macromechanical level. The evaluation of effective mechanical and strength properties of composites appoints the operational merits of those.

38. Further evolution and elaboration of the theory of reinforcement must be taken on the base of construction of data-set for optimal structures and the components of composite, taking into account the physical and chemical properties of surfaces and potentials of interactions in order to prognosis the reinforcement effect either concrete properties of material. It is important to attend to the using of nanoparticles as reinforcement filler and technology the distribution of those inside the matrix.

Milestones Completed

Current technical status - on schedule

Cooperation with foreign collaborators
We discussed with the Partner the current questions under the project, some corrections of the Work plan from the point of view of the account of concrete parameters at modelling. The questions connected to experimental researches, questions of correction of the plan of works also are discussed, from the point of view of realization of additional quantum-chemical researches.

Problems encountered and suggestions to remedy
We hope in the near future to discuss the last results received during work under Project.

Perspectives of future developments of the research/technology developed
We hope to continue our researches in framework collaboration with Air Force Research Laboratory.

Attachment. Papers and reports published during present stage of work

1. Lurie S., Belov P., Tuchkova N. The Application of the multiscale models for description of the dispersed composites// Int. Journal "Computational Materials Science" A., 2004, 36(2):145-152.
2. Sergey A. Lurie and Alexander L. Kalamkarov General Theory of Defects in Continuous Media// Solid and structures, 2005,(accepted for print)
3. Evtushenko Y.G, Lurie S., Volkov-Bogorodsky D, Zubov V. I. Numerical - analytical modelling of scale effects at research of deformations for disperse reinforced nanocomposites with use of the block method of multifields//Comput. Math. And Math Phys. 2005 (accepted for publication)
4. Obraztsov I.F., Lurie S.A., Belov P.A., Volkov-Bogorodsky D.B., Yanovsky Yu.G., Kochemasova E.I., Dudchenko A.A., Potupcik E.M., Shumova N.P. Elements of theory of interphase layer. Composite Mechanics and Design, 2004, v.10, N3, pp.596-612.
5. Lurie S, Belov P, Volkov-Bogorodsky D, Tuchkova N, Nanomechanical Modeling of the Nanostructures and Dispersed Composites, Int. J. Comp Mater Scs 2003; 28(3-4):529-539
6. Lurie, P.A. Volkov-Bogorodskii D.B.and N.P. Tuchkova N. P, Mathematical model of the interphase layer. Mathematical and numerical modeling of the composites// Int. Symp. On Trend in applications of Mathematics to Mechanics (STAMP"2004) Aug. 2004, Seeheim, Germany. pp.28-29
7. Lurie S., Hui D. and Kireitseu M. Multiscale Modeling of the Interphase Layers in the Mechanics of Materials, Proceedings Book of 11th International Conference on Composites/Nano Engineering, Hilton Head, S. Carolina, August 8-14, 2004. pp. 784-786
8. Lurie S., Leontiev A., Tuchkova N. One algorithm of the solution of the fracture mechanics problems for the finite elastic bodies//Mechanics of composite materials and structures. 2004, v.10. N3
9. S A Lurie, N P Tuchkova, V I Zubov The Application of the Interphase Model for the Description of the Filled Composite Properties with Nanoparticles. Identification of the Parameters of the Model // The 2nd International Conference on Composites Testing and ModelIdentification Comptest 2004 held on the 21st - 23rd September 2004, hosted by the Department of Aerospace Engineering, University of Bristol, U.K. (http://www.aer.bris.ac.uk/comptest2004/proceedings)
10. Vlasov A.N. Averaging of mechanical properties of heterogeneous media. Composite Mechanics and Design, 2004, v.10, N3, pp.424-441.
11. Yanovsky Yu.G., Zgaevskii V.E. Mechanical properties of high elastic polymer matrix composites filled with rigid particles: Nanoscale consideration of the interfacial problem. Composite Interfaces, 2004, v.11,N3, pp.245-261.
12. Yanovsky Yu.G. Multiscale Modeling of Polymer Composite Properties. International. Journal for Multiscale Computational Engineering, 2005, v.3, N2.
13. Obraztsov I.F., Vlasov A.N., Yanovsky Yu.G. Calculating Method of Strength Properties of Heterogeneous Media. Doklady Physics, Moscow, 2005 (in press).

14. Yanovsky Yu.G. Multiscale Modeling of Polymer Composite Properties. Proceedings of the Sixth World Congress on Computational Mechanics, Tsinghua University Press and Springer, Beijing, China, Eds. Z.Yao, M.Yuan, W.Zhong, 2004, pp.758-762.
15. Nikitina E.A., Yanovsky Yu.G. Quantum Mechanical Investigation of the Microstructure and Mechanical Characteristics of Nano-Structured Composites. Abstracts of the Sixth World Congress on Computational Mechanics, Tsinghua University Press and Springer, Beijing, China, Eds. Z.Yao, M.Yuan, W.Zhong, 2004, p.626.
16. Teplukhin A.V. Monte-Carlo Modeling of Atomic and Molecular Mesoscopic Composite Systems. Abstracts of the Sixth World Congress on Computational Mechanics, Tsinghua University Press and Springer, Beijing, China, Eds. Z.Yao, M.Yuan, W.Zhong, 2004, p.627.
17. Vlasov A.N., Yanovsky Yu.G. Numerical Modeling to Determine Constitutive Relations of Jointed Rock. Abstracts of the Sixth World Congress on Computational Mechanics, Tsinghua University Press and Springer, Beijing, China, Eds. Z.Yao, M.Yuan, W.Zhong, 2004, p.628.
18. Yanovsky Yu.G., Basistov Yu.A., Filipenkov P.A. Problem of identification of rheological behavior of heterogeneous polymeric media under finite deformation. Proceedings of the XIV International Congress on Rheology, ISBN 89-950057-5-0, The Korean Society of Rheology, 2004, SO18-1 – SO18-3.
19. Yanovsky Yu.G. Multiscale Modeling of Polymer Composite Mechanical Properties and Behavior. Abstracts of the International Conference on Heterogeneous Material Mechanics, Chongqing University and Yangtze River/Three Gorges, China, 2004, p.252.

ATTACHMENTS
Summary of Personnel Commitments
Dorodnicyn Computing Centre of Russian Academy of Sciences:
Lurie S.A. (task 2; tasks 4; tasks 5;   task 6;   task 7);
Belov P.A.(Tasks 4; 6);
Evtushenko U.G. (Task 7)
Moiseev E.I (Task 6.)
Zubov V.I. (Task 7)
Tuchkova N.P. (Task 6);
Goldshtein R.V.(Tasks 4; 5);
Ustinov K.B. (Tasks 4);
Perelmuter M.N. (Task 5)
Institute of Applied Mechanics of Russian academy of Sciences
Yanovskiy Y.G. (Tasks 1; 5;);
Levin Y.K. (Task 5);
Vlasov A.N. (Task 7)
Volkov-Bogorodskiy D.B. (Task 2).
Karnet Y.N. (Tasks 1, Tasks 5);
Filipenkov P.A. (Task 3)
Nikitina K. A. (Tasks 1)
Tepluchin A.V. (Tasks 1)

2. Major Equipment Acquired   - Non

Manager of the Project   Sergey Lurie